Deutsche Rohstoffagentur
Bundesanstalt für Geowissenschaften und Rohstoffe

50 DERA Rohstoffinformationen

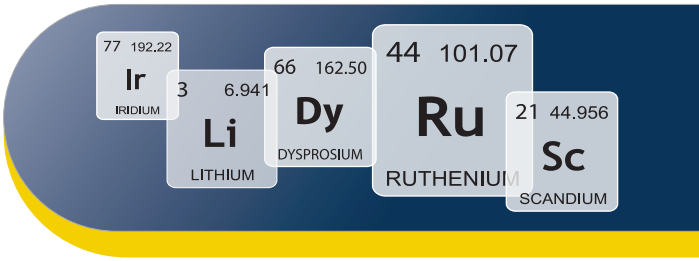

Raw materials for emerging technologies 2021

A commissioned study

Impressum

Editors: German Mineral Resources Agency (DERA) at the
Federal Institute for Geosciences and Natural Resources (BGR)
Wilhelmstr. 25–30
13593 Berlin, Germany
Phone: +49 30 36993 226
dera@bgr.de
www.dera.bund.de

Authors: Frank Marscheider-Weidemann, Sabine Langkau, Elisabeth Eberling, Lorenz Erdmann, Michael Haendel, Michael Krail, Antonia Loibl, Christoph Neef, Marius Neuwirth, Leon Rostek, Saeideh Shirinzadeh, Denis Stijepic, Luis Tercero Espinoza
Fraunhofer Institute for Systems and Innovation Research ISI
Breslauer Str. 48
76139 Karlsruhe

Sarah-Jane Baur, Mathilde Billaud, Otmar Deubzer, Franziska Maisel, Max Marwede, Jana Rückschloss, Max Tippner
Fraunhofer Institute for Reliability and Microintegration IZM
Gustav-Meyer-Allee 25, building 17/3
13355 Berlin

Contact DERA: Ulrike Dorner | ulrike.dorner@bgr.de
Viktoriya Tremareva | viktoriya.tremareva@bgr.de

Layout: deckermedia GbR

Date: August 2021

Reference: Marscheider-Weidemann, F.; Langkau, S.; Baur, S.-J.; Billaud, M.; Deubzer, O.; Eberling, E.; Erdmann, L.; Haendel, M.; Krail, M.; Loibl, A.; Maisel, F.; Marwede, M.; Neef, C.; Neuwirth, M.; Rostek, L.; Rückschloss, J.; Shirinzadeh, S.; Stijepic, D.; Tercero Espinoza, L.; Tippner, M. (2021): Raw materials for emerging technologies 2021. – DERA Rohstoffinformationen 50: 348 p., Berlin.

ISBN: 978-3-948532-61-1 (print version)
ISBN: 978-3-948532-62-8 (pdf)
ISSN: 2193-5319

Berlin, 2022

Federal Ministry for Economic Affairs and Climate Action

The Federal Institute for Geosciences and Natural Resources is the central geoscientific authority providing advice to the German Federal Government in all geo-relevant questions. It is subordinate to the Federal Ministry for Economic Affairs and Climate Action (BMWK).

Fraunhofer ISI

Fraunhofer IZM

Raw materials for emerging technologies 2021

A commissioned study

Commissioned by the German Mineral Resources Agency (DERA) at the Federal Institute for Geosciences and Natural Resources (BGR), Berlin

Preface

Mineral raw materials are essential for industrial value chain technological progress and the preservation of our prosperity. They make an important contribution to the future transformation of our society at all levels of economy, ecology and socio-cultural development.

With reference to the Federal Government's Raw Materials Strategy of 2010 and 2020 and its measures to increase security of supply, the German Mineral Resources Agency (DERA) carries out monitoring of potentially critical mineral raw materials, which are indispensable for the technological progress of our economy. This study was undertaken by the Fraunhofer Institute for Systems and Innovation Research ISI and the Fraunhofer Institute for Reliability and Microintegration IZM on behalf of DERA as part of it's raw materials monitoring.

The aim of DERA's raw materials monitoring is to inform German companies and political stake-holders about current demand, supply and price trends for primary mineral raw materials and intermediate products of the first stages of the value chain. Critical developments on the international commodity markets can thus be recognised at an early stage and possible alternative strategies can be developed within the companies.

The study analyses raw material demand from key and emerging technologies. The focus is on the question of which raw materials can be expected to experience possible increases in demand due to future technological developments over the next 20 years. Unexpected surges in demand due to technological changes on the market can have a significant impact on future commodity price and supply risks. The study is therefore updated every five years in close discussion with the German industry.

Dr. Peter Buchholz

Head of the German Mineral Resources Agency (DERA) at the
Federal Institute for Geosciences and Natural Resources (BGR)

Table of contents

List of figures

List of tables

Executive Summary

While emerging technologies have the potential to improve efficiency in existing systems, they can also potentially enable all new technology systems. They can thus trigger revolutionary innovation impulses beyond the boundaries of individual economic sectors. However, technological change can have a significant impact on the demand for individual mineral raw materials. The study “Raw materials for emerging technologies” was commissioned by the Federal Ministry for Economic Affairs and Energy (BMWi) in 2009 to investigate the demand impulses of future technologies (Angerer et al. 2009). Together with a follow-up study commissioned by DERA and published in 2016, results helped bridge considerable knowledge gaps with regard to raw material demand for emerging technologies (Marscheider-Weidemann et al. 2016). With innovation constantly accelerating, the present study updates the state of knowledge on the mineral raw material requirements of technological change.

In contrast to the previous studies in which emerging technologies were assigned to industrial branches, the 33 technologies in this study are presented according to clusters. The clusters are “Mobility and aerospace”, “Digitisation and Industry 4.0”, “Energy technologies and decarbonisation”, “Recycling and water management”, and “Power and data networks”. Therefore, the clusters also examine technologies that are not emerging technologies, but are essential for the clusters, like electricity networks.

In order to be able to map the future development of the various technologies as consistently as possible, the Shared Socioeconomic Pathways (SSPs), which were created as part of the 5th Assessment Report of the Intergovernmental Panel on Climate Change (IPCC) for climate policy issues, are used as framework scenarios (Kriegler et al. 2012). For the selected scenarios SSP1 (Sustainability), SSP2 (Middle Path), and SSP5 (Fossil Path), the narratives for the individual clusters are supplemented and backed up with data if these could not be taken directly from the SSP database of the International Institute for Applied Systems Analysis (IIASA no date).

In line with the two previous studies, results depend very much on the respective technologies and their market diffusion. For eleven metals, the estimated demand in 2040 from emerging technologies could be as high as or higher than their 2018 production (see Figure 0.1). However, it can also be seen in the figure that demand strongly depends on the respective scenarios (see the presentation of results in Section 5). For example, the demand in SSP1 (Sustainability) is very high for scandium due to its use in hydrogen technology, or for lithium from the higher demand in electromobility, while the raw material demand of these two metals in SSP5 (Fossil Path) is below the production volume in 2018. At the same time, the demand for ruthenium and platinum in SSP5 is particularly high, as large data volumes and storage capacities in data centers are assumed in this scenario in 2040. Table 0.1 summarises the most important emerging technologies and their demand for a number of raw materials. Raw material requirements for technologies outside the scope of this study were not considered.

The figures presented for the SSPs do not represent forecast values, but illustrate various future possibilities that appear realistic given what is known now. The overall scope of this study is to identify relevant fields of technologies and raw materials in order to encourage further work to address potential challenges and help develop measures to address those. The following measures can help contribute to a secure supply of mineral raw materials:

– increase capacities and improve efficiency in mining and processing,
– substitution at the material and technology level,
– resource efficiency in production and application,
– recycling, including design for recycling, return strategies, and efficient recycling technologies.

When developing new technologies, identifying options for securing raw materials should be considered. Current raw material prices depend on many factors; they are not a measure of the long-term physical or economic availability of a raw material. Therefore current prices should not be the sole basis for long-term decisions.

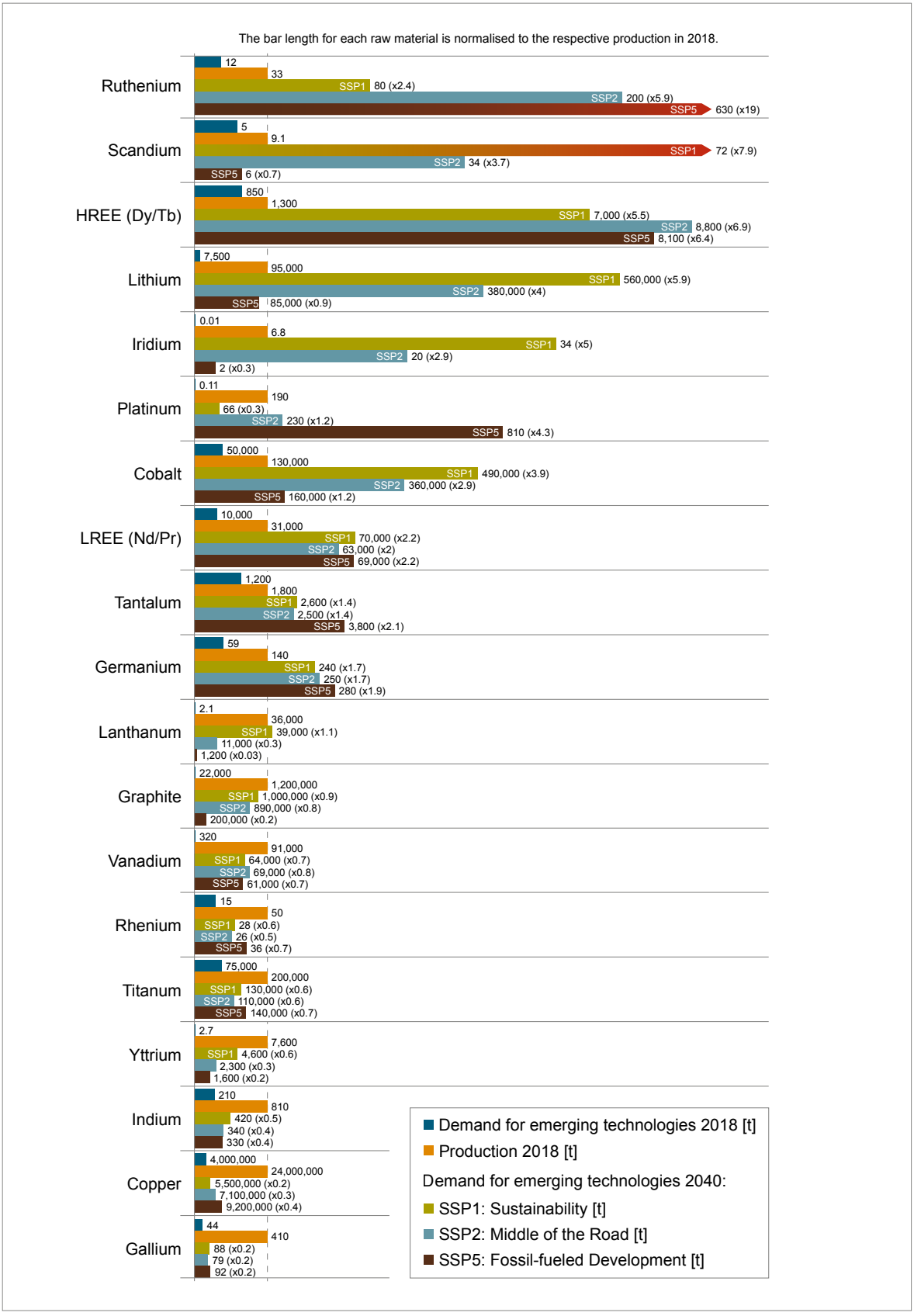

Figure 0.1: Demand for different raw materials for selected emerging technologies in 2018 and in the three scenarios in 2040 compared to the primary production of the respective raw materials in 2018

Table 0.1: Global raw material demand as a ratio of production in 2018 for the 33 analysed emerging technologies

Raw material	$Demand_{2018}$ / $Production_{2018}$	$Demand_{2040}$ / $Production_{2018}$			Emerging technologies with high demand
		SSP1 Sustain-ability	SSP2 Middle Path	SSP5 Fossil Path	
Ruthenium	0.4	2.4	5.9	19	Data centers, super alloys, synthetic fuels
Scandium	0.5	7.9	3.7	0.7	SOFC – Stationary fuel cell, water electrolysis
HREE	0.6	5.5	6.9	6.4	Electrical traction engines for motor vehicles, wind turbines
Lithium	0.1	5.9	4	0.9	Lithium-ion high-performance electricity storage, solid-state batteries, alloys for airframe lightweight construction
Iridium	0	5.0	2.9	0.3	Water electrolysis
Platinum	0	0.3	1.2	4.3	Data centers
Cobalt	0.4	3.9	2.9	1.2	Super alloys, lithium-ion high-performance electricity storage, solid-state batteries
LREE	0.3	2.2	2	2.2	Electrical traction engines for motor vehicles, wind turbines, high-performance permanent magnets, data centers
Tantalum	0.7	1.4	1.4	2.1	Super alloys, microelectronic capacitors, radio frequency microchips, data centers
Germanium	0.4	1.7	1.7	1.9	Fiber optic cable
Lanthanum	0	1.1	0.3	0.03	Solid-state batteries, water electrolysis, SOFC – Stationary fuel cell
Vanadium	0	0.7	0.8	0.7	CCS – Carbon capture and storage, redox flow batteries
Rhenium	0.1	0.6	0.5	0.7	Super alloys
Titanium	0.3	0.6	0.6	0.7	Alloys for airframe lightweight construction, superalloys, solid-state batteries, additive manufacturing of metal components (“3D printers”), water electrolysis, seawater desalination
Yttrium	0	0.6	0.3	0.2	Automatic piloting of road vehicles, water electrolysis, SOFC – Stationary fuel cell
Graphite	0	0.9	0.8	0.2	Lithium-ion high-performance electricity storage
Indium	0.3	0.5	0.4	0.4	Indium tin oxide (ITO) in display technology, optoelectronics/photonics, thin-film photo-voltaics
Copper	0.2	0.2	0.3	0.4	Power grid expansion, electrical traction engines for motor vehicles, wind turbines, solid-state batteries, water electrolysis
Gallium	0.1	0.2	0.2	0.2	Radio frequency microchips, thin-film photo-voltaics

1 Framework scenarios for global socioeconomic development

1.1 Background: The Shared Socioeconomic Pathways

The five Shared Socioeconomic Pathways (SSPs) were created from 2011 onwards as part of the 5th Assessment Report of the Intergovernmental Panel on Climate Change (IPCC) for climate policy issues (Kriegler et al. 2012). Given the great uncertainty surrounding future development, the SSPs represent different global socioeconomic developments for the 21st century.

The SSPs serve as a basis for and components of scenarios (Pachauri & Meyer 2014) and are one element of the huge range of potential socioeconomic trajectories into the future. Each SSP comprises a narrative or storyline and, initially, quantifications split into various global models for population (International Institute for Applied Systems Analysis, IIASA (Kc & Lutz 2017)), gross domestic product (GDP, separate implementations into individual models produced in each case by IIASA (Crespo Cuaresma 2017), OECD (Dellink et al. 2017) and Potsdam Institute for Climate Impact Research, PIK (Leimbach et al. 2017)) as well as urbanisation (National Center for Atmospheric Research, NCAR (Jiang & O'Neill 2016)). Within this, the development of population is a central driver for the development of GDP. Above and beyond this, additional parameters, such as energy consumption and land use, have been quantified into various global Impact Assessment Models (so-called IAMs) on this basis (Lutz et al. 2019). From the total of five plausible SSPs, there are four extreme scenarios and one scenario illustrating the middle ground between these extremes (see Figure 1.1). The narratives of all five SSPs are presented below.

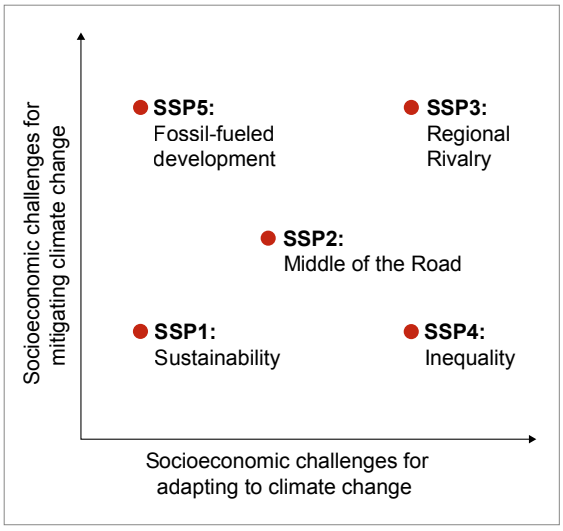

Figure 1.1: The five Shared Socioeconomic Pathways (source: O'Neill et al. 2017)

SSP1 Sustainability – Taking the green road (low challenges to mitigation and low challenges to adaptation)
"The world shifts gradually, but pervasively, toward a more sustainable path, emphasizing more inclusive development that respects perceived environmental boundaries. Management of the global commons slowly improves, educational and health investments accelerate the demographic transition, and the emphasis on economic growth shifts toward a broader emphasis on human well-being. Driven by an increasing commitment to achieving development goals, inequality is reduced both across and within countries. Consumption is oriented toward low material growth and lower resource and energy intensity." (Riahi et al. 2017).

SSP2 Middle of the Road (medium challenges to mitigation and medium challenges to adaptation)
"The world follows a path in which social, economic, and technological trends do not shift markedly from historical patterns. Development and income growth proceeds unevenly, with some countries making relatively good progress while others fall short of expectations. Global and national institutions work toward but make slow progress in achieving sustainable development goals. Environmental systems experience degradation, although there are some improvements and overall the intensity of resource and energy use declines. Global population growth is moderate and levels off in the second half of the century. Income inequality persists or improves only slowly and challenges to reducing vulnerability to societal and environmental changes remain." (Riahi et al. 2017).

SSP3 Regional Rivalry – A Rocky Road (high challenges to mitigation and high challenges to adaptation)
"A resurgent nationalism, concerns about competitiveness and security, and regional conflicts push countries to increasingly focus on domestic or, at most, regional issues. Policies shift over time to become increasingly oriented toward national and regional security issues. Countries focus on achieving energy and food security goals within their own regions at the expense of broader-based development. Investments in education and technological development decline. Economic development is slow, consumption is material-intensive, and inequalities persist or worsen over time. Population growth is low in industrialized and high in developing countries. A low international priority for addressing environmental concerns leads to strong environmental degradation in some regions." (Riahi et al. 2017).

SSP4 Inequality – A Road divided (low challenges to mitigation, high challenges to adaptation)
"Highly unequal investments in human capital, combined with increasing disparities in economic opportunity and political power, lead to increasing inequalities and stratification both across and within countries. Over time, a gap widens between an internationally-connected society that contributes to knowledge- and capital-intensive sectors of the global economy, and a fragmented collection of lower-income, poorly educated societies that work in a labor intensive, low-tech economy. Social cohesion degrades and conflict and unrest become increasingly common. Technology development is high in the high-tech economy and sectors. The globally connected energy sector diversifies, with investments in both carbon-intensive fuels like coal and unconventional oil, but also low-carbon energy sources. Environmental policies focus on local issues around middle and high income areas." (Riahi et al. 2017).

SSP5 Fossil-fueled development – Taking the highway (high challenges to mitigation, but low challenges to adaptation)
"This world places increasing faith in competitive markets, innovation and participatory societies to produce rapid technological progress and development of human capital as the path to sustainable development. Global markets are increasingly integrated. There are also strong investments in health, education, and institutions to enhance human and social capital. At the same time, the push for economic and social development is coupled with the exploitation of abundant fossil fuel resources and the adoption of resource- and energy-intensive lifestyles around the world. All these factors lead to rapid growth of the global economy, while global population peaks and declines in the 21st century. Local environmental problems like air pollution are successfully managed. There is faith in the ability to effectively manage social and ecological systems, including by geo-engineering if necessary." (Riahi et al. 2017).

1.1.1 Selection of several SSPs as framework scenarios for the Raw Materials for Emerging Technologies 2021 study

The two extreme scenarios SSP1 and SSP5 as well as the Middle of the Road scenario SSP2 were selected as framework scenarios for this study and are presented in more detail below. While overall SSP2 represents the moderate Middle of the Road scenario it is not the midway point between SSP1 and SSP5 because to a certain extent it also takes account of aspects from the SSP3 and SSP4 extreme scenarios (see Figure 1.1). In particular, SSP1 and SSP5 include very significant and/or very rapid global development of education, economy and technology. However, they differ in terms of their focus and objective: in SSP1, the international community is striving for sustainable development taking ecological limits into consideration. In contrast to this, confidence in technological innovations and competitive markets to solve ecological problems dominates in SSP5 where development is accompanied by fast economic growth based on fossil fuels. SSP2 sees an interplay between fossil fuel-based growth and efforts to develop sustainably, continuing historical developments to date. However, global development of education, economy and technology are slower and weaker overall than in SSP1 and SSP5. They are constrained by tendencies towards regional rivalry and protectionism as well as inequalities, each of which is considered to an even more extreme degree in SSP3 and SSP4. These are important and plausible potential future developments. However, given the

extreme constraint of technology development, they are less relevant for this study than SSP1, 2 and 5. Therefore, SSP3 and 4 are not included in the technology synopses on the grounds of capacity constraints.

1.1.2 Overviews of the selected SSPs

The tables below once again illustrate the key differences and common features of the selected framework scenarios SSP1, 2 and 5.

1.1.3 Further assumptions relating to climate policy

In their basic form (basic scenarios), SSPs 1–5 do not include any assumptions on future climate policy measures. Yet without such measures, the international climate protection goals will be missed in all five SSPs.

Within this context, failure seems plausible for SSP5 as a result of which no international climate policy successes are assumed (**SSP5 baseline**). For SSP2, in addition to the basic scenario, this study assumes that the 2 °C goal and/or limiting radiative forcing to 2.6 W/m² is achieved through climate policy measures (**SSP2-26**). For SSP1, in addition to the basic scenario, it is assumed that the 1.5 °C goal and/or limiting radiative forcing to 1.9 W/m² is achieved through a very ambitious climate policy (**SSP1-19**).

Table 1.1: Population development in SSP1, 2 and 5 (source: Riahi et al. 2017)

Indicator	SSP1 Sustainability	SSP2 Middle of the Road	SSP5 Fossil Path
Population growth	Relatively low	medium	Relatively low
Urbanisation	high	medium	high
Education level	high	medium	high
Health level	high	medium	high

Table 1.2: Development in relation to economy and technology in SSP1, 2 and 5 (source: Riahi et al. 2017)

Indicator	SSP1 Sustainability	SSP2 Middle of the Road	SSP5 Fossil Path
International cooperation	Effective	Comparatively weak	Effective for development goals, weak for environmental goals
Environmental policy	Better management of local and global problems, stricter regulation of harmful substances	Moderate successes	Focus on local problems with direct link to wellbeing, low efforts to address global problems
Policy focus	Sustainable development	Weak focus on sustainability	Economic development, free markets
Institutions	Effective	Uneven, modestly effective	Increasingly effective, focus: free markets
Environment	Conditions improve with time	Continued deterioration of conditions	Highly technical solutions, successful for local problems
Land use	Strong regulation	Medium regulation	Medium regulation

Table 1.3: Development in relation to policy and environment in SSP1, 2 and 5 (source: RIAHI et al. 2017)

Indicator	SSP1 Sustainability	SSP2 Middle of the Road	SSP5 Fossil Path
Income growth per capita	high in medium- and low-income countries, medium in high-income countries	medium, irregular	high
Economic inequalities	reduced between and within countries	moderate, uneven reduction between and within countries	significantly reduced, especially between countries
International trade	medium	medium	high, regional specialisation in production
Globalisation	connected markets, regional production	semi-open globalised economy	strong globalisation and interconnectedness
Consumer behaviour	low growth in material consumption	material-intensive	materialism, status consumption, tourism, mobility
Meat consumption	low	medium	high
Technology development	fast	medium, irregular	fast
Technology transfer	fast	slow	fast
Energy technologies	focus: efficient and renewable	investment in renewables but continued fossil dependence	fossil, no active pursuit of alternatives
Carbon intensity	low	medium	high

1.2 Energy scenarios

Overall, the SSPs represent very different energy futures, exhibiting a broad spectrum of potential energy demand developments and energy supply structures. This spectrum results from different assumptions of the framework conditions for energy systems, such as costs and the availability of future fossil fuel resources, technological change, economic growth and new energy services etc.

The extent and structure of future energy technologies in the SSP scenarios are key determinants of the challenges of mitigating and adapting to climate change. For example, the SSP5 basic scenario is hugely dependent on fossil fuels and includes an increasing share of coal in the energy mix. In contrast to this, SSP1 includes an increasing share of renewable energies and other low-carbon energy sources. Compared with the other SSPs, the “Middle of the Road” picture in SSP2 results in a more balanced energy development based on a continuation of the current energy mix and its dominance of fossil fuels. This is continuously improved through the use of biomass and renewable energies. As can be seen in Figure 1.1, in SSP2 medium challenges result in terms of both adapting to the consequences of climate change and also avoiding and reducing greenhouse gas emissions.

The SSP5 scenario exhibits a more than threefold increase in energy demand over the course of the century (driven primarily by rapid economic growth), see Figure 1.2. As a result, SSP5 is characterised by serious challenges to mitigating climate change. Energy demand in the SSP1 scenario is particularly low, peaks in around 2080 and then falls due to the successful implementation of energy-efficiency measures and changes in behaviour. This results in a global decoupling between energy demand and economic growth. In line with the intermediate challenges, demand for

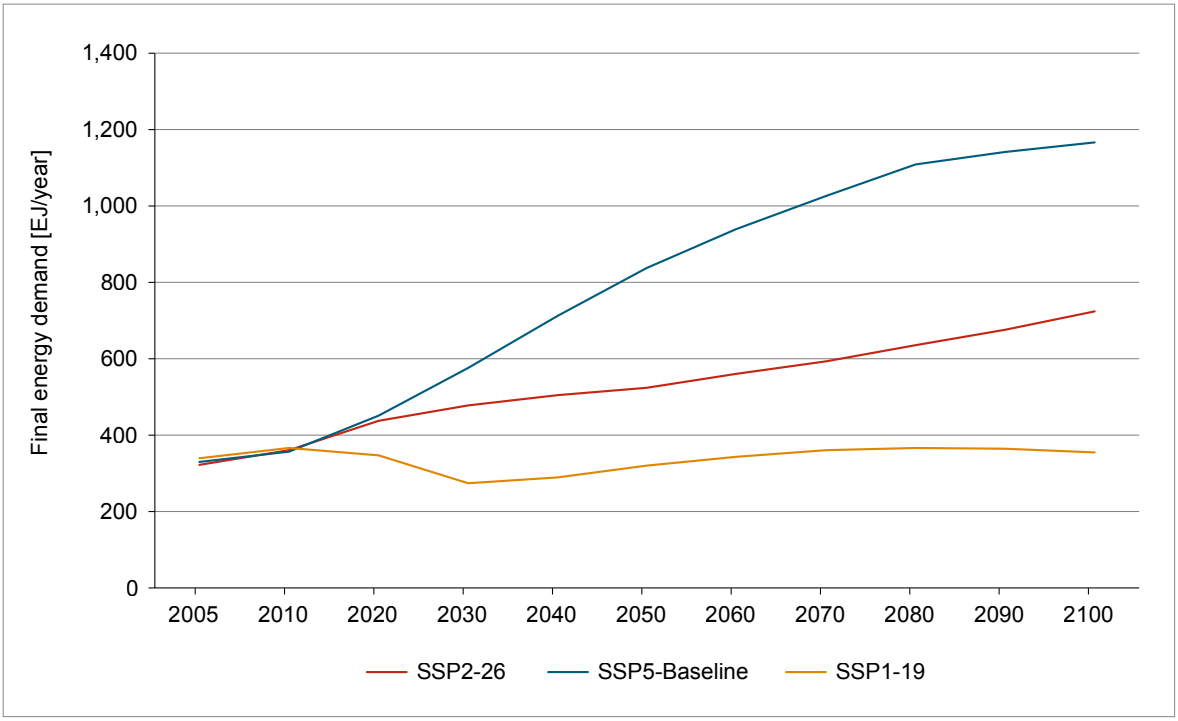

Figure 1.2: Final energy demand of the three selected SSP scenarios (source: IIASA database, no date)

ultimate energy in the SSP2 scenario doubles in the long term (2100), indicating a middle ground pathway.

The SSP database of the International Institute for Applied Systems Analysis (IIASA no date) contains explicit details of the development of technologies in the SSPs, such as details for wind energy, solar energy, hydrogen generation, CCS and the production of synthetic fuels (Riahi et al. 2017). We have used these to describe the market potential in the year 2040 in the corresponding technology chapters. The database was produced between 2012 and 2018. Where useful and possible, short-term influences, such as the COVID-19 pandemic or current discussions on decarbonisation, have also been taken into account.

1.3 Mobility scenarios

We have produced various mobility scenarios on the basis of the Shared Socioeconomic Pathways (SSPs) (Riahi et al. 2017) in order to describe new registration figures and therefore vehicle sales and production. The source of data analysed to describe general new registration figures and technology-specific new registration figures (this relates to electric vehicles: EV) was the internal xEV database of the Fraunhofer ISI. The database was developed in 2014 by Fraunhofer ISI and has been updated annually ever since. The last update was in April 2020. The database covers the global production and sales figures for conventional vehicles and xEV models, itemised by country, as well as information about the battery capacity and range of the vehicles. The database aggregates information made available by Marklines Co, Ltd (MARKLINES CO Ltd 2020), the International Organization of Motor Vehicle Manufacturers (OICA 2020), the European Automobile Manufacturers Association (ACEA 2020), the EV sales blog (EV Sales Blog 2020) and other online sources (e.g. websites of automotive OEMs). The ISI xEV database was compared with the European Alternative Fuels Observatory (EAFO 2020) and found to be a good match.

Modelling of the new registration figures on the basis of GDP development in the SSP scenarios is illustrated below. We have described market diffusion of electric vehicles with the aid of the Bass diffusion model and adapted to the SSP scenarios.

1.3.1 Development of vehicle markets

In the past, we have been able to see that new registration figures and vehicle markets grow in parallel with global GDP (see Figure 1.3). Since 2017, new registration figures have deviated from the GDP growth trend. The reason for this is not clear. On the one hand, the growth of vehicle markets can be seen to be clearly slowing down, in Europe for example, which could indicate that the market is potentially saturated. In 2019, the registration figures in China also showed a distinct drop, which doesn't necessarily indicate market saturation and could only be a temporary effect. Over the last few years and during the COVID-19 pandemic in 2020 in particular, vehicle sales have not therefore been a clear driver of GDP growth. However, the data does not allow us to conclude whether the new registration figures translate into saturation globally and are therefore decoupling from GDP growth in the long term.

Despite the current deviations, we selected GDP as a key input parameter for modelling the mobility scenarios and new registration figures. This approach simplifies the interdependency between GDP and vehicle sales which is currently evident in reality. GDP growth was used as an exogenous variable for describing the vehicle market in the modelling.

Continued proportional development of the vehicle markets and predicted GDP were presumed in the “Middle of the Road” (SSP2) and “Fossil Path” (SSP5) scenarios. In the “Sustainability” (SSP1) scenario, which explicitly presumes that economic activities will transition to low-resource and energy-efficient practices, modelling of the vehicle markets was only linked to the development of GDP to a disproportionately low extent. While in this scenario, we have assumed the same growth rates for GDP and vehicle markets up until 2019, GDP growth up until 2040 only results in growth in the vehicle markets of up to 50 % in this model. In the transitional period between 2020 and 2040, a linear decrease in the proportionality from 100 to 50 % is presumed.

As a result of growth of the vehicle market decoupling from growth in GDP in the SSP1 scenario, we see smaller vehicle markets than in the SSP2 and SSP5 scenarios. The total market outlined in SSP1 thereby grows globally to around 135 mil-

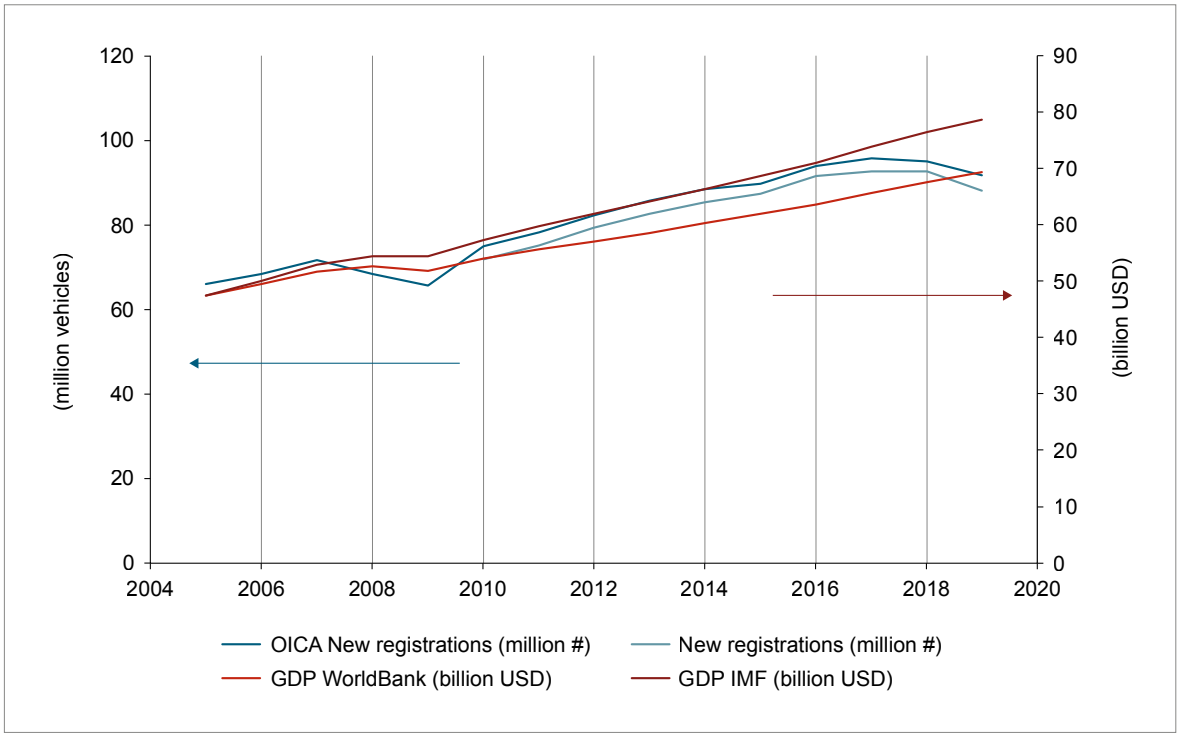

Figure 1.3: Trend in global new vehicle registrations since 2005 (left-hand scale) and global GDP (right-hand scale)

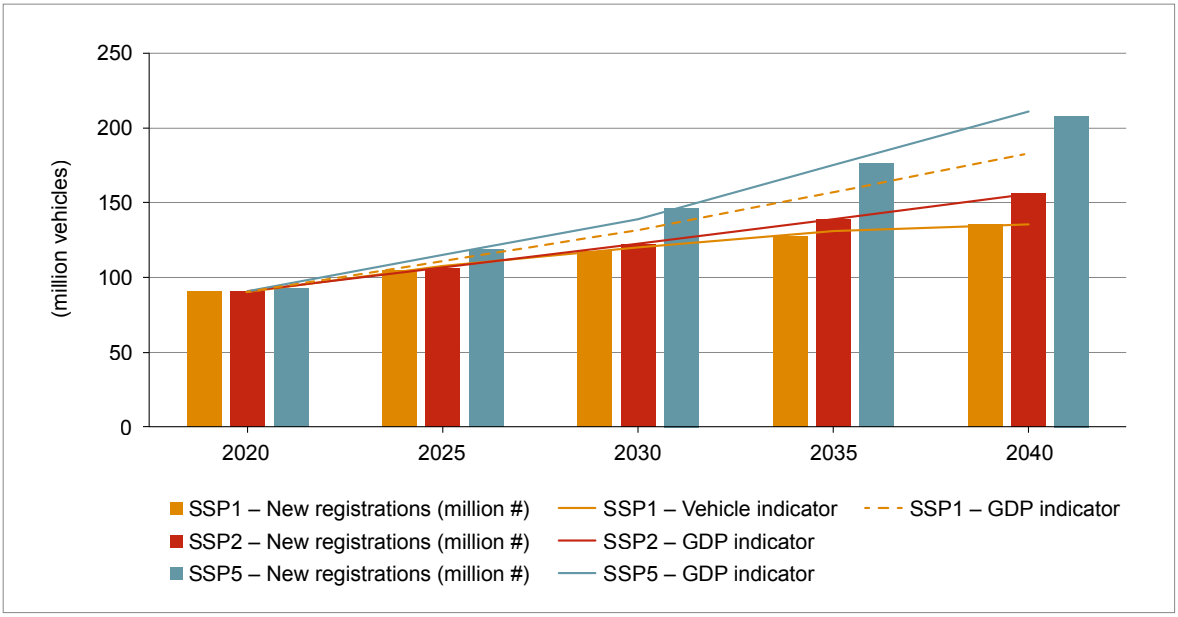

Figure 1.4: Predicted trend in vehicle markets and comparison to GDP growth from SSP scenarios

Note: The SSP indicators were standardised for comparison with the size of the vehicle market in 2019.

lion vehicles by 2040. In the SSP5 growth scenario, the total market in 2040 is around 210 million vehicles (see Figure 1.4).

As well as modelling the total volume of vehicles, the market shares of small cars (mini, segments A, B), compact class cars and vans (compact, segments C, M) and premium class vehicles (premium class, segments D, E, F and SUV segments) also vary. In the SSP2 and SSP5 scenarios, the trend observed over the last few years of a shift in market shares towards premium class vehicles has been continued. In contrast, in the sustainability scenario (SSP1) we have presumed that growth of the premium class segment will flatten off and even fall from 2030 onwards. On the other hand, we have assumed correspondingly greater growth in the mini and compact categories.

While the decoupling of new car registration figures from GDP growth contained in the SSP1 scenario is motivated by the personal purchase decisions of individuals, more complex consideration must be given to utility vehicle markets. The issue of sustainability may bring about a drop in the level of goods traffic and therefore low growth of the utility vehicle segment, but this would not reflect the rising GDP otherwise expected in SSP1.

Given the assumptions made, growth of the passenger car markets in the SSP1 scenario are not a significant driver of growth in GDP. Stimuli for growth would therefore have to come from other sectors of the economy. To be able to illustrate

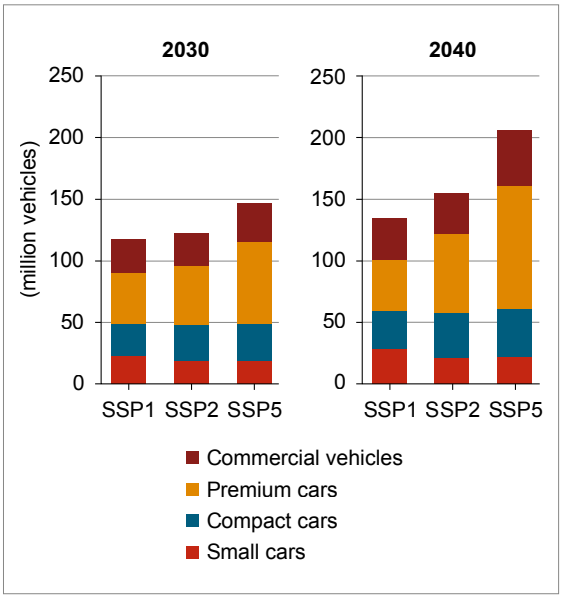

Figure 1.5: Market shares of different vehicle categories in SSP1, SSP2 and SSP5 scenarios for 2030 and 2040

Table 1.4: Modelling parameters to represent the SSP scenarios as vehicle markets and to describe the market diffusion of electric vehicles

Model parameters to represent the SSP scenarios			
Parameter	**"Sustainability" (SSP1)**	**"Middle of the Road" (SSP2)**	**"Fossil Path" (SSP5)**
GDP dependence, passenger car markets	Decreasing linearly, 100 % in 2019 up to 50 % in 2040	proportional, 100 %	
GDP dependence, commercial vehicle markets	proportional, 100 %		
Vehicle segments	Slowing of growth in premium segments, higher growth for small and compact	Continued high growth in premium segments, stagnation for small and compact	
BEV addressable passenger car market (share of total market, a)	75 %	75 %	10 %
PHEV addressable passenger car market (share of total market, a)	100 %	80 %	33 %
FCEV addressable passenger car market (share of total market, a)	60 %	50 %	–
xEV addressable commercial vehicle market (share of total market, a)	60 %	50 %	–
Market diffusion EV (p, q)	fast	medium	slow

goods traffic rising in line with GDP growth, the growth rates of the utility vehicle categories in the SSP1 scenario have continued to be linked proportionally to growth in GDP.

Compared with the status quo (2019), the share of utility vehicles in the total vehicle market increases in the SSP1 scenario (21 % in 2019 to more than 25 % in 2040). In the SSP5 growth scenario on the other hand, the share of utility vehicles remains constant over time at around 21 %. The same applies to the SSP2 Middle of the Road scenario.

1.3.2 Diffusion of the market by electric vehicles

Predicting how the market for electromobility (xEV) will develop in the long term and predicting the resultant demand for energy storage capacities is complex. While we can now look back over several years of development (battery electric vehicles (BEV) and plug-in hybrid electric vehicles (PHEV) have been around since 2010), there are various influencing factors. For example, development of the size of the total market potential for electromobility, development of mobility concepts, battery technology development (including technical performance parameters and costs), type, scope and intensity of political framework conditions, acceptance by society and users and social changes, usage and service models.

After the exponential or logistical diffusion model, the diffusion model proposed by Bass (1969) is the simplest model for describing the market launch and diffusion of innovative products taking account of the effects of innovation and imitation. This model reproduces with sufficient accuracy the global development of electric car sales between 2010 and 2019 in particular and reflects the range of existing market forecasts for the future (Thielmann et al. 2018). The model considers the share of initial purchases based on the novelty of the product (innovators, innovation coefficient p) and/or based on its distribution (imitators, imitation coefficient q).

Figure 1.6 shows an example of development of global new registration figures between 2010 and 2019 for battery electric vehicles (BEV) in the mini

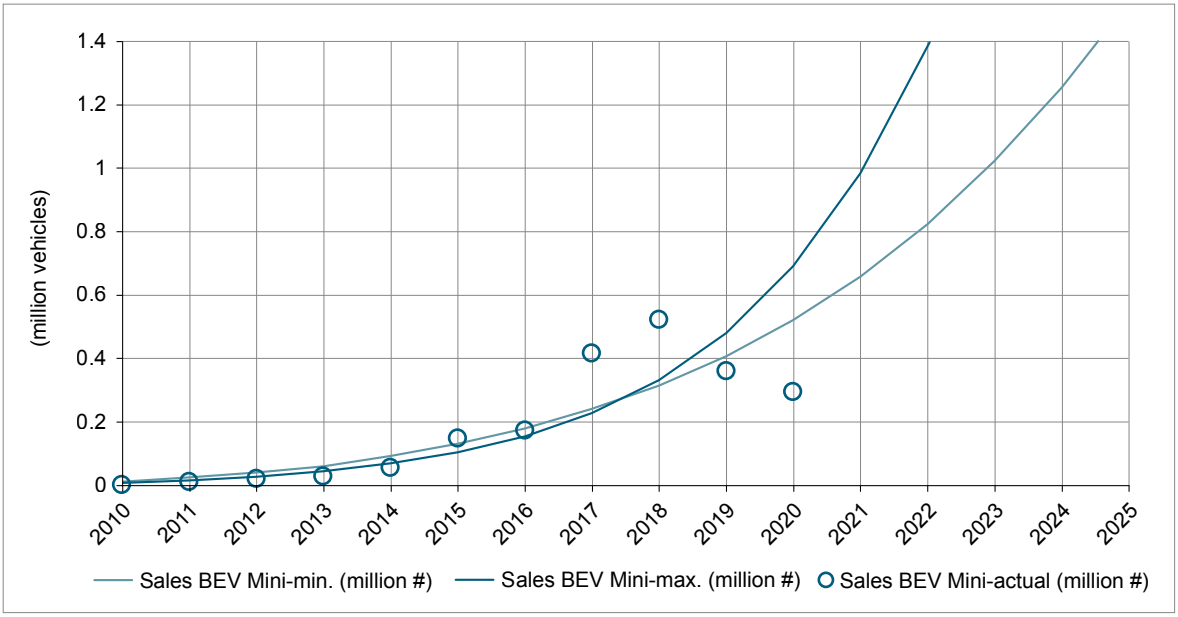

Figure 1.6: Trend in new registrations for BEV vehicles in the small car category since 2010 and minimum and maximum model fit

category. As with Figure 1.7, we have adapted parameters p and q of the diffusion model for all types of electric drive and vehicle categories to the best possible fit based on the data available for up to 2019. This fit ignores the previous distinct drop in new registration figures caused by the COVID-19 situation in 2020 and therefore presents an optimistic scenario (maximum model, rapid diffusion). Initial forecasts for the develop-

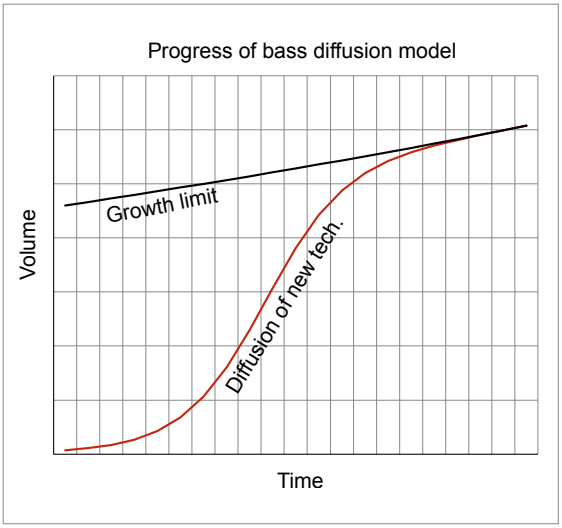

Figure 1.7: Schematic representation of Bass diffusion model with dynamic growth limit

Table 1.5: Vehicle markets by vehicle category for SSP1, SSP2 and SSP5

	2025	2030	2035	2040
SSP1 New registrations (million #)	104.5	116.9	127.4	135.5
Small cars	19.3	22.3	25.4	28.5
Compact cars	23.9	26.4	28.8	31.3
Premium cars	37.5	41.1	42.6	41.5
Utility vehicles	23.7	27.1	30.6	34.2
SSP2 New registrations (million #)	106.0	122.1	138.9	156.4
Small cars	17.1	18.5	20.1	21.5
Compact cars	25.8	29.4	33.3	37.3
Premium cars	39.9	47.6	55.7	64.2
Utility vehicles	23.2	26.7	29.9	33.4
SSP5 New registrations (million #)	118.5	146.4	176.3	208.2
Small cars	17.2	18.9	20.6	22.3
Compact cars	25.4	29.7	34.1	38.8
Premium cars	51.3	67.0	83.8	101.7
Utility vehicles	24.6	30.8	37.8	45.5

ment of the vehicle and electric vehicle markets in 2020 assume a strong double-digit percentage decline for 2020 as a whole (BLOOMBERGNEF 2020). To describe the minimum model (slow diffusion), we have used a corresponding model fit with a hypothetical data point for 2020, which assumes an 18 % decline in the EV markets.

In order to describe potential market saturation in the model, when modelling market diffusion of electric vehicles, we further assumed that the new registration figures across all types of drive (electric vehicles (EV) and vehicles with a combustion engine (ICE), see Table 1.5) depict a natural maximum limit for growth of the xEV market.

It is however conceivable that battery electric vehicles (BEV) and plug-in hybrid electric vehicles (PHEV) may not be directly accessible for the entire vehicle market. Given range or usage requirements in particular, e.g. with regard to utility vehicles, the diffusion of BEV and PHEV could only extend to sub-markets in the long term, which can be described by an appropriately adapted maximum growth limit within the framework of the Bass diffusion model. Alongside the innovation and imitation coefficients (p, q), in the model the addressable share of total market (a) was selected as a third input parameter in the model description. The assumptions for parameter a for SSP1, 2 and 5 scenarios are listed in Table 1.4. In the SSP1 scenario, we have assumed that 75 % of the entire car market could be substituted by BEV. In the SSP2 and SSP5 scenarios, the figures are just 55 and 10 % respectively because in these scenarios electromobility is not promoted internationally (SSP2) or is of less importance overall (SSP5). Higher substitution potential overall of 100, 80 and 33 % was assumed for PHEV because these vehicles do not have range limits and remain highly compatible with fossil fuel energy sources. From 2025 onwards, we have also assumed diffusion of the market by fuel cell electric vehicles (FCEV) in the SSP1 and SSP2 scenarios. Because continued use of fossil fuels means that there is no clear driver for the development of this technology, we have assumed no market launch in the SSP5 scenario. Following a similar argument, we have rated the potential for EV substitution in the utility vehicle sector as 60 or 50 % (SSP1, 2), while ignoring potential substitution in the SSP5 scenario.

The applied model prioritises the sale of BEV amongst drive technologies as the market grows.

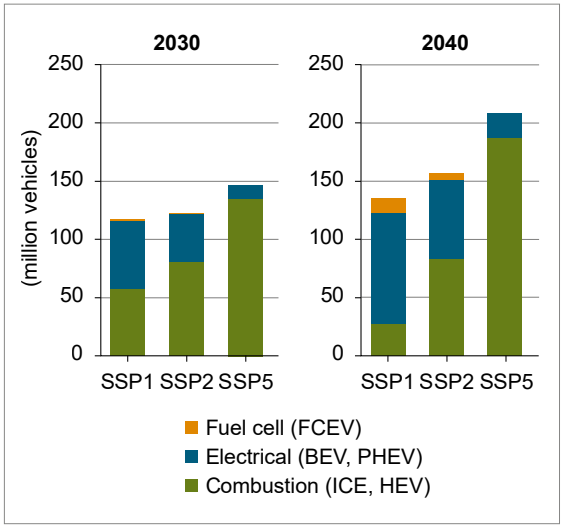

Figure 1.8: Market shares of electric (BEV, PHEV), fuel cell (FCEV) and combustion engine (ICE and HEV) drive technologies in SSP1, 2 and 5 scenarios for the years 2030 and 2040

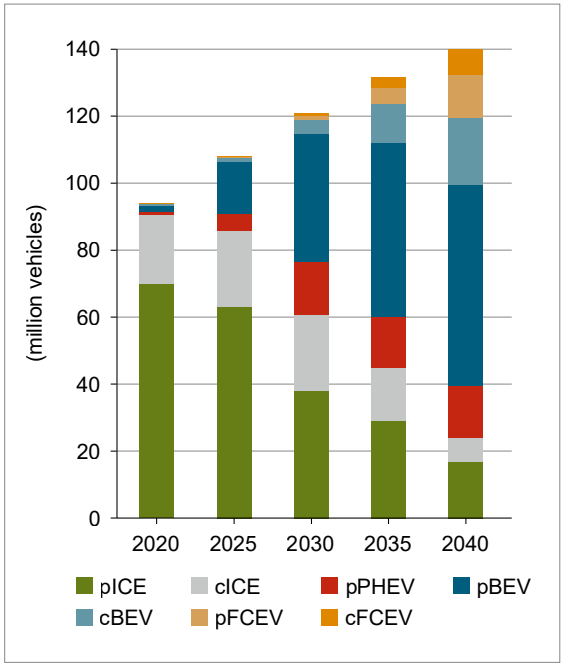

Figure 1.9: Market shares and sizes for different drive technologies in the SSP1 scenario until 2040 for passenger cars (p) and commercial vehicles (c)

Table 1.6: New registrations by drive technology in the SSP1 scenario, in million units

SSP1	2025	2030	2035	2040
BEV Small cars	2.54	9.17	17.47	22.50
BEV Compact cars	0.77	2.20	5.49	11.15
BEV Premium cars	12.18	26.55	28.86	26.47
PHEV Small cars	0.04	0.07	0.12	0.19
PHEV Compact cars	0.47	1.30	3.30	7.61
PHEV Premium cars	4.64	14.75	11.67	7.73
FCEV Small cars	0.00	0.04	0.17	0.54
FCEV Compact cars	0.02	0.09	0.30	0.89
FCEV Premium cars	0.03	0.21	1.00	3.63
BEV Light utility vehicles	0.84	3.65	10.65	17.92
BEV Heavy-duty vehicles	0.01	0.04	0.11	0.31
BEV Buses	0.36	0.70	1.13	1.53
FCEV Light utility vehicles	0.01	0.11	0.58	2.37
FCEV Heavy-duty vehicles	0.08	0.56	2.36	4.80
FCEV Buses	0.01	0.04	0.20	0.52

Table 1.7: New registrations by drive technology in the SSP2 scenario, in million units

SSP2	2025	2030	2035	2040
BEV Small cars	2.19	5.21	7.29	8.27
BEV Compact cars	0.67	1.55	3.20	5.54
BEV Premium cars	8.29	16.71	21.12	24.53
PHEV Small cars	0.02	0.04	0.05	0.07
PHEV Compact cars	0.32	0.64	1.28	2.49
PHEV Premium cars	4.62	10.22	10.53	12.45
FCEV Small cars	0.00	0.03	0.09	0.25
FCEV Compact cars	0.01	0.05	0.16	0.46
FCEV Premium cars	0.01	0.10	0.37	1.10
BEV Light utility vehicles	0.81	3.64	8.08	13.97
BEV Heavy-duty vehicles	0.01	0.02	0.06	0.15
BEV Buses	0.15	0.25	0.35	0.43
FCEV Light utility vehicles	0.00	0.04	0.42	2.95
FCEV Heavy-duty vehicles	0.00	0.09	0.32	0.88
FCEV Buses	0.00	0.00	0.02	0.08

BEV can diffuse the market unhindered until their addressable market share a is reached. Sales of PHEV (and HEV, not considered any further in this study) therefore fall in the model as soon as market saturation by electric vehicles (xEV) is achieved and there is direct competition between the three forms of electric drive technology (HEV, PHEV, BEV). The scenarios developed therefore differ not just in terms of the speed of diffusion of electric drive technologies (xEV compared with ICE), but also in terms of the relative shares of the three electric drive technologies. In the SSP1 scenario where BEV diffuse the market rapidly, the market shares of PHEV and HEV fall early on. In the slow scenario (SSP5) where BEV are able to directly access a smaller market, PHEV and HEV retain higher shares of the market in the medium term.

Although the market potential of fuel cell-driven vehicles (FCEV), which are a type of hybrid of fuel cell and battery electric vehicle, can still not be clearly predicted today, bringing FCEV to the market has been prioritised over all other drive tech-

Table 1.8: New registration figures by drive technology in the SSP5 scenario, in million units

SSP5	2025	2030	2035	2040
BEV Small cars	0.25	0.61	0.99	1.26
BEV Compact cars	0.10	0.22	0.45	0.82
BEV Premium cars	0.99	3.15	4.81	6.06
PHEV Small cars	0.01	0.01	0.02	0.03
PHEV Compact cars	0.08	0.15	0.24	0.38
PHEV Premium cars	1.91	7.51	10.01	12.08

nologies in the model. No more justifications can be provided for this assumption, but it will have no major impact on the market shares of the HEV, PHEV and BEV drive technologies given the time period under consideration of up to 2040.

1.4 Digitisation scenarios

1.4.1 Basic understanding: Digital transformation and its technological stimuli for demand for raw materials

Definition

In this study, "digitisation" or "digital transformation" is understood to mean radial change brought about through the use of computer systems and the networking of all areas of society and the economy (Köhler et al. 2018). The digital revolution can be classed as the third major change in the sociological history of mankind after the neolithic and the industrial revolution (Stengel et al. 2017). Its origins can be traced to the 1980s and the invention and initial spread of the Internet (Stengel et al. 2017). In light of the comprehensive digitisation of industrial production that we are currently witnessing, the term Industry 4.0 or the Fourth Industrial Revolution has been coined in Germany. However, these process should actually be viewed as the second phase of the digital revolution because micro-electronics remain the technical basis for these changes (Hirsch-Kreinsen et al. 2018).

Figure 1.10 shows how digitisation or digital transformation can be viewed with a focus on demand for raw materials. Here, we see a split into an economic/social level and a physical level. The physical or material basis of the digitisation system is micro-electronics (integrated circuits) and micro-system technology (miniaturised, multifunctional and independently operating sensor/actuator systems for recording, disseminating and transferring data). Out of this emerges the "digital infrastructure", which can be sub-divided into end devices, data transfer networks as well as data storage and processing centres (data centres). Transmission networks and data centres can be described under the umbrella term of "central digital infrastructure". Key figures are therefore storage capacity or stored volume of data, transmission capacity or traffic as well as computing capacity or annual computing volume (Hilbert & López 2011).

The combination of new trends and paradigms (e.g. networking, automation, artificial intelligence, big data, virtual reality), which require the digital infrastructure to be expanded, and innovation-based capacity expansion of the digitisation infrastructure, which makes these new trends/paradigms possible in the first place, are key to the past and future development of digitisation (see Figure 1.10). For example, artificial intelligence (AI) is currently making great progress because the fundamental infrastructure components it requires are currently in place and we were already aware of the main approaches for developing AI. In a similar way, 5G is now enabling Industry 4.0 to be implemented on a wide scale.

Relationship between the "Digitisation context scenarios" and the "Digitisation technology synopses"

Figure 1.10 outlines various digitisation trends at a social/economic level. Huge transformational potential is being attributed to combinations of these trends (World Economic Forum 2018). These digital future trends have no particular abiotic raw material demand but as a result of data and computing requirements may represent exceptional demand stimuli for computing infrastructure (e.g. AI and big data, cloud computing, virtual realities). These trends are not therefore considered in individual technology synopses, rather their demand stimuli for the digital infrastructure are analysed as part of the "Digitisation context scenarios" section.

Above and beyond this, several digital emerging technologies are linked to specific hardware components and therefore specific (abiotic) raw material demands. These are examined in individual technology synopses (e.g. "Devices in the Internet of Things (IoT)" in Section 3.2.8, "Industrial robotics and Industry 4.0" in Section 3.2.6). What's more, these technologies also have demand stimuli for the central data infrastructure, which are in turn considered in the context scenarios.

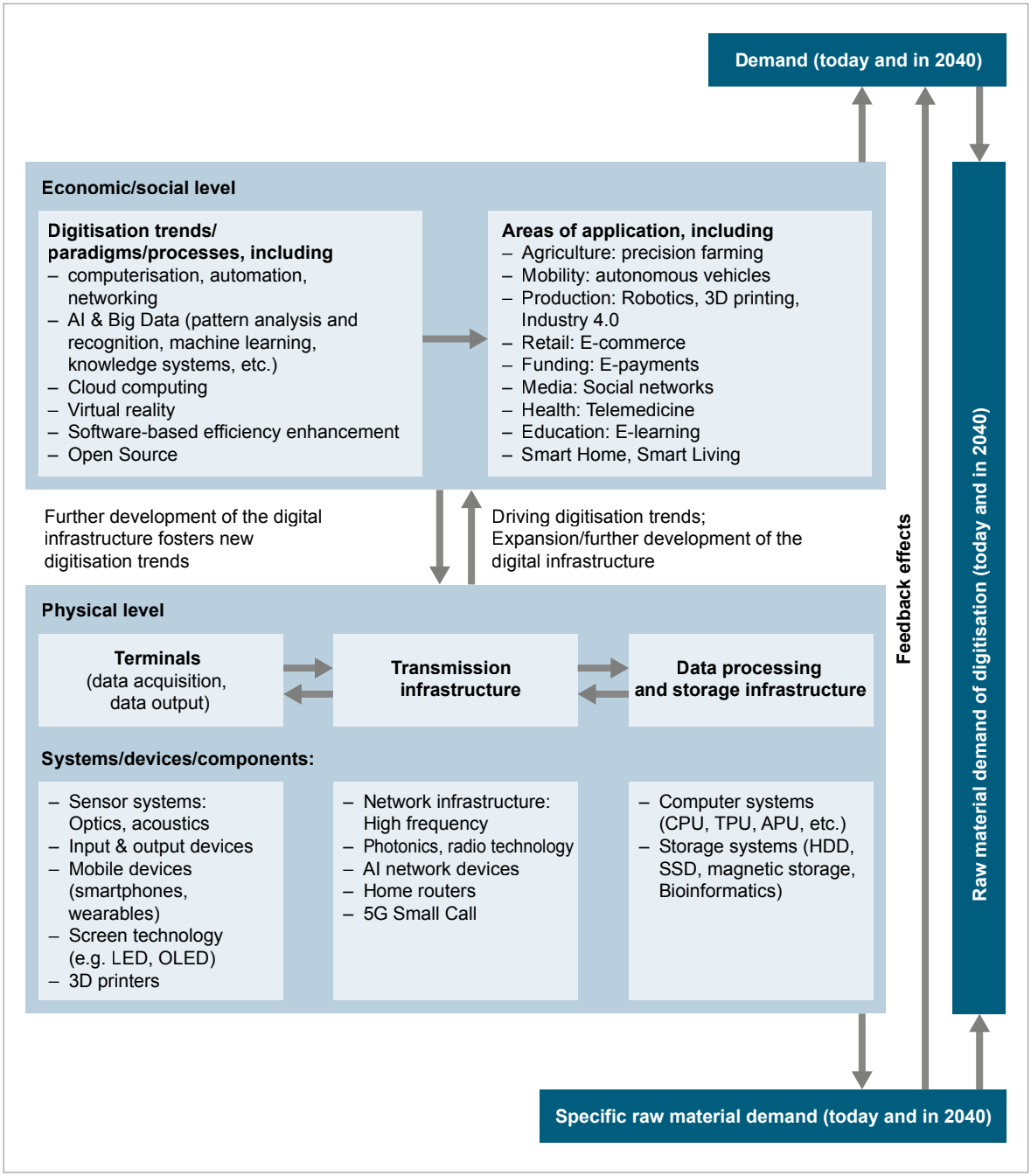

Figure 1.10: Understanding of the digitisation system with a focus on raw material demand (source: own representation)

Finally, several technology synopses address key material-intensive basic technologies of the digital infrastructure (e.g. data centres, fibre-optic cables, 5G/6G). Even though these technologies are not brand new, should these infrastructure elements grow in an exceptional manner, this may result in exceptional demand stimuli for raw material markets, which are analysed in the technology synopses. Context assumptions on growth of the key figures relating to digital infrastructure (data transmission, storage, computation) which are consistent across all synopses are key to this and are explained in the following sub-chapters. The purpose of the digitisation context scenarios is therefore to compare assumptions from technology synopses on digital infrastructure elements and explain common drivers.

Three digitisation trends have particular potential to increase data volumes today and in the future and thereby drive infrastructure expansion: AI including machine learning, IoT including Industry 4.0, and cloud computing including edge computing. (As explained at the outset and depicted in Figure 1.10, conversely, you could say that these three major trends are made possible thanks to current advances in the digital infrastructure). There is a separate technology synopsis on IoT and Industry 4.0; artificial intelligence and cloud computing are described in more detail in this chapter under the drivers of expansion of the digital infrastructure.

Some conventional digital end devices have already reached a certain degree of market saturation such that exceptional demand stimuli are not expected of them for 2040 (Hilbert 2015; Cisco 2019). Devices, such as smartphones, tablets, PCs, laptops and clients are not therefore made the subject of individual technology synopses. Specific components are covered in other synopses (e.g. “5G (6G)” in Section 3.5.3 and “Microelectronic capacitors” in Section 3.2.4).

1.4.2 Historical trends and existing future scenarios

This study is most interested in how past and/or current digitisation trends continue in the future. The references contain data on past development, descriptions of the current situation as well as scenarios and predictions for the near future (up until 2025, e.g. Hilbert (2015), Reinsel et al. (2018), Cisco (2019)). For the medium-term future up until 2030, you will find firstly an analysis of possible economic and social developments (Stone et al. 2016; Rao & Verweij 2017; Bughin et al. 2018), and secondly quantitative forecasts of energy demand. The latter are based mainly on an extrapolation of current trends without further rationalisation, e.g. Andrae & Edler (2015). Only more general scenarios, such as the SSPs and the World Energy Outlook, exist for the period up until 2040. These provide no or very scant detail of digitisation trends (Riahi et al. 2017; IEA 2019). In the following section, we summarise significant trends and draw conclusions for the individual scenarios up until 2040.

Data and forecasts of the development of central key figures relating to the digital infrastructure between 1985 and 2025: Capacities and volumes of data storage, transmission and computation

Generally speaking, we see a diffusion of new technologies such that the portfolio of related products (including systems, service units, etc.) produces an S-shaped curve over time (see Section 1.5). This empirical finding can be explained using various models, whereby the epidemiological model and cost/benefit model illustrate two fundamental patterns. With the cost-based models, we assume that the costs for an innovation fall over time due to the effects of scale etc., meaning that people with different available budgets choose to make purchases at different times. This produces a trend depicting an S-shaped curve. Following this explanatory approach, the diffusion of technology following an S-shaped curve is always linked to technological advancement and corresponding cost reductions.

With many digital technologies, market diffusion also overlaps with technological advancement but happens on different scales in comparison to non-digital technologies. The typical example of this is Moore's law, which states that the number of circuitry components on an integrated circuit or the number of transistors per unit area doubles at regular intervals. Initially (1965–1970), this interval was roughly every twelve months and then slowed to 24 months. It remained at this high level for decades, doubling every two years between 1970 and 2020. Moore's law is key to the level of computing power available.

Similarly, Edholm's law predicts that the available bandwidth doubles every 18 months. The work of Hilbert & López (2011) and Hilbert (2015) investigates the exponential development of capacity available globally for storing and transmitting data, initially between 1986 and 2007, and then updated up until 2014. This work shows that in the 21 years between 1986 and 2007 data storage capacity grew at a compound annual growth rate (CAGR) of 31 %, which is roughly five times that of the global economy. In 2014, global storage capacity reached 4.6 zettabytes (1 ZB = 10^{21} bytes) while it had been just 2.6 exabytes (1 EB = 10^{18} bytes) in 1986. Global capacity to transmit data using information and communi-

cation technology (ICT) grew from 7.5 petabits (1 Pb = 10^{15} bits) in 1986 to 25 exabits (1 Eb = 10^{18} bits) by 2014 at a CAGR of 35 %. These estimates include all available devices along with all of their maximum capacities and assume that all data is compressed as much as possible (Hilbert & López 2011). It therefore represents the theoretical maximum potential that is not fully utilised in reality but can be used to describe development over several decades using constant indicators. The growth rates result from the overlap between advancement and diffusion of technology described above. Technological advancement can then be split once more into hardware development and software development. Technological advancements in software are an important and often under-appreciated driver. For example, in 2007 the same hardware was able to transmit three times as much data as in 1986 thanks to formats such as ZIP, GIF, JPEG, MPEG (Hilbert 2014). According to Hilbert (2014), the technological advancement of hardware and software is around 2 to 6 times more relevant to the annual growth rates of storage and transmission capacity than the diffusion of technology, in other words the further proliferation of storage and transmission components. We can therefore conclude that storage and transmission capacity is growing much faster than the raw material demand needed for it.

Cisco (2017) provides historical data on traffic, in other words the amount of data actually transmitted, see Figure 1.11. These values also result from the overlapping of the diffusion of technology, i.e. the further proliferation of components, and technological advancement, i.e. the greater possibilities available per component thanks to hardware and software innovations. For example, the CAGR for data transmitted via a fixed Internet for the 20 years between 1997 and 2017 is 67 %. This is similar to the current growth rates for mobile traffic (e.g. 2012–2017: 68 % CAGR). We can also see from Figure 1.11, however, that annual growth rates are falling, which produces a trend depicting an S-shaped curve. This is no surprise because transferred data have a very short life (close to 0) (see Figure 1.13 in Section 1.5). We would expect to see a similar trend in growth rates for the amounts of energy needed, although it will be slightly curbed because the increases in efficiency/performance made possible through hardware and software innovations grow at a slower rate. This curbing also affects the raw material demand for the corresponding components. However, we should also note that these components have a long life (Belkhir & Elmeligi 2018), meaning that the curve trend over time should correspond more to the first derivative of a compressed curve as in Figure 1.12, see also Figure 1.13 in Section 1.5.

It therefore follows that compared with the development of transferred quantities of data, the development of raw material demand is curbed significantly, firstly by advancements in efficiency and secondly by the fact that data is being transmitted permanently while infrastructure components are only replaced over longer intervals.

This difference is also obvious if we compare the growth in annual global investment in data centres. Depending on the source used, for the period between 2010 and 2014 we find a CAGR of 15 % (DatacenterDynamics 2015) and for the period between 2012 and 2019 a CAGR of 6 % (Gartner 2020).

Forecasts for the near future (until around 2025) contain similarly impressive growth rates for data transmission and also the generation of data (Reinsel et al. 2018; Cisco 2019), as seen in the historical data. For example, Cisco (2018) predicted growth in data centre traffic between 2016 and 2021 from 6 ZB to 19.5 ZB, including data from both business and consumers (CAGR 27 %). Busy-hour traffic dictates expansion of infrastructure and is growing by a factor of 4.6 (Cisco 2019). The amount of data stored in data centres grew over the same period at a CAGR of 36 % to 1.3 ZB in 2021. Big data's share of this data increased from 18 % to 30 %. According to Cisco (2018), 5.9 ZB of data was stored on end devices in 2021. Figure 1.11 shows that current forecasts indicate continued growth at ever decreasing rates. Therefore, historical trends indicate that we will probably see high, but ever decreasing growth rates for the amounts of data transmitted and stored in the future.

In parallel to this, the data centre market is forecast to grow at lower rates. Technavio (2019) anticipates a CAGR of 17 % for the global data centre market between 2019 and 2023. Market Research Future (2021) assumes growth at a CAGR of 11 % between 2017 and 2023. This confirms the effect described previously; namely that

improvements in technological efficiency translate into lower growth for infrastructure components than volumes of data.

This is even more striking in the scenarios for infrastructure components themselves. Berwald et al. (2015) assume that the number of servers in Europe will increase from 9.3 million in 2014 to 12.8 million in 2030, yet admittedly the computing power of these servers cannot be compared.

Current and future drivers for expansion of digital infrastructure

In order to better understand the development of volumes of data and underlying infrastructure components, it is worth looking at the historical, current and future drivers of technology diffusion and technological advancement at a global level. A basic distinction can be made here between (A) fundamental access to the digital infrastructure and (B) intensity of use. The roles of fundamental access to the digital infrastructure and intensity of use for the development of transmitted and stored data can be better understood if we distinguish between various countries depending on their level of income. By analogy with Hilbert (2015; 2019) as well as Dutta & Lanvin (2019) we use the World Bank classification of assigning countries to four income groups: (1) high, (2) upper-middle, (3) lower-middle and (4) low.

Participation in the global, digital infrastructure correlates closely with the income level of the respective countries. Hilbert (2015; 2019) calls this the "digital divide" and uses the ratio of the shares of countries with a high income level to the rest of the world as an indicator. In terms of fundamental access to infrastructure, this ratio has been constantly falling for a long time such that we can talk of widespread global diffusion. Because comparably large numbers of people have access, this growth is gradually flattening off. It is driven by macroeconomic development and not technological innovation. In 2018, for example, 51 % of the world's population had access to the Internet and, according to Cisco (2019), that figure will rise to 66 % in 2023, which represents a CAGR of 6 %. The percentage of people who own a mobile phone is set to grow from 66 % of the world's population in 2018 to 71 % in 2023 (CAGR 2 %, (Cisco 2019)). In countries with a low level of income, more people have a mobile phone than fixed access to the Internet meaning that smartphones have a major role to play in primary Internet access.

With regard to the available bandwidth, the ratio of applicable shares in countries with a high income compared with the rest of the world ("digital divide") also fell up until the year 2000, which can be explained by the global diffusion of 2G and narrow brand transmission. In the years between 2001 and 2008, the digital divide increased due to the introduction of broadband technology (both fixed and mobile) in countries with a high level of income. Since 2008, we can see the digital divide falling away again thanks to the global diffusion of broadband technology. A similarly staggered development is also likely for future infrastructure innovations. In 2007, countries with a high income level had 18 times more broadband per capita while the same figure for 2017 was just 2.6 times more.

According to Dutta & Lanvin (2019), countries with a high level of income will also be better equipped to profit from digital transformation. Not only have they invested more in ICT in the past, but will continue to do so in the near future. What's more, they have better opportunities for identifying emerging technologies and investing in them. Dutta & Lanvin (2019) therefore believe that a general trend emerges: the lower a country's level of income, the lower its network readiness index. Furthermore, countries with a high income level are also more incentivised to invest in automation etc. because they have higher labour costs (Rao & Verweij 2017; Bughin et al. 2018). AI technologies are therefore adopted to a much lesser extent and/or much more slowly in countries with a lower income level. On the other hand, they have huge potential for leapfrogging (Rao & Verweij 2017): as they develop their economies, today's low-income countries can jump certain phases which today's high-income countries have had to pass through. For example, their first mobile phone could well be a smartphone or rather than paper-based distance learning, they may go straight to e-learning.

Alongside the level of income, political measures also have a major impact on the opportunities that different countries have for digital participation (Hilbert 2015). For example, at the start of 2000 Japan and South Korea invested huge amounts

in expanding their fibre-optic infrastructure. Bandwidth in China and Russia has also risen sharply since 2010 (Hilbert 2015). China has a pronounced AI strategy and already ranks second to the USA in terms of the number of AI patents held (Bughin et al. 2018). Rao & Verweij (2017) anticipate that the USA will continue to dominate AI in the near future but will then be overtaken by China. China is also expected to be able to gain the most globally from AI technologies because its economy is heavily focused on production and it will be able to tap into the great potential offered by automation and digitisation.

SSP2 maps out a path where the differences we currently see between various countries continue while SSP1 and SSP5 assume greater alignment and/or countries with a lower income level catching up rapidly.

In 2017, countries with a high income made up 25 % of access but 43 % of broadband (Hilbert 2019) while being home to 15 % of the world population. New technological applications, which are generally data intensive, are the main growth drivers for volumes of data in countries with a high income (Cisco 2018; Cisco 2019). While growth rates are similar in all regions of the world (approx. 30 % up until 2023, (Cisco 2016)), the growth of data in countries with a high income level, driven by innovation, will have a greater impact on global data growth because while it may grow at a similar CAGR it is starting from a much higher base level. The most important developments in countries with a high income level are explained below.

Cloud computing

Cloud computing describes the central provision of storage space, computing power or application software on servers, which is made available on end devices through the use of digital transmission infrastructure. These capacities no longer need to be available on individual end devices and can also be accessed from various end devices.

Cloud computing is currently considered the main driver of growth in data traffic and expanding data storage in data centres (Cisco 2018). Contrary to this, local data storage is increasingly diminishing in importance (Reinsel et al. 2018). This in turn is down to the greater number of opportunities afforded by enhanced transmission technologies, currently e.g. 5G, as well as new architectures such as multicloud and hybrid cloud, making them attractive, especially for business (Technavio 2019). Back in 2014, 20–40 % of all data was stored on the cloud according to Hilbert (2015). Current trends also include a decentralisation of cloud storage, firstly in the form of semi-central storage systems (edge computing), and secondly in the form of the increasing proportion of cloud services outside the USA, meaning that data centres are more spread around different parts of the world. Both improve latency periods, scope for monitoring and make data transport more efficient. Further improvements in efficiency are expected from increased use of hyper-scale data centres. These improvements in efficiency in turn pave the way for greater overall demand as prices fall and make new applications possible such that we can expect to see traffic and storage increase overall. According to Cisco (2018), cloud applications made up 88 % of overall traffic in 2016; this figure is predicted to rise to 95 % for 2021. Again here distinctions should be made as stored data is a holding which is added to year on year whereas traffic isn't permanent but instead represents annual volume. Streaming, gaming and social media make up the lion’s share of cloud traffic generated by consumers, and these figures are growing all the time (Cisco 2018).

The Internet of Things (IoT)

Technical details and developments relating to the IoT can be found in Section 3.2.8. High growth stimuli for volumes of data are expected of the IoT because many applications include video functions as well as it needing a high resolution and low latency (e.g. autonomous driving). Indeed the volume of data generated is two orders of magnitude greater than the volume of stored data (Cisco 2018). Nonetheless, we expect that IoT applications will be powerful drivers for cloud storage (Reinsel et al. 2018).

Video applications

Collectively, we expect video applications to act as the greatest growth stimuli for data storage and transmission. In China, according to Reinsel et al. (2018), video monitoring will assume a key role

in video applications. In contrast, we expect the greatest growth in countries with a high income level to be in the entertainment sector, caused by streaming, gaming and social media. Cisco (2019), for example, assumes further uptake of smart TVs with ever higher resolutions: 66 % of all the new TVs purchased in 2023 are expected to be capable of UHD (CAGR 30 %). UHD (Ultra High Definition) or 4K offers twice the resolution of HD (High Definition), which in turn provides 9 times the resolution of SD (Standard Definition). According to Cisco (2019), this trend is set to continue beyond 2023 with 8K and wall TV. As described at the outset, new applications need better transmission rates and more storage and/or faster rates of transmission, and better storage capabilities make new applications possible. In theory, this causal relationship could continue for ever and saturation does not seem to be in sight. It is conceivable that the trend will diminish if there are interesting developments in other consumer markets in the future. For example, we have already seen applications in the robotics sector where there was a low level of purchase interest (Stone et al. 2016). The growth trend may, however, also weaken if consumption is limited to a level within sustainable limits. This latter scenario can be seen in SSP1, while unlimited consumption can be seen in SSP5.

Mobile data

The trend in mobile data transfer basically maps the development of data transmission via fixed Internet connections (see Figure 1.11). Because this technological development started later, the growth rates are currently still higher. Again, video applications are the main driver for data traffic, representing 59 % of mobile data transmission in 2017. Compared with transmission using the fixed Internet, mobile data transfer is much more energy intensive. According to Cisco (2019), between 2018 and 2023 IoT devices on mobile networks (e.g. GPS in cars, mobile monitoring of goods in production and transport, patient monitoring) grew at a CAGR of 30 %. Smartphones, however, only grew at a CAGR of 8 % with other types of mobile phone actually falling globally resulting overall in a CAGR of 8 % for devices on mobile networks (Cisco 2019). The diffusion of smartphones since 2014 has also resulted in bandwidths increasing overall in countries with upper-middle incomes in Asia.

In terms of the speeds of transmission as an enabler for new developments in streaming, gaming and social media, the following increases are predicted (Cisco 2019) between 2018 and 2023:

– broadband 46 Mbps → 110 Mbps,
– mobile data 13 Mbps → 44 Mbps,
– WiFi 20 Mbps → 92 Mbps.

In countries with a high level of income, Low-Power-Wide-Area networks (LPWA) could become established as a new network system for IoT applications. These place few demands on broadband but require a high level of geographical coverage (e. g. for monitoring pets).

Artificial intelligence

The term artificial intelligence (AI) is used differently by different stakeholders. Rao & Verweij (2017) provide a good description of various aspects. They understand AI to be computer systems, which are able to perceive their surroundings, and are able to learn, make decisions and perform actions on the basis of these perceptions and their programmed objectives. Sensor technology, e.g. for recording videos, therefore also falls under the term AI. The first distinction made within these systems is whether they support human actions or decisions or act completely autonomously. The second distinction relates to whether the systems are continually learning and adapting or whether their reactions are fixed. The automation of routine tasks that is now very widespread is therefore also considered as artificial intelligence. Huge potential in the future is however ascribed to the possibilities of machine learning based on neuronal networks. This includes pattern recognition and reinforcement learning. The recognition of patterns in large volumes of data can be used, for example, in natural language processing, recognising peculiarities in medical images and traffic planning in cities. Reinforcement learning describes a scenario in which a computer system works out its capabilities through trial and error on the basis of basic settings. Machines can therefore learn to make the right decisions within defined limits or assist with decision-making. Perhaps the most well-known example is AlphaGoZero, which has used trial-and-error learning to become the world's best chess system. Other than gaming clients, we still need to establish the practical

applications of reinforcement learning; for example, certain forms of process optimisation may be conceivable (World Economic Forum 2018). Some of the successes achieved by artificial intelligence are impressive but the capabilities of an AI system are limited to very specific applications (Stone et al. 2016). We are not yet able to transfer what one system has learnt to a slightly different task (World Economic Forum 2018). Stone et al. (2016) also include crowdsourcing projects like Wikipedia under the term AI. This shows just how hard it is to define the scope of the term. According to the World Economic Forum (2018), AI is the most pervasive, most fundamental digitisation trend and therefore the trend which will have the most far-reaching implications.

Developments in the sphere of artificial intelligence are still very much in their infancy and will display more and more potential in the medium to long term (Stone et al. 2016; Rao & Verweij 2017; Bughin et al. 2018). Rao & Verweij (2017) forecast that AI applications will allow global GDP to grow by 14 % by the year 2030. Around 40 % of this will be due to increases in productivity, which are the focus for the near future, and around 60 % will be due to new purchasing stimuli, which will gain in importance in the more distant future. The new purchasing stimuli can be put down to personalised and optimised products, with the time savings gained through increased automation etc. being of less importance according to Rao & Verweij (2017). “More intelligent” products can in turn collect more or different data, which in turn leads to the development of new products such that the development is self-reinforcing. Bughin et al. (2018) are even anticipating a net increase in global GDP of 16 % by 2030 and this is after transaction costs have been deducted, meaning that pure growth is forecast to be 26 %. They assume that by 2030 around 70 % of businesses will have implemented at least one AI application, while less than 50 % of businesses will have exhausted all the AI opportunities available to them. 7 % growth in GDP is expected from innovative products alone. These scenarios of course all come with huge levels of uncertainty; the diffusion of AI technologies could progress at a slower rate, for example (Rao & Verweij 2017). Despite this, it is generally assumed that AI technologies will realise their full potential over the next few decades (Herweijer et al. 2020).

The reasons given for why now or the near to more distant future is considered the right time for widespread market diffusion of AI technologies in the mass market include the following (Stone et al. 2016; Bughin et al. 2018; World Economic Forum 2018):

– increase in data, this includes structured data (tables and databases) as well as unstructured data (text, images, video, audio), e.g. GPS data and sensor data from mobile phones and vehicles,
– the processing of these large volumes of data becomes possible, thanks to cloud computing, new hardware systems, such as GPU (Global Processing Unit) rather than CPU (Central Processing Unit), SoM (System on a Module) and SoC (System on a Chip), making more complex systems possible in mobile applications,
– new algorithms → machine learning,
– better global networking → faster transfer of knowledge, crowdsourcing, open source,
– the pressure of competition.

Hardware innovation, especially neuromorphic systems will be of relevance to future development up until 2040; after which quantum computers (see Section 3.2.2) will have a role to play (World Economic Forum 2018).

Until 2030, the development of artificial intelligence will continue to be restricted to specific applications and progress will vary greatly by economic sector and application (Stone et al. 2016; Rao & Verweij 2017):

– health sector: diagnostic support through pattern recognition, especially in imaging methods, patient monitoring and coaching,
– mobility: autonomous driving and maintenance, traffic planning,
– financial sector: automation of processes, security of transactions, personalised financial advice,
– retail: personalised products, demand forecasts, stock management
– entertainment and communication: personalised advertising, automated media generation, virtual reality,
– production: on-demand, optimisation, maintenance,
– agriculture: precision farming,

– energy: smart metering, grid optimisation, predictive maintenance,
– logistics: autonomous driving, controlling traffic,
– robotics: delivery, cleaning,
– education: personalised offerings for the general public (improved efficiency and effectiveness, reduced costs, new opportunities for countries with a low level of income),
– security: visual monitoring (especially in China (Reinsel et al. 2018), USA (Stone et al. 2016)).

Generally speaking, development in areas with a high proportion of hardware (e.g. robotics) will advance more slowly than in other areas because hardware cannot be developed and scaled up as quickly and cheaply as software (Stone et al. 2016). It is also harder to create a suitable and secure learning environment for robots. For example, the first robot vacuum cleaners were launched in 2001; but the product still hasn't gained widescale acceptance. It therefore seems plausible that the latest trends we see today will be able to gain significant shares of the market by 2040 and be of relevance for raw material demand. Regulations and a lack of trust amongst the population may also slow down developments.

Alongside specific further development for certain applications, if incremental, continuous further development is typical for AI, we can expect to see neither radical leaps in innovation nor the emergence of a super intelligence by 2040 (Stone et al. 2016).

Overall, we therefore expect to see far-reaching and long-term impacts (beyond 2040) from AI technologies. Different speeds of diffusion are covered within the scenarios with SSP2 depicting slow development and SSP1 and SSP5 very fast development.

Digitisation to attain Sustainable Development Goals (SDGs)

If digital transformation is to contribute to the attainment of the United Nations' Sustainable Development Goals (SDGs), it must be steered in the right direction by politicians, technology developers, investors, economists and civil society through the use of appropriate governance (World Economic Forum 2018; Dutta & Lanvin 2019; WBGU 2019). Otherwise it threatens to contribute to the goals being missed (TWI2050 2018; WBGU 2019). The areas covered by the SDGs include education, health, economic development and environmental protection. It is generally assumed that levels of prosperity are raised by digital technologies, but not necessarily evenly distributed. This applies in particular to the loss of jobs brought about by automation and digitisation, which puts the issues of a fair distribution of wealth and universal basic income on the agenda (Stone et al. 2016; Rao & Verweij 2017; Bughin et al. 2018). Overcoming differences in how people partake in digital opportunities between different countries is also a significant challenge (see above).

The SSP2 scenario assumes a continuation of historical trends, in other words, differences remaining between different countries. In contrast, SSP1 and SSP5 presume that countries with a low level of income will massively catch up such that they also assume that digitisation will contribute globally to rapid improvements in the areas of health, education and ensuring a level of prosperity to secure people's livelihood.

Environmental protection is not usually mentioned in general scenarios and forecasts on the future development of digitisation (Stone et al. 2016; Bughin et al. 2018). Potential energy savings achieved through gains in efficiency are the features most likely to be mentioned but mainly just in passing. Studies specifically dedicated to the potential of digitisation to protect the environment also focus on these potential savings (World Economic Forum 2018; Herweijer et al. 2020), while stating that they should be viewed in relation to the resulting increase in demand and the energy and resource demands of digitisation itself (Köhler et al. 2018). Indeed, the huge gains in efficiency achieved in the past have always resulted in increased output and greater demand, in turn producing increasing levels of energy and resource consumption overall (Gossart 2015). Herweijer et al. (2020) predict that the potential of AI applications for environmental protection will cut greenhouse gas emissions by 1.5–4 % and raise GDP by 3.1–4 % by 2030. Comparing this with the fact that the same institution (Rao & Verweij 2017) forecast GDP to rise generally as a result of AI by 14 % clearly shows the minor role assigned to environmental applications. The

greatest prospects for applications are anticipated in Europe (Herweijer et al. 2020). Above and beyond direct potential savings, the potential for environmental protection is often seen to arise from improved monitoring, e.g. World Economic Forum (2018). It should be remembered that in many areas of environmental protection there is no lack of awareness of problems but simply no measures to tackle them.

SSP1 assumes that technical development will progress at roughly the same speed as that in SSP5, in other words much faster than in SSP2. The focus in SSP1 is much more on environmental protection applications while the volumes of data overall in SSP2 and SSP5 are the same. SSP1 also assumes that we will not run applications which consume vast amounts of resources and energy but deliver little added value or only slightly contribute to the attainment of the SDGs. This includes, for example, streaming and gaming at ever higher resolutions, which contributes greatly to the overall amounts of data transmitted and stored. So an alternative development path is indicated here in which future improvements in efficiency actually result in savings in the sense of lower growth rates rather than continuous growth fuelled by increased output and greater demand. SSP1 therefore assumes that data transmission and storage will grow to a lesser extent than in SSP2 and SSP5.

Scenarios beyond 2030

The IEA (2019) describes how we should expect electricity demand for digital technologies to increase up until 2040 and how in countries with a high level of income this increase roughly corresponds to the savings that can be achieved through efficiency measures in all economic and social areas. To a certain extent, we can interpret this as a macroeconomic rebound effect: the savings achieved through efficiency measures are reinvested in new applications. At the same time, the IEA (2019) sees digitisation technologies as an enabler for efficiency measures and optimisation.

1.4.3 Scenarios for the development of digitisation and data volumes in SSP1, SSP2 and SSP5

Table 1.9 illustrates several assumptions on the future development of digitisation within the three context scenarios SSP1, SSP2 and SSP5 (see Section 1.1).

SSP2

In SSP2, the general future development follows the historical pattern, which is also assumed to apply to digitisation in this scenario. Improvements in the efficiency of digital technologies brought about through cost reductions also continue to fuel rising demand and greater productivity and/or new digitisation trends, which collectively produces a further increase in data storage, transmission and processing. Figure 1.11 illustrates the continuation of historical developments for data transmission: the growth rates continue to drop off but remain at a very high level overall. The “digital divide” is gradually reduced, but still present: countries with a low level of income only slowly catch up in line with the historical pattern.

SSP5

Thanks to international cooperation, SSP5 envisages a rapid alignment of the digital connectivity in countries with a low income level, which contributes to a more rapid improvement in economic conditions. Digital technologies also enable rapid progress to be made in the areas of health and education, by making leapfrogging possible, for example. Overall, technological development still gathers speed. Even in countries with a high income level, digital consumption increases unchecked, while the rest of the world adopts this consumption pattern as best it can. Figure 1.11 shows how this could result in accelerated or greater growth in volumes of data compared with historical patterns (SSP2).

SSP1

SSP1 also assumes faster technological progress than SSP2, as a result, in particular, of good inter-

Table 1.9: Assumptions related to the development of digital technologies

	SSP1	SSP2	SSP5
Technological progress (technology generations and leaps)	very high (focus on sustainability)	medium	very high
International interconnectedness	very high	medium	very high
Use of digital technologies	medium high oriented to sustainability goals	unevenly distributed, dependent on income growth	very high, all that is possible
Data volumes	medium high	medium, varying in different countries	very high, all that is possible
Trend in demand for digital products/technologies	medium high	medium	very high
Level of digitisation of industrial sectors	high	medium	very high
Increase in material efficiency	very high	medium	high (profitable potential fully exploited)
Recycling	very high	medium	high where profitable, otherwise medium
Expansion of fibre-optic cable in countries with previously weak digital infrastructure	very high	medium	very high
Expansion of fibre-optic cable in countries with already strong digital infrastructure	low	low-medium	medium high

national cooperation. However, unlike SSP5, further development here focuses on applications in health, education and environmental protection. In particular, potential for saving energy and raw materials through digital technologies is fully exploited. Given the good international cooperation, countries with low or middle income levels rapidly make progress in catching up in terms of their economies and technologies. On the other hand, the level of consumption in countries with a high income level does not continue to rise unchecked. This is the point at which this scenario deviates from the historical pattern. In the past, increases in the efficiency of digital technologies have always resulted in greater demand and productivity, but not to absolute energy and raw material savings in the sector. In SSP1, it is assumed that gains in efficiency lead for the first time to a decoupling of economic growth from energy and raw material demands.

The greatest driver for transmitted and stored volumes of data is video applications (Cisco 2019). These cover a series of applications of relevance to health (e.g. telemedicine, patient monitoring) and education (e.g. online teaching) as well as environmental protection (e.g. precision farming, environmental monitoring, smart energy supply networks). These applications will grow more in SSP1 than in SSP2. At the same time, streaming, gaming and social media in an ever increasing resolution and the rising level of consumption makes up the lion's share of data volumes and are also seen as the greatest future factors for growth in volumes of data. The sustainability potential of increasing resolution levels and greater use of these applications is considered to be low compared with their consumption of resources meaning that these applications grow less strongly in SSP1 than in SSP2. Overall, this results in the lowest growth of data volumes in SSP1 (see Figure 1.11). Compared with the fixed Internet,

growth in mobile data is also weaker because mobile data has a worse environmental footprint. After 2028, growth in SSP1 once again diminishes more clearly than in the other scenarios because at roughly this date the greatest potential for resource efficiency has been fully exploited and new products are coming to the fore (Rao & Verweij 2017).

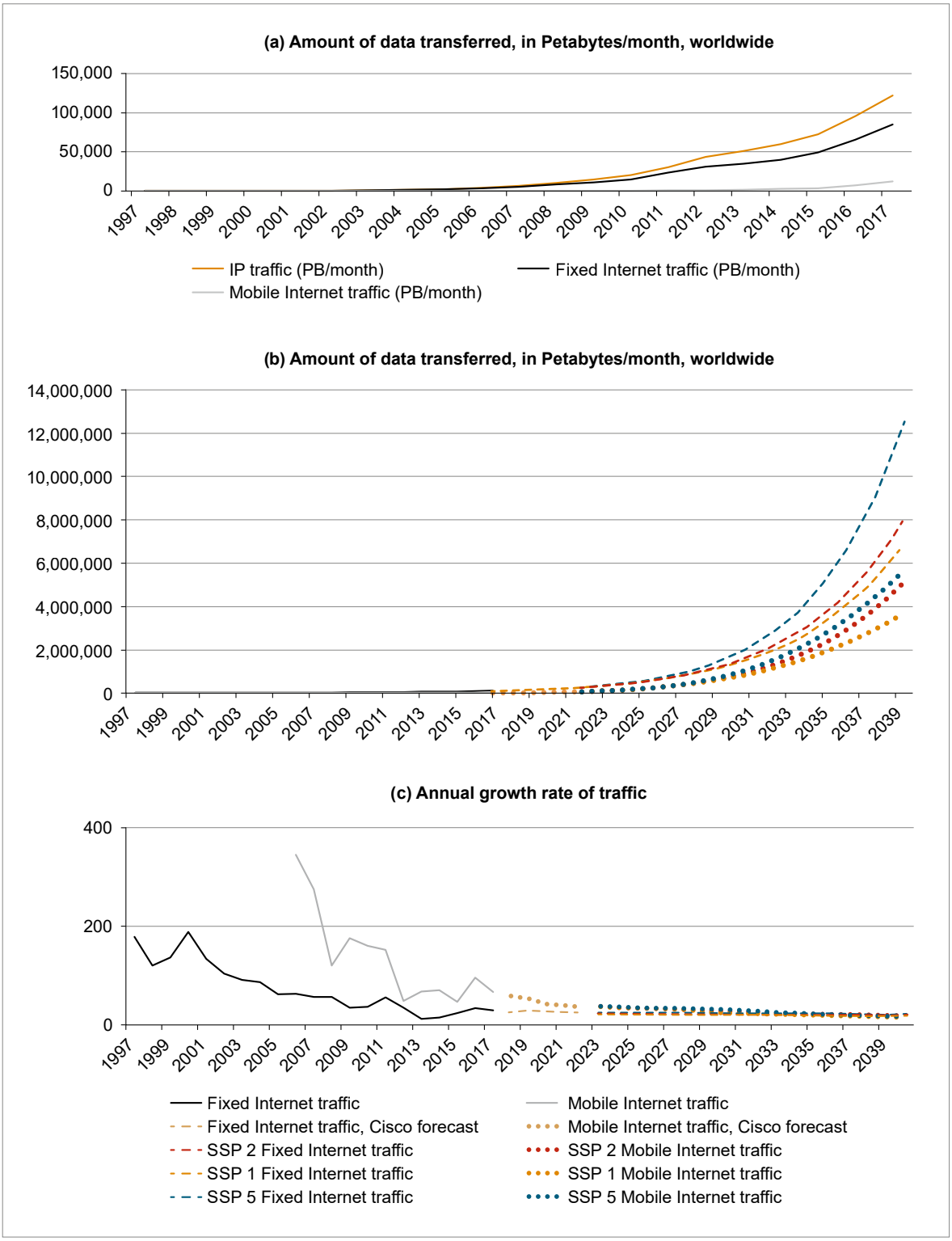

Figure 1.11: Growth of transmitted data volumes (a) historical; (b), (c) historical + scenarios

Other conceivable developments

A diminishing of growth resulting from less economic growth and weaker technological development is also conceivable, but is not considered here in more detail because exceptional stimuli for raw material demand would not be anticipated in such a scenario (similar to SSP3 & 4 with the higher-level scenarios).

The scenarios serve to illustrate possible developments and are not forecasts. Growth in demand for raw materials cannot be derived directly from the scenarios because firstly we expect huge improvements in efficiency driven by hardware and software innovations and secondly transmitted data volumes are accrued afresh every year while the underlying infrastructure is retained for longer periods and only changes if added to, replaced or modernised.

1.5 Diffusion scenarios

The method used to estimate future raw material demand was described in BMWI (2007). The influences of technical and economic development are considered separately and then combined as factors:

(1) $B = b \cdot A$

- B Raw material demand of one particular application, in tonnes/year
- b Specific raw material demand of the application (tonnes/unit)
- A Rate of activity (production volume) of the application (units/year)

(2) $$\frac{B_{2040}}{B_{2018}} = \frac{b_{2040}}{b_{2018}} \cdot \frac{A_{2040}}{A_{2018}}$$

The ratio of raw material demand for the year 2040 to the raw material demand of the year 2018 is calculated in (2). The factor $\frac{b_{2040}}{b_{2018}}$ describes the change in specific raw material demand per application brought about by technological change and the factor $\frac{A_{2040}}{A_{2018}}$ describes the influence of economic development between the base year of 2018 and the target year of the projection 2040.

The application units in this study may include km of fibre-optic cable, number of battery-powered vehicles, kW of installed capacity in wind turbines. The number of application units produced in 2018 (A_{2018}) and the specific material demand per unit (b_{2018}) are data, which theoretically can be calculated with accuracy. However, in reality recording global production figures proves difficult due to the many different manufacturers, product types and markets etc. In some cases, data could not therefore be established, while in other cases, deviating estimates were found to exist. Determining the material demand per application unit also proved to be problematic in many cases. The specific material demand differs by manufacturer and type of technology and is sometimes guarded as a trade secret. When determining specific material demand, consideration needs to be given to not just the material contained in the product unit but also production waste and rejects.

The corresponding data for 2040 cannot be determined. This study attempts to use scenarios to forecast which future developments are possible or probable on the basis of what we know today.

The development of specific material demand up until 2040 (b_{2040}) differs greatly for different technologies and is established in each case on the basis of research and questioning of experts. Some general basic considerations are explained below. Generally speaking, increasing demands on performance and functionality result in higher specific material demands. In contrast with this trend, increases in efficiency and substitution lead to a reduction in specific material demand. We would expect greater potential savings in this regard for technologies, which are still at an early stage of development. What's more, the greater the potential savings, the greater the awareness of the problem and the more research effort is made in the respective sectors. The more specific the function of the material for the application in question, the more unlikely there is to be a substitution. Despite this, an unforeseeable innovation (for example, substitution by a new, more suited material) may dramatically change the specific material demand.

The forecast of application units produced in 2040 (A_{2040}) is also provided individually for all technologies because the technologies differ greatly in terms of criteria of relevance to global market development. The most important criterion for the prevalence of a technology is its benefit. There are some technologies which provide a totally new and additional benefit and some which may take

the place of existing technologies because they offer benefits over the old ones. The benefits of such displacement technologies may be so great that they fully capture an existing market (e.g. flatscreen TVs/CRT TVs). However, several technologies may also be in permanent competition because all offer certain benefits, which take effect to different extents in different applications (e.g. different generator technologies for wind turbines). In addition to the prevalence of the application in 2040, we also need to produce scenarios for the market share of the different technologies in these cases. We should also bear in mind that today's emerging technologies may also be displaced in the near future by unforeseeable innovations.

The way in which a technology market grows globally also depends on the extent to which it spreads exclusively or predominantly in certain regions, cultures or socioeconomic spheres. The openness of users to new products and the infrastructure required for the actual prevalence of emerging technologies are key here. What's more, the development of some of the technologies under consideration depends greatly on political support (e.g. wind turbines, traction motors for electric cars).

We have economic models depicting the diffusion of new technologies. These initially show exponential growth, which flattens off as a saturation value is approached, resulting in S-shaped curves (see Figure 1.12). These curves describe the development of the total stock. The development of annual sales figures only follows this curve for products with a very short life (virtually 0, e.g. as with energy raw materials). With very long product lives (virtually infinite), annual sales

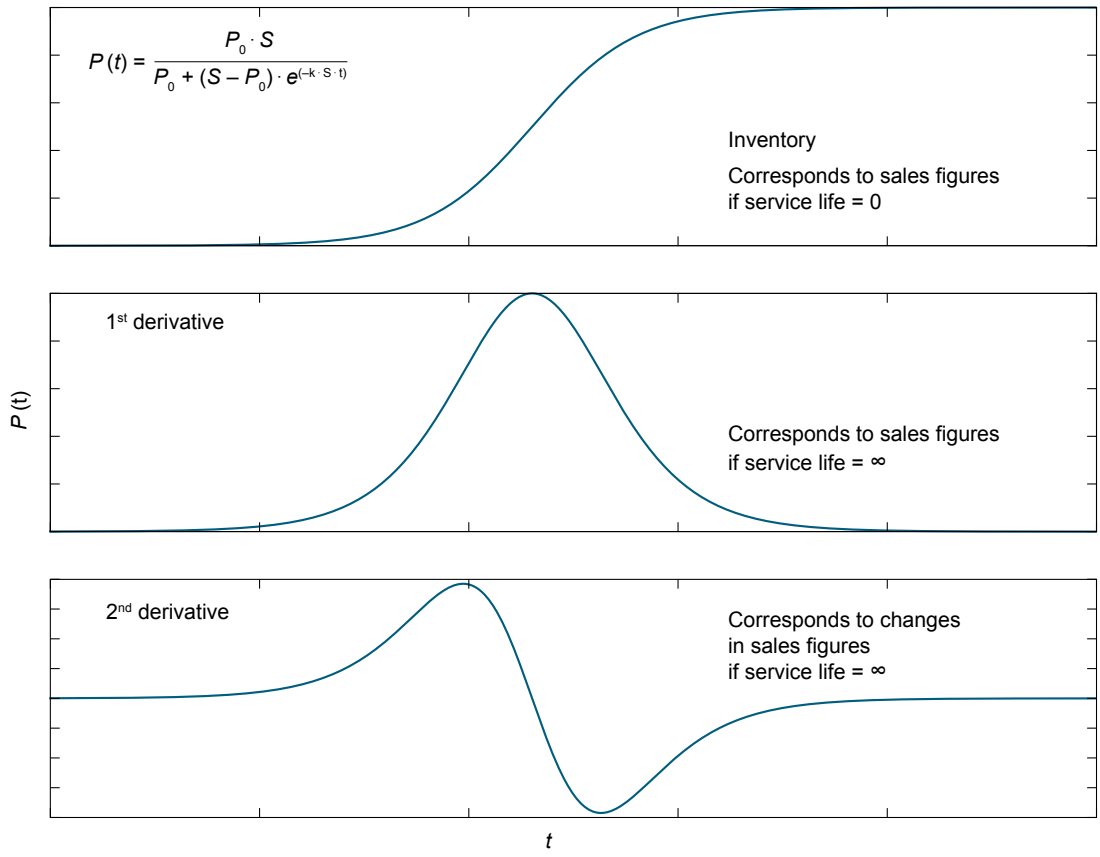

Figure 1.12: Diffusion of a technology as per the saturation model (source: own representation)

figures illustrate the first derivative of the stock curve (see Figure 1.12). Figure 1.13 illustrates the theoretical progress of lives between 0 and infinity. The compound annual growth rates (CAGR) frequently cited in market studies are the change in sales figures and therefore the first derivative of sales figures. They also correspond to the second derivative of stock when the product's life is infinite. Figure 1.12 clearly shows that the CAGR falls and may even become negative as the product becomes more mature even though stock is continuing to grow.

We often don't know what the level of saturation is or when it will be reached. At the end of the day, even complex model calculations are therefore only as good as the assumed coefficients. Given these huge uncertainties, we will restrict ourselves to simple models.

On a global scale, a distinction needs to be made between regions with different levels of development, infrastructures and cultures. The global growth in demand for a technology is therefore the overlap of growth in different regions as it occurs at different points in time.

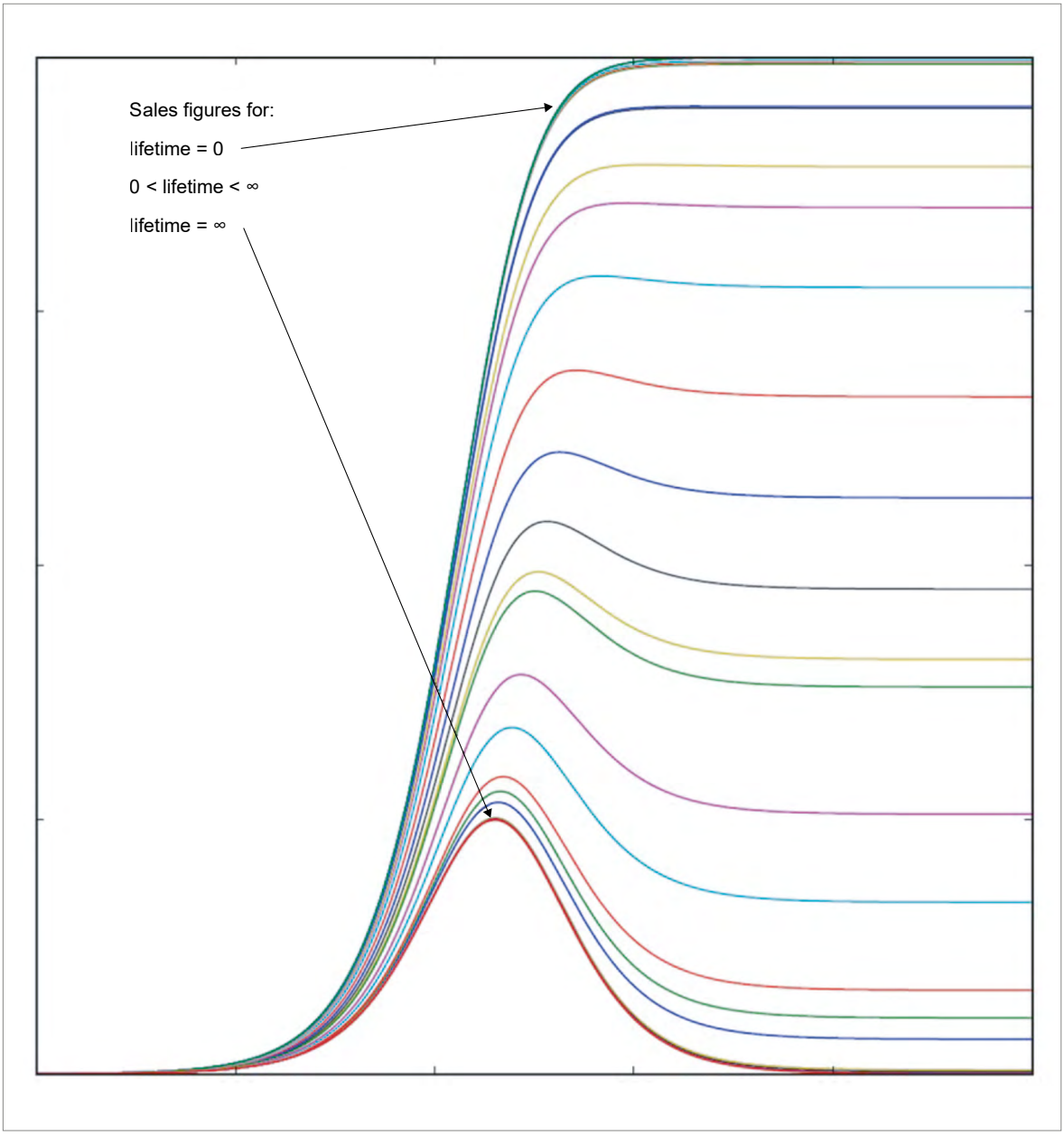

Figure 1.13: Trend in sales figures over time for different lifetimes (source: own representation)

The early growth phase of new technologies is generally marked by exponential growth with high exponents for stock and sales figures (see Figure 1.12). Growth of the global economy also impacts on the growth of emerging technologies. The development of GDP in the various SSPs outlined in Section 1.1.2 serves as a basis for predicting market diffusion. However, this applies to different extents for different technologies and depends, for example, on whether we are talking about a general technology, which is contained in many other technologies, or a special technology with one individual and very specific application. Exceptional stimuli for raw material demand stem mainly from technologies, which grow with growth exponents way beyond that of the global economy over a certain period of time.

2 Selection of the emerging technologies

Selection of technologies for a detailed analysis

The technologies which are presented and analysed in depth in the following sections were selected on the basis of a list of potential emerging technologies. Emerging technologies are defined as technical capabilities which can be exploited by industry and trigger revolutionary boosts in innovation far exceeding the boundaries of individual economic sectors. This list was produced for the preceding study and contains 168 emerging technologies (Marscheider-Weidemann et al. 2016). Targeted research into emerging technologies was used to update this list.

A workshop of experts, held at the German Mineral Resources Agency (DERA) in November 2019, also added to the list of technologies. Representatives from industrial associations in the metal industry, raw material manufacturers and industrial firms which use highly critical raw materials attended this workshop. One of the fundamental findings of this workshop was that the selection of emerging technologies and their market developments should focus on the 1.5 degrees goal of the Paris Agreement (United Nations 2015). The technologies should also be presented in clusters in order to contribute to appropriate discussion in other areas, such as that relating to raw material demand during the energy transition in Germany.

The technology synopses in this study are therefore presented in clusters and not listed by affected industries, as has previously been the case. Technologies which are not considered innovative but are essential to a cluster, are therefore also analysed in this report. Overviews of the clusters in diagram form were produced, as can be seen in Figures 2.1 to 2.3, for the “Mobility and aerospace”, “Digitisation and Industry 4.0” and “Energy technologies and decarbonisation” clusters in order to analyse how essential they are. The technologies investigated in this study are highlighted in blue. You can see that some technologies are used in several clusters and that some technologies provide an essential basis for other technologies to work. These technologies were arranged in the two clusters “Recycling and water management” (desalination of sea water and raw material recycling) and “Power and data networks” (expansion of the power grid, fibre-optic cable, 5G (6G), data centres and inductive transmission of electric energy).

The following criteria also applied to selection of the ten new technology synopses: What was the status of the technology in the 2018 base year? Is there potentially a future market for the technology in 2040? What will the raw material demand and recycling potential look like in 2040? Technologies which do not require inorganic mineral raw materials are not considered, such as DNA synthesis, artificial intelligence and browser technologies. 33 technologies were selected at the end of the process.

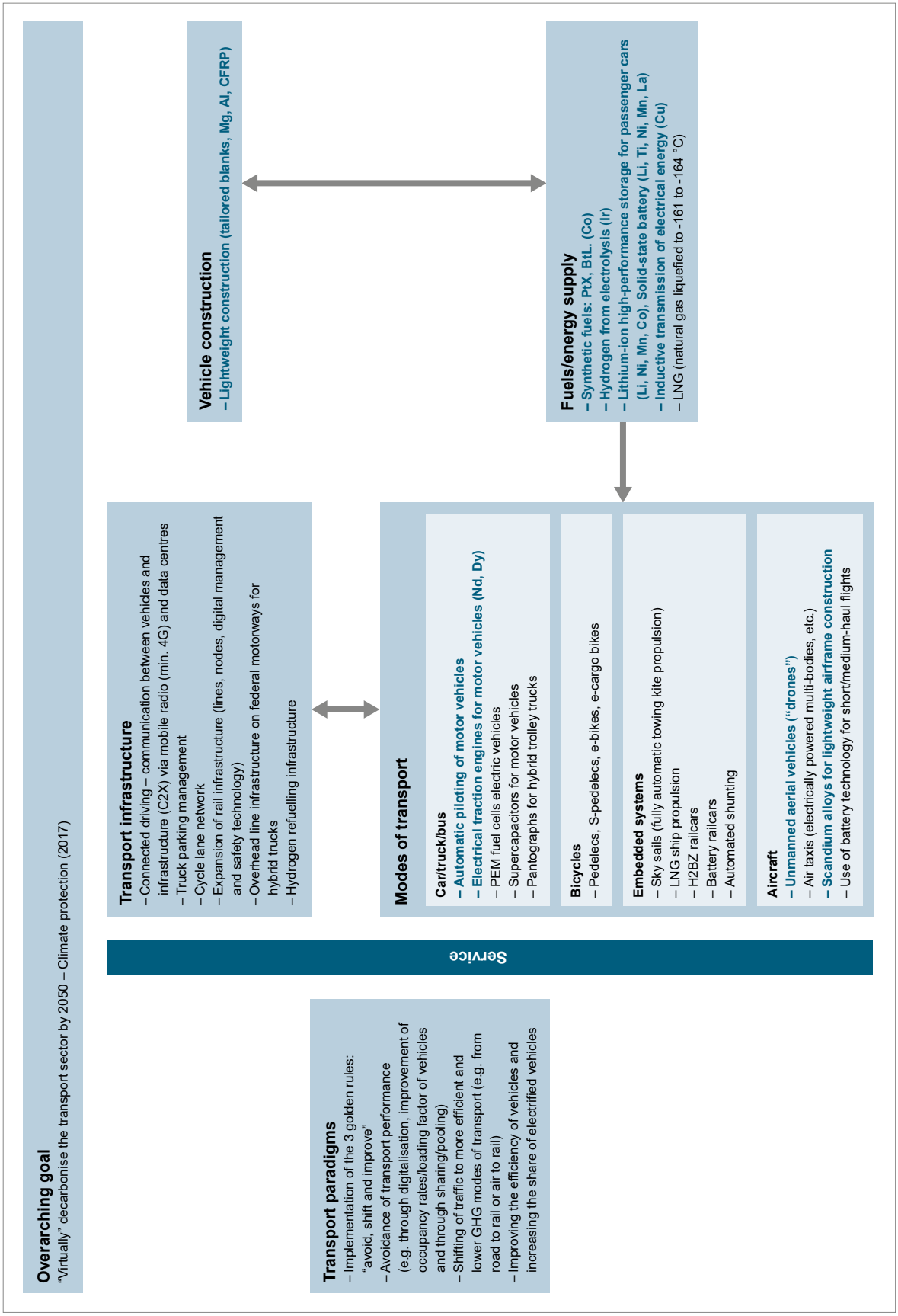

Figure 2.1: Schematic overview of the mobility and aerospace cluster (source: own representation)

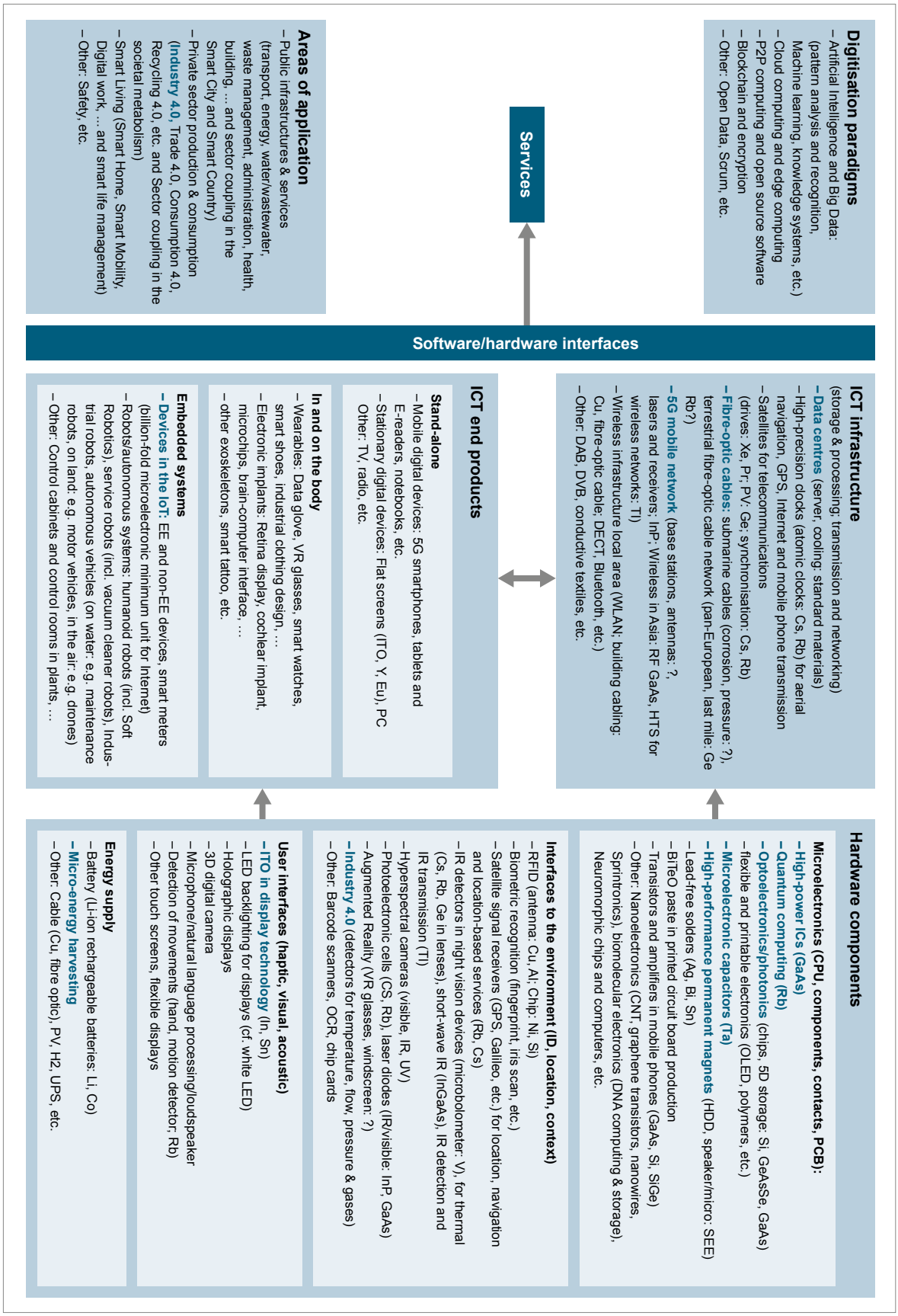

Figure 2.2: Schematic overview of the digitisation and Industry 4.0 cluster (source: own representation)

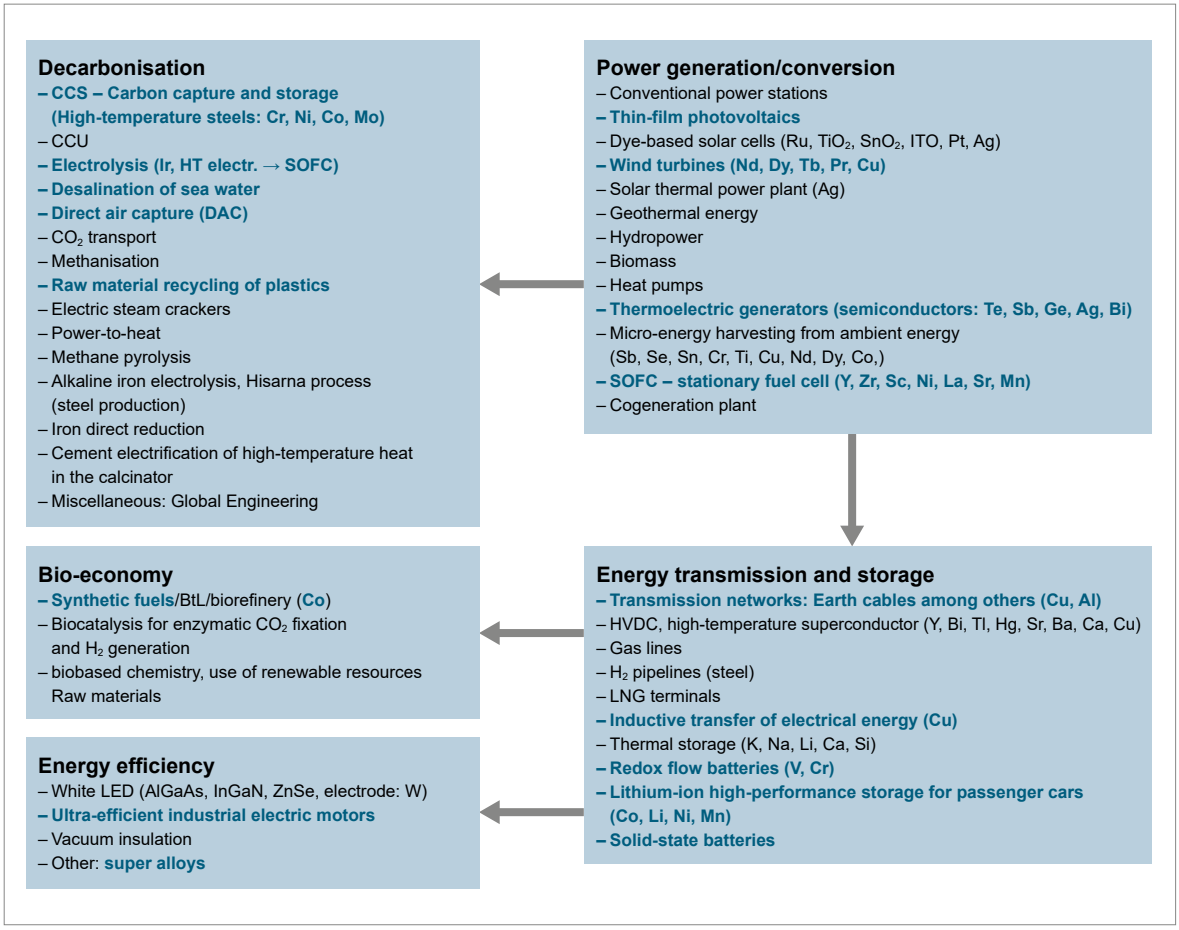

Figure 2.3: Schematic overview of the "Energy technologies and decarbonisation" cluster (source: own representation)

3 Technology synopses

3.1 Cluster: Mobility and aerospace

3.1.1 Lightweight car construction

3.1.1.1 Technology description

Reducing the weight of vehicles is a permanent challenge for vehicle manufacturers, one which has become even more important due to efforts to protect the environment and increase the range of electric vehicles. The vehicle resistance is composed of the air, rolling, climbing and acceleration resistance. Except for air resistance, all of these are directly proportional to the vehicle's mass. This means that, with increasing vehicle mass, greater drive power is also required. A reduction in the vehicle weight of 100 kg lowers the fuel consumption of conventional passenger cars by an average of 0.5 l/100 km and reduces CO_2 emissions by 12 g/km (Klein 2012).

Legislation and customer demands are increasing the requirements for safety technology and comfort features, resulting in the average vehicle weight rising sharply in the past. In passenger cars, for example, these features include the side impact protection, ABS, ESP, the exhaust gas catalytic converters, but also air conditioning systems and motors for window lifters, seat adjustment and other comfort devices. Due to the increasing weight of the vehicle, higher engine outputs are also required to avoid any loss of vehicle dynamics. The increasing engine power in turn results in a higher engine weight, creating a continuing weight spiral and so the mass of new vehicles steadily increases. To counteract this weight spiral, lightweight construction is increasingly being used in vehicle construction. For battery-powered electric vehicles in particular, lightweight construction is an essential success factor to counteract the range problem caused by limited battery capacities. With decreasing body weight, either the total weight of the vehicle can be reduced, resulting in reduced energy demand due to decreasing vehicle resistances, or a larger battery can be used while keeping the total weight the same. In both cases, the range of an electric vehicle can be increased through lightweight construction, even if there are limits to lightweight construction for reasons of technology, economy and safety.

There are various lightweight construction strategies designed to reduce the mass of structures while maintaining the same mechanical stress capacity (Friedrich 2013):

– Lightweight material construction: in lightweight material construction, weight reduction is achieved by substituting the original material with a material of lower density while maintaining the same shape. When high-strength steel replaces conventional steel, this is referred to as lightweight steel construction. Other metals for lightweight material construction are aluminium or magnesium, which can achieve weight savings of 40 % and 49 %, respectively. Audi in particular relied on lightweight aluminium construction with the Audi Space Frame, which reduced the body weight of the 2015 Q7 model by 71 kg (Audi 2017). In addition to metallic materials, fibre-reinforced composites such as GRP (glass fibre) with a lightweight construction potential of 20 % or CFRP (carbon fibre) with a lightweight construction potential of over 50 % can also be used. In the Mercedes Benz SL 500, for example, 4.5 kg of weight could be saved in the tailgate alone by making it out of GRP instead of steel while maintaining the same shape (Friedrich 2013). BMW also uses composite materials, for example in the BMW i3 electric vehicle.

– Lightweight manufacturing: lightweight construction measures, which are made possible by the production process, are grouped together under lightweight manufacturing. The further development of laser welding, for example, has led to new possibilities in joining technology. The new flow-forming process allows material to be consolidated during forming in such a way that weight savings of up to 15 % can be achieved in rim production. Using gas or water injection technology, hollow plastic components can be manufactured in one step, replacing the original solid components and thus saving weight (Friedrich 2013).

– Lightweight mould construction: in lightweight mould construction, the material of a com-

ponent is distributed in such a way that it is adapted to the stress so that material can be saved at less stressed points. Design measures for reinforcement include, for example, ribs, beading or a shell shape. The structural simulation (e.g. finite element method) of components under load allows the shape to be perfectly adapted to the load.

– Conditional lightweight construction: external influencing factors such as stress capacity, legislation or expected service life have an impact on the weight of vehicles. Through conditional lightweight construction, these are adapted to implement lightweight construction.

– Conceptual lightweight construction: conceptual lightweight construction refers to the construction method, which is differentiated into differential, integral and integrating construction methods. In the differential construction method, several components are assembled additively by joining to form a structure, whereas in the integral construction method, the aim is to create a structure from just one component, which then has a higher form complexity. The integrating design combines integration and differentiation (Klein 2012).

Many real-world approaches to lightweight vehicle construction cannot be fully ascribed to a lightweight strategy. The steel industry developed a lightweight construction approach with tailored blanks, with the Thyssen Stahl AG doing the pioneering work. The technology began in 1985 with the welding of large-format steel sheets that were wider than could be produced with the rolling equipment of the time. With the advent of laser beam welding, the possibility was recognised of joining sheets of different thickness, strength and surface coating into a pre-product, which is subsequently deep-drawn into a body component on the customer's site (Mertens & Koch 2003). With this technology, sheets in thicknesses of 0.6–3 mm are adapted to the different local mechanical requirements on the finished component. High-strength steel is inserted where the local load requires it and the sheet thickness is reinforced where high stiffness is needed. By adapting the material, the material quality and the surface finish to the local loads occurring in the component, the sheet thicknesses can be reduced, while reinforcing parts and flanges for overlap joints are no longer required. Tailored blanks thus have elements of lightweight material, lightweight manufacturing and conceptual lightweight construction. The different processes for producing tailored blanks are described below (Merklein et al. 2014):

– Tailor-welded blanks: welding of sheets with different material properties.
– Patchwork blanks: Local reinforcement by overlapping sheets.
– Tailor rolled blanks: Sheets which have a continuous change in thickness due to a rolling process.
– Tailor heat-treated blanks: Locally different heat treatment of sheets.

The technology is used for the production of doors, tailgates, side panels, A- and B-pillars, roofs, wheel arches, floor panels, side members, engine mounts, bumpers and strut mounts. Today, all major steel manufacturers supply tailored blanks, including Salzgitter Europlatinen GmbH, from whose website Figure 3.1 is taken. The graphic shows the body shell of a car and highlights the components that are subject to particular stress.

The technology of laser-welded, customised sheet metal blanks allows weight savings on the body shell of 25 %. For a VW Golf class vehicle with a body weight of 360 kg, this equates to 90 kg. So as well as reducing weight, tailored blanks also help conserve resources compared to conventional sheet metal construction. Using tailored blanks can also reduce costs because material is saved.

Technology development is still in flux. In the meantime, even sheet metal joints that are not straight can be welded. The laser beam follows the curve of any joint contours. The joining of steel and aluminium sheets to form hybrid tailored blanks is also being experimented with and was successfully implemented back in 2004 by the Chair of Forming Technology and Foundry Engineering at the TU Munich using laser roll seam joining. Other processes for producing hybrid tailored blanks are friction stir welding and the cold metal transfer process (Friedrich 2013). When steel is welded to aluminium by conventional methods, an intermetallic phase forms in the joining zone that has brittle properties. As a result, the part can only be formed or deep-drawn to a limited extent, making it unsuitable for most automotive body applications. To avoid intermetallic phase formation, the

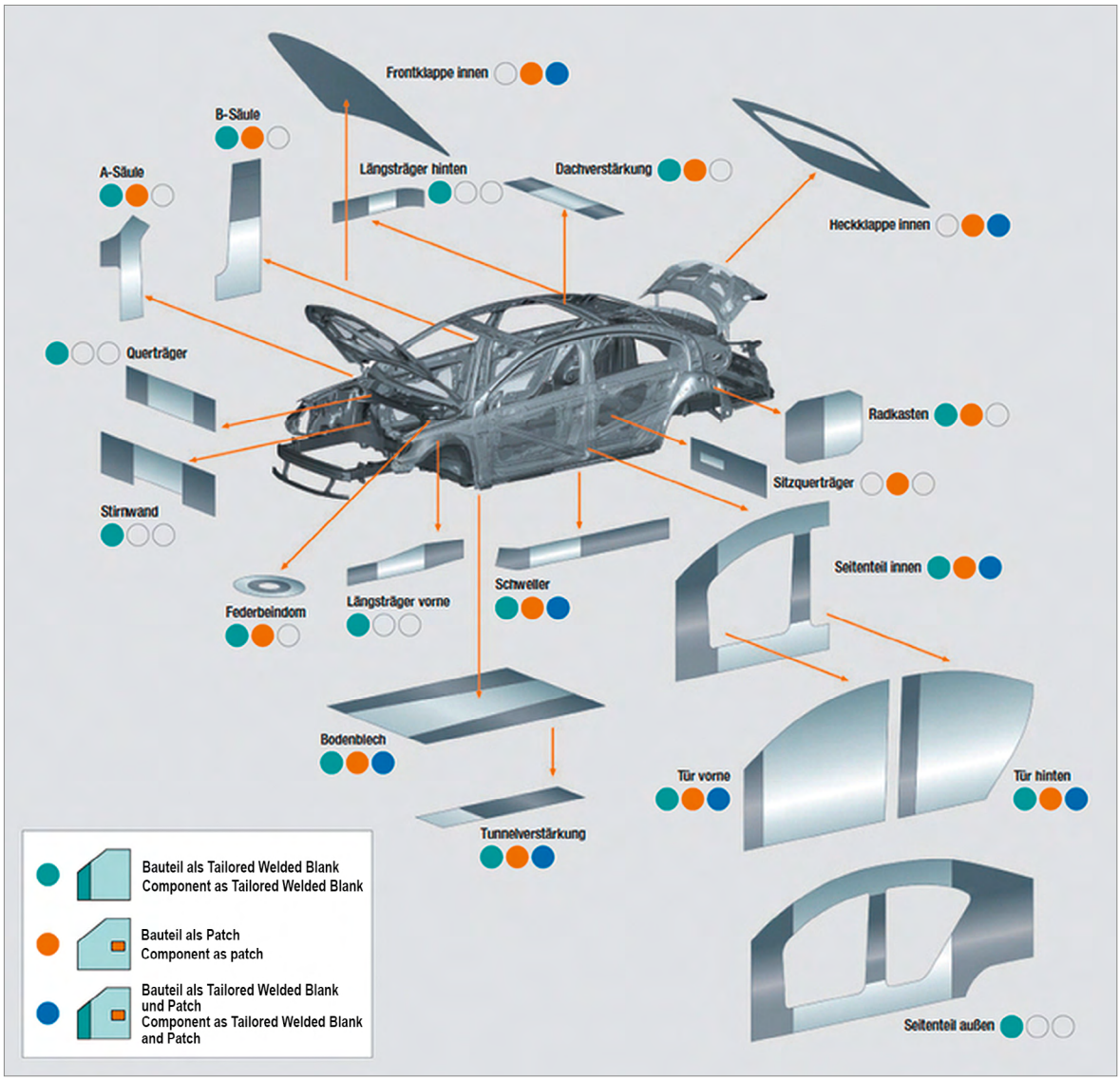

Figure 3.1: Potential applications of tailored blanks (source: SALZGITTER EUROPLATINEN GMBH)

Fraunhofer IWS developed a special process for joining aluminium and steel. For this, an intermediate joining element (known as a transition joint) is produced, which is a steel-aluminium bimetallic strip. This is produced in a rolling process with simultaneous heating by means of laser radiation in the joining zone. By precisely adjusting the thermomechanical conditions, a material bond with an extremely thin intermetallic phase is created. As a result, the transition joint has excellent deformation properties and strength. The transition joint is then used as an intermediate element of the sheets to be joined by welding the steel part to the steel component and the aluminium part to the aluminium component (WAGNER et al. 2014).

The underlying new lightweight construction strategy is multi-material design, the aim of which is to use the best material for the application at every point (KLEIN 2012). The use of aluminium in tailored blanks allows the weight of components to be reduced even further; for example, the weight of a bumper could be reduced by 30 % with almost unchanged deformation behaviour in the event of a crash (WAGNER et al. 2014).

Since tailored blanks play an essential role in car body construction at present and in the future and will have an impact on the future raw materials market due to the use of metals, only tailored blanks will be examined below.

3.1.1.2 Raw material content

Classic tailored blanks are made of different steels, i.e. an alloy of iron and carbon, to which further alloying elements may be added. Weldable and high-strength steels to absorb local load peaks have a key role to play in tailored blanks. They are a prerequisite for the weight saving because they make it possible to reduce the sheet thicknesses at the load point and also at the other less stressed points. The high-strength steels used have tensile strengths of around 1,000 N/mm^2 and more. The strength of steel can be increased by increasing the carbon content, heat treatment and mechanical deformation. However, with a carbon content of more than 0.22 %, weldability and toughness decrease rapidly (Dubbel 1983). Both of these properties are indispensable for welded and deep-drawn tailored blanks. The strength of weldable steels is therefore increased by the formation of a fine-grained microstructure. On the one hand, this is done by adding minute quantities of alloying elements that refine the grain, including aluminium, niobium and vanadium in proportions of less than 0.1 wt%. On the other hand, the microstructure is influenced by heat treatment and rolling. The batch annealing stage after cold rolling plays a major role in the formation of the microstructure and properties of car body panels.

Names such as TRIP steel (Transformation Induced Plasticity), DP steel (dual-phase steel), CP steel (complex-phase steel) and others have emerged for the optimised high-strength special steels used in vehicle construction. What they have in common is that martensitic islands are formed in a ferritic (DP) or ferritic-austenitic (TRIP) matrix by special heat treatment and mechanical forming, which increase the tensile strength and at the same time keep the yield strength low for good formability during deep drawing. Important alloying elements of dual-phase steel are manganese (0.8–2 %), silicon (0.1–0.5 %) and aluminium (up to 0.2 %). Austenitic steels, including TRIP steel, additionally contain austenite formers such as nickel, cobalt and manganese. Materials development is still very much in flux. High-strength manganese-boron steels are a more recent development (Vollmers 2008; Bartos 2014).

3.1.1.3 Foresight industrial use

In 1991, Volkswagen's Golf III was the world's first vehicle to use tailored blanks in series production. Large manufacturers of tailored blanks include, for example, Salzgitter Europlatinen and Bao Steel, which, with Wisco Tailored Blanks, took over the pioneer in this field, ThyssenKrupp Tailored Blanks. Currently no study on the market penetration of tailored blanks could be located. Therefore, the current share of tailored blanks can only be estimated, so it is assumed to be 40 % of the body shell.

The mastery of laser beam welding of any seam shape opens up further applications for the technology and additional potential for weight reduction. The costs of tailored blanks are also expected to fall in the future due to an increase in expertise and large-scale production. Since tailored blanks are particularly advantageous for components with inhomogeneous loads, it cannot be assumed that the entire car body will be made up of tailored blanks in the future. Therefore, it is estimated that the share of tailored blanks in the body shell will double to 80 % by 2040.

Hybrid tailored blanks are currently still the subject of research and are therefore not yet used in series production in vehicles (Hildenbrand 2019). Challenges with different materials are the reduction of electrochemical corrosion and the control of different thermal expansion coefficients. Since it is not yet foreseeable when and whether hybrid tailored blanks will become established on the market, they are not included in the scenario for the raw material demands of car bodies.

The main area of application for tailored blanks is the automotive industry. However, there is also potential for use in other sectors, such as the household appliance industry, mechanical engineering and plant construction.

3.1.1.4 Foresight raw material demand

To estimate the raw material demand for tailored blanks in the future, the mobility scenarios SSP1, SSP2 and SSP5 are used, which have already been described in more detail in this report. The current and future vehicle production figures

Table 3.1: Global production (BGR 2021) and calculated raw material demand for tailored blanks

	Unit	Production in 2018	Demand foresight for 2040		
			SSP1 Sustainability	SSP2 Middle of the Road	SSP5 Fossil Path
Vehicle production	million units	85.1	135.5	156.4	208.2
Demand for auto body sheet	kilotonnes	39,799	56,328	65,017	86,550
Crude steel production	kilotonnes	1,820,366			

are shown in Table 3.1 and include both private and commercial vehicles. It is assumed that the average newly registered vehicle weighs around 1,800 kg (Abuelsamid 2019) and that the body makes up 25.5 % of the total weight of the vehicle (Lutsey 2010). The composition of vehicle bodies is assumed as described in the Foresight industrial use. Only the crude steel without alloying elements is considered, as the alloying elements used and their concentrations in the steel vary greatly depending on the application and production technology.

In 2018, the production of vehicle bodies accounted for 2.2 % of total crude steel production. By using tailored blanks, an average weight saving of 11 % can be achieved compared to current vehicle bodies. The demand for raw materials for car bodies thus increases by only 42 %, 63 % or 117 % depending on the scenario, while the number of vehicles produced increases by 59 %, 84 % or 145 % in the period under consideration. In addition to a positive effect of the weight reduction on the energy requirement for vehicle operation, tailored blanks can also reduce the raw material demand per vehicle. With crude steel production on the rise, it is therefore possible to reduce the share of vehicle bodies in the total demand for steel. This is an example of the potential of lightweight construction strategies to decouple economic growth from the demand for raw materials.

3.1.1.5 Recycling, resource efficiency and substitution

Tailored blanks, like other steel products, are fully recyclable. The elimination of sealing compound creates advantages in the recycling process compared to conventional car bodies (Friedrich 2013). The recycling effort increases for hybrid tailored blanks made of several metals, for example aluminium and steel, as they contain different raw materials within one component which then have to be separated mechanically or metallurgically for recycling. However, by heating the joining zone, a type of intermetallic phase growth can be generated in the transition joint which is accompanied by a brittle failure of the joining zone even at low loads, so that a mechanical separation is made easier by the embrittlement of the joining zone (Wagner 2020).

3.1.2 Electrical traction engines for motor vehicles

3.1.2.1 Technology description

Based on the scenarios for future vehicle sales and fleet shares of the electric drive concepts (Section 1.3), the material requirements for electrical traction engines are analysed in this technology synopsis. Only passenger cars are considered, not commercial vehicles, trains and buses.

Requirements for traction engines for e-cars

In general, efficiency is a motor's most important quality feature. In motor vehicles, high engine efficiency should be ensured over a wide range of speeds and torques. It is also important for the overall efficiency of the vehicle that the traction engine takes up as little space as possible and contributes as little as possible to the overall mass. An essential criterion is therefore a high power and torque density of the engine. Low maintenance, high reliability and low noise are also among the basic requirements. Cost com-

petitiveness and availability of materials also need to be considered in engine selection (Bradshaw et al. 2013b; Chau & Li 2014a).

Types of traction engine for e-cars

In the past, DC motors were used in electric vehicles because it was a simple and mature technology. Their biggest disadvantage, however, is the rectifier, which requires a lot of maintenance and wear and also produces carbon dust (Bradshaw et al. 2013b). In the future, DC motors will therefore at most be used in motor vehicle concepts aimed at simplicity (Chau & Li 2014a). Three-phase machines will dominate. Synchronous and asynchronous motors, as well as switched reluctance motors, are used in electric vehicles.

Synchronous and asynchronous motors work according to the principle of the Lorentz force. Copper coils on the stator generate a rotating magnetic field so that the rotor, to which a magnetic field is also applied or induced, is set in motion. If it rotates synchronously with the magnetic field of the stator, it is a synchronous motor. If the rotor rotates more slowly, it is called an asynchronous motor.

Asynchronous motors (ASM) are also referred to as induction motors. Their rotor ("squirrel cage rotor" or "cage rotor") usually consists of a short-circuited cage made of aluminium or copper embedded in sheet iron (see Section 4.6). The main advantage of asynchronous motors is their low cost. They are also low-maintenance, efficient and technologically mature. The main disadvantage is that the mass and volume are large compared to other engine types with the same power output (Bradshaw et al. 2013a; Chau & Li 2014b).

The magnetic field on the rotor of a synchronous motor can be generated by permanent magnets or induced electrically by copper coils. A combination of both is also conceivable (Burkhardt et al. 2014). The permanent magnets can be surface mounted (SPM) or integrated (IPM). **Electrically excited synchronous motors (ESM)** are associated with lower costs, but also have lower efficiency compared to permanent-magnet excited synchronous motors and are larger and heavier for the same power.

Permanent magnet excited synchronous motors (PSM) feature the highest power density and are also low-maintenance and very efficient. However, the neodymium-iron-boron magnets used (NdFeB magnets, cf. Section 3.3.9) cause high costs due to the rare earth elements neodymium and dysprosium they contain. Moreover, PSMs cannot be switched off, but always recuperate when they are not driving the axle. However, recuperation is only desired when braking, not, for example, when driving at a constant speed on the motorway when neither braking nor accelerating. Therefore, the ASM can be particularly advantageous for frequent long-distance journeys (Oppenheimer 2020).

Reluctance motors are based on the alignment of a ferromagnetic rotor in the magnetic field of the stator caused by magnetic resistance (reluctance). Switched reluctance (SR) motors are used as traction engines in electric motor vehicles, in which a rotating magnetic field is created at the stator by switching copper coils on and off. Switched reluctance motors are low-maintenance, efficient and low-cost, but have a lower power density than permanent magnet excited synchronous motors. A major disadvantage is their high noise level (Chau & Li 2014a). The decisive factor for their future market penetration will therefore be the extent to which this volume can still be reduced in the further development of the relatively new technology.

Hybrid engines (HSM) combine the reluctance principle with the use of permanent magnets. However, the magnets are located on the stator. Compared to PSM, these motors have the advantage that they can be switched off and thus do not cause unwanted recuperation (Merwerth 2014). Their power density and efficiency are higher than that of ASM and ESM (Merwerth 2014; Kane 2020).

3.1.2.2 Raw material content

The specific material requirements of a motor vehicle's traction engine depend greatly on the engine size, which in turn is influenced by the segment (small to luxury cars) and the drive technology (HEV, PHEV, BEV, FCEV, REEV). The raw material demands of the different engine types differ too.

In conventionally combustion-engine powered motor vehicles, smaller quantities of copper are needed for the starter motor and generator. By contrast, electric traction engines generate significant additional demand for copper. Copper coils are used to generate magnetic fields on the stator of an electric motor and on the rotor of electrically excited synchronous motors. The squirrel-cage rotor on the rotor of the asynchronous motors is made of copper or aluminium.

Neodymium-iron-boron magnets (NdFeB magnets), which contain the rare earth element neodymium (Nd), are used in permanently excited synchronous motors and hybrid motors. To optimise the magnetic properties (see Section 3.3.9), part of the neodymium is substituted by the rare earth element dysprosium (Dy).

Current information regarding the magnetic mass per traction engine fluctuates between 1.2–3 kg. Table 3.2 provides an overview of the magnetic masses used by vehicle segment and drive technology based on Glöser-Chahoud & Tercero Espinoza (2015). This is based on the non-linear relationship between motor power and magnet mass.

Information on the dysprosium content varies greatly in some cases, but is usually between 6.6 % and 12 % Dy. The mean value of 8.3 % Dy calculated in Glöser-Chahoud & Tercero Espinoza (2015) is assumed, resulting in 23.7 % Nd (with a total of 32 % rare earth elements). The partial substitution of Nd and Dy by praseodymium (Pr) and terbium (Tb) is possible, which is discussed in more detail in Section 3.3.9.

Table 3.2: Magnet mass per engine in kg for various drive technologies and vehicle segments (source: Glöser-Chahoud & Tercero Espinoza 2015)

	HEV	PHEV	BEV/FCEV
Small cars	1.2	1.7	1.7
Compact cars	1.5	2.3	2.5
Premium cars	2.0	2.8	3.0

3.1.2.3 Foresight industrial use

The number of xEVs sold in 2040 is taken directly from the electric mobility framework scenarios. For the corresponding demand for the rare earths Nd/Pr and Dy/Tb, the extent to which the various motor concepts for traction engines become established will be crucial. The engine concepts currently used and the market positions of the companies behind them, which are examined below, provide indications of this.

Relevant manufacturers

The manufacturers with the highest market shares in the PHEV and BEV segments in 2020 are (Pontes 2021):

- Tesla, Inc.
- SAIC Motor Co Ltd (formerly Shanghai Automotive),
- Volkswagen AG,
- Renault SA – Nissan Motor Co., Ltd,
- BYD Co Ltd,
- BMW AG.

Other manufacturers with relevant xEV sales figures are Hyundai, Audi, Volvo, Chery, Wuling, BAIC (Beijing Automotive) and Great Wall Automotive. The high number of Chinese automotive companies (SAIC, BYD, Wuling, Great Wall Automotive, Chery) is striking. Other Asian countries such as India, Indonesia, Thailand and Vietnam also have increasingly relevant automotive production. Companies such as SAIC and Hyundai are planning major investments in India (Mordor Intelligence 2020b). Globally, most cars are produced in China, with resident automotive companies focusing on increasing production and sales of xEVs domestically (Mordor Intelligence 2020b). Many Chinese companies have joint ventures or partnerships with foreign companies, e.g:

- Volkswagen/General Motors – SAIC/Wuling,
- BMW – Great Wall Automotive,
- Daimler – BYD,
- Daimler – BAIC,
- Jaguar Land Rover – Chery,
- Volvo – Geely.

Table 3.3: Market shares of various engine technologies in different price segments in 2040

BEV categories	ESM	PSM	ASM	HSM	PSM + ASM	HSM + ASM
Small cars	0.3	0.3	0	0.4	0	0
Compact cars	0	0.45	0	0.45	0	0.1
Premium cars	0	0.15	0.2	0.2	0.15	0.3

Tesla is the only foreign company that sells xEVs in China without having a joint venture with a Chinese company. Tesla itself has large production facilities in China for this purpose. Overall, it can be assumed that the xEVs produced in China use similar technologies to the foreign companies.

Current technology choice

Currently, the following variants are used in commercially available xEVs (for technical details, see technology description):

- permanent magnet excited synchronous motors (PSM),
- inductively excited synchronous motors (ESM),
- electrically excited asynchronous motors (ASM),
- Hybrid motors (HSM), which operate with permanent magnets on the stator according to the reluctance principle.

ESMs are more likely to be used in the price-sensitive segment, i.e. in small cars such as the Renault Zoe and Smart, due to their lower costs but have disadvantages with regard to extreme driving performance (Oppenheimer 2020).

PSMs are used in almost all hybrid cars due to their advantages in efficiency and power density (Oppenheimer 2020). Many manufacturers also use these powerful but comparatively expensive motors for fully electric cars; for example, the Nissan Leaf, Hyundai Ioniq, Hyundai Kona, BYD Qin, BYD e6, BYD F3DM, JAC iEV6E and SAIC Roewe E50 all run on PSM.

ASMs are used primarily in the high-price segment, e.g. in the Audi e-tron, due to their advantages for long-distance journeys. Also popular in the high-price segment are combinations of PSMs and ASMs, through which the respective advantages of both concepts are exploited to the full (Lang 2019; Oppenheimer 2020).

In 2013, BMW was the first company to use series-production-ready **HSMs** (Merwerth 2014) which had market-relevant distribution in the BMW i3 model. In the past, Tesla relied on asynchronous motors as a matter of principle; the company's name honours the inventor of the asynchronous motor. Since 2019, however, hybrid engine technology has also been used. The newer models each have one engine on the front axle and 1 to 2 engines on the rear axle. ASM and HSM are used for this purpose (Lambert 2018; Kane 2020).

Scenarios for future industrial use

In the assumptions on the future use of different engine concepts (Table 3.3) for BEVs, the strengths and weaknesses of the different concepts are considered with regard to the different price segments. It is also assumed that the comparatively new concepts of hybrid engines and the combination of different engines will gain in importance in the future. For HEVs and PHEVs, on the other hand, it is assumed that PSM technology will be used 100 % here. These vehicles have to accommodate an electric and a conventional drive motor, so the advantages of PSM in terms of power density and efficiency take clear priority.

3.1.2.4 Foresight raw material demand

The average quantities of magnets required are based on the assumptions regarding the share of different engine technologies in 2040 in different price segments (Table 3.3) and the magnet quantities required in different price segments (Table 3.2). It is assumed that an HSM requires only 60 % as much magnetic material as a PSM (Blagoeva et al. 2019). A combination of ASM and

PSM also halves the amount of magnet required. With a combination of HSM and ASM, the amount of magnet required is thus only about 30 % of the amount needed with a pure PSM solution.

For the specific dysprosium demand in 2040, the scenarios shown in Table 3.4 are considered due to numerous research efforts to reduce the dysprosium content in NdFeB magnets. Since dysprosium and neodymium substitute for each other in magnetic materials, a reduction in dysprosium means an increase in the neodymium content in all material science approaches. It is assumed that there is little effort in SSP5 towards material efficiency in general, but at the same time general scientific progress is rapid and there is sufficient incentive for material efficiency improvement due to the high prices for dysprosium. Similar savings are assumed in SSP2, although scientific progress is slower here, however moderate savings should still be possible by 2040. In the sustainability scenario SSP1, a stronger focus on material efficiency and thus a significant reduction of the Dy content is assumed.

This synopsis only considers the raw material demand for traction engines of e-cars. For information on the demand for NdFeB magnet material for other automotive applications, see Section 3.3.9 on high-performance permanent magnets.

Table 3.4: Scenarios for the development of the Dy component in NdFeB magnets for engines in EVs (Dy component in 2014) (source: Glöser-Chahoud & Tercero Espinoza 2015)

Scenario	Reduction in Dy component through advances in R&D	Dy component in NdFeB magnets in EV engines 2040	Nd component in NdFeB magnets in EV engines 2040
SSP1	[Dy percentage 2014] – 50 %	4.2 %	27.8 %
SSP2	[Dy percentage 2014] – 25 %	6.2 %	25.8 %
SSP5	[Dy percentage 2014] – 25 %	6.2 %	25.8 %

Table 3.5: Specific copper demand for various electric motors in kg/kW

	ESM	PSM	ASM	HSM	PSM + ASM	HSM + ASM
Copper	0.16	0.09	0.16	0.04	0.125	0.1

Table 3.6: Global production (BGR 2021) and calculated raw material demand for electrical traction engines for motor vehicles, in tonnes

Raw material	Production in 2018	Demand in 2018	Demand foresight for 2040		
			SSP1 Sustainability	SSP2 Middle of the Road	SSP5 Fossil Path
Neodymium / praseodymium	23,900 (R) 7,500 (R)	1,430	34,050	31,350	31,960
Dysprosium / terbium	1,000 (R) 280 (R)	500	5,140	7,530	7,680
Copper	20,590,600 (M) 24,137,000 (R)	33,200	800,000	816,000	772,600

M: Mine production (tonnes of metal content)
R: Refinery production (tonnes of metal content)

Table 3.6 shows the demand resulting from the scenarios for the rare earths neodymium (or substitute praseodymium) and dysprosium (or substitute terbium, for details see Section 3.3.9) in 2040. The aggregate extraction volume of rare earths in 2018 was 151,200 tonnes in metal content, according to BGR (2021). The very similar values for Nd in all three scenarios result from the overlapping of different effects. Thus, while there are significantly more BEVs in SSP1 in 2040, there are also significantly fewer HEVs than in SSP2 and SSP5. Due to the dominance of PSM engine technology in HEVs and PHEVs, the overall demand expectations for neodymium are comparable. For dysprosium, the demand expectations in SSP2 and SSP5 are even significantly higher than SSP1, since in SSP1 a stronger reduction of the Dy content in the magnets is assumed due to efficiency efforts. The values for 2018 were also calculated from estimates for the current share of different engine technologies and the sales figures of the mobility framework scenarios.

To calculate the copper demand for electrical traction engines, a study by IDTechX for the Copper Association is used (ICA 2020) in which average specific copper demands of between 0.04 and 0.16 kg/kW are given for different motor types, compare Table 3.5. Assuming engine outputs of 50, 85 and 150 kW in 2040 for the mini, compact and luxury class vehicle segments and the registration figures for electric vehicles from Section 1.3.2, the copper requirements are calculated as shown in Table 3.6.

3.1.2.5 Recycling, resource efficiency and substitution

In Germany, traction engines from electric cars that are to be disposed of are currently generally fed into the copper recycling stream (Bast et al. 2015). It is technically possible to remove the NdFeB magnets from the motors without destroying them and to reuse them. However, the use of different geometries and alloys and the continuous development of magnet and motor technologies make direct reuse more difficult. However, if NdFeB magnets can be collected by type in a separate waste stream, material recycling through hydrogen embrittlement is possible, but this leads to losses in remanence (residual magnetisation) of approx. 3 %. Through raw material recycling using hydrometallurgical processing, pure rare earths can be recovered as oxides. In Germany, however, the reduction of these oxides to pure metals is currently not technically possible (Bast et al. 2015).

In 2040, the recycling of NdFeB magnets after their use in electric car traction engines in Germany is likely to be economical, although this will depend on volume, raw material prices and the share of the more expensive heavy rare earth elements dysprosium and terbium (Bast et al. 2015).

3.1.3 Alloys for lightweight airframe construction

3.1.3.1 Technology description

The airframe represents the mechanical structure of an aircraft. It includes the fuselage, wings, engine nacelles, cowling, tail and landing gear (see Figure 3.2 and Aviation Safety Bureau 2007). The optimisation of the materials used for the airframe plays a significant role in the development of new aircraft models. The basic requirements for a suitable material are high corrosion and fatigue resistance, damage tolerance, rigidity and strength. It is particularly important that the density of the material is as low as possible, which leads to a reduction in the weight of the aircraft and thus to fuel savings. The performance, weight and cost of suitable materials must then be considered. Due to their lightness, aluminium alloys have been the dominant materials in lightweight airframe construction for decades. However, they face strong competition from composites, which increasingly make up a large proportion of the aircraft structure in newly developed airframes (Frost & Sullivan 2016; AIRBUS 2018; Frost & Sullivan 2019).

Figure 3.2: Schematic diagram of the airframe of a passenger aircraft, consisting of fuselage, wings, engine nacelle, cowling, tail and undercarriage (source: by kind permission of E. Tercero Daschner)

3.1.3.2 Raw material content

Alloys

Aluminium alloys have proven themselves in lightweight airframe construction. Despite the considerable increase in the use of composites in newer aircraft models (see below), aluminium alloys remain the most widely used material in aircraft construction (Frost & Sullivan 2016; Frost & Sullivan 2019). This is due to the large number of short- and medium-haul aircraft (e.g. the Airbus 320 family and Boeing 737) compared to wide-body aircraft (see Figure 3.3). On regional aircraft, aluminium is also at least partly preferred in more recent developments (Mraz 2014; Morimoto et al. 2017).

Conventional aluminium materials have to be riveted. However, recent developments, especially aluminium-lithium alloys (Al-Li), allow welding with lasers and/or friction stir welding, which enables

Table 3.7: Alloy components of some commercially available aluminium-lithium alloys (sources: Constellium 2017a, Constellium 2017b, Constellium 2017c, Constellium 2017d, Constellium 2017e, Constellium 2017f, Constellium 2017g)

Alloy	Li	Cu	Mn	Mg	Ag	Zr
2098	0.8 to 1.3 %	3.2 to 3.8 %	Max. 0.35 %	0.25 to 0.80 %	0.25 to 0.60 %	0.04 to 0.18 %
2195	0.8 to 1.2 %	3.7 to 4.3 %	Max. 0.25 %	0.25 to 0.80 %	0.25 to 0.60 %	0.08 to 0.16 %
2065	0.8 to 1.5 %	3.8 to 4.7 %	0.15 to 0.50 %	0.25 to 0.80 %	0.15 to 0.50 %	0,05 to 0.15 %
2198	0.8 to 1.1 %	2.9 to 3.5 %	Max. 0.50 %	0.25 to 0.80 %	0.10 to 0.50 %	0.04 to 0.18 %
2196	1.4 to 2.1 %	2.5 to 3.3 %	Max. 0.35 %	0.25 to 0.80 %	0.25 to 0.60 %	Max. 0.35 %
2050	0.7 to 1.3 %	3.2 to 3.9 %	0.20 to 0.50 %	0.20 to 0.60 %	0.20 to 0.70 %	0.06 to 0.14 %
2297	1.1 to 1.7 %	2.5 to 3.1 %	0.10 to 0.50 %	Max. 0.25 %		0.08 to 0.15 %

Notes: All of the alloys shown also contain up to 0.12 % Si and up to 0.15 % Fe; most of them also contain up to 0.10 % Ti and up to 0.35 % Zn.

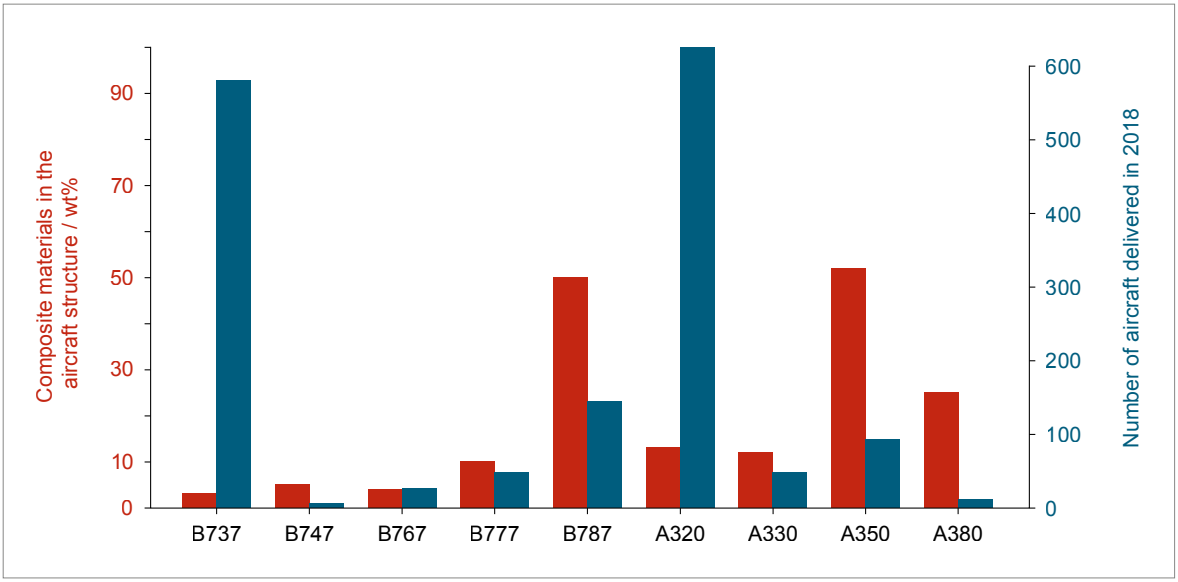

Figure 3.3: Proportion of composite material in the airframe of current Airbus and Boeing models and the numbers of each model delivered in 2018

considerable cost savings (Angerer et al. 2009; e.g. see Constellium 2017c; Constellium 2017f). The addition of scandium (Sc) also allows welding with lasers (Angerer et al. 2009). However, due to the high price of scandium, Al-Sc alloys are currently not competitive in aircraft construction and are only used on niche markets (Djukanovic 2017; Dorin et al. 2018).

Unlike Al-Sc alloys, Al-Li alloys are gaining importance and are used commercially as sheets, plates or castings, e.g. in the Boeing 787 and Airbus A350 XWB and A380 (Constellium n.d.; Constellium 2013; Aluminium Fair 2014; Arconic 2020). The weight-saving aluminium components can be added to existing series with no or only minor changes to the aircraft design (Aluminium Fair 2014). The composition of some commercially available Al-Li alloys is shown in Table 3.7.

Titanium and its alloys also have a definite place in aircraft construction due to their low density, high corrosion resistance and strength, even at elevated temperatures (Frost & Sullivan 2016; Pervaiz et al. 2019). Titanium alloys are preferred in composite structures because corrosion occurs at the junction between aluminium and composite components. Consequently, the use of titanium increases as the use of composites increases (AIRBUS 2018). From a weight share of less than 10 % in the past (Sibum et al. 2003-2020), the weight share of titanium and titanium alloys in the composite-rich Boeing 787 and Airbus A350 XWB reaches 14–15 % (Dursun & Soutis 2014; Frost & Sullivan 2016).

The processing of metal components for aircraft construction is traditionally subtractive: solid metal semi-finished products are often milled to the desired final shape (López de Lacalle et al. 2011). This removes well over 80 % of the material (López de Lacalle et al. 2011; AIRBUS 2018). This is changing at the moment through the use of additive manufacturing processes (AIRBUS 2018). Titanium alloys as well as aluminium alloys are being developed for this purpose and are already commercially available (Apworks n.d.; AIRBUS GROUP 2015; Metal AM 2020).

Carbon fibre-reinforced plastics (CFRP)

High-performance Al alloys remain an important component in civil airframe construction, but are losing their clear dominance due to the increased use of composites, mainly carbon fibre-reinforced plastics (Dursun & Soutis 2014). At around 50 wt% (AIRWISE 2013), these composite materials are already the main components of the Boeing 787 Dreamliner wide-body aircraft (maiden flight: 2009) and Airbus A350 (maiden flight: 2013). Al alloys now account for only 20 wt%.

Completed before the A350, the Airbus A380 (maiden flight: 2005) still consists of 25 wt% composites, of which 85 wt% are CFRPs (Woidasky & Jeanvré 2015). Figure 3.3 shows the composite content of various Airbus and Boeing aircraft models. Since narrow-body aircraft also require thinner sheet metal for the outer skin, the weight saving from using composites is also lower there (Sloan 2020), and these smaller, much more frequently sold models are mainly made of aluminium alloys (see Figure 3.3). The production of composite parts in the required quantities for the Airbus A320 family and Boeing 373 series is also not possible with the technology that is currently dominant. The development of corresponding solutions is being driven forward (Sloan 2020).

3.1.3.3 Foresight industrial use

The three aircraft manufacturers Airbus, Boeing and Bombardier provide and publish detailed forecasts for the global aircraft markets. In the latest editions, all three assume strong and steady growth in aircraft demand, supported mainly by economic growth and a variety of other drivers (Bombardier 2017; AIRBUS 2019a; Boeing 2019a). The expectation is a little more than doubling of the aircraft fleet over the next 20 years. The growth of the aircraft fleet is mainly driven by narrow-body aircraft, which are even expected to expand their large share (currently approx. 70 %) of the aircraft fleet.

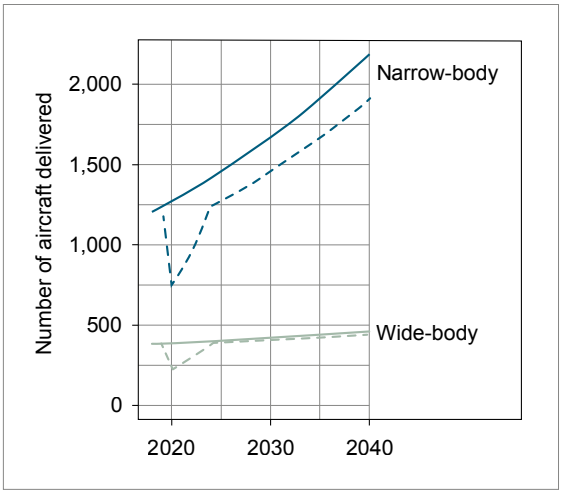

Figure 3.4: Assumed aircraft deliveries up to 2040 in the SSP2 scenario (source: adapted from AIRBUS (2019a) and Boeing (2019a); see explanations in the text)

Even before the outbreak of the COVID-19 pandemic, Airbus and Boeing addressed the resilience of the aviation sector using historical data from past geopolitical and economic crises (AIRBUS 2019a; Boeing 2019a). These crises had the effect that passenger numbers stagnated or declined slightly for 1 to 3 years, only to show the same or even stronger growth again afterwards. However, the COVID-19 pandemic is different and has so far led to a sharp drop, not stagnation, in passenger numbers. Aircraft production at both major manufacturers has fallen sharply in the first half of 2020 (about 40 % for Airbus, over 50 % for Boeing in Q1 2020; Argus Media 2020). It is therefore to be expected that the effects will be more pronounced and longer-lasting, so that the only recently published forecasts appear rather optimistic from today's perspective, despite the sector's historical resilience.

The following assumptions were made for the estimation of the passenger aircraft market:

– Aircraft categories like Boeing (Boeing 2019a): Narrow-body and wide-body aircraft, as these correlate better with aircraft composition than the categories used by Airbus (small, medium, large), because the medium category includes not only aluminium but also CFRP-heavy aircraft.

– Growth rate of aircraft deliveries: 2.7 % for narrow-body and 0.9 % for wide-body aircraft based on AIRBUS (2019a) and Boeing (2019a) forecasts.

– COVID-19 adjustment: 40 % drop in aircraft deliveries in 2020, with the drop in narrow-body aircraft being greater than in wide-body aircraft, and an upwards climb to “normal” by 2024. This results in a total of 11 % fewer aircraft deliveries in 2040 (about 1,900 narrow-body as well as about 440 wide-body aircraft) compared to the projections in AIRBUS (2019a) and Boeing (2019a) and comparable to Boeing (2020).

– It is assumed that the aircraft manufacturers' forecasts correspond most closely to the SSP2 scenario. Since aircraft deliver-

ies correlate well with economic growth, the scenario in Figure 3.4 is first scaled using the GDP scenarios (Dellink et al. 2017; Riahi et al. 2017). In the SSP5 "Fossil Path", a much higher increase in air traffic is expected, driven by very strong economic growth coupled with weak environmental awareness (cf. Table 1.2), resulting in a demand for approximately 3,250 (instead of 2,350 in SSP2) aircraft in 2040. In the SSP1 scenario, the increase in air traffic is not as strong despite high economic growth due to significant environmental awareness, so that the need for new aircraft is put at a total of about 2,200.

3.1.3.4 Foresight raw material demand

The aviation industry will continue to use a wide mix of materials until 2040 (cf. AIRBUS 2018). Currently, a certain dichotomy is emerging in which wide-body aircraft prefer to use composite materials and narrow-body aircraft prefer to use aluminium materials. However, redesigns of the top-selling Airbus A320s and Boeing 737s (for narrow-body aircraft) are expected during this period, and these may involve increased use of composites at the expense of aluminium (Sloan 2020). However, weight is not the only factor in the choice of materials; recent developments in narrow-body aircraft also rely on aluminium instead of composites (Morimoto et al. 2017; AIRBUS 2018). The increased use of 3D printing in aircraft manufacturing is creating new opportunities for metal alloys (AIRBUS 2018).

It is therefore assumed that aluminium materials will dominate airframe construction in the narrow-body aircraft segment by 2040. It is also assumed that Al-Li alloys will replace conventional aluminium materials by 2040. For the wide-body segment, it is assumed that the dominance of composites will consolidate by 2040 and the material mix will approximate that of the A350 XWB and B787.

The exact proportions of alloying elements in Al-Li alloys are usually a trade secret. To determine an approximate order of magnitude of the lithium requirement for Al-Li alloys in airframe construction, the product data in Table 3.7 is used as a guide, covering a wide range of tasks in airframe

Table 3.8: Assumptions relating to airframe composition (proportions of aluminium alloys, steel, titanium and titanium alloys and composite materials in 2040)

Category	Unladen weight	Al	Steel	Ti	Composite materials
Narrow-body	40 tonnes	72 %	10 %	12 %	6 %
Wide-body	110 tonnes	20 %	8 %	15 %	51 %

Table 3.9: Global production (BGR 2021) and calculated raw material demand for lightweight alloys for airframes, in tonnes

Raw material	Production in 2018	Demand in 2018	Demand foresight for 2040		
			SSP1 Sustainability	SSP2 Middle of the Road	SSP5 Fossil Path
Copper	20,590,600 (M) 24,137,000 (R)	11,000	12,000	13,000	18,000
Lithium	95,170 (M)	low	4,200	4,400	6,200
Silver	28,083 (M)	low	1,200	1,300	1,800
Titanium	260,548 (R)	57,000	75,000	80,000	110,000

M: Mine production (tonnes of metal content)
R: Refinery production (tonnes of metal content)

construction. The mean values of the indicated concentration ranges are 1.2 % Li, 3.5 % Cu, 0.25 % Mn, 0.5 % Mg, 0.35 % Ag and 0.1 % Zr. For simplification purposes, titanium alloys are considered to be titanium.

The impact of the COVID-19 pandemic is modelled in a simplified way as follows: 40 % decline in aircraft manufacturing in 2020 compared to 2019, with a return to pre-crisis levels in 2024. Growth is then calculated based on the growth forecasts of the major aircraft manufacturers (see Figure 3.4). The difference in raw material demands between the aircraft manufacturers' pre-COVID-19 forecasts and the simple COVID-19 adjustment in the SSP2 scenario is 9–12 % in 2040, depending on the material.

The interplay of these assumptions and scenarios results in requirements of 330,000 to 480,000 tonnes Al, 4,200 to 6,200 tonnes Li, 12,000 to 18,000 tonnes Cu, 1,700 to 2,600 tonnes Mg, 1,200 to 1,800 tonnes Ag and 75,000 to 110,000 tonnes titanium for 2040. Copper is already being used today in aluminium alloys. These estimates refer to the raw materials required for aircraft fuselage production, not to the raw material content of the aircraft. A lot of production waste is generated, especially in the case of metallic materials (AIRBUS 2018).

3.1.3.5 Recycling, resource efficiency and substitution

The recycling of aluminium alloys from aircraft construction is already well established. This follows from the unfavourable ratio between purchased material and material in the final product (the buy-to-fly ratio, as it is known, AIRBUS 2018) as well as the high intrinsic value of the alloys. Aluminium suppliers for aircraft construction therefore only use about 25 % primary aluminium and 75 % production scrap (Michaels 2018). Aluminium recycling from old products is also well established. The disposal of old aircraft or their components is mainly shaped by strict regulations or traceability and documentation. The value of reusing the parts is many times higher than the material value. The recovery of high-quality aluminium alloys from old aircraft is possible through identification and separation. However, these are not reused in structural parts (Woidasky & Jeanvré 2015; Woidasky et al. 2017). In addition, the alloys evolve over time and are therefore not necessarily usable today for their originally intended function.

The scrapping of larger quantities of aircraft with significant proportions of composites is not expected until after 2030. At present, therefore, it is mainly production scrap from composite materials that is produced, but its quantity is estimated to be comparatively small (AIRBUS 2018). In addition, the recycling or disposal of composites is generally associated with many technical difficulties. There are parallels in this area to the construction of wind turbines. Active research is currently going on into the recycling of these materials.

It is expected that the greater use of additive processes will lead to better buy-to-fly ratios (AIRBUS 2018). Given the high recycling rates for production scrap, the effect on primary demand should remain low.

3.1.4 Automatic piloting of motor vehicles

3.1.4.1 Technology description

If a computer-controlled system takes over the driving task from the driver in any means of transport, then the technical term used is “automated driving” or the “automatic piloting of motor vehicles”. Colloquially, however, the term "autonomous driving" is still often used. The extent to which driving tasks are taken over can vary greatly because the majority of vehicle manufacturers and suppliers are introducing automated driving in evolutionary stages. In this context, vehicle manufacturers have settled on the following five stages of automated driving, based on the work of the SAE (Society of Automotive Engineers):

Stage 1 – Assisted driving
The preliminary stage on the way to automated driving is assisted driving using driving assistance systems. Here, within certain limits, either the longitudinal or lateral guidance of the vehicle is taken over, although the driver must constantly monitor the system and be ready to intervene.

Stage 2 – Semi-automated driving
In semi-automated driving, the system takes over both the longitudinal and lateral guidance of the vehicle for a certain period of time or in specific situations. However, the driver must still monitor the system permanently and be able to take over the driving completely at any time.

Stage 3 – Highly automated driving
The main distinguishing feature of highly automated driving functions compared to the previous automation levels is that the vehicle takes over longitudinal and lateral guidance for a limited period of time or in specific situations and the driver no longer has to permanently monitor the system. However, he must always be able to take over the driving again completely and safely with an appropriate time reserve when called upon to do so.

Stage 4 – Fully automated driving
In fully automated driving, the system takes over the driving of the vehicle completely in a defined practical situation and handles all related situations automatically.

Stage 5 – Driverless driving
In driverless driving, the highest level of automation, the system takes over complete control of the vehicle from start to finish on all types of roads, at all speeds and in all environments and weather conditions. All persons in the vehicle thus become passengers.

The automatic piloting of motor vehicles thus starts with the partial automation stage according to the 5-stage scheme. Today, motor vehicles on the road are already on the threshold of level 3, highly automated driving, to level 4, fully automated driving. 2018 saw the launch of the Audi A8, the first series vehicle to offer Stage 3. Waymo has already been working with fully automated vehicles in taxi operations (Waymo One) in various cities in the USA since autumn 2020. In rail and air transport, on the other hand, fully automated systems have been in place for many years. However, the introduction of automation in road traffic began with a variety of driver assistance systems (ADAS – Advanced Driver Assistance Systems) in the 1950s with the standard introduction of brake boosters and power steering. In 1958, Chrysler offered cruise control in a series vehicle for the first time. The anti-lock braking system (ABS) and, derived from it, the anti-slip control (ASR) and the automatically shifting all-wheel drive have been available in series vehicles since 1985. In 1987, Toyota launched the first GPS-guided navigation system and Electronic Stability Control (ESP) has been available since 1995. Today, numerous control units are installed in new vehicles, in addition to the engine control, especially for assistance systems. The speed of innovation in assistance systems has developed very dynamically in recent years. A major reason for this is the parallel development of automated motor vehicles outside the classic automotive industry. Large IT companies such as Google (with Waymo) and Apple, but also new players in the automotive industry such as Tesla, are setting a fast pace. The classic OEMs and suppliers want to and have to keep up in order not to be degraded to mere producers of the driveable shell. From a technical point of view, the main drivers of this dynamic development are the increasing performance of processors and memories, sensors and actuators, the development of algorithms for handling big data in combination with artificial intelligence and the constantly falling prices of these components.

Table 3.10 shows examples of assistance systems grouped according to their stage of development. The overview shows the technological diversity of support functions, but does not claim to be exhaustive. Individual systems are listed along with clusters that bundle several individual systems, as is the case with “semi-automated driving”. “On the market” means that the system can be ordered from vehicle manufacturers as equipment for series vehicles.

Assistance systems as well as all of the automation functions required for piloted driving depend on powerful sensors and control units that provide valid information about the vehicle environment at all times and under all general conditions and weather situations. OEMs sometimes take very different approaches to the composition of these system components in order to meet the requirements for a particular level of automation. While Tesla, for example, currently relies on the interaction of up to eight cameras, one long-range and one short-range RaDAR as well as nine ultrasonic sensors for the full self-driving function (corresponding to automation level 4), Audi equips its vehicles such as the A8 for auto-

Table 3.10: Driver assistance systems (source: own research)

	System	State of development
1.	Power brake (servo brake)	On the market since the 1950s
2.	Power steering	Market launch 1951
3.	Cruise control	Market launch 1958
4.	ABS	Market launch 1985
5.	Traction control (ASR)	Market launch 1985
6.	Automatic four-wheel drive	Market launch 1985
7.	GPS navigation	Market launch 1987
8.	ESP	Market launch 1995
9.	Adaptive cruise control (ACC)	On the market
10.	Hill start assist	On the market
11.	Parking assist	On the market
12.	Driver alertness assistant	On the market
13.	High beam assistant	On the market
14.	Pedestrian protection system	On the market
15.	Infrared camera for night vision	On the market
16.	Curve light assistant	On the market
17.	Emergency brake assist (collision avoidance system)	On the market
18.	Tyre pressure monitoring	On the market
19.	Rear view camera	On the market
20.	Side wind assist	On the market
21.	Safety belt pretensioners	On the market
22.	Lane-keeping assistant	On the market
23.	Lane change assistant	On the market
24.	Semi-automated driving	On the market
25.	Phone assistant	On the market
26.	Blind spot assistant	On the market
27.	Traffic sign detection	On the market
28.	Wrong-way warning system	On the market
29.	Accident assistant (location reporting etc.)	On the market
30.	Platooning for lorries	In market launch
31.	Remote-controlled automatic parking	On the market
32.	Intelligent speed limit adaptation	On the market
33.	Automatic junction assistant	On the market
34.	Highly automated driving	On the market
35.	Fully automated driving	In market launch
36.	Driverless driving	In development

Table 3.11: Average number of system components required (source: KRAIL et al. 2019)

Components	Level 1	Level 2	Level 3	Level 4	Level 5
Ultrasound	9	9	9	9	9
Radar	2	4	4	8	8
LiDAR	0	0	1	1	1
Camera	0	2	5	5	5
DSRC	1	1	1	1	1
GNSS positioning	1	1	1	1	1
V2X module	1	1	1	1	1
Controllers	1	1	2	3	3

mation level 3 with five cameras, four mid-range RaDARs, one long-range RaDAR, twelve ultrasonic sensors and one laser scanner (LiDAR). However, with the exception of Tesla, all other OEMs currently rely on at least one LiDAR when equipping vehicles with sensors. Based on expert interviews and the evaluation of secondary literature, KRAIL et al. (2019) estimated the most frequent distribution and number of system components required per automation level (see Table 3.11).

The information about the driving environment in the available series production vehicles, but also in the prototypes of the OEMs, suppliers and other manufacturers (Waymo, etc.) is thus currently obtained by optical cameras in the visible and IR light wave spectrum using ultrasonic sen-

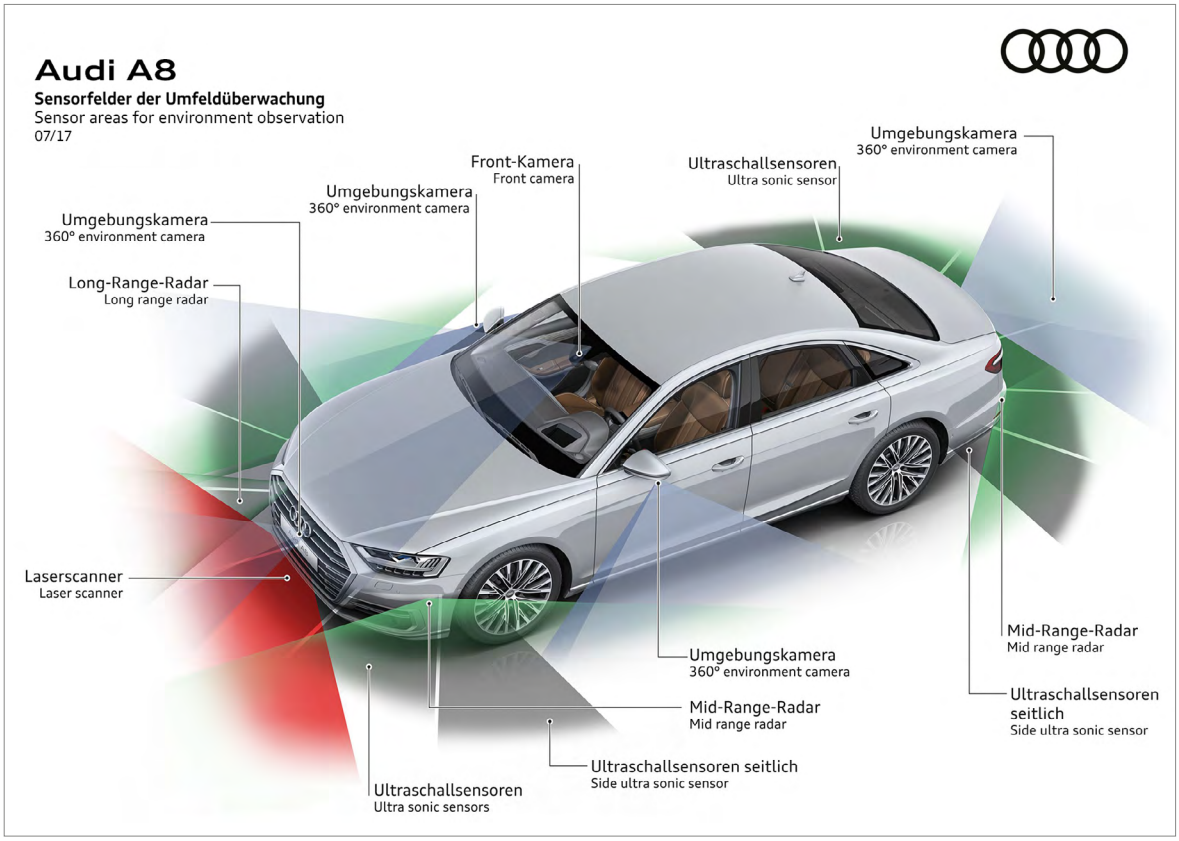

Figure 3.5: Example of sensors in a highly automated series-production vehicle (source: Audi AG)

sors, radar sensors and laser scanners or LiDAR sensors. Figure 3.5 shows the sensor equipment of the first highly automated series production vehicle available with level 3, the Audi A8.

A central component for obtaining data to create a spatial image of the surroundings is the laser scanner. The laser scanner is technically a LiDAR (Light Detection And Ranging), which can measure distance and speed in the near and far range by optical means using monochromatic laser radiation. The LiDAR's evaluation processor calculates a centimetre-precise image of the vehicle's surroundings by comparing the emitted and reflected laser radiation. LiDARs are powerful but still comparatively expensive components. Google's first autonomous test vehicle is equipped with the HDL-64E High Definition LiDAR from California-based Velodyne Lidar, Inc (Figure 3.6). It has a maximum range of 120 m, measures with an accuracy of less than 2 cm and still cost more than USD 70,000 in 2015. In the meantime, LiDARs have been significantly optimised in terms of size, performance and price (between USD 10,000 and 18,000). Velodyne now installs Alpha Prime LiDARs in Ford vehicles with ranges of up to 245 m and significantly smaller dimensions.

Conventional LiDARs work with a laser. The generated laser beam is then directed onto the measuring surface via oscillating rotating mirrors. The Velodyne Alpha Prime VLS-128 does without rotating mirrors, but is equipped with 128 lasers that generate a vertical beam fan. The rotation of the laser head scans the 360° field of view. Class 1 lasers are used with a beam power of less than 1 mW, which is harmless to the human eye. The laser operates at a wavelength of 905 nm in the invisible infra-red range (Velodyne 2020). It is not clear from Velodyne's information what kind of lasers are installed, but they could be InGaAs lasers whose material composition and geometry are not known.

Control units are the components in automated vehicles where sensor data is converted into commands for the actuators in the vehicles. These must already be very powerful for automation levels 2 and 3 and be able to perform up to 30 trillion TOPS (operations per second). For fully auto-

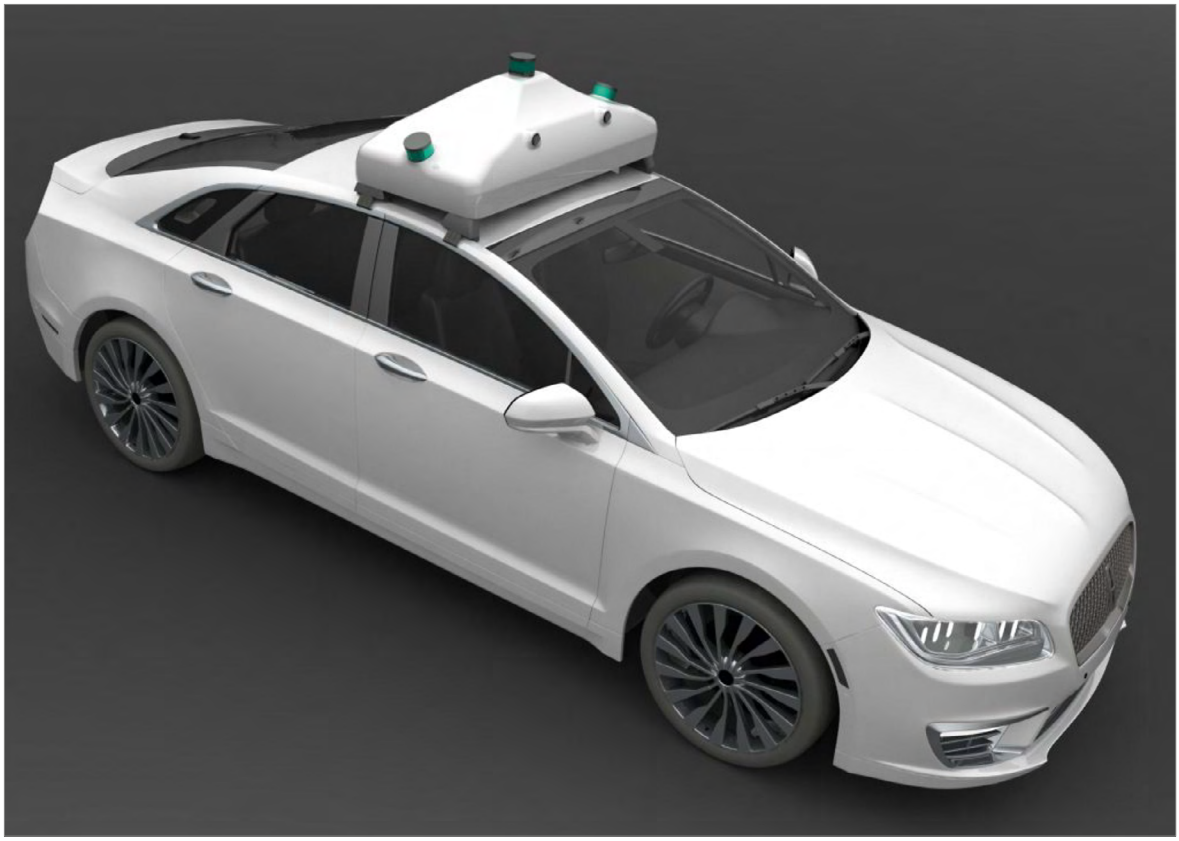

Figure 3.6: Fully automated test vehicle with LiDAR technology (source: Velodyne)

mated and driverless driving, the control units must be even more powerful. Nvidia, as one of the most significant manufacturers of CPU units in the control units of automated vehicles, currently offers the NVIDIA Drive AGX Pegasus platform for this purpose. According to the manufacturer, it can execute up to 320 trillion TOPS. While automation levels 2 and 3 require a CPU (with eight processor cores), a GPU, a DLA (Deep Learning Accelerator), a PVA (Programmable Vision Accelerator), an ISP (image signal processor) and a 256-bit LPDDR4 memory, levels 4 and 5 require twice the amount of these units plus a further two graphics processors.

3.1.4.2 Raw material content

LiDARs in highly and fully automated vehicles are designed with solid-state or semiconductor lasers. Neodymium-doped YAG lasers (Nd:YAG lasers) are commercially widely available. This solid-state laser uses a transparent yttrium-aluminium-garnet single crystal ($Y_3Al_5O_{12}$) as the host material. The active material is neodymium, which replaces about one atomic per cent of yttrium. During doping, Y^{3+} ions are replaced by Nd^{3+} ions. The energetically dominant laser radiation of the Nd:YAG crystal is in the infra-red range and has a wavelength of 1064 nm, which can be brought to 532 nm by frequency doubling. 532 nm is perceived by the eye as a greenish light. Gallium arsenide laser diodes are used for pumping, emitting light at a wavelength of 808 nm into the YAG crystal. In addition, Peltier elements, for example bismuth telluride (Bi_2Te_3), are present on the pump laser and the YAG crystal for temperature stabilisation. The frequency is fine-tuned using piezo-ceramic technology by subjecting the YAG crystal to a mechanical voltage. Lead zirconate titanant ($Pb[Zr_xTi_{1-x}]O_3$, $0 \leq x \leq 1$), for example, is used as the piezo ceramic. The mineral potassium titanium oxide phosphate with the summation formula $KTiOPO_4$ is suitable for frequency doubling (Eichenseer 2003).

Radar sensors for distance measurement, for example for parking assistants, can now be built in a highly integrated way. A consortium of KIT, Robert Bosch GmbH and other partners has developed a miniaturised radar sensor that can be mass-produced at a cost of less than one Euro. The high-frequency components, the transmitting and receiving antennas and the evaluation electronics are housed on an 8 x 8 mm SiGe chip. The sensor works with electromagnetic waves at a frequency of 122 GHz. According to the developers, the distance of objects at a distance of several metres can be determined with an accuracy of less than 1 mm (KIT 2012).

Ultrasonic sensors for distance measurement use piezoelectric ceramics or piezoelectric plastics for sound generation and detection. In this process, the piezoelectric material is made to vibrate by alternating voltage (piezo loudspeaker). The reverse principle is used for the detection of the reflected wave. The incoming wave hits piezoactive material. The transmitted vibration generates electrical signals that are interpreted by the evaluation electronics.

In addition to the active semiconductor materials of the various sensors, copper, solder, gold as contact material, circuit boards as circuit carriers and a large number of passive components such as ohmic and inductive resistors and capacitors are used for the electronic circuits. However, the amounts of material required for the electronic components and their sensors are far from critical.

3.1.4.3 Foresight industrial use

The market for assistance and/or automation systems has been developing very dynamically for several years. While in the meantime the optimism of a rapid market introduction of automation level 4 has given way to realism due to some accident-related setbacks and partly hasty or poorly prepared market launches of autopilot systems on the road, the current efforts of some manufacturers are already showing the first signs of success. Based on expert interviews with decision-makers from the automotive industry, the introduction of automation level 4 can be expected as early as within the next few years. Roadmaps from various associations, such as the VDA or the European ERTRAC, confirm these expectations. However, experts question whether and when the final automation level 5 can be realised. However, as the functionalities between level 4 and level 5 do not differ significantly and the scope of automated driving is only limited by the framework conditions (road conditions, weather situation, availability of high-resolution maps

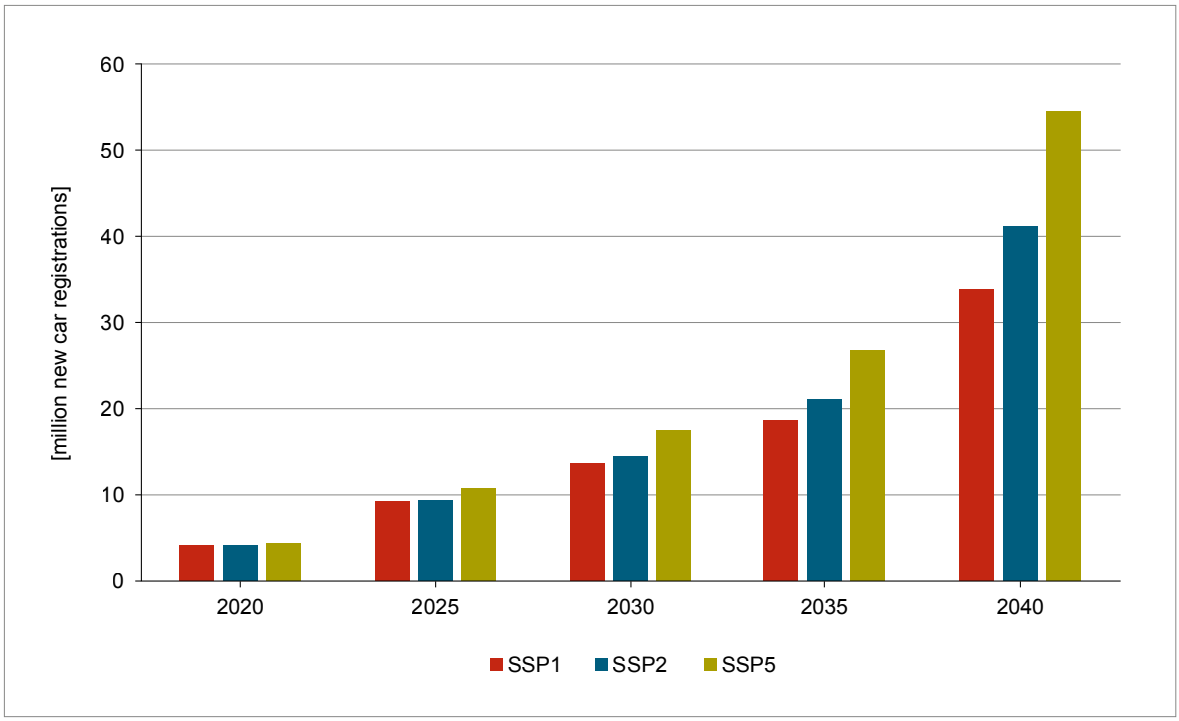

Figure 3.7: Global new registrations of automated cars, levels 2 to 5 (source: Fraunhofer ISI)

and coverage with fast mobile radio) at level 4, the introduction of level 5 is not crucial for the development of the technology and with it the demand for raw materials.

Krail et al. (2019) have estimated possible market ramp-up curves for cars, trucks and buses in different size classes and for the five automation levels for the German market on the basis of learning curves at system component level and the acceptance around or willingness to pay a premium. If the findings on market ramp-up are transferred to the global market for passenger cars and commercial vehicles, the result is the outlined market ramp-up for passenger cars and commercial vehicles that will be equipped with systems of automation levels from 2 (partially automated driving) to 5 (driverless driving) and newly registered worldwide by 2040.

The basis for the calculation is first an estimate of the development of new registrations of passenger cars and commercial vehicles (CVs) by 2040. This estimate assumes an increase in global new car registrations from 74.2 million in 2019 to 99.6 million cars in 2040, and for commercial vehicles from 18.7 million in 2019 to 24.7 million in 2040. Assuming that only the markets in industrialised countries follow the same path or the same speed of market ramp-up, and that markets in emerging and developing countries follow with a time lag of five and ten years respectively, the following picture emerges (see Figure 3.7 and Figure 3.8). For passenger cars, the estimate suggests that between 34 million (for scenario SSP1) and 54.6 million passenger cars (for scenario SSP5) could be equipped with systems that enable piloted driving with different levels of automation by 2040. For commercial vehicles, the number of new registrations of automated vehicles climbs to figures of between 17.8 million (for scenario SSP2) and 24.2 million commercial vehicles (for scenario SSP5) by 2040.

3.1.4.4 Foresight raw material demand

The technical concept of the Velodyne LiDAR Alpha Prime VLS-128, which is already close to the implementation stage, is to be used as the basis for estimating future raw material demands. It contains 128 laser systems. It is further assumed that, as in the previously mentioned BMW i3 self-parking research vehicle, four LiDAR are used per vehicle (Priemer 2015). The geo-

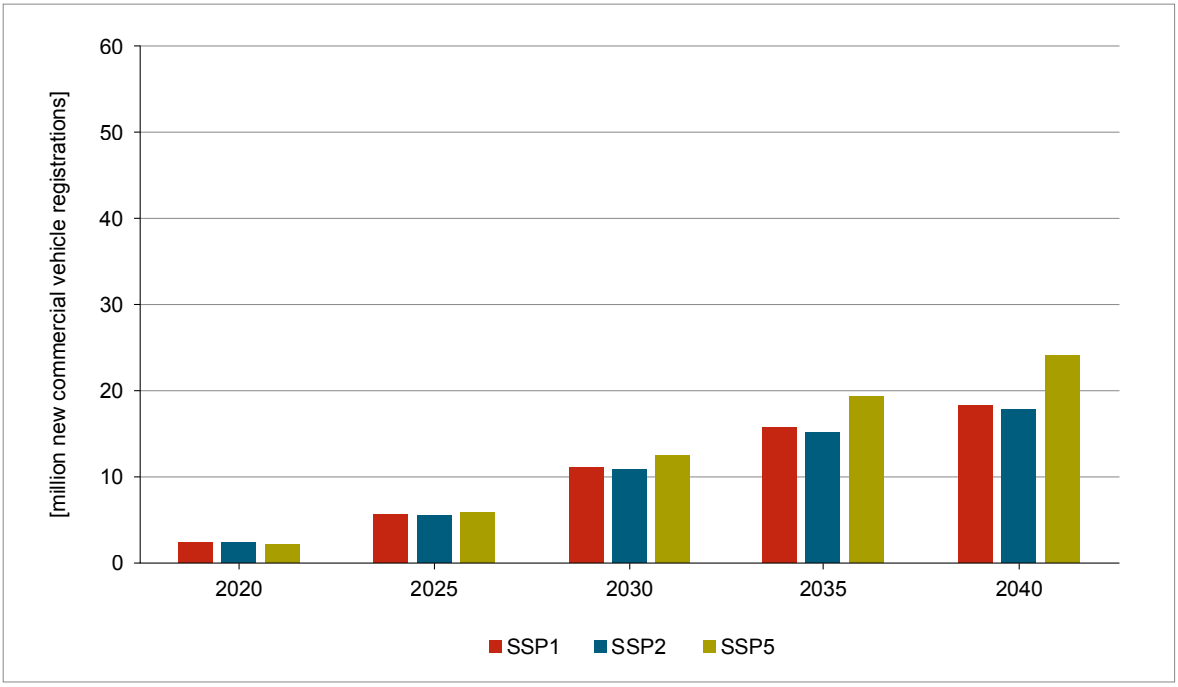

Figure 3.8: Global new registrations of automated commercial vehicles, levels 2 to 5 (source: Fraunhofer ISI)

metric dimensions of the lasers in the Alpha Prime VLS-128 are not known. The assumptions set out in Table 3.12 are used as a basis for estimating the future demand for raw materials.

With these assumptions, the weight of the individual YAG crystal is calculated to be 0.32 g, or 40.96 g YAG per LiDAR and per vehicle with 128 lasers installed. Accordingly, equipping 78.8 million passenger cars and commercial vehicles with LiDAR laser scanners creates an annual demand for YAG crystal of 3,228 tonnes.

The chemical summation formula for YAG doped with 1 atomic % neodymium is $Y_{2.97}Nd_{0.03}Al_5O_{12}$. The molecular weight of this material is 595.3 g. According to Table 3.13, it contains 0.72 wt% neodymium and about 44 wt% yttrium. Based on the assumptions made, this results in an annual demand of about 14.7 to 22.2 tonnes of neodymium and 928 to 1,401 tonnes of yttrium, if the vehicles produced in 2040 according to the estimates in scenario SSP1 (about 52.2 million) and in SSP5 (about 78.8 million) were to be equipped with laser scanners (Table 3.14). To account for the uncertainties, the formulated scenario is an estimate of potential and represents the upper limit for the application's expected raw material demand.

Table 3.12: Assumptions made to estimate raw material demand

YAG host crystal	
Active material	1 atomic % Nd
YAG dimensions	Diameter 3 mm, length 10 mm
YAG density	4.55 g/cm^3
No. of lasers per LiDAR	128
No. of LiDAR per vehicle	1
Vehicle production in 2040	52.2 to 78.8 million vehicles per year

The comparison of the expected raw material volume potential for laser scanners with global production shows that no critical demand segment is emerging in this application. This assessment also applies to the other vehicle sensors.

Based on the estimated number of vehicles (passenger cars and commercial vehicles) for 2040, the demand for control units is 105–160 million CPUs and 210–320 million GPUs.

Table 3.13: Percentage by weight of raw materials in Nd:YAG solid-state laser

Element	Atomic weight g/Mol	No. of atoms	Molecular weight g/Mol	Percentage by weight wt%
Yttrium	88.9	2.97	264.0	44.35
Neodymium	144.2	0.03	4.3	0.72
Aluminium	27.0	5	135.0	22.68
Oxygen	16.0	12	192.0	32.25
Nd:YAG		20	595.3	100.00

Table 3.14: Global production (BGR 2021) and calculated raw material demand for laser scanners for autonomous driving of road vehicles, in tonnes

Raw material	Production in 2018	Demand in 2018	Demand foresight for 2040		
			SSP1 Sustainability	SSP2 Middle of the Road	SSP5 Fossil Path
Neodymium	23,900 (R)	~0	14.7	16.2	22.2
Yttrium	7,600 (R)	~0	928	1,050	1,401
Aluminium	63,756,000 (R)	~0	480	540	720

R: Refinery production (tonnes of metal content)

3.1.4.5 Recycling, resource efficiency and substitution

The laser scanner is one of the central sensor components for making the piloted driving of road vehicles possible. By quickly scanning the vehicle's surroundings around 360° with numerous laser beams (laser scanners with up to 128 lasers are now available on the market), a reliable and high-resolution image of the surroundings can be generated in combination with other sensors. Laser radiation is monochromatic and can therefore be focused very effectively. This means that, even at greater distances, the scanning beam is narrow and able to resolve fine structures. To date, the laser scanner has been an elementary component in almost all automated vehicle concepts developed, as the performance of low-cost ultrasonic and radar sensors has not been able to be increased to such an extent that they can generate the required high-precision image of the vehicle environment on their own. The only alternative would be pattern recognition methods that evaluate the image from optical stereo cameras. Tesla is the only manufacturer to rely heavily on camera technology, but has also added laser scanners to its systems following a number of accidents.

It is possible to create the LiDAR of laser scanners with different semiconductor and solid-state laser systems. Ford's research vehicles use laser scanners from the Velodyne Laser Incorporation, which presumably use InGaAs semiconductor lasers to generate the 903 nm laser radiation. But even with the common Nd:YAG solid-state laser, wavelengths close to the InGaAs laser radiation can be created with 946 nm and 1,064 nm.

For the disposal of used cars, the End-of-Life Vehicles Ordinance sets demanding recycling targets. Since 1 January 2015, 95 % of the empty weight must be reused or recycled for materials or energy. Energy recovery is limited in that at least 85 % must be reused or recycled (End-of-Life Vehicles Ordinance 2016). The legal requirements are being circumvented to a considerable extent by exporting very old used vehicles, including, it is assumed, scrap cars, to developing countries and Eastern Europe (EUWID 2015). Sensors, actuators and processors cannot be reused at the end of a car's life because technological change

does not allow this after more than a decade. For this complex electronic waste, the options for material recovery are also unsatisfactory for technical and economic reasons. It is to be expected that a not inconsiderable proportion of these components will be recycled for energy (circuit boards, insulation, plastic housings) or disposed of.

A central accompanying effect of piloted driving is accident avoidance. Initial field studies with automated vehicles at European level (e.g. the EU projects euroFOT, AdaptiVe or L3Pilot) have confirmed on the basis of millions of test kilometres that 90 to 100 % of accidents can be avoided by automated systems in motor vehicles. The avoided scrapping and reconditioning of accident vehicles improves raw material efficiency. Assistance systems help to avoid traffic jams, make better use of parking space (depaving) and support disabled and elderly people with limited sensory abilities. They improve energy efficiency and reduce CO_2 and pollutant emissions by steering the vehicle drive around the best operating point (see Krail et al. 2019).

Moreover, automated driving can usher in a revolutionary surge of innovation that will reach its culmination with driverless cars on the road. It will be associated with considerable social implications, characteristic of an emerging technology. Taxis will become driverless robot taxis that are requested by smartphone and given the destination by voice command. Car sharing or car pooling services are becoming increasingly flexible and enable convenient door-to-door journeys without waiting times. The requested vehicle drives up to the house at the specified time without a driver and is ready to board. At the end of the journey, it automatically heads for the next job. The user hardly notices any difference compared to owning a car and switches to car-sharing without any loss of comfort.The existing vehicle fleet is utilised more efficiently, while new production and the amount of raw materials required decrease. Such effects on the demand for raw materials cannot be assessed with the necessary certainty even today, as numerous other aspects that drive or slow down this development are not yet clear. These are, on the one hand, the technical framework conditions especially in urban traffic, the legal framework conditions as well as the question of acceptance and aspects such as the desire for privacy.

3.1.5 Aircraft for 3D mobility (eVTOL)

3.1.5.1 Technology description

The terminology for aircraft for 3D mobility is very inconsistent. 3D mobility is used for passenger transport, sometimes including freight transport. Often unmanned aerial vehicles (UAV) are called “drones”, but manned aerial vehicles are called “air taxis/flying cars” or “passenger drones”. By referring to urban areas, the term “urban air mobility” excludes the respective applications of the same technology in rural areas. In this technology synopsis, the term 3D mobility is used and covers both manned and unmanned areas of application.

3D mobility is achieved with small and light aircraft that can take off and land vertically or over short distances. In contrast to large aircraft with jet engines, these small aircraft require only small infrastructure units for take-off and landing. Vertical take-off and landing aircraft (VTOL) can take the form of multicopters, dual-phase, tilt-wing and modular car quadrocopters, while short take-off and landing (STOL) can be achieved with gyrocopter and roadable aircraft. Possible propulsion types are electric (battery and fuel cell), hybrid propulsion, distributed propulsion, helicopter propulsion and turbo-electric (Duwe et al. 2019). 3D aircraft are controlled by pilots, semi-automatically or autonomously (Xu 2020). For simplification, the text below refers to electric VTOL aircraft (eVTOL aircraft), including short and vertical take-off and landing.

In recent years, the power density of batteries has been increasing and with it their widespread use in various applications, including eVTOL aircraft. The electric propulsion of eVTOL aircraft causes significantly lower noise emissions and no local pollutant emissions compared to conventional jet or helicopter engines. For this reason, deployment scenarios for eVTOL aircraft are also being developed for densely populated areas (cf. Figure 3.10). Central to achieving economically attractive flight speeds and ranges are lightweight construction concepts for both the airframe and the moving parts such as rotors or extendable wings.

Figure 3.9: Unmanned 3D aircraft for application of plant protection agents (source: https://commons.wikimedia.org/wiki/File:4X-UHJ_Agridrones_d.jpg; licence: CC BY-SA 4.0)

In passenger transport, there are several potential uses for eVTOL aircraft. Core areas are passenger mobility, for example, in individual aircraft for commuting and private transport, security and rescue (including air ambulances), and commercial travel purposes and services (including urban air taxi, inner-city air transport, flying airport shuttle or ferry alternative), compare Figure 3.10. Typically, aircraft for 3D mobility have space for two to four people.

Aircraft for 3D mobility are being developed in collaborations by major manufacturers and by over 80 start-ups with financially strong partners, including Kitty Hawk and Joby Aviation, and in Germany Volocopter and Lilium.

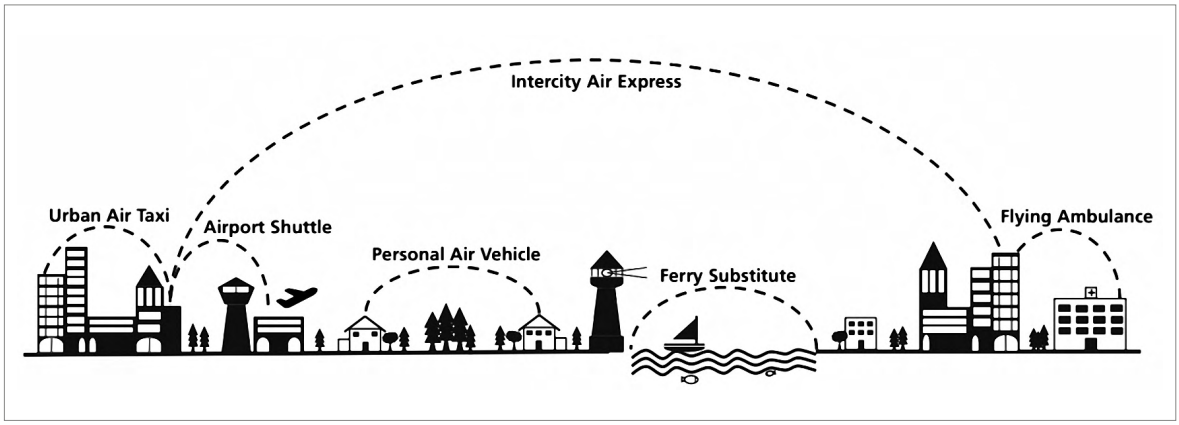

Figure 3.10: Selected application scenarios for manned 3D mobility – © Fraunhofer IAO (source: Duwe et al. 2019)

In terms of their main function, unmanned civil eVTOL aircraft can be divided into three types (DRONEII 2020):

- Transport of goods (e.g. for the delivery of parcels)
- Spraying (e.g. of pesticides or seedlings)
- Image recording (e.g. for inspection/maintenance, monitoring, mapping, observation, film/photography, localisation/detection)

The main motives for the use of unmanned eVTOL air vehicles are savings in time and costs as well as improvements in quality and occupational health and safety (DRONEII 2020). Unmanned eVTOL aircraft for civil use are divided into the weight classes 'Micro' and 'Nano' (lighter than 2 kg), 'Mini' (lighter than 20 kg) and 'Small' (heavier than 20 kg), based on their take-off weight. The sizes 'Medium' (150–600 kg) and 'Large' (over 600 kg) are predominantly or exclusively used for military purposes (BMVI 2020). Most models are developed or manufactured for unmanned aerial vehicles in the “Mini” size class.

The global civilian drone market (recreational and business) is currently dominated by DJI and its competitors Parrot and Yuneec, which however have been suffering from DJI's aggressive pricing strategy (Global Data 2019). Important developers and providers of unmanned aerial systems in Germany are Microdrones and HeightTech. Active companies in the freight transport sector include DHL, Deutsche Post AG, Zookal, Google, Amazon and FedEx.

3.1.5.2 Raw material content

Table 3.15 shows an overview of the raw materials used in unmanned eVTOL aircraft.

The raw material spectrum and its areas of application in eVTOL air vehicles are heterogeneous. eVTOL air vehicles are among the systemic innovations that combine several components already established or further developed on the market. In view of the large number of different system configurations and thus also raw materials in their

Table 3.15: Raw materials in unmanned eVTOL aircraft (source: European Commission 2020a, adapted)

Raw material	Areas of application
Be	Alloys, communication equipment and integrated wiring networks, electrooptical systems and undercarriage
Cu	Super alloys and CuBe alloys, communication systems
Ga	GaAs and GaN for communication, identification and electrooptical systems
Ge	On-board electronics, inertial navigation systems and identification systems for combat
In	Components for electrooptical systems
Al	Lightweight high-performance alloys for airframe, drive housing and avionics
Hf	NiHf super alloys for high-strength, high-temperature applications
Fe	Special steels for structural and mechanical parts
Mg	High-performance AlMg alloys
Ni	Ni and NiTi alloys (ductile and corrosion-resistant) for turbine and mechanical parts
Nb	Ferroniobium for high-strength structural parts
Sc	AlSc alloys for lightweight, high-strength parts and moulded parts
Ti	Ti alloys for lightweight and high-strength reinforcements, e.g. in 3D printing, airframe, wings, fans and compressors
Nd, Pr, Dy (SEE)	Electric motors with electronic speed control (rotors)
Li	Lithium-ion batteries
Co	Lithium-ion batteries

components, a selection of components and purposes must be made for an assessment of the raw material content. Essential main components are the airframe and the wings/rotors, the electric motor, the battery, the avionics and – if the mission purpose is to record images – the camera.

For competitive reasons, only a few quantitative technical specifications are given for eVTOL aircraft. There are currently over 40 development projects for the wingless multi-rotor concept, over 20 for the aeroplane-like lift & cruise concept and over 50 for the tilt-wing/rotor concept (Heckmann 2020). Lilium's electric jet (5-seater), with its 36 swivelling electric motors (2,000 HP), is expected to eventually fly at up to 300 km/h and have a range of 300 km. The weight is around one and a half tonnes, the wingspan is 11 metres. The Volocopter (2-seater) has 18 rotors (Münder 2017). For the prototype of a smaller model (2-seater), an empty weight of 440 kg (maximum take-off mass 640 kg), a range of 300 km and a top speed of 300 km/h are stated, with the 36 electric motors together producing 320 kW (Mattke 2020).

The electric drive with battery limits the payload and range due to their high weight, which is why eVTOL aircraft are manufactured using lightweight construction. Carbon fibre-reinforced polymers in particular are used for this purpose due to their low specific weight and strength (Xu 2020). Although projections for composites (airframes, wings and rotors) point to strong growth, the unmanned aircraft segment will remain a small share of the composites market for aviation as a whole.

In the field of airborne passenger transport, safety aspects play an even greater role than in the field of unmanned aerial vehicles (including crash tests, collision with birds, loading conditions, flight envelope, shielding of rotors, information about abnormal operating conditions). The Volocopter and Lilium systems are therefore designed with a high degree of redundancy: they have several motors and numerous battery cells operating independently of each other to enable a safe landing if individual components fail (Jetzke 2018).

The order volume for unmanned aircraft propulsion systems is relatively small. For this reason, in the past, an existing electric drive was usually used and adapted. The new development of drive concepts is subject to strict secrecy (Hegmann 2019), which is why no information on the use of copper and NdFeB is available for this.

The mass deployment of eVTOL aircraft could possibly trigger significant demand impetus for lithium batteries. The battery contributes about one third of the empty weight (Xu 2020). The development goal is to increase the energy density from 220 Wh/kg in the finished package to more than 500 Wh/kg in 2025. A 420 kg battery would then be able to provide at least 210 kilowatt hours of electricity on board of a Lilium jet (Hegmann 2019).

The components for eVTOL's avionics are not very specific for 3D aircraft. 3D aircraft can operate via GNSS/GPS positioning (+/–0.5 to 1.5 m) or line-of-sight positioning (+/–0.1 to 0.3 m) in the environment. The “Paketcopter” micro drone uses magnetometers for navigation, which measure the earth's magnetic field in its spatial extent. Other magnetometer technologies include fluxgate magnetometers, superconducting quantum interference devices, proton magnetometers, helium-3 and helium-4 magnetometers and alkali magnetometers (K, Cs, Rb) (Hovde et al. 2013). GNSS/GPS and magnetometers are also combined into units. In sensor technology, including barometers, gyrometers and accelerometers, there is a strong trend towards micro-electromechanical systems (MEMS), mostly silicon-based. In avionics, manufacturers are increasingly relying on automation and artificial intelligence, especially machine learning.

For the growth segment of remote sensing for the targeted cultivation of agricultural land (precision agriculture), IR and multi-spectral sensors are mainly used (Colomina & Molina 2014). Germanium has an important role to play in IR and optical sensors. Such germanium-containing camera lenses can also be used for other image recording purposes. Recreational drones are assumed to be equipped with a camera as standard (SESAR 2016).

3.1.5.3 Foresight industrial use

The main drivers of and barriers to 3D mobility include the availability of end-to-end solutions (“Drones as a Service”), the Internet of Things

(IoT) and legislation (Global Data 2019). In Germany, the Air Traffic Act and air traffic regulations, among others, regulate the use of manned and unmanned aviation systems. Accordingly, no permit is required for drones weighing up to 5 kg. Permission can be granted for the operation of unmanned aerial vehicles with a total mass of no more than 25 kg within sight of the controller if the flight altitude is no more than 100 metres above ground and the craft does not fly over crowds of people, residential properties, police operations sites, etc. (BMVI 2020).

In a survey of drone manufacturers and users, 54 % said the COVID-19 pandemic would tend to have positive effects on the drone industry in the long term, 17 % expected negative effects and 29 % had no opinion (DRONEII 2020).

For both unmanned and manned 3D aircraft, there are a number of market studies (by Frost&Sullivan, Roland Berger and Meticulous Research, Grandview Research, among others) looking at the development of unit numbers. Science-based studies for unmanned 3D aircraft are available for the USA (FAA 2020) and Europe (SESAR 2016). For manned 3D aircraft, two studies make important differentiations, one for the USA (NASA 2018) and one from a global perspective (Grandl et al. 2018).

It is currently not foreseeable which technologies and systems will become established for unmanned and manned 3D mobility in the long term. In 2018, rotary wings dominated the market for commercial drones in Germany; rigid wings and hybrid concepts accounted for the remainder, amounting to about one-eighth and less than one-sixteenth of the market, respectively (Grand View Research 2019).

Table 3.16: Projections of volume of eVTOL aircraft traffic in various studies

Context	Object of scenario and assumptions made	Year referred to	Projected traffic
Unmanned eVTOL in USA (FAA 2020)	Recreational drones: 1.32 million units in existence Commercial: 385,000 units in existence; strong growth	2019/ not determined	Recreational drones saturation: 1.5 million units
Unmanned eVTOL in EU (SESAR 2016)	Recreational: 1–1.5 million drones in existence Commercial and state: 10,000 drones in existence Strong growth; scenarios deviating from baseline: conservative and high acceptance	2035/2050	7 million recreational drones in existence; market saturation with 1 million sales per year achieved in 2025. 200,000 (2025), 395,000 (2035), 415,000 (2050) drones for commercial and state use in existence; conservative (230,000 and 265,000) and high acceptance (830,000 and 910,000)
Manned eVTOL globally (Grandl et al. 2018)	Market entry 2025 with 500 passenger drones in existence, diffusion in 2035 in Asia (45 %), Europe (35 %) and America (20 %) / theoretical potential with full expansion of infrastructure (including vertiports)	2035/ not determined	15,000 passenger drones in existence; theoretical potential: 200,000 passenger drones in existence; realistic potential: 40,000–75,000 passenger drones for megacities and major urban centres (upper value with enlarged vertiport infrastructure)
Manned eVTOL in US cities (NASA 2018)	Air metro (standardised air travel routes, autonomously piloted, with an average of three passengers)	2030	740 million passenger trips with 23,000 aircraft, 100–300 vertiports per city (3–6 VTOL in parallel)

For comparison (Grandl et al. 2018): In 2035, the global number of automobiles is expected to reach 1.7 billion and the number of aircraft with more than 100 seats or payload of more than 10 tonnes is expected to reach 42,000.

3.1.5.4 Foresight raw material demand

For the estimation of future raw material demands, three typical configurations of eVTOL aircraft have been defined which differ primarily in terms of their payload and thus also their weight.

The identification of the material composition was based on a life cycle assessment for a freight transport drone (Koiwanit 2018). According to this source, the copper content of the electric motors is 35 %, while the magnetic material content $Nd_2Fe_{14}B$ is 10 %. The weight percentage of neodymium in $Nd_2Fe_{14}B$ is 27 wt%, whereby neodymium can also be replaced by praseodymium up to a maximum of one quarter for price reasons (Marscheider-Weidemann et al. 2016). The quantity shares for electric motors were transferred to the other 3D aircraft.

The quantities of lithium polymer batteries were estimated for the eVTOL aircraft from various sets of data[1]. The lithium content in lithium-polymer batteries for lithium-ion high-performance storage for passenger cars is around 80–120 g Li/kWh; cf. Section 3.1.7. The batteries' energy storage quantity can be used to estimate the lithium requirement per eVTOL aircraft[2]. For the germanium content, GoPro cameras are assumed. These action cameras are also multi-spectral or equipped for night vision. For the IR/multi-spectral cameras, a value of 4.2 g of germanium per lens was identified from a life cycle assessment for lens manufacturing for night vision systems (Bhutto & Jalbani 2012).

For 3D aircraft used for inspection flights or recreational purposes, the estimated lifetime is 7 years (SESAR 2016), for transporting goods 11 years (AUVSI 2013) and for transporting people 15 years.

The following specific assumptions were made:

- eVTOL aircraft for commercial and government purposes are distributed in the 2040 inventory as follows: 25 % for cargo and 75 % for image capture, based on the quantity structure of SESAR (2016).
- 25 % of the eVTOL aircraft in agriculture will be used for pesticide and seed delivery (cargo) and 75 % for image capture in 2040.
- Of the eVTOL aircraft for image capture in 2040, 100 % in agriculture, 50 % in industry/infrastructure, 25 % for government and 5 % for recreation have a multi-spectral/IR camera with a germanium lens.
- The global unit numbers of 3D aircraft in 2040 were projected using the future unit numbers for Europe (SESAR 2016) and Europe's share

Table 3.17: Assumptions relating to the weight distribution of components in eVTOL aircraft in kg

	eVTOL aircraft type		
	Imaging	**Freight (goods transport and spraying)**	**Passenger transport**
Payload	Camera	10 kg load	6 passengers
Weight without payload	1	10	1,000
Airframe and propeller	0.25	8	300
Motors	0.1	0.5	150
Battery	0.5	1	500
Avionics	0.1	0.25	25
Unspecified	0.05	0.25	25

[1] 350 g (LiPo) and 90 g for a camera drone (RIT camera), 297–468 g for a consumer drone (DJI 2020), 440 g for an 8.8 kg drone for spraying agricultural chemicals (FPV 2020), 680 g for a delivery drone (Koiwanit 2018) and about a 200 kg battery for a 530 kg passenger drone (Khavarian and Kockelman 2020).

[2] 1,000 kWh batteries are assumed for passenger transport (80–120 kg Li per aircraft), 100 Wh batteries for image capture (8–12 g Li per aircraft) and 1 kWh battery for freight transport (80–120 g Li per aircraft).

of global built-up area in 2040 (for government purposes and freight transport), global agricultural area in 2040 (for agricultural land) and GDP (for other commercial purposes) in the SSP scenarios. The projections of the stock of eVTOL aircraft for recreational purposes in 2040 are based on the classification of the population by low, middle and high-income countries (United Nations 2019)[3].

With regard to the metal requirements for the motors and batteries, different material efficiency progress has been assumed for the different SSPs (see Section 1.1), but not for the germanium requirements of the mature infra-red (IR) and multi-spectral cameras.

Taking these assumptions into account, the raw material demands for 2040 are calculated according to each scenario (see Table 3.19).

Table 3.18: Assumptions relating to the number and efficiency of eVTOL aircraft under the conditions of selected SSP scenarios

Factor	Unit	Scenario		
		SSP1 Sustainability	SSP2 Middle of the Road	SSP5 Fossil Path
eVTOL State purposes	units in the 2040 inventory	1,400,000	1,200,000	1,000,000
eVTOL Agriculture	units in the 2040 inventory	1,000,000	1,500,000	2,000,000
eVTOL Goods transport	units in the 2040 inventory	400,000	1,400,000	2,400,000
eVTOL Other commercial purposes	units in the 2040 inventory	666,667	666,667	666,667
eVTOL Recreational purposes	units in the 2040 inventory	7,312,586	12,604,181	20,312,069
eVTOL Passenger transport	units in the 2040 inventory	10,000	30,000	50,000
Material efficiency Motors and batteries	Change 2018–2040	50 %	35 %	20 %

Table 3.19: Global production (BGR 2021) and calculated raw material demand for 3D aircraft, in tonnes

Raw material	Production in 2018	Demand in 2018	Demand foresight for 2040		
			SSP1 Sustainability	SSP2 Middle of the Road	SSP5 Fossil Path
Copper	20,590,600 (M) 24,137,000 (R)	n/a	150	390	900
Neodymium	23,900 (R)	n/a	11	30	70
Lithium	95,170 (M)	n/a	210	660	1.630
Germanium	143.1 (R)	n/a	0.76	1.3	1.5

M: Mine production (tonnes of metal content)
R: Refinery production (tonnes of metal content)

[3] In SSP1, the figures for the degree of equipment are 0.25 %, 0.1 % and 0.01 %; in SSP2, 0.5 %, 0.15 % and 0.03 %; and in SSP5, 1 %, 0.2 % and 0.05 %.

Compared to electric cars, the future raw material demands in terms of lithium, copper and neodymium for eVTOL air vehicles are very low. This is in particular due to the relatively small number of units that go on sale each year. For germanium alone, the demand in the SSP5 scenario for 2040 is about 1 % of the refinery production in 2018 and for lithium about 2 % of the mine production. Also in the SSP5 scenario, the induced demand for raw materials would be easily met, all other things being equal.

The demand for germanium for the IR/multi-spectral lenses could experience a noticeable boost in demand in the future when 3D aircraft are used en masse for agricultural imaging, surveillance and recreational purposes. The rather conservatively calculated germanium demand should be easily covered if no other technologies disruptively influence the germanium market.

For other raw materials not investigated in Table 3.19 (cf. Marscheider-Weidemann et al. 2016), significant relative demand is only possible in the case of special metals with small production volumes. However, this presupposes a dedicated research interest in the special metals, for example for avionics, and a corresponding availability of data, which is not available in sufficient quantity today.

3.1.5.5 Recycling, resource efficiency, substitution

Currently, many technologies and components compete on the markets for manned 3D aerospace systems. The field of unmanned systems is more mature, but even here there are a multitude of possible material configurations. The influence of raw material prices or bottlenecks on the design of eVTOL air vehicles currently seems to be of secondary importance compared to the achievement of functionality.

No meaningful information is available on the recycling and resource efficiency of eVTOL aircraft. The loss of unmanned eVTOL aircraft through crashes is likely to be an important gap in the material cycle, while safety requirements for manned systems should minimise crashes. The low specific material quantities compared to aircraft and the use of composite materials make recycling difficult.

3.1.6 Super alloys

3.1.6.1 Technology description

Super alloys are materials with a complex composition for high-temperature applications. These are usually nickel, cobalt or iron-based alloys to which a large number of other alloying elements are added, in some cases also in higher concentrations. Important alloy components include in particular platinum, chromium, molybdenum, tungsten, rhenium, ruthenium, tantalum, niobium, aluminium, titanium, manganese, zirconium, carbon and boron. Super alloys are mostly resistant to scale and high temperatures. Unlike other alloys, super alloys are designed to have high strength, corrosion resistance, creep resistance and surface stability, even at high temperatures. This extends the application range of super alloys compared to steels, for example. They can be produced either using melting metallurgy or powder metallurgy.

The quality of a thermodynamic cycle, as it is technically achieved in combustion engines, turbines and jet engines, is determined by the Carnot efficiency:

$$(1)\ \eta_C = 1 - \frac{T_0}{T_E}$$

η_C: Carnot efficiency
T_0: Outlet temperature
T_E: Inlet temperature

The equation shows that the efficiency of the driven machine is better the lower the outlet temperature T_0 and the higher the inlet temperature T_E of the process. Since the outlet temperature cannot usually be lowered below the ambient temperature, the only way to improve efficiency is to increase the inlet temperature. Materials development is therefore striving to increase the materials' heat resistance. The carbon-based fuels used today – oil, gas, coal and biomass – release CO_2 when burned. Improving efficiency and thus reducing fuel consumption is therefore always a contribution to climate protection.

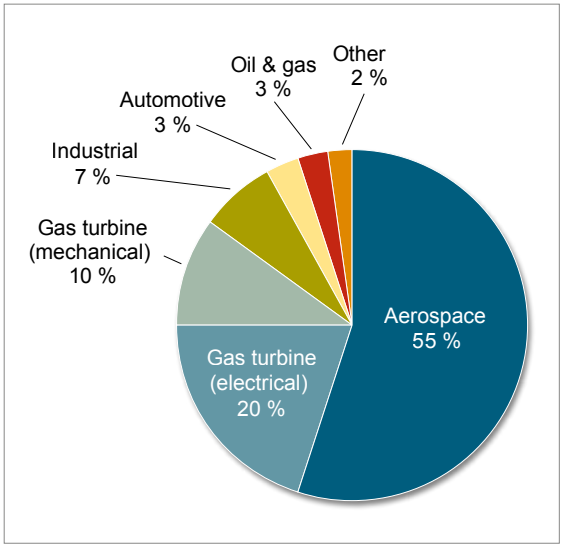

Figure 3.11: Super alloys by end use in 2012 (source: own representation based on Bedder & Baylis 2013)

The application limit of high-temperature steels is around 850 °C. With ferritic stainless steels, service temperatures of up to 1,350 °C can be achieved, however the strength at these temperatures is low. These steels are thus heat-resistant (corrosion-inhibiting), but not creep-resistant (i.e. without good mechanical properties). For higher strength requirements, super alloys and composites of ceramics and metals (cermets) are used. The working temperatures of creep-resistant nickel-based super alloys in gas turbines today reach 1,230 °C.

To achieve an economically attractive service life of the components, creep-resistant materials have to meet further requirements in addition to high strength. These include resistance to oxidation, corrosion, abrasion and a low tendency to creep. The term “super alloy” has become established for materials that meet these demanding requirements at high working temperatures.

High-temperature applications are of great economic importance in numerous sectors, processes and products. In aerospace engines, stationary gas and steam turbines, diesel and petrol engines for motor vehicles, boilers for heating buildings, in the iron and steel industry, non-ferrous metal production, metal processing and machining, the chemical and petrochemical industry, in the melting of glass products and in the burning of cement and lime, to name but a few. Figure 3.11 indicates the demand for super alloys according to the sectors described.

3.1.6.2 Raw material content

Nickel and cobalt-based alloys are described below as common super alloys. Titanium alloys and cermets are also listed as other high-temperature materials.

Nickel-based alloys

There are a large number of high-temperature super alloys. The most economically significant are the nickel-based alloys. They were originally developed for jet engines to improve their performance (thrust) and fuel consumption. The rotor blades and guide vanes of the gas turbine on these engines reach peak temperatures of over 1,000 °C. Today, they are made of nickel-based super alloys, as are the turbine rotor in the combustion chambers and the exhaust unit with the jet pipe.

Figure 3.12 shows an older jet engine with the main components clearly visible. Today, turbofan engines are used with separate coaxial shafts for the compressor and turbine stages.

Super alloys have moved from aerospace into many other applications. Examples include exhaust valves in internal combustion engines, components of automotive exhaust catalytic converters, high-temperature springs, forging tools, drilling tools in oil and gas production and heat exchangers. Brand names for nickel-based super alloys are Inconel®, Incoloy®, Hastelloy®, Nimomic®, Waspaloy®, Cronifer® and Nicrofer®. The composition of nickel-based alloys is shown in Table 3.20 as an average of common alloys.

The high chromium content provides corrosion and scale resistance (oxidation), but has a negative effect on the material's creep resistance (Strassburg 2019). Molybdenum, tungsten and cobalt are added to increase strength. Titanium and aluminium hinder the creep of the material through the formation of intermetallic phases. Small amounts of cerium, hafnium, zirconium and yttrium are also used as cor-

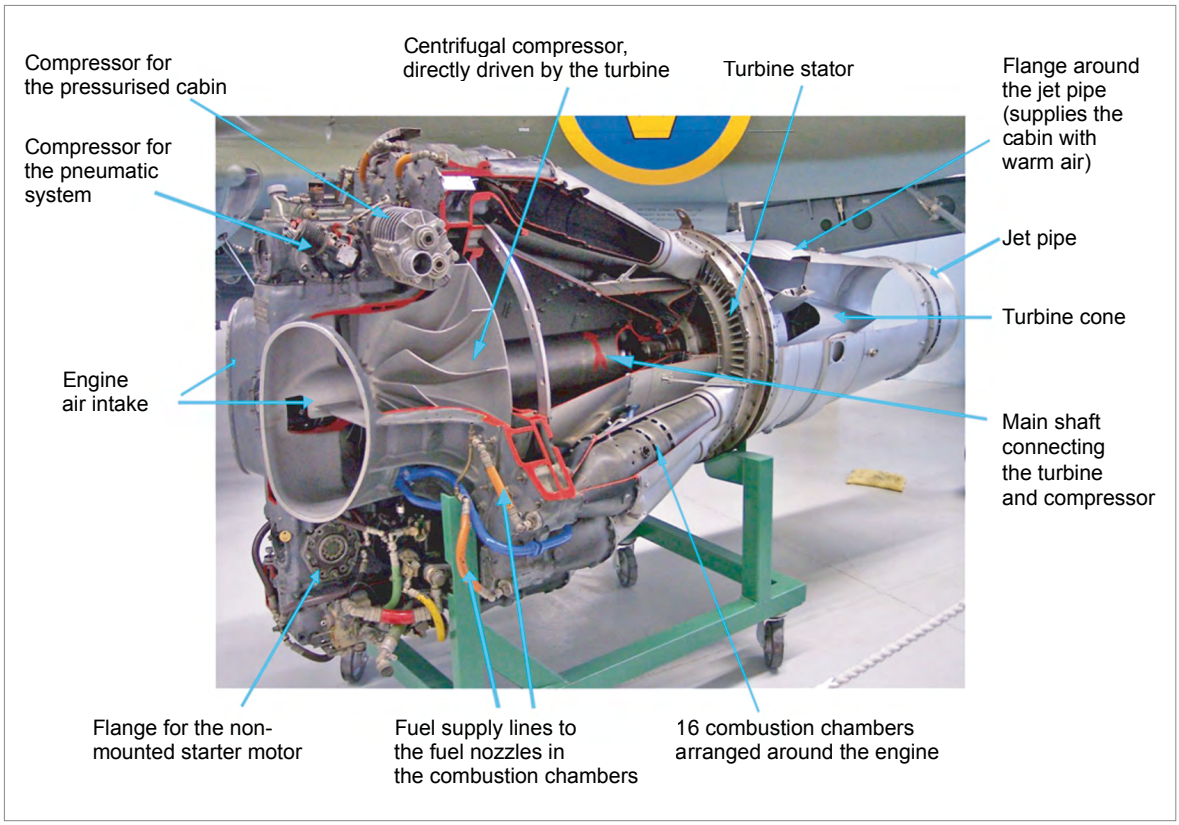

Figure 3.12: Jet engine (source: Ian Dunster, Wikimedia, CC BY-SA 3.0)

rosion inhibitors (Dubbel 1983). Rhenium, a metal with the second highest melting point after tungsten, is added in proportions of 3–6 % as an alloy component for certain highly stressed components, e.g. in jet engines (Konter 2012).

Table 3.20: Average composition of nickel-based super alloys (source: European Commission 2020a; European Commission 2020b)

Alloying element	Percentage by weight [wt%]
Nickel	57
Chromium	17
Cobalt	10
Iron	1.4
Molybdenum	3
Aluminium	1.7
Titanium	1.6
Niobium	1.3
Carbon	0.07

Bedder & Baylis (2013) assume that 75 % of the rhenium is consumed in nickel-based alloys, which is why continuous efforts are being made to save rhenium.

Cobalt-based alloys

Another group of super alloys are the cobalt-based alloys. They are characterised by high abrasion resistance, and their resistance to abrasion and corrosion is not lost even at higher temperatures. However, the creep strength is lower than that of the nickel-based alloys. The creep strength is the tensile stress that causes a material to break at a certain temperature (e.g. 600 °C) over a certain period of stress (e.g. 10,000 hours). The creep strength determines a component's permissible operating life.

One of the main alloying components of cobalt-based alloys is chromium. Depending on the application, molybdenum, tungsten, nickel and other metals are added. They are used for components that are exposed to high abrasion loads,

Table 3.21: Average composition of cobalt-based super alloys (source: Donaldson & Beyersmann 2012)

Alloying element	Percentage by weight [wt%]
Cobalt	55
Chromium	21.5
Molybdenum	0.4
Tungsten	8.4
Iron	2.6
Nickel	8.3
Tantalum	1.7
Niobium	0.4
Titanium	0.5
Boron	< 0.4
Zirconium	0.1
Carbon	< 0.85

such as cutting tools, chain saw rails, gun barrel linings and sliding couples of artificial joints. Table 3.21 shows the average composition of common cobalt-based alloys.

Titanium alloys

The use of titanium alloys began around 1950, 50 years after the first experiments with nickel and cobalt-based alloys. Originally confined to the aerospace industry, titanium's unrivalled strength-to-weight ratio has seen it make its way into countless applications. Today, high-temperature, corrosion-resistant titanium alloys are available for working temperatures up to 600 °C (Sibum et al. 2017). They thus almost reach the application limit of high-temperature steels. Table 3.22 shows the composition of the titanium alloy IMI 829 for high-temperature technologies. Other alloying elements used in specific applications are copper, manganese, vanadium and others.

Table 3.22: Composition of a heat-resistant titanium alloy (source: Meetham 2012)

Alloying element	Percentage by weight [wt%]
Titanium	86.45
Aluminium	5.50
Tin	3.50
Zirconium	3.00
Niobium	1.00
Silicon	0.30
Molybdenum	0.25

Cermets

Cermets are another material for creep-resistant and abrasion-resistant materials. These are metal-ceramic composites in which ceramic substances or carbides are embedded in a metal phase, for example tungsten carbide in cobalt, titanium carbide in nickel, aluminium oxide (Al_2O_3) in chromium or thorium oxide (ThO_2) in tungsten. The use of metal as a binder eliminates the brittleness that is typical of pure ceramics. Cermets are used as hard metals in cutting tools for metal and stone, for high-temperature applications such as thermocouple protection tubes, as cathodes in electron beam tubes and as a gliding ball in ball-point pens, to name a few. They are produced by powder metallurgy.

3.1.6.3 Foresight industrial use

The use of nickel-chromium alloys dates back to the beginning of the 20th century. Their use has increased steadily since then, and more recently they have received new impetus from efforts to contribute to climate protection with energy efficiency and lightweight construction and to offset the sharply rising costs of fuel. Applications of super alloys have been discussed in the previous sections. They are extremely diverse and are difficult to quantify in terms of the volume of their current and future use. The world trade statistics of the United Nations (UN COMTRADE) also do not provide any usable information for estimating the global demand for super alloys.

Super alloys combine several advantageous properties that have already been pointed out. Their application sometimes leads to enormous improvements in product development. According to G. W. Meetham, of Rolls-Royce plc, UK, the use of a high-temperature titanium alloy in a jet engine,

for example, reduced fuel consumption by 13 % and weight by 18 % and increased thrust by 42 % compared to steel (MEETHAM 2012). For diesel engines, the same source considers an increase in efficiency from 38 to 65 % possible through the use of high-temperature ceramics (MEETHAM 2012).

The material development of super alloys is by no means complete, as can be seen from the fact that the number of patents on super alloys increased steadily by 24 % between 2015 and 2019 (FROST & SULLIVAN 2020b). The focus of past research has shifted towards nickel-based alloys over the last five years, with a significant increase in interest, while the number of research papers on cobalt and iron-based alloys has declined (FROST & SULLIVAN 2020b). In addition to the further development of new alloys, the machining of super alloy components is also being investigated in greater depth, as this often proves difficult due to their high heat resistance and strength. The particular focus here is on methods for mechanical processing (THELLAPUTTA et al. 2017) and for welding super alloys (SASHANK et al. 2020).

The proliferation of super alloys is creating demand for nickel, chromium, cobalt and titanium in particular. Figure 3.13 shows that the composition of super alloys evolves significantly over time. One obstacle to the growth of super alloys is the increasingly complex material composition. To the increasing requirements in terms of mechanical properties and corrosion resistance, the proportions of expensive elements such as rhenium or ruthenium are increasing, pushing up the costs of super alloys (FROST & SULLIVAN 2020b).

3.1.6.4 Foresight raw material demand

Global demand for 2018 is reported by NETL (2019) to be 287 kilotonnes of nickel-based super alloys. According to BEDDER & BAYLIS (2013), 95 %

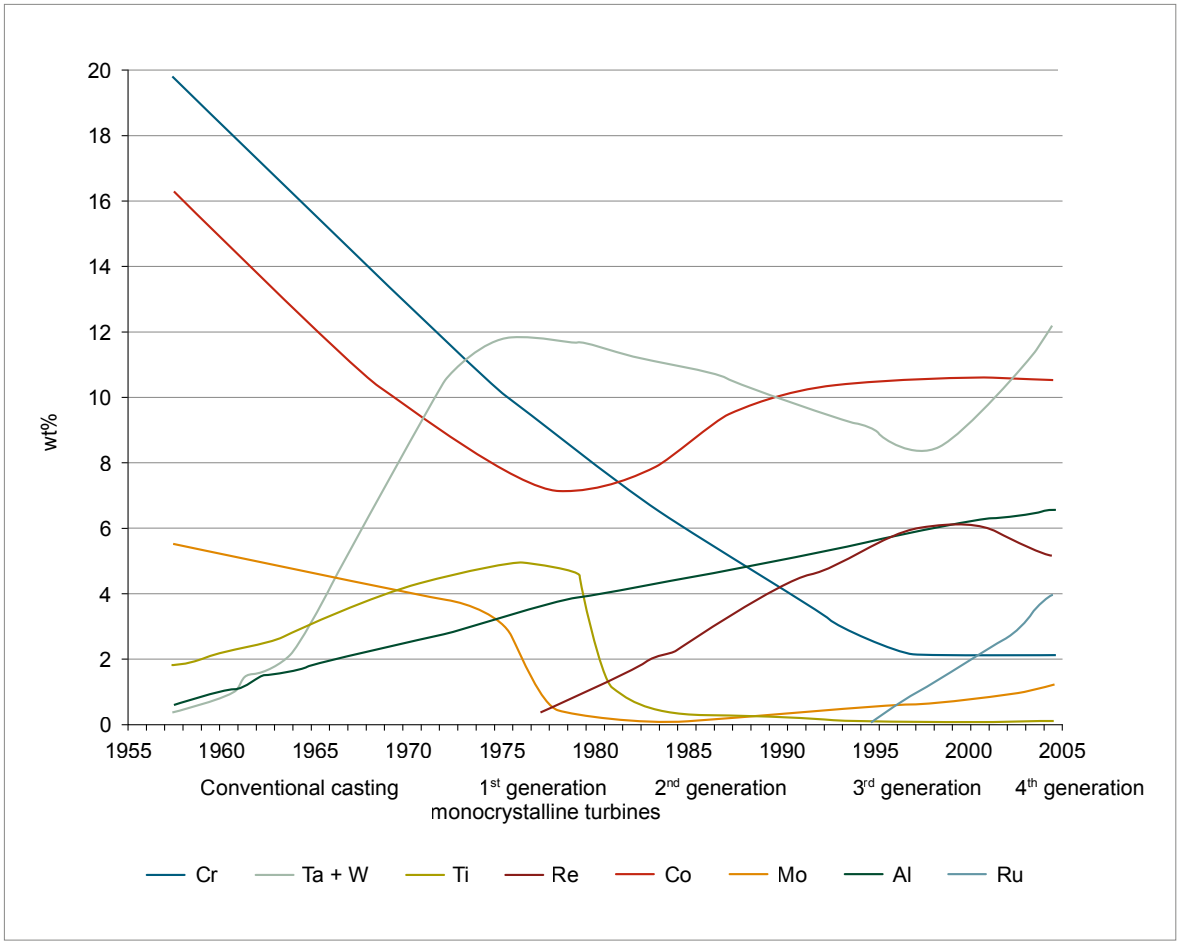

Figure 3.13: Material development in jet engine construction (source: adapted from CLIFTON 2013)

of the super alloys used are also nickel-based alloys. Within the raw material demand scenario formed, it is assumed that the remaining 5 % are cobalt-based alloys, as iron-based alloys are rather rare among the super alloys. This results in a demand of 15 kilotonnes of cobalt-based alloys in 2018.

Based on the average compositions of the nickel- and cobalt-based super alloys, which are shown in Table 3.20 and Table 3.21, the demand for the respective alloying elements can be calculated for 2018. This is shown in Table 3.23 and is compared to the metal production of the same year.

To estimate the growth of the super alloy market, a distinction is made between the areas of application for super alloys as given in Figure 3.11. The use of super alloys for aerospace is assumed to be constant to the number of aircraft produced as described in Section 3.1.3. Use in the other areas of application is considered to grow constantly with GDP based on to individual scenarios.

The raw material composition of the super alloys is assumed to be constant over the period considered, but may change in reality due to new alloy constituents and compositions. With the assumed growth, the estimated demand for 2040 is just under 520 to 720 kilotonnes of super alloys. This results in the raw material demand forecast shown in Table 3.23. The demand for raw materials proves to be particularly critical in scenario SSP5, as the largest growth in aircraft construction is assumed within this scenario. For cobalt, for example, the SSP5 scenario results in a critical demand for 2040 of about 70 % of the annual production of 2018. In contrast, however, there is a trend towards more nickel-based alloys instead of cobalt-based alloys, which could not be taken into account any further within the scenario. However, cobalt is also used for nickel-based alloys with a mass fraction of up to 20 % (Strasbourg 2019). In the SSP5 scenario, high demands for nickel and tantalum also have to be considered, which correspond to 18 % and 33 % of the current production, respectively. There will also be smaller impacts on the market for niobium (13 % of 2018 production) and molybdenum (8 %

Table 3.23: Global production (BGR 2021) and calculated raw material demand for super alloys, in tonnes

Raw material	Production in 2018	Demand in 2018	Demand foresight for 2040		
			SSP1 Sustainability	SSP2 Middle of the Road	SSP5 Fossil Path
Nickel	2,189,313 (R)	164,000	301,000	283,000	392,000
Chromium	27,000,000 (M)	52,000	95,000	89,000	124,000
Cobalt	126,019 (R)	37,000	68,000	63,000	88,000
Niobium	68,200 (M)	4,000	6,900	6,500	9,000
Iron	1,520,000,000 (M)	4,000	8,100	7,600	10,500
Molybdenum	265,582 (M)	9,000	16,000	15,000	21,000
Aluminium	63,756,032 (R)	5,000	8,900	8,400	11,600
Titanium	260,548 (R)	5,000	8,500	8,000	11,100
Tungsten	77,080 (M)	1,300	2,300	2,200	3,000
Tantalum	1,832 (M)	260	470	440	610
Boron	N/A[1]	60	110	100	140
Zirconium	1,256,362[2] (M)	20	28	26	36

M: Mine production (tonnes of metal content)
R: Refinery production (tonnes of metal content)

[1] *No meaningful data available, as production data for individual countries is based on different boron products/boron content*
[2] *Production of zirconium minerals*

of 2018 production). The SSP1 and SSP2 scenarios each have lower raw material demands, with the SSP2 scenario being the lowest despite a higher volume of aircraft production due to the lower assumed economic growth.

In the assumptions described above, the composition of the super alloys is assumed to remain constant. In the future, however, up to 4 % rhenium and 5 % ruthenium could be added to nickel-based alloys (Frost & Sullivan 2020b). Table 3.24 shows that, in the SSP5 scenario, 58 % of current global rhenium production could be used for super alloys by 2040, so a significant impact on the rhenium market could be expected if this alloy became established. Even more critical is the ruthenium demand forecast, where the estimated demand for super alloys in the 2040 SSP5 scenario is 109 % of 2018 mine production. All three scenarios are expected to have a significant impact on the rhenium and ruthenium markets in particular.

3.1.6.5 Recycling, resource efficiency and substitution

Since super alloys, as shown above, are used in large turbines, among other things, and their composition is known partly, they can be efficiently collected for recycling. However, the complex composition and change of alloy components, which is shown in Figure 3.13, represent a major technical and consequently also economic challenge for the recycling of super alloys. Nevertheless, the high price of raw materials and the scarce availability of some alloy components of super alloys are drivers for recycling. In addition to remelting with primary material to produce new super alloys, there are also pyro- and hydrometallurgical processes available to recover the individual metals of the super alloy (Srivastava et al. 2014). Particularly scarce metals such as ruthenium and rhenium could be substituted in the future.

3.1.7 Lithium-ion high-performance electricity storage (for mobile applications)

3.1.7.1 Technology description

Electromobility has been a growing sector for years and also receives a lot of attention from the media. Due to current political debates such as the diesel driving ban and political goals to make Europe climate-neutral by 2050, a mobility turnaround is also necessary, which includes the promotion and expansion of electromobility (European Commission 2019). Unlike combustion engines, electric vehicles do not cause local greenhouse gas emissions such as CO_2 or other air pollutants such as nitrogen oxides when in use. While fossil fuels are generally still used to produce electricity today, emission-free use may be possible in future if “green energy sources” are used to generate electricity. When examining the life cycle of an electric vehicle compared to a diesel or petrol car, many studies conclude that electric vehicles already have a positive climate balance, which will improve further with an expansion of CO_2-neutral electricity generation (Agora Verkehrswende 2019a; Reuter et al. 2019). Some critical voices see it as more sensible, among other things, to use green power in the

Table 3.24: Global production (BGR 2021) and calculated raw material demand, in tonnes; on the assumption that ruthenium and rhenium become established in super alloys

Raw material	Production in 2018	Demand in 2018	Demand foresight for 2040		
			SSP1 Sustainability	SSP2 Middle of the Road	SSP5 Fossil Path
Ruthenium	33[1] (R)	15	28	26	36
Rhenium	50 (M)	12	22	21	29

M: Mine production (tonnes of metal content)
R: Refinery production (tonnes of metal content)

[1] *Source: JM 2020*

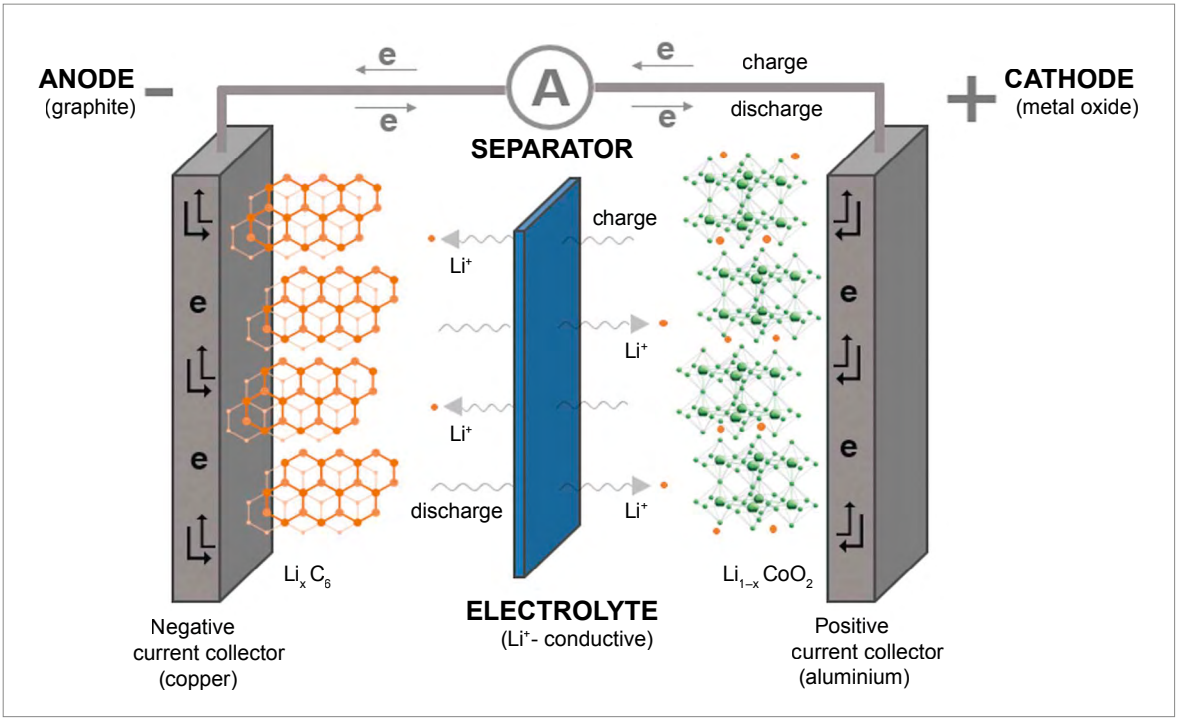

Figure 3.14: Schematic construction of a lithium-ion battery (source: own representation)

electricity grid in the medium term and thus substitute coal-fired power, for example. The promotion of electric cars with the current energy source mix in the electricity grid should therefore lead to approx. 75 % more GHG emissions for electric cars compared to diesel vehicles (Schmidt 2020). In scientific discourse, however, these calculations are contradicted (Wietschel 2020).

The four main components of a lithium-ion cell are the cathode, the anode, the electrolyte and the separator (Figure 3.14). During the discharging process, the cathode acts as the positive electrode and the anode as the negative electrode, which is reversed during the charging process (Korthauer 2013).

Depending on the application, amorphous carbon (hard and soft carbon), graphite, lithium titanate (LTO) or silicon composites are currently used as anode materials. Amorphous carbon as well as graphite occur naturally, but can also be produced synthetically (Korthauer 2013).

Transitional metal layer oxides are predominantly used as the positive electrode material at the cathode (Kurzweil & Dietlmeier 2018). Conventional cathode materials for mostly small electronic applications such as smartphones, laptops or tablets use lithium cobalt oxide (LCO). Due to the low thermal stability of cobalt oxide and its high material price, it is not used in electromobility (Zubi et al. 2018). The following electrode materials are used for this purpose:

- Lithium manganese oxide (LMO)
- Lithium nickel manganese cobalt oxide (NMC)
- Lithium nickel cobalt aluminium oxide (NCA)
- Lithium iron phosphate (LFP)

A battery pack required for electric vehicles consists of individual cells which in turn are made up of cell components that contain certain metals as chemical compounds (Figure 3.15).

In contrast to nickel-cadmium (NiCd) and nickel-metal hydride (NiMH) batteries with energy densities of up to 60 Wh/kg and 80 Wh/kg, today's 3.7 V lithium-ion batteries achieve specific energy densities of up to 270 Wh/kg (Table 3.25) (Kurzweil & Dietlmeier 2018). A high energy density is particularly important for mobile applications such as mobile phones, laptops or electric vehicles, since the greater the energy density, the lighter or smaller the battery becomes while the capacity remains the same (Rahimzei et al. 2015).

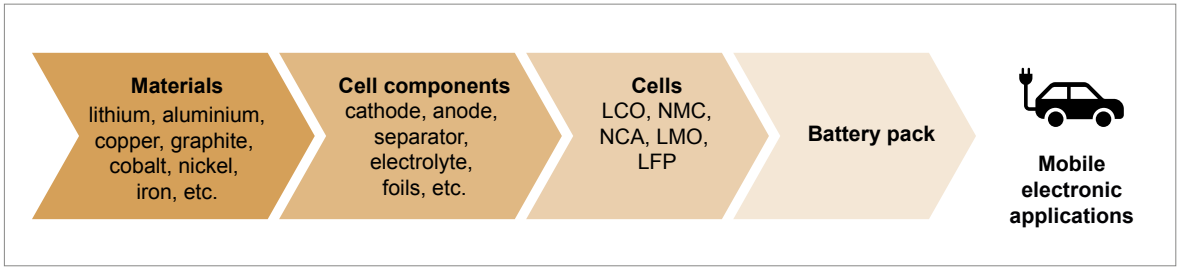

Figure 3.15: Construction of battery packs for electronic applications (source: Zubi et al. 2018)

Table 3.25: Characteristics of various cathode materials for lithium-ion batteries (source: Kurzweil & Dietlmeier 2018, Zubi et al. 2018, Reinhardt et al. 2019, Battery University 2020, Duan et al. 2020, Durmus et al. 2020)

Cathode	LCO	LMO	NMC	NCA	LFP
Empirical formula	$LiCoO_2$	$LiMn_2O_4$ (spinel)	$LiNi_xMn_yCo_{1-x-y}O_2$	$LiNiCoAlO_2$	$LiFePO_4$
Energy density at cell level [Wh/kg]	150 to 200	100 to 140	150 to 270	200 to 270	90 to 120
Thermal runaway [°C]	150	250	210	150	270
Cell voltage [V]	3.6 to 3.9	3.7 to 4.0	3.6 to 3.7	3.6 to 3.8	3.1 to 3.3
Practical capacity [Ah/kg]	145	120	150 to 180	190 to 200	160
Costs	high	low	medium	medium	low
Safety	low	medium	high	–	very high

In contrast to the classic lithium-ion battery, the lithium-sulphur and the lithium-air battery are seen as emerging technologies, which have a fundamentally different cell structure and can have a higher energy density (Korthauer 2013). Lithium-sulphur batteries can have energy densities of 300–350 Wh/kg, while lithium-air batteries could reach energy densities of 700–1,700 Wh/kg (Korthauer 2013; Kim et al. 2019). These battery types are not included in the forecast for 2040, as their introduction by then and their use in electromobility is unclear.

3.1.7.2 Raw material content

For NMC batteries, there are different compositions within their formula, related to the content of nickel, manganese and cobalt. In addition to the classic NMC 111 with equal proportions of nickel, manganese and cobalt, there are also NMC 433 (ratio 4:3:3), NMC 532 (ratio 5:3:2), NMC 622 (ratio 6:2:2), NMC 811 (ratio 8:1:1) (Thielmann et al. 2015). Research is being conducted into further cobalt savings, right through to cobalt-free batteries.

The high nickel content improves the capacity of the battery, increasing that of an NMC 811, for example, by almost 50 % compared to NMC 111 to around 200 mAh/g (Research Interfaces 2020). While this does not represent a major leap compared to the classic NMC cathodes of the current generation, it is nevertheless predicted that NMC, with a wide variety of compositions, will dominate 75 % of the battery market in 2030 (Zhao 2018).

Calculations of the cathode material and metal requirements per kWh were carried out below on the basis of typical formation losses as they occur today in graphite anodes. The results are displayed in Table 3.26.

Table 3.26: Quantities of specific metals in battery cathodes [kg/kWh]

Cathode material	Li	Co	Ni	Mn	Fe	P	Al	O
NMC 111	0.120	0.333	0.333	0.312	0	0	0	0.550
NMC 433	0.117	0.298	0.395	0.278	0	0	0	0.539
NMC 532	0.121	0.205	0.512	0.191	0	0	0	0.558
NMC 622	0.104	0.176	0.525	0.164	0	0	0	0.476
NMC 811	0.096	0.082	0.653	0.076	0	0	0	0.445
HE-NMC 2030	0.123	0	0.106	0.491	0	0	0	0.456
NCA15	0.098	0.125	0.661	0	0	0	0.019	0.451
NCA 5	0.095	0.065	0.725	0	0	0	0.011	0.439
LFP	0.084	0	0	0	0.674	0.374	0	0.772
LMO	0.080	0	0	1.266	0	0	0	0.738

3.1.7.3 Foresight industrial use

As things stand today, lithium-ion technology is best able, out of the storage technology systems available, to meet the high requirements of a large storage system in the electric vehicle sector in terms of service life, safety and power and energy density (Kampker et al. 2018).

The trend in cathode materials for LIBs is towards low-cobalt and high-nickel raw materials in order to reduce material costs and substitute potentially critical materials as much as possible. With a high nickel content, the electrical conductivity and the Li^+ diffusivity also increase, which increases material performance (Thielmann et al. 2018).

NMC 622 represents the state of the technological art in the automotive industry. NMC 811 is currently being commercialised due to its higher specific energy density (Ding et al. 2019). In addition to the increased energy density through the use of NMC 811, the battery costs are significantly reduced due to the reduction of cobalt in NMC 811 (10 wt%), which is currently more expensive than nickel, in contrast to NMC 111 (33.3 wt%) (Ding et al. 2019).

High-energy NMC (HE-NMC) are lithium-rich "integrated" composite materials that aim to increase energy density and also offer a price advantage over nickel-rich materials due to their high manganese content (Rozier & Tarascon 2015; Thielmann et al. 2017). The technology could enter the market in 2025, provided that the current difficulties are overcome (Thielmann et al. 2017).

LFP cathodes, which have been the focus of attention for many years, do not currently appear to be realistic competitors in the automotive sector in the medium term due to the low energy density of 90–120 Wh/kg that can be achieved at cell level, but they could experience a revival if ecological criteria become more important (Zubi et al. 2018; Wu et al. 2020). Today, the LFP battery plays a marginal role in electric vehicles, while it achieves better success in e-bikes as well as offering great potential for use in off-grid and grid-connected power systems (Zubi et al. 2018).

Among the four main chemistries for LIB, LMO shows moderate safety and relatively low specific energy (Ding et al. 2019). Although LMO cells were originally used in some electric vehicles, interest in this material has waned (Zubi et al. 2018). Based on these trends, an estimate was carried out of the shares of cathode materials by 2040 (Figure 3.16).

In contrast to the sole use of graphite as anode materials in LIBs, silicon-carbon composites are regarded as promising. Si-based admixtures are already being used in LIBs today. A continuous increase in the Si content can be expected. The maturity of Si-rich technologies and their implementation in production technology is expected by 2025 (Thielmann et al. 2017).

3.1.7.4 Foresight raw material demand

To calculate the future demand for raw materials, the average battery size is determined from extensive literature research into drive technologies and vehicle segments (Table 3.27) and an estimate carried out of the shares of cathode materials by 2040 (Figure 3.16).

The subsequent calculation of the raw material demand is carried out using the specific metal quantities of the battery cathodes, the proportions of the cathode materials and the total capacities of the scenarios calculated in Section 1.3 (Table 3.28).

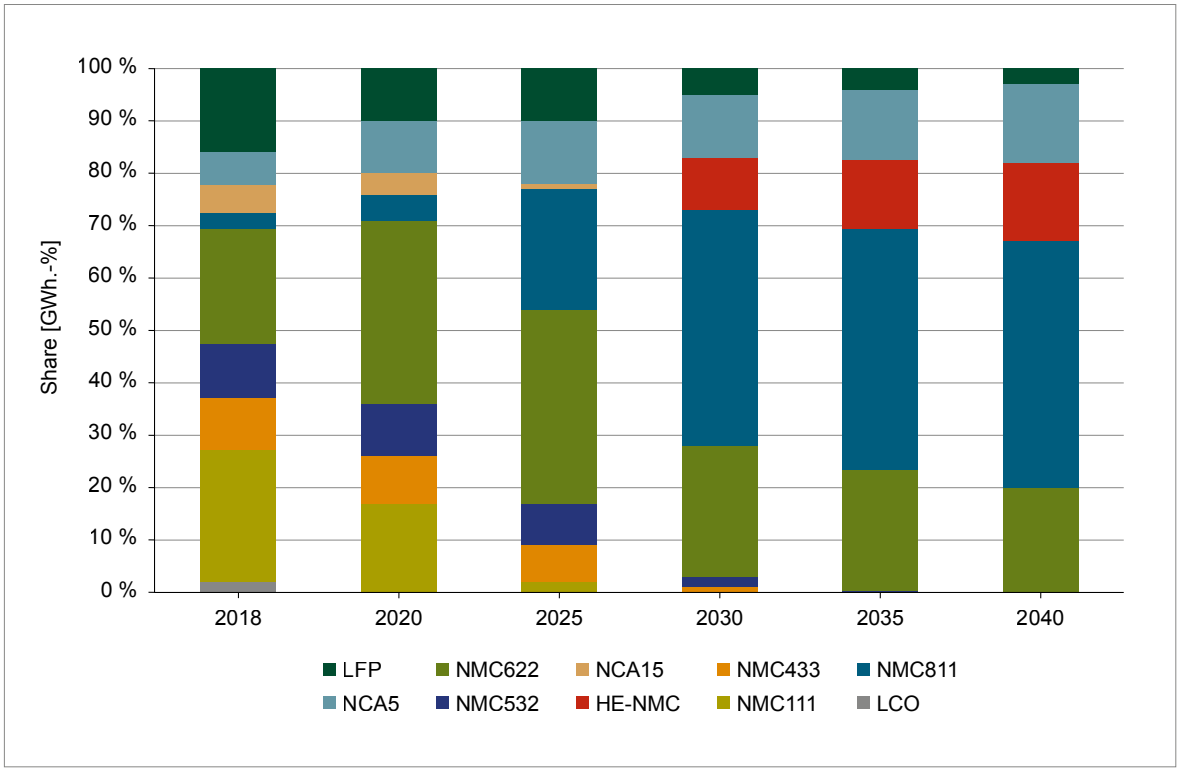

Figure 3.16: Estimated proportions of cathode materials to 2040 (source: own representation)

Table 3.27: Battery sizes by drive technology and size segment in kWh (rounded values)

Vehicle segment	HEV until 2020	HEV after 2020	PHEV until 2020	PHEV after 2020	BEV until 2020	BEV after 2020	FCEV until 2020	FCEV after 2020
	Average battery capacity [kWh]							
Small cars	–	1	24		25	30	1*	1.6*
Compact cars	1	1	11	12	35	51	1*	1.6*
Premium cars	–	2	12	14	83	83	1	1.6
Light utility vehicles	–	–	14		29	50	1*	1.6
Heavy duty vehicles	–	–	41		307		10*	
Buses	–	–	–	–	193		10*	

** estimated*

Table 3.28: Global production (BGR 2021) and calculated raw material demand for lithium-ion high-performance batteries, in tonnes

Raw material	Production in 2018	Demand in 2018	Demand foresight for 2040		
			SSP1 Sustainability	SSP2 Middle of the Road	SSP5 Fossil Path
Cobalt	151,059 (M) 126,019 (R)	12,750	311,000	270,400	59,830
Nickel	2,327,499 (M) 2,189,313 (R)	32,320	2,003,000	1,742,000	385,400
Manganese	20,300,000 (M)	11,140	530,500	461,300	102,000
Lithium	95,170 (M)	7,460	377,300	328,100	72,600
Flake graphite (natural)	1,156,300 (M)	21,900	1,019,000	886,400	196,000
Graphite (synthetic)	1,573,000				

M: Mine production (tonnes of metal content)
R: Refinery production (tonnes of metal content)

3.1.7.5 Recycling, resource efficiency and substitution

Most existing recycling plants for lithium-ion batteries focus mainly on the recovery of cobalt, nickel and copper, but not lithium. The reasons for this are, firstly, that recycling plants have to focus on recovering older LIBs (mainly LCO), which are now reaching the end of their life, and secondly, that cobalt is by far the most valuable metal in lithium-ion batteries and thus responsible for the profitability in recycling (Or et al. 2020). Table 3.29 lists a number of recycling plants without any claim to completeness. Some recyclers recover “black mass” as an intermediate product containing electrode-active materials and conducting salts and which is further processed by other companies.In the near future, NMC 111 will be increasingly replaced by NMC 622 and NMC 811. The optimised cells will contain lower amounts of cobalt and a higher nickel content. Recycling plants should therefore be able to handle all cathode chemistries with high efficiency in the future, if possible, in order to fully exploit the recycling potential. At present, the technical feasibility of lithium recovery is still difficult. Given the background of the long-term forecast requirements for LIBs, recovery should also be striven for here. Ideally, recycling plants should also use processes that have lower energy use and environmental impact. The proposal for a regulation on batteries and waste batteries, repealing Directive 2006/66/EC and amending Regulation (EU) 2019/1020, published in December 2020, also provides for recycling efficiencies for lithium-ion batteries and material recovery rates for their contained raw materials cobalt, nickel, lithium and copper (European Commission 2020c).

Graphite is and will remain an essential component of lithium-ion batteries and will also be used in the future as a combination with high-performance compounds such as silicon or silicon-metal alloys (Asenbauer et al. 2020). Although the recycling of graphite from spent lithium-ion batteries plays an important role in terms of environmental protection and future graphite resource shortages, it has not yet attracted much attention because recycled graphite is not suitable for reuse in batteries (Gao et al. 2020; Liu et al. 2020b). The Australian company EcoGraf Limited has developed a promising purification process that aims to recover high-purity anode material for batteries from used lithium-ion battery materials (EcoGraf 2020).

Table 3.29: Recycling plants for LIB worldwide (sources: Mayyas et al. 2019, Velázquez-Martínez et al. 2019, Or et al. 2020, Sojka et al. 2020)

Recycling plant	Input stream	Recovered materials	Lithium recovery
Umicore Battery Recycling (BE)	LIB, NiMH	Co, Ni, Cu, Fe, $CoCl_2$	No
Inmetco (US)	LIB, NiMH, NiCd	Co, Ni, Fe	No
Nickelhütte Aue (Germany)	LIB, NiMH	Ni, Cu, Co	No
Accurec Recycling GmbH (Germany)	LIB, NiMH, NiCd	Copper alloy Black mass	Li_2CO_3
Sumitomo-Sony (Japan)	LIB	CoO	No
Recupyl S.A.	LIB, primary Li	$LiCO_2$	Li_2CO_3, Li_3PO_4
Retriev Technologies (Toxco)	LIB, primary Li	MeO	Li_2CO_3
Akkuser (Finland)	LIB	Co, Cu powder, Fe	No
Battery Resources	LIB	$NMC(OH)_2$	Li_2CO_3
LithoRec (Duesenfeld) (Germany)	LIB	Metal oxides	Li_2CO_3
OnTo (USA)	LIB	Cell cathode powder	Li_2CO_3
Aalto University (Finland)	LIB	CoC_2O_4, Al	Li-Ni solution
Sung Eel (Korea)	LIB	Co, Mn, Ni	Li_2CO_3
Kyoei Seiko (Japan)	LIB	Ni, Co, Cu	No
Dowa (Japan)	LIB	Ni, Co, Cu	unknown
Brunp (China)	LIB	$NMC(OH)_2$	unknown
GEM (China)	LIB	Co, Ni	No
Huayou Cobalt (China)	LIB	Co, Ni	No
Ganzhou Highpower (China)	LIB	Co and Ni salts	Li_2CO_3

3.1.8 All-solid-state batteries

3.1.8.1 Technology description

All-solid-state batteries (ASSB) are electrochemical systems in which the ionic and electronic charge transport and storage is carried out exclusively by solids. Compared to conventional lithium-ion batteries (Section 3.1.7), ASSB differ in particular in the electrolytes used in the cell concepts (Thielmann et al. 2017; Thielmann et al. 2019).

Many of the safety hazards in conventional LIBs stem from the use of liquid, highly flammable or explosive electrolytes. The compatibility of many active materials in the electrochemical system is also determined by the properties of the electrolytes. The organic solvents and salts commonly used, for example, limit the cell voltage that can be achieved in practice. Many of the ageing effects in LIBs are the result of the interaction between the electrolyte and the particle surface of the active materials.

Using solid electrolytes and thus enabling solid batteries can both improve the safety properties of the cells and enable new material combinations and thus improve the batteries' performance parameters. In particular, the use of metallic lithium as an anode in Li-based ASSB promises enormous increases in energy density up to values of over 1,000 Wh/l or over 350 Wh/kg (Thielmann et al. 2017; Green Car Congress 2019; Ruffo 2019). Solid electrolytes could enable metallic anodes, as their hard structure could suppress the dendritic growth of lithium during cycling, which can otherwise lead to short-circuiting and create huge safety problems.

Table 3.30: Selection of ceramic solid-state electrolytes of phosphate, oxide and sulphide types studied in research

Material	LATP	LAGP	LLZO	LLTO	LGPS	LSPS1	LSPS2	LPS
Empirical formula	$Li_{1,4}Al_{0,4}Ti_{1,6}(PO_4)_3$	$Li_{1,5}Al_{0,5}Ge_{1,5}(PO_4)_3$	$Li_7La_3Zr_2O_{12}$	$Li_{0,34}La_{0,51}TiO_{2,94}$	$Li_{10}Ge_{0,5}Sn_{0,5}P2S_{12}$	$Li_{3,4}Si_{0,4}P_{0,6}S_4$	$Li_{9,54}Si_{1,74}P_{1,44}S_{11,7}Cl_{0,3}$	$Li_{9,6}P_3S_{12}$
Type	NASICON	NASICON	Garnet	Perovs-kite	LISICON	LISICON	Tetragonal	Tetra-gonal
Density (g/cm³)	2.93	3.42	5.02	4.82	2.03	1.93	1.90	1.91
Ionic conduc-tivity at room temperature (mS/cm)	2	4	3	0.9	9	6.7	25	1.2

Different classes of solid electrolytes are currently still being investigated in research and industry. These include glasses, inorganic ceramics (SCE solid ceramic electrolytes) and also polymer-metal salt complexes (SPE solid polymer electrolytes) (Takada 2013). Some of the known oxide ceramics show high voltage stability and thus allow the use of high-voltage cathodes. A general weakness of oxide ceramic solid-state batteries results from the frequently low ionic conductivity and the high interface resistances between cell components. Such batteries often have to be operated at increased temperatures. Sulphidic solid electrolytes sometimes exhibit significantly higher conductivities, which facilitates their use at room temperature. However, the materials often do not have good chemical stability, which places special demands on their processing and protective coatings. In addition to oxides and sulphides, phosphates, for example, are being investigated for their suitability as solid electrolytes.

Table 3.30 lists examples of various ceramic solid electrolytes and their properties. Among the systems investigated, those that have a high ionic conductivity (sulphides, e.g. LSPS, lithium tin phosphorus sulphide) or can be produced from inexpensive raw materials (e.g. LATP, lithium aluminium titanium phosphate) are particularly interesting. In particular, compounds containing germanium, for example, are therefore ruled out for commercial application from a cost perspective.

Polymers can be made ion-conductive by complexing them with Li salts. In the process, the salts are dissolved in the polymer chains. Ion transport occurs via the mobility of the polymer chains. The best-known representative of this class is polyethylene oxide (PEO) in combination with lithium bis(trifluoromethanesulfonyl)imide (LiTFSI) salt. SPE usually have a low ionic conductivity at room temperature, which prevents their practical use. Examples from literature, for example, describe the complex formation of PEO and a $LiNO_3$ or LiTFSI salt with a concentration of ethylene oxide groups to Li of 20:1 to 10:1 and ionic conductivity of 0.1 to 1 mS/cm. Polymer electrolytes promise high compatibility with established manufacturing processes in battery cell production, as roll-to-roll processes could be applied.

The conductivity of polymer electrolytes can be significantly increased by combining them with ceramic or metallo-organic nanoparticles to form composite electrolytes (CPE composite polymer electrolytes). SPE/CPE polymer electrolytes are distinct from so-called gel polymers, as they are already used in LIBs today. These are electrolyte formulations which are very similar to conventional liquid electrolytes. By using CPE with ion-conducting ceramic filling materials, the transition from polymer electrolytes to ceramic electrolytes becomes fluid. In use, a combination of polymer matrix, which supports processability, and ceramic fillers, which increase the conductivity and prevent the growth of Li dendrites, could prevail. However, from today's perspective, it is still unclear which of the materials and combinations mentioned can ultimately lead to the commercial use of solid-state batteries.

Various options are also conceivable for the cell design. In principle, all common formats are possible, at least for polymer electrolyte cells, since the

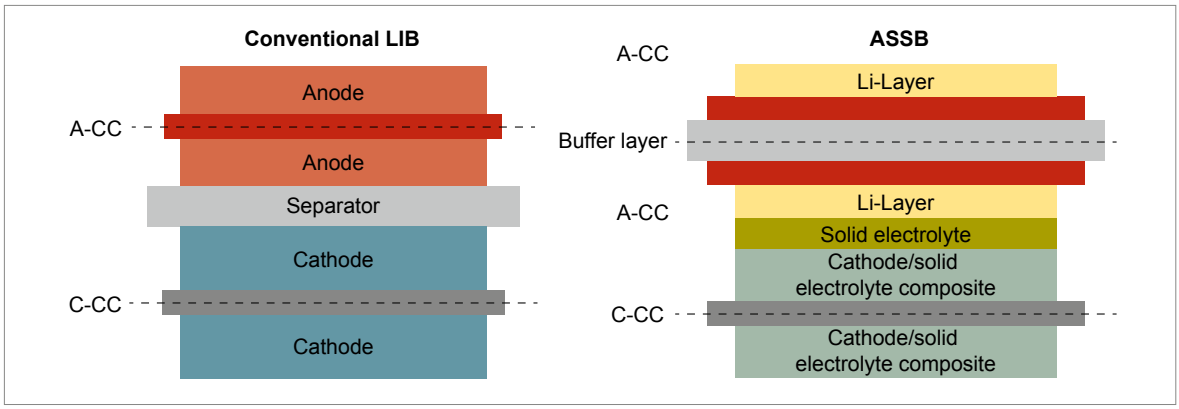

Figure 3.17: Schematic representation of the structure of conventional LIB (left) and solid state battery cells (right) (source: Thielmann et al. 2019)

Notes: In a conventional LIB, the liquid electrolyte permeates the porous system comprising anode, separator and cathode. In an ASSB the cathode consists of an active material/solid electrolyte composite. The metallic Li layer could be of dense construction. The change of volume in the Li layer during cyclization may require a buffer layer.

electrolyte can be wound. Purely ceramic electrolyte layers could require stacking of the electrodes. As shown in Figure 3.17, the volume change of the anode during cycling could require a buffer layer. In this case, double-sided use of the current collector foils, as used in liquid electrolyte LIBs, is not possible, at least for one of the electrodes.

3.1.8.2 Raw material demand

The raw material demand for the metals lithium, titanium, lanthanum, copper, manganese, cobalt and nickel (aluminium was not considered) for ASSB results from the use in the active materials, the solid electrolyte and the current collectors of the battery cells. The raw material demand for the battery module or at pack level was not considered. Compared to conventional, liquid electrolyte-based LIBs, there are changes in the raw material demands for the anode, the electrolyte and, if necessary, also the cathode.

In ASSB, similar cathode materials are to be used as is the case with liquid electrolyte LIBs. Although the chemical reactivity of some of the solid electrolytes investigated with respect to many current cathode materials still precludes these material combinations, it can be assumed that suitable protective coatings can be developed (Culver et al. 2019). This should allow materials such as NMC and high-voltage spinel (LMNO) in particular to be used in future ASSB.

The raw material demand per Wh by the cathode active materials is thus basically the same as the demand for conventional LIBs described in Section 3.1.7. In the future, however, this may no longer apply. The dimensioning of the cathode and anode in LIBs must be designed not only for suitable reversible surface capacities but also for irreversible chemical reactions. If silicon-containing high-capacity anodes are used in the future, irreversible chemical reactions at the anode could dominate during cell formation. The underlying processes consume Li, which would have to be introduced into the cell by an excess of cathode material (Aravindan et al. 2017).

In solid-state batteries with a metallic Li anode, on the other hand, the amount of cyclable Li in the cell could be controlled not only by the cathode but also by the thickness of the initial Li metal layer. As a result, better utilisation of the cathode capacity could be possible, especially over the later course of the battery lifetime, which translates into lower demand for cathode material per Wh.

At present, there is no final concept for the design of metallic Li anodes. It is possible that, in the future, initially Li-free anodes (Lee et al. 2020) will be installed in ASSBs, which in turn means that all the lithium required for the electrochemical reactions must be introduced through the cathode. However, initial thin Li layers (e.g. a few µm) on the anode current collector foils are also conceivable. Compared to conventional liquid electro-

Table 3.31: Comparison of SCE, SPE and liquid electrolyte battery cells and parameters for the calculation of raw material demand

Comparison of the lithium requirements of different electrolyte systems			
System	**SCE**	**SPE**	**Liquid**
Material combination	As a mix of 25 % LLZO, 25 % LATP and 50 % LSPS	PEO:LiTFSI	EC/DMC/DEC:LiPF6
Concentration of Li in the electrolyte	See molecular formulas As a mix, 8.3 wt%	15:1(EO:Li) corresponding to 0.73 wt%	1M corresponding to 0.55 wt%
Concentration of Ti, La in the electrolyte	See molecular formulas. As a mix, 5 wt% (Ti) or 12.5 wt% (La)	–	–
Assumptions: Electrolyte	SCE layer 5 µm, 25 % porosity	SPE layer 10 µm	Electrolyte requirement 2 g/Ah at cell level
Assumptions: Cathode	SCE 20 % by volume in cathode composite	SPE 20 % by volume in cathode composite	
	6 mAh/cm^2 area loading		
Assumptions: Anode	Metallic Li, 5 µm		–
Assumptions: Anode current collector	Cu, 5 µm, coated on one side		Cu, 6 µm, coated on both sides
Raw material demand Li g/kWh	15 (anode) 27.2 (electrolyte)	15 (anode) 1.3 (electrolyte)	3.1 (electrolyte)
Raw material demand Ti g/kWh	16.3 (electrolyte)	–	–
Raw material demand Cu g/kWh	210 (current collector)		126 (current collector)
Raw material demand La g/kWh	40.9 (electrolyte)	–	–

Note: For SCE, the raw material demand was calculated as a material mix with equal proportions of LLZO, LATP and LSPS.

lyte LIBs with graphite anodes, this variant has a higher raw material demand for lithium for the anode. In the calculations in Table 3.31, a thin initial lithium layer was assumed.

The biggest changes in terms of raw material demand result from the change of electrolyte. The concentration (e.g. 1 mol/l) of Li salts in liquid electrolytes corresponds to a small weight share of lithium. Compared to the proportion of lithium in the cathode materials, the raw material demand for lithium through the electrolyte is therefore almost negligible.

The situation is similar with solid polymer electrolytes (SPE), whose salt concentration in the electrolyte is of a similar order of magnitude. However, by using a more or less smooth Li metal anode in SPE, the amount of electrolyte needed to fill the pores of the (graphite) anode can be saved compared to liquid electrolyte LIBs.

Solid ceramic electrolytes (SCE) with one or more Li atoms per formula unit, on the other hand, have a significantly higher Li concentration. Especially in the case of sulphide electrolytes, lithium accounts for more than 10 wt%. Depending on the specific compound, other raw materials considered in this study may be required by the use of solid ceramic electrolytes, e.g. lanthanum in LATP.

Overall, this results in a comparable raw material demand for liquid electrolyte LIBs and pure SPE LIBs. Ceramic SCE or hybrid forms of SPE and SCE can have a significantly higher Li demand.

3.1.8.3 Foresight industrial use

Solid-state batteries are currently still a topic of research and development. Large-scale industrial use and production in particular pose some challenges, starting with the selection of material systems and ending with the development of a manufacturing process for the battery cells that is suitable for mass production. Compared to conventional LIBs, significant adjustments have to be made to the production processes in terms of material production, electrode production and stacking as well as formation. Nevertheless, solid-state batteries are now an integral part of the technology roadmaps of major international cell and automotive manufacturers.

In the USA in particular, several start-ups such as Ionic Materials (Ionic Materials 2020), Pathion (PATHION 2020) or TeraWatt (TeraWatt Technology 2020) are involved in the development and production of solid electrolytes and solid battery cells. Likewise, companies already fully established in the LIB value chain, such as Toray or Asashi Kasei, are involved in the development of solid-state batteries. Among car manufacturers, Toyota in particular communicates its commercialisation goals and development progress to the public. For example, small-scale production of battery cells is planned for 2025 (Steffen 2020). Their use in Toyota vehicles could possibly take place in a few years' time.

The first commercial uses of solid-state cells for electric vehicles could therefore be between 2025 and 2030. If the development goals in terms of energy density and safety can be implemented, solid-state batteries will likely be able to gain significant market share in the automotive sector. The speed of market penetration will also depend on the investments required in production infrastructure, so that even when the technology reaches a high level of technical maturity, a sudden switch from conventional to solid-state batteries cannot be expected.

The differentiation of the three SSP future scenarios allows the modelling of possible ranges of market penetration for ASSB. In sustainability scenario SSP1, significant research work in the area of battery storage and electromobility can be assumed, so that the market maturity of ASSB could be reached very early. By 2040, a market share of 25 % solid batteries is assumed on the electromobility market. In the SSP5 growth scenario, the commercialisation of solid-state batteries could be delayed or limited to niche segments due to a lack of incentives. By 2040, a market share of 5 % was assumed for ASSB. In the moderate scenario SSP2, a market share of 10 % for ASSB was assumed accordingly. According to the mobility scenarios and vehicle battery sizes discussed in Section 1.3, the resulting market sizes are shown in Table 3.32.

As discussed, the material combinations and solid electrolytes suitable for commercial use are still under development today. To map different trends with regard to the fast-charging capability, costs and processability of the materials, a mix of 75 % ceramic materials and 25 % polymer electrolytes (here PEO:LiTFSI) was assumed for the use of solid electrolytes in 2040. Among the ceramic materials, a mix of 50 % of a sulphidic material (LSPS), 25 % of an oxidic material (LLZO) and 25 % of a phosphate (LATP) was assumed. The purpose of putting a stronger emphasis on sulphidic material is to take into account the currently promising results on this class of material from research. The assumed mix is intended to represent the uncertainties for subsequent industrial use and is not to be understood as a combination of materials within a single battery cell.

Table 3.32: Market volumes for solid state batteries in electromobility in 2040 for different SSP scenarios

	SSP1 Sustainability	SSP2 Middle of the Road	SSP5 Fossil Path
Market volume ASSB 2040	1,244 GWh (25 % of total market volume)	360 GWh (10 % of total market volume)	38 GWh (5 % of total market volume)

Note: The remaining market shares (95 % in SSP5 to 75 % in SSP1) are covered by conventional LIBs (see 3.1.7).

Table 3.33: Global production (BGR 2021) and calculated raw material demand for solid-state battery cells in electromobility applications, in tonnes

Raw material	Production in 2018	Demand in 2018	Demand foresight for 2040		
			SSP1 Sustainability	SSP2 Middle of the Road	SSP5 Fossil Path
Lithium	95,170 (M)	–	177,000	47,000	5,000
Titanium	260,548 (R)	–	15,000	4,400	500
Manganese	20,300,000 (M)	–	187,000	49,000	5,100
Cobalt	151,059 (M) 126,019 (R)	–	109,000	28,000	3,000
Nickel	2,327,499 (M) 2,189,313 (R)	–	702,000	183,000	19,000
Copper	20,590,600 (M) 24,137,000 (R)	–	261,000	76,000	8,000
Lanthanum	35,800 (R)	–	38,000	11,000	1,200

M: Mine production (tonnes of metal content)
R: Refinery production (tonnes of metal content)

3.1.8.4 Foresight raw material demand

For the calculation of the future raw material demand, the same cathode materials were assumed as for conventional LIBs (see Section 3.1.7). The raw material demands for battery cells for the assumed material mix of solid electrolytes are shown in Table 3.33.

3.1.8.5 Recycling, resource efficiency and substitution

Similar to the recycling of conventional LIBs, processes can be used for solid-state batteries that allow the recovery of the transition metals or even the lithium. Possible processes concentrate on the cathode and the solid electrolyte, as there is practically no metallic lithium on the anode when the cells are discharged.

Basically, there are different requirements for the recycling process of ASSB due to the absence of organic solvents. When mechanically crushing vehicle batteries, the flammability of organic liquid electrolytes poses a safety risk that does not exist for solid electrolytes. In today's established processes, the liquid electrolyte is first evaporated by heating and thus the electrochemical system is also inactivated. Reuse of the electrolyte is therefore not possible. This step could be omitted for solid-state cells. The metallic components of solid electrolytes, like those of the cathode, are accessible through pyro- or hydrometallurgical recycling processes. The higher proportion of lithium per kWh, especially of the ceramic solid-state cells, could increase the incentives to also recover this metal in the process. For all-solid-state batteries, however, there is also the fundamental possibility of recovering the electrolyte materials directly, processing them and using them to produce new battery cells (Tan et al. 2020b). So far, however, there are no studies that investigate the practical separability of cathode and electrolyte materials (Tan et al. 2020a).

From an industry perspective, it is unlikely that separate recycling processes will be set up for conventional LIB and solid-state batteries, as this would require further pre-sorting of batteries and delay the achievement of economic efficiency due to large batch sizes. With a significant return of used solid-state cells, e.g. from 2040, recycling processes may need to be adapted for appropriate compatibility.

As already demonstrated, many different solid electrolytes are currently being investigated and optimised with regard to their technical suitability for use in batteries. Ceramic electrolytes in particular differ greatly in their content of different

metals and thus also in the specific material costs. Similar to the development of cathode materials in the last ten years, material developments are therefore also likely in the long term which aim to reduce the costs per kWh of solid-state batteries.

3.2 Cluster: Digitisation and Industry 4.0

3.2.1 Indium tin oxide (ITO) in display technology

3.2.1.1 Technology description

The world nowadays is characterised by mobile information transfer and processing, which is very much dependent on the visualisation of multimedia data and user input. In this day and age, challenges are predominantly being overcome by high-resolution, electronic thin-film transistor (TFT) displays that are increasingly touchscreen-based, because they simply have the largest information transfer density. Various display technologies have thus become an absolutely indispensable part of modern society and are being used as more than just everyday communication and information portals; applications also include security, healthcare, entertainment, industry and commerce (Chen et al. 2016).

Cathode ray tubes (CRTs) have dominated the market for over a century since they were first invented. It was only the development of flat-panel displays (FPDs; also known as flat screens) – starting with segmented liquid crystal displays (LCDs) for mass production – that heralded the gradual decline of this first display technology. The years that followed saw passive-matrix LCDs with an initially poor resolution further developed until LCD technology finally achieved its breakthrough in the late 1990s with the mass production of active-matrix LCDs based on thin-film transistor (TFT) technology (Chen et al. 2016). Liquid crystal displays (LCDs) have dominated the display market since manufacturers stopped making plasma screens in 2013 and 2014 (Katzmeyer 2014). Organic light-emitting diode (OLED) technology, which was first demonstrated in 1987 and has since become the mainstream in entertainment technology, is another competitor to LCD technology. OLED technology's advantages include the likes of its self-illuminating capabilities, transparency, improved colour display and high resolution, not to mention the possibility of a flexible or a bendable design. But these benefits command higher prices (Salehi et al. 2019). So the display market is currently dominated by these two technologies, with the scales significantly tipped in LCDs' favour. We are in a transition period at present, where the deciding factors with regard to market dominance are LCDs' innovation potential and OLED technology's price potential (Blankenbach 2016). Both this aspect and unpredictable technology innovations make forecasting a highly complicated business, especially up to the year 2040.

Transparent conducting oxides (TCOs) that are doped ZnO or SnO_2 in most cases are used as transparent electrodes. ZnO is doped with aluminium, for example, and SnO_2 with indium (indium tin oxide, or ITO for short) or fluorine. A British consortium has developed a procedure for printing antimony-doped tin oxide (ATO) as a transparent electrode on glass as another, more affordable alternative to ITO. ATO is 90 % tin and 10 % antimony, which is more affordable and more readily available than indium (Bush 2006).

ITO is used to produce the electrode layers in LCDs, OLEDs, PDPs and FEDs. The structural principles of LCDs and OLEDs are described below.

Liquid crystal displays (LCDs)

LCDs are made in lots of process steps to structure and apply the various functional layers. The ITO layer is applied to the front and back glass plates as an electrode (Figure 3.18). Then, a polymer layer is applied to a glass substrate. This layer is structured so that it helps with the LC molecules' alignment later on. The two glass plates are aligned, joined together to form a panel and cured in the hot press furnace. The next step is to add liquid crystals and apply the polarising foils (Fraunhofer Institute for Reliability and Microintegration (IZM) 2007, Steinfeldt et al. 2004).

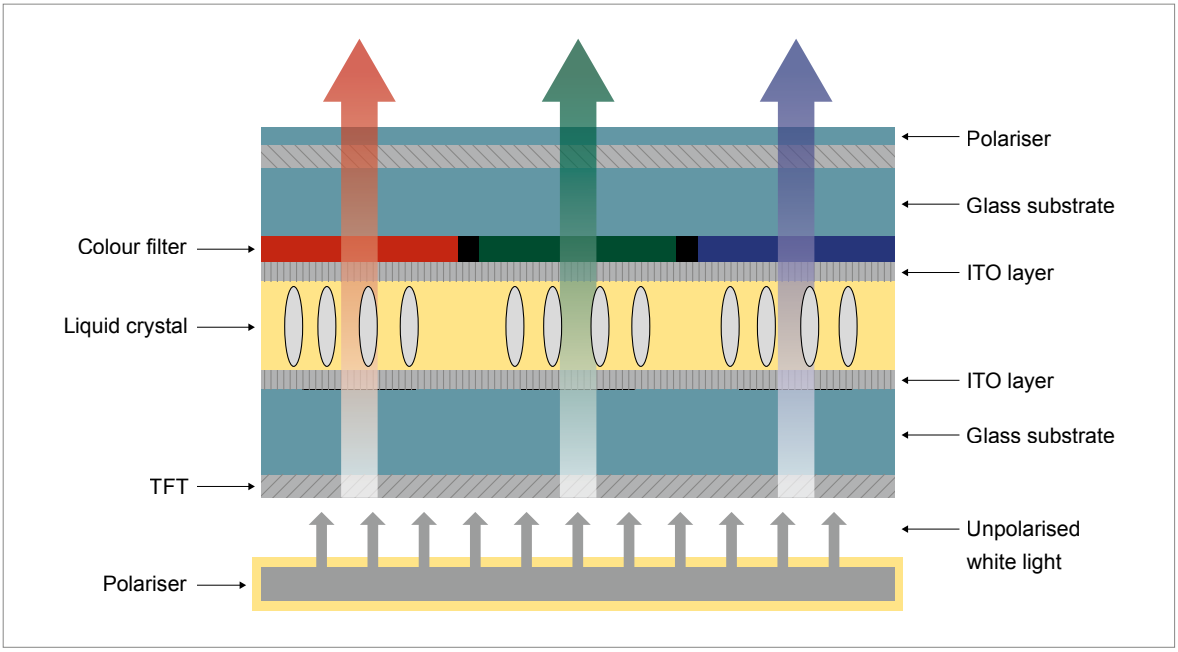

Figure 3.18: Schematic construction of an LCD (source: Fraunhofer IZM 2007)

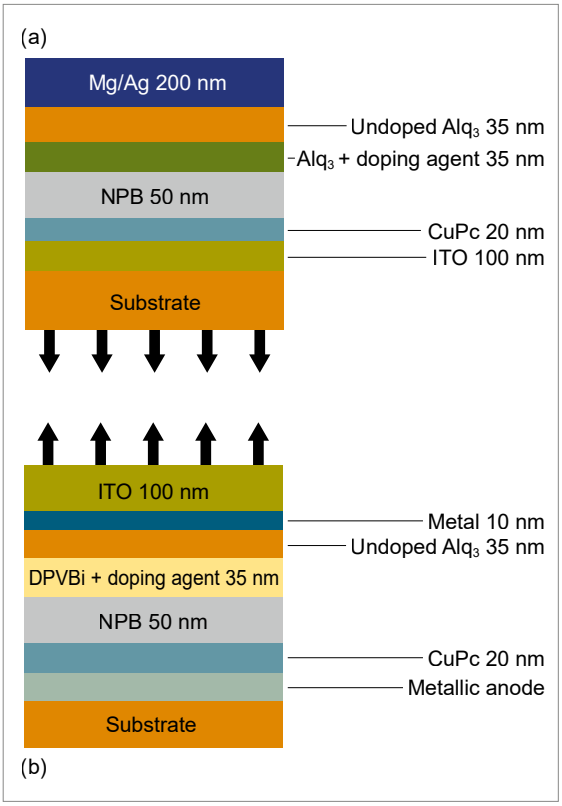

Figure 3.19: Schematic construction of an OLED, a) down-emitting stack, b) up-emitting stack (source: own representation based on Steinfeldt et al. 2004)

Organic light-emitting diode displays (OLED displays)

During the OLED display manufacturing process, the transparent ITO layer is applied to a glass substrate for each stack (see Figure 3.19). The next steps involve applying all the other organic and metallic layers (including silver) by evaporation. Afterwards, the front panel is attached, and the whole thing is encapsulated so that it is airtight (Fraunhofer IZM 2007, Steinfeldt et al. 2004).

3.2.1.2 Raw material content

A study conducted by the German Federal Environment Agency found that there are variations of indium area density – both between individual device types and their panel sizes (Wolf et al. 2017). In the case of LCDs, which use two ITO layers to display images, analyses conducted as part of the German Federal Environment Agency's e-Recmet project revealed an area density of 613–931 mg/m² for various sizes of PC monitors, laptops and flat-screen TVs (Böni et al. 2015). These values are in line with the ones provided in the previous report. A blanket average of 700 mg/m² is the assumption incorporated for LCD panels in the following calculations. This is based on an

analysis conducted by Rasenack & Goldmann (2014), also for various devices.

The assumed area density for OLED displays was 350 mg/m², since the data sample was only small. This basis of this assumption was OLED panels' structure. As has been mentioned previously, OLED screens use just one transparent electrode layer (i.e. one ITO) instead of two. The assumption here, therefore, is that OLED devices have on average only half (i.e. 350 mg/m²) of the indium area density compared to LCDs.

3.2.1.3 Foresight industrial use

The square meterage of global OLED and LCD panel sales was used to calculate the global indium demand for display panels. No distinctions were made regarding the device type they were used for, since the total area produced could not be determined using the sales figures for the device types (TV, mobile phone, etc.) in conjunction with the associated panel size and display technology.

Display Daily (2020a) and IHS Markit (2019) provided data for the total flat screen area from 2014 to 2019. A display area of 424 million m² in 2040 was modelled using an s-curved progression based on the average growth rate of 6.9 % in 2018. The data on the current spread of OLED and LCD displays was collected from Display Daily (2020b) and JPCIC (2020). The technology spread in 2040 was also modelled based on the growth that both technologies are experiencing at present. OLED technology's current trend of rapid growth lasts longer in Scenario A, while it tapers off more rapidly in Scenario B. Scenario A thus describes the technology spread as 30 % LCD and 70 % OLED in 2040, whereas in Scenario B the market is dominated by 80 % LCD and OLED technology trails behind with only 20 %. Diagrams depicting both scenarios can be found in Figures 3.20 and 3.21. As has been discussed previously, it is difficult to make an exact prediction, which is why these forecasted scenarios aim to cover a wide range.

Table 3.34 lists the display areas for 2018 (the base year) and the various scenarios for the year 2040.

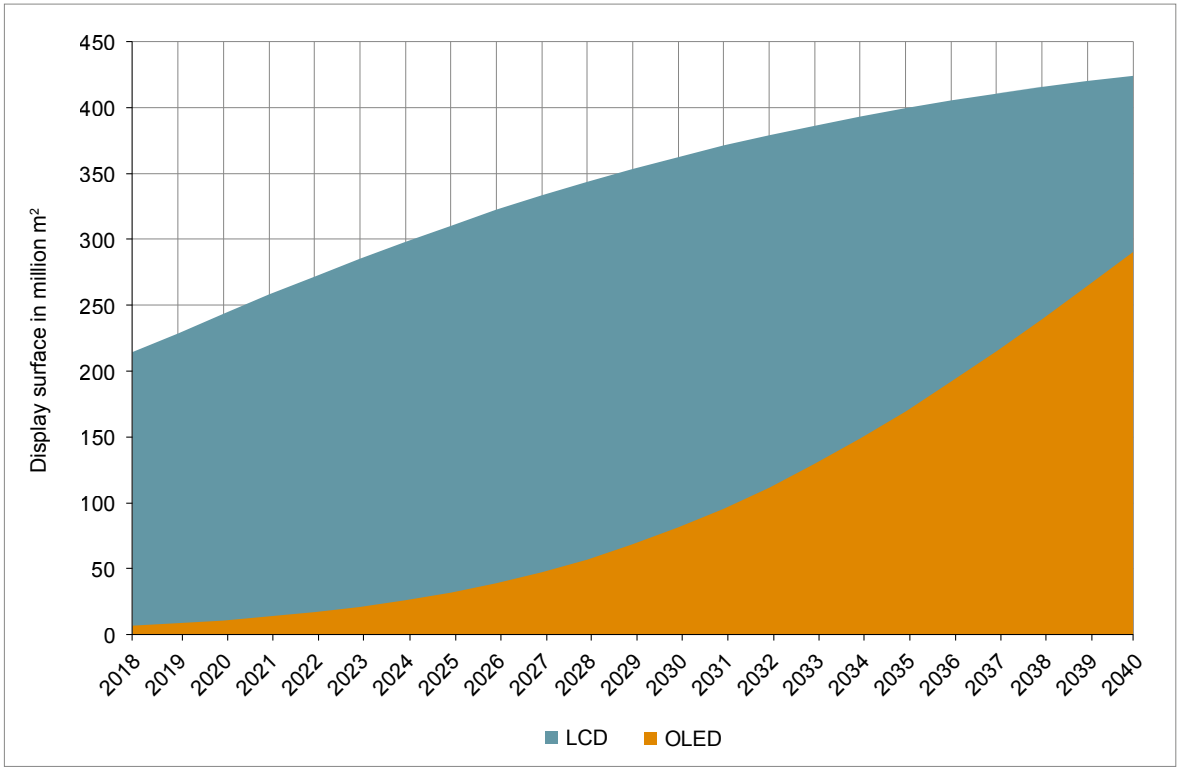

Figure 3.20: Scenario A – total flat screen surface area with LCD and OLED distribution (source: own representation)

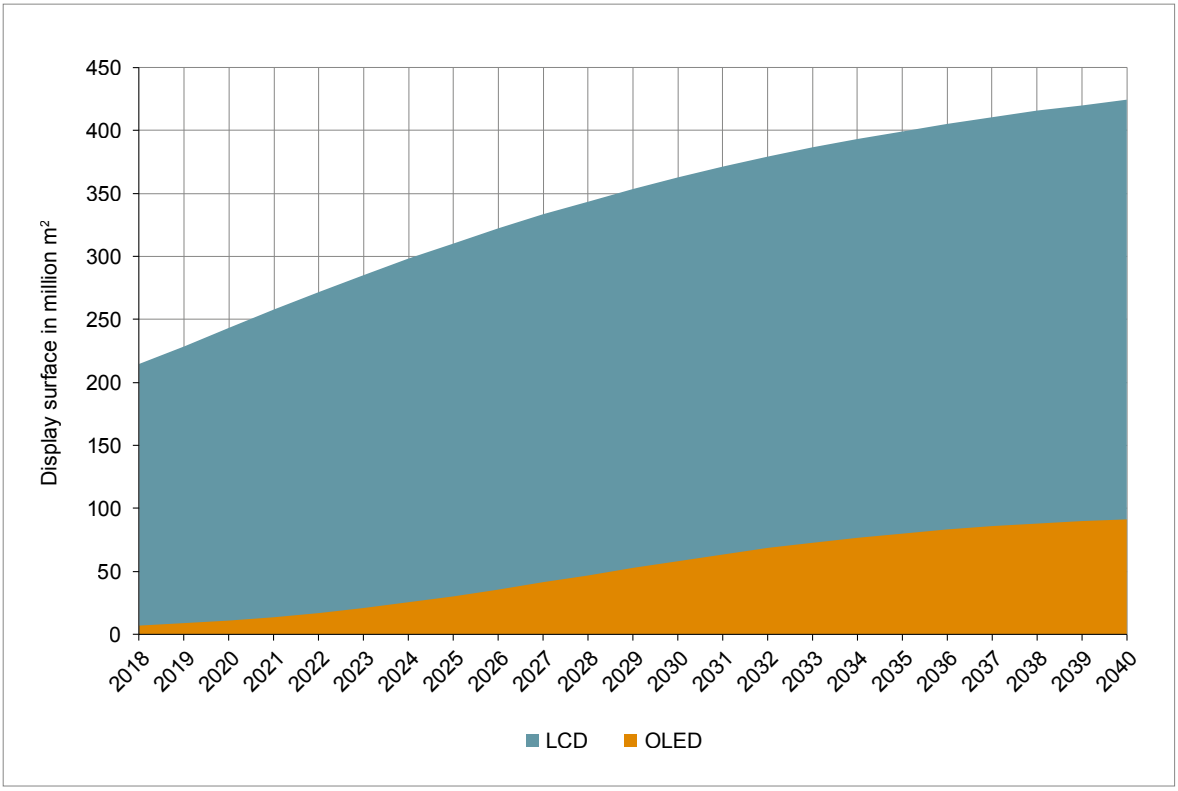

Figure 3.21: Scenario B – total flat screen surface area with LCD and OLED distribution (source: own representation)

Table 3.34: OLED and LCD surface area sold (sources for baseline year of 2018: DISPLAY DAILY 2020a, IHS MARKIT 2019)

	Baseline year	Scenario A	Scenario B
Year	**2018**	**2040**	**2040**
OLED (million m²)	6.7	297	85
LCD (million m²)	207.7	127	339
Total (million m²)	**214.4**	**424**	**424**

3.2.1.4 Foresight raw material demand

It is possible to calculate the displays' raw material content using the LCDs' or OLEDs' square metre numbers with the corresponding area density. Studies conducted by MARWEDE & RELLER (2014) established the net efficiency of the sputtering processes for display production to be at 80 % for 2018 (the base year). So, of the total material usage (material in the sputtering target), approx. 20 % is neither recycled (production waste recycling of overspray and target residues), and nor is it incorporated in the product (in other words, it is disposed of). Technological advancement and improving recycling measures within the manufacturing processes resulted in an assumed 90 % net efficiency for all three scenarios in 2040. These 20 % or 10 % have to be added to the displays' indium content to reveal the actual production demand.

Table 3.35 lists the global indium production and the demand for both products and in production for 2018 (the base year). The different scenarios' projected demand is shown too.

The calculated data leads to the hypothesis that indium demand within display production accounts for a significant percentage of global production. The indium demand that is actually consumed (in production) amounts to 23% in 2018 (the base year). Compared to the previous report (MARSCHEIDER-WEIDEMANN et al. 2016), which considered 2013 as the base year, this is an additional

Table 3.35: Global production (BGR 2021) and calculated raw material demand for indium in display technology, in tonnes

Raw material	Production in 2018	Demand in 2018	Demand foresight for 2040	
			Scenario A	Scenario B
Indium	808 (R)	148 tonnes (in products) 185 tonnes (in products)	193 tonnes (in products) 214 tonnes (in products)	267 tonnes (in products) 297 tonnes (in products)

R: Refinery production (tonnes of metal content)

indium demand in excess of approx. 68 tonnes, taking the mean value at that time into account. Reasons for this rapid rise include this report's methodical approach to data collection. The previous report, for instance, used sales figures to determine screen panels' total area, potentially causing some screen sizes or device types to be excluded. This report has taken data on the sold displays' total area into consideration.

Since an identical total display area was assumed for both scenarios, the higher indium demand in Scenario B can only be attributed to the different technology spread. As explained above, OLED has a lower indium area density, so the forecasted indium demand in Scenario A is far lower. These projections would result in a global indium demand of 27 % in Scenario A and 37 % in Scenario B, relative to global production in 2018. These figures are roughly in line with the ones provided in the previous report for the year 2035. The difference here, however, is that the indium area density for OLED displays was assumed to be considerably higher and the total display areas smaller; they have been revised sharply downwards here. Scenario B with the higher demand of 297 tonnes is included in the estimated indium demand; see Section 4.4.4.

It is becoming clear that, as display area sales figures continue to rise, we ought to better exploit opportunities for minimisation, substitution or improved raw material recycling. These points are addressed in the final chapter of this technology synopsis.

3.2.1.5 Recycling, resource efficiency and substitution

The flat screen industry is aware of just how critical indium is and of its associated price fluctuations. So it is focusing its research and development efforts on finding alternatives to ITO. Material-intrinsic factors are playing a role too, and ITO's rarity and associated value aren't the only reasons why it is worth looking for alternatives. Although ITO is advantageous in that it offers low sheet resistance and high transparency, it has poor mechanical properties, toxicity and high processing costs, not to mention the high metal price (Chen et al. 2016; Zhang et al. 2018).

While ITO still has a 90 % share of the market at present, in the TFT segment at least (Zhang et al. 2018), there are alternatives, indium-free TCOs. Examples particularly include aluminium-doped zinc oxide (AZO) or fluorine-doped tin oxide (FTO). Both of these alternatives are industrially produced at a cheaper cost than ITO. However, they are not equally suitable. While new, amorphous TCOs like indium gallium zinc oxide (IGZO / IZGO), indium zinc oxide (IZO) and zinc tin oxide have similar or even better properties than ITO, they are still five years away from market maturity and some still use indium to some extent. TCOs aren't the only possible solutions. Development is ongoing on a number of other transparent and conductive thin-film technologies that could offer an alternative to ITO in the future:

– Ultra-thin metal foils and zinc metal oxide multilayers.

– Carbon nanotubes (CNTs): Industrial experience of this technology in this field. CNTs could equal ITO's performance with peak val-

ues. But this might not be enough as a direct competitor to ITO, which is why the industry is particularly keen to capitalise on the material's high flexibility (Ghaffarzadeh 2018).

– Metal nanowire foils: Silver nanowire foils in particular have a certain chance of success as an alternative to ITO (Zhou & Lee 2020) and are moving towards achieving commercial breakthrough. They are already being used in low-cost mobile phones and in large multi-touch displays. Since the sales market for foldable mobile phones is growing, an opportunity to become established could emerge in the medium to long term (Ghaffarzadeh 2018).

– Organic transparent conductors (PEDOT:PSS): Poly-3,4-ethylenedioxythiophene is a transparent, electrically conductive polymer that has also been touted as an alternative to ITO for some time. But previous generations' properties were poor. Research into improvements continued because of the material's low price. But PEDOT could never quite match ITO's properties. At the time when PEDOT showed noticeable improvements, the price of ITO dropped too, so it was eliminated as an alternative (Ghaffarzadeh 2018).

– Printed metal lattice: Here, too, there have already been successful attempts to establish the market. The likes of Microsoft was already using this technology in its Surface model, as were other major laptop manufacturers. It should be noted in this regard that printed metal lattice is not a technology in its own right. Rather, it is merely an umbrella term that covers various manufacturing processes designed to produce metal lattice films. Although they are not listed below, each procedure has different advantages, disadvantages and levels of market maturity (Ghaffarzadeh 2018).

The search for alternatives to ITO started from the new field of flexible electronics (e.g. OLEDs on foils). ITO's low mechanical stability limits display flexibility. An organic, transparent and conductive PEDOT:PSS with printed silver contacts is replacing ITO in a flexible OLED display prototype. The rigid OLED displays on glass (which are already being used for mobile phones at present) still use ITO. Alternatives to ITO-free displays are LED displays for signs or large 'screens'. However, InGaN is used for the blue and white diode. In conclusion, there is currently no alternative to ITO for the flat screen display industry (Tercero Espinoza et al. 2014).

Display recycling with subsequent indium recovery is not taken into account in the above considerations. In the case of LCD panels, which have dominated the market to date and of which the likes of conventional LCD CCFL televisions and LCD CCFL monitors each have an average lifetime of ten and eight years respectively, and which accounted for 96.9 % and 98.8 % of sales figures up to 2009, the volume of waste disposed of in Germany was projected to be 11 million units for 2020 (Wolf et al. 2017). With an average indium content of 180 mg per LCD TV screen and 60 mg per LCD monitor, this would generate a considerable volume for this market segment alone. In the OLED devices segment, we cannot currently predict what future disposal volumes will be like. This is due to the constantly improving and initially low lifetime of 10,000 operating hours on the one hand, and a highly dynamic market on the other (Wolf et al. 2017). In the indium recycling segment, there are already several patents in place that specifically deal with extracting the valuable metal from end-of-life LCD panels. China, South Korea and Taiwan are pioneers in this area (Amato & Beolchini 2018). Unfortunately, recovery is not considered to be economical given the small amount of indium produced as a target element per device unit (Wolf et al. 2017). A Swiss study conducted by Groesser & Brechbuehler-Peskova (2015) came to the same conclusion, but found that this was only partly true. If indium recovery were considered in isolation, a procedure would not be economically viable; on the other hand, the costs would be moderate if indium recycling were integrated into the existing recycling system. Indium in particular is most likely to meet the recycling requirements when compared to the metals found in electrical and electronic equipment (Groesser & Brechbuehler-Peskova 2015). This gives us good reason to hope for extensive indium recovery in the near future – both in ecological and economical interests and with the gradual goal of resource self-sufficiency in mind. Since the return flow quantities will continue increasing in the future, economies of scale

could make the recycling of indium from displays economical – possibly in combination with other waste streams containing indium like CIGS solar cells or production waste.

Coating waste is already being recycled today. In the future, two advances in technology will significantly enhance the efficiency of raw materials. Firstly, the use of rotating instead of planar sputtering targets means that more material is removed. Secondly, optimised process control means more material can land on the substrate.

3.2.2 Quantum computers

3.2.2.1 Technology description

Quantum computers are considered to be the new generation of computers that, until now, have incorporated conventional microprocessors. Classic computer systems based on CMOS[4] transistors, which have been around since 1971, use Boolean logic to process data on electronic circuits developed mainly on silicon substrates. In simple terms, the architecture comprises input and output devices for receiving data and retrieving information, a processor as the computing core, memories and paths that enable data exchange. Computation is performed by manipulating the electrical voltage so the transistors are switched between two voltage values known as binary bits: the binary values logical 1 and logical 0.

Quantum computers use a computing paradigm that extends beyond Boolean logic, the foundations of which lie in quantum physics. Quantum computers' basic computing units are called 'quantum bits' or 'qubits'. Qubits adopt energy states that can be measured as 0 or 1, in a similar way to classic computers. However, before the measurements are performed, qubits' energy states are 0, 1 or any value in between. This is referred to as 'superposition'. These simultaneous intermediate states made possible by quantum phenomena allow much more information to be stored and processed compared to binary systems.

In other words, a single qubit enables two simultaneous calculations. This translates into a higher degree of parallel computation, which doubles with each additional qubit and thus increases exponentially. For example, three qubits permit eight calculations in parallel, while four qubits allow double that (16 calculations). With 275 qubits, a quantum computer can perform more calculations than there are atoms in the visible universe (Villanueva 2009). So quantum computers are more powerful than ordinary ones, and they can potentially solve highly complex problems that no classic computer can solve in a limited period of time. This concept is called 'quantum supremacy'.

To achieve quantum supremacy, a certain number of qubits have to be created, but this is challenging for several reasons. Qubits can experience decoherence, meaning they lose their quantum behaviour and this suppresses the computational advantage. A qubit can become decoherent due to internal imperfections or weak interactions with its surroundings. During operations involving qubits, mistakes can occur as a result of decoherence and quantum noise. A viable strategy for correcting mistakes is to distribute the information of one qubit (logical qubit) to several qubits (physical qubit) simultaneously. In this way, disturbances that affect each qubit individually have less of an impact on the quantum state as a whole (IBM n.d.). However, this involves a significant overhead that may require thousands of physical qubits to encode an error-tolerant logical qubit (Massimo et al. 2018).

Applications

Quantum computers have the potential to revolutionise computing and are enabling new computational discoveries in many areas of scientific and practical interest that aren't possible with classic computers. Finance, machine learning, communication systems, quantum cryptography, virtual quantum experiments, chemistry and materials science all stand to benefit greatly from quantum computers. However, many of these applications require a large number of (several hundred or thousand) qubits, and this prospect simply is not in sight yet. Quantum computers that are powerful enough to solve these challenging problems require scalable quantum computer development (Grumbling & Horowitz 2019).

[4] Complementary metal oxide semiconductor

Qubit technologies

There are various qubit technologies, including superconducting, trapped ion, photonic, semiconductor spin and topological technologies. The leading candidates among these technologies are superconducting and trapped ion qubits (Savage 2018). Superconducting qubits cooled down to nearly absolute zero can be monitored and integrated into circuits more easily than other types of qubits. However, as the number of qubits increases, they are more likely to interact with the outside world and lose their coherence (Savage 2018).

The trapped ion quantum computer uses high-precision, isolated atomic particles and uses lasers to perform operations. Trapped ions as qubits have a better coherence time compared to superconducting qubits (Ferraro & Prati 2020). However, mastery of this technology is not at the level of superconducting qubits yet, and they are operated at lower speeds.

Photons are non-interacting and so, as qubits, they do not suffer from the short coherence time caused by interaction with their surroundings. But this property makes performing two-qubit operations difficult. The qubits enable these operations by interacting with one another, and these operations are essential for quantum computation (Georgescu 2020). Photonic quantum computers may also need additional devices like optical quantum memories to delay or store photons. Each of these considerations requires additional resources, creating a large overhead (Slussarenko & Pryde 2019).

Semiconductor spin qubits offer a longer coherence time, which makes them suitable for mass scalability (Ferraro & Prati 2020). On the downside, though, they require virtually perfect materials and have to be operated with extreme precision. The technology is not mature yet, and its performance needs to be improved so connections can be established between multiple qubits (IBM n.d.).

Topological quantum computation is a quantum information processing approach that eliminates decoherence on account of its immunity to all forms of noise. So the technology promises fundamental breakthroughs if and when physical implementation is successful. The models of topological qubits are only theoretical at present.

3.2.2.2 Raw material content

Quantum computers' raw material demand is determined from various sections. This report focuses on the key areas of raw material demand in qubit production and the cooling vacuum systems needed to run quantum computers.

Raw materials for qubits

Superconducting qubits are widely used in existing quantum processor implementations. The components consist of what is known as a 'Josephson junction' with a nano-thin insulator layer arranged between two superconducting electrodes.

Superconducting qubits for digital quantum computing and quantum simulation are most commonly made from aluminium wiring and aluminium/aluminium oxide/aluminium junctions on silicon or sapphire substrates. Aluminium is widely used as a non-conducting layer in the middle of the junction. Commercial versions of superconducting quantum processors with a large number of qubits use either aluminium or niobium for the wiring and the metal electrodes (Grumbling & Horowitz 2019).

Ytterbium atoms were used in a commercial version for trapped ion qubits. Ytterbium is a rare earth metal whose atoms are all identical and can maintain their states over long periods of time (IonQ no date). Basic ion capture and ion control have been demonstrated with almost all alkaline earth and alkaline earth-like ions, which offer different trade-offs for quantum systems. Strontium, cadmium, beryllium, barium, calcium and magnesium are other elements that are most commonly used in quantum computers in ionised form.

Different materials offer certain advantages when it comes to creating a photonic quantum computer. Lithium niobate, a material that is already well established in classic integrated photonics, has advantageous properties for optical quantum computers too. The material is an efficient and flexible platform for photon sources that enables fast on-chip electro-optical modulation. Silicon

photonics also provides high component density, low losses, advanced integration technologies and industrial potential. Extensive research is being conducted into many other material platforms that are useful for optical quantum computers (Slussarenko & Pryde 2019).

Topological quantum computers use non-Abelian forms of matter like Majorana fermions and anyons to store quantum information. The most promising developments in topological quantum computing can be traced back to a non-Abelian mesh of Majorana fermions.This is a massless fermionic particle proposed long ago in theoretical physics (Lian et al. 2018; The Quantum Daily 2020).

Raw material for cooling and vacuum systems

The qubits and, accordingly, the metal parts that they consist of are on the nanoscale. Although they form the computational heart of quantum computers, it is small volumes that make up the entire system. For example, roughly 10^{-13} g aluminium is used for superconducting on-chip qubit designs made from pure aluminium (Winkel et al. 2020).

Most of quantum computers' physical volume is required for cooling systems, since the devices have to be completely isolated from all sources of noise and cooled down to nearly absolute zero to prevent mistakes (D-Wave Systems Inc. 2015). Cooling systems are also required for other qubit technologies like trapped ions and semiconductor spin qubits. However, different quantum computers' exact operating temperatures vary; they are in the extremely low milli-Kelvins for superconducting technologies.

These cooling systems contain various metallic components like copper, aluminium, high-grade steel and other materials (Prouvé et al. 2007; Marx et al. 2014; Micke et al. 2019). The volume of materials required depends on the cooling systems' size, performance and type.

This study shows that rough estimates of the average low and high copper requirements (copper being the main raw material based on various cryogenic cooling systems that are used for quantum computing) could range from 12 to 240 kg.This estimated amount for the quantum computer production volume under consideration may be lower if the technology develops more robust qubits that are capable of operation at higher temperatures.

3.2.2.3 Foresight industrial use

While quantum computers are still in the early stages of development, they have made rapid progress in recent years. The number of qubits has been steadily increased, reaching 128 in 2019 and exceeding previous expectations. The diagram below (Figure 3.22) illustrates the rise in the number of qubits, incorporating various technologies, that has been achieved in recent years.

Progress in quantum computing allows us to solve problems that classic computers cannot. This may potentially translate into considerable growth in various branches of industry and service sectors as quantum computers give rise to new products and highly optimised product development approaches. Extensive trial-and-error-based calculations are essential – particularly in the fields of material design, the chemicals industry and the pharmaceutical industry. This adds to the time needed to design and model new products. The situation may change completely if quantum simulation could support these laboratory processes, thereby reducing trial and error and speeding up the discovery of new material combinations and products (Langione et al. 2019).

In its report, the Boston Consulting Group (BCG) predicts (Langione et al. 2019) that quantum computers will undergo three phases of progress. Faulty qubits are expected to remain an issue in the next progress phase (i.e. in the next three to five years). During this phase, improvements in error prevention techniques will be highly significant in moving towards and maximising the utility of medium-scale quantum computers. We can expect growth in global value creation in various end consumer industries, including material-focused industries, financial services, computational fluid dynamics, pharmaceuticals and other segments like transport, logistics, energy and metrology (Langione et al. 2019).

Quantum computers' second progress phase would take place in the next 10 to 20 years. There are expectations that high quantum scalability

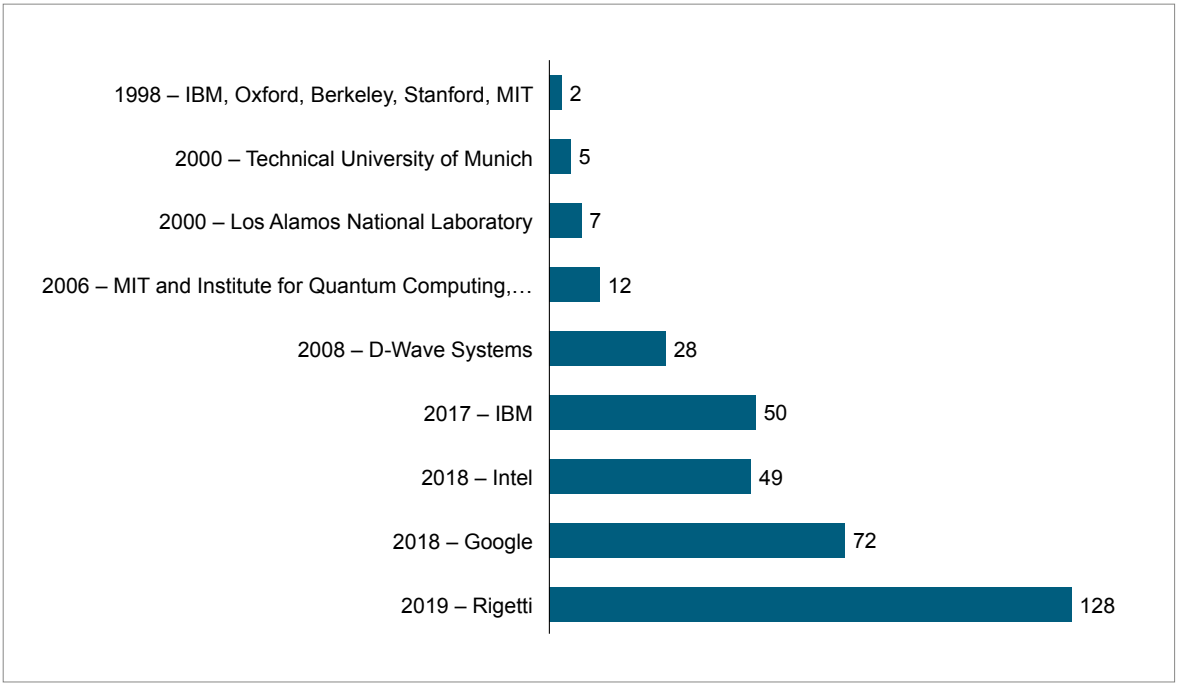

Figure 3.22: Growth in the number of qubits (source: diagram based on FELDMAN 2019)

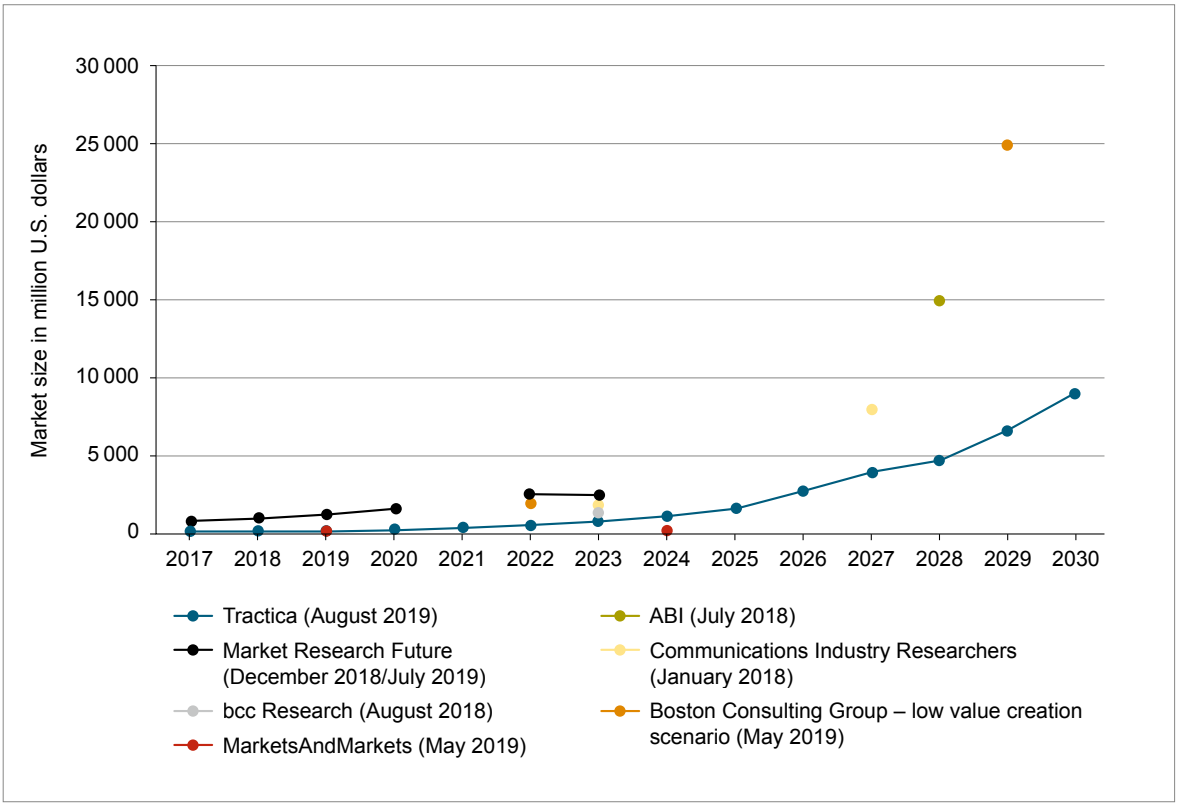

Figure 3.23: Comparison of selected market size forecasts and projections for the global quantum computer market from 2017 to 2030 (in million USD) (source: STATISTA 2019c)

Table 3.36: Global production (BGR 2021) and calculated demand for copper for quantum computers, in tonnes

Raw material	Production in 2018	Demand in 2018	Demand foresight for 2040
Copper	20,590,600 (M) 24,137,000 (R)	0.3 – 6	57 – 1,153

M: Mine production (tonnes of metal content)
R: Refinery production (tonnes of metal content)

and reliability will be achieved during this period, enabling significant experimental advantages. This scenario is followed by a third period of extensive progress, leading to fully scalable and error-tolerant quantum computers. These advances would promise a huge reduction in computational complexity and deliver considerable capacity for various industrial sectors. For this scenario, it is expected that operational income will rise significantly, in the range of hundreds of billions of USD, by 2050.

The scenarios discussed above are based on the assumption that improvements in materials, production and qubit control would continue smoothly. In the more optimistic case, quantum computers may see higher growth due to breakthroughs that are capable of revolutionising the field and its industrial end user sectors. Since quantum computers are still at an early stage of development and are not marketable yet, market growth forecasts cannot be compared with one another and the impact is difficult to predict. Figure 3.23 shows a comparison of different predictions and illustrates two things. On the one hand, the market is usually predicted to be worth billions of USD; on the other, the expected market size varies considerably.

Various scenarios developed based on expert opinions include initial quantum computer applications ranging from one qubit to several thousand in the near to medium term (Moore & Nordrum 2018; Budde & Volz 2019). At this level of predicted progress, it is expected that by 2040 many laboratories, data centres and companies around the world will be kitted out with quantum computers. Accordingly, Yole Développement's market forecast, which predicts a moderate growth rate, appears to be a solid basis. Yole is predicting a 27 % compound annual growth rate (CAGR) until 2030 for the quantum hardware sector (Yole Développement 2020d).

3.2.2.4 Foresight raw material demand

Research into existing quantum computers reveals that, in 2018, there were about 25 industrial quantum computers, including superconducting and trapped ion technologies. Table 3.36 outlines the estimated copper demand for quantum computers in 2040. The estimate is based on a copper demand of 12–240 kg for each quantum computer's cooling and vacuum systems and the assumption that the average annual growth rate until 2040 is about 27 % (Yole Développement 2020d).

3.2.2.5 Recycling, resource efficiency and substitution

The materials used in dilution refrigerators for quantum computers are not currently recycled because the technology is new and undergoing further development. Generally speaking, over 70 % of the copper in end-of-life products is recycled (EuRIC aisbl 2020).

3.2.3 Optoelectronics / photonics

3.2.3.1 Technology description

Optoelectronics is based on the quantum mechanical effects that light has on electronic materials, especially semiconductors. Optoelectronics is the study and application of electronic devices that source, detect and modulate photons to electrons in an electrical circuit (Sweeney & Mukherjee 2017).

Optoelectronic devices have already made their way into many different aspects of our lives. Examples include barcode scanning systems in supermarkets, the CDs, DVDs and Blu-ray discs

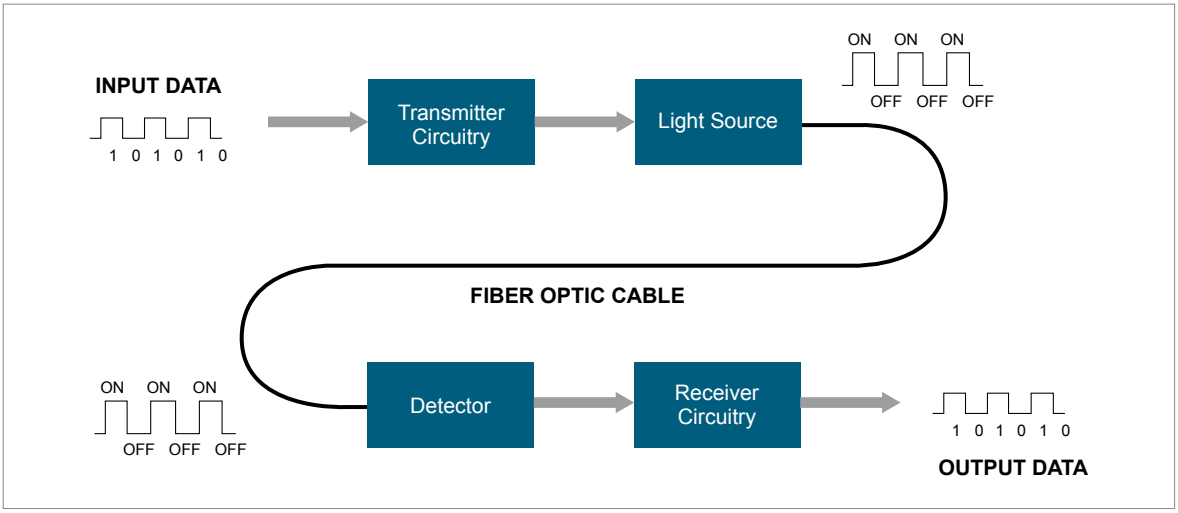

Figure 3.24: Principle of optical communication (source: Massa 2000)

we watch at home, computer mouse positioning solutions, the laser printers we use in our offices, and so on. The best-known optoelectronic object is the light-emitting diode (LED): an LED can emit a brilliant light by applying an electric current that travels through its multiple, complex semiconductor layers. All optoelectronic devices are based on the same type of electron/photon interaction in a semiconductor. Not only do they emit light (LED or laser diode); they modulate (modulator) and detect (photodiode) it too.

Optoelectronic devices are mainly used in:

- lighting (general lighting, automotive, horticulture and display lighting)
- sensing (LiDAR, cameras, gas sensors, etc.)
- telecommunications (optical transceivers)
- photovoltaics (solar cells)

Telecommunications

In this report, we will focus on the telecommunications application, and more specifically on optical telecommunication, since it is based on optoelectronic components. “Optical telecommunication” refers to the transmission of information over distances in the form of light.

An optical telecommunication system consists of:

- a transmitter that receives the electrical signal, which it converts into an optical signal
- a transmission medium that carries the signal (optical fibre)
- a receiver that receives the optical signal, which it converts back into an electrical signal

The principle of optical communications is summarized in Figure 3.24 (Massa 2000).

The materials used in fibre-optic cables are listed in Section 3.5.2 on fibre-optic cables.

Optical transceivers

An optical transceiver contains a transmitter and a receiver in a single housing. An example is shown in Figure 3.25. An optical transceiver contains, among other things, a controller chip, an RF (radio frequency) circuit, lenses and mirrors, as well as a light source (laser diode) and a light detector (photodiode). The last two components are photonic parts, and their composition will be outlined further. According to Yole Développement (2020c), the laser diode makes up 20 to 30 % of the module, and the photodiode 5 to 20 %.

The laser diode as a light source: VCSEL and EEL

A laser diode can directly convert electric current into photons of light by exploiting the unique properties of some semiconductor devices. These

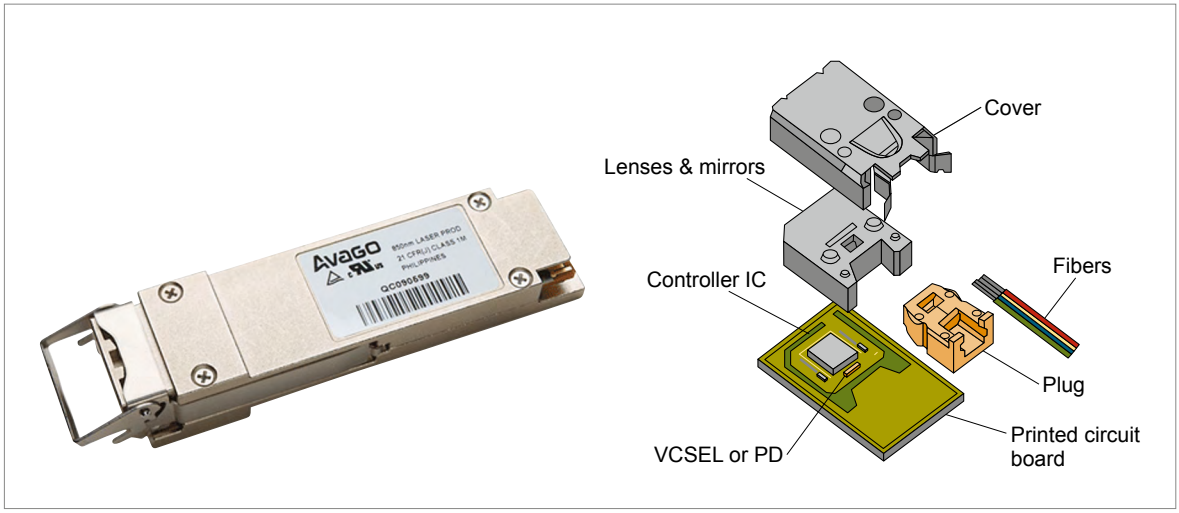

Figure 3.25: Left: an optical transceiver from Broadcom, right: diagram showing the main components of an optical transceiver from Murata (sources: left: Broadcom 2020, right: Murata 2007)

are known as "III – V compounds" and include the likes of GaAs, InP, GaSb, GaN and their alloys (Sweeney & Mukherjee 2017). The III–V active layer (whose properties define the laser characteristics) is built up on a substrate ('wafer'). While the substrate is mainly used as a physical carrier, its properties must also be compatible with the active layer (crystal lattice and coefficient of thermal expansion). This is why a wide range of wafers are used in optoelectronics.

There are two laser diode technologies available on the market:

– Vertical-cavity surface-emitting laser (VCSEL)
– Edge-emitting laser (EEL)

VCSELs emit light from the top of the chip, while EELs emit light from the edge of the structure, as illustrated in Figure 3.26.

A VCSEL consists of two highly reflective distributed Bragg reflectors (DBRs), which are mirror structures with an active region comprising one or more quantum wells for laser light generation (Figure 3.27). The DBR mirror structure is made up of layers of high- and low-refractive-index materials. The two mirrors provide very high reflectivity of the light back into the active layer, allowing the VCSEL to amplify the optical performance. The light thus oscillates perpendicular to the layers and escapes through the top (or bottom) of the device (Princeton Optronics, no date). This structure is much more complex than an EEL's.

In contrast, an EEL is made up of bars that have been cleaved from the wafer. Due to the high contrast in refractive index between air and the semiconductor material, the two cleaved parts act as mirrors. In the case of an edge-emitter, the light thus oscillates parallel to the layers and escapes sideways. There are several EEL designs:

– Fabry Pérot (FP) lasers
– Distributed Bragg Reflector (DBR) lasers
– Distributed feedback (DF) lasers
– Quantum cascade lasers

The type of laser diode used for an optical transceiver depends on the reach distance (Yole Développement 2020b):

– short reach (0–100 m): GaAs VCSEL laser diode
– intermediate reach (500 m–10 km): silicon photonics and InP EEL laser diode
– long reach: InP EEL laser diode (> 10 km)

GaAs EELs are also used for telecommunications in fibre sensors and in telecom instrumentation systems. But GaAs is still mainly used for 850 nm VCSELs for the purpose of data communication (i.e. telecommunication over short distances and using glass fiber) (Mutig 2010). GaAs EELs are

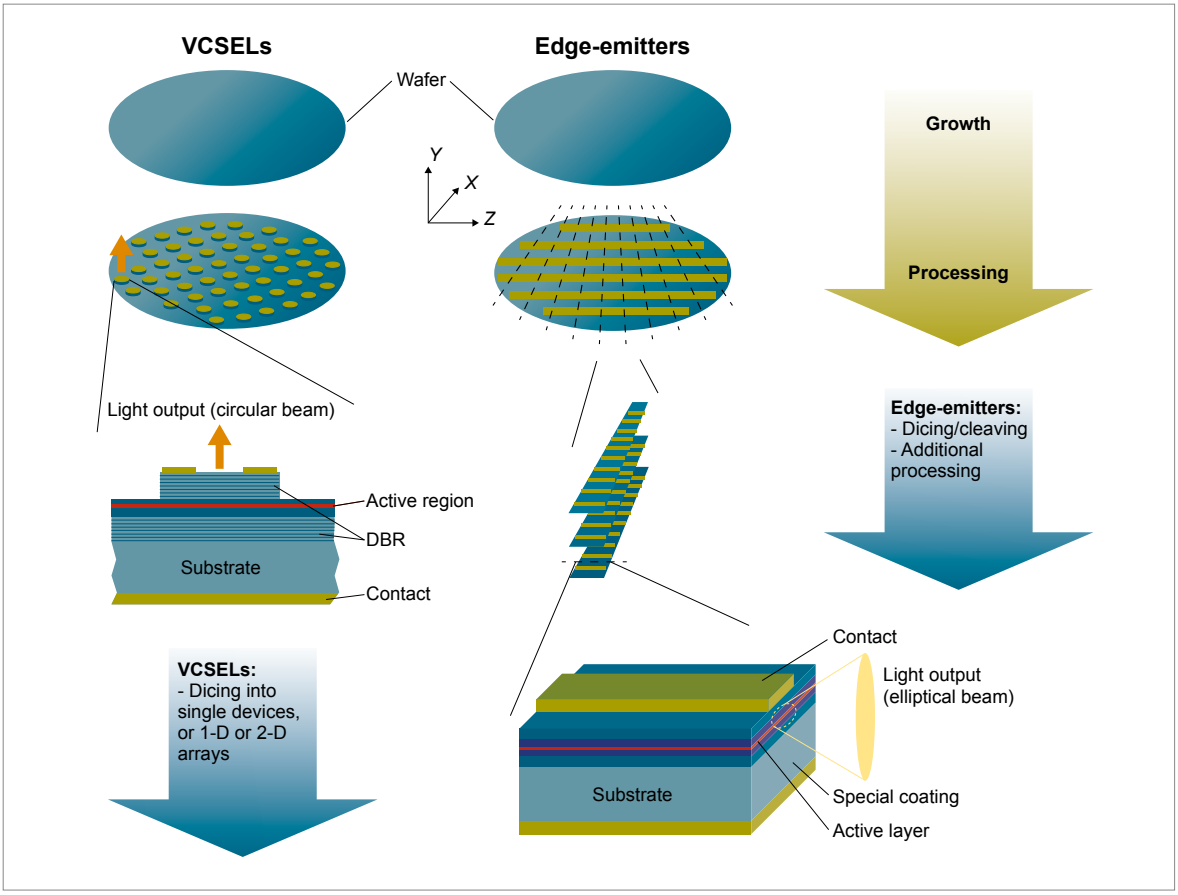

Figure 3.26: Comparison of the function of VCSEL and EEL lasers (source: Princeton Optronics, no date)

associated with data centres in particular. The transceiver types for GaAs-based data communication are Ethernet, fibre channel and optical interconnects (Yole Développement 2019a).

The photodiode as a light detector

A photodiode detects the optical signal and converts it into an electrical signal. The photodiode responds to different wavelength ranges depending on the semiconductor type. In telecommunications, there are two types of photodiode:

– The PIN diode is the most common optical detector. Its structure is shown in Figure 3.28. The absorbed photons create carriers (electrons or holes) that generate a current.
– An avalanche photodiode (APD) is used for long-distance and low-power detection. An "avalanche process" occurs in this type of photodiode, i.e., excited carriers can generate

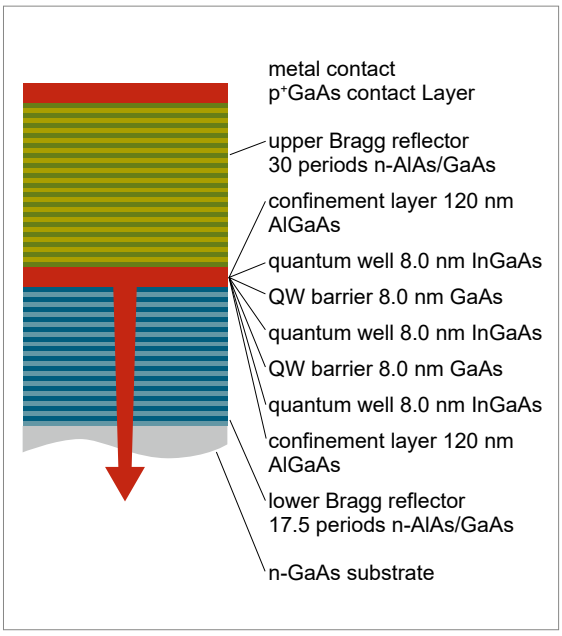

Figure 3.27: Structure of a distributed Bragg reflector (DBR) (source: Enlitech no date)

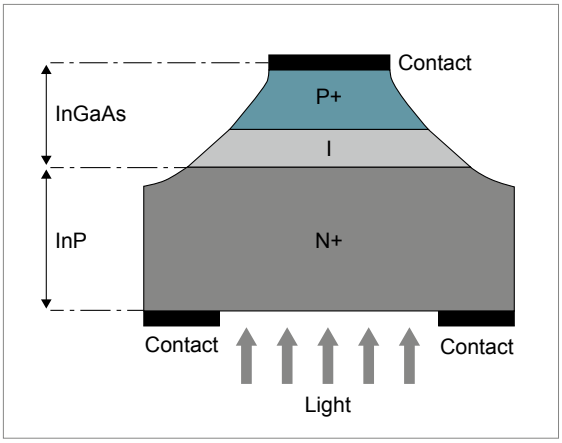

Figure 3.28: PIN photodiode structure (source: ELECTRONICSNOTES 2021)

other new carriers and thus effectively amplify the electrical signal (RP PHOTONICS ENCYCLOPEDIA 2019).

For telecommunication purposes, InP and GaAs are the two types of substrate used to develop the photodiode devices. The InGaAs on InP wafer is now the standard material used for high-speed applications. While silicon and germanium are also used for photodiodes, they are more used for other applications than telecommunications.

Photonic integrated circuits (PICs): InP and silicon photonics

A PIC is a device that integrates at least two photonic functions. The most widely used platform for PIC is InP substrates, which allows the integration of active functions (e.g. light emission, detection, amplification) with passive functions (light guiding, filtering, coupling). The biggest advantages of InP-PICs are low loss and high optical performance, as all functions are integrated on a single chip. The disadvantages of this approach are, firstly, the high costs and, secondly, the limited size of the InP wafers (SMIT et al. 2019).

Another platform that is currently used for optical transceivers in particular is the silicon platform. In silicon photonics, optical components based on InP (laser and detector) are integrated into a silicon chip. This approach reduces the amount of III – V materials incorporated into the optical transceiver (see Section 3.2.3.5 under "Substitution") and increases the production capacity by manufacturing on 300 mm silicon wafers. While other platforms like silicon nitride (SiN), glass, polymer, silicon dioxide (SiO_2) and $LiNbO_3$ exist, they are less versatile than silicon and InP.

3.2.3.2 Raw material content

The production of laser diodes and photodiodes requires a substrate (GaAs, InP in the case of telecommunications) that multiple and complex active layers are built up on (InGaAsP, InP, AlGaAs, GaAs, etc.). This crystal growth is called epitaxy. Depending on the device, the epitaxy layer can be up to 12 µm thick (GUINA et al. 2017). Since the epitaxy layers are still much thinner than the substrate thickness, we will take into account in this report only the material contained in the substrate. However, it must be pointed out that the material utilisation during epitaxy can be very low. A 2013 report explains that a MOVPE (metal organic vapour-phase epitaxy) reactor can lead to around 30 % atom-for-atom utilisation of the III sources (indium and gallium) and to 20 % atom-for-atom utilisation for the V sources (arsenic and phosphorus) (WOODHOUSE & GOODRICH 2013). Moreover, the complexity of some lasers can also generate a low manufacturing yield. For example, a GaAs VCSEL can be up to 10 µm thick with up to 400 layers (YOLE DÉVELOPPEMENT 2020b). The epitaxy process itself leads to significant material loss, but the complexity and variety of layer composition mean we cannot cover it in this report.

This is why we will exclude the epitaxy materials from the following calculation and only count the substrates. The net amount of Ga, As, In and P is calculated based on the wafer thickness (AXT 2020; FREIBERGER COMPOUND MATERIALS 2020a), the GaAs and InP densities (5.315 g/cm³ and 4.81 g/cm³ respectively) and the molecular weight (see Table 3.37). The gross percentage of the semiconductor element takes into account the material loss during wafer production. In GaAs production, the material utilisation rate is around 45 % (CLEMM et al. 2017). This figure includes inner loop recycling, where intermediate waste is reintroduced in wafer synthesis. No data could be found on material utilisation for InP wafer production, which is why we assumed the rate would be the same as for GaAs wafer production.

Table 3.37: Quantity of Ga, As, In and P per wafer (gross demand)

	GaAs Wafers	InP Wafers
Wafer size	6”	4”
Thickness	675 µm	600 µm
Material utilisation rate in wafer production	45 %	45 %
Gallium demand per wafer	70.1 g	
Arsenic demand per wafer	75.3 g	
Indium demand per wafer		42.7 g
Phosphorus demand per wafer		115 g

Note: Gross demand is the amount needed for wafer production, including material losses during production.

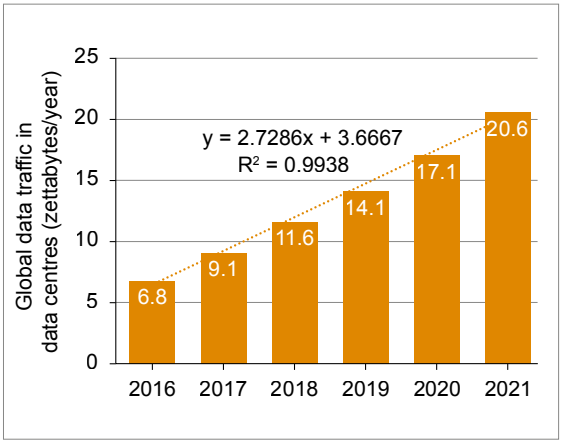

Figure 3.29: Growth in worldwide data traffic in data centres (zettabytes per year) according to CISCO and trend used for forecast until 2040 (source: Cisco 2018)

3.2.3.3 Foresight industrial use

Market for data communication

The forecast in this study is based on Yole’s estimate to 2025. The trend towards high-speed optical transceivers is expected to boost InP sales, since this material is particularly advantageous for high performance. The compound annual growth rate (CAGR) of InP wafer sales is 31 % for data centre communications between 2017 and 2023 alone (Yole Développement 2019a). The CAGR for InP wafer sales for optical transceivers with a data rate above 100 GB/s is experiencing very strong growth: 149 %, from 150 to 90,000 InP wafer units between 2017 and 2023. The growth in data centre traffic forecast by Cisco (2018) is taken into account to forecast wafer sales from 2026 to 2040; it is expected to increase from 6.8 zettabytes (ZB) in 2016 to 20.6 ZB in 2021 (Figure 3.29). This study assumes that this growth will continue in a linear fashion until 2040. Wafer sales will not follow the growth in data centre traffic shown in Figure 3.29 exactly, so it will be reduced with an additional raw materials ratio, which is different for GaAs and InP wafers. For GaAs, it is the ratio of wafer market growth to data centre traffic growth in 2019 and 2020, and is equal to 0.3. The ratio is identical for InP, but it is 0.8 for the market growth in 2023 and 2024.

Figure 3.30 shows projected GaAs wafer sales for VCSELs in optical transceivers, which could double by 2040 and potentially reach 28,000 wafers that year. Wafer sales for VCSELs remain small compared to the RF market (see Section 3.2.5 ‘Radio frequency microchips’) with potentially 1.5 million wafers in 2040. Figure 3.31 shows the amount of InP wafers that will be required in future for data communication (in blue). This forecast is based on the current market segmentation between InP and silicon photonics. The silicon photonics market could grow faster than InP and gain market segments against InP in the future. But silicon photonics is still dependent on InP wafers for the active components (light source and detection). This forecast should be viewed as a worst-case scenario, where InP use remains the core technology. The volume of InP wafers for data communication will grow rapidly until 2024 (2017–2024 CAGR = 31 %) according to Yole Développement (2019a). In 2040, InP wafer sales could reach 27,000 wafers annually if demand for optical transceivers in data centres remains this high.

Market for telecommunications

5G technology will lead to many more base stations than 4G. This will require tens of millions of transceivers, which will consume a significant number of InP wafers used for laser detectors and photodetectors alike. This study expects

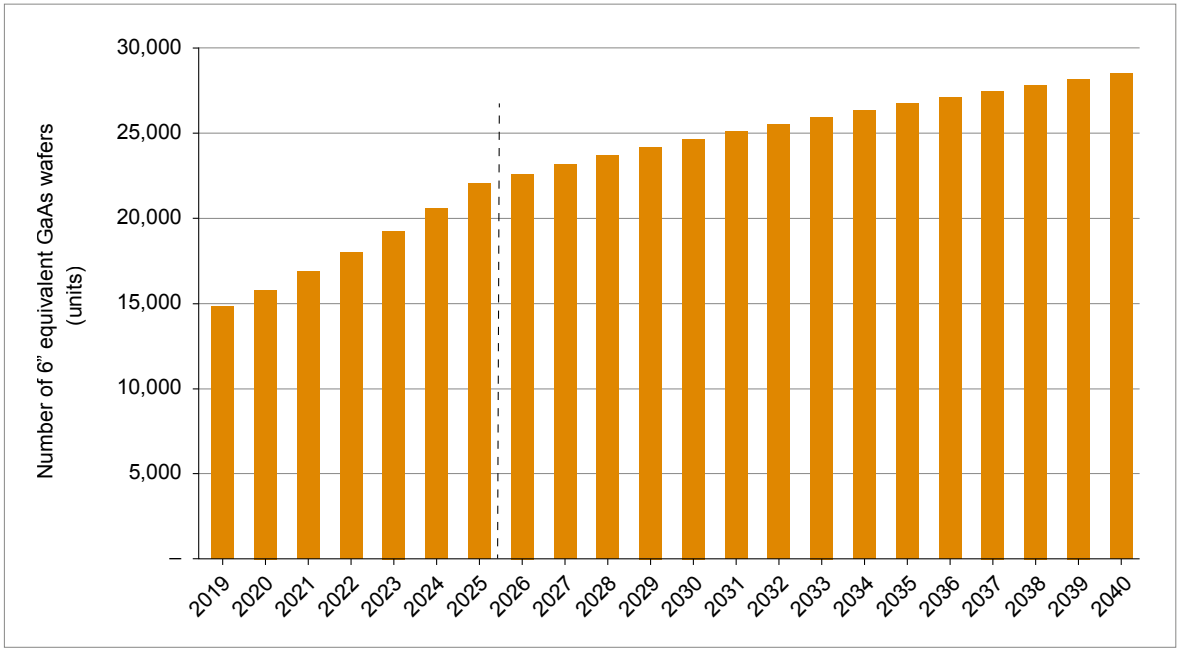

Figure 3.30: Market for GaAs wafers in units sold (source: 2019 to 2025: Yole Développement 2019a, 2026–2040: own forecast)

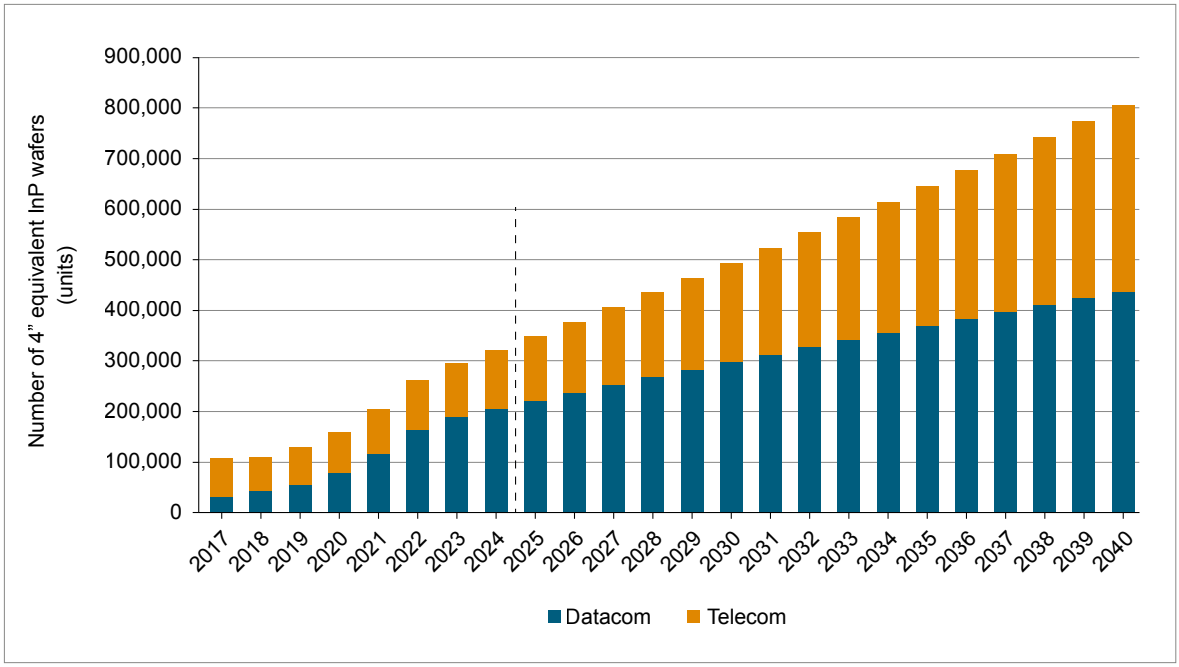

Figure 3.31: Market for InP wafers in units sold (source: 2017 to 2024: Yole Développement 2019a, 2025–2040: own forecast)

the InP wafers for telecommunications market to develop identically to the RF devices market (see Section 3.2.5 'Radio frequency microchips'), since 5G is the main driver. Yole is forecasting 9 % annual growth between 2019 and 2024, driven by 5G applications (Yole Développement 2019a). Between 2025 and 2040, sales of InP wafers for telecommunications are expected to follow mobile internet data's annual growth (see Section 1.4 'Digitisation scenarios'). Since wafer

sales will not follow this growth exactly as shown in the data centre graph, it will be reduced with an additional raw materials ratio, which is the ratio of wafer sales growth to mobile internet traffic in 2023 and 2024 and is equal to 0.3. Figure 3.31 shows sales forecasts for InP wafers designed for data centres and telecommunications. Given that the three scenarios do not differ significantly from one another with respect to mobile internet traffic's growth rates, only one scenario is considered in this calculation.

3.2.3.4 Foresight raw material demand

Based on wafers' raw material demand (Table 3.37) and on wafer forecasts (Figures 3.30 and 3.31), we can estimate the raw material demand for 2040 below.

Table 3.38 compares global production in 2018, the amount of material for the optical transceiver market in 2018 and the demand forecast for 2040 for each element. The amounts of gallium and arsenic are not expected to increase significantly in the future. Volumes in wafer sales remain small compared to the RF market (see Section 3.2.5 'Radio frequency microchips'). Then again, demand for indium, which is essential for photodiodes and laser diodes, will triple by 2040. This forecast is based on a worst-case scenario in which InP technology will remain the main platform. Silicon photonics is currently replacing the InP platform to cut costs and boost performance (see Section 3.2.3.5 under 'Substitution'). Since there is no specific evidence from the SSP narratives and the amounts are comparatively small, the SSPs make no further distinction.

3.2.3.5 Recycling, resource efficiency and substitution

Recycling

Gallium and indium from end-of-life electronic products are not recycled at present. The reasons for this include the greater economic incentive to pyrometallurgically recycle the precious metals that the components contain (European Commission 2020b). The hydrometallurgical recycling of gallium from production waste from photovoltaic production is technically feasible (Marwede 2013). So far, however, there have been no attempts to determine whether extraction from components is also possible. The multitude of chemical elements in the component, the low gallium and indium concentrations in the component and the need previously to identify and separate the components from the electronic scrap cast doubt on the economic feasibility. The fine distribution of these elements in different products and components also makes it difficult to collect sufficient quantities for recycling.

However, pre-consumer recycling (from industrial waste) is an important secondary source of gallium and indium. Closed loop recycling often occurs in the industry, mainly for economic reasons. The manufacturing processes of GaAs and GaN wafers are considered the most important secondary source of the metal, with about 60 % scrap being produced and recycled in a "closed loop" (Licht et al. 2015; European Commission 2020b). A material flow analysis of GaAs wafer production conducted by Freiberger Compound Materials GmbH reveals that 55 % of the Ga and As introduced in the manufacturing process is not

Table 3.38: Global production (BGR 2021) and calculated raw material demand for GaAs and InP for the optical transceiver market, in tonnes

Raw material	Production in 2018	Demand in 2018	Demand foresight for 2040		
			SSP1 Sustainability	SSP2 Middle of the Road	SSP5 Fossil Path
Gallium	413 (R)	1	2	2	2
Arsenic	32,783 (M)	1	2	2	2
Indium	808 (R)	5	35	35	35

M: Mine production (tonnes of As_2O_3 content)
R: Refinery production (tonnes of metal content)

contained in the wafer. Gallium can be extracted from this waste by electrochemical processes and reused (Clemm et al. 2016).

Substitution and resource efficiency: Silicon photonics

Another platform that is currently used for optical transceivers in particular is the silicon platform. In silicon photonics, optical components based on InP (laser and detector) are integrated into a silicon chip. The biggest advantages of InP-PICs are low loss and high optical performance, as all functions are integrated on a single chip.

Silicon photonic PICs use III–V materials for the active functions only and use silicon for the others. As a matter of fact, Si-based lasers are very inefficient emitters and detectors of light. This approach reduces the amount of III–V materials incorporated into the optical transceiver and increases the production capacity by manufacturing on 300 mm silicon wafers. While other platforms like silicon nitride (SiN), glass, polymer, silicon dioxide (SiO_2) and $LiNbO_3$ exist, they are less versatile than silicon and InP.

3.2.4 Microelectronic capacitors

3.2.4.1 Technology description

Capacitors are used to store electrical charge and their uses include maintaining a steady current in integrated circuits (ICs). The miniaturisation trend in microelectronics favours compact designs and thus, indirectly, dielectrics in capacitors with a high dielectric constant.

Electrolyte and ceramic-based capacitor technologies are an important line of distinction. There are electrolytic capacitors with aluminium, tantalum or niobium electrodes. Tantalum electrolytic capacitors achieve the highest charge density per volume, while ceramic-based capacitors are the most affordable. Electrolytic capacitors with Ta_2O_5 as dielectric have been on the market for five to six decades now. The first components suitable for surface mounting (SMDs) were introduced in the 1980s. The extremely cyclical market trends with corresponding price and availability issues – not to mention ethical concerns regarding tantalum (a conflict metal) – have given rise to efforts to find substitutes since around 2007 (ZVEI 2019). For example, multilayer ceramic capacitors (MLCCs) have replaced tantalum capacitors in many applications, especially in portable ICT devices, on account of technical improvements and the associated expansion of the range of applications (Roskill 2018; Zednicek 2019; ZVEI 2019). However, the industry's high innovation dynamics have presumably already led to the substitution potential being highly exploited (Damm 2018).

Figure 3.32 shows sample applications of different capacitor technologies as a function of voltage and capacitance.

In tantalum-based electrolytic capacitors' performance range (i.e. low voltage with medium capacitance), there are overlaps particularly with niobium-based electrolytic capacitors, not to mention aluminium-based electrolytic capacitors and ceramic capacitors.

Below is a description of the design and working principle of the two main types of tantalum-based/niobium-based electrolytic capacitors (Figure 3.33) and MLCCs (Figure 3.34).

The relative dielectric constant of Ta_2O_5 and Nb_2O_5 is 27 and 41 respectively. However, Nb_2O_5's greater dielectric constant is more than compensated for by the thicker oxide layer, so the designs containing tantalum can be more compact. In case of the tantalum electrolytic capacitor (Ta capacitor), the anode is made from tantalum, on which a uniform, dielectric tantalum pentoxide layer was created by anodic oxidation. A liquid or solid electrolyte like manganese dioxide forms the cathode. A conductive polymer (polypyrrole (PPy) or polythiophene (PEDOT)) replaces the electrolyte in polymer capacitors (Avnet Abacus 2020).

Comparing tantalum and niobium capacitors reveals the following suitability preferences (Zednicek 2006):

– Tantalum capacitors with MnO_2 electrodes are suitable for high-temperature applications (up to 200 °C), high voltages (up to 50 V) and reliability requirements. This is why they can particularly be found in segments that have high qualification requirements – in the likes

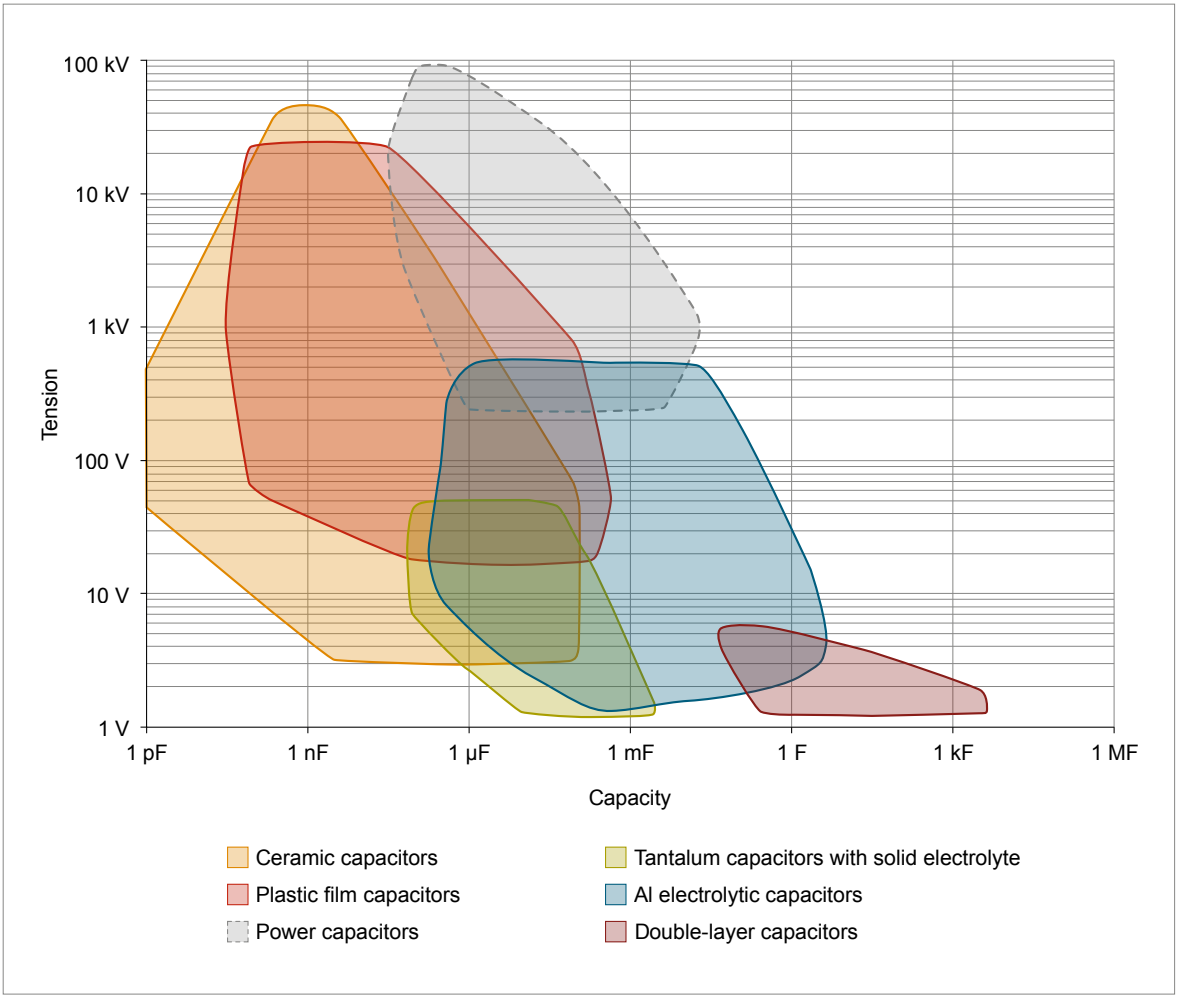

Figure 3.32: Examples of applications of various capacitor technologies (source: Elcap, Cepheiden, Wikimedia)

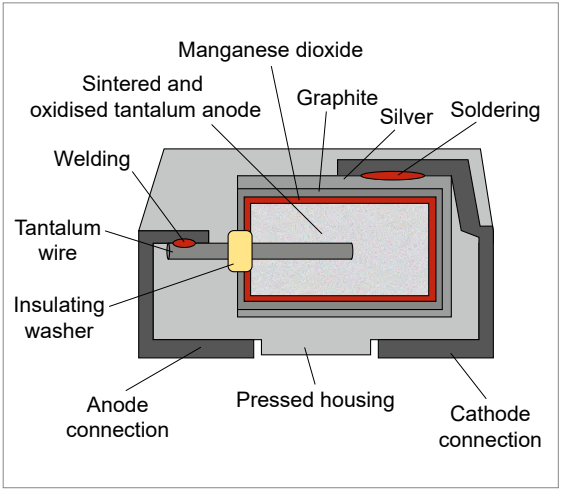

Figure 3.33: Structure of a tantalum-/niobium-based electrolytic capacitor (source: Elcap, Wikimedia)

of commercial and military aerospace, medical applications and sub-sectors of industrial electronics (ZVEI 2019).

– Before the turn of the millennium, various manufacturers developed capacitors with a conductive polymer as the cathode material (polymer capacitors). Here, the manganese dioxide (MnO_2) that was used previously was substituted by a conductive plastic material (ZVEI 2019). Tantalum capacitors with polymer electrodes are suitable for applications with lower electrical requirements, such as DC/DC converters in notebooks, PDAs, telecommunications and other applications (ZVEI 2019).

– Niobium oxide capacitors are an alternative to tantalum capacitors and offer good value for money. Given their reliability, they are used in more than just the consumer segment; they can be found in the high-end segment too. However, niobium capacitors still have limited dielectric strength at present (Stenzel 2021), which is why Stenzel (2021) assumes that niobium will not do away with tantalum on a large scale, partly due to the limited number of manufacturers.

An MLCC capacitor consists of a multitude of individual ceramic capacitors that are layered one on top of the other and contacted via the connection surfaces. The starting material for all MLCCs is a finely ground mixture of ferroelectric base materials like barium titanate ($BaTiO_3$) that are modified by adding zirconium, niobium, magnesium, cobalt and strontium, which foils are made from. They are then further processed by electrode pressure, lamination, sintering, and so on. It is vital that manufacturers of ceramic capacitors are familiar with the composition and size of the powder particles.

With regard to MLCCs' electrode material, silver-palladium electrodes have lost their share of the market to nickel electrodes and copper electrodes. Pd-based MLCCs' share of the market has declined from around 85 % in the mid-1990s to 10–15 % in the late 2000s (Nassar 2015). Nowadays, palladium in MLCCs is only used in high-end products in automotive, medical and military applications, so even a slight decline in demand from the electronics sector could be observed here (JM 2019). In the previous report 'Raw materials for emerging technologies' (Marscheider-Weidemann et al. 2016), it was still assumed that 50 % of MLCC capacitors have AgPd electrodes. So, in the 2016 forecast, out of all the materials used for MLCCs only the projected amount of palladium in 2035 was significant compared to global production in 2013. Since MLCCs with AgPd electrodes are only used in special applications nowadays, no demand scenarios are being created for MLCCs in this update. Silver and manganese from Ta capacitors and niobium from Nb capacitors inconsequential in the forecasts too, so only tantalum in tantalum capacitors is considered in this report.

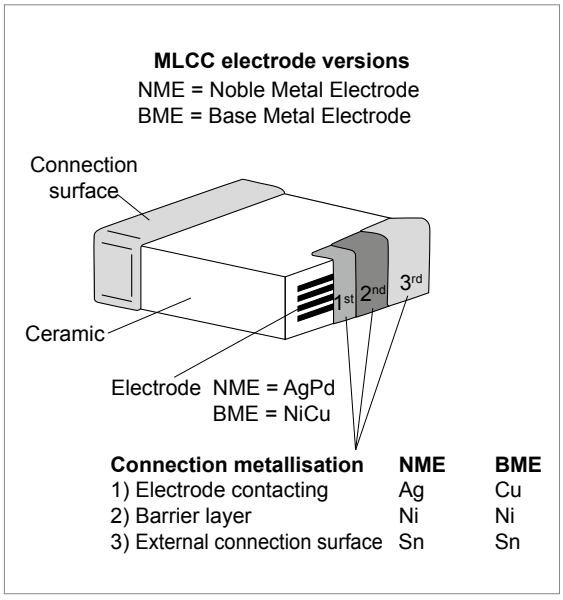

Figure 3.34: Structure of a multilayer ceramic capacitor (MLCC) (source: Elcap, J. Both, Wikimedia)

3.2.4.2 Raw material content

According to investigations conducted by the German Mineral Resources Agency (DERA), a tantalum content of 53 wt% was determined for a tantalum capacitor measuring 3.9 mm x 3.1 mm x 2.3 mm (L x W x H). But since only two measurements were performed, the value should not be considered representative (Bookhagen et al. 2018). Further analyses of tantalum capacitors from smartphones measuring 2 mm x 1.25 mm x 1 mm (L x W x H) revealed a maximum tantalum content of 40 wt% per capacitor (Reinhold 2020). This value validates the maximum content of 42.6 wt% tantalum per capacitor (ZVEI 2003).

Since there are no publicly available market figures on the capacitor market's turnover (measured in capacitors sold) and the fluctuation margin of tantalum volume per capacitor is also very high due to the different sizes or capacities, the amount is estimated using the cap-grade Ta powder sold. Not all the manufacturers are represented in the statistics published by the 'Tantalum-Niobium International Study Centre' (TIC). The TIC (2020b) states that 573 tonnes of cap-grade Ta powder were sold in 2018. However, there was a shortage of MLCC capacitors in 2018 (Stenzel 2021) and thus greater demand for capacitors, so the quantity sold in 2018 is rather high. The numbers fluctuate a lot. This is why, in the context of this study, it is assumed that demand has

grown by 3.1 % on average since 2009 based on the (TIC 2020b) figures. Taking the 475 tonnes of cap-grade Ta powder in 2009 as the reference year (TIC 2020b), approximately 630 tonnes of cap-grade tantalum were sold in 2018. Additionally, there is demand for tantalum wire, which Reinhold (2020) believes accounts for about 9 % of the capacitor's total content. Stenzel (2021) instead assumes that the wire has a 15–20 % mass percentage due to the ever smaller size. This brings the calculated total demand to approx. 725–760 tonnes in 2018. This study assumes an average of 740 tonnes. As mentioned previously, demand was particularly high in 2018. This results in a numerical gap of about 130 tonnes compared to the 815 tonnes of tantalum required for capacitors in 2018 that Roskill (2018) stated.

3.2.4.3 Foresight industrial use

Roskill is of the opinion that capacitors are tantalum's main application market (Roskill 2020c). Given that vehicles and households will be electrified in future, tantalum capacitors will still be increasingly important then too since they are highly reliable in harsh environments, despite costing more. The main application markets are medical applications like hearing aids and pacemakers, automotive applications, and ICT terminals and cell towers (TIC 2020a). The likes of 5G will raise the requirements placed on the electronics used in smartphones, demanding faster downloads and response times (Roskill 2020b; Roskill 2020c).

The lack of data on the market as a whole and the future of the capacitor market means that the material flows can only be roughly quantified (Damm 2018). The "Tantalum-Niobium International Study Centre" association publishes annual sales figures for various tantalum materials, including cap-grade Ta powder, which is essential as a sintered product for capacitors (TIC 2020b). The numbers fluctuate a lot. However, if we assume that these figures reflect the demand market, it has grown by of 3.1 % annually on average in the period from 2010–2018. This figure is almost equal to the global 3 % growth in GDP over the same period, which suggests that the Ta capacitor market is dependent on global market growth. However, there was a peak in demand in 2018 caused by the MLCC shortage, which explains why Stenzel (2021) is assuming a 2 % annual growth rate of instead. Despite the COVID-19 crisis, the market is not expected to slump in 2020; instead, there are expectations that demand will be stronger given the digitisation trend (terminal devices and infrastructure) (Damm 2020; Stenzel 2021).

3.2.4.4 Foresight raw material demand

It is believed that growth will not decline sharply in 2020; rather, it assumptions are that will continue to rise by 2 % on account of the strong digitisation trend during the COVID-19 crisis. From 2020 onwards, reference is made to the global GDP growth figures that form the basis of the SSPs (Riahi et al. 2017); they range from 2.5 to 5.1 % depending on the scenario and time period. So SSP1 and SSP5 in particular fit the corridor of 4–5 % annual demand growth of total tantalum demand from all applications until 2026 as maintained by DERA (Damm 2018; TIC 2020c). SSP2 is expected to have the lowest average market growth (3.1 %).

According to the scenarios, the tantalum demand for capacitors in 2040 may increase to 94–110 % of today's global production. However, these forecasts are subject to high levels of uncertainty, because it is difficult to predict which capacitor technologies or materials (e.g. niobium) will prevail in the long term and in which applications. Additionally, there are still uncertainties regarding how the storage density will develop (tantalum farad / weight); this has roughly been raised by 6 % per year in the last seven years (from 100 µF per capacitor in 2013 (Zogbi 2013) to 150 µF, with the size staying about the same (AVX 2021). This means that, when the market is measured by the number of capacitors sold, it has grown far faster than the demand for tantalum as a raw material. These gains in material efficiency will also have an impact on future raw material demand. Compared to the projections as outlined by Marscheider-Weidemann et al. (2016), the forecasted tantalum demand is significantly higher – partly because the demand for 2013 (130 tonnes) was significantly underestimated. The demand for cap-grade Ta powder alone was 540 tonnes in 2013 according to TIC (2020b).

Table 3.39: Global production (BGR 2021) and calculated raw material demand for microelectronic capacitors, in tonnes

Raw material	Production in 2018	Demand in 2018	Demand foresight for 2040		
			SSP1 Sustainability	SSP2 Middle of the Road	SSP5 Fossil Path
Tantalum	1,832 (M)	740	1,716	1,459	2,013

M: Mine production (tonnes of metal content)

3.2.4.5 Recycling, resource efficiency and substitution

Tantalum is hardly recycled from end-of-life waste, and the global tantalum recycling rate is less than 1 %. Production waste recycling is, in contrast, one of the common processes, and about 10 to 25 % of the primary raw materials can be replaced with recycled production waste (Wilts et al. 2014). Recycling of tantalum from end-of-life scrap mainly focuses on post-industrial and post-consumer scrap, where tantalum is produced in larger quantities (e.g. as a super alloy in turbine blades, sputtering targets from the semiconductor industry, components for plant engineering, process scrap such as production waste and tantalum carbides from the carbide industry) (Gille & Meier 2012; Damm 2018). Post-industrial waste is produced during production or manufacturing, while post-consumer waste is created by end consumers. According to the Federal Institute for Geosciences and Natural Resources (BGR) (2018), 275 tonnes of tantalum were extracted from secondary production in 2016. Tantalum recovery from electrical devices like mobile phones is not economically feasible at present since the valuable metal is highly diluted, there is a lack of process developments and collection rates are low (Damm 2018). Gille & Meier (2012) believe that the low tantalum concentration in ICT terminal devices (i.e. the high dissipation) is a huge challenge for efficient material recovery. There are no industrial-scale facilities, because high concentrations and purities are required for recycling tantalum capacitors and separating the components from printed circuit boards (Sander et al. 2018). Solutions for automated component removal, recognition and sorting have been developed by the European research project ADIR (Noll et al. 2020).

3.2.5 Radio frequency microchips

3.2.5.1 Technology description

Radio frequency communication

Radio frequency (RF) chips are used for wireless telecommunications and are based on an electromagnetic signal as a form of communication. The radio frequencies range from 3 kHz to 300 GHz. RF technology is used in many applications, including cell phones, WLANs, satellites and remote sensing. The wide range of applications is shown in Figure 3.35.

Figure 3.36 illustrates a simplified model of RF wireless communication. The source supplies the information to the transmitter (audio, video, data). Once signal processing is complete, the transmitter sends information to the receiver through an antenna. The transmitter's process functions might include the likes of modulation, encoding and analogue-to-digital conversion, while the receiver's process functions would be the reverse (decoding, demodulation, etc.). For both transmission and receipt to be effective, the transmitter and receiver also perform signal amplification, frequency filtering, signal translation from one frequency to another, etc.

RF semiconductor devices

An RF system requires two types of hardware subsystem to transfer the information: a transmitter and a receiver. They consist of many components; the main ones are:

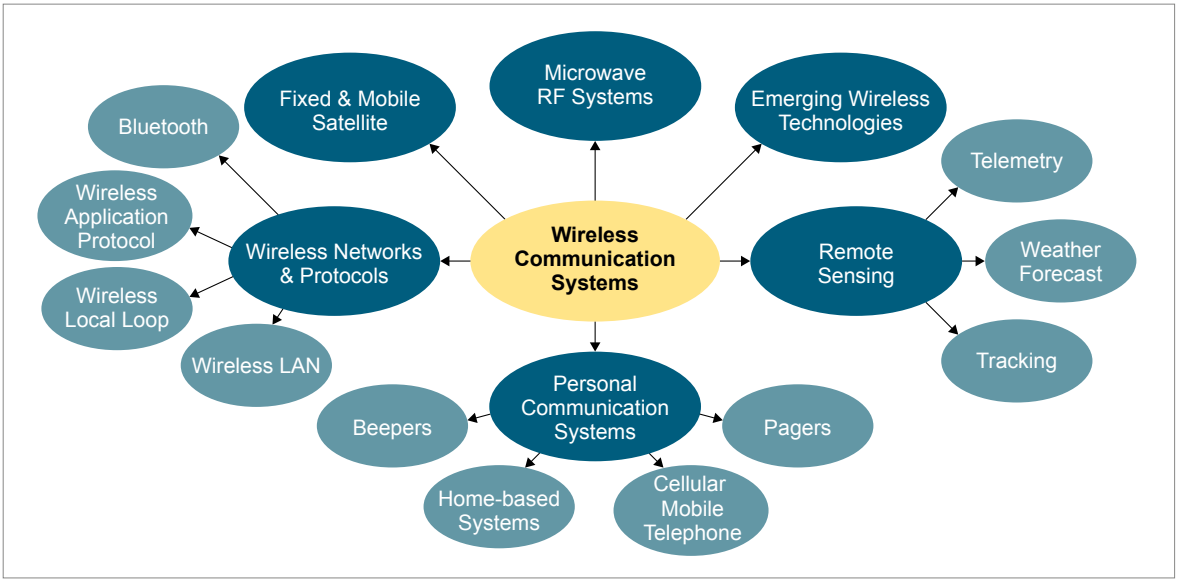

Figure 3.35: Applications of RF communication (source: Ugweje 2004)

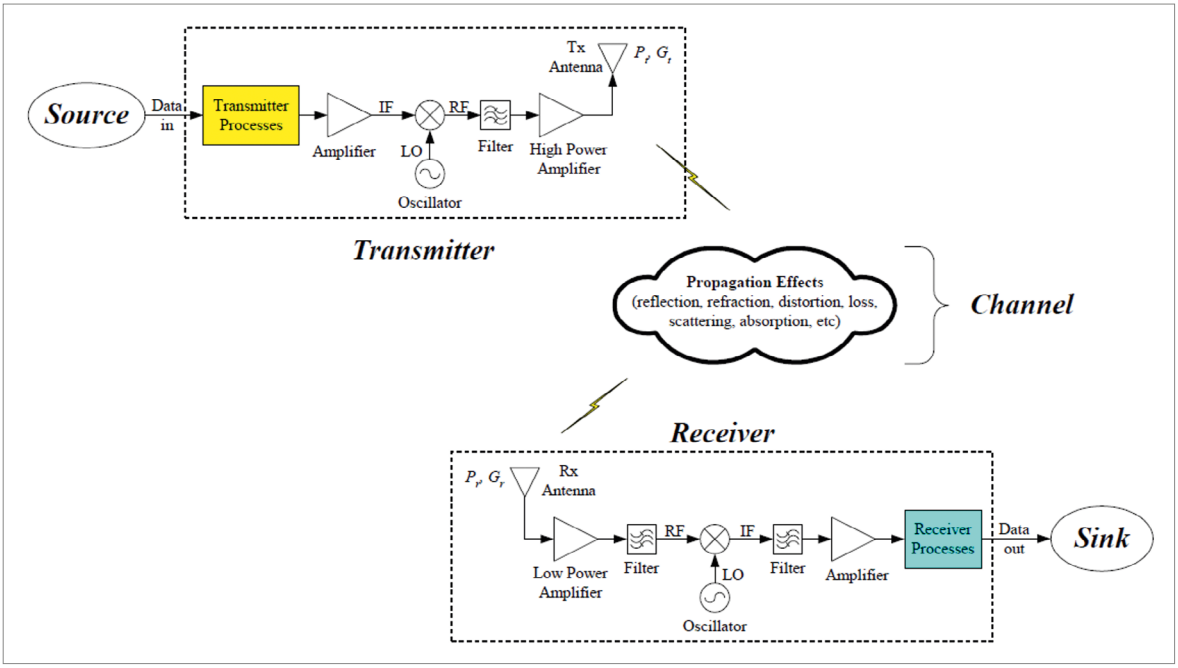

Figure 3.36: Simplified model of terrestrial wireless RF communication (source: Ugweje 2004)

– Power amplifiers, which amplify the outgoing signal, making it strong enough to reach the base station
– Low-noise amplifiers, which amplify the incoming signal
– Filters, which select the signals according to their frequencies
– Switches, which move signals from one RF path to another

There are obviously many more components in RF systems, but we will focus on these ones, since they contain critical materials. These components are integrated circuits based on semiconductor devices. The transistor is the main semiconductor device. Many types of transistors exist, depending on the application.

Integrated circuits are made in and on wafer surfaces. The area on the wafer that the semiconductor device or integrated circuit occupies is called a chip, microchip, die or bar. The transistors and other electronic components are manufactured on the wafer surface at the front end of the line (FEOL). Companies use four basic operations in a variety of sequences and variations to produce microchips. These are material deposition, patterning, doping and heat treatment.

Active layers / substrates for RF

Integrated circuit manufacturing requires a substrate (Si, GaAs, InP, SiC or sapphire) that an active layer is grown on. This crystal growth is called epitaxy. An example is shown in Figure 3.37. In this case, the substrate is GaAs and the active layer is GaAs or InGaAs. The active layer's properties define the device's performance. The substrate is used as a physical support to build the device, but its physical properties (crystal lattice constant, coefficient of thermal expansion) must also be adapted to the active layer to obtain the best crystal quality and device performance. This is why a wide variety of substrates is used. In the case of GaN, Si or SiC, substrates are used in production, since GaN substrates are very expensive and limited in size. The main substrates per type of substrate are listed in Figure 3.37. RF devices are based on many semiconductors, including silicon (Si and SOI, silicon-on-insulator), gallium arsenic (GaAs), gallium nitride (GaN), silicon carbide (SiC), indium phosphide (InP) and silicon germanium (SiGe).

The piezoelectric materials used are lithium niobate and lithium tantalate ($LiNbO_3$ and $LiTaO_3$). They are produced as bulk wafers (Nakamura 2012).

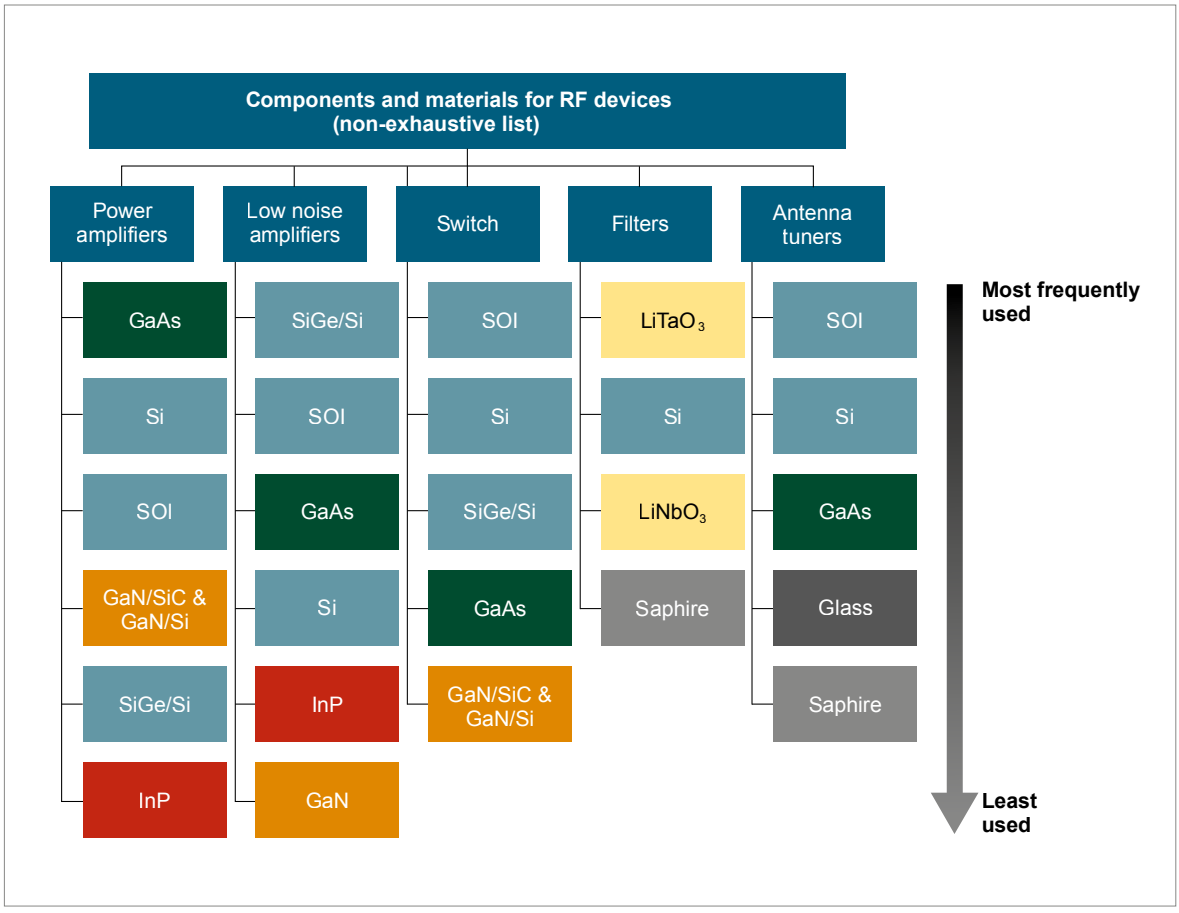

Figure 3.37: List of substrates used for the main components of RF devices (source: own representation)

Note: SOI means 'silicon on insulator'. GaN/Si means that a GaN layer was applied to a Si wafer.

Considering the thickness of materials deposited on the wafer (a few nanometres to few micrometers), most of the materials actually come from the wafer itself (around 500–700 µm thick). It must, however, be considered that the epitaxy processes can sometimes be very inefficient, leading to high material losses (up to 70 % material loss) (Horowitz et al. 2018). But these losses are only small amounts compared to the material needed for wafer production. This is why we will only consider the wafer in the sections that follow.

Gallium arsenide (GaAs)

Some of gallium arsenide's (GaAs) electrical properties are better than silicon's electrical properties. The electron velocity and electron mobility are higher, meaning that transistors that operate at several hundred GHz can be produced. They also have less noise than silicon devices at these high frequencies and can operate at higher power levels because they have a higher breakdown voltage. Gallium arsenide components are ten times faster than silicon ones. They are also less susceptible to faults and have lower energy requirements. Because of these properties, GaAs circuits (GaAs ICs) are particularly suitable for high-frequency power applications in mobile phones, for wireless local area networks (WLANs) and global positioning systems (GPSs). GaAs ICs are also used in microwave electronics, cable TV receivers, telecommunication devices and military and space applications (Yole Développement 2020b). Figure 3.38 is a diagram of a GaAs transistor.

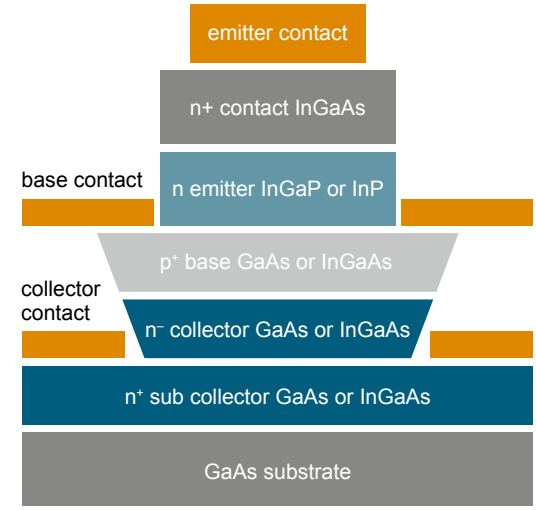

Figure 3.38: Diagram of an HBT (heterojunction bipolar transistor) on a GaAs substrate (source: Freiberger Compound Materials 2020b)

Indium phosphide (InP)

InP-based heterojunction bipolar transistors (HBTs) and high electron mobility transistors (HEMTs) offer performances that are far superior to GaAs (superior electron mobility, better thermal dissipation than GaAs), making them ideal for high-speed RF applications. Figure 3.39 shows a cross-section of an InP HEMT device. But their high costs and limited substrate size restrict the InP market to the RF niche market and low volumes. InP HF devices are currently used in automatic test equipment, military and defence applications, radar equipment and security applications.

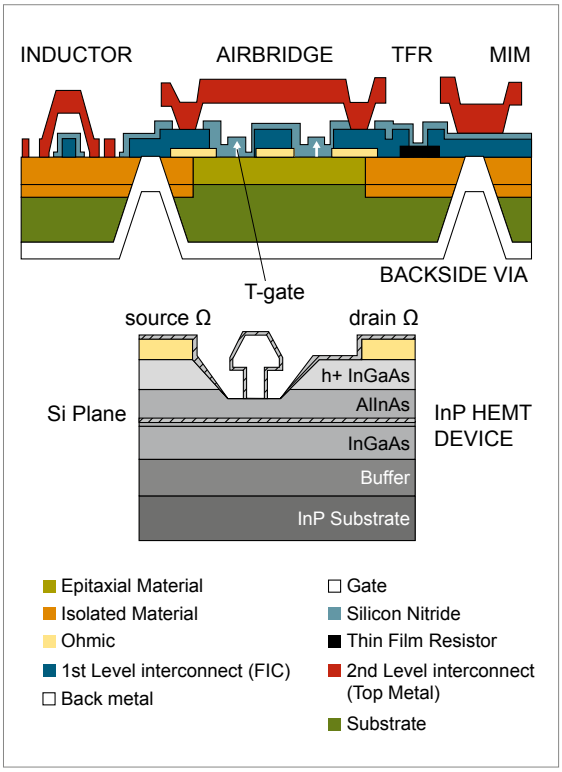

Figure 3.39: Cross-section of an InP HEMT device (source: Deal 2014)

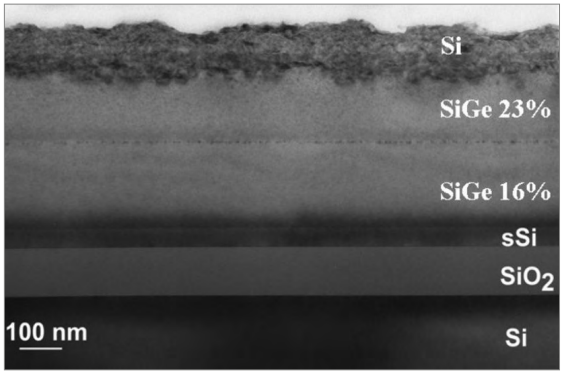

Figure 3.40: Cross-section of SiGe layers of different molar ratios on a silicon wafer (source: Cisco 2018)

Germanium (Ge)

Pure germanium wafers are mainly used as substrates for III–V solar cells. Ge wafers measuring 300 mm in diameter can be produced using the Czochralski crystal growth process. If germanium is grown epitaxially on silicon wafers, we call them 'epitaxial Ge wafers'. Ge or SiGe is deposited on a silicon substrate by chemical vapour deposition (see Figure 3.40). Silicon germanium (SiGe) refers to the alloy Si1-xGex, which consists of a molar ratio of silicon and germanium.

SiGe components are used for wireless devices, wireless local area networks (WLANs), optical communication systems, hard drives, automotive chips and global positioning systems (GPSs). SiGe transistors are small, produce little noise and are energy efficient, so they extend mobile devices' battery lives.

They operate more stably at high temperatures and in the ultra-high frequency range. Very fast SiGe chips can be produced with known production technologies, like those in the silicon chip industry. While SiGe processes are similarly expensive to those for silicon complementary metal oxide semiconductor (CMOS) production, they are cheaper than other heterojunction technologies like GaAs.

Gallium nitride (GaN)

Gallium nitride devices are attractive for high-power applications at low frequency ranges. Most GaN RF devices are power amplifiers. GaN-based low noise amplifiers (LNAs) and switches are also available, but more for niche markets (mainly military applications). The wireless infrastructure will be the main driving market in the GaN RF business in future (Yole Développement 2019b) (see Section 3.5.3 '5G / 6G'). 5G and 6G developments will increase in the coming years and boost the volume of GaN.

Silicon (Si)

Silicon is the main material used in RF communications, and it is also a critical material according to the EU (European Commission 2020b). Despite this, silicon is used in all types of integrated circuit, not just RF. While it would indeed make sense to calculate the amount of Si for global microelectronic manufacturing, not just RF, this is not the scope of this synopsis.

Lithium niobiate (LN) and lithium tantalate (LT)

Lithium niobate ($LiNbO_3$) (also referred to as "LN") and lithium tantalate ($LiTaO_3$) (also referred to as "LT") are piezoelectric materials that can convert an electrical signal into mechanical energy, like sound waves, and back. The filters can be produced on 4.5" or 6" bulk LN or LT wafers. Most wafers use $LiTaO_3$ as the base material. A new piezoelectric-on-insulator (POI) approach, an $LiTaO_3$ exclusive, was recently launched by SOITEC (Butaud et al. 2020). The POI volume remains small for now, but might increase in future. SOITEC signed an agreement with Qualcomm in July 2020 regulating the supply of POI substrates for 4G and 5G RF filters (Joosting 2020). A bulk LT wafer is bonded on an Si wafer. After debonding, only a thin layer of LT remains on the Si wafer for device production. The rest of the LT wafer can theoretically be reused to prepare a new POI substrate (see Figure 3.41). This might be a solution in future to encourage more sparing use of lithium tantalate-based materials, but no information about material reuse could be found. The process is also limited to $LiTaO_3$ and SAW (surface acoustic wave) filters.

It is worth noting that yttrium (a rare earth element) and thallium (a highly toxic material) are also used in what are known as "high-temperature filters" (HTFs) thanks to their microwave super-

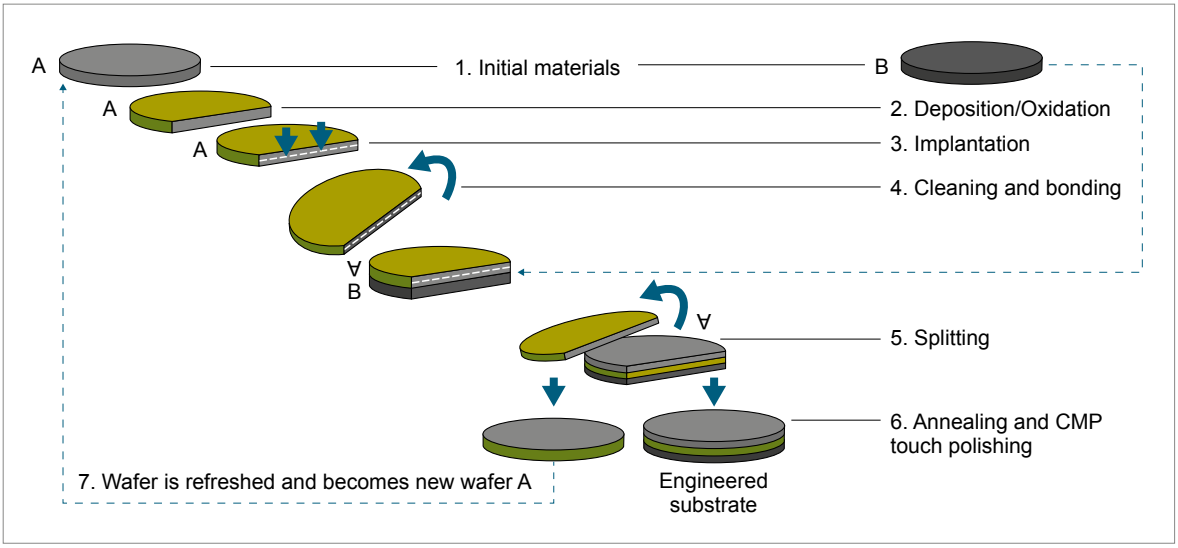

Figure 3.41: Piezoelectric on insulator (POI) smart cut™ process diagram from SOITEC (source: Butaud et al. 2020)

conducting properties. $YBa_2Cu_3O_{7-\delta}$ (YBCO) or $Tl_2Ba_2CaCu_2O_8$ (TBCCO) layers are deposited on ceramic substrates like $LaAlO_3$, MgO or sapphire (2" substrate for volume production). What makes HT filters attractive is their enhanced sensitivity to improve signal reception and their exceptional selectivity to reject interfering signals. They also demonstrate a very low level of resistance, so devices that are much more compact than the equivalent devices designed with traditional materials can be built. However, HT filters must be combined with a cooling system, since they operate at low temperatures (Simon et al. 2004). HT filters are primarily used in mobile communication base stations, in radar systems and in radioastronomy (Sun & He 2014). While it was not possible to estimate the amount of yttrium and thallium, it should still be small compared to gallium and arsenic.

3.2.5.2 Raw material content

We will focus on the GaAs, InP and piezoelectric substrates.

Semiconductor wafers

The net amount of Ga, As, In and P is calculated based on the wafer thickness (AXT 2020; Freiberger Compound Materials 2020a), the GaAs and InP densities (5.315 g/cm³ and 4.81 g/cm³ respectively) and the molecular weight (see Table 3.40). The gross percentage of the semiconductor element takes into account the material loss during wafer production. In GaAs production, the material utilisation rate is around 45 % (Clemm et al. 2017). This figure includes inner loop recycling, where intermediate waste is reintroduced in wafer synthesis. No data could be found on material utilisation for InP wafer production, which is why we assumed the rate would be the same as for GaAs wafer production.

Table 3.40: Quantity of Ga, As, In and P per wafer for RF application (gross demand)

	GaAs-wafers	InP-wafers
Wafer size	6"	4"
Thickness	675 µm	600 µm
Material utilisation rate in wafer production	45 %	45 %
Gallium demand per wafer	70.1 g	
Arsenic demand per wafer	75.3 g	
Indium demand per wafer		42.7 g
Phosphorus demand per wafer		11.5 g

Note: Gross demand is the amount needed for wafer production, including material losses during production.

Table 3.41: Amount of Li, Nb and Ta per ceramic wafer (net content)

	$LiNbO_3$-wafer	$LiTaO_3$-wafer
Wafer size	6”	6”
Thickness	500 µm	500 µm
Lithium	n: 2.0 g	n: 2.0 g
Niobium	n: 26.6 g	
Tantalum		n: 52.2 g

Note: Net content is the mass of the elements contained in the wafer. It is not the mass required for production.

Table 3.42: Quantity of Ga per wafer for RF application (gross demand)

	GaN on Si	GaN on SiC
Wafer size	6”	4”
GaN thickness	5 µm	3 µm
Ga mass in wafer	0.5 g	0.1 g
Material utilisation rate in wafer production	80 %	80 %
Production yield	70 %	90 %
Gallium demand per wafer	0.6 g	0.2 g

Note: Gross demand is the amount needed for wafer production, including material losses during production.

Ceramic wafers

The net amount of Li, Nb and Ta considered in Table 3.41 are calculated based on the wafer size and thickness, as well as on the material density (4.64 g/cm^3 and 7.46 g/cm^3 for $LiNbO_3$ and $LiTaO_3$ respectively). We were unable to calculate the gross element amount, since no information on material utilisation during the wafer production process could be found.

3.2.5.3 Foresight industrial use

InP

InP RF devices are currently used in automatic test equipment, military and defence applications, radar equipment and security applications. Due to the limited size and high costs, there is currently no market pressure for high-volume RF applications. There are no expectations that InP will enter the mass market before 2040, so the amount of InP wafers for this application is likely to be very low and remain stable until 2040 (Yole Développement 2019a). The mass of indium required for the actual InP production for RF chips is estimated at around 1 tonne for 2018 and should remain stable. InP wafers are primarily used in optoelectronic components.

GaN

Gallium nitride (GaN) crystal growth is still in its infancy at present. GaN is not available yet as a substrate for semiconductor electronics. GaN components are built on silicon (6 inch) or silicon carbide (SiC) (4 inch) wafers. The GaN layer on SiC is about 3 µm. On Si, a buffer layer of $Al_xGa_{1-x}N$ is needed to make up for the lattice mismatch between GaN and Si, so the AlGaN / GaN layer is thicker (~5 µm). The production yield is then lower too, since the epitaxy is more complex. The Ga mass per wafer is calculated as per the parameters set out in Table 3.42. The number of silicon and silicon carbide wafers for GaN devices remains small compared to GaAs wafers. In 2018, roughly 48,000 SiC wafers and 400 silicon wafers were sold for GaN RF devices. The market is expected to grow rapidly in the next few years due to 5G (see Section 3.5.3 ‘5G / 6G’) with a 116 % CAGR between 2018 and 2024.

As a worst-case scenario for 2040, it can be assumed that the market for GaN devices is directly linked to the growth in mobile phone sales presented in the ‘5G / 6G’ technology synopsis (see Section 3.5.3). Indeed, GaN components should be extensively adopted in 5G / 6G infrastructure (see Section 3.5.3). If the number of Si / SiC wafers sold is correlated with this growth, it can be estimated that between 1 and 2 tonnes of Ga (depending on the SSP1-2-5 scenario) will be required for GaN RF components in 2040. Even considering an extreme increase in wafer sales due to the exponential growth of mobile internet traffic, the amount of Ga associated with GaN RF devices remains low compared to GaAs devices.

GaAs

According to Yole Développement (2020b), the demand for frequency filters with GaAs-based amplifiers is largely dependent on the number of mobile phones, as approximately 93 % of these filters are used in mobile phones. In recent years, the number of mobile phone connections has strongly and steadily increased (Statista 2021a), although growth rates have dropped considerably over the last decade. The number has hardly increased since 2019. With approx. 8.2 billion connections, it exceeds the global population of approx. 7.8 billion people (Statista 2019b). The growth in connections in recent years has been driven primarily by countries in Asia and Africa. In contrast, Europe and North and Latin America saw only slow growth in the number of mobile phone connections. The market in these parts of the world has now become saturated. Due to this development of the mobile phone market in recent years and due to the fact that the number of mobile phones considerably exceeds the world's population, it is assumed for the calculations of the raw material demand for GaAs-based amplifiers in mobile phones that the total number of mobile phones will increase with the population growth from 2026 onwards.

Yole Développement (2020b) is forecasting 6 % average annual growth from 2019 to 2025 for GaAs semiconductors in mobile devices. For the period from 2019 to 2025, an 81 % average annual growth rate for 5G-capable mobile phones has been calculated from sales forecasts of different-generation mobile phones (Yole Développement 2020b). So this growth in 5G handsets is causing the 6 % annual growth in GaAs amplifiers.

The Yole forecast is used for the period from 2019 to 2025 to determine the demand for gallium in 2040 in the various SSPs. On this basis, it is assumed that the different data traffic of the digitisation scenarios SSP1, SSP2 and SSP5 will determine the growth of 5G-capable mobile phones and thus GaAs semiconductors after 2025, when 5G networks are expected to be widely expanded. The following growth rates between 2025 and 2040 were assumed for the individual scenarios:

– SSP5: the share of 5G-enabled mobile phones in mobile phone sales increases by an average of 81 % annually from 2019 to 2025, starting with 19 million units. This continues after 2025 until market saturation, i.e. 100 % of new mobile phones sold are 5G-enabled. According to Yole Développement (2020b), this growth corresponds to an average annual increase in GaAs amplifiers of 6 %. By introducing 6G from 2030, these growth rates are repeated, so that from 2039 all mobile phones sold are 6G-capable. Alternatively, since the amplifiers can also be manufactured with silicon technology for frequencies above 6 Hz, as of 2030 the growth in 5G/6G mobile phones is only expected to be 0.7 %, corresponding to annual global population growth in this period. The annual increase in GaAs semiconductors is therefore 0.14 % over this period.

– SSP2: The 5G-compatible mobile phones' share of sales grows by an average of 40 % per year after 2025 until the market becomes saturated. From 2030 onwards, the share of 6G-compatible mobile phones is expected to increase by an average of 40 % per year, starting with 9.5 million units, until market saturation. Alternatively, there are assumptions that from 2030 onwards the further increase will only be in line with global population growth, since the 6G-specific frequencies beyond 6 GHz will be implemented in or integrated with silicon-based technology.

– SSP1: The share of 5G-compatible mobile phones is only seeing 0.7 % annual growth after 2025, which equates to the rise in the global population according to Statista (2019b). The introduction of 6G from 2030 to 2036 causes an annual increase of 40 % starting with 9.5 million units, as in SSP2. Thereafter the proportion of these phones will again grow analogously to global population in this period.The alternative scenario described in SSP2 and SSP5 is also considered here, so that from 2030 continued annual growth in GaAs amplifiers is 0.14 %, resulting from the growth in global population.

The GaAs wafer sales forecasts (with the 'without integration in silicon technology' scenario) are shown in Figure 3.42.

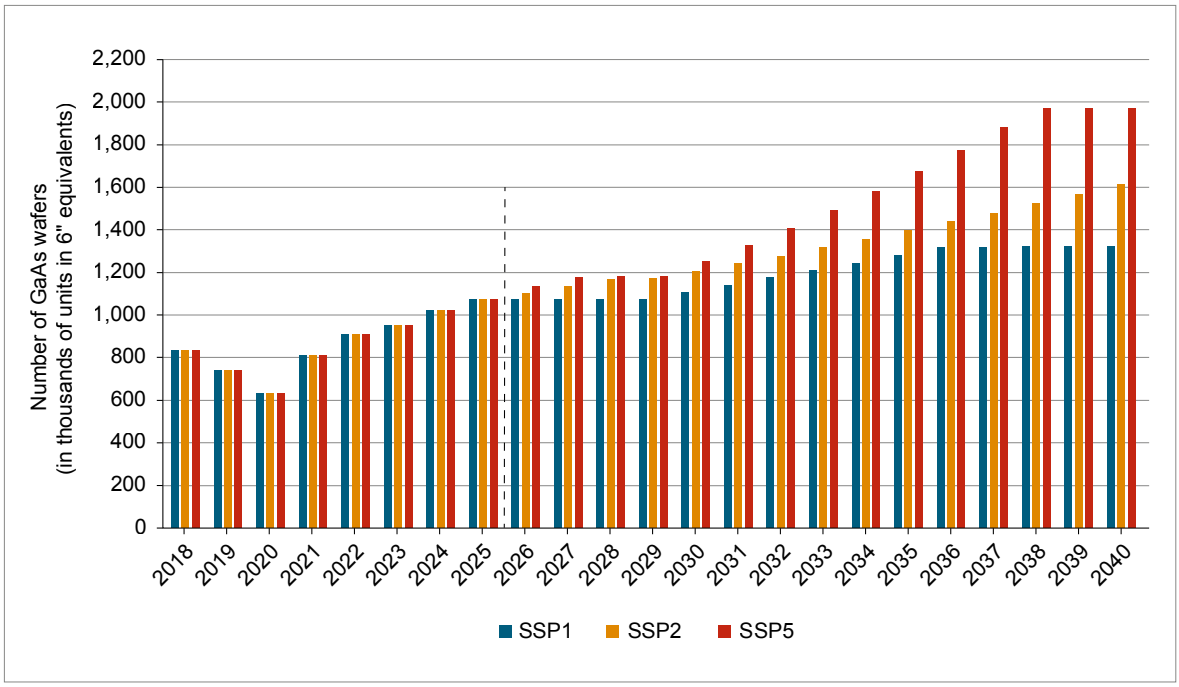

Figure 3.42: Market for GaAs wafers (scenario without integration in silicon technology) in thousands of units sold (source: 2018 to 2025: Yole Développement (2020b), 2026 to 2040: own forecast)

$LiTaO_3$/$LiNbO_3$

LT/LN substrates will still form a key part of wafer consumption, but the ratio of LT / LN wafers compared to the rest of wafer consumption will decrease due to silicon-based filters (Yole Développement 2020a). The $LiTaO_3$ and $LiNbO_3$ wafer sales forecasts (in 6" equivalence) can be found in Figures 3.43 and 3.44. Yole is forecasting 6 % and 17 % CAGR for $LiTaO_3$ and $LiNbO_3$ respectively between 2020 and 2025 in the RF market. The same scenarios (SSP1-2-5) as described for GaAs wafers (see above) are considered for the 2026–2040 period.

3.2.5.4 Foresight raw material demand

Based on the raw material demand for wafers (Table 3.40 and Table 3.41) and on wafer demand forecasts (Figures 3.42, 3.43 and 3.44), we can estimate the amount of raw materials required for 2040. The annual gallium demand is illustrated in Figure 3.45. During the production of GaAs semiconductors, according to Clemm et al. (2016), only about 45 % of the gallium used goes into the product. This is why the quantities that are not incorporated in the product during production (55 %) are shown in addition to the gallium in the wafers. According to Clemm et al. (2016), waste containing gallium is treated in recycling processes and gallium is also recovered in the process. However, it is not known what the gallium recycling rates are here. So the gallium demand in Figure 3.45 is a worst-case scenario, assuming that this gallium is not recycled or is only recycled to a very small extent, since the gallium in the GaAs semiconductors has not been recycled to date either. The gallium content in the semiconductors thus represents the "best case" under the assumption that gallium is recycled from the production residues at very high rates and thus hardly any gallium is consumed net via the gallium demand in the GaAs semiconductors.

Table 3.43 compares global production in 2018, the amount of material for the RF market in 2018, and the 2040 demand forecast for various materials. The largest quantities of semiconductor materials for RF components are silicon (this report does not contain any estimated volumes) and GaAs. Sales with GaAs power amplifiers are identical to those in Section 3.5.3 '5G (6G)', since the mobile phone is the main market for GaAs.

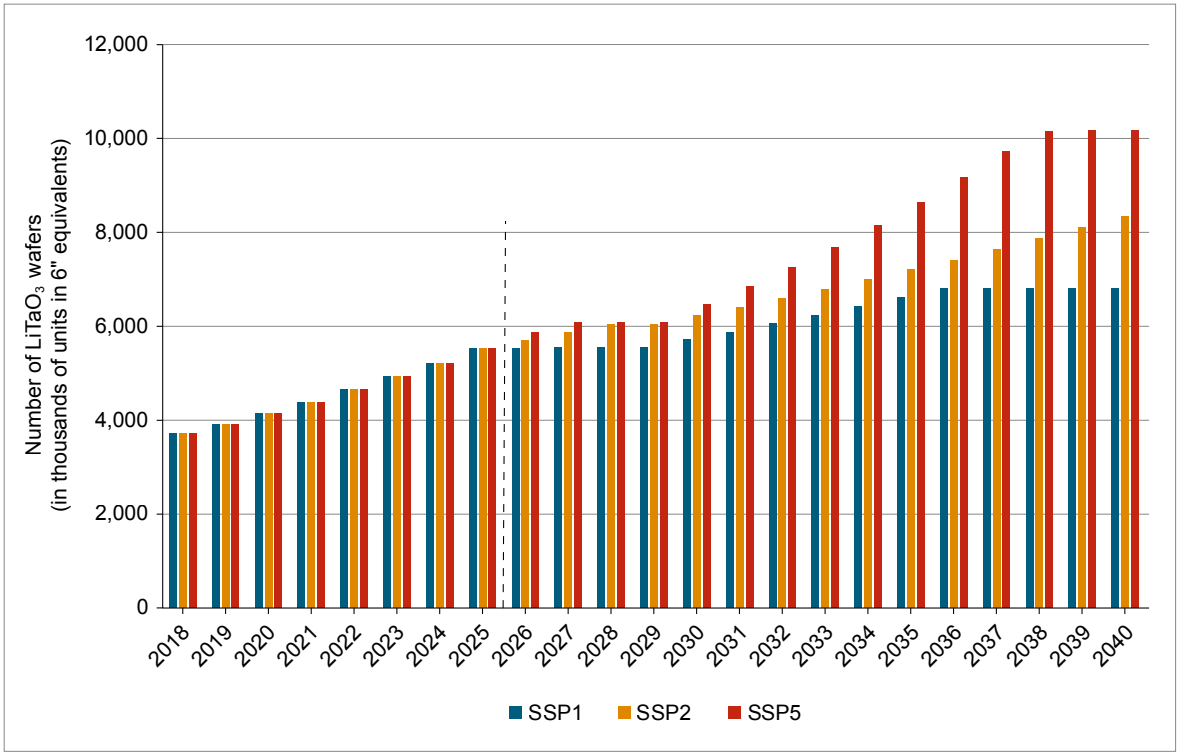

Figure 3.43: Market for $LiTaO_3$ wafers in thousands of units sold (source: 2018 to 2025: Yole Développement (2020b), 2026 to 2040: own forecast)

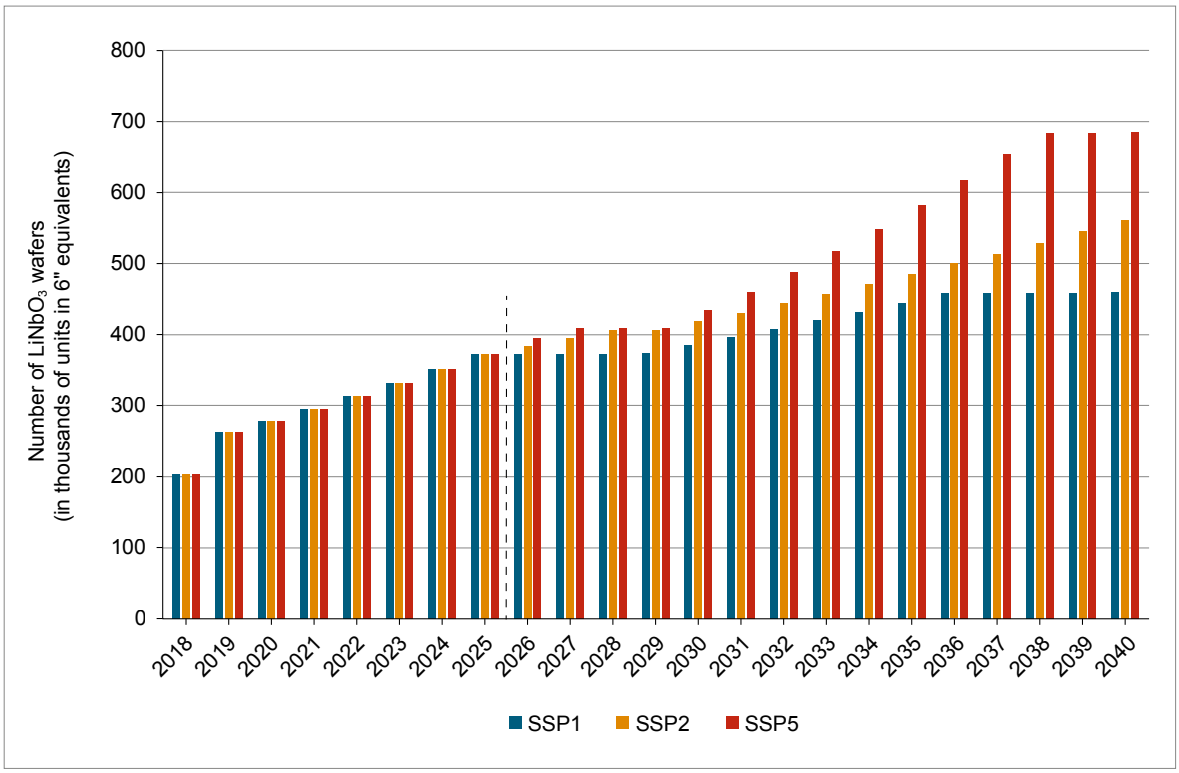

Figure 3.44: Market for $LiNbO_3$ wafers in thousands of units sold (source: 2018 to 2025: Yole Développement (2020b), 2026 to 2040: own forecast)

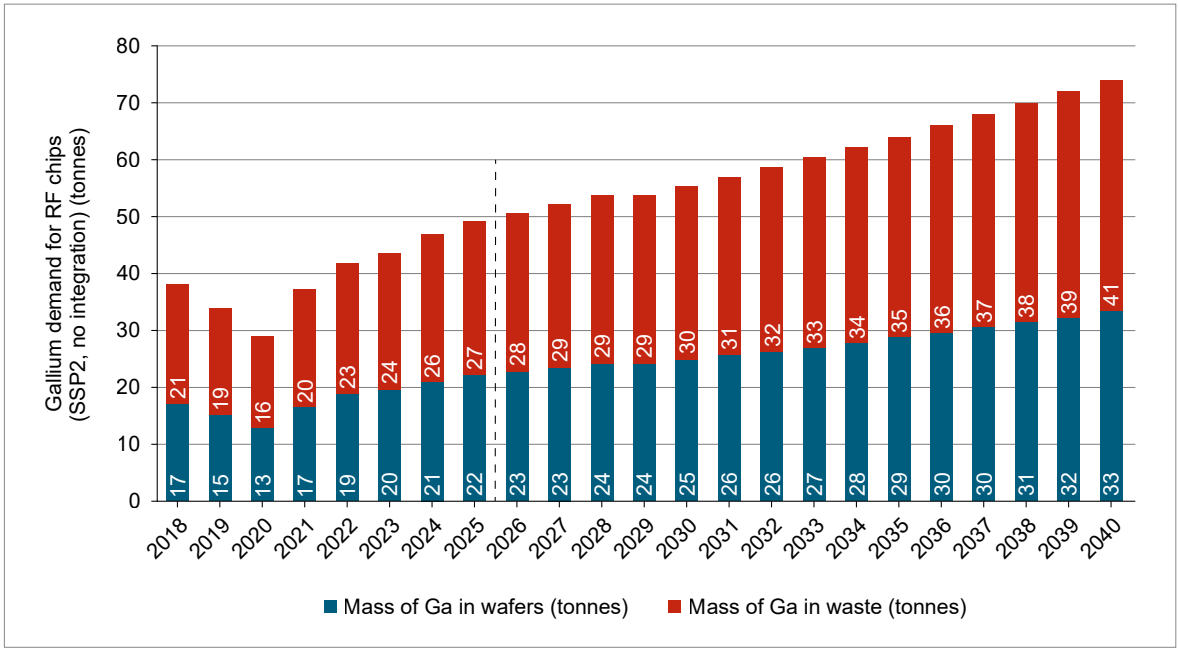

Figure 3.45: Trend in gallium demand for RF chips (source: 2018 to 2025: YOLE DÉVELOPPEMENT (2020b), 2026 to 2040: own forecast)

Table 3.43: Global production (BGR 2021) and calculated raw material demand for GaAs, $LiTaO_3$ and $LiNbO_3$ wafers, in tonnes

Raw material	2018		2040 (no integration)			2040 (with integration)		
	Production in 2018	Demand in 2018	SSP1	SSP2	SSP5	SSP1	SSP2	SSP5
Gallium (total)	413 (R)	38	60	74	90	49	54	54
Ga in semi-conductors		17	27	33	41	22	24	24
Ga in waste (min.)		21	33	41	50	27	30	30
Lithium	95,170 (M)	8	15	18	22			
Niobium	68,200 (M)	5	12	15	18			
Tantalum	1,832 (M)	194	356	435	531			

M: Mine production (tonnes of metal content)
R: Refinery production (tonnes of metal content)

Gallium is also used in GaN layers in some RF components. However, this amount of gallium was not calculated in this estimate because it is very small.

Piezoelectric materials make up a significant amount of materials too, even though they are only used in one type of component (the filter). It should be noted that only the net quantity (only the material contained in the wafer) is taken into account for tantalum, niobium and lithium, whereas the gross quantity (taking manufacturing losses into account) is indicated for semiconductors. This forecast probably underestimates the actual amount of lithium, tantalum and niobium needed for RF chips.

3.2.5.5 Recycling, resource efficiency and substitution

Recycling

Gallium, indium, lithium and niobium from end-of-life electronic products are not recycled at present. The reasons for this include the greater economic incentive to pyrometallurgically recycle the precious metals that the components contain (European Commission 2020b). The hydrometallurgical recycling of gallium from production waste from photovoltaic production is technically feasible (Marwede 2013).So far, however, there have been no attempts to determine whether extraction from components is also possible. The multitude of chemical elements in the component, the low gallium and indium concentrations in the component (Clemm et al. 2016) and the need previously to identify and separate the components from the electronic scrap cast doubt on the economic feasibility. The fine distribution of these elements in different products and components also makes it difficult to collect sufficient quantities for recycling.

However, pre-consumer recycling (from industrial waste) is an important secondary source of gallium and indium. Closed loop recycling often occurs in the industry, mainly for economic reasons. The manufacturing processes of GaAs and GaN wafers are considered the most important secondary source of the metal, with about 60 % scrap being produced and recycled in a “closed loop” (Licht et al. 2015; European Commission 2020b). A material flow analysis of GaAs wafer production reveals that 55 % of the Ga and As introduced in the manufacturing process is not contained in the wafer. Post-industrial waste from GaAs wafer production can be treated for gallium recovery operations (Clemm et al. 2016). However, the recycling rates achieved for gallium during this process are unknown (Licht et al. 2015).

Resource efficiency

As can be seen from Figure 3.37 of the technology description (3.2.5.1), there are many technologies for all the RF components. Some of them do not include the critical materials mentioned in this study. However, GaAs, InP, $LiTaO_3$ and $LiNbO_3$ have special properties that currently meet the market’s requirements. But this market can be highly volatile, and one technology can be rapidly replaced by another as costs are cut or performance is improved. Predicting which material will be used in future is almost impossible.

It is also worth mentioning that GaAs, InP and piezoelectric wafers could be replaced by silicon wafers that a thin layer of GaAs, InP or piezoelectric material is deposited on. In actual fact, the most important part of the material is the surface layer that the component is made on. Piezoelectric substrates-on-insulator (POI) and GaN on Si are already in production (made by SOITEC, as shown in Figure 3.41). Intense research is also ongoing into the manufacture of GaAs or InP on a silicon substrate, mainly as a cost-cutting endeavour and either by heteroepitaxy (Li & Lau 2017) or by layer transfer (Di Cioccio et al. 2005). These two approaches could be a way of significantly reducing the amount of III–V elements, but would also increase the demand for silicon, which is also a critical material according to EU specifications.

Substitution

The possibility of substituting gallium and indium in ICs is also limited, since III–V-based ICs were developed specifically for applications that silicon-based semiconductors are inadequate for, so these components cannot be substituted without impairing function or performance (Graedel et al. 2014).

3.2.6 Industrial robotics and Industry 4.0

3.2.6.1 Technology description

The term ‘Industry 4.0’ was coined in Germany in 2011. Industry 4.0 refers to the mass connection of information and communication technologies with industrial production facilities. In addition to this technical transformation, an organisational and cultural transformation is required to turn the vision of an agile business with a high degree of automated decision-making and execution into reality (Schuh et al. 2020).

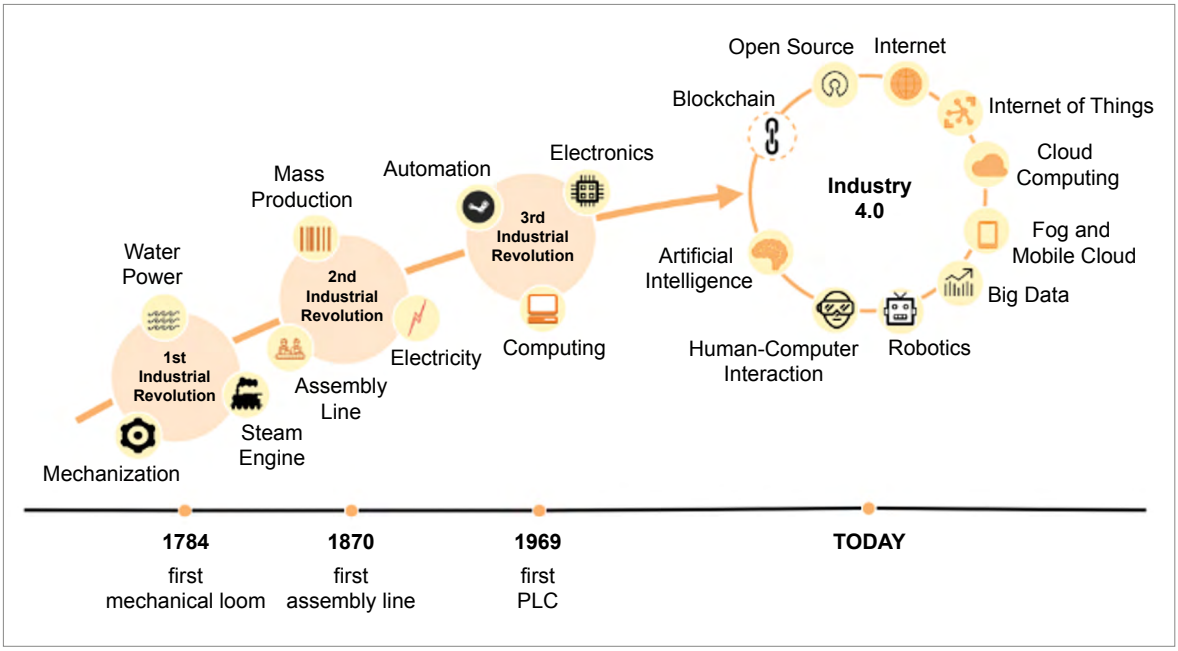

Figure 3.46: Technologies that drove the various industrial revolutions (source: Aceto et al. 2019)

Note: Blockchain technology is still in the research and introduction phase and is therefore shown with a dashed line.

From a technological standpoint, Industry 4.0 does not refer to a single piece of technology; rather, it can only be implemented through the interaction of many technologies. Figure 3.46 shows a schematic timeline of the four industrial revolutions and the associated triggering technologies. The figure shows that Industry 4.0 is driven by many different technologies, all of which are constantly evolving and are often difficult to demarcate. At the same time, they are closely intertwined and cannot be clearly distinguished from each other, partly due due to their historical development (Aceto et al. 2019).

Some constituents of Industry 4.0 are covered by other technology synopses, including Section 3.2.8 'Devices in the Internet of Things (IoT)', Section 3.5.3 '5G/6G' and Section 3.5.4 'Data centres'. There are also overlaps with the technology summaries entitled 'Autonomous driving of vehicles' (Section 3.1.4) and 'Aircraft for 3D mobility (eVOTL)' (Section 3.1.5). In the following, industrial robots are examined as an important aspect of Industry 4.0.

Definition

The VDI Guideline defines industrial robots as follows: 'Industrial robots are universally applicable motion automata with several axes, sequence and direction or angle of movement being freely programmable (i.e. without any need for mechanical intervention) and, in some cases, sensor-guided. They can be equipped with grippers, tools or other manufacturing equipment and can execute manipulation and/or production processes' (VDI Association Technologies of Life Sciences 2013).

Areas of application

Robots are used in many different industries, including automotive manufacturers and suppliers, aerospace, the food and beverage industry, textiles, wood and furniture, printing and paper, rubber and plastics, chemicals and pharmaceuticals, household appliances, precision mechanics, construction, foundry, ceramics and stone, as well as in agriculture. They are used for lots of different activities like welding, picking, painting, laser cutting, dismantling or measuring. In the non-industrial sector, robots can be found,

for example, in the field of medical technology, in the entertainment business or in service robotics, (DGUV 2015). This paper only examines the case of industrial robots, however.[5]

Design of an industrial robot

Industrial robots usually have three main axes and three secondary axes. We distinguish between different types of robots depending on how they can move their axes (translatory and rotatory). Serial kinematics involve a number of arms connected with joints; the last joint holds the tool. In contrast, a parallel robot's arms are mounted on the same plate and come together in an end effector, thus enabling three-dimensional movement (DGUV 2015). There are also stationary and mobile industrial robots (Oubbati 2007).

An industrial robot is usually built following the structure outlined below. It has a drive for moving the various limbs and for locomotion (if the robots are mobile). The drive consists of a controller, a gearbox and a motor. Acquired information is processed and actions are specified using the control system. The internal sensors collect on-board data about the robot's position and orientation, about the effector, and even about the general operating state (e.g. the battery charge level). External sensors provide feedback on the surrounding area, allowing responses to unforeseen environmental conditions. Examples include image processing systems, light barrier functions or ultrasonic sensors. The robot's tool is called an 'effector' and is usually a gripping, machining or assembly tool. The manipulator (the robot arm) makes the effector's movements in space (Oubbati 2007; DGUV 2015).[6]

Types of industrial robots

Within the industrial robots segment, we distinguish between caged robots and collaborative robots ('cobots'). Caged robots are traditional industrial robots developed for use in mass production; they can perform repetitive tasks with extreme precision. They are often stationary and fenced to prevent any risks of personal injury to employees (Mewawalla 2019). In contrast, cobots are designed to work with humans in specific tasks such as assembly, packaging or soldering. They are often much smaller, more mobile and can slow down movements more quickly, minimising the risk of injury. Unlike traditional industrial robots, they have a multitude of sensors that enable them to interact with their surroundings. Cobots are usually easy to program. As a result, users are not required to have extensive programming knowledge (rggroup 2020) and can manually guide cobots to teach them a movement (Kräusslich 2020). However, research by TU Berlin shows that cobots are being used statically and in coexistence at this moment in time, in a similar way to classic industrial robots, rather than in collaborative work (Kluy 2020).

3.2.6.2 Raw material content

Literature compiling raw material and material requirements for robots was hard to find; there were almost no sources available. In its publication entitled 'Materials dependencies for dual-use technologies relevant to Europe's defence sector', the JRC (Joint Research Centre, EU Commission) presents an overview of required raw materials, processed materials and components for robots in general; see Figure 3.47.[7] The authors list 44 raw materials for robot production.[8] Raw materials that are considered critical (i.e. that are at risk of supply shortages) are shown in red (Blagoeva et al. 2019).

In 2020, the JRC's publication entitled 'Critical raw materials for strategic technologies and sectors in the EU' again addresses the 2019 overview of raw materials and supplements it with a figure that allocates relevant raw materials for robots to

---

[5] Traditionally, the robotics market is split into two large segments: industrial robots and service robots. Service robots are all human support robots, such as robots used in the medical field and in households, logistics robots, drones or autonomous vehicles (Mewawalla 2019; Blagoeva et al. 2019). In contrast, industrial robots are ones that automate part of the production process. However, the transitions between the two categories are becoming increasingly smooth (Mewawalla 2019).

[6] This technology synopsis does not consider the topic of robots networking with one another and with a central control system; see the IoT technology synopsis regarding this matter.

[7] However, the JRC also seems to be facing inadequate sources; its citations include the site 'battlekit' as a source for production materials required for robots used in the defence and security sectors (Blagoeva et al. 2019), page 98.

[8] Rare earths are included as one raw material in this list

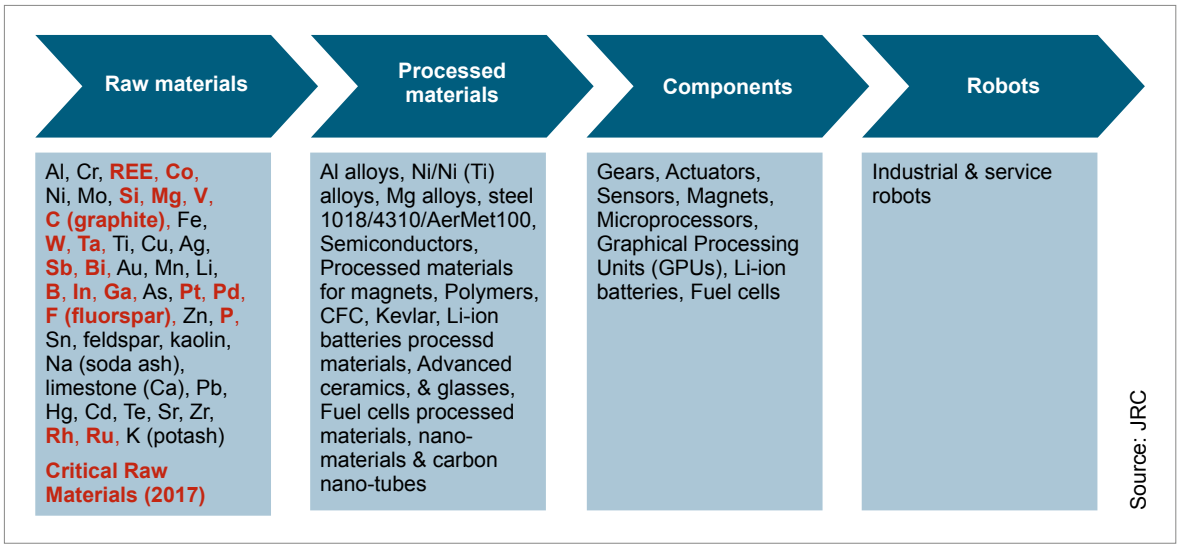

Figure 3.47: Robots: an overview of raw materials, processed materials and components (source: Blagoeva et al. 2019)

individual components; see Figure 3.48. However, it is not obvious what criteria it used to select the relevant raw materials.

The raw materials required for individual components are illustrated in this figure[9]:

- Electronic cables: Cu
- Electro-optical systems: Be, Ga, In
- Energy system: Ga
- Electroplating: Ni
- Manipulator: Ti
- Permanent magnet: B, Dy, Nd, Pr
- Sensors: In

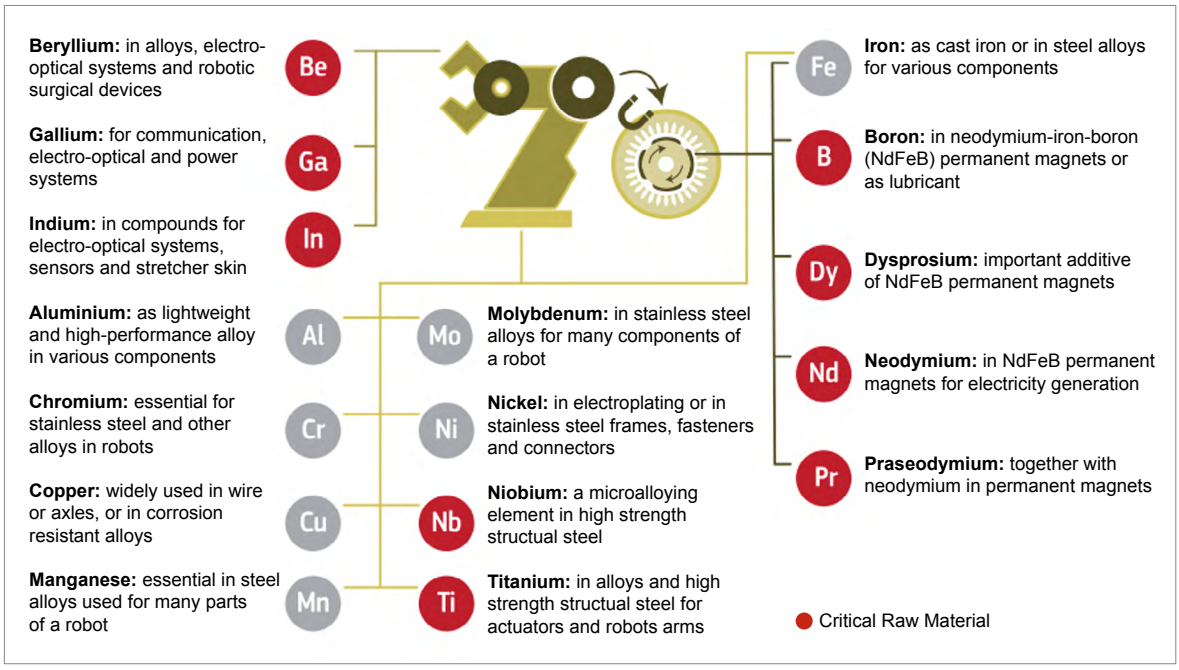

Figure 3.48: Relevant raw materials in robots (source: European Commission 2020a)

[9] Components and raw materials needed for other types of robots (e.g. medical robots used in surgery) are not listed.

– Various components[10]: Al, Cr, Cu, Fe, Mn, Mo, Nb, Ni

Kopacek & Kopacek (2013) dispute industrial robots' end-of-life management processes. To this end, they disassemble a Sony SRX-611 SCARA and report on its components and the materials it contains. The essential materials are steel, aluminium, plastic and cables. The authors describe the Sony SRX-611 SCARA as being comparable with a standard robot as regards recycling.[11] According to KUKA, a manipulator is essentially made from aluminium, cast iron, steel and plastic materials (KUKA 2021). The lower a robot's dead weight, the higher the payload it can carry. This is why KUKA has, for a long time now, been working with fibre composites to reduce the dead weight. However, fibre composites also have disadvantages compared to other materials, including complex processing, the fact that they are difficult to bond to other materials and their relatively high price (Schmirgel 2021).

The previous remarks illustrate the strong need for research into the raw material demand for the minimum components of industrial robots. Additionally, it is important to distinguish between robot types (min. collaborative robots and traditional industrial robots), since the raw materials needed vary greatly depending on the configurations. Industrial robots networking and sensory equipment requirements are still on the rise too; see the following section.

3.2.6.3 Foresight industrial use

Technological trends

A list of current trends in (industrial) robotics is provided below:

– New materials: smaller and lighter components, e.g. vanadium-based materials or lightweight metal alloys made from titanium, aluminium or magnesium (European Commission 2020)

– Energy generation from the environment, material sciences (OECD 2021)

– Soft robotics: "(...) class of deformable and compliant robots that can squeeze, stretch, climb, shape-change and self-heal (Terryn et al. 2017). Research in soft robotics aims to further develop abilities to grow, evolve, self-heal and biodegrade (Laschi et al. 2016). Many developments in soft robotics are inspired by examples from the natural world." (OECD 2021)

– Laser systems with an improved range and angle resolution, sensors (OECD 2021)

– LiDAR technology as an anti-collision system, originally used in autonomous vehicles; it is increasingly being used in robots. However, it is unclear whether it will become just as widely accepted as 3D cameras and ultrasound (Mewawalla 2019).

– Cloud-based robots and predictive control (Mewawalla 2019; OECD 2021)

– Edge computing (Mewawalla 2019)

– Neuromorphic processors: particularly suitable for recognising and analysing patterns, low energy consumption (Mewawalla 2019)

– More sensitive grippers, actuators (OECD 2021)

– Miniaturisation: "(...) In one of the most striking examples of miniaturisation to date, researchers at MIT recently built self-powered robots the size of a human cell. These robots are able to follow pre-programmed instructions, as well as sense, record and store information about their environment, gathering data that can be downloaded once a task is completed. While these robots are at the laboratory stage, potential uses exist in medical diagnostics and industry." (OECD 2021; Chandler 2918).

[10] This figure does not provide a more accurate classification.
[11] However, the Sony SRX-611 was made back in 1990. The authors claim there are no statistics on the robots' age; they estimate that it is 12 years old on average based on their experience.

– Intelligence: “Combining AI with other innovations is conferring a myriad of new capabilities on robots, including greater autonomy. Major developments include better vision, learning transfer between robots and across robot swarms, learning in virtual environments, learning by doing, learning by curiosity, emotional awareness, better object manipulation and more collaborative robots (‘cobots’).” (OECD 2021). Self-learning robots reduce the time and effort required for programming, especially to set parameters (Schmirgel 2021).

– Cobots: “With the ability to work in tandem with humans, modern robotic systems are able to adapt to a rapidly changing environment. The range of collaborative applications offered by robot manufacturers continues to expand. Currently, shared workspace applications are most common. Robots and workers work alongside each other, completing tasks sequentially. Applications in which the human and the robot work at the same time on the same part are even more challenging. Research and Development (R&D) focuses on methods to enable robots to respond in real time.” (Heer 2020). According to Götz (2018) and Schmirgel (2021), many industrial companies’ aim is to use robots without protective fences, since they are inflexible and take up lots of space. We can also distinguish between several levels of ‘human-robot collaboration’, with the degree of collaboration increasing with each level: separate workspaces, coexistence, cooperation and (finally) collaboration. However, the last stage (collaboration, working on a part at the same time) is still very rare in industry. A different level is suitable depending on the activity to be automated. It is now also possible to work with larger industrial robots without a protective fence (e.g. in final assembly in the automotive industry). The production stations of tomorrow will therefore be designed as a function of various influencing variables, such as cycle times, batch sizes, employee availability and processes (Götz 2018). If the number of humans working with robots is only set to increase in future, this will also require robots to be simple and intuitive to use (Schmirgel 2021).

Market development

According to the IFR (2020), 373,240 industrial robots worth USD 13.8 billion in total (excluding software and peripherals) were installed globally in 2019, with an estimated inventory of 2,722,077 industrial robots. Since 2010, the demand for industrial robots has been steadily increasing; growth between 2014 and 2019 averaged 11 %. In 2019, however, global sales figures fell by 12 % in the two main sales sectors especially (i.e. the automotive and electronics industries). This reflects the ‘difficult times’ that these two sectors are facing, and is also related to the trade conflict between the USA and China. Nevertheless, the automotive industry is still the largest consumer of industrial robots in 2019 (28 %), followed by electronics (24 %), metal and mechanical engineering (12 %), the plastics and chemicals industry (5 %), food (3 %), other (8 %) and no specific industry (20 %) (Statista 2019a; IFR 2020). There are five (main) sales markets for industrial robots, where 73 % of all industrial robots were installed in 2019: China, Japan, the USA, South Korea and Germany.

The International Federation of Robotics’ 2020–2023 sales forecasts are vague; it is expecting sales to nosedive in 2020 due to the COVID-19 pandemic. It is expecting a digitisation boom and therefore excellent industrial robot sales prospects in the medium term. Tractica is forecasting a turnover of USD 18.25 billion in 2025; the forecast is from 2018 (Statista 2020); see Figure 3.49. Taking its turnover into account, this would result in an average annual growth rate of 4.03 % between 2019 and 2025. In contrast, Frost & Sullivan (2020a) are estimating a turnover of USD 38.3 billion with an average annual growth rate of 12.2 % between 2019 and 2024; see Figure 3.50. Frost & Sullivan (2020a) are thus predicting more than double the revenue for 2024, and their projected annual growth rates are steadily increasing, with 2024 having the highest rate (18.3 %). Tractica’s growth rates, on the other hand, are steadily declining to a projected 1.33 % growth rate for 2025.[12]

Cobots’ share of the industrial robots segment is approx. 4.83 % in 2019 according to the IFR (2020). But cobots are the fastest-grow-

[12] Certain differences can probably be explained by different system limits (e.g. to what extent software is included). Tractica is assuming USD 13.85 billion, and Frost & Sullivan USD 19.43 billion for the 2018 turnovers (which are not estimates).

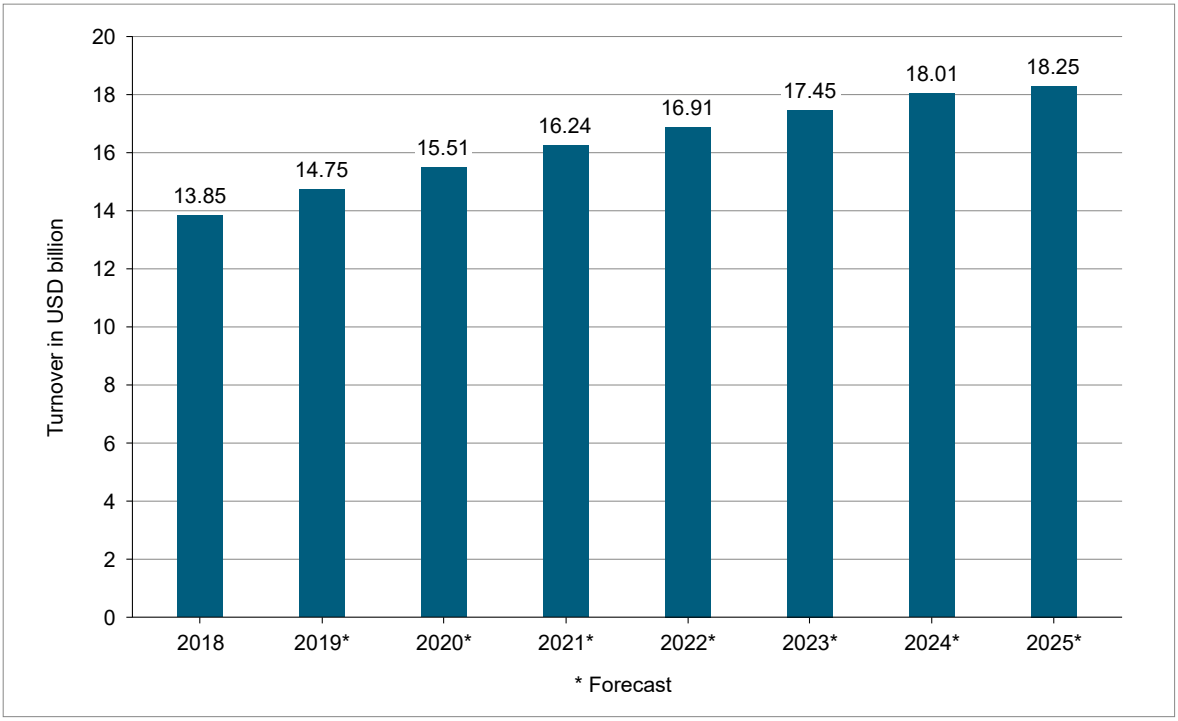

Figure 3.49: Sales volume for industrial robots worldwide between 2018 and 2025 (in USD billion) (source: STATISTA 2020)

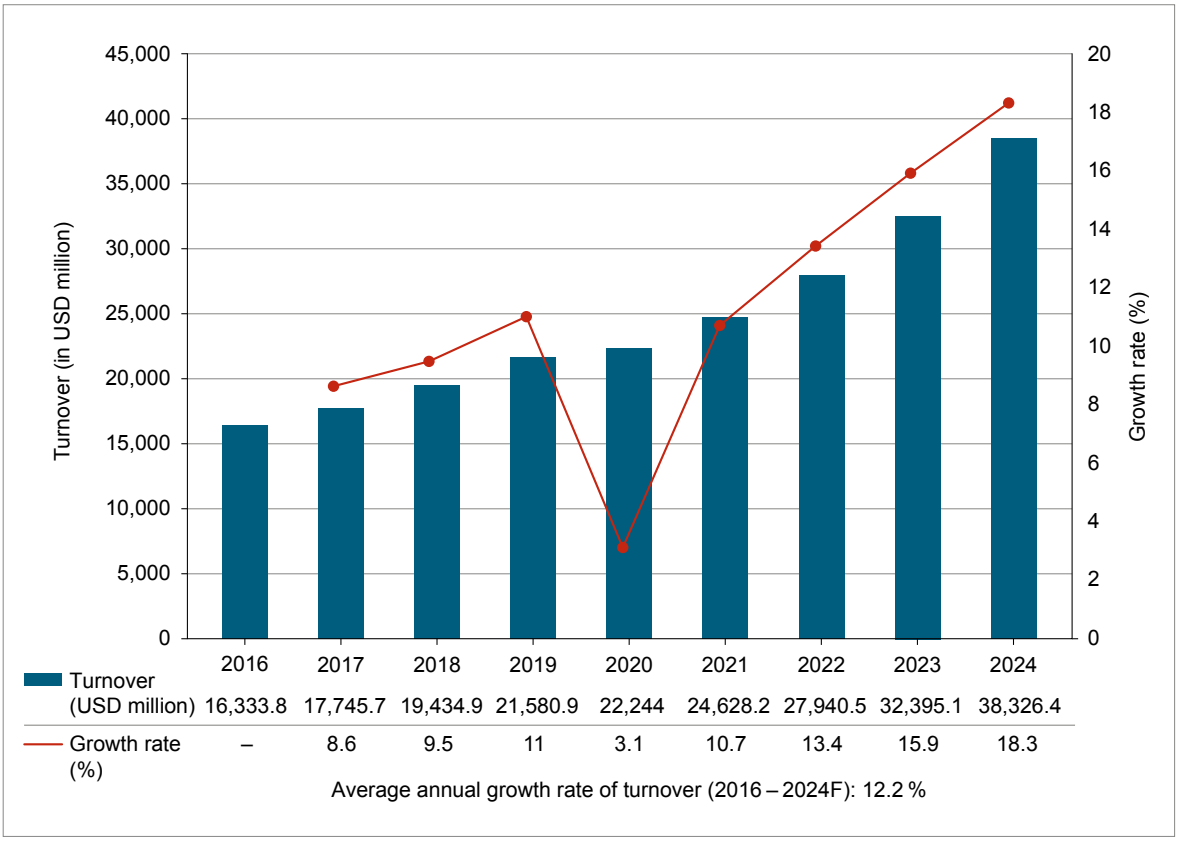

Figure 3.50: Sales forecast for industrial robots worldwide between 2016 and 2024 (in USD million) (source: FROST & SULLIVAN 2020a)

ing segment within the industrial robots sector (Mewawalla 2019). Neumeier (2020) and Schmirgel (2021) believe that the trend towards cobots is clear to see, especially given that they are easy to use and program and can be set up quickly. Cobots are also becoming more attractive from a 'value for money' standpoint, and technology is improving at the same time too (Schmirgel 2021). Frost & Sullivan (2020a) are showing exponential growth for cobots within their forecasts until 2024. But since they are still relatively new compared to traditional industrial robots, their share of the industrial robotics market remains low despite their high growth (Mewawalla 2019).

Leading industrial robotics companies are ABB, Fanuc, Kuka, Yaskawa, Estun and Siasu. Companies operating in the field of robotics software and hardware development are important too (Mewawalla 2019; Frost & Sullivan 2020a).

Table 3.44: Sales trend for industrial robots worldwide to 2040 (source: Riahi et al. 2017)

Year	SSP1		SSP2		SSP5	
	Turnover in USD billion	Growth rate	Turnover in USD billion	Growth rate	Turnover in USD billion	Growth rate
2018	13.85	–	13.85	–	13.85	–
2019*	14.75	6.50 %	14.75	6.50 %	14.75	6.50 %
2020*	15.51	5.15 %	15.51	5.15 %	15.51	5.15 %
2021*	16.24	4.71 %	16.24	4.71 %	16.24	4.71 %
2022*	16.91	4.13 %	16.91	4.13 %	16.91	4.13 %
2023*	17.45	3.19 %	17.45	3.19 %	17.45	3.19 %
2024*	18.01	3.21 %	18.01	3.21 %	18.01	3.21 %
2025*	18.25	1.33 %	18.25	1.33 %	18.25	1.33 %
2026	19.01		18.84		19.18	
2027	19.81		19.46		20.16	
2028	20.63	4.18 %	20.09	3.26 %	21.19	5.11 %
2029	21.50		20.75		22.27	
2030	22.39		21.43		23.41	
2031	23.26		22.02		24.54	
2032	24.16		22.64		25.73	
2033	25.10	3.87 %	23.27	2.79 %	26.97	4.83 %
2034	26.07		23.92		28.27	
2035	27.08		24.59		29.64	
2036	28.00		25.21		30.88	
2037	28.95		25.85		32.18	
2038	29.93	3.40 %	26.51	2.54 %	33.53	4.19 %
2039	30.95		27.18		34.93	
2040	32.00		27.87		36.40	

*Notes: The figures for 2018–2025 come from Tractica; years marked with * are sales forecasts. From 2026 onwards it was assumed that sales would develop in line with global growth in GDP in the given SSP. Growth rates are taken from the relevant publicly accessible database. The database reports growth rates at five-year intervals; to calculate the sales forecasts for each SSP, these were split into average annual growth rates.*

Turnover development until 2040

The development of global industrial robot turnover until 2040 was determined as a function of the three framework scenarios (SSP1, SSP2 and SSP5). The procedure is described below. Data from Tractica was used for the years 2018–2024. The 2018 global turnover of USD 13.85 billion for industrial robots is in line with the IFR's figures.[13] For the years 2025–2040, the assumption was that global industrial robot turnover will develop in line with global GDP in the respective SSP. Industrial robots' different growth rates can be made plausible as follows: For SSP5, it is assumed that the industrial sector will experience a very high level of digitisation; this also includes industrial robots (highest growth rates until 2040 in the relative scenario comparison). For SSP1, it is assumed that the industrial sector will experience a high level of digitisation; this will particularly focus on technologies and innovation to reduce energy and resource consumption (the growth rates are slightly lower than for SSP5). For SSP2, it is assumed that the industrial sector will experience a medium level of digitisation (the growth rates are lowest in the relative comparison).

3.2.6.4 Foresight raw material demand

It was not possible to work out the raw material demand in 2040 due to the diversity of industrial robots, a lack of data concerning industrial robots' raw material demand and the required raw material quantities for each industrial robot, not to mention a lack of sales forecasts for the number of industrial robots.

According to KUKA (2021), the essential components of a manipulator (i.e. aluminium, cast iron, steel and plastic materials) will remain readily available in the future. In an initial approximation, there are no significant differences between (traditional) industrial robots and cobots. Unlike the mechanical components, the electronic components contain raw materials that are significantly rarer (KUKA 2021). Depending on the component and the raw materials it contains, more in-depth analyses are required here to assess the availability of raw materials and the demand.

3.2.6.5 Recycling, resource efficiency and substitution

As early as 2013, Kopacek & Kopacek (2013) wrote that robot manufacturers will have to contend with end-of-life laws and regulations for robots, not to mention ethical environmental protection principles. The European Commission is also recommending that eco robot designs should be incentivised to enable more efficient use of materials and energy, easy component disassembly, material identification, reuse and recycling (European Commission 2020a).

According to its website, ABB has been recycling robots for over 25 years to extend their lives. In doing so, it would prevent old robots from being scrapped or simply not used. For its clients, this particularly translated into their return on investment being maximised. Recycling is taking place in the Czech Republic, the USA, China, Brazil, Mexico, Germany and Vietnam (O'Donnell 2020). KUKA is also offering used, refurbished industrial robots and spare parts. Used robots are also available for special applications in the likes of the gas-shielded welding, casting, palletising, loading and unloading, assembly, insertion and placement segments. Used industrial robots can be rented, bought or even sold to KUKA. This allows smaller companies to use industrial robots at lower costs too (Schmirgel 2021).

Kopacek & Kopacek (2013) believe that, in theory, a robot's lifetime is unlimited. But what cuts it short is the the control hardware and software and the mechanical design. In their estimation, it is mainly little-used industrial robots more than 10 to 15 years old that are dismantled, because most components (like gears, controllers or grippers) have a reasonably high price on the spare parts market. Based on their dismantling of the Sony SRX-611 SCARA, they deduce that the mechanical parts, motor axles, harmonic drives, gearboxes and some other parts are reusable in most cases. Furthermore, most components can be efficiently recycled with the recycling and dismantling technologies that are available at present. Only electric gearboxes, control panels and certain cables from the control unit cannot currently be affordably recycled.

[13] In view of this agreement, Tractica's turnover forecasts were used instead of Frost & Sullivan's.

3.2.7 Additive manufacturing of metal components ('3D printing')

3.2.7.1 Technology description

Additive manufacturing refers to various procedures in which materials are joined together one layer at a time to form a component. In contrast, subtractive manufacturing produces components by removing material from a solid body (e.g. by drilling, punching or cutting).

Additive manufacturing is particularly suitable for producing small quantities and/or customised products (mass customisation), production on demand (e.g. pilot series) or on-site production (e.g. close to the customer), production of spare parts (e.g. older series products), rapid prototyping (e.g. to shorten product development) and the production of delicate and geometrically complex structures with a low specific weight (e.g. for lightweight construction). In addition to the improved functionalities, the expiry of patent protection for important procedures, the acceleration of the production speed, the wide range of applications from one-off to series production and the drop in equipment and material prices are driving the spread of additive manufacturing.

Additive manufacturing of plastic, metal and ceramic components is a state-of-the-art process in numerous industrial sectors. Relevant markets include medical technology, aerospace, automotive and other industries, plus retail. The fastest growth rate is in medical technology (dentistry and orthopaedics) and aerospace (structural and machine parts), where additive manufacturing is used to reduce weight and thus cut transport costs (Auer 2019).

According to VDI (2014), additive manufacturing usually takes place in four phases (Figure 3.51): First, a three-dimensional model of the component is created using CAD (I), supported by the 3D scanning of an existing component as an option. Data processing (II) includes the separation of the component into superimposed layers ('slicing'), process preparation and parameter setting in the system's control computer. In the actual additive process (III), the component is manufactured by means of phase transition of a liquid or powdery material into the solid state. This is usually followed by post-processing, such as cleaning, post-curing, coating and mechanical finishing (IV).

A variety of additive manufacturing methods are available for the actual additive process, including: VAT photopolymerisation, powder bed fusion (PBF), direct energy deposition (DED), material extrusion, binder jetting, material jetting and sheet lamination. When discussed publicly, all of these methods are often referred to as '3D printing'; however only binder jetting is 3D printing in the narrower sense of the phrase.

While polymers are used more in additive manufacturing than metals, the gap is narrowing and metals could overtake polymers from 2021 onwards (Global Data 2019).

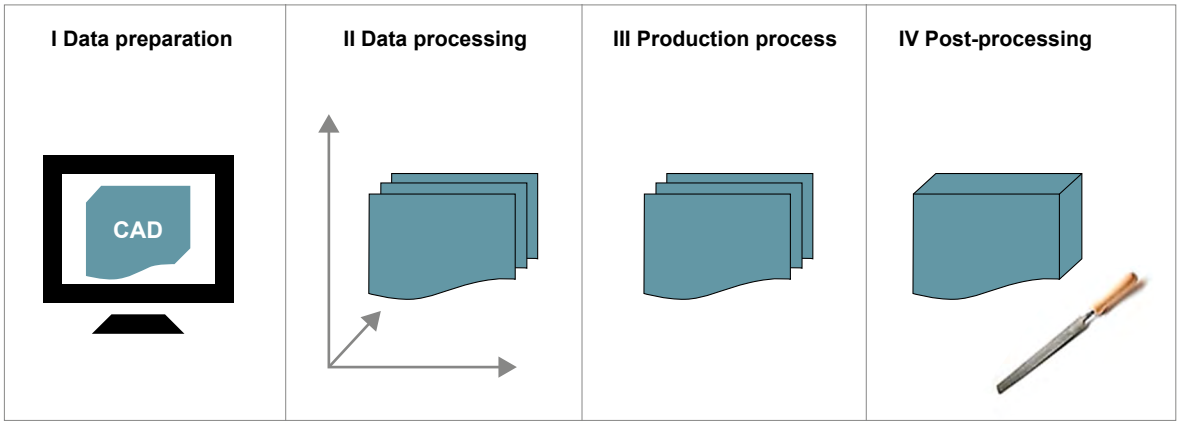

Figure 3.51: Phases of additive manufacturing (source: own representation, based on VDI guideline 3405, VDI 2014)

This technology synopsis focuses on the additive manufacturing of metallic components. At present, components made from metal alloys can be additive manufactured using powder bed fusion, direct energy deposition, binder jetting or sheet lamination; fluidic force microscopy might also be an option in the future (Caviezel et al. 2017). In principle, a wide range of components can be considered for additive manufacturing. Examples of the two growth sectors (medical technology and aerospace) are:

– Hip joints with titanium alloy bases
– Fuel nozzles for aircraft made from cobalt-chromium alloys

The basis for additive manufacturing of metal components is predominantly precursors in powder form, but they come in filament form, too. At present, about 4,500 tonnes of metal powder are produced each year for additive manufacturing. This amount is comparatively small given that some 700,000 tonnes of metal powder are produced per year (MPIF & APMI International 2020).

The overall market for additive manufacturing can be split into hardware, materials, software and services. Leading hardware companies include Desktop Metal, GE Additive, Markforged, EOS, HP, 3D Systems, Ultimaker, EnvisionTEC and Stratasys, while the top materials companies are BASF, Henkel, GKN, Sandvik, Solvay and Höganäs (Global Data 2019).

The players in the value chain of additive manufactured metallic components include VDM Metals (unalloyed pure metals), Heraeus (powder and filament), EOS and ExOne (additive manufacturing systems) and Thyssen Krupp and Airbus (component manufacturers).

3.2.7.2 Raw material content

Table 3.45 shows an overview of the raw materials used for additive manufacturing (European Commission 2020a).

Table 3.45: Raw materials for additive manufacturing (source: European Commission 2020a)

Raw material	Einsatzgebiete
Al	Al alloys for aerospace, lightweight and rigid cabin interior
Fe	Corrosion-resistant Fe alloys for structural and mechanical parts
Ni	Ni and NiTi alloys, ductile and corrosion-resistant, for turbine and mechanical parts
Ti	High-strength Ti alloys for aerospace and medical applications
Mg	High-performance AlMg alloys
Cr	Corrosion-resistant CoCr alloys in gas turbines, machinery, and medical and dental applications
Co	Super alloys, corrosion-resistant CoCr alloys in gas turbines, machinery, and medical and dental applications
Cu	Super alloys, Ni alloys
Hf	Ni-based super alloys, high-strength high-temperature applications
Mn	Ni alloys
Mo	Ti alloys to increase stability
Nb	Super alloys, TiAlNb alloys, in machinery, blades, valves and rotors
Sc	Lightweight, high-strength components and moulded parts
Si	AlMg alloys
W	Heat-resistant super alloys, in corrosion-resistant and tool steels, turbine blades and baffle plates
V	TiAl alloys
Zr	Ti alloys, metallic glass, toothed rings, springs, gear units and sensors

Metal powders and filaments for additive manufacturing can be based on very different alloys. We need to focus on specific alloys in specific areas of application to estimate the future raw material demands.

EOS has steel, nickel, cobalt/chrome, copper, titanium, aluminium and tungsten-based metal alloys in its portfolio (EOS 2020). The material's specific properties are the results of alloying the base metal with other elements:

Further information about alloy compositions can be found in the product data sheets for metal powders designed for use in additive manufacturing, including those from GKN for Ti6Al4V and AlSi10Mg.

The metal alloy's special composition gives the additive manufactured component the desired product properties and the material the process properties required for shaping it with the technical method in question.

Table 3.46: Material composition of selected metal alloys for additive manufacturing [wt%] (source: Kreft & Jackel 2019)

Raw material	EOS Ni Hx	EOS Ti
Co	0.5–2.5	
Ni	Balance	
Fe	17–20	0.3
Ti		Balance
Cr	20.5–23	
Mo	8–10	
Mn	1.0	
W	0.2–1.0	
Cu		
Nb		
Other	a)	b)

Notes: a) C 0.1 %, S 1.0 %; b) C 0.08 %, H 0.015 %, O 0.25 %

Aerospace technology

Huang et al. (2016) estimate additive manufacturing's weight-saving potential for a 40.6 tonne passenger aircraft to be 9–17 %. 4–5 % can be ascribed to aluminium alloys, 2–5 % to nickel alloys, 3–6 % to titanium alloys and 0.4–1 % to steel alloys. The Ti6Al4V alloy is used especially for the additive manufacturing of turbine blades on account of its combined properties – namely high strength, fracture toughness, low density and low coefficient of thermal expansion. Additive manufactured components with precious metal bases (gold, silver, platinum group metals) are also used in aircraft construction (Yusuf et al. 2019).

Hettesheimer et al. (2018) consistently use Ti6Al4V as their assumption to estimate the energy demand for the aerospace sector. The titanium content is estimated as being 7 % for long-haul aircraft weighing 145 tonnes and for short-haul aircraft weighing 40 tonnes. The weight saved as a result of additive manufacturing is estimated as being 20 % per component.[14] Verhoefa et al. (2018) give a similar value of 21.3 % weight saved per component. The reference model here is an Airbus A320 weighing 42.4 tonnes.

For titanium use in the aerospace sector, projections are simulated for a business-as-usual development and for a development adjusted with additive manufacturing. The correction curve is only a few percentage points below business-as-usual in 2018, but by 2028 additive manufacturing is already expected to save over 15 % of titanium demand in the aerospace sector (Titanium USA 2018).

The alloys for subtractive or formative manufacturing and additive manufacturing are not necessarily identical for a base metal, which is why the alloy components might still experience additional boosts in demand despite demand for base metals dropping.

[14] Similarly, the procedure for the automotive sector, including tractors, with AlSi10Mg. Estimates place the aluminium content of vehicles weighing 1.6 tonnes and tractors weighing 8 tonnes to be 9 wt% respectively. As is the case with aircraft components, the weight saved thanks to additive manufacturing is 20 %.

Orthopaedic technology

Additive manufacturing in vascular surgery covers three main applications: anatomical models, surgical tools, and implants and prostheses (Marti et al. 2019). Orthopaedic technology is all about additive manufactured implants and prostheses.

A conventional hip prosthesis weighs approximately 450 to 900 g in total, depending on the choice of material and size (DePuy Orthopaedics 2008). Knee joint prostheses weigh around 280 to 425 g (bonesmart.org 2015), or up to 500 g if they include cement (Lee et al. 2005). Cobalt- and titanium-based alloys are used for both types of conventionally manufactured prostheses (Marscheider-Weidemann et al. 2016).

3.2.7.3 Foresight industrial use

Global demand for metals used in additive manufacturing was reported as being 780 tonnes of powder and 62 tonnes of filament for 2017. With an average annual growth rate of 33.5 % and 27.8 %, demand is expected to reach 7,872 tonnes of metal powder and 445 tonnes of filament in 2025 (Kreft & Jackel 2019).

Demand in 2017 was dominated by aerospace and defence technology with 41.6 wt% and medical and dental technology with 29.9 wt%. By 2025, aerospace and defence technology's share is expected to increase significantly to 48.2 %, while the other customer sectors' relative shares will decline (medical and dental technology, automotive industry) or stagnate (others) (Kreft & Jackel 2019).

The main alloy metals for additive manufacturing in 2017 were titanium and nickel with 38.1 wt% and 29.0 wt% share of the total demand, respectively. In 2025, this quantitative dominance is expected to increase further to 43.4 wt% (3,612 tonnes of titanium-based alloys) and 30.9 wt% (2,570 tonnes of nickel-based alloys) respectively (Kreft & Jackel 2019).

Aerospace technology

Huang et al. (2016) simulate the time availability and adoption of additive manufactured components in aircraft. In its slowest variant, the adoption rate of 80 % additive manufactured parts is reached after 28 years (only for new aircraft); the additive manufacturing of components replaced in service is also taken into account in the other variants (5–15 years until the 80 % adoption rate is reached).

A commercial aircraft's typical lifetime is around 20 to 30 years. Hettesheimer et al. (2018) specify a lifetime of 26 years for both short-haul and long-haul aircraft. The annual registration of about 20 long-haul and 125 short-haul aircraft is calculated with an inventory of 500 short-haul and 125 long-haul aircraft – excluding replacement purchases.[15] Verhoefa et al. (2018) specify a 4 % annual increase in global fleet size for 2036–2050, which would result in a fivefold increase in the global aircraft fleet compared to today.

Scheduled maintenance must also be considered for the demand for additive manufactured components. There are typically over 30,000 individual components in an aircraft's engine system alone that require regular maintenance and repair (Matthews 2018).

The titanium industry is expecting demand to exceed 40,000 aircraft between 2018 and 2038 (Titanium Asia 2018) and is discussing the demand-reducing effects that additive manufacturing has on each aircraft and how low-titanium aircraft are gaining more shares of the market.

Orthopaedic technology

In the previous study entitled 'Raw materials for emerging technologies 2016', the development of demand for orthopaedic implants was estimated based on the projected rise in the number of hip joint operations between 2005 and 2030 (Wittenauer et al. 2013). As a result, (Marscheider-Weidemann et al. 2016) assume there will be 3 million hip operations and 2.7 million knee joint operations in 2035.

[15] Cars' lifetime is stated as being as nine years, and tractor units' as 4.2 years. Annual production of 5.7 million cars (3.2 million annual registrations) and 125,000 tractor units is assumed for scaling up to Germany.

The rule of thumb for the lifetime of dental implants is 15 years. Artificial hip and knee joints (endoprostheses) have a lifetime of 15–20 years, and in some cases even 25 years or longer.

Total titanium usage for medical devices was estimated at 1,700 tonnes in 2017. Growth for medical-grade titanium is expected to be 3–5 % per year over the next few years (Titanium Asia 2018).

3.2.7.4 Foresight raw material demand

In light of the multitude of additive manufacturing methods, processed materials, uncertain future developments and multi-layered effects on the demand for raw materials, an estimate of the raw material demand for components in this study can only be illustrative, not predictive. The projection focuses on the aerospace and orthopaedic technology markets with nickel- and titanium-based alloys.

The near projections for titanium and nickel alloys stated by Kreft & Jackel (2019) are used to calculate the 2018 demand, and the individual metals' mass contents are calculated based on the composition of the alloys EOS Ti and EOS Ni Hx (for bandwidths: mean value of minimum and maximum value). The alloys are not allocated to the user industries, which is why a differentiated extrapolation of the market potential is used instead of an analysis of the maximum market potential.

A simplified assumption is made from delayed growth compared to Kreft & Jackel (2019)'s theory for the future raw material demand. This delayed growth then saturates until market potential is reached. This market potential in the reference case (SSP2) is about three times the value forecast for 2025. Replacement purchases in healthcare are scheduled to be made at 15 years, and at 20 years in the aircraft sector. With regard to material demand, a simplified assumption that the alloys' material composition will remain unchanged in 2040 is made.

Assumptions from Table 3.47 lead to differences between the projection for raw material demand under the conditions set out for the three SSP scenarios (SSP1, SSP2 and SSP5). These assumptions are taken into account to calculate the demands for 2040 shown in Table 3.48.

Overall, this estimated 2040 raw material demand for additive manufacturing shows clear incentives to demand for metals in relation to demand for 2018 (the base year); however, they are only very moderate relative to global production in 2018. The differences between the scenarios are inconsistent but small.

The 2040 demand forecast is only considerable for titanium: Depending on the scenario, the future surge in demand is 3.3–3.5 % of titanium sponge production or 2.5–2.7 % of titanium refining production in 2018. For all the other raw materials examined, the future surge in demand is significantly below 0.5 % of the 2018 reference values.

While this is certainly a conservative estimate, even if demand doubles in 2040 there should not be any serious rises in demand for the nickel and titanium alloys used today. If the substitution potential of components from formative or subtractive manufacturing by additive manufacturing is taken into account, net reductions in demand can even be expected for the metals examined here.

Table 3.47: Assumptions relating to future raw material demand subject to the conditions of selected SSP scenarios

Factor	Scenario		
	SSP1 Sustainability	SSP2 Middle of the Road	SSP5 Fossil Path
Market potential: titanium-based, relative to SSP2	120 %	100 %	80 %
Market potential: nickel-based, relative to SSP2	120 %	100 %	80 %
Increase in material efficiency 2018–2040	50 %	35 %	20 %

Table 3.48: Global production and calculated raw material demand for additive manufacturing in the aerospace and medical technology industries, in tonnes

Raw material	Production in 2018	Demand in 2018	Demand foresight for 2040		
			SSP1 Sustainability	SSP2 Middle of the Road	SSP5 Fossil Path
Titanium	198,050 (sponge) 260,548 (R)	308	6,460	6,998	6,890
Nickel	2,327,500 (M) 2,189,313 (R)	108	2,153	2,333	2,297
Chromium	27,000,000 (M)	50	2,012	1,677	1,342
Iron	1,520,000,000 (M)	43	1,712	1,426	1,141
Molybdenum	265,582 (M)	21	833	694	555
Cobalt	151,060 (M) 126,019 (R)	3.5	138.8	115.7	92.5
Manganese	20,300,000 (M)	2.3	92.5	77.1	61.7
Tungsten	77,080 (M)	1.4	55.5	46.3	37

M: Mine production (tonnes of metal content)
R: Refinery production (tonnes of metal content)

3.2.7.5 Recycling, resource efficiency, substitution

In January 2016, the Federation of German Industries published a position paper on the implications that 3D printing would have on raw materials security for German industry (BDI 2016). Positive effects compared to subtractive production include low-waste production and lightweight construction. Negative effects include unclear item recyclability, increased production due to simple manufacturing, the production of defective products or 'crapjects' (Kreiger & Pearce 2013; IÖW 2014).

The energy and materials required in the component production phase depend on a number of the components' technical and morphological specifications, machine parameters and production settings, particularly layer thickness, geometry, positioning and production time (Bourhis et al. 2013). Production waste from metallic alloy processing can in principle be recycled well from a technical standpoint, and economically too in most cases (Meteyer et al. 2014).

Since the additive manufactured components in the applications examined have long lifetimes, end-of-life recycling estimates are fraught with a great deal of uncertainty, because to date we have had next to no experience with end-of-life recycling of additive manufactured implants and aircraft components. A major barrier is likely to be collecting components for end-of-life recycling, while metallurgical recycling seems plausible assuming that secondary raw material prices are acceptable.

3.2.8 Devices in the Internet of Things (IoT)

3.2.8.1 Technology description

ISO/IEC 20924 (2018) defines the Internet of Things (IoT) as an "infrastructure of interconnected entities, people, systems and information resources together with services, which processes and reacts to information from the physical world and virtual world". The IoT can be construed as all the components, layers and platforms that add value compared to the Internet of People. The scope of the IoT, its applications and technical solutions is wide and heterogeneous (cf. Krause et al. 2017).

This technology synopsis mainly focuses on the physical IoT modules; there are different classifications to categorise them.

Special requirements are placed on IoT devices: long reach, low data transfer rate, low energy consumption and cost-effectiveness (according to Mekki et al. 2019). Ojo et al. (2018), for example, categorise IoT devices as low-end, middle-end and high-end with respect to their performance. Low-end IoT devices are mostly used for simply recording information and the smallest control processes. Middle-end IoT devices offer advanced processing capabilities, such as algorithms for simple visualisations, and can host more than one communication technology. High-end IoT devices are mostly single-board computers (SBCs) that can perform more sophisticated edge computing (e.g. machine learning) and have high connectivity and high-quality interfaces to the surrounding area (e.g. cameras). High-end IoT devices are also used as IoT gateways.

According to Mekki et al. (2019), IoT communication technology can be split into short-range technologies (e.g. Zigbee, Bluetooth, Bluetooth Low Energy (BLE), near-field communication, radio frequency identification (RFID)), cellular communication (Wi-Fi, 2G (GSM), '2.5G' (GPRS), 3G (UMTS), 4G (LTE), 5G (NR)) and wireless low-power wide area networks (LPWAN). Satellites are viewed as being potentially potential game-changing for the IoT (Urlings 2019).

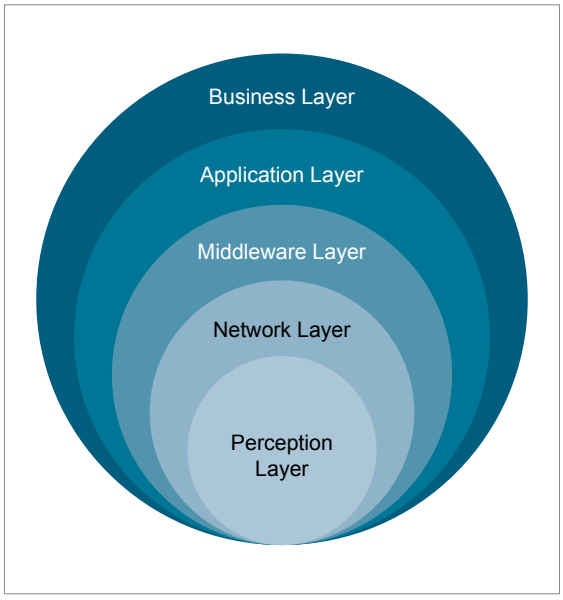

Figure 3.52: Reference model for the IoT architecture (source: Antão et al. 2018)

At present, the following technologies are particularly important:

– BLE is a Bluetooth variant specifically for low-power IoT devices (Sainathan 2018). Compared to passive RFID, BLE's reader range is far greater, but tag costs are significantly higher.

– LPWAN describes communication solutions that enable wireless long-range communication over 10–40 km rurally and 1–5 km in urban areas. The form of communication is comparatively energy-efficient and affordable. The technologies are widely used and researched today: Sigfox, LoRa and NB-IoT.

– 5G is expected to significantly drive IoT market development. 5G's advantages over 4G include its low latency and high data transfer rates, while its disadvantages include its shorter range. There is a separate technology synopsis for 5G (see Section 3.5.3).

According to Krause et al. (2017), a distinction is made between three types of networking: '(1) Connection of a product to a manufacturer, user or another product (one-to-one, like vehicles' diagnostic functions). (2) A central system that permanently / temporarily connects to multiple products (one-to-many, like additional smart services for predictive maintenance and updates). (3) Connection of many products to other products and external sources of information to create ecosystems (many-to-many, like using weather data to predict and optimise energy consumption).'

The IoT's data processing architecture is summed up by the terms 'edge computing', 'cloud computing' and 'fog computing'. Data can be processed locally, near where it is collected (edge computing), or centrally (cloud computing). Decentralised pre-processing followed by centralised processing can take place too (fog computing). The decision as to what architecture will be chosen is taken with costs and efficiency development in mind (McKinsey & Company 2019; Chiang & Zhang 2016).

IoT applications can be found in a wide range of industries even today. From a turnover perspective, Statista (2018) reckons that connected cities (USD 38.8 billion) and industrial internet (USD 35.9 billion) are the largest segments, well ahead of wearable systems (USD 11.8 billion), connected vehicles (USD 4.5 billion) and connected homes (USD 2.9 billion) (2018 data in each case). In terms of IoT device unit numbers, the image for 2018 is as follows: smart cities (473.2 million), industrial IoT (440.8 million), personal IoT (472.6 million), medical IoT (125.4 million), connected vehicles (64.7 million) and connected / smart homes (1.2 billion). The smart agriculture, commercial transport, intelligent retail, smart energy management and smart buildings fields are named too, but not quantified (Columbus 2018).

According to Global Data (2018), the following companies are active market players for the four main IoT layers: Qualcomm, Intel, NXP, Infineon, Microchip, Analog Devices and STMicroelectronics at device level; Cisco, Nokia, Ericsson and Huawei, as well as AT&T, NTT and Vodafone, at network level; Amazon, Microsoft, Google, SAP, Software AG and Alibaba at data level; and Apple and Google in consumer internet, and GE and IBM in industrial internet.

Given its sheer breadth and complexity, the 'Devices in the IoT' technology synopsis contains numerous references to other technology synopses. At this point, the focus is narrowed down to minimum components for IoT devices – firstly to do justice to the IoT's special mass nature and, secondly, to avoid overlaps with technology synopses like data centres (Section 3.5.4), radio frequency microchips (Section 3.2.5) and autonomous driving of vehicles (Section 3.1.4).

3.2.8.2 Raw material content

According to Krause et al. (2017), the following minimum components are required for IoT objects: sensors for recording information, a microprocessor appropriate for the specific task, a device for energy supply, a networking component and, if necessary, actuators that trigger actions based on evaluated sensor information, depending on the field of application. All the embedded systems are also equipped with a unique ID (e.g. RFID or IP address). In future, it will theoretically be possible to kit out all sufficiently large physical objects with the minimum IoT components.

Table 3.49 will give readers an idea of the IoT devices' physical nature in a basic configuration, their power supply and connectivity, and the estimated cost development.

This list is not exhaustive; there are other and more recent systematisations. However, what makes this systematisation (Sparks 2017) advantageous is that it is the only one available for free that contains a long-term quantitative estimate of the IoT minimum components.

We encounter a number of difficulties in determining the raw material content of the minimum components for IoT objects. While we could use standard electronics to come close to the material composition of IoT beacons, IoT receivers and IoT gateways, the first (Angerer et al. 2009) and second edition (Marscheider-Weidemann et al. 2016) of the study entitled 'Raw materials for emerging technologies' illustrated that the market breakthroughs hoped for at single unit level (especially for supermarket and drug store items, i.e. 'fast-moving consumer goods' or 'FMCGs' for short) failed to materialise for the smart tags sub-segment of the RFID sector, and that Industry 4.0 sensor technology could not be quantified either due to insufficient information. Data on all minimum IoT components is patchy (e.g. on BLE, Bluetooth Low Energy) and often outdated (e.g. low-end microchips). The IoT's broad scope of potential implementations does not at present permit for a plausible breakdown of the market shares of the basic technical concepts for the individual minimum components. Additionally, numerous new material developments that make estimating 2040 raw material demands appear shortsighted from today's perspective are plausible. Using this, we can formulate a demand to determine the required materials for current and future IoT minimum components.

The only free source at present on the IoT's raw material demand focuses on storage technology. While storage technology is not specific to devices in the IoT, it particularly extends to data centres (see Section 3.5.4). Although HDDs and flash memories can be considered established

Table 3.49: Basic configuration of the IoT (source: Sparks 2017)

Module type (1)	Energy supply	Connectivity	BOM costs for a basic IoT module (2)	
			Actual situation in 2017	Projection for 2035
Smart Tag	RF Energy Harvesting	NFC or RFID	USD 0.40	USD 0.15
Smart sensor	Solar cells, button cell	Unlicensed radio frequency (3) or LPWAN (4)	USD 4	USD 1.5
Smart camera	Power grid	WiFi, LTE or Ethernet	USD 8	USD 3
IoT beacon	Solar cells, button cell	Unlicensed radio frequency (3)	USD 3	USD 1
IoT receiver	Solar cells, button cell	Unlicensed radio frequency (3) or LPWAN (4)	USD 3	USD 1
IoT gateway	Power grid	Unlicensed radio frequency (3) or Internet connection	USD 8	USD 3

Notes: (1) Smart tags for the IoT generate data for analysis in real time. Smart sensors measure the characteristics of their immediate environment and forward this information for processing. Smart cameras are visual smart sensors, and smart tags could also progress to a kind of smart sensor if combined with sensors and data loggers. An IoT beacon repeatedly transmits a small signal such as an ID number or web address. If there is a compatible IoT object in proximity to the beacon, an action is automatically triggered. A controlled IoT object receives its control instruction from an IoT receiver, which can also operate with long-wave radio frequencies if necessary. IoT objects operating in unlicensed radio frequencies connect to the Internet via IoT gateways. (2) BOM – bill of materials, i.e. not including manufacturing costs; (3) Bluetooth, WiFi, Zigbee; (4) Low Power Wide Area Network, e.g. NB-IoT, LoRa, Sigfox.

Table 3.50: Raw material demand for various storage technologies in the IoT, in tonnes/ZB (source: Ku 2018)

Storage technology	Component (selection)	Material (selection)	tonnes/ZB
Ferroelectric RAM	Control gate	Pt or Ir	Ir: 49 to 246 Pt: 47 to 236 Zr: 14 to 54
	Iron layer	$Pb(Zr_xTi_{1-x})O_3$	
	Electrode	Pt	
Magnetic RAM	Conductor	TaN	Ta: 7.7
	Pinning/antipinning	$Fe_{60}Co_{40}$ / $Ir_{20}Mn_{80}$	Co: 0.5 to 0.6 Ir: 0.9 to 2.7
	Electrode	W	W: 7.7
PCM	Phase change material	$Ge_2Sb_2Te_5$	Ge: 0.05 Sb: 0.08 Te: 0.21
3D XP	PC element	SiGe	Ge: 0.1 to 0.3
Resistive RAM	Dielectric	HfO_2	Hf: 3.3

Notes: Other chalcogenide glasses are also used for PCM but the cumulative raw material demand is of a low order of magnitude.

baselines, FeRAM (ferroelectric), MRAM (magnetic), PCM (phase exchange material), 3D XP (stacked PCM) and RRAM (resistive) are emerging technologies.

Table 3.50 outlines the raw material demands for different storage technologies (material content) in tonnes/ZB:

Ku (2018) shows that there may be notable effects on raw material demand, beyond the well-known issue of FeNdB demand for HDDs, if FeRAM spreads massively on platinum group metals. The use of RRAM in the zettabyte range is capable of noticeably increasing demand for hafnium. All other storage technologies appear to be straightforward in terms of raw material demand. The emerging technologies PCM and 3D XP, not to mention MRAM, are already powerful alternatives to the established HDD and flash storage technologies without triggering major boosts in raw material demands.

The author Ku (2018) concludes that the materials required due to IoT storage technologies are not too alarming, and that it is unclear whether storage technology is causing the most urgent material problems in terms of ICT upscaling, as opposed to the likes of data processing or data transfer. Against this backdrop, this study does not provide an independent estimate on the raw material demand for storage technologies. Nevertheless, the quantitative future projections for IoT objects formulated in the section below can be used to specify the need for a component-based analysis of IoT objects' raw material content. However, this would require an independent investigation.

3.2.8.3 Foresight industrial use

Estimates of how IoT components market will develop vary greatly depending on what is attributed to the IoT and which time periods are covered.

There are few long-term estimates for the IoT components' unit numbers:

- ARM Limited (Sparks 2017) estimates cumulative potential production from 2017 to 2035 to be 1 trillion units, of which 500 billion are expected to be tags, followed by 250 billion sensors, 10 billion cameras, 100 billion IoT beacons, 120 billion IoT receivers and 20 billion IoT gateways.
- According to DBS Bank (Columbus 2018), the installed active IoT unit base in 2016 was 6.4 billion units (consumer devices: 62 %). By 2030, this figure is expected to reach 125 billion units (consumer devices: 60 %).
- Transforma Insights (Morrish 2020) puts the installed active IoT device base at 7.6 billion units at the end of 2019. This figure is expected to reach 24.1 billion units by 2030 (CAGR: 11 %). In this period from 2019 to 2030, the shares of short-range technologies (Wi-Fi, Bluetooth and Zigbee) are expected to change from 74 % to 72 %, public networks (mainly cellular networks) from 16 % to 20 %, and private networks from 10 % to 8 %.

The International Data Corporation (IDC) estimates that there will be 41.6 billion connected devices generating 79.4 zettabytes (ZB) of data traffic as early as 2025 (IDC 2019).

Certainly, we should only take such illustrative estimates with a pinch of salt. However, they still give an impression of the sheer number of IoT devices we might expect in the future.

3.2.8.4 Foresight raw material demand

Different forms of IoT adoption and raw material content are conceivable depending on the SSP scenario. However, the 'raw material content' and 'foresight – industrial use' information situation is inadequate even for an illustrative estimate of future raw material demand.

3.2.8.5 Recycling, resource efficiency, substitution

Some initial studies are examining the IoT's environmental impact. However, they are focusing on energy consumption and circular economy issues (cf. International Telecommunication Union & WEEE Forum 2020, etc.) and not on material content and resource efficiency matters.

The essential characteristics of IoT's minimum components is that they are miniaturised, widespread and embedded in other objects. Printable electronics with minimal material content are being developed and used for the mass market for cost reasons. There are only minimal market incentives for recovering the IoT minimum components' constituents, and the high entropy makes the ecological sense doubtful too.

The introduction of IoT minimum components into other recycling material streams may lead to material incompatibilities under certain circumstances. Then, the IoT minimum components' design would be important for recycling, as they would have to be separated from the main objects or made suitable for the mass stream.

3.3 Cluster: Energy technologies and decarbonisation

3.3.1 Thermoelectric generators

3.3.1.1 Technology description

Thermoelectric generators (TEGs) convert temperature differences directly into electrical energy. In doing so, they do not need any moving parts or consumables (and, consequently, no maintenance). They are reliable and long-lasting and do not emit any noise (Champier 2017). Many technical processes, especially combustion processes, produce waste heat, which can serve as a source of energy for TEGs. This field of application, waste heat utilization, holds great potential for aspects such as fuel savings in vehicles or greater efficiency in combined heat and power units and central heating systems in buildings (Fraunhofer Institute for Physical Measurement Techniques (IPM) 2017). Small TEGs are used in the case of what is known as energy harvesting. For example, they can supply electricity to sensors from existing heat sources such as heating pipelines or even body heat. In aerospace engineering, radioisotopes have been connected to TEGs as a heat source to supply power to satellites and sensors for decades (Champier 2017; Beretta et al. 2019; Freer & Powell 2020; Jouhara et al. 2021).

The process to convert heat into electrical power using thermoelectric generators is based on the Seebeck effect: An electric potential difference (voltage) will arise between two points in a conductive material if these points have different temperatures. The electrons responsible for electrical conduction move faster in regions with higher temperatures than they do in those with lower temperatures. This leads to an accumulation of electrons in the colder region. The difference in potential produced causes a return flow of electrons, which counterbalances the accumulation. This creates a characteristic voltage for the conductive material concerned. A thermoelectric material should deliver as high a voltage as possible at a certain temperature difference to ensure optimum efficiency. To ensure this is the case, its electrical conductivity should be as high as possible to guarantee an adequate electron flow. At the same time, the thermal conductivity should be as low as possible to maintain the temperature difference. The dimensionless ZT value is usually specified as an index for thermoelectric performance (Beretta et al. 2019):

$$ZT = \alpha^2 \frac{\sigma}{\kappa} T$$

- α Seebeck coefficient in V K^{-1}
- σ Electric conductivity in Ω^{-1} m^{-1}
- κ Thermal conductivity in W m^{-1} K^{-1}
- T Mean value of the temperatures on the hot and cold sides in K

The ZT value is therefore not only dependent on the material; it is also dependent on the temperature. For specific applications, it is thus essential that the material's temperature-dependent ZT value is also high in the relevant temperature range.

It is rare to find materials suitable for thermoelectric generators which have a high electrical conductivity but a low thermal conductivity since good electron conduction is generally paired with effective thermal conductivity. For example, thermal and electrical conductivity are high in metals and low in insulators. Semiconductors exhibit average values for both variables and achieve the best ZT values as shown in Table 3.51. Painstaking research is currently being conducted into materials to maximise ZT values (Freer & Powell 2020).

Thermoelectric generators use n- and p-conducting semiconductor layers in which additional conduction electrons (n-conductors) or holes (p-conductors) are created using foreign atoms in a crystal lattice. These semiconductor layers are linked via wires and connected in series electrically, thus allowing a continuous current flow. The electrical circuit is located perpendicular to the temperature gradient (see Figure 3.53). Heat exchangers are used to transmit heat to the gen-

Table 3.51: Thermoelectric properties of insulators, metals and semiconductors at room temperature (source: SPARKS 2017)

	Unit	Insulators	Metals	Semiconductors
Seebeck constant α	10^{-6} V K^{-1}	1,000	5	200
Electrical conductivity σ	Ω^{-1} m^{-1}	10^{-10}	10^{8}	105
Thermal conductivity κ	W m^{-1} K^{-1}	0.1 – 1	10 to 1,000	1 to 100
ZT value	–	10^{-14}	10^{-3}	0.1 to 2.2

erator's hot side and cool or transfer heat away on the cold side (JAZIRI et al. 2020). The thermoelectric modules must withstand large temperature gradients and related stress loads and deformations during many heating and cooling processes. They must also be stable within the operating environment (chemical, mechanical) (FREER & POWELL 2020).

It is thus important to optimise the entire module design in addition to the properties of the thermoelectric materials (see Section 3.3.1.2). This includes electric connecting elements (wires), heat exchangers and the power inverter to convert the generated direct current into an alternating current (CHAMPIER 2017). Key parameters for TEGs are the power density (indicated in W cm^2; the greater the power density, the lighter the thermoelectric generator is) and the cost per unit of power (€ per watt).

Thermoelectric generators have a low efficiency compared to other technologies used to convert waste heat into electricity. However, a thermoelectric generator's simple structure offers an advantage since it ensures high reliability, a long service life and low maintenance. Moreover, thermoelectric generators are scalable and their use can be adapted individually to the specific application concerned. They are also suitable for applications which do not include moving parts and are silent in their operation. Thermoelectric generators are unrivalled for temperatures below 100 °C (WIETSCHEL et al. 2010).

3.3.1.2 Raw material content

Different materials each have both advantages and disadvantages with regard to the suitability criteria specified in Section 3.3.1.1. Materials based on PbTe, Bi_2Te_3, BiSb and SiGe are already in commercial use. PbTe and SiGe are used in the space industry while only Bi_2Te_3 is relevant for commercial use in other applications such as heat utilisation (CHAMPIER 2017;

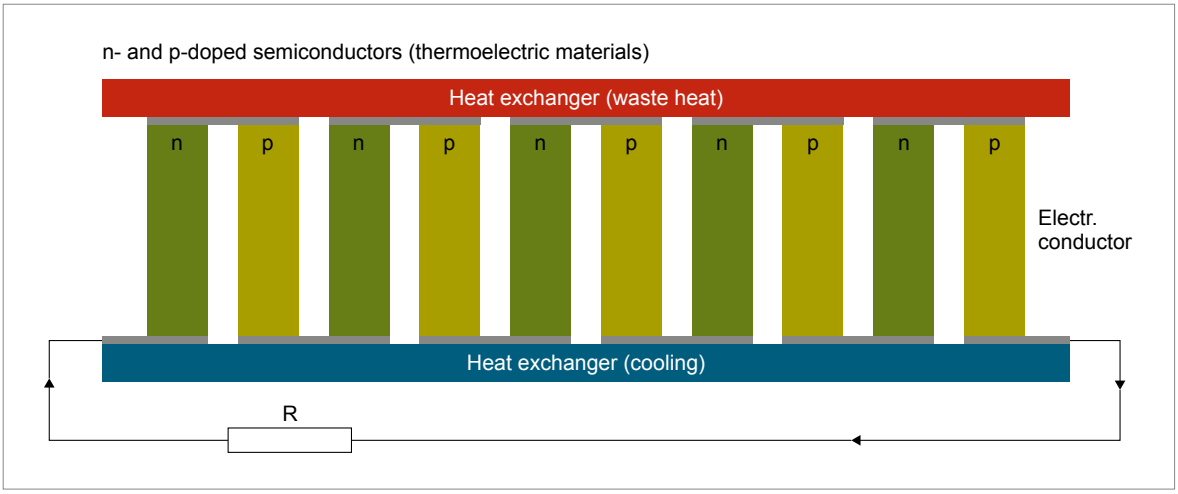

Figure 3.53: Structure of a thermoelectric generator (source: own representation)

Cramer et al. 2018; Jouhara et al. 2021). The following material classes are undergoing research and development (Beretta et al. 2019; when [X,Y, Z] is written, it means that X, Y and Z can substitute one another and are therefore contained in variable quantities; see Freer & Powell 2020):

- Oxide, e.g. $Zn_{0.96}Al_{0.02}Ga_{0.02}O$, $NaCo_2O_4$
- Silicides, e.g. $FeSi_2$, $Mg_2[Si,Ge,Sn]$; $Ru_{0.1}Mn_{0.9}Si_y$; $MnSi_{1.73}$
- Skutterudites, $X_yCo_4Sb_{12}$, X: Sr, Ba, La, Yb, Ce, Nd, Er, In; $Yb_{12}Ca_2MnSb_{11}$
- Half-Heusler materials, [Hf,Zr][Co,Ni,Fe][Sn,Sb]
- Sulfosalts, e.g. $Cu_{12}[S|(SbS_3)_4]$
- Nanostructured silicon
- Polymers.

ZT values of around 1 are achieved in thermoelectric generators in commercial use. This also leads to overall efficiency levels of 2–8 % due to contact systems in need of improvement among other things. ZT values of up to 2.4 have already been achieved in research. However, higher values (ZT values > 3) are required for large-scale TEG applications (Freer & Powell 2020; Jouhara et al. 2021).

Current applications for TEGs outside the aerospace industry are based exclusively on Bi_2Te_3 (Champier 2017; Cramer et al. 2018). Very different materials are currently under consideration for future thermoelectric generators and may again contain many different elements. Most of the aforementioned materials are also at an early stage of development, so it is not possible to predict which particular raw materials will be important for TEGs in the future. Some of the materials listed above contain elements which are regarded as potentially critical raw materials (Te, Sn, Co, In, Ga, Er, Ru, Hf). Both toxicity (e.g. Pb) and potential limitations due to the availability of raw materials (e.g. Te) are currently a key concern in research into thermoelectric materials (Jouhara et al. 2021; Ying et al. 2021).

3.3.1.3 Foresight industrial use

The use of thermoelectric generators in potential mass markets such as the automotive industry is technically possible (HEATRECAR Consortium 2013). TEGs based on Bi_2Te_3 in commercial use currently achieve real efficiencies of 2–8 %. This results in costs of around €3–8/W. The costs for the thermoelectric material here are considerable, e.g. 20 % for bismuth telluride (HEATRECAR Consortium 2013). Thermoelectric generators are regarded as competitive when costs are €1/W or less (Wietschel et al. 2010) with higher (up to €3/W) or lower costs (€0.5/W or less) being specified depending on the application (HEATRECAR Consortium 2013). According to König et al. (2015), the price for TEG-generated electricity can be reduced to about USD 0.5 per W through economies of scale and improvements in performance (savings on materials, improvements to materials, modules and generators). Various research projects and demonstrators have shown that this is technically feasible (HEATRECAR Consortium 2013; e.g. Champier 2017). However, the anticipated breakthrough in waste heat utilisation for vehicles has not come to fruition in recent years. The subject-matter is being further advanced in research but it depends on new thermoelectric materials being developed (Cramer et al. 2018; Beretta et al. 2019; Freer & Powell 2020). The time frame for using thermoelectric generators in vehicle construction is closely linked to the use of internal combustion engines, which are currently gradually being replaced by electric power systems.

Applications in industrial plants include both direct conversion of waste heat (e.g. from steel production, Kuroki et al. 2015) and its use as a power source for sensors and actuators. Both are possible and have already been demonstrated. However, TEG manufacturers' product portfolios indicate that the latter has the greater commercial relevance (EnOcean 2021; TEC Microsystems 2021; e.g. TEGnology 2021). Measuring and control system applications are also relevant in the buildings sector and are already being marketed commercially (EnOcean 2020). However, this area of application remains a niche market since small sensors and actuators can generally also be powered by batteries or electrical circuits. Despite higher costs, TEGs can offer advantages and be used in cases where this is impractical (e.g. due to frequent battery replacement) (Perpetua 2021).

To ensure suitability for future mass applications, the highly encouraging ZT values for the thermo-

electric materials currently being tested in laboratories also need to be put to practical use. In addition to developing these materials, it is also important to optimise the entire module and generator structure. Thermoelectric generators can also be used in power plants, production facilities and data centres. The crucial factor here is whether there are suitable TEGs for the temperature level in the system or plant concerned. Large-scale TEGs are potentially highly suitable for using waste heat in many industrial plants.

End user applications are also being discussed as future areas of application for TEGs. These include TEG-driven cooking sensors to save energy, watches and smartphones powered by body heat, clothing with sensors to monitor body functions and similar. Studies are currently being conducted on flexible substrates (Du et al. 2018; Wang et al. 2019; Fan et al. 2021).

3.3.1.4 Foresight raw material demand

Thermoelectric generators offer great potential in different application segments. The market originally anticipated in the motor vehicle sector based on the utilisation of waste heat from internal combustion engines has disappeared due to the shift towards sustainable means of transport. At present, it is the measuring and control systems sector which offers an attractive niche market (based on Bi_2Te_3), but it is dependent on new materials before it can expand further. Although thermoelectric applications account for around 30 % of the demand for Te (European Commission 2020a), this mainly involves Peltier coolers (e.g. for cooling PCR devices for gene sequencing) or digital cameras for special applications (Gärtner et al. 2003; cf. Selenium-Tellurium Development Association 2021) and not TEGs. Use in the space sector also continues to exist but the raw material demand is low in this case. Due to the early development stage and the various competing material systems for the next generation, the raw material demand cannot be reliably estimated for 2040.

3.3.1.5 Recycling, resource efficiency and substitution

Although recycling is possible in principle, the more complex the chemical composition of thermoelectric materials is, the more costly and time-consuming it will be. The aforementioned materials can substitute one another.

3.3.2 Thin-film photovoltaics

3.3.2.1 Technology description

Thin-film technologies refer to processes in which solid substances are deposited in micro- or nanometre thin or monomolecular layers. These substances exhibit physical behaviour (strength, optical properties, electric conductivity and similar) which differs from a solid body made of the same material. Thin-film technologies not only comprise the deposition process itself but also the subsequent processing or structuring of the deposited layers.

Thin film technology has developed into a key, pioneering surface engineering technology in many industrial segments. This is why thin-film technology can be regarded as a cross-sector technology. The chart below gives a rough overview of the differentiation between the various thin-film technologies and examples of their application in photovoltaics (PV).

In contrast to the solid cells produced using crystalline silicon wafer technology, the photovoltaically active material is deposited on a substrate. While the substrate provides mechanical stability, the thickness of the photovoltaic material is designed to absorb as much light as possible. In its most simple form, the structure of a thin-film cell consists of a substrate, an electrode, semiconductor I, semiconductor II and an electrode. At least one of these electrode layers must be transparent.

There are a variety of photovoltaically active materials in thin-film cells. Not only p-n junctions are used for charge separation; heterojunctions are also used between the different semiconductors. A heterojunction, also called a heterostructure, refers to the interface between two dissimilar materials which do not conduct perfectly (semi-

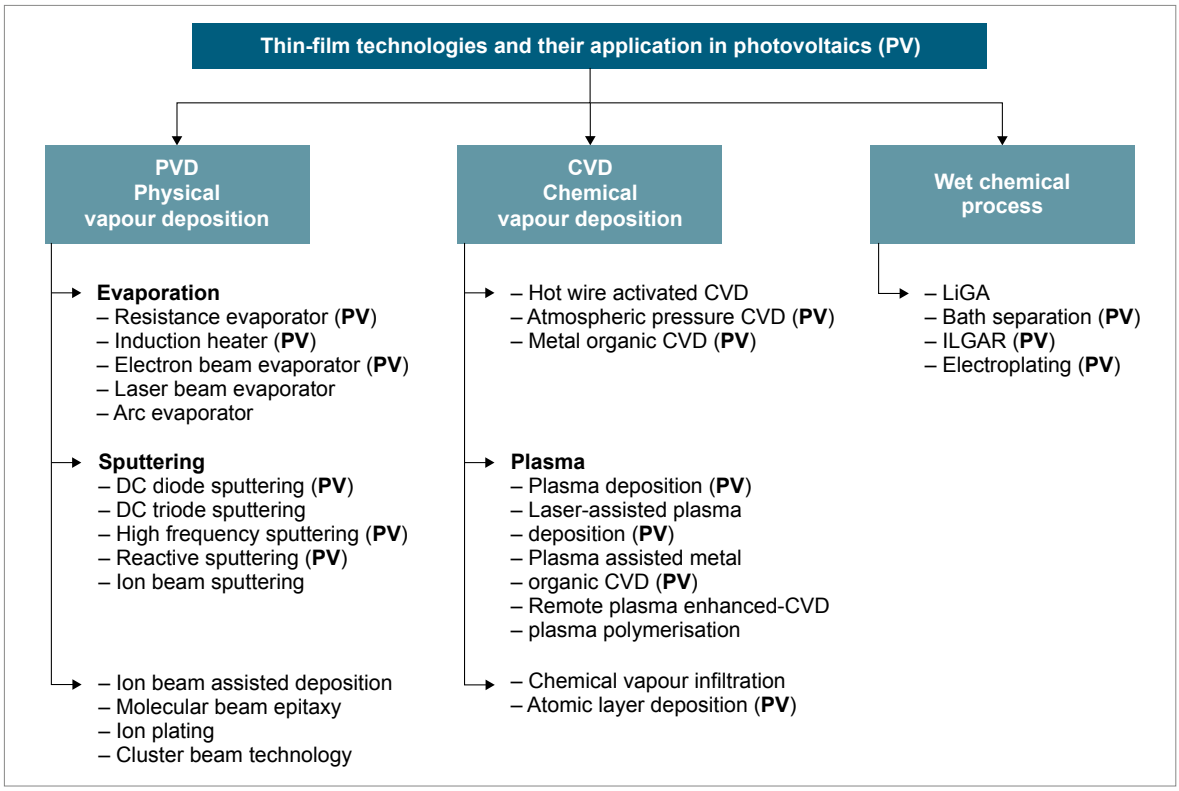

Figure 3.54: Overview of the various thin-film technologies (source: own representation based on Chen et al. 1996 and Kamalasanan 1996)

conductor materials). Unlike in a p-n junction, it is not the doping method which is different here; it is the material type. Semiconductors therefore usually have a different energy in the band gap. Heterojunctions are found in III-V semiconductors or II-VI semiconductors. A distinction is made between the following variants:

- Amorphous silicon (a-Si) with a p-n transition or with a heterojunction to a-Si:C
- Crystalline Si with a p-n transition
- CdTe with a heterojunction to CdS
- $CuInSe_2$ (In is replaced by Ga and Se by S to a certain extent) with a heterojunction to CdS (CIS)
- GaAs with p-n junction or with a heterojunction

Greater potential has long been attributed to thin-film technologies within the photovoltaics sector. However, solar cells made of silicon wafers currently dominate the photovoltaic market with almost 96 % of supplied modules containing silicon wafer solar cells in 2018. However, thin-film cells offer technological advantages (Fraunhofer ISE 2020). The genuine advantages notably include the low material and energy intensities in production and the consequential cost advantages. Another advantage is the relatively variable cell size. Whereas the size of solid cells is restricted to the wafer size and thus to around 21 cm (M12 module size), thin-film solar cells can be manufactured in large dimensions with the size of the coating equipment being the only limitation. The wide variety of options available with regard to substrate materials also brings advantage, including roll-to-roll processes and the production of transparent cells which are particularly suitable for building integration.

The advantages that thin-film cells offer may also be regarded as disadvantages. The market is thus very heterogeneous and production processes and module sizes are not standardised, unlike in conventional PV systems. This could have a restrictive effect on future market development for thin-film technology (Von Ardenne GmbH 2020). The thin-film cell types CdTe, CI(G)S and a-Si had a market share of 4 % on the overall PV market in 2018 (Fraunhofer ISE 2020); see Figure 3.55.

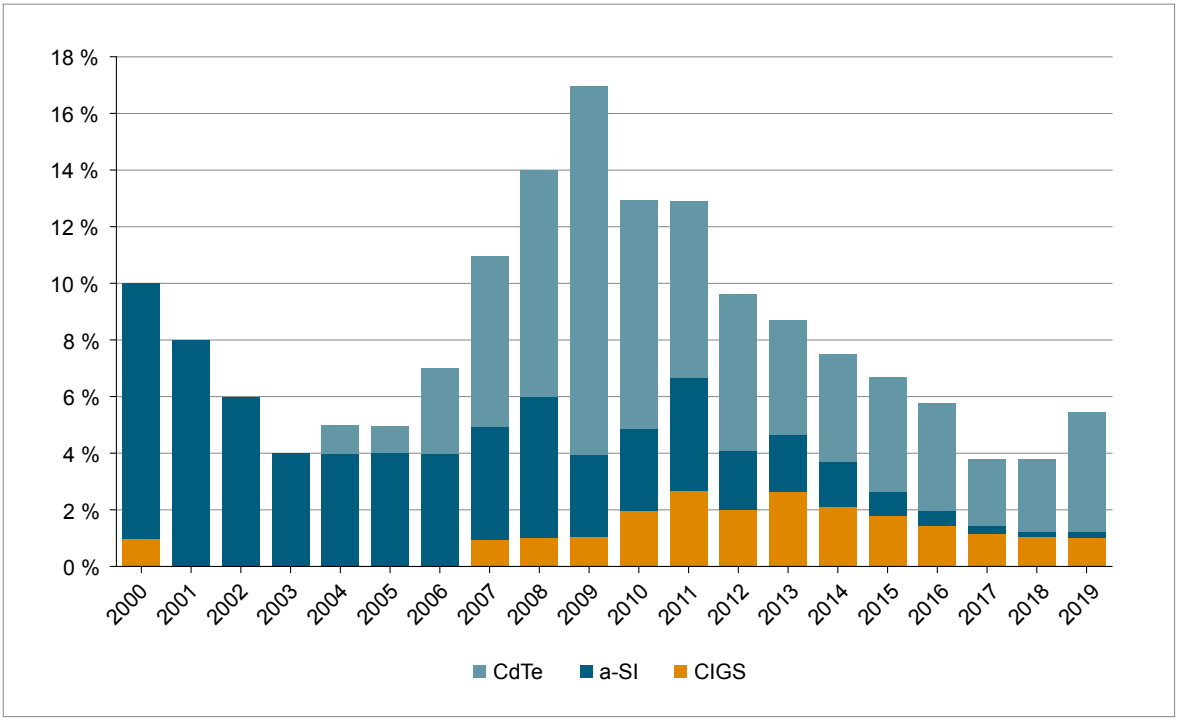

Figure 3.55: Share of the total PV market represented by various thin-film cell types (light blue: CdTe; dark blue: a-SI; orange: CIGS) with a total global PV production of 102 GWp in 2018 (sources: Fraunhofer ISE 2020, Statista 2021b)

The different thin film technologies are described in detail below.

3.3.2.1.1 Thin-film cells made of amorphous silicon (a-Si)

The structure of a typical thin-film PV cell made of amorphous silicon (a-Si) differs from that of a crystalline solar cell in that the silicon layer is much thinner and an intrinsic silicon layer is interposed between the p- and n-conducting silicon, serving as an absorber. Amorphous silicon cells can be very thin because the absorption coefficient for light is much greater than for crystalline silicon. The substrate comprises glass, through which the cells are illuminated. As shown in Figure 3.56 below, current, conventional a-Si cells or modules usually feature ZnO or aluminium-doped ZnO (AZO) as the TCO (transparent conductive oxide) instead of the indium tin oxide (ITO) used previously. Production of a-Si cells are subject to lower price risks thanks to the use of base metals (Kowsar et al. 2019).

An essential characteristic of a-Si cells is degradation due to light exposure (Staebler-Wronski effect). As a result, efficiency decreases permanently by an absolute 2 or 3 % after a few hours or days of irradiation. The efficiency of 1 cm² laboratory cells is 13.4 % when non-stabilised (Kowsar et al. 2019) and 9.5 % when stabilised. Commercial modules achieve an efficiency of around

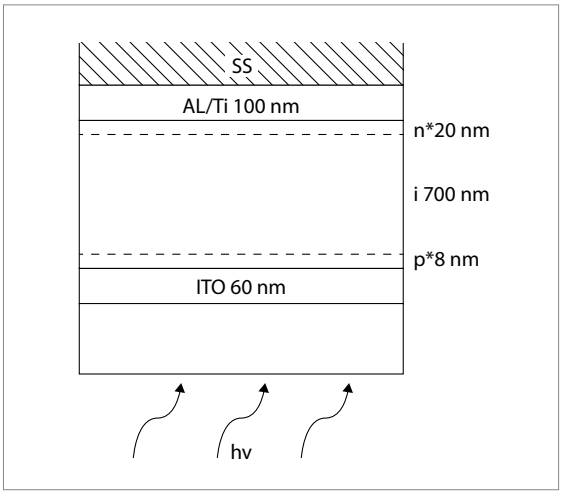

Figure 3.56: Structure of an amorphous silicon solar cell (source: own representation based on Falk 2006)

7.5 % when stabilised (Mahmoudi et al. 2019). The trend is moving towards developing tandem or stack cells where a number of cells with different band gaps are interconnected. Amorphous silicon cells are most commonly used for smaller output capacities, such as power supply to pocket calculators. a-Si cells dominate the market completely in this power segment. They are rarely used for higher output capacities. Due to the very low energy requirements for a-Si cells production, their energy return on investment period is at one year only half as long as for crystalline cells despite low efficiency.

3.3.2.1.2 Crystalline silicon thin-film cells

The development of thin-film cells made of crystalline cells is motivated by the desire to produce them as cost-effectively as amorphous silicon cells and achieve the efficiency that polycrystalline solid cells offer. The advantages of the two conventional silicon cell types could thus be combined and their respective disadvantages eliminated.

A major challenge of this technology is the question of the correct grain size and the required layer thickness. A distinction must be made between two development strategies here: one is seeking to produce large grains; the other is seeking to reduce recombination at the grain boundaries of small grains through passivation, mostly by saturating with hydrogen.

Glass is used as a substrate for the cells. They usually have a similar structure to cells made of amorphous silicon. TCO is used as an electrode on the one side with a metal layer, usually aluminium, used on the other. At a few µm, the layer thickness is relatively narrow since the effective absorption coefficient is high in this material, particularly due to the amorphous material between the grains, and the dispersion on the small grains extends the light path. Cells of this type have already achieved an efficiency of 13.4 % (Kowsar et al. 2019).

3.3.2.1.3 Gallium arsenide cells (GaAs)

Gallium arsenide is an ideal material for solar cells. Its energy gap is optimal for sunlight and as a direct semiconductor GaAs completely absorbs light in layers just a few µm thick. However, gallium arsenide crystal growth is complex from a technical perspective despite methods being constantly improved. GaAs modules are used in the space sector to generate energy for satellites since they are highly resistant to cosmic radiation and also achieve optimum levels of efficiency. Today, GaAs cells are crystalline thin-film cells that achieve an efficiency of 30 % and more on 4 cm^2 in the laboratory. Polycrystalline GaAs cells offer significantly poorer performance since the grain boundaries in GaAs cannot be passivated as easily as in silicon and there is thus a higher incidence of surface recombination. The most favourable variant consists of thin crystalline GaAs layers on a crystalline germanium wafer, where epitaxy is possible thanks to the similar lattice constants. Zn(p) or Te(n) is used for doping since they can be added as ethyl compounds in a gaseous form.

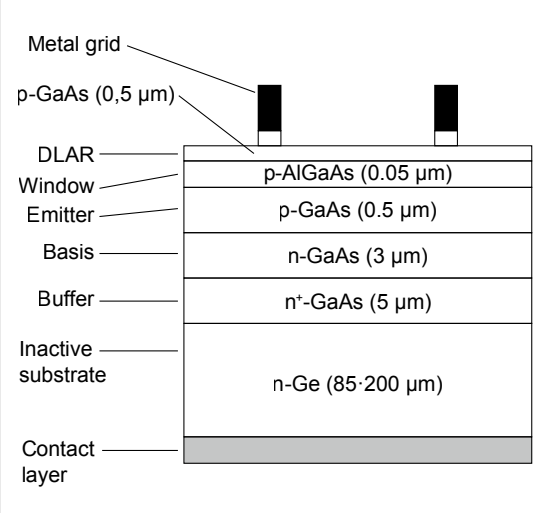

Figure 3.57: Structure of a GaAs cell (source: own representation based on Falk 2006)

Note: DLAR is an anti-reflection layer used with high-efficiency multi-junction GaAs technology, e.g. on a base of TiO_2/MgF_2 or ZnS/MgF_2. As well as the variants mentioned here there are many other combinations, such as gallium indium phosphide, (Ga, In), P/gallium arsenide and GaAs/germanium.

3.3.2.1.4 Cadmium telluride cells (CdTe)

Cadmium telluride is a direct semiconductor with an advantageous band gap and a high absorption coefficient. The advantage of CdTe cells is their lower temperature sensitivity and their high sensitivity to diffuse solar radiation.

In previous CdTe configurations, a CdS interface was deposited on the molybdenum substrate using vacuum gas-phase deposition while a CdTe layer was deposited using chemical gas-phase deposition. Superstrate configurations have replaced a substrate configuration in modern CdTe cells. The TCO layer now acts as a window and CDs are used as a buffer layer. SnO_2, In_2O_3: Sn, ZnO, Cd_2SnO_4 are often used as a TCO in references. The TCO serves as a front contact and side conductor. The CdS window layer can be applied using wet-chemical bath deposition, sputtering and a closed-space sublimation process (CSS). The CdTe absorber layer is often deposited onto the substrate using CSS and then treated using CSS with $CdCl_2$ vapour. $CdCl_2$ treatment increases the grain size, which leads to a significant increase in efficiency (Kowsar et al. 2019).

The cadmium content is unsuitable for receiving the CdTe cells. Intensive research is being conducted into finding a substitution for cadmium due to its toxicity. However, the heavy metal cadmium is relatively immobile in a CdTe cell, although cadmium may become mobilised in extreme situations such as a building fire. There are also toxic risks during the production of modules and recycling of used modules.

A typical CdTe solar cell consists of five individual layers: one CdTe absorber layer around < 2 µm thick, a CdS intermediate layer around 100 nm thick and two tellurium and antimony telluride (Sb_2Te_3) layers 20 or 100 nm thick. Figure 3.58 shows a structural model of a CdTe cell.

3.3.2.1.5 CIGS-PV

CIS (copper indium diselenide or disulfide) or CIGS (copper indium gallium diselenide or disulfide) is used in a thin-film photovoltaic cell based on chalcopyrite compound semiconductors ($Cu(In, Ga)(Se, S)_2$). The basic structure of a conventional CIS solar cell is shown in Figure 3.58.

Cells are generally assembled on molybdenum-coated glass substrates. The molybdenum layer serves as the rear contact in this case. The molybdenum layer also ensures that unabsorbed light is reflected back into the absorber layer. The interface between the p-conducting $Cu(In, Ga)Se_2$ or $CuInS_2$ layer and the poorly n-conducting layer made of CdS or ZnS form the heterojunction. CdS is transparent and acts as a window. The transparent second electrode is located on top as a front contact. Transparent, n-conducting ZnO acts as the front contact.

A cathode sputtering method deposits the molybdenum layer onto the substrate during the manufacturing process. The p-doped CIGS absorber layer is applied to the molybdenum layer. Using the latest technical standards for highly efficient CIGS solar cells, this layer is applied using physical gas-phase deposition at high temperatures (~600 °C), which is continued with a two-stage

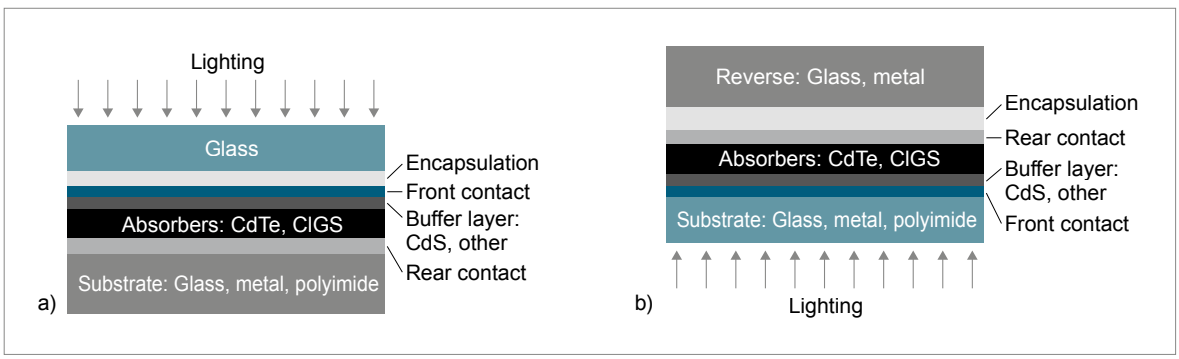

Figure 3.58: Structure of a) substrate and b) superstrate of chalcogenide solar cells (CdTe, CIGS) (source: Marwede 2013)

process. e.g. sputtering followed by selenization with SE vapour or H_2Se gas (Kowsar et al. 2019). Both the ZnO front contact and the molybdenum rear contact are sputtered.

3.3.2.1.6 Other thin-film cells

In addition to the cells listed here, there are other cell types that also form part of the thin-film family. Organic solar cells are particularly worthy of a mention here. The reason behind developing this cell type is the use of significantly more favourably priced materials and manufacturing processes during which expensive raw materials such as platinum and ruthenium are used to a certain extent. However, efficiency levels have been very low so far and the service life is also really short at around 5,000 hours. There are no cells or modules using this technology available on the market yet. One example of this cell type is the dye-sensitised solar cell (DSSC). Also known as the Grätzel cell, this cell type uses organic dyes in a similar way to photosynthesis to convert light into electrical energy. These cells are mostly purple and provide the best efficiency among all organic solar cells at over 15 %, although they also have a limited service life due to aggressive electrolytes. The latest research into polymers or metal foils as a replacement for glass substrates could help DSSC cells to make a commercial breakthrough in the future (Kowsar et al. 2019).

Another thin-film technology from recent years which has attracted a great deal of attention is perovskite solar cells (PSC). With initial efficiencies of around 10 % and 500 hours of stable operating time, these cells are not competitive yet. Due to their photoelectric properties, which may include a high absorption coefficient, a long carrier diffusion length and low exciton binding energy at times, the perovskite solar cell makes an ideal candidate for providing light-absorbing materials. Cells with 25.2 % efficiency have now been produced on a laboratory scale (Zhang & Park 2020). Moreover, perovskite solar cells scored the best sustainability during an environmental performance evaluation of several emerging thin-film technologies (Gok 2020).

3.3.2.2 Raw material content

Only CI(G)S and CdTe technologies are considered in the text below, because they have been commercially available for several years and are dependent on key raw materials. Moreover, they currently represent by far the largest share of the market with 97 % of the thin-film PV modules sold (Fraunhofer ISE 2020). Figure 3.59 provides a rough composition of CdTe or CIGS thin-film modules.

Figure 3.59 shows that glass and the frame structure are the main components in modules. In contrast, the proportion of semiconductor compounds, included under “thin-film elements”, is relatively low. Only part of the target material used ends up on the substrate, especially during sputtering processes. One part is not removed and remains on the target, which is then recycled. Another part of the target material is deposited on the chamber walls and/or panels, which can also be recycled to some extent. The substrate size is thus decisive for material efficiency during sputtering among other things. As material is sprayed over the substrate edge (around 0.15 m) during sputtering (overhang), the ratio between the overhang and substrate size determines how much of the material actually ends up on the substrate. A greater substrate size would improve this ratio. However, there are technical limits to the substrate size to be sputtered (Von Ardenne GmbH 2020).

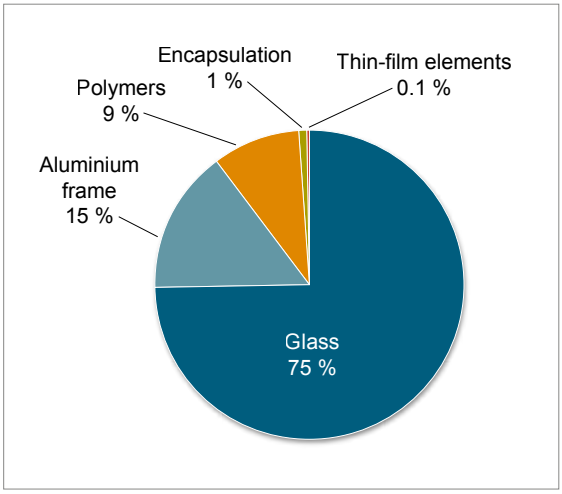

Figure 3.59: Composition of a thin-layer PV module (source: Sander et al. 2007)

Finally, you also need to take into account that the front electrode on some PV cells consists of an ITO layer instead of ZnO, which constitutes another component that uses indium in such cases. Marwede & Reller (2014) developed scenarios for material efficiency throughout the life cycle of both thin-film technologies. They also looked at material losses during coating or due to rejects and the recycling of these losses. In doing so, they defined material utilisation during production as a product-specific raw material demand due to the use of raw materials for production minus the materials recycled from production waste. This means that credit is given for the recycled material. The calculated material utilisation efficiencies can be used to determine how much the raw material demand for production exceed the actual material content in the modules.

The product-specific raw material content per Wp depends on the layer thickness, the stoichiometric composition of the layers, the solar cell efficiency and the material efficiency. A value of 1,000 W/m² was assumed for the solar constant. The formula below was used for calculations.

The degree of efficiency determines how many square metres of space are required per watt of nominal output. Small CIGS modules (841 cm²) can now achieve 19 %, as Solar Frontier has demonstrated. Values of 15 % can be achieved for larger MiaSolé modules, which are manufactured on a surface measuring 9,703 cm². It has also been established that the stability of modules is comparable, if not higher even that in c-Si modules (Shah 2020). A module efficiency of 17 % is being used for the current calculations for CIGS in 2019. However, the efficiency of finished CdTe modules can exceed 18 % (First Solar modules measuring 7,038 cm²) (Shah 2020) up to 19 % (Fraunhofer ISE 2020). In the past, there were problems with the durability of solar cell efficiency; this was related to the diffusion of copper, which is required to provide a suitable rear contact. However, this problem has now been practically resolved by embedding copper into a ZnTe layer. This improvement is evident in the high reliability of First Solar modules (Shah 2020). As a result, a efficiency of 19 % is also expected for current calculations in 2019.

Current material efficiencies in established manufacturing processes are 70 %. Both personal information and own estimates based on different studies have been used to calculate these values (Zuser & Rechberger 2011; Cichy 2017). This value does not include material recycling rates for manufacturing waste recovery. For this reason, calculations used a net material efficiency of 80 % for 2018, based on the research findings of Marwede & Reller (2014). A net material efficiency of 95 % is assumed for the SSP1 scenario and 90 % for the SSP2 scenario for the year 2040.

As there is also a wide variation in the absorber layer thickness between the manufacturers and the manufacturing processes, a linear decrease in the layer thickness was taken from the previous report for CIGS (1.4 µm) and CdTe (1.7 µm) in 2018. The values of 0.5 µm and 1.0 µm from the previous report for 2035 were used again for the fast and slow development of the two models for 2040. This is because of the enormous uncertainty of a forecast over such a long period of time. These figures contradict previous references, e.g. the extensive research by Cichy (2017), which predicted a layer thickness of 0.8 µm for 2040. However, the EU research project ARCIGS-M is

$$W_{p,x} = \frac{\rho_{A,x}}{\sigma \cdot \eta_M \cdot \eta_{MNE}}$$

Symbol	Description	Unit
$W_{p,x}$	Product-specific raw material content of element x depending on output	tonnes/GW
$\rho_{A,x}$	Mass per unit area of element x depending on layer thickness and stoichiometric occurrence	g/m²
σ	Solar constant	GW/m²
η_M	Module efficiency	%
η_{MNE}	Production-specific net material efficiency	%

already undertaking research with CIGS absorber layer thicknesses of 0.5 µm. These figures are reached using a layer of silver instead of a molybdenum layer since this unabsorbed light is transmitted back into the absorber layer and a more complete absorption of sunlight is produced (European Union 2020). Diermann (2019) also reports in PV-Magazine that similar research can also be applied to CdTe. A nano-structured rear mirror is also used in this design with the aim of keeping light in the semiconductor for longer.

The aforementioned data can be used to derive parameters for calculating the production-specific raw material demand for 2018. These are the starting points for developing two different technology scenarios for the year 2040 (see Table 3.52).

The data in Table 3.52 are based on the exemplified examination of common coating processes for CdTe and CIGS modules. The cell-specific contents of semiconductor materials are governed by considerable uncertainties overall. Layer thicknesses and coating processes have a significant impact on the actual demand for semiconductor material and vary from manufacturer to manufacturer. Moreover, they differ significantly between laboratory scale systems and pilot plants and also change when processes are subsequently developed into mass production systems.

3.3.2.3 Foresight industrial use

Effective and significant demand effects from thin-film photovoltaics for high-purity semiconductor materials crucially depend on the market growth for thin-film photovoltaics. Future market development for thin-film photovoltaics also very much depends on the overall development of energy demand (prices for fossil fuels among other things), renewable energy sources in particular (including funding for advancing technology and feed-in tariff conditions) and very specifically the photovoltaics (including the current standard of thin-film technology. IMAGE SSP1-19 and the MESSAGE-GLOBIOM SSP2-26 scenario are used to preview industrial use here; compare Section 1.1.1. No additional photovoltaic capacity will be installed between 2030 and 2040 in the REMIND-MAGPIE SSP5 baseline (Bauer et al. 2017a).

In 2018, global solar cell production amounted to 102 GWp (Statista 2021b). The market share of CdTe was 2.6 % (with 2.7 GWp) while CIGS took a share of 1.1 % (with 1.2 GWp) (Fraunhofer ISE 2020). To estimate future raw material demand, it was assumed that, in SSP1-19, both technologies will each achieve a market share of 8 % of the annual installed capacity of 390 GW_p in 2040. In SSP2-26, both the overall market and the thin film market expand at a slower rate: it is thus assumed that each technology will achieve a market share of 2 % of the annual installed volume (65.7 GW_p) in 2040.

Table 3.52: Production-specific raw material demand depending on absorber layer thickness, efficiency and material inefficiency

	2018		2040			
			SSP1 Sustainability		SSP2 Middle of the Road	
	CIGS	CdTe	CIGS	CdTe	CIGS	CdTe
Absorber layer thickness	1.4 µm	1.7 µm	0.5 µm	0.5 µm	1 µm	1 µm
Efficiency	17 %	19 %	25 %	25 %	21 %	22 %
Material efficiency	80 %		95 %		90 %	
Raw material demand [tonnes/GWp]	Cu: 11.3 In: 14.3 Ga: 3.8 Se: 27.8	Cd: 27.5 Te: 31.3	Cu: 2.5 In: 2.9 Ga: 0.8 Se: 5.9	Cd: 5.9 Te: 6.7	Cu: 6.1 In: 7.8 Ga: 2.2 Se: 15.6	Cd: 15.0 Te: 17.2

Note: Stoichiometry Cu(In0,7Ga0,3)Se2

Table 3.53 summarises the global annual installed capacity of PV and annual additions for the thin-film PV cell types CIGS and CdTe studied in depth. No meaningful projections could be made for increased use of GaAs cells, which are mainly used for space-related applications.

3.3.2.4 Foresight raw material demand

The future demand for raw materials (Table 3.54) can be calculated by multiplying the production-specific raw material (Table 3.52) by the annual installed power capacity (Table 3.53).

If we look at the raw material demand for the individual absorber layer materials in 2018 in Table 3.54 in comparison to recent years or the figures for 2013 in the previous study (Marscheider-Weidemann et al. 2016), we see they have decreased. This can be attributed to the three advances in thin-film technologies while taking into account the formula for the product-specific raw material content per Wp. First of all, the efficiencies of CIGS and CdTe PV plants have improved considerably; efficiencies of just 12 % were estimated for both technologies in 2013. We can now assume efficiencies of 17 % (CIGS) and 19 % (CdTe) for good modules. Furthermore, continuous innovations have made absorber layers thinner, which has resulted in a lower area density for the individual elements. There have also be considerable advances in manufacturing processes, which means material efficiencies of 80 % can be assumed today. There is also the fact that the annual installed capacity of CIGS and CdTe has decreased slightly in direct comparison to the previous study. However, this is not the case if we refer to the historical data provided by Fraunhofer ISE (2020). It is thus supposed that the estimated figures for 2013 were too high.

A reduction in raw material demand is expected for the requirements forecast in SSP1-19 compared to the breakdown scenario 2035, even if this reduction is only slight. If we compare the SSP2-26 scenario with the scenario at that time

Table 3.53: Annual installation of CdTe and CIGS solar modules in megawatt peak in SSP1-19 and SSP2-26 scenarios

Annual installation	2018	2040	
		SSP1-19 Sustainability	SSP2-26 Middle of the Road
CdTe (MWp)	2,700	31,200	1,300
CIGS (MWp)	1,200	31,200	1,300

Table 3.54: Global production (BGR 2021) and calculated raw material demand for thin-layer PV, in tonnes

Raw material	Production in 2018	Demand in 2018	Demand foresight for 2040	
			SSP1 Sustainability	SSP2 Middle of the Road
Copper	20,591,000 (M) 24,137,000 (R)	14	79	8
Indium	808 (R)	17	92	10
Gallium	413 (R)	5	26	3
Selenium	3,677 (R)	33	184	20
Cadmium	26,670 (R)	74	184	20
Tellurium	595 (R)	84	210	22

M: Mine production (tonnes of metal content)
R: Refinery production (tonnes of metal content)

("slow development" in 2035), we can detect a significant reduction, which is due to the very low sales figures in the market forecast in the SSP2-26 scenario.

However, a marked discrepancy can be found between the raw material demands in the two scenarios with regard to the estimations for 2040 (Table 3.54). Despite the poorly predicted absorber layer thicknesses, material efficiencies and efficiency for "slow development" (SSP2-26), the annual installed capacity is decisive for the raw material demand. Whereas the scenario model SSP2-26 estimates an annual installed capacity of 1,300 MWp, the forecast for "rapid development" (SSP1-19) is 31,200 MWp, which represents a difference by a factor of 24. All forecasts for raw material demands for the SSP2-26 model consist of a virtually constant or lower demand in relation to global production for 2018 compared to 2018. As a result, the "rapid development" and the associated increased raw material demands for the SSP1-19 model are discussed in more detail below.

Due to the sharp increase in sales figures for CdTe for the SSP1-19 model compared to the annual installed capacity for 2018, the demand for tellurium increases considerably compared to the quantity required in 2018. In this case, 14 % of world production was used for CdTe in 2018 and an increase to 35 % of the world production in 2018 was forecast for 2040. A potential bottleneck in tellurium supply for mass production of CdTe modules is discussed critically here. However, model calculations which take into account all aspects of recycling and different market developments showed that there would be sufficient tellurium to install an accumulated capacity of 2 TWp up to 2050 (Powalla et al. 2018). Fthenakis (2009) expects that the Tellurium supply will be significantly expanded in the future thanks to the growth of copper production, during which tellurium is obtained as a by-product. This means the future raw material demand for photovoltaics can be met.

Similarly, the demand for cadmium is expected to increase sharply. The forecast demand for photovoltaic technologies of 74 tonnes/year (2018) is likely to increase to 184 tonnes/year (2040). However, both values in the different scenarios represent only a fraction of 0.1 % or 0.7 % of the annual global production in 2018. The issue of toxicity in the semiconductor compound CdTe plays a part in this respect. There has not been sufficient research into toxicity to date. CdTe-PV is not (yet) subject to the ban under the European RoHS Directive (RoHS Directive 2011) at the present time. If there is a ban on putting CdTe-PV modules onto the market in Europe in the future, this will have a direct impact on raw material demand. This will be of particular consequence for tellurium since the CdTe PV industry is one of its main consumers.

Forecasts predict a significant increase in demand for the absorber materials indium, gallium and selenium for CIGS modules for 2040. Nonetheless, according to the European Commission's Foresight study, tellurium and indium in particular have the most critical demand-to-supply ratio in keeping with the predictions made here (European Commission 2020a).

Future development of CIGS thin-film photovoltaics also depends on how the raw material demand for indium and gallium evolves for other technologies such as LEDs, displays or ICs. For instance, LCD TV manufacturers are likely to absorb increases in indium prices far more easily since the value percentage of indium in relation to the purchase price is significantly lower than it is for CIGS solar modules. LCD manufacturers can also use possible substitutes if indium prices rise too much. CIGS manufacturers can only substitute indium to a limited extent: if gallium is used instead of indium, the band gap is worse and gallium is also as expensive and critical as indium to a similar degree.

3.3.2.5 Recycling, resource efficiency and substitution

The use of photovoltaic systems is growing rapidly worldwide. The modules manufactured today are expected to reach the end of their service life in 25 to 30 years' time and 78 million tonnes of PV waste will be generated or vast quantities of modules will be taken out of service by 2050. First Solar, the world's largest PV module recycler with extremely high on a vast scale, recovers glass, metals and plastic from manufacturing process scrap and waste CdTe modules using a combination of mechanical and chemical processes.

First Solar recycles 25,000 tonnes of used CdTe modules every year. A recycling rate of 95 % is achieved for cadmium and tellurium (Ravikumar et al. 2020). Safe recovery and good recycling methods are urgently needed for CdTe modules since the high toxicity of semiconductor materials is important factor to take into consideration.

One major benefit of recycling CIGS modules is that the critical, valuable metals gallium and indium can be extracted from old modules. As there is a high concentration of both elements – 600 ppm (Ga) and 90 ppm (In) – used CIGS modules have a higher concentration of these elements than in ores. Current research has already shown recovery rates of 90 % on a pilot scale and thus provides a starting point for further trials and consideration to recover indium and gallium more effectively than secondary raw materials. However, here, we are also faced with the problem that it will be a few decades before used modules are returned in large quantities if we assume an average life span of 25 years. Again, it is not only the valuable metals that make it essential to recycle; modules also contain a great number of toxic substances. A more effective network needs to be built up between CIGS manufacturers and recyclers in the future to pursue the targets of the recycling economy (Amato & Beolchini 2019). With the European Commission taking on a pioneering role in providing new statutory and regulatory frameworks to help advance towards a recycling economy for PV plants, such rules may also over CIGS in the near future. CIGS cells are ideal for meeting the standards for recirculation of raw materials (ESS 2017; Heske et al. 2019).

The concentration of gallium and indium in CIGS solar modules is too low to ensure their cost-effective recovery. Recyclers are thus studying the option of combining recycling of LCDs (Indium) with the recycling of CIGS solar cells, which could make the process viable in the short term (EU 2014). Moreover, the aim is to recycle the substrate glass to a high standard so that a raw material important in terms of quantity can be brought back onto the market.

Solar cells using cheaper, more readily available semiconductor compounds such as CuZnSnS, CuN or FeS_2 are being developed as an alternative to GIGS and CdTe. There are also other technologies to choose from, such as organic and dye-sensitised solar cells. Perovskite solar cells in particular impress with low energy requirements, low production costs, high efficiency and, consequently, a shorter energy return on investment period compared to other conventional PV technologies. They also bring advantages in terms of environmental compatibility (Zendehdel et al. 2020).

The European Commission's Foresight study on critical raw materials for PV production also critically addressed the issue of how to counteract any bottlenecks in raw material procurement. According to the study, the EU could benefit from having already defined joint recycling and recovery targets. However, further standardised waste classifications would be desirable for PV plants (European Commission 2020a).

3.3.3 Water electrolysis

3.3.3.1 Technology description

Water electrolysis uses electrical energy to break water down into its constituent parts oxygen and hydrogen. This emission-free process to produce hydrogen using renewable energies is considered one of the key technologies for decarbonising energy systems further. In the past, however, high hydrogen production costs compared to alternative technologies meant that water electrolysis was only used in very isolated cases, such as the Aswan dam in Egypt and in the Peruvian city of Cuzco. A change in circumstances have recently led to an increasing interest in the technology.

The basic principle behind water electrolysis involves connecting a power source to two electrodes in water and establishing an electrical circuit thanks to ion migration. As a result, hydrogen will appear on one electrode and oxygen on the other. Figure 3.60 shows the basic operating principle. It is thus the reverse principle of the fuel cell when oxygen and hydrogen are added to it. In a similar way to fuel cells, we also subdivide electrolysis based on the electrolytes or membranes that it uses. The alkaline electrolysis and polymer electrolyte membrane electrolysis (PEM electrolysis) available for large-scale industrial use are particularly worthy of mention here. Solid oxide electrolysis is not quite as well developed.

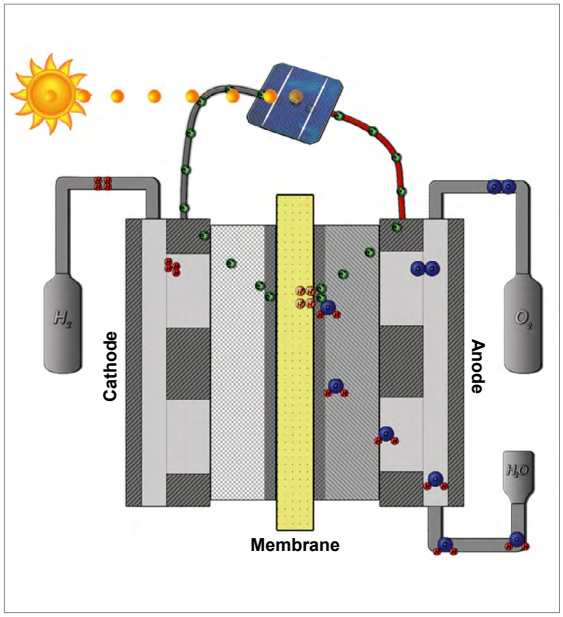

Figure 3.60: Design and working principle of a PEMEL (source: Davidlfritz, PEM Elektrolyse 5, Wikimedia, CC BY-SA 3.0)

We also refer more frequently to anion exchange membrane electrolysis (AEM electrolysis), which attempts to combine the benefits of alkaline electrolysis and PEM electrolysis without their disadvantages. However, this section does not look at this technology any further due to its early stage of technological development. IRENA (2020a) gives a an overview of the currently available technologies.

Alkaline electrolysis uses an alkaline electrolyte, which often consists of a 20–40 % KOH solution. A non-conductive porous membrane, what is known as a diaphragm, links the anode and cathode. The diaphragm is permeable to OH^- ions, but is electrically non-conductive and is impermeable to oxygen and hydrogen. When a current is applied to the electrodes, OH^- ions are formed as hydrogen is separated on the cathode. These OH^- ions migrate to the positively charged anode through the diaphragm, where they form oxygen as they release an electrical charge. This creates twice as many hydrogen molecules as oxygen molecules. The current densities are usually between 0.2–0.8 A/cm^2 in this process. The gas bubbles formed at high current densities increase electrolyte resistance, thus constituting a limitation. We can only reduce the diaphragm thickness to a limited extent since it would otherwise allow the product gases to diffuse through it. Efficiencies between 50 and 78 % can be achieved at temperatures of 70–90 °C and pressures of less than 30 bar. Using an alkaline solution means there is little corrosion on the cell and there is no need to use precious metals.

PEM electrolysis features a proton-permeable solid polymer membrane generally made using sulfonic acids. An H^+ ion is formed on the precious metal acting as a catalyst on the anode immersed in water. This ion migrates along the membrane to the cathode when electrical energy is applied. The charged particle flowing into the porous electrode produces hydrogen there. Fully desalinated water is generally used in order to prevent contamination, which would reduce the service life of electrodes. When PEM electrolysis is used, the direct contact of the electrodes on the membrane can lead to higher current densities than with alkaline electrolysis at 1–2 A/cm^2. The higher current densities also allow a more compact design. Efficiency lies between 50 and 83 % at pressures similar to alkaline electrolysis. The operating temperature is slightly lower at 50–80 °C. This particular process can usually achieve slightly higher hydrogen purities. PEM electrolysis is also able to respond more effectively to load fluctuations and can be put to used more quickly. Due to historical development, many cell types are still based on the PEM fuel cells with similar materials normally used.

Since solid oxide electrolysis can often also be operated in reverse mode, as in a solid oxide fuel cell (SOFC; see Section 3.3.5), the functional principles, the materials used and the designs are often identical. However, adding water onto both the anode and the cathode makes it interesting to concentrate on the anode-based cell structure, as this can reduce ohmic losses in the electrolyte. A solid oxide is used as an electrolyte, just like in an SOFC. Water is decomposed into hydrogen and an O^2 ion on the cathode. The ion migrates to the anode through the electrolyte, forming oxygen when the electrical charge is released. High operating temperatures of 700–850 °C are required to ensure that the electrochemical reaction can take place. However, the high operating temperatures mean that high efficiencies can be expected in the long term, even though these are currently between 45 and 55 %. Current densities

of 0.3–1 A/cm² are anticipated for solid oxide electrolysis. The use of waste heat, which is sometimes possible, can reduce the power requirement to a certain level. Current stack sizes are still significantly smaller than with alkaline electrolysis and PEM electrolysis, though. This also applies to the service life, which is considerably lower at less than 20,000 hours.

A comparison between these three water electrolysis technologies shows that there are many overlapping areas of use for three options and that each of these technologies can often be substituted with one of the others. This particularly applies to alkaline electrolysis and PEM electrolysis. This can also offset material demands to a certain extent. However, alkaline electrolysis can be considered to have benefits in that it currently brings financial advantages regarding investment and we are able draw on many years' experience with the technology. The maximum stack sizes have also been somewhat larger to date. PEM electrolysis can feature a significantly more compact design and can respond more effectively to load changes. This is regarded as highly beneficial when integrating fluctuating renewable energies. However, the use of precious metals makes it difficult to scale on a cost-efficient basis. Due to its high operating temperature, solid oxide electrolysis offers great potential for achieving efficiencies, although low-priced heat sources need to be available to make it financially viable. Fluctuations in load also produce high thermal loads, which is why the aim is to achieve continuous operation with the solid oxide electrolysis. Current research activities indicate that we can expect further harmonisation of alkaline electrolysis and PEM electrolysis in particular in the long term.

Manufacturers have increasingly repositioned themselves in recent years. Fuel cell manufacturers are trying to extend their product range. Start-ups, smaller firms and experienced manufacturers hope to be able to grow rapidly based on the increasing demand. Established producers on the gas market such as Linde or Air Liquide are seeking strategic partnerships or entering into joint ventures. Some companies such as ThyssenKrupp or Siemens are focusing on one technology such as alkaline electrolysis or PEM electrolysis. Other manufacturers such as NEL are trying to offer both technologies. It can be said that the Europeans are promoting PEM electrolysis heavily on the global market while other countries such as China are focusing more on alkaline electrolysis. Despite the growing demand, there seem to be no problems or only slight limitations in manufacturers' production capacities for solid oxide electrolysis, as revealed in a survey (NOW GmbH 2018). Newly built electrolysers can now be significantly larger than 100 MW thanks to their modular design.

3.3.3.2 Foresight industrial use

The water electrolysis capacities installed to date have been limited compared to alternative technologies due to financial challenges. According to IEA (2020b), added capacities have only amounted to around 10 MW per year in recent years. However, starting in 2019, the number of pronouncements regarding output capacities to be installed have increased rapidly, which means that added capacities should more or less double every year until 2023; see Figure 3.61. We should also bear in mind that further installations may be announced for this period.

Alkaline electrolysis was mainly used in the past. However, PEM electrolysis has managed to gain market share continuously since 2000 and currently has a share of around 45 %. New announced capacities predominantly use PEM electrolysis. There are only a few individual solid oxide electrolysis plants to date with most existing as a demonstration plant only (Staffell et al. 2019; IEA 2020c).

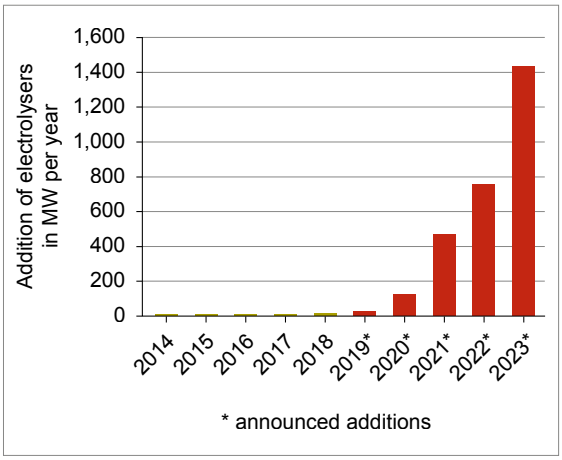

Figure 3.61: Addition of electrolysis capacities (source: IEA 2020b)

As we can see from pronouncements regarding the expansion of new electrolysis capacities, significant market growth can be expected in the next few years, not least due to increased subsidies. However, this anticipated market growth is unlikely to continue over the coming years. For this reason, this study assumes somewhat more conservative values. There are also considerable doubts regarding the long-term demand and, consequently, the future importance of water electrolysers.

For this study, the installed future capacities are determined based on the green hydrogen generation in the SSP scenarios; see Section 1.1. The SSP scenarios are designed to represent the widest development corridor possible, which takes into account the development assumptions from other studies, e. g. Weltenergierat – Deutschland e. V. & Frontier Economics (2018), Irena (2020a). It is assumed that the electrolysers will be operated for 3,500 full load hours on a long-term basis. A constant technology mix of 85 % alkaline electrolysis, 10 % PEM electrolysis and 5 % solid oxide electrolysis is assumed. This is because solid oxide electrolysis is not currently operated on an industrial scale and market growth should only be expected in the medium term, the raw materials (iridium and platinum) for PEM electrolysis are not available in sufficient quantities despite the projects currently planned and alkaline electrolysis currently offers financial advantages in terms of investment costs.

The assumptions regarding installed output capacities and the electrolysers added each year can be found in the SSP scenarios in Figure 3.62. The demand in 2040 is significantly lower in SSP5 with a supply of around 100 GW than in SSP1-19 at around 1,700 GW. SSP2-26 comes between the two at 430 GW, which corresponds to the required annual increase in SSP1-19 around the same time. The scope between the scenarios is therefore very wide as a result.

The possible different market developments also have a sizeable influence on further development of technologies. With large quantities of electrolysers, more significant progress is to be expected and also necessary regarding design and saving materials. The regulatory framework also has a direct impact on market development. Different political goals could thus lead to different developments on a local level. Alternative technologies such as direct electrical processes can help reduce the need for electrolysis in the long term.

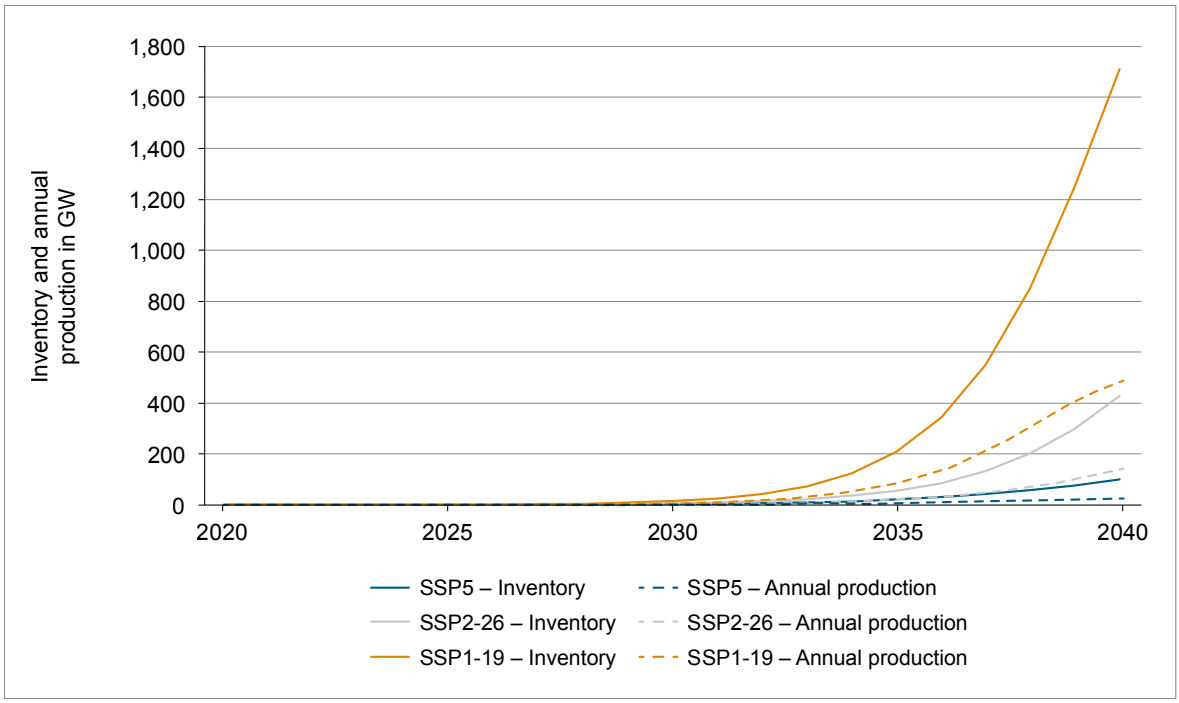

Figure 3.62: Production and expansion of electrolyser stock for SSP5, SSP2-26 and SSP1-19 scenarios (source: own representation)

3.3.3.3 Raw material content

The three electrolyser types impose different requirements on the raw materials and especially catalysts (Khan et al. 2018). Non-precious metals can be used for alkaline electrolysis (David et al. 2019). An aqueous caustic potash solution is generally used as an electrolyte. A sodium hydroxide solution can also be used, however. Zirfon (coated polysulfone matrix with ZrO_2) is normally used for the diaphragm. Alternative materials or polymer membranes have not managed to find acceptance here to date. However, no major savings can be expected in material thickness (250 µm) due to the requirements for gas permeability. Mainly nickel-based materials, such as Raney nickel, or coated high-grade steel are used for both the anode and cathode. However, precious metals are also included in the studies and further developments to increase the current densities and improve dynamic behaviour. This can also mean platinum is used in the electrodes, for example.

PEM electrolysis generally uses a Nafion variant (perfluorosulfonic acid (PFSA)-polytetrafluoroethylene (PTFE) copolymer) as the electrolyte. Hydrocarbon-based materials can be used as an alternative. Unlike alkaline electrolysis, PEM electrolysis is dependent on precious metals due to the acidic environment around the membrane. The anode usually requires iridium oxide (IrO_2) as a result. Iridium is currently also considered to be irreplaceable since no alternative material has yet offered the required properties, e.g. ruthenium oxide (RuO_2) which features a significantly higher corrosion rate. However, efforts are being made to reduce the electrode load and save material due to the scarcity of material. In the case of both Ir and Ru, 0.5–1.5 g/kW of material is required whereas roughly 1 g/kW is currently needed. Platinum group metals are mainly used in the cathode with platinum in particular often used with carbon carrier material in quantities of 0.05–0.2 g/kW. There is also a continuous reduction in this case. Platinum offers effective corrosion protection and good conductivity. Palladium or suitable alloys are also used as an alternative (Shiva Kumar & Himabindu 2019). Platinum and titanium are usually also required for the transport layers and bipolar plates on the electrodes.

As solid oxide electrolysis and SOFCs often only differ in the way they operate, the required materials are the same as for SOFCs (Chen & Jiang 2016; Hussain & Yangping 2020; Beiderbeck et al. 2020). This means that a yttrium-stabilised zirconium dioxide (YSZ) can generally be used as the electrolyte. Nickel-YSZ materials are used for the anode while perovskite materials such as lanthanum strontium manganite (LSM) are used for the cathode. If further developments for anode-based cells advance favourably, there may be a slight shift toward anode-supported solid oxide electrolysis from a materials perspective as this can eliminate ohmic losses. However, the mean operating temperature currently targeted for solid oxide electrolysis also makes it possible to use options such as scandium-stabilised zirconium dioxide (ScSZ)/scandium-cerium-stabilised zirconium dioxide (ScCeSZ) for the electrolyte.

The values indicated in Table 3.55 were based on the specific loads on the PEM electrolysis electrodes and the LCA studies in Koj et al. (2015), Häfele et al. (2016), Koj et al. (2017), Bareiss et al. (2019), Carmo et al. (2019), Shiva Kumar &

Table 3.55: Specific raw material demand for water electrolysers in g/kW (sources: Koj et al. 2015, Häfele et al. 2016, Koj et al. 2017, Bareiss et al. 2019, Carmo et al. 2019, Shiva Kumar & Himabindu 2019, Lotrič et al. 2021)

Raw material	g/kW
Iridium	0.1
Platinum	0.01
Titanium	28.3
Aluminium	112.6
Copper	229.1
Zirconium	83.7
Scandium	0.1
Yttrium	5.9
Lanthanum	0.8
Nickel	423.1
Cobalt	0.3
Manganese	0.9
Cerium	9.3
Chromium	131.1

Himabindu (2019), Lotrič et al. (2021). The findings for SOFCs were also taken into account for solid oxide electrolysis and mean values were then calculated. Extreme values were not considered and assumptions were made regarding reduced material usage in electrochemical cells to represent future development.

3.3.3.4 Foresight raw material demand

Table 3.56 shows the following raw material demand for water electrolysers. It is based on the assumptions regarding the specific raw material demand and the defined scenarios for hydrogen demand and the resulting production quantities. It is clear that most raw materials on their own are not critical for the quantities produced. However, this is not the case with iridium and scandium. In the case of iridium, the demand for 2040 in two scenarios (SSP1 and SSP2) is significantly higher than for production in 2018. If the assumptions are correct current demand (also see Section 3.3.5 on SOFCs), significantly more scandium will be required in Scenario SSP1 in 2040 than is currently being produced. We should also bear in mind that the scenario assumed that the proportion of solid oxide electrolysis cells for which it is used will be small.

Since the different water electrolysis processes require different raw materials, although usage requirements overlap to a certain extent, material bottlenecks can be eased to some degree by using an alternative water electrolyser type. With solid oxide electrolysis in particular, there are materials which are generally used as an alternative for scandium or can even replace it entirely.

It should be noted that research activities have increased significantly in recent years, especially on improving cost efficiency for water electrolysers. To ensure construction becomes more viable

Table 3.56: Global production (BGR 2021) and calculated raw material demand for water electrolysers, in tonnes

Raw material	Production in 2018	Demand in 2018	Demand foresight for 2040		
			SSP1 Sustainability	SSP2 Middle of the Road	SSP5 Fossil Path
Iridium	6.8[1] (R)	0.01	34	10	2
Platinum	190 (M)	0.00	6	2	0.33
Titanium	260,548 (R)	3.55	13,600	3,900	720
Aluminium	63,756,000 (R)	14.20	54,200	15,400	2,900
Copper	20,591,000 (M) 24,137,000 (R)	28.80	110,400	31,300	5,800
Zirconium	1,256,362[2] (M)	10.50	40,300	11,400	2,100
Scandium	9.1 (M)	0.01	24	7	1
Yttrium	7,600 (R)	0.74	2,800	800	150
Lanthanum	35,800 (R)	0.10	370	100	20
Nickel	2,327,500 (M) 2,189,313 (R)	53.20	203,870	57,900	10,800
Cobalt	151,060 (M) 126,019 (R)	0.04	160	40	8
Manganese	20,300,000 (M)	0.12	450	130	24
Cerium	58,800 (R)	1.20	4,490	1,270	240
Chromium	27,000,000 (M)	16.50	63,200	17,900	3,300

M: Mine production (tonnes of metal content)
R: Refinery production (tonnes of metal content)
[1] Source: JM 2020
[2] Production of zirconium minerals

financially, reductions in the demand for precious metals are unavoidable. We can thus assume that this will have a positive effect on future raw material demand.

3.3.3.5 Recycling, resource efficiency and substitution

Due to the similarity between water electrolysis and fuel cells, their use of materials is comparable in some respects. As a general rule, the cell type and design have a major influence on the recycling rate due to the use of different materials. Different manufacturing processes and sizes also lead to different material losses. In the case of alkaline electrolysis and PEM electrolysis, material loss tends to be in the low single-digit percentage range. Recycling efforts are considerable if a material used has a high value. Since this does not include ceramics, they are usually disposed of for second use as a filling material, although recycling rates of up to 100 % can be achieved for most metals. However, there are still difficulties with transition metals with a recycling rate of just 30 % and with platinum metals with a rate of 50–90 % (Environment Park SPA et al. 2018; Environment Park SPA et al. 2019; Lotrič et al. 2021). Nonetheless, recycling rates of more than 90 % can be achieved for platinum and iridium when new processes are used (Carmo et al. 2019). If there are sizeable quantities of used systems, we can assume that recovery will be improved even further in the case of solid oxide electrolysis if there are suitable economic incentives.

3.3.4 Direct air capture (DAC)

3.3.4.1 Technology description

Direct air capture (DAC) refers to the filtering of CO_2 from the ambient air with a plant, an example of which is shown in Figure 3.63. DAC can be used to reduce the CO_2 content in the atmosphere, which counteracts the greenhouse effect responsible for global warming. The filtered CO_2 can be used for different purposes. One option is to store CO_2 for the long-term, thus removing it permanently from the atmosphere. In such a case, we talk about “negative emissions”. Storage of greenhouse gas has the potential to help considerably in meeting the Paris Climate Agreement

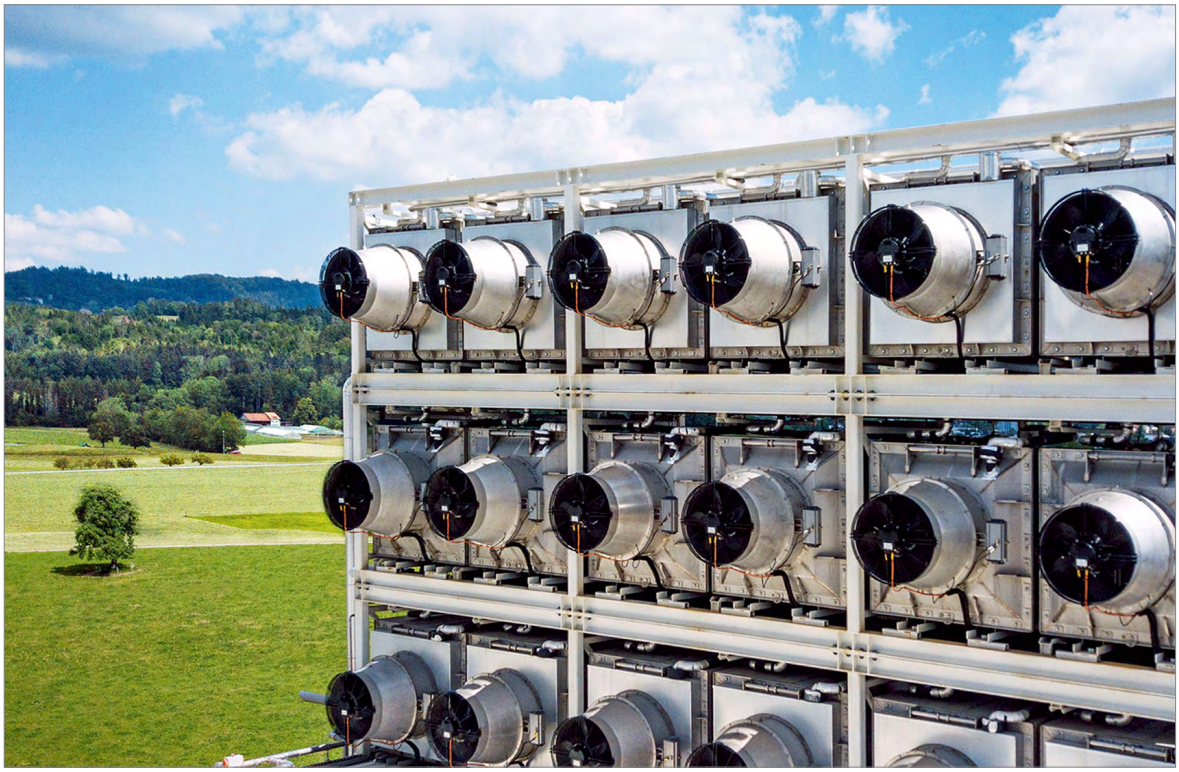

Figure 3.63: Direct air capture plant (source: Climeworks)

(Gambhir & Tavoni 2019). Feasible long-term CO_2 storage options include geological deposits such as deep salt rocks or basalt where the CO_2 is mineralised, thus placing it in safe, long-term storage (Fasihi et al. 2019). The CO_2 can also be used to manufacture synthetic fuels or hydrocarbons for plastics manufacture. Fischer-Tropsch synthesis is used to produce fuels such as petrol, diesel, kerosene or others from the CO_2 and hydrogen (Liu et al. 2020a). Admittedly, these fuels produce emissions locally again when they undergo combustion. However, the entire carbon cycle can be closed if renewable energy is used to produce the hydrogen. A more climate-neutral and thus more environmentally friendly alternative can thus be created for means of transport that are difficult to electrify, such as aeroplanes. The captured CO_2 can be used to enrich the air in greenhouses, where the CO_2 is absorbed by the plants through their metabolism, leading to a fertilizer effect. Another option to make use of the CO_2 is enhanced oil recovery. During this process, CO_2 is pumped into oil deposits to bring the oil to the surface. This is currently a profitable possible use, especially in the USA, since tax relief on negative emissions reduces the price of oil obtained by using enhanced oil recovery in conjunction with DAC (Mulligan & Lashof 2019; IEA 2020a). However, there are concerns about the safety and stability of this storage system, which need to undergo further research (IEA 2015).

Fans draw large quantities of air into the DAC system to push it through a sorbent to remove the CO_2 from the ambient air. There are currently two different methods to filter CO_2 from the air – the adsorption method and the absorption method. In the adsorption method, the CO_2 is deposited on the surface of a solid. It is thus adsorbed. After a certain period of time, the CO_2 on the surface reaches a saturation state, meaning the adsorption bodies need to be regenerated. For regeneration, the saturated solid is replaced by an unsaturated one and then scrubbed to extract the CO_2 (Martin et al. 2017). The process thus runs discontinuously.The adsorption process incurs comparatively low costs, consumes relatively little energy and does not use fossil fuels, unlike the absorption process.

The absorption process uses two interconnected circuits – a brine circuit and a calcium circuit – so that the CO_2 is first chemically bound and then extracted. The process is based on absorbing CO_2 in an aqueous alkali solution, usually a caustic potash solution.The alkali solution is fed into and removed from a brine circuit (on left in Figure 3.64) on a continuous basis. The CO_2 dissolved in the brine reacts with the caustic potash solution, which is channelled to a reaction unit for regeneration. This unit forms the interface between the two circuits. In this unit, the carbon is deposited in the form of calcium carbonate, which is transferred into the calcium circuit (on right in Figure

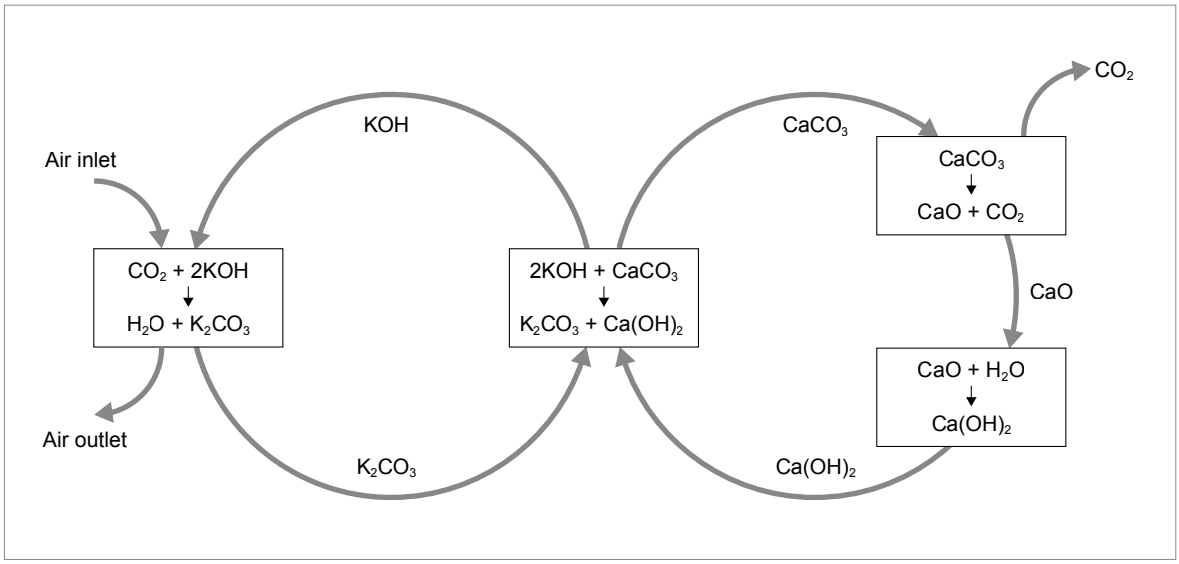

Figure 3.64: Chemical process of the two cycles of the absorption process for direct air capture (source: own representation based on Keith et al. 2018)

3.64) while the resulting caustic potash solution is channelled back to the absorption unit. The calcium carbonate is then heated in the next step to extract the CO_2, which can then be separated. During this step, natural gas is normally used to generate heat. This accounts for most of the energy input in the process. However, the DAC system can separate the CO_2 released during combustion so that no additional emissions are produced. Efforts are being made to electrify this process step in the future so that it is not dependent on fossil fuels. The calcium oxide produced during the heating process is hydrated to calcium hydroxide in order to close the second circuit (Keith et al. 2018). The absorption method is thus a continuous process, unlike the conventional adsorption method. This method is also easier to scale and its sensitivity to air pollution is lower.

Dittmeyer et al. (2019) developed a concept for small-scale use of DAC. This concept aims to use existing ventilation systems in larger buildings for DAC. For example, air conditioning systems in urban high-rise buildings could be used to filter CO_2 from the air. This concept could save on some of the required resources and energy since suitable ventilation systems already exist and are in operation. The disadvantage compared to a large-scale DAC plant, however, is the low-scale sorption and regeneration unit.

Figure 3.65: Permanent storage of CO_2 through mineralisation in a suitable geological deposit (source: Carbfix, photo by Sandra O. Snaebjornsdottir)

In addition to DAC, another of the technologies used for negative emissions is carbon capture and storage (CCS). In the case of CCS, the CO_2 is not taken from the ambient air. It is removed from point sources such as exhaust gases in power stations and then stored. As the CO_2 concentration in these exhaust gases is significantly higher than in the atmosphere, the energy input is lower compared to DAC. However, CCS only reduces the greenhouse gas emissions from power plants but does not change the CO_2 content in the atmosphere. The influence that DAC has on climate warming is therefore more immediate. You will find a closer look at the emerging technology CCS in Section 3.3.6. Figure 3.65 shows an example of how negative emissions are created by storing CO_2 in rock.

3.3.4.2 Raw material content

The demand for materials for an absorption method DAC plant with a capacity of 1 Mt CO_2 per year are derived from the basic scenario constructed by Jonge et al. (2019). This does not include the compression, transport and storage of the CO_2. It only refers to the DAC plant itself used to filter the CO_2 from the ambient air. Table 3.57 shows the raw material demand. The raw material content in DAC plants which function based on the adsorption method cannot be determined at present since development of this technology is at an early stage. Due to a more complicated scalability and the discontinuous process, which requires a large number of adsorption bodies, the raw material demand for the adsorption process

Table 3.57: Material demand of DAC plants using the absorption process with a capacity of 1 Mt CO_2/a (source: IEA 2020b)

Material	Unit	Material demand: absorption
High-grade steel	tonnes	32
Low alloy steel	tonnes	5,000
Concrete	m^3	117,000
PVC	tonnes	14,000
Polypropylene	tonnes	15
Glass fibre-reinforced polyurethane	tonnes	70

is estimated to be higher than the raw material demand for the absorption process specified in Table 3.57.

3.3.4.3 Foresight industrial use

There are currently 15 DAC plants in use worldwide, which together capture 9,000 tonnes of CO_2 out of the atmosphere (IEA 2020a). In Germany, no companies or research institutions have been directly involved in the development of DAC to date, although the required expertise does exist there (Viebahn et al. 2019). Relevant international DAC companies are presented in brief below. In addition to selling CO_2, a common business model for these companies involves selling negative emissions to other companies or individuals so that they can improve their carbon balance.

– Carbon Engineering (CE) is a Canadian company that uses the high-temperature absorption method. CE has been operating a DAC test facility which absorbs 1 tonne of CO_2 per year since 2015 (Keith et al. 2018). It is currently planning to build a commercial DAC plant with a capacity of 1 million tonnes of CO_2 per year with construction scheduled to start in 2021. The aim is to use the captured CO_2 for enhanced oil recovery in cooperation with Occidental Petroleum (Carbon Engineering 2019).

– Climeworks is a Swiss company which merged with the Dutch DAC company Antecy in 2019. In contrast to Carbon Engineering, Climeworks uses the adsorption method in its DAC plants. It currently operates two such plants. With a capacity of 900 tonnes of CO_2 per year, the plant operated in Switzerland is designed to capture CO_2 to sell for use in beverage production or greenhouses. The second plant is located in Iceland due to the low energy costs and is designed for a capacity of 50 tonnes of CO_2 per year. It uses the waste heat from a geothermal plant used for energy supply to increase overall efficiency. The CO_2 is permanently stored in the ground after mineralisation to generate negative emissions (Geoengineering Monitor 2018).

– Global Thermostat is a US-based company and, like Climeworks, uses the adsorption method. A test facility in California filters 730 tonnes of CO_2 per year from the atmosphere (Viebahn et al. 2019). Working in cooperation with Siemens Energy and Porsche AG, it is planning to build a plant for synthetic fuel production in Chile. This plant will use CO_2 from the ambient air and H2 produced in a electrolytic system and will be operated with wind energy (Fialka 2021).

– Other, smaller DAC companies include Skytree and Infinitree.

A current barrier to greater growth in DAC is the high costs due to the high energy consumption and the technology being at an early stage of development. The current estimated costs vary widely depending on the source. The National Academies of Sciences, Engineering, and Medicine (2019) specify USD 199–357 per tonne of CO_2 for the absorption method and USD 88–228 per tonne of CO_2 for the adsorption method. According to estimates by Fasihi et al. (2019), costs could fall to around USD 56 per tonne of CO_2 (€50 per tonne of CO_2) by 2040 thanks to the anticipated market diffusion and further technological developments.

Another obstacle to the growth of DAC is the environmental impact caused by the materials used, setting up and installing plants and the required equipment and operating materials. Power consumption in particular can be linked with high emissions from electricity generation. Deutz & Bardow (2020) concluded that DAC plants can already generate negative emissions today if the entire value chain is taken into account. They looked at two plants in their study: one operated in Switzerland and one in Iceland. Their study asserts that the actual net emissions are highly dependent on energy production and energy efficiency. This means that, due to the regional electricity mix, DAC is unable to contribute to climate neutrality in many places at the moment. In fact, the opposite is true: they are actually responsible for greenhouse gas emissions.

According to the IEA's Sustainable Development Scenario, DAC will capture 9.67 Mt CO_2 per year from the atmosphere by 2030. If DAC capacity continues to grow, DAC will filter around 34 Mt CO_2 per year in 2040. In this case, the capacity increase for DAC in 2040 is around 3.04 Mt CO_2.

3.3.4.4 Foresight raw material demand

As DAC is still at an early stage of development and there are just a few test facilities, the current raw material demand for DAC is not relevant compared to global raw material production. However, this may change in the future if the use of DAC increases. The scenario described in Section 3.3.4.2 on DAC capacity and the specified raw material content of DAC plants is used to calculate the accumulated materials input up to 2040. As the specific raw material demand for the adsorption process has not yet been published in references, the scenario assumes that the absorption process will provide the total capacity increase for DAC. However, a parallel expansion of both technology variants should be expected. Depending on the source, the service life of DAC plants is indicated to be 20–50 years (Fasihi et al. 2019), so existing plants are not expected to need replacement before 2040, meaning they are not relevant for raw material demand. Table 3.58 shows the estimated raw material demand for DAC until 2040. You can see that we expect only a small proportion of current crude steel production to be needed to produce DAC plants until 2040. For this reason, the emerging DAC technology is anticipated to have no significant influence on the raw materials market.

3.3.4.5 Recycling, resource efficiency and substitution

The steels used in DAC are fully recyclable at the end of a plant's service life, meaning the raw materials are not removed from the metal cycle. It is not expected that the steel used for a DAC plant's supporting structure will be substituted since iron is cheap and the most widely used metal. As a result, neither material costs nor raw material availability require a substitution. Resource efficiency can be enhanced where necessary in the future by using larger-scale plants and drawing on improved technical expertise.

3.3.5 Stationary solid oxide fuel cells (SOFCs)

3.3.5.1 Technology description

Fuel cells come under the energy converter category and generate electricity through low-temperature combustion. The solid oxide fuel cell (SOFC) is a type of fuel cell that is operated at high temperatures and contains a solid electrolyte in contrast to other fuel cell types, such as the PEM fuel cell. SOFCs are used in both stationary and portable applications. Further developments are increasingly enabling their mobile use as well. This section, however, focuses on stationary operation, which has also been the main field of application for SOFCs in the past. Stationary SOFCs are mainly used for stand-alone electricity generation and combined heat and power generation. Most units are currently used for this purpose in the USA and South Korea (Weidner et al. 2019).

While there has been greater consolidation worldwide in recent years, interest from OEMs has recently increased once more, as the activities of Bosch, Weichai and Cummins show (Weidner et al. 2019). Most SOFCs are currently being built by

Table 3.58: Global production (BGR 2021) and calculated raw material demand for DAC plants using the absorption process, in tonnes

Raw material	Production in 2018	Demand in 2018	Demand foresight for 2040
High-grade steel		–	97
Low alloy steel	1,820,366,000	–	15,220
Concrete		–	356,159
PVC		–	42,617
Polypropylene		–	46
Fibreglass		–	213

Bloom in the USA with a capacity of some 80 MW. These are primarily large stationary units. Other main producers are SOLIDpower in Europe and Aisin in Japan (E4TECH (UK) Ltd 2019b). Unlike conventional heat engines, which are limited by Carnot efficiency, SOFCs can generate electricity directly and very efficiently in an electrochemical process while also providing heat in the form of waste heat. This enables combined efficiency levels of up to 90 % to be achieved with electrical efficiency typically being around 50–60 %. Another advantage lies in the fact that a wide variety of fuel types can be used, such as hydrogen, hydrocarbons or carbon monoxide. A modular design allows good scalability for small and larger systems without needing to accept major losses in efficiency. Other advantages compared to conventional energy conversion systems are reliability, low noise and low emissions.

SOFCs consist of electrochemical cells connected to each other by electrical interconnectors to form a stack. The cell itself contains a dense ion-conducting electrolyte, which separates two porous electrodes, the cathode and the anode, from one another. The operating principle is shown in Figure 3.66 to give an idea of how it works. The oxygen fed to the cathode reacts with the electrons coming from the external electric circuit to form oxide ions (O^{2-}), which then migrate to the anode (fuel electrode) through the ion-conducting electrolyte. In the anode, the oxide ions recombine with hydrogen (and/or carbon monoxide) in the fuel to form water (and/or carbon monoxide). Electrons are released during this process and flow from the anode to the cathode via the external electrical circuit.

There are typically two different SOFC stack designs: a planar and a tubular design. The planar design is a surface cell design, which can also be found in the other fuel cell types. The cell is constructed in a tubular shape in the tubular design; cf. Figure 3.67. The particular advantage here is the easier sealing compared to the planar design. Longer current paths and lower current densities tend to be considered as disadvantages of the tubular design. There are different versions for each variant with manufacturers generally focussing on specific individual variants. A distinction can also be made between the variants based on their anode- or electrolyte-based design. In the past, it was the electrolyte-based variant which dominated the market since it allowed easier fuel gas supply and despite higher ohmic losses caused by the thicker electrolyte. However, research activities initiated into solid oxide electrolysis (SOEL) means more work is being carried out on anode-based variants again.

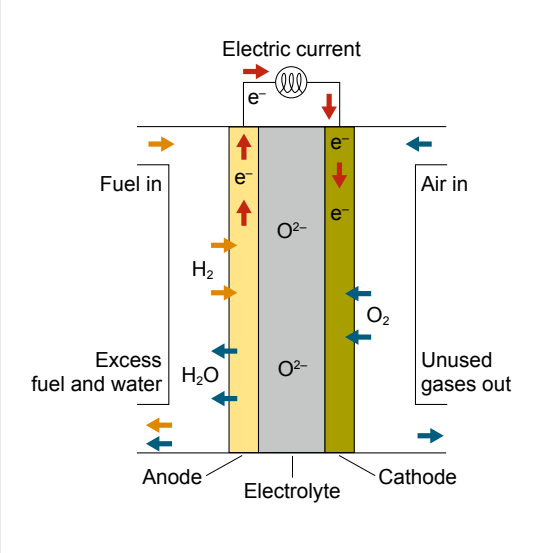

Figure 3.66: Design and working principle of a solid oxide fuel cell (source: Sakurambo, Sunspeanzler, Wikimedia, CC BY-SA 3.0)

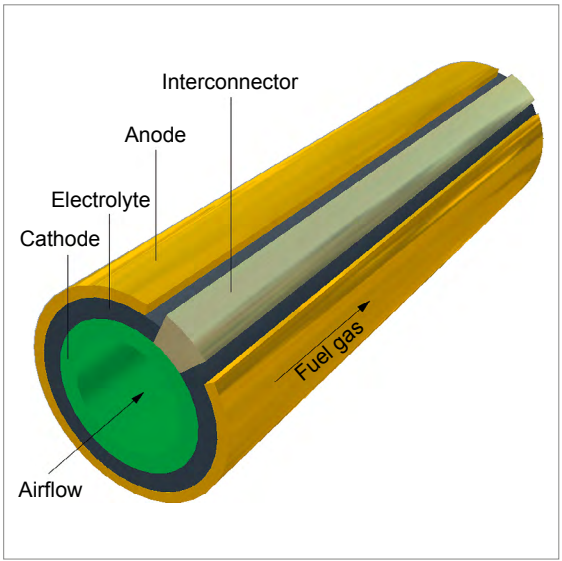

Figure 3.67: Design and working principle of a tubular solid oxide fuel cell (source: Jmsanta, Degree, Wikimedia, CC BY-SA 3.0)

The required operating temperature depends on the materials used and is between 500 and 1,000 °C. Efforts to reduce costs and make SOFCs more flexible have ensured that increasingly lower operating temperatures have become possible in recent years. Working temperatures have thus been reduced from 900–1,100 °C to 500–750 °C. To ensure that the electrochemical reactions also take place efficiently at lower temperatures, material thicknesses needed to be reduced or materials replaced to ensure ionic conductivity. It is therefore often beneficial to select materials in advance on the basis of their electrical and ionic conductivity for new developments with the aim of achieving specific operating temperatures, structural shapes or purposes for the SOFCs. Different advantages and disadvantages of individual materials and/or combinations of materials have contributed to the fact that many different materials are used in building SOFCs and each manufacturer has a preference for specific materials.

3.3.5.2 Foresight industrial use

E4TECH (UK) Ltd (2016) and E4TECH (UK) Ltd (2019b) describe the historical development of the SOFC market, which is shown in Figure 3.68.

In the initial years up to 2017, SOFC production increased continuously, although growth rates had already started to fall. In the last three years, growth has stagnated with SOFC production delivering around 85 MW per year.

In general, however, the market is expected to continue to expand with mid-term growth rates between 10 % and 25 %. The analyses in this study are based on the percentage market development for stationary applications in the three scenarios predicted by E4TECH (UK) Ltd (2019a) combined with the SSP assumptions on hydrogen; see Section 1.2. It is also assumed that only hydrogen will be used as a fuel in the long term. Annual SOFC production outputs since 2010 are taken into account to determine the current plant capacity.

These assumptions have been combined into a single trend for plant capacity and annual production; see Figure 3.69. SSP5 expects that plant capacity will grow very slowly in 2040 and will be about 10 GW. SSP2-26 and SSP1-19 expect annual production to continue to increase with production in SSP2-26 being half the size of production in SSP1-19. Plant capacities are forecast to be 33 GW for SSP2-26 and 52 GW for SSP1-19 in 2040.

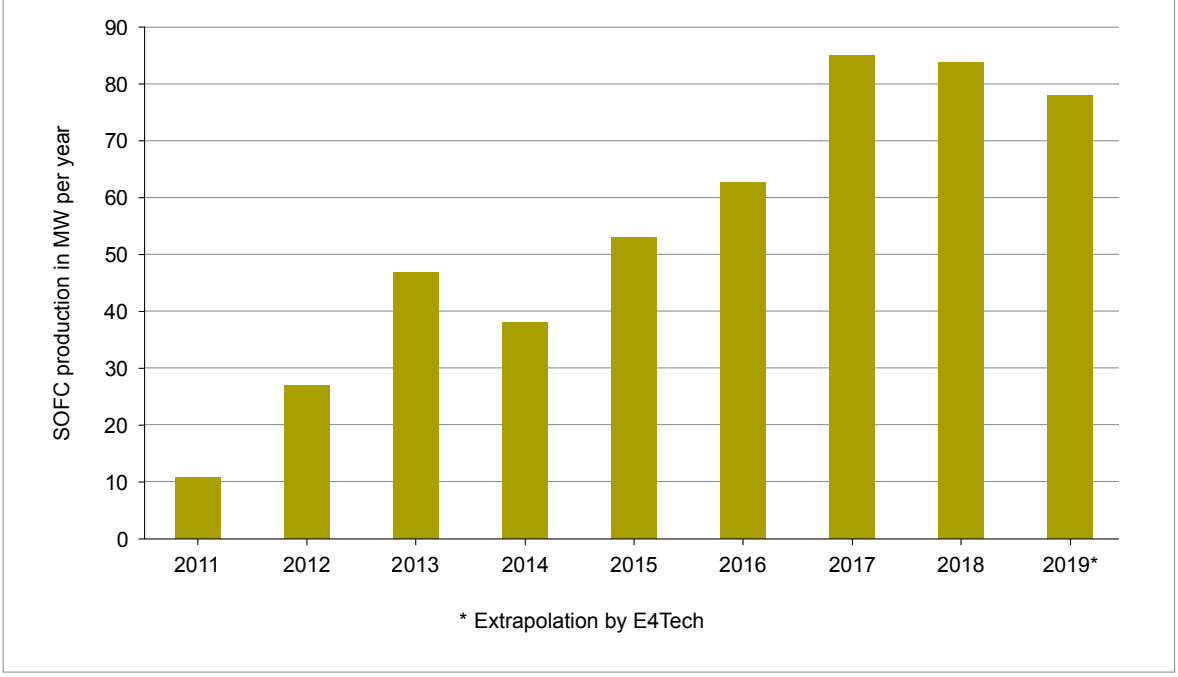

Figure 3.68: Production of SOFCs (sources: E4TECH (UK) Ltd 2016, E4TECH (UK) Ltd 2019b)

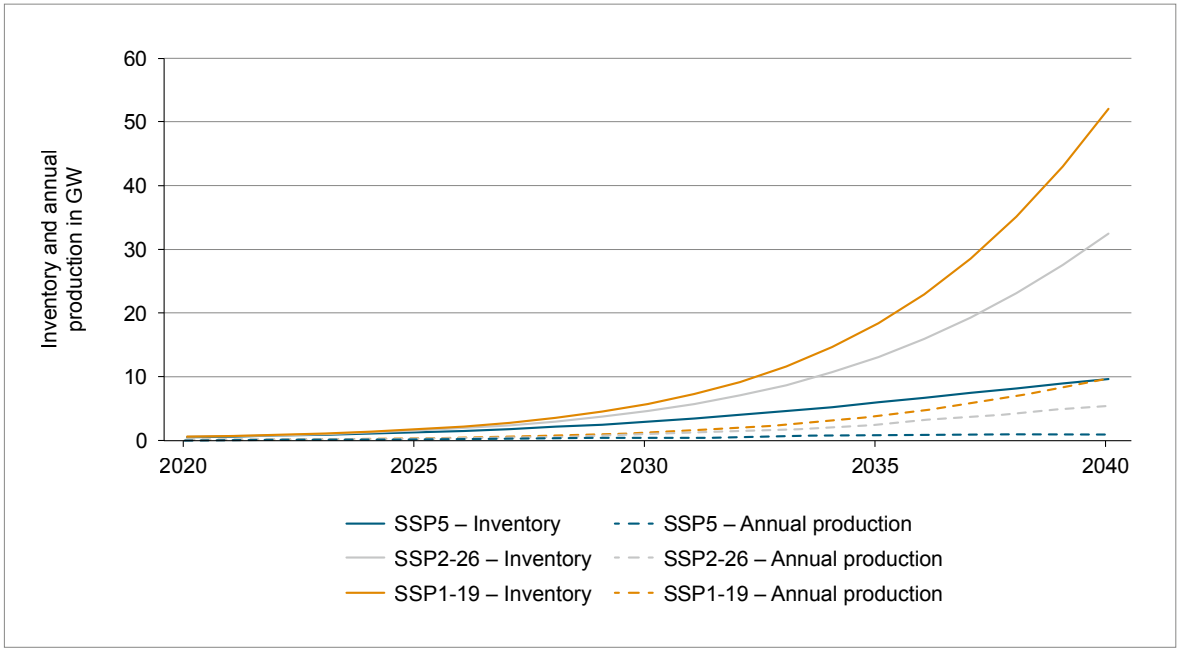

Figure 3.69: Production and expansion of SOFC stock for SSP5, SSP2-26 and SSP1-19 scenarios (source: own representation)

The fuel cell market depends very much on the general political situation, research funding and the economic possibilities. However, there is also uncertainty contingent on the development of other fuel cell types and alternative technologies. This will inevitably lead to changes in design and material selection for SOFCs due to the market environment. Moreover, a manufacturer may gain market shares, which can lead to a higher demand for certain alternative materials than expected.

3.3.5.3 Raw material content

The electrolyte material selected often determines the specific design and the other materials used. In principle, a wide variety of materials can be used. Four commonly used materials are yttria-stabilised zirconia (YSZ), scandium-stabilised zirconia (ScSZ), gadolinium-stabilised ceria (GDC) and cerium-gadolinium oxide (CGO). YSZ has been used for a long time and is currently still the most frequently used electrolyte material. However, it has low ionic conductivity at lower temperatures below 700 °C. ScSZ has better conductivity and greater stability but it is not so widely available and is more expensive. GDC and CGO offer sufficiently high conductivity even at low temperatures below 600 °C but are not as chemically and mechanically stable (Da Silva & Souza 2017; Hussain & Yangping 2020; Zhang et al. 2020).

Birnbaum et al. (2019) provide an overview of the materials which are mainly used in different cell types. The main material used for the electrolyte is YSZ with dosing components of 3–10 mol%. Scandium-cerium-stabilised zirconia (ScCeSZ) is specified as an alternative. Nickel-YSZ materials are very commonly used for the porous anode in combination with nickel-ceria and Ni-ScCeSZ. There is a slightly larger variety of choices for the cathode of lanthanum strontium cobalt ferrite (LSCF) and lanthanum strontium manganite (LSM) with YSZ or, alternatively, lanthanum strontium cobaltite (LSC) and lanthanum strontium ferrite (LSF). Stainless steels and iron-chromium-yttrium alloy (CFY) or FeCrAlY are used for the interconnects. Higher operating temperatures here often require more complex alloys to prevent corrosion and ensure adequate thermal stability.

The structural design and the cell type have a direct influence on the material requirements. For example, the anode-based layer is usually between 200–300 µm thick and the electrolyte-based layer about 150 µm thick. The non-load-bearing electrolyte layer can otherwise be considerably thinner at 5–15 µm and benefit from lower

Table 3.59: Specific raw material demand for SOFC in g/kW (sources: Strazza et al. 2015, Gandiglo et al. 2019, Smith et al. 2019, Bicer & Khalid 2020)

Raw material	g/kW
Nickel	1,070
Yttrium	87
Zirconium	289
Lanthanum	28
Manganese	37
Chromium	2,728
Aluminium	629
Cobalt	6
Scandium	5

ohmic losses. The cathode and anode vary in thickness between 20 and 50 µm.

Depending on the design of the cells, current densities of 2 W/cm² can also be achieved at low temperatures, although these are typically around 0.5 W/cm² (Kendall & Kendall 2016). Mean values were calculated for the expected specific material requirements in Table 3.59 based on the studies in Strazza et al. (2015), Gandiglio et al. (2019), Smith et al. (2019), Bicer & Khalid (2020). High extreme values were not taken into account for the materials in the electrochemical cell to reflect future technological development. It is assumed that the typically used and aforementioned materials will be used.

If we include information regarding the use of extracted scandium, it is currently primarily used for SOFCs, especially by the largest manufacturer Bloom Energy (Grandfield 2018), which requires around 92 g/kW. So as not to ignore this demand, a specific demand for scandium is also shown under technological development and thus material savings. It would primarily substitute the demand for yttrium in the electrolyte in the overall view.

3.3.5.4 Foresight raw material demand

In the case of stationary SOFC systems, the raw material demands as shown in Table 3.60 are calculated based on the specific raw material demand per g/kW and the scenarios for the

Table 3.60: Global production (BGR 2021) and calculated raw material demand for stationary SOFC systems, in tonnes

Raw material	Production in 2018	Demand in 2018	Demand foresight for 2040		
			SSP1 Sustainability	SSP2 Middle of the Road	SSP5 Fossil Path
Nickel	2,327,500 (M) 2,189,313 (R)	84	10,350	5,800	1,100
Yttrium	7,600 (R)	2	842	470	90
Zirconium	1,256,362[1] (M)	23	2,798	1,570	300
Lanthanum	35,800 (R)	2	270	150	29
Manganese	20,300,000 (M)	3	360	200	38
Chromium	27,000,000 (M)	213	26,400	14,800	2,800
Aluminium	63,756,000 (R)	49	6,100	3,420	650
Cobalt	151,060 (M) 126,019 (R)	1	63	35	7
Scandium	9.1 (M)	5	48	27	5

M: Mine production (tonnes of metal content)
R: Refinery production (tonnes of metal content)

[1] *Production of zirconium minerals*

production figures. None of the raw materials is critical with the exception of scandium. Existing production capacities are also nominally adequate for the demand in 2040. However, production needs to be expanded significantly for scandium or material savings if usage does not change to a considerable extent. This also reflects the fact that the largest proportion of extracted scandium is already used in SOFC production.

The difference in demand between the three different SSPs is relatively wide with a factor of around 9 between SSP5 and SSP1-19. This difference plays a major role, especially in the case of scandium or scarce raw materials used as an alternative. This could have a significant influence on market development in SSP2-26 (2040: three times the demand compared to production in 2018) and SSP1-19 (2040: five times the demand). We would then assume that alternative materials need to be used if the application allows their use from a technical and financial perspective. Materials which are associated with low operating temperatures and may be more critical include gadolinium and cerium among others.

3.3.5.5 Recycling, resource efficiency and substitution

Current material losses are assumed to be high, especially for strategic metals, due to prevailing waste disposal practices, even if materials could be recycled in principle (Ökopol GmbH 2016). The manufacturing process, cell geometry and its size also have an impact on material loss. In the past, material loss were estimated to total up to 50 % (Lilley et al. 1989). However, more recent works state that they can also be just 10–30 % (Lee 2015; Mehmeti et al. 2016).

A high recycling rate of up to 99 % is possible with a nickel anode. There are no recycling processes available for lanthanum strontium manganite in the cathode and lanthanum chromite in the interconnect, which provides electrical connection for the cells and ensures gas is transferred to the electrodes. Accordingly, higher recycling rates could be achieved with a planar SOFC compared to a tubular one. The complex recycling of ceramic materials, the high energy requirements and their low value mean that they are only used for secondary recycling as a filling material in the construction industry or in cement and clinker brick production (Environment Park SPA et al. 2018). However, if we assume that there is a larger market for old systems and an increase in value, we can expect that such processes will also be used more for recycling.

3.3.6 CCS – Carbon capture and storage

3.3.6.1 Technology description

CO_2 from industrial combustion processes can be captured and permanently stored in a geological formation. This can reduce the increasing contamination of the atmosphere with greenhouse gases. The International Energy Agency considers the use of CO_2 separation methods to be absolutely crucial in achieving climate targets (IEA 2016). The technology as a whole is commonly referred to as carbon capture and storage (CCS) (Fischedick et al. 2015). The process can be divided into three individual steps (Figure 3.70): CO_2 capture, CO_2 transport to the deposit site (in tanker ships, tanker trucks and pipelines) and CO_2 storage.

Separation technologies have been used in the chemical industry and refineries for decades but their technical application in the energy sector remains challenging. Different CO_2 separation methods on a power-plant scale are under debate, although their system components are already fully developed. A crucial differentiating factor is the stage when CO_2 emissions are captured (Fischedick et al. 2015): post-combustion capture, oxy-fuel combustion and pre-combustion. Two other methods whose technical development is even less advanced in the energy sector are the membrane process and the chemical looping process.

Only the post-combustion and oxy-fuel processes can be retrofitted to existing systems. In the case of the pre-combustion process, the entire system needs to be specially designed, so it is only suitable for new systems. Figure 3.71 shows the three carbon capture processes in a chart.

Post-combustion

If the CO_2 is separated after combustion, we refer to a post-combustion process. During this process, the fuel is first combusted as normal. Combustion produces nitrogen oxides, sulphur oxides and other pollutants. Existing power plants therefore have suitable flue gas cleaning systems that filter and separate contaminants. In the case of the post-combustion process, an additional cleaning step is added after the flue gas cleaning system. The following processes are currently used to separate CO_2 from flue gas: the absorption method (chem. and phys. absorption), adsorption method, membrane method and cryogenic method. The most common method is chemical absorption by means of amine scrubbing, generally also known as gas sweetening. During this process, usually based on the counterflow principle, the flue gas is replaced by a liquid solvent (e.g. an amine-based fluid such as monoethanolamine), which absorbs or binds the CO_2 from the flue gases. Heat is added and the CO_2 previously bound is outgassed again in another reactor. Pressure change can also be used to produce such regeneration by desorption. The regenerated solvent is returned to the process circuit and the CO_2 can be transported further. In the case of membrane technology, the CO_2 is separated using specially selective membranes (Fischedick et al. 2015).

Compared to the other processes described, chemical absorption offers the highest standard of technological development for separating CO_2 from the power plant process. Being an end-of-pipe technology, the post-combustion process has the advantage that it can be retrofit to existing

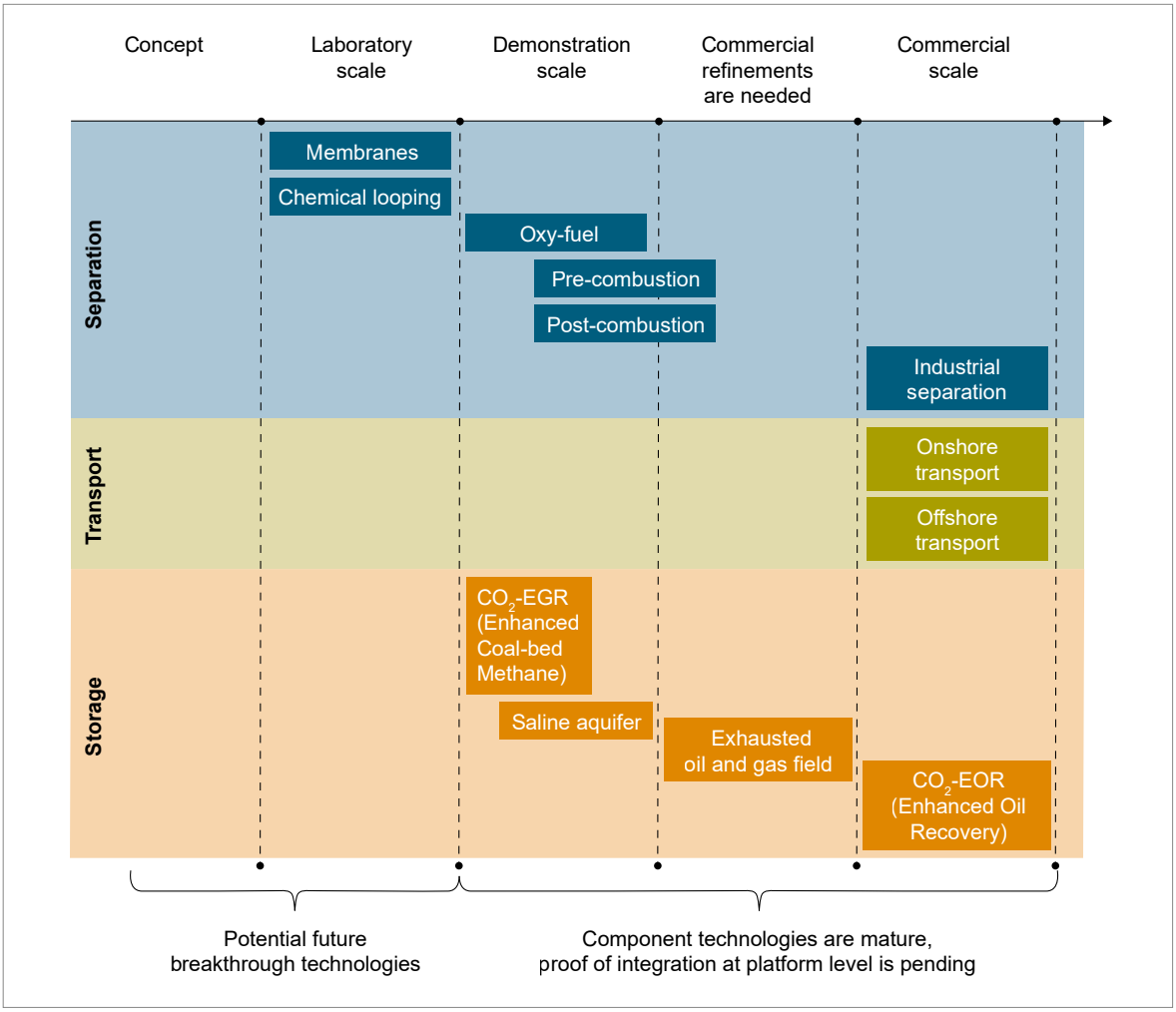

Figure 3.70: Development stages of CCS system components (source: own representation based on IPCC 2005 and McKinsey & Company 2008)

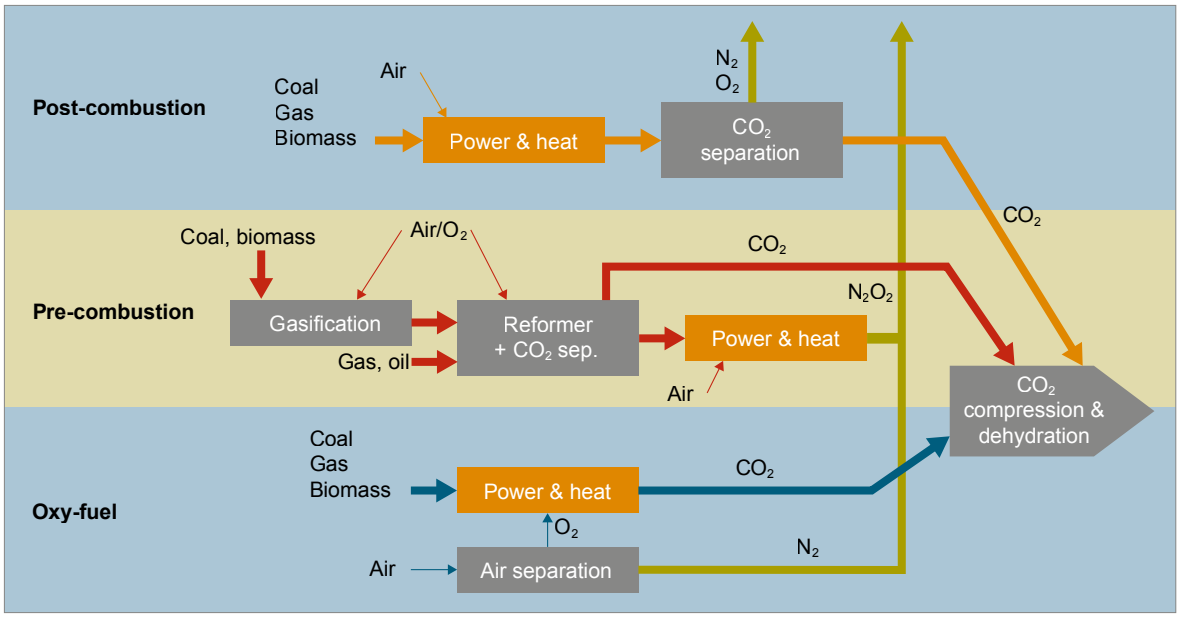

Figure 3.71: Schematic representation of the three carbon capture methods (source: adapted from IPCC 2005)

power plants. As far as the power plant structure is concerned, the use of a chemical scrubbing process does not involve any changes to the technologies used such as boilers, turbines and pre-combustion chambers. However, the entire plant needs to be adapted since additional heat energy must be provided for regenerating the solvent. Moreover, the scrubbing system and the required piping must be included in the plant geometry and topology. The post-combustion method offers optimum flexibility with regard to the power plant's controlled load utilisation. Disadvantages include the high energy requirement, which is mainly related to solvent regeneration, and the increased space requirement for the entire plant (Fischedick et al. 2015; Wietschel et al. 2015).

Pre-Combustion

In pre-combustion capture, CO_2 separation takes place before the actual combustion process. IGCC (integrated gasification combined cycle) technology is used as an example here. During this process, the fuel is converted into synthesis gas by adding oxygen at temperatures of about 900 °C in a gasification reactor. The unwanted gas components (H_2S, COS, HCN, NH_3) are then removed. The synthesis gas, which mainly comprises hydrogen and carbon monoxide, is converted into CO_2 and more hydrogen by means of hydrogen conversion in a shift reactor, where steam is added. This produces a synthesis gas from the main components hydrogen and CO_2. The high partial pressure in the CO_2 enables the CO_2 to be separated from the H_2/CO_2 mixture using membranes or physical scrubbing. If physical scrubbing is used, the CO_2 is dissolved in a scrubbing solution such as methanol. Membrane technology (hydrogen membranes) for CO_2 separation will also increasingly become an option in the future. It has the advantage that it consumes less energy. The residual hydrogen can then be used to generate electricity for gas or steam turbine power plants (Fischedick et al. 2015). IGCC power plants offer the advantage that they are highly flexible in their utilisation and fuel use. As a result, other alternative energy sources such as biomass or special fuels can be used for gasification in addition to coal. A considerable disadvantage of this technology, however, is that it cannot be retrofit to existing power plants (Fischedick et al. 2007; Fischedick et al. 2015).

Oxy-fuel

The oxy-fuel process is based on burning a fuel in pure oxygen and not in a conventional way in ambient air. This produces a flue gas, which pri-

marily consists of CO_2 (around 80 %) and steam. Combustion in pure oxygen does not produce nitrogen oxides, which eliminates the need for complex denitrification systems. During the following condensation step, the CO_2 in the flue gas is separated from the steam. As pure oxygen is used during combustion, extremely high combustion temperatures are produced. Part of the flue gases is channelled back into the process to reduce and regulate the temperature. The remaining exhaust gas can then be removed from other contaminants, such as sulphur oxide, to be scrubbed. The main separation work involves producing the pure oxygen in an air separation plant. As a result, this is when the most energy is consumed. The best available technology for this process is cryogenic air separation, during which the air is first liquefied and then the oxygen and nitrogen are separated by distillation. The use of high-temperature membranes to produce oxygen could significantly reduce energy consumption. However, these special polymer membranes are not state-of-the-art technology (Cremer 2007). In addition to the membrane process, the chemical-looping process can also be regarded as a promising solution (Kuckshinrichs 2013; Fischedick et al. 2015).

Chemical looping combustion (unmixed combustion)

The chemical looping process (CLC) is a new technology. The energy input for separating the CO_2 from the exhaust gas flow is significantly lower than for other CO_2 separation methods. It comprises an indirect combustion process, during which the fuel is combusted without direct contact with the air. The required oxygen is not produced during energy-intensive cryogenic air separation. It is provided by an oxygen carrier instead (Orth 2014). The CLC process essentially consists of two interconnected fluidised bed reactors, an air reactor and a fuel reactor. The bed material circulating between the two reactors acts as an oxygen carrier and generally consists of metal oxide (MeO). The oxygen carrier is oxidised with air in the air reactor. The flue gas from the air reactor is composed of nitrogen and oxygen. The oxygen carrier reacts with the fuel in the fuel reactor downstream, thus removing the oxygen from the metal oxide once more. The flue gas flow produced in this way mainly consists of carbon dioxide and steam. A pure CO_2 gas flow remains once the steam has condensed. When the reaction in the fuel reactor is complete, the reduced metal oxide is transported back to the air reactor and regenerated with oxygen (Orth 2014). Figure 3.72 shows how the CLC process works in simplified form.

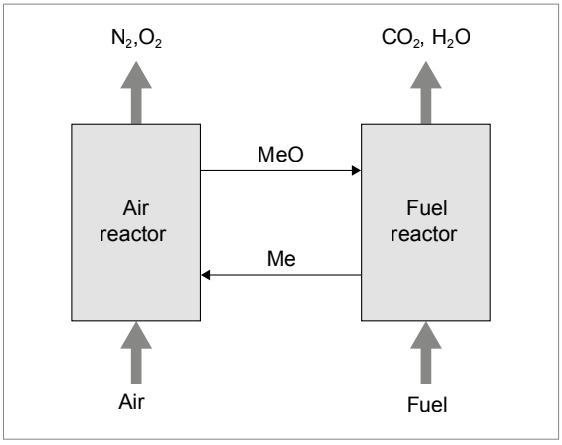

Figure 3.72: The chemical looping process (source: Orth 2014)

CO_2 transport

After separation in all processes, the CO_2 is either compressed to 110 bar (supercritical condition) for transport in pipelines, the preferred means, or liquefied, so it can be transported in ships or trucks in small quantities. It is then stored in deep geological formations on- or offshore. Valuable experience has already been gained in oil extraction, where CO_2 can be used for EOR (enhanced oil recovery) or can be stored in depleted oil and gas fields.

CCS technology development

Due to efficiency losses of 6–13 % caused by CCS technologies in power plants (Wuppertal Institut, ISI, IZES 2017), power plants require 40 % more primary energy (IPCC 2005), depending on the type of plant. These losses are also associated with high CO_2 emissions. 85–95 % of these CO_2 emissions are then separated and can be stored, meaning CCS can reduce the total emissions to the atmosphere by 80–90 % overall.

An increase in efficiency in the basic power plant process is thus an essential development task. All processes have the potential to reduce efficiency

losses through their efficient integration into the overall power plant process and the development of new processes and materials. The fact that all separation processes have already achieved a CO_2 purity of over 99 % holds promise. The combustion process is by far the most advanced technology for separating CO_2 emissions during the power plant process (Kuckshinrichs 2013; Wietschel et al. 2015; Wuppertal Institut et al. 2017).

There are already a few CCS systems in operation worldwide. Some of them are large-scale systems. In Europe, there are currently two large-scale plants with a total combined CCS volume of 1.7 million tonnes of CO_2 per year. There are also ten more plants at different development stages in Europe: one in Norway, one in Ireland, two in the Netherlands and six in the UK. These ten plants have the capacity to separate a total of 20.8 million tonnes of CO_2 per year. The storage capacity in Europeis estimated to be about 300 gigatons of CO_2 (Global CCS Institute 2019). Figure 3.73 contains former, on-going and future CCS projects (Global CCS Institute 2020).

3.3.6.2 Raw material content

Cormos et al. (2013) studied the three different types of power plants: natural gas and combined-cycle coal-fired power plants with integrated gasification (NGCC, IGCC and PF) with and without CCS. They found that twice the amount of concrete and steel is required to build power plants with CCS in the case of coal-based power plants. When it comes to gas-fired power plants, the CCS variant only increases the demand for low-alloy steels by 64 %.The presented figures are based on reference concept power plants with a capac-

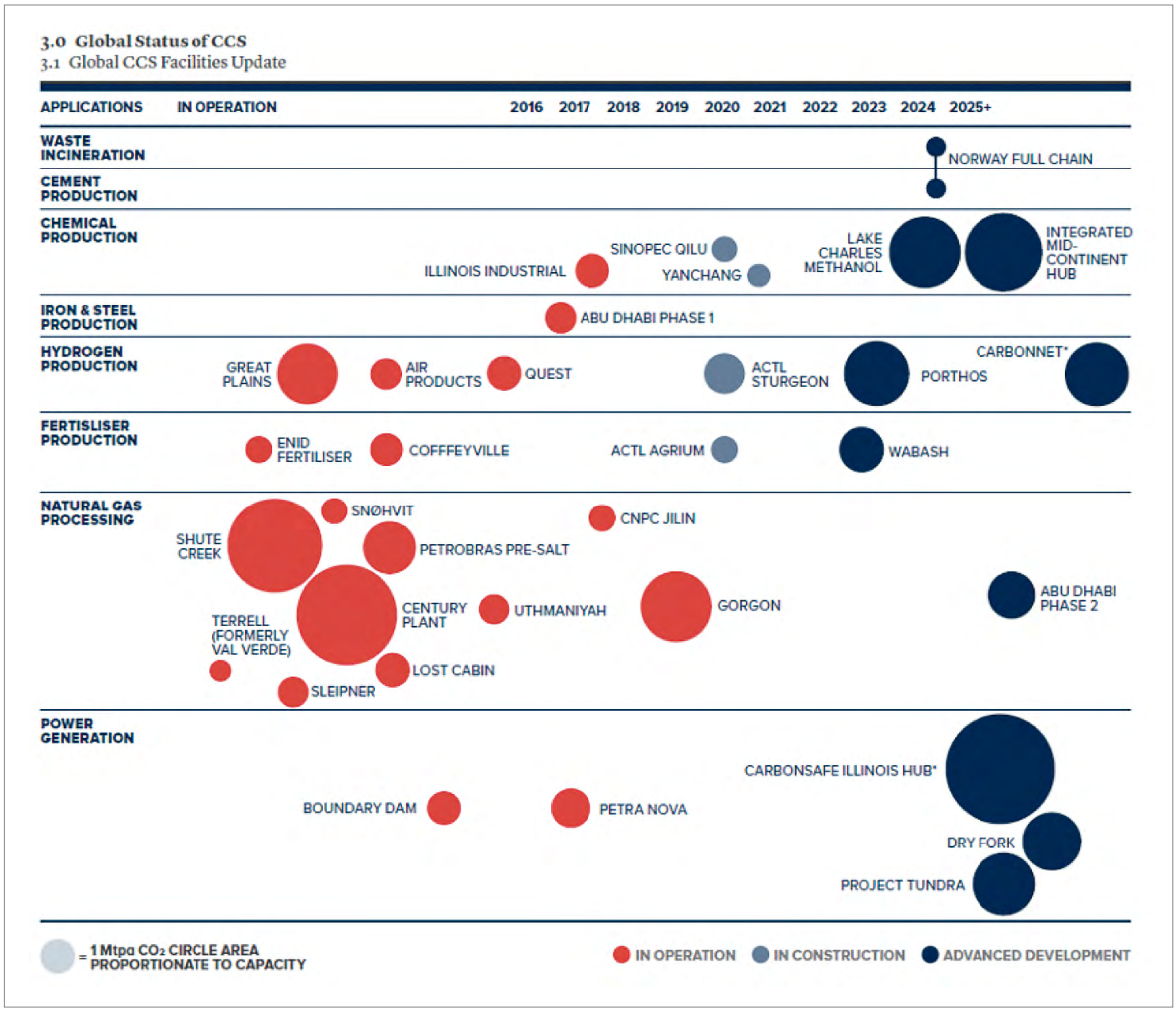

Figure 3.73: Global CCS projects (source: Global CCS Institute 2020)

Table 3.61: Quantity of alloying elements for CCS technologies in kg/MW_{el} (source: Moss et al. 2011)

Alloying element	kg/MW
V	100
Nb	100
Ni	1,145
Mn	3,761
Cu	692
Co	7.5
Cr	362
Mo	1

ity of between 400–500 MW and a minimum CO_2 separation rate of 90 %. According to Cormos et al. (2013), these figures are valid compared against references. Simulations were added where required. The most efficient power plants were then compared with one another with the design parameters taken from reference works.

A JRC study (Moss et al. 2011) analysed CCS alongside other energy technologies with regard to the quantities of material needed to comply with the Strategic Energy Technology (SET) plan. In Table 3.61 lists the identified alloying elements for CCS technologies. In addition to the demand for the CCS system itself, these figures also include the quantities of steel for pipes to transport the CO_2 to the storage location (Moss et al. 2011).

Besides the construction materials with the required alloying elements, CCS technologies also need materials for the CO_2 separation process on an on-going basis. These materials are listed by CO_2 separation method in Table 3.62. In the case of post-combustion, aqueous alkanolamine solutions such as monoethanolamine (MEA) and carbonated adsorbates are currently used for CO_2 scrubbing. According to an estimate in Fischedick et al. (2007), the following quantities of chemicals are required per separated tonne of CO_2 during MEA scrubbing: 2.25 kg MEA solvent, 0.0826 kg activated carbon and 0.152 kg NaOH.

In the long term, the implementation and reliable operation of a power plant with 700 °C technology will be an essential pre-requisite for scrubbing CO_2 from flue gases and placing it in suitable deposits while also taking financial aspects into account. Current fossil-fuel-fired power plants with a mean efficiency of around 38 % are not suitable for operation with CO_2 flue gas scrubbing if we wish to handle primary fossil energy

Table 3.62: Materials for CO_2 separation methods (source: D'Alessandro et al. 2010)

		Post-combustion	Pre-combustion	Oxyfuel combustion
Absorption	– Chemical (alkanolamines) – Physical (ionic liquids)	■	■	
Adsorption	– Microporous materials (zeolites, metal oxides, metal-organic materials, carbon-containing adsorbents) – Pressure/temperature swing adsorption	■	■	■
Low-temperature distillation		■	■	■
Membranes	– Inorganic (ceramic, hydrogen transport, ion transport) – Polymer – Hybrid membranes	■	■	■
Gas hydrates		■	■	
Chemical looping	– Metal oxides		■	■

sources responsibly. Apart from higher fossil fuel consumption, considerably more CO_2 would also need to be separated and stored if flue gas scrubbing is used (VGB 2011).

3.3.6.3 Foresight industrial use

Roadmaps indicate the target year 2030 as the date when CCS will be commercially available on a power-plant scale (EUROPEAN COMMISSION 2015). Having said that, the period during which CCS can contribute to climate protection not only depends on the separation technologies themselves being available but also on the available storage capacity and the required transport infrastructure (GRÜNWALD 2007). However, new pilot plants (cf. MIT 2015) and commercial CCS projects with a capacity of over 60 MW are still being planned and built (cf. GLOBAL CCS INSTITUTE 2020).

It is difficult to estimate future development of CCS technology since it is not expected to be put into routine, commercial use until 2030. The roadmap in (IEA 2013a) predicts a strong increase in CCS capacity between 2030 and 2040 under the conditions defined in a 2 °C scenario for global warming. In a more recent study, the IEA Sustainable Development Scenario up to 2040 expects a worldwide power plant capacity of 315 GW electricity generation to be equipped with CCS, accounting for 5 % of the world's power plant capacity (IEA 2020a). This corresponds to an increase in average retrofitted and newly built CCS capacities of 15 GW per year over the next two decades (IEA 2020a).

The data on power generation in the SSP models (RIAHI et al. 2017) (also see Table 3.63) can be used to estimate the power plant output for different years by converting them into TWh, based

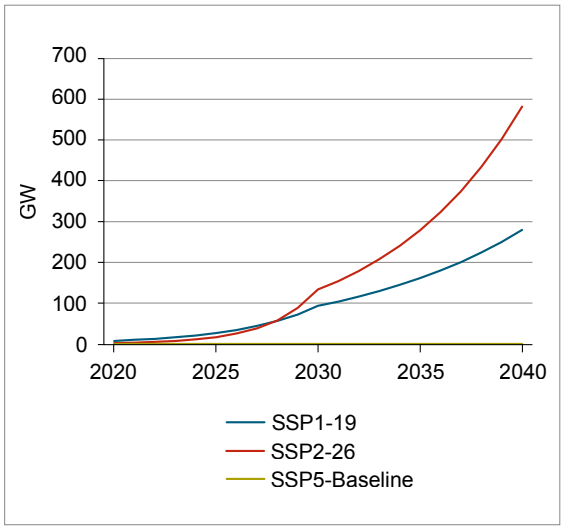

Figure 3.74: Output of power plants with CCS in GW (source: own representation)

Table 3.63: Power generation with CCS for the year 2040 in the selected SSPs (source: RIAHI et al. 2017)

Power generation with CCS by energy source [EJ/y]	SSP1-19 Sustainability	SSP2-26 Middle of the Road	SSP5 Fossil Path
Coal	1.30	1.80	0
Gas	7.97	17.39	0
Biomass	6.66	0.13	0
Sum	**15.93**	**19.32**	**0**

Table 3.64: New CCS capacities for power plants to be installed in 2040 [GW]

	SSP1-19 Sustainability	SSP2-26 Middle of the Road	SSP5 Fossil Path
Power generation output with CCS [GW]	32.2	88.3	0

on the annual operating time and a (very high assumed) power plant availability of 95 %; see Figure 3.74. When looking at the scenarios, it is interesting to note that no CCS technologies are included in the power supply until 2040 in the base SSP5 “Fossil Path” scenario.

This can be used to anticipate the newly installed power plant capacities with CCS for 2040; see Table 3.64.

3.3.6.4 Foresight raw material demand

It is difficult to make reliable assumptions to calculate raw material demand based on the best available technology (demonstration systems). First of all, steel alloys for highly efficient coal-fired power plants are still at the testing stage. Secondly, reductions are expected in the demand for materials thanks to further development of processes. Lastly, new membrane technologies could replace current air separation systems for the oxy-fuel process or physical processes to separate CO_2 before combustion. There may be a demand for rare earths in this case. However, since there are some potential material combinations, other materials could be used in the future as the result of potential shortages or cost issues. The future expansion of CCS technology is also still difficult to estimate.

This technology synopsis estimates the raw material demand for alloying elements for CCS for 2040. If we combine the assumptions about the specific raw material demand with the values in Table 3.61 and the power plant capacities with CCS in Table 3.64, we have the demand quantities for CCS technologies for 2040; cf. Table 3.65.

The calculations in this technology synopsis indicate that all alloying elements will account for a very small share of world production at less than one percent. The study for the cement industry (Vatopoulos & Tzimas 2012) comes to a similar conclusion. In this sector, the CCS technologies studied also have no effect on the raw material demand to manufacture clinker bricks individually and thus also worldwide.

3.3.6.5 Recycling, resource efficiency and substitution

Since CCS is still at an early stage of its development and further developments of processes are still expected, it is difficult to make conclusions about recycling and substitutability of raw materials with regard to CCS. The construction materi-

Table 3.65: Global production (BGR 2021) and calculated raw material demand for CCS, in tonnes

Raw material	Production in 2018	Demand in 2018	Demand foresight for 2040		
			SSP1 Sustainability	SSP2 Middle of the Road	SSP5 Fossil Path
Vanadium	90,661 (M)	n. v.	3,200	8,800	0
Niobium	68,200 (M)	n. v.	3,200	8,800	0
Nickel	2,327,499 (M) 2,189,313 (R)	n. v.	36,900	101,200	0
Manganese	20,300,000 (M)	n. v.	121,300	332,300	0
Copper	20,590,600 (M) 24,137,000 (R)	n. v.	22,300	61,100	0
Cobalt	151,059 (M) 126,019 (R)	n. v.	200	700	0
Chromium	27,000,000 (M)	n. v.	11,700	32,000	0
Molybdenum	265,582 (M)	n. v.	30	100	0

M: Mine production (tonnes of metal content)
R: Refinery production (tonnes of metal content)

als for CCS technologies are certainly similar to those for conventional power plant components: the copper, aluminium and chromium they contain will therefore also be recycled in the future (European Commission 2015). It will also be possible to recycle catalysts or replace catalysts with vanadium and replace wolfram with calcium carbonate (for SO_2 retention) (IEA 2012).

3.3.7 Redox flow batteries

3.3.7.1 Technology description

Redox flow batteries (RFB) were developed in the 1970s. They store electrical energy in salts and are thus related to storage batteries. Unlike in conventional storage batteries, the two energy-storing electrolytes circulate in two separate circuits, between which ions can be exchanged via a membrane within the cell (Oertel 2008). The energy-retaining electrolytes are stored outside the cell in separate tanks. This means the stored energy quantity does not depend on the size of the central reaction unit for the charging or discharging process. The tanks can be filled easily by hand and the battery can be filled from them. The tank size determines the energy content in the battery (kWh) while the charging/discharging unit determines the power output (kW). The two parameters power output and storage capacity can be scaled separately from one another, something which is not possible with conventional batteries. Pumps move the electrolyte into the reaction unit, where the redox reaction takes place. The ions are transported through the membrane while the electrons are conducted through an external electricy circuit. Electrical power is fed into this electrical circuit during charging and removed from the circuit during discharging. The redox reaction causes the two electrolytes to change their oxidation stage. A movable separator is located within the tanks to physically separate the fluids and prevent the “charged” and “discharged” electrolytes from mixing (Wietschel et al. 2015). Since each individual cell only produces a low voltage, many individual cells are connected in series to produce a combined high voltage. A reaction unit thus consists of many individual cells. As the salts are typically not very soluble, the unit achieves energy densities similar to lead-acid batteries

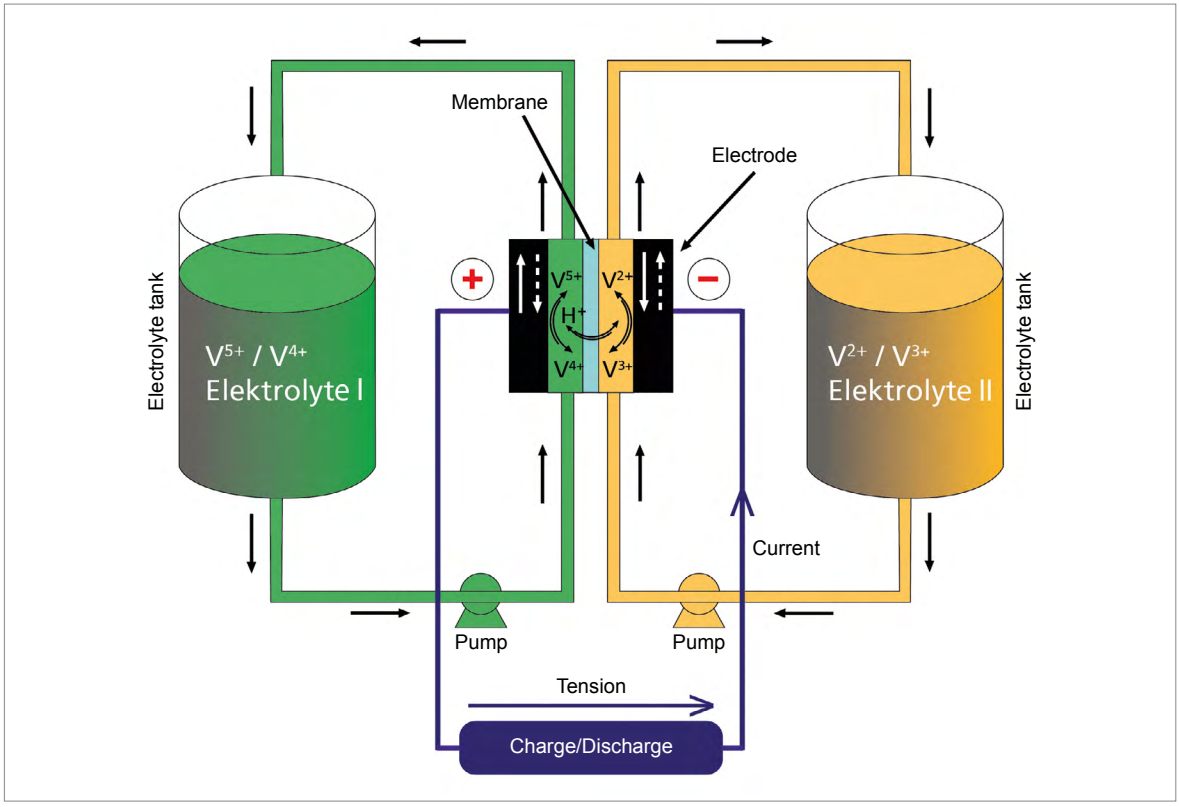

Figure 3.75: Design and working principle of a redox flow battery (source: Fraunhofer UMSICHT)

Table 3.66: Typical technical parameters of a vanadium RFB (source: Wietschel et al. 2015)

Technical parameters	Today	2025	2050
Gravimetric energy density (Wh/kg)	6 to 10	20	40
Volumetric energy density (kWh/m³)	4.2 to 6.25	12	24
Gravimetric power density (W/kg)	1 to 3	10 to 30	–
Volumetric power density (kW/m³)	0.42 to 2.4	4.2 to 24	–
No. of full charge cycles (in thousands)	13 to 20	–	–
Lifetime (a)	20	–	–
Self-discharge (%)	< 1 %/a	–	–
Operating temperature (°C)	+20 to +35	–	–
Efficiency (%)	70 to 80	–	–

(Wietschel et al. 2010). Due to their low volumetric and gravimetric energy density, redox-flow batteries are unsuitable for mobile applications such as electric vehicles. However, redox flow batteries are able to produce large energy quantities compared to electrochemical battery storage systems, meaning that they are particularly suitable for use as large stationary batteries to compensate for fluctuating energy generation or demand.

Vanadium redox flow batteries (V-RFB) have triumphed on the market thanks to their good properties in relation to energy density and service life. Moreover, this technology variant does not cause contamination in the electrolytes if ions diffuse through the membrane unintentionally. Vanadium is used at different oxidation stages for both electrolytes in these batteries. When the battery is charging, reduction takes place on the negative electrode and oxidation on the positive electrode. The protons diffuse through the membrane and the electrons are transported via the external circuit. When the battery discharges, the reaction is reversed, meaning electrical power can be drawn (Chen et al. 2017a).

$V^{2+} \leftrightarrow V^{3+} + e^-$ (negative electrode)

$VO_2^+ + 2H^+ + e^- \leftrightarrow VO^{2+} + H_2O$ (positive electrode)

The technical parameters for V-RFBs can be found in Wietschel et al. (2015) and are shown in Table 3.66. The predicted parameters for 2025 and 2050 are also given where available to provide an insight into the development goals.

Another promising technology variant is all-iron redox flow batteries (I-RFB), which are currently under development and are not available on the market yet. As in V-RFBs, a metal with different oxidation stages is used in both electrolytes. However, iron is used instead of vanadium in both electrolytes in I-RFBs, meaning the electrolytes are not contaminated in I-RFBs either if there is unintentional diffusion through the membrane. The following reaction takes place in I-RFBs when charging (left to right) and discharging (right to left) (ESS 2017):

$Fe^{2+} + 2e^- \leftrightarrow Fe^0$ (negative electrode)

$2Fe^{2+} \leftrightarrow 2Fe^{3+} + 2e^-$ (positive electrode)

3.3.7.2 Raw material content

Electrolyte makes up the most part of an RFB's total weight. V-RFBs require water and sulphuric acid for the electrolyte in addition to vanadium as the ions need to dissolve. Copper is used for the electrodes and steel is used in components such as the pumps which circulate the electrolyte. Polymers are used for the tanks and in seals among other components. You will find the average raw material demands for V-RFB in Table 3.67. The specific material requirement refers to the energy which can be stored over the entire life cycle. The specific energy calculated for a cycle is an average of 19.9 Wh/kg. The vanadium requirement calculated for a cycle is assumed to be 3.02 kg/kWh. According to Peither (2020), the iron requirement for the electrolytes in an I-RFB is around 4.4 kg/kWh.

Table 3.67: Average raw material demand of a V-RFB (source: Díaz-Ramírez et al. 2020)

Raw material	Specific material demand (g/kWh)	Percentage by weight [wt%]
Vanadium pentoxide	1.62	10.07
High-grade steel	1.72	10.7
Copper	0.13	0.78
Carbon	0.04	0.26
Polysulphone	0.07	0.44
Polypropylene, rubber	0.64	3.94
Sulphuric acid	4.18	25.95
Water	7.71	47.85

3.3.7.3 Foresight industrial use

At present, there are redox flow batteries with a capacity of 70 MW installed worldwide, in which 250 MWh of energy can be stored. There are almost exclusively medium to large battery storage systems (Colthorpe 2020). The IEA expects the installed battery power to increase to 330 GW by 2040 in the Stated Policies Scenario and to 550 GW in the Sustainable Development Scenario (IEA 2019). However, these scenarios do not make further specifications on the battery type and storage capacity.

Vanadium RFBs are now ready for the market. Their advantages over other storage batteries are their very long service life, high number of cycles and low self-discharge. This means that RFBs are particularly suitable for large stationary battery storage systems. Compared to other RFBs, V-RFBs have undergone development for a long time now so that they have reached a higher stage of development than alternative cell chemistries. One of the main idea generators is this system's original developer, the University of New South Wales (UNSW) in Sydney. In 2005, VFuel Pty Ltd was founded as a spin-off from the university, which currently no longer produces its own battery systems. Battery specialist Gildemeister installed a CellCube FB 30-130 at the UNSW in 2015. Used with for research purposes, it has an output of 30 kW and a storage capacity of 130 kWh. The largest V-RFB manufacturer according to its own figures is Infinity Energy, which supplies large battery storage systems with an output of up to 10 MW and a capacity of 40 MWh. Other major suppliers are China-based Prudent Energy Inc., Cellenium Company Ltd (Thailand), Sumitomo Electric Industries (Japan) and VRB Energy. A commercially available V-RFB by German firm VoltStorage serves as a home battery storage system with a capacity of 6.2 kWh and a maximum power output of 2 kW. It is specially designed to link to privately owned PV systems and can also be connected in series to other systems to increase performance and capacity (VoltStorage GmbH). Volterion is a spin-off from the Fraunhofer Institute for Environmental, Safety, and Energy Technology UMSICHT and supplies V-RFBs with a maximum output of 15 kW with a capacity of 13 kWh (Volterion 2020).

A sharp increase in I-RFBs is expected in the future since these incur significantly lower material costs. Moreover, there use the highly non-critical metal iron instead of vanadium while the energy density and other battery properties are similar to competing V-RFBs. One I-RFB manufacturer is US-based ESS, which collaborates with BASF among other partners. According to ESS, an I-RFB achieves a similar high cyclic and calendrical service life as a V-RFB (ESS 2017). Yang et al. (2020) examine another cell chemistry for RFB, also based on iron. The V-RFB manufacturer VoltStorage is also expected to switch over to I-RFB in the future (Peither 2020).

At present, there are also various projects in Germany which use vanadium RFBs:

– Braderup: conducted by Robert Bosch GmbH and the Braderup-Tinningstedt cooperative wind farm, this project comprises a hybrid battery storage system connected to six wind

turbines. The storage system was installed in 2014 and contains Sony lithium-ion batteries (with a capacity of 2 MWh and a power output of 2 MW) and a Vanadis Power GmbH redox flow battery (1.3 MWh and 0.3 MW) (Bosch 2014).

– RedoxWind: the Fraunhofer Institute for Chemical Technology (ICT) has developed and operates a large-scale redox flow battery with a power output of 2 MW and a capacity of 20 MWh. The RFB is connected directly to the DC intermediate circuit of a wind turbine to form a single unit comprising a generating unit and a storage battery as a pilot plant (Fraunhofer ICT 2015).

– EnergyKeeper: funded by the EU through the Horizon 2020 programme, this research programme ran from 2017 to 2019 and studied organic RFBs. The project aimed to build an organic RFB which would achieve an power output of 100 kW and a capacity of 350 kWh (Radziukynas 2020).

– Sonar Redox: commenced in early 2020, the SONAR research project is studying potential active materials for RFBs under the coordination of the Fraunhofer ICT. The aim is to create a screening method based on a model. The method will be used to evaluate different organic active materials with regard to their suitability for use in RFBs. The project thus seeks to identify a selection of alternatives to vanadium using a variety of evaluation criteria (Krapp 2020).

– A battery for the world: funded by the German Federal Ministry of Education and Research, this innovation competition for an inexpensive, environmentally friendly battery storage system designed for use worldwide started in 2020. Landshut University of Applied Sciences developed an I-RFB in cooperation with VoltStorage (Landshut University of Applied Sciences 2020).

3.3.7.4 Foresight raw material demand

Irena (2017) estimates an annual growth in storage capacity of 20 GWh. The specified specific raw material demands can be used to calculate the total demand for the active materials for RFBs, which are listed in Table 3.68. The raw material demand is specified for both V-RFBs and I-RFBs while assuming for both that the one cell chemistry will prevail over the other. The cumulative raw material demand assumes that only V-RFBs are currently installed since I-RFBs and organic RFBs are currently still under development. It is estimated that 8 % of the cumulative demand can be attributed to system construction in 2018.

Table 3.68: Raw material demand for redox flow batteries

System	All vanadium	All iron
Amount of material required [kg/kWh]	3.02	4.4
Accumulated demand in raw materials in 2018 [in tonnes]	756	0

Table 3.69: Global production (BGR 2021) and calculated raw material demand for redox flow batteries, in tonnes

Raw material	Production in 2018	Demand in 2018	Demand foresight for 2040	
			All vanadium	All iron
Vanadium	90,661 (M)	60	60,500	–
Iron	1,520,000,000 (M)	–	3,200	88,000

M: Mine production (tonnes of metal content)

According to the specified scenario, the demand for vanadium for RFB in 2040 amounts to about two-thirds of mine production in 2018. The use of redox flow power storage batteries is expected to stimulate the demand for vanadium significantly. If I-RFBs becomes standard by 2040, no impact can be expected on the iron market since the amount of iron used in I-RFBs is proportionally much lower than the total production volume. As it is not certain that I-RFBs will emerge as the pre-eminent format over V-RFBs by 2040 and the SSPs do not provide any direct data on battery storage technologies, no individual demands are indicated for the three SSPs. A total demand for vanadium of 60,500 tonnes is assumed for all three scenarios instead; see Section 4.14.4.

3.3.7.5 Recycling, resource efficiency and substitution

The metals in the electrolytes in redox flow batteries do not change over their service life and can be fully recycled. The electrolyte can either be pre-processed in such a way that it can be reused as electrolyte or the salts are extracted from the electrolyte to be used in a different application. RFB manufacturers are obliged to take back the batteries once their useful life has come to an end, so it is expected that recycling channels will become established for RFBs in the future. RFBs can be dismantled after decommissioning, so that the other components in the battery can also be recycled in addition to the electrolyte (Gouveia et al. 2020).

There are numerous research and development projects on vanadium-free RFBs, which could help to avoid potential supply bottlenecks for vanadium caused by the sharp increase in demand. At present, these projects also focus on organic RFBs in addition to the I-RFBs already described. In metal-free organic RFBs, aromatic compounds are used as electrolytes to store the energy. Varying the molecular composition can influence battery properties such as potential, temperature resistance, cycle stability and water solubility. The very high number of possible molecules allow a response to changes in boundary conditions (CMBlue Energy AG 2020). However, organic RFB development has not reached the same level as that of V-RFBs, so organic RFBs are not ready for the market yet. Both the service life and the energy density of organic RFBs are expected to be significantly inferior to those of V-RFBs or I-RFBs. Companies which are currently engaged in developing organic RFBs include CMBlue Energy and Jena Batteries, for example.

3.3.8 Wind turbines

3.3.8.1 Technology description

Generating electrical power from wind is an established, time-tested technology. However, high growth rates are still expected worldwide to meet the challenges of climate change. Increases in its use are therefore expected until 2040. New generator technologies may bring about a change in the demand for materials during this time. Figure 3.76 shows the structure and dimension of a wind turbine.

Generator technologies

Wind forces striking perpendicularly rotate the specially shaped blades of a wind turbine through dynamic lift. The mechanical energy in the rotation movement is converted into electrical energy in a generator. A magnetic field is created on the generator rotor to do so. The rotation of the magnetic field induces a current in the surrounding stator's conducting windings, so that electrical power can be generated. If the rotor and magnetic field run in synchronisation, it is called a synchronous generator. If the rotor runs faster than the magnetic field, it is referred to as an induction generator. In the case of generators excited by permanent magnetisation, the magnetic field on the rotor is ensured by attaching permanent magnets (NdFeB magnets; also see Section 3.3.9). In electrically excited generators, the magnetic field is induced via live copper coils (Lorentz force). Electrical energy is required to do so but this electrical energy is significantly less than the electrical energy produced as a final result.

In the case of directly driven and, consequently, gearless wind turbines (direct drive), the generator is directly connected to the rotor shaft and thus operates at the same speed as the rotor blades in the wind turbine. Greater speeds in what are known as high-speed wind turbines are accom-

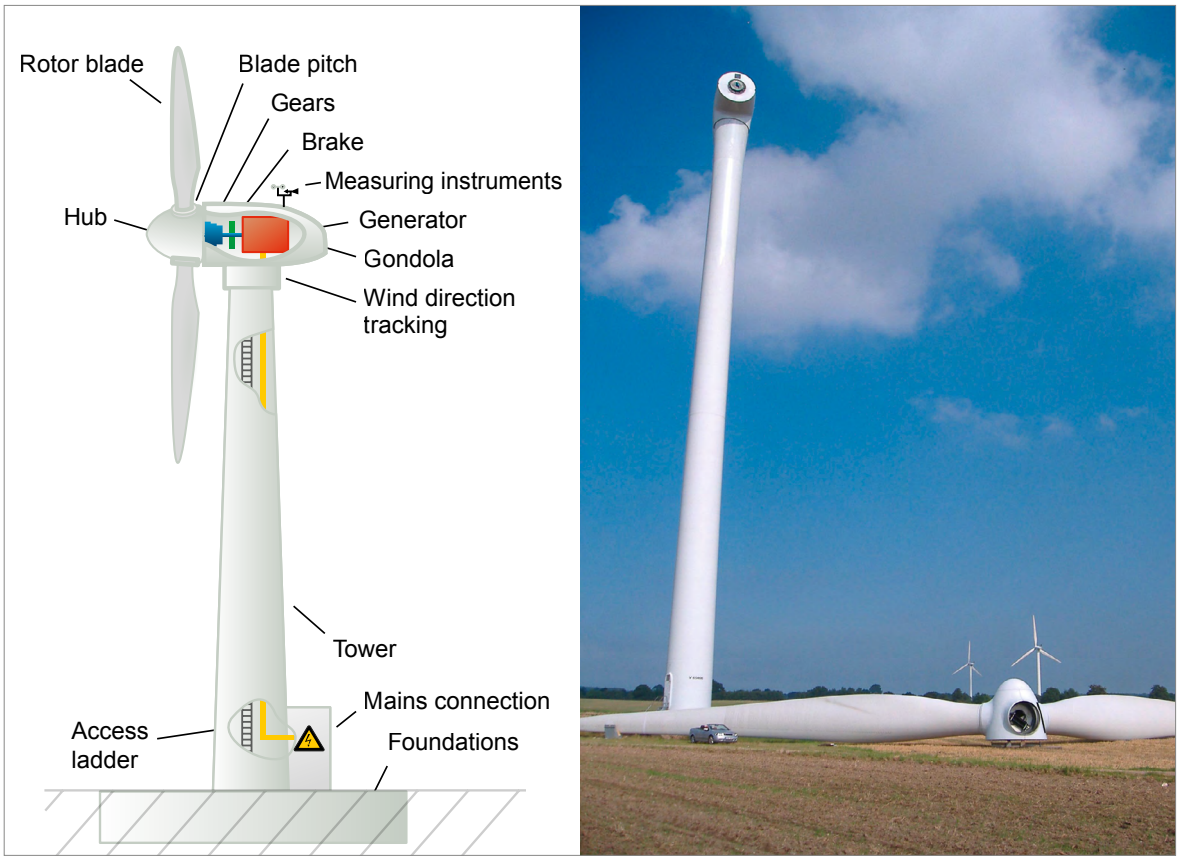

Figure 3.76: Components of a wind turbine (left) and dimensions of a wind turbine with a car for scale (right) (sources: image on left: Arne Nordmann CC BY-SA 3.0; image on right: Karle Horn CC BY-SA 3.0)

plished by a gear between the rotor and the generator. This allows space, weight, materials and costs to be reduced in the generator design. However, a gear can account for 25 % of the costs for a wind turbine, reduces power generation efficiency and increases the plant's maintenance needs and susceptibility to faults (Viebahn et al. 2014). Medium-speed wind turbines with a low-gear transmission and a coupling not prone to malfunction are regarded as a hybrid between direct drive and high-speed wind turbines.

Wind turbine generators are currently being developed in which the windings to generate the magnetic field consist of high temperature superconductors (HTS). Since these high-temperature superconductors have a much lower electrical resistance than copper, their use increases the magnetic field strength and, consequently, the generator output with the same weight. The generator could weigh 50 % less in a 10 MW wind turbine compared to a permanently magnetic direct-drive wind turbine, for example (Buchert 29/08.11; BINE Informationsdienst 2011; BINE Informationsdienst 2011; Viebahn et al. 2014).

Reluctance generators are also under development. Their effect is not based on the Lorentz force but on magnetic resistance (reluctance) instead (Viebahn et al. 2014). Table 3.70 contains the generator technologies currently used or under development for wind turbines. Generator types that are not relevant for wind turbines or are no longer used in new wind turbines are not included.

Characteristic variables

The usual characteristic variable of a wind turbine is its maximum power output (power rating). The actual output produced by a wind turbine depends on the wind and, consequently, on the location and on seasonal and daily fluctuations. A capacity fac-

Table 3.70: Various drive technologies currently in use in wind turbines (black) or in development for wind turbines (blue)

	Gearbox (GB)	Direct Drive (DD)
Electrically **e**xcited	Double-fed asynchronous machine (GB-DFIG)	Synchronous generator (DD-EESG)
		High **T**emperature **S**uperconductor
Permanent-**m**agnet-excited	Synchronous generator (GB-PMSG)	Synchronous generator (DD-PESG)
Reluctance gears		**R**eluctance generator

tor therefore indicates the ratio between the average generated output and the maximum output (IEA 2013c). The crucial characteristic variables also include the hub height and rotor diameter.

Onshore and offshore

Wind turbines on land (onshore) are already in widespread use. Offshore wind turbines have been establishing a new technology segment for some years now. Since high growth rates are expected on a sustained basis in both segments, this section looks at both technology segments. As a result of differing external conditions, the market shares for the generator technologies contained in Table 3.70 are different in both segments, as discussed in more detail in paragraph 3.3.8.3.

Offshore wind power generation offers advantages due to the higher and more constant wind speeds at sea. The disadvantages are higher costs for installation (transport, foundations), maintenance, network connection (Bradshaw et al. 2013b; IEA 2013c) and greater stress on components due to the salty air (Moss et al. 2011). Conventional offshore wind turbines are anchored in the sea bed using a monopile (steel pile), enabling them to be used in shallower waters up to 50–60 m deep. Floating foundations are currently being developed for wind turbines to provide greater flexibility in their location. A first wind farm using floating foundations was installed in Scotland in 2017 with a total installed capacity of 30 MW (IEA 2019).

Offshore wind turbines achieve capacity factors of 40–50 %. When turbines are located away from the coast, the capacity factor increases but the costs for installation, maintenance and network connection also increase (IEA 2019). Yearly average capacity factors of 20–35 % are typical for onshore wind turbines. Highly suitable installation locations can achieve 45 % or more (IEA 2013b).

Offshore wind turbines are particularly interesting for countries such as Germany, where economically viable onshore locations are considered to have already been almost fully utilised. As a result, any further expansion must be mainly provided by offshore turbines or repowering. Repowering refers to the replacement of existing wind turbines with newer models with a higher power rating.

3.3.8.2 Raw material content

Material demand for mass raw materials

Figure 3.77 shows roughly which materials are used in different parts of wind turbines. Composite materials are not examined in detail in this study focusing on metals since they are crude-oil-based raw materials. In Table 3.71 contains estimates of required material quantities per installed power rating in megawatts (MW). There are differences in the individual technology variants due to the generator excitation types and the use of gears for transmission. Onshore wind turbines usually have a concrete foundation whereas offshore turbines are often anchored to the sea bed with steel piles, which also leads to different raw material demands.

According to Harmsen et al. (2013), in addition to the demand for copper for the wind turbine, 5.7 tonnes/MW of copper is also required for high-voltage DC cables and 2.2 megatonnes (Mt) of copper are needed per exajoule (EJ) of transported power to expand the transmission grid. This means that 95 % of the copper requirement

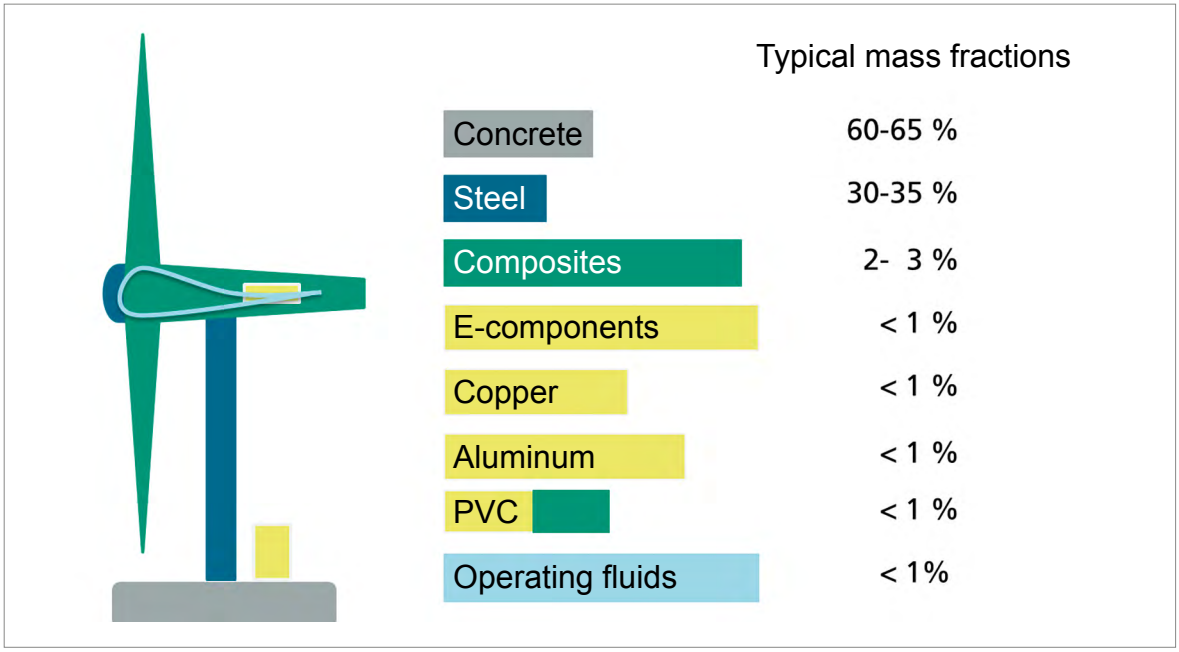

Figure 3.77: Material demand of a wind turbine (source: Seiler & Woidasky 2013)

for wind energy is not needed for turbine construction but to expand the network instead. This is because favourable locations for generating wind power can be far away from the consumers acquiring the generated power. Since the power generated fluctuates sharply over time depending on the wind strength, additional material requirements may arise for voltage transformers and local storage to compensate for peak loads (IEA 2013).

As the size of wind turbines increases, the material requirement and thus the cost per installed power output decrease. This is because the rotor diameter of a wind turbine has a quadratic relationship with the generated electrical power output. The wind speed, which increases as the hub height increases, even has a cubic relationship with generated output. However, there are physical limits to the trend towards increasingly larger wind turbines which has existed for years (Rohrig 2014) due to the maximum achievable blade peak speeds and nacelle weights (Viebahn et al. 2014). Structural innovations may also reduce the specific material demand. One example is the tower's sandwich structure in which two smaller interlocking steel pipes with a composite material such as expoxide resin are used instead of one thick steel pipe (VDI ZRE 2014). On the other hand, the market share is increasing for offshore turbines. These have a higher material content due to the more challenging conditions. There are also currently proposals to use steel instead of composites to manufacture rotor blades for offshore wind turbines (VDI ZRE 2014). For the sake of simplicity due to the different trends, it is assumed that the specific material demands in Table. 3.71 will remain constant until 2040.

Material demand for rare earth elements

NdFeB magnets are used in wind turbine generators with permanent magnet excitation (see Table 3.70). These may not only contain neodymium but also the rare earth elements dysprosium, terbium and praseodymium (see Section 3.3.9). Gearless direct drive wind turbines require significantly greater magnetic masses than high-speed and medium-speed wind turbines with gears due to the large generator. In Table 3.72 contains the specific raw material demands for rare earths for the different technology variants, in tonnes/GW.

It is assumed that these values will not change before 2040, although a reduction may be feasible due to an optimisation of the generator design, for example.

Table 3.71: Material demand for wind turbines, in tonnes/MW (source: Carrara et al. 2020)

Specific raw material demand	DD-EESG (onshore)	DD-PMSG (offshore)	GB-PMSG (onshore)	GB-DFIG (onshore/offshore)
Steel	132	119.5	107	113
Cast iron	20.1	20.1	20.8	18
Aluminium	0.7	0.5	1.6	1.4
Copper	5	3	0.95	1.4
Nickel	0.34	0.24	0.44	0.43
Zinc	5.5	5.5	5.5	5.5
Chromium	0.525	0.525	0.58	0.47
Manganese	0.79	0.79	0.8	0.78
Molybdenum	0.109	0.109	0.119	0.099
Concrete	369	243	413	355
Polymers	4.6	4.6	4.6	4.6
Glass/carbon fibre reinforced plastic	8.1	8.1	8.4	7.7
Boron	0	0.006	0.001	0

Table 3.72: Demand for rare earths for wind turbines, in tonnes/GW (source: Carrara et al. 2020)

Specific raw material demand	DD-EESG (onshore)	DD-PMSG (offshore)	GB-PMSG (onshore)	GB-DFIG (onshore/offshore)
Neodymium	28	180	51	12
Dysprosium	6	17	6	2
Praseodymium	9	35	4	0
Terbium	1	7	1	0

Some sources state that no dysprosium will be needed for NdFeB magnets in wind turbines since there is adequate space for cooling (Roskill Information Services 2011). Most sources, however, assume that the proportion of dysprosium in magnets will be around 2 %. To calculate the raw material demand, the demand for dysprosium is determined based on the specific demand in Table 3.72.

The high-temperature superconductor wind turbines (HTS) under development require yttrium, lanthanum and cerium. Nonetheless, the demands of around 0.002 tonnes/MW are very low compared to permanent magnet technology (Buchert 2011).

3.3.8.3 Foresight industrial use

In 2018, worldwide wind turbine capacity increased by 50 GW with 4.3 GW corresponding to offshore turbines and the remaining capacity to newly installed onshore turbines (IEA 2019). Onshore wind turbines thus accounted for more than 91 % of the growth in installed wind energy power output in 2018. In the same year, a total energy of 67 TWh was generated in offshore wind turbines and 1,198 TWh in onshore wind turbines, meaning that only 5 % of the energy generated by wind power was produced offshore (IEA 2019).

The political situation is regarded as the largest growth driver for further expansion of wind power

Table 3.73: Scenarios for the energy production and installed output of wind turbines (sources: Fricko et al. 2017, Kriegler et al. 2017, Van Vuuren et al. 2017, IEA 2019, Irena 2020b, Irena 2020c)

Scenario	Year	Primary energy [EJ/a]	Onshore capacity [GW]	Offshore capacity [GW]
	2018	1.3	540	23.6
SSP1-19	2040	16.5	1,022	51.1
SSP2-26	2040	28.3	2,433	14.7
SSP5	2040	5.0	538	0

Table 3.74: Additional wind turbine output installed in 2040 due to capacity increase and repowering, in [GW/a]

Scenario	Location	Repowering	Actual capacity increase	Total capacity increase
SSP1-19	Onshore	63.98	54.62	118.60
	Offshore	0.72	41.61	42.33
SSP2-26	Onshore	63.98	89.12	153.06
	Offshore	0.72	6.81	7.53
SSP5	Onshore	63.98	-2.16	61.82
	Offshore	0.72	0	0.72

generation. The greatest obstacle is considered to be the adaptation of general technical conditions (electricity distribution network, electricity storage systems) to weather- and location-dependent electricity generation by wind turbines (IEA 2013).

The expansion of wind energy is estimated based on the three scenarios SSP1-19, SSP2-26 and SSP5, which are described in Section 1.1. Table 3.73 contains the annual energy production and the installed capacity for these scenarios.

The increase in wind turbine capacity is needed to estimate the raw material demand for wind turbines for one year. Repowering, which consists of replacing old wind turbines with new ones, also needs to be taken into account here. According to Carrara et al. 2020), the lifetime of wind turbines is increasing and is currently 25 years for onshore turbines and 30 years for offshore turbines. Repowering in 2040 is therefore assumed for onshore turbines with the increase in capacity in 2015 and for offshore turbines with the increase in 2010 since, on average, turbines from these construction and installation years will have reached the end of their lifetime in 2040. The capacity increases for 2010 and 2015 are taken from Irena (2020b) and are shown in Table 3.74. A linear interpolation of the capacity in 2030 and 2040 is used to calculate the real capacity increase without repowering. The capacity increase is shown in Table 3.74. SSP5 expects more turbines to be dismantled than new ones built in 2040.

Market shares of different technologies

The raw material demand for wind turbines depends on the market share of the drive technologies. The demand for rare earths particularly depends on the type of generator excitation since no permanent magnets are required in electrically excited machines (see Table 3.70). Different raw demands also arise for construction materials for the various technologies – for example, due to the use of steel foundations instead of concrete ones, the size of the generator or possible use of a gearbox. Table 3.71 and Table 3.72 take into account the specific raw material demands for the different variants.

Electrically excited high-speed asynchronous generators with gears continue to hold significant market shares for both on- and offshore, but the newer technologies will take over to a certain extent. This is demonstrated by the world's three largest wind turbine manufacturers (GWEC 2019; IRENA 2019). The Danish company Vestas (20.3 % market share) used to build induction generator wind turbines only but has also been offering permanent-magnet-excited high-speed wind turbines with gears for a few year (VIEBAHN et al. 2014). Siemens Gamesa (12.3 % market share) has also built induction generator wind turbines in the past but has now opted to produce direct drive turbines with permanent magnet excitation, just like the Chinese supplier Goldwind (13.8 %). In contrast, the German manufacturer Enercon (5.5 % market share) has been building direct drive turbines with electric excitation since 1992 and is not planning to change its concept.

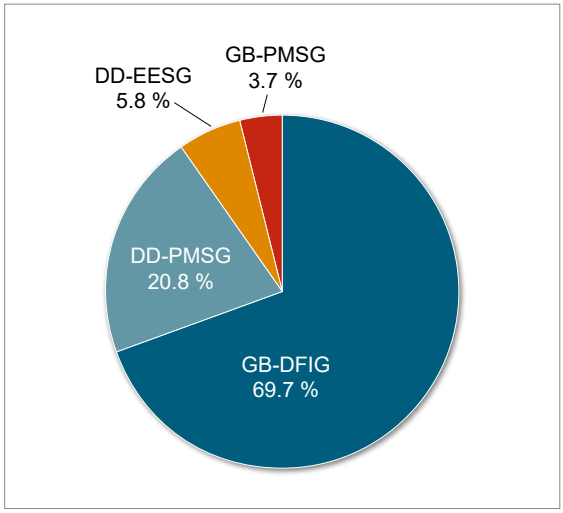

Figure 3.78: Market shares of technology variants in 2018 (source: GWEC 2019 in IRENA 2019)

Direct drive technology accounted for a 26.6 % market share of the wind turbines built worldwide in 2018. However, some of the direct drive wind turbines are also electrically excited while hybrid turbines use permanent magnets despite gears connected upstream. The market share of wind turbine technologies using permanent magnets was 24.5 % in 2018 (GWEC 2019; IRENA 2019).

However, many factors will determine what market share different technologies will manage to capture in the future. The availability and prices of rare earths will play a major role in this process. We should note that China is likely to be the market leader in wind power in 2035 with a 30 % global share in wind turbine production (IEA 2013). Since China currently accounts for almost 75 % of global rare earth mining, we should assume that the availability of these materials will be regarded as less critical in China. As a result, technologies based on NdFeB magnets will probably be more widely used than in Europe, for example.

Furthermore, the choice of location (on- or offshore) will have a significant influence on the choice of technology. In 2040, around 20 % of primary power generated by wind turbines will come from offshore wind turbines. In 2018, it was just 5.4 % (IRENA 2020c). It is expected that the cost of generating electricity will decrease by 60 % for offshore wind turbines between 2018 and 2040 (IEA 2019). Due to this increasing market share of the total plant capacity, we assume that offshore turbines are likely to account for more than 20 % of the turbines newly built in 2040. Direct drive wind turbines with permanent magnet excitation are expected to have a great future, especially in this segment. This is because their low maintenance requirements in the offshore sector is a decisive advantage due to the high cost for offshore maintenance. This advantage can compensate for the higher costs of the technology. However, medium-speed permanent magnet wind turbines are also likely to gain in importance in the offshore segment (VIEBAHN et al. 2014). In contrast, direct drive turbines with electrical excitation and turbines with intermediate gears will be important mainly in the onshore segment. If the high-temperature superconductor wind turbines (HTS) currently under development are ready for the market by 2040, they will mainly compete for market share with permanent magnet direct drive wind turbines (VIEBAHN et al. 2014). Figure 3.78 shows the market shares of the technology variants for 2018.

Figure 3.79 shows the shares of the technology variants for the wind turbines which are newly built in 2040. All new wind turbines are taken into account here so that repowering is also included. The technology market shares shown are calculated based on the assumption that the market for onshore wind turbines is composed as it is currently (see Figure 3.78) while permanent magnet direct drive technology becomes the standard

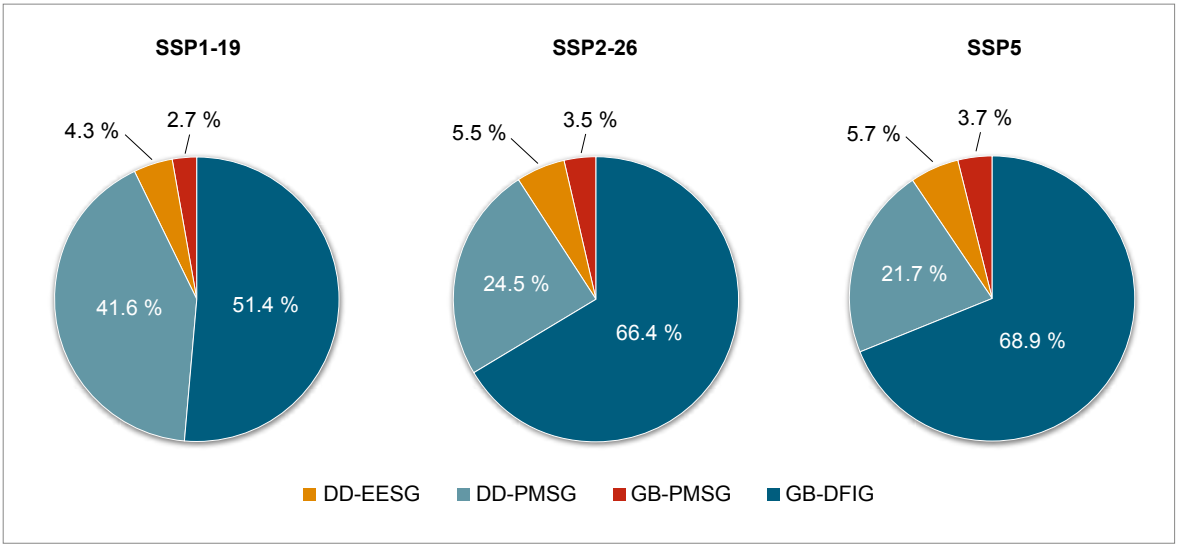

Figure 3.79: Assumptions relating to technology shares in 2040 for global newly built wind turbines in the different scenarios (onshore and offshore including repowering) (source: own representation)

for offshore wind turbines. This technology offers advantages with regard to lifespan and maintenance intervals. These properties are particularly important in the offshore segment due to difficult accessibility. This is likely to increase the demand for rare earths. Market penetration by new technologies such as the reluctance generator or generators with high-temperature superconductors is not foreseeable yet and, as a result, is not taken into account in the scenarios.

3.3.8.4 Foresight raw material demand

The specific raw material demand in Table 3.71 and Table 3.72, the scenarios for the wind turbine capacity expansion in Table 3.73 and Table 3.74 and the distribution of capacity among the different technology variants in Figure 3.79 are used to calculate the raw material demand, which is shown in Table 3.75 andd Table 3.76. Future increased material efficiency due to optimisation processes could further reduce the specific material demands. However, this is ignored in the scenarios since it is difficult to estimate progress in this area. In Table 3.75 shows the demand for bulk raw materials in scenarios SSP1-19 and SSP2-26 differs only slightly. However, depending on the raw material, the demand for bulk raw materials in scenario SSP5 is about 55–66 % lower than in the other two scenarios and at a similar level to the raw material demand in 2018. The expansion of wind energy is unlikely to have a major impact on the raw materials markets in the case of mass raw materials.

A different picture emerges in the case of rare earths, as we can see in Table 3.76. A significant increase in the demand for rare earths is expected in scenario SSP1-19 due to the anticipated major expansion in offshore wind turbines. The demand for rare earths for wind turbines will thus increase five- or six-fold in this scenario compared to 2018. The expansion of wind energy may have a significant impact on the market for rare earths with the low global production volumes of these raw materials in comparison to mass raw materials. The demand for rare earths also increases significantly in Scenario SSP2-26 but considerably less than in Scenario SSP1-19. Scenario SSP5 does not contemplate a further expansion of offshore wind turbine capacity so that the demand for rare earths remains almost the same as in 2018. According to the Federal Institute for Geosciences and Natural Resources (2021), the aggregate production volume of rare earths was 151,200 tonnes in 2018.

Table 3.75: Global production (BGR 2021) and calculated raw material demand for WKA, in tonnes

Raw material	Production in 2018	Demand in 2018	Demand foresight for 2040		
			SSP1-19 Sustainability	SSP2-26 Middle of the Road	SSP5 Fossil Path
Steel	1,820,366,000	5,695,000	18,725,000	18,540,000	7,209,000
Cast iron	1,520,000,000 (iron)	922,000	3,064,000	3,008,000	1,168,000
Aluminium	63,756,000 (R)	58,300	161,000	184,000	73,300
Copper	20,591,000 (M) 24,137,000 (R)	95,100	355,000	317,000	121,000
Nickel	2,327,500 (M) 2,189,313 (R)	19,100	55,900	60,800	24,000
Zinc	12,800,000 (M) 13,110,000 (R)	272,000	858,000	883,000	344,000
Chromium	27,000,000 (M)	24,200	80,000	78,800	30,600
Manganese	20,300,000 (M)	38,700	126,000	126,000	49,000
Molybdenum	265,582 (M)	5,100	16,800	14,500	6,400

M: Mine production (tonnes of metal content)
R: Refinery production (tonnes of metal content)

Table 3.76: Global production (BGR 2021) and calculated demand for rare earths for wind turbines, in tonnes

Raw material	Production in 2018	Demand in 2018	Demand foresight for 2040		
			SSP1-19 ustainability	SSP2-26 Middle of the Road	SSP5 Fossil Path
Neodymium	23,900 (R)	2,430	13,470	8,900	3,180
Dysprosium	1,000 (R)	270	1,370	970	350
Praseodymium	7,500 (R)	390	2,420	1,480	520
Terbium	280 (R)	76.7	480	290	100

R: Refinery production (tonnes of metal content)

3.3.8.5 Recycling, resource efficiency and substitution

If supply bottlenecks should occur for the rare earth elements terbium, neodymium, dysprosium and praseodymium in the future, this will not necessarily affect the expansion of wind energy production globally. It will favour a switch to technologies that require little or no rare earth elements instead. Resource efficiency is expected to increase slightly in the future thanks to the trend towards higher and more powerful wind turbines.

The long lifespans of wind turbines (about 25–30 years) means there are currently only a few wind turbines requiring disposal or recycling. In Germany in the past, turbines dismantled during repowering tended to be taken apart on site and then exported to emerging and developing countries (VDI ZRE 2014). The recycling rate for the entire turbine currently stands at 80–90 % (Seiler & Woidasky 2013). Research is currently being undertaken to improve recycling of the composite materials used in the blades (Seiler & Woidasky 2013). The large magnet mass of 0.3 to 3 tonnes

per turbine is favourable for recycling rare earth elements compared to other applications. Dismantling the generator and separating steel and copper scrap for recycling makes financial sense and is technologically and logistically feasible.

3.3.9 High-performance permanent magnets

3.3.9.1 Technology description

Permanent magnets and high-performance permanent magnets

Permanent magnets have magnetic forces of attraction and repulsion. Unlike electromagnets, permanent magnets have and retain these magnetic forces without the need for current flow. Permanent magnets are made of hard magnetic materials such as FeCoCr alloys, hard ferrites, samarium cobalt and neodymium-iron-boron among others and are produced by applying an external magnetic field. During this process, the existing magnetic domains (white areas) within the material are aligned along the external magnetic field. When these domains are aligned, the material remains magnetised when the external magnet field disappears. Soft magnetic materials, such as soft ferrites (NiZn), have strong magnetic properties when in an external magnetic field but lose their magnetism after the external field is removed.

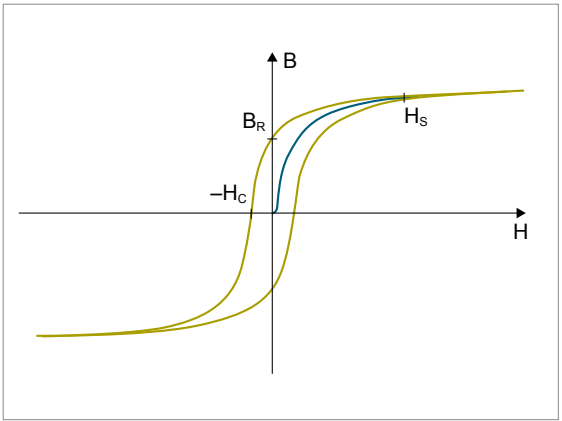

Figure 3.80: Hysteresis curve of a permanent magnet: B: magnetic flux density, H: magnetic field strength, BR: remanence, HC: coercitivity (source: Walter Dvorak, Wikimedia, public domain)

The properties of a hard magnetic material that determine its suitability as a permanent magnet are visualised in Figure 3.80 and explained below:

– High BR remanence: BR remanence is the magnetisation remaining in a magnet when the external magnetic field is removed (magnetic flux density B).

– High coercive field force: the coercive field force HC corresponds to the H field force which must be used to completely demagnetise magnets. The higher the coercive field force is, the greater the magnet's resistance to external magnetic fields is.

– High energy density: the product of B and H equates to the magnetic field energy. The energy density is obtained based on the volume. The maximum energy density of a magnetic material is considered a crucial performance criterion.

– High maximum operating temperature: magnets are exposed to high temperatures in many applications such as motors. However, each permanent magnet is characterized by a maximum operating temperature above which the orientation of the white areas and, consequently, the permanent magnetism are noticeably and irreversibly lost. This maximum operating temperature is significantly lower than the Curie temperature above which ferromagnetic properties (i.e. the ability to be attracted by a magnet) in a material such as iron or in a neodymium-iron-boron magnet (NdFeB magnet) is lost.

NdFeB magnets are considered high-performance permanent magnets because their maximum energy density $(BH)_{max}$ is far higher than the maximum energy density of standard magnets made of ferrites or aluminium-nickel-cobalt alloys. They also have around twice the energy density of samarium-cobalt magnets (SmCo magnets) (Schmal 2010).

Types and production of NdFeB magnets

Sintered or bonded NdFeB magnets can be used, depending on the application type. Bonded NdFeB magnets are cheaper but are less temperature-resistant and less powerful. They are used in electrical appliances, for example, while only sintered magnets are suitable for challenging applications such as drive motors in vehicles or generators in wind turbines.

An NdFeB alloy is produced in an induction furnace to manufacture sintered NdFeB magnets. The alloy is pulverized and milled to form powder, which is then formed and sintered based on the alignment of the grains in the magnetic field. The magnets produced in this way are then cut and ground into the required shape and then magnetized in the preferred direction (Schmal 2010). According to Liu & Chinnasamy (2012), 20–30 % of the material is lost during grinding and cutting. However, grinding debris and rejected magnets are recycled. It is therefore assumed that, when estimating raw material demand, the mass of the NdFeB magnets contained in a product approximately equals the demand.

Bonded magnets can be produced using HDDR (hydrogenation, disproportionation, desorption and recombination).

NdFeB magnet applications

In principle, high-performance permanent magnets can be used in all magnet applications. In particular, their use in brushless permanent magnet three-phase synchronous motors opens up many fields of application. However, NdFeB magnets are only actually needed in areas where it is essential to combine high performance with a low mass or low volume. Low-cost ferrites are a widely used alternative when requirements are less stringent regarding the magnetic energy density. Moreover, NdFeB magnets are not suitable for temperatures above 200 °C. That is why SmCo magnets are used in high-temperature applications. Whether NdFeB magnets are used in all areas in the future or exclusively for applications with more stringent requirements will greatly depend on the price and availability of the integral components.

NdFeB magnets are used in the following sectors worldwide (Roskill Information Services 2011; Imarc 2020):

- Conventional automotive industry
- Electric vehicles
- Aeronautics
- Medical technology
- Electrical equipment (heat exchangers, large appliances, small appliances, information and telecommunications technology such as data storage units)
- Electric measuring instruments
- Energy generation
- Military
- Industry

The electrical appliances area of application consists of many different applications with NdFeB magnets very often forming a very small part of each purchased product. However, high sales figures for mass applications result in large quantities of magnetic material overall. Electrical appliances are divided into the six categories according to the German Electrical and Electronic Equipment Act (ElektroG): heat exchangers, screens and monitors, lamps, large appliances, small appliances, and small information and telecommunications technology devices (Stiftung EAR not date).

The large appliances and small appliances categories include many applications, such as children's toys and locking and fastening mechanisms, where NdFeB magnets can be substituted by weaker magnets. Their use in motors should not be considered essential for items such as washing machines either. However, the excellent properties of NdFeB magnets are required in motors in items such as battery screwdrivers or electric razors. In the heat exchanger category, NdFeB magnets are increasingly used in air-conditioning units to improve energy efficiency due to stricter energy-saving regulations. They mainly contained ferrites in the past.

HDD, CD and DVD drives are considered main applications in the small information and telecommunications technology devices category. NdFeB magnets are contained in the swing arm actuator (HDD) and in the rotation motor (HDD, DVD and CD) in this case. CD and DVD drives will become less important due to online data transfer and HDD hard drives in terminal devices are being increas-

ingly replaced by SSD hard drives, which work without moving parts and therefore do not require magnets. However, HDD hard drives will continue to play an important role in the future (see Section 3.5.4 on data centres). Loudspeakers in items such as laptops will also feature largely. NdFeB magnets are also used in stepper motors. Overall, NdFeB magnets can thus be found in laptops, desktop computers, servers, central data storage units, printers, fax machines, photocopiers and similar. NdFeB magnets are also encountered in loudspeakers and drives in consumer electronics such as televisions, audio devices, laptops, tablets, computers, portable audio/DVD players, game consoles, watches, clocks, digital cameras and smartphones (Bookhagen et al. 2020).

Another major application field is the conventional automotive industry. Here, NdFeB magnets are spread over a wide variety of individual applications in motors, actuators and sensors. These include interior equipment elements such as speed indicators, air conditioning systems, power windows, windscreen wipers or seat adjusters and also for engine components, power-assisted steering, ABS and eddy current brakes. Figure 3.81 shows an example.

In addition to these applications, electric and hybrid cars (see Section 3.1.2) and electrically powered bikes feature comparatively large NdFeB magnets in their drive motor. Electric and hybrid cars are regarded as the application with the greatest growth potential.

Another important application field for NdFeB magnets are industrial applications such as motors for robots and injection moulding machines (see Section 3.2.6) and also traction motors. NdFeB magnets may also feature in industrial air conditioning systems. Magnetic separation devices to process metals (recycling) and minerals (mine production) also use NdFeB magnets.

NdFeB magnets are also found in many small individual applications in aviation, medicine and measurement instrumentation. In the medical technology field, MRI scanners are a common application featuring relatively large NdFeB magnets. However, MRI scanners mostly contain ferrites. Other mass applications with small NdFeB magnets include pacemakers, insulin pumps and sleep apnoea devices (Mordor Intelligence 2020b).

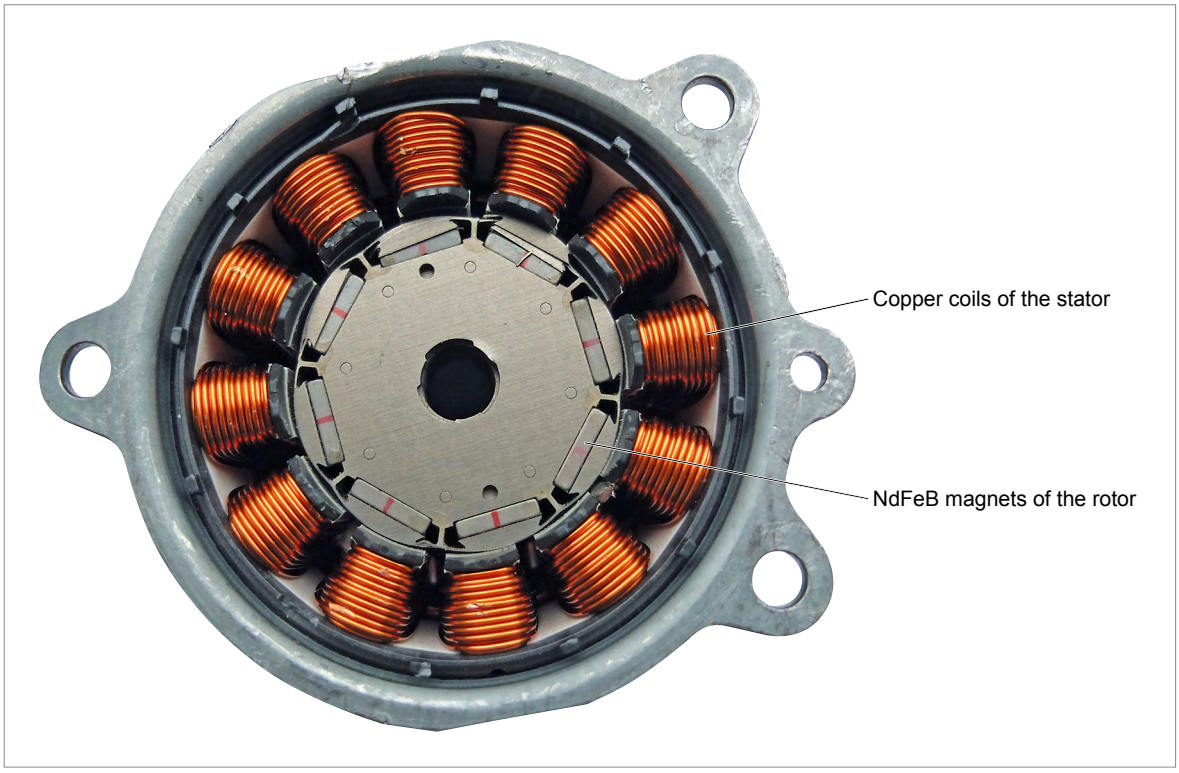

Figure 3.81: Steering motor of a car (source: Fraunhofer ISI)

In the defence sector, NdFeB magnets are used for radar systems, acceleration sensors, night vision glasses and remote steering of missiles. Countries such as the USA therefore consider these raw materials strategically important and are building storage facilities for them.

Another growth market for NdFeB magnets is their use in generators for wind turbines (see Section 3.3.8). They are also used to a lesser extent in run-of-river and tidal power plants.

Another emerging technology where NdFeB magnets can be used is magnetic refrigeration systems, which are being developed for cryogenic refrigeration in research and for refrigerators for home and industrial use. Magnetic refrigeration systems save 50–60 % more energy than conventional refrigeration units (Schüler et al. 2011). However, these refrigeration systems are still at the research stage (Podbregar 2019).

3.3.9.2 Raw material content

NdFeB magnets may contain numerous other elements in addition to the three main components iron, boron and neodymium. Adding cobalt improves the corrosion resistance in NdFeB magnets. Corrosion resistance can be further improved using a protective nickel or epoxy resin coating.

Praseodymium (Pr) can be used as a substitute for neodymium (Nd) for reasons of cost but only up to a ratio of Nd:Pr = 3:1 since higher PR content would affect the magnetic properties (Buchert et al. 2012). According to Roskill (2011), the demand for Nd and Pr for NdFeB magnets corresponded to a ratio 3:1 in 2010. 5:1 is often specified as the average or usual ratio (Buchert et al. 2012; Glöser-Chahoud & Tercero Espinoza 2015).

The maximum operating temperature of NdFeB magnets can be increased from a mere 80 °C to 200 °C by substituting part of the neodymium with dysprosium (Dy) or terbium (Tb). This is why NdFeB magnets containing dysprosium are used in electric car motors and wind turbine generators (Hoenderdaal et al. 2013). Dysprosium also enhances the corrosion resistance in magnets and increases the coercive field force.

Terbium has the same positive effect on magnets but it does not reduce their remanence, unlike dysprosium (Schüler et al. 2011). Lighting technology used to generate high demand for Tb, thus driving up prices with the result that terbium was hardly ever used in NdFeB magnets. LED technology has become standard and does not use terbium. Consequently, the availability of terbium and thus its use as a replacement for dysprosium in NdFeB magnets could increase.

According to Roskill (2011), some Chinese manufacturers add gadolinium (Gd) to NdFeB magnets to reduce costs but this also impairs their magnetic properties.

The pure magnet phase $Nd_2Fe_{14}B$ is composed of 27 % neodymium, 72 % iron and 1 % boron. In magnets, sintered grains in this phase are surrounded by a rare-earth phase so that the total fraction of rare earth elements has a mass percentage of around 32 %.

3.3.9.3 Foresight industrial use

Emerging technologies that will increase the demand for NdFeB magnets enormously are electric cars and wind turbines (Research and Markets 2019; Green Car Congress/Adamas Intelligence 2020; Mordor Intelligence 2020b; Roskill 2020a), which are analysed in Sections 3.1.2 and 3.3.8. Numerous market studies have also identified consumer electronics as a key driver behind increases in future demand (Research and Markets 2019; Imarc 2020; Mordor Intelligence 2020b; Technavio 2020). The Asia-Pacific region is the principal region with an increasing demand for magnets for consumer electronics. According to Technavio (2020), the Asia-Pacific region will account for 86 % of global growth in the rare earth market between 2020 and 2024. Many major global electronics producers are based in Japan, India and South Korea (Mordor Intelligence 2020b). A marked increase in electronic device production is also expected in India due to additional investments and government incentive programmes (Mordor Intelligence 2020b). As the world's largest manufacturer of electronic equipment, China produces for both export and the domestic market. Substantial increases in demand for consumer electronics is expected both within China and in countries

which import from China (Mordor Intelligence 2020b). China thus continues to dominate the demand for rare earths and their production (Roskill 2020a).

Besides consumer electronics, medical technology, which includes MRI, pacemakers, insulin pumps and sleep apnoea devices, is also identified as a growth market for NdFeB applications (Research and Markets 2019; Imarc 2020; Mordor Intelligence 2020b; Technavio 2020). Major investment in the health sector is not only expected in the Asia-Pacific region, but also in Africa and the Middle East (Mordor Intelligence 2020b).

Uncertainties regarding stable supply or demand-related bottlenecks and concerns about social injustices and environmental and judicial abuses related to rare earth mining are identified as potential growth inhibitors (Research and Markets 2019; Mordor Intelligence 2020b; Technavio 2020). Both may lead to a widened search for replacements for NdFeB.

Overall, the annual demand for rare earth for magnets increased by 6.4 % on average between 2015 and 2019 while demand dropped by 9.3 % in 2020 due to the Covid-19 crisis (Green Car Congress/Adamas Intelligence 2020). All current market studies forecast a rapid recovery of the market. Roskill (2020a) assumes a compound annual growth rate (CAGR) of around 10 % in the total demand for rare earth oxides (SEOs) between 2020 and 2030 with the proportion of magnet applications expected to grow from 29 % to 40 % during the same period. This leads to a growth in demand for magnetic applications with a CAGR of 13.5 % between 2020 and 2030. Green Car Congress/Adamas Intelligence (2020) expect an increase in demand for magnet applications with a CAGR of 9.7 % until 2030. Garside (2020) forecasts a CAGR of 11 % for magnet applications between 2019 and 2025. All CAGR percentages listed here include the growth for electrical traction engines for motor vehicles and wind turbines, which has already been examined separately in Sections 3.1.2 and 3.3.8. For this reason, scenarios for the future development of demand for magnet applications in the consumer electronics sector only are analysed below. These are based on the framework scenarios regarding digitisation (cf. Section 1.4). Scenario SSP2 assumes that historical trends will continue. The progressive spread of internet connections worldwide and increasing data volumes will not only lead to higher demands for established consumer electronics devices but also for further developed and new devices. This will be accompanied by a growth in demand at a CAGR of 7 % between 2021 and 2040. In contrast, SSP5 forecasts an acceleration and intensification of growth (CAGR 8 %). In SSP1, development is also accelerated compared to SSP2. However, it also takes sustainable consumer behaviour into account (e.g. longer use, reuse and repair of consumer electronics), resulting in a CAGR of 6.8 %.

3.3.9.4 Foresight raw material demand

According to Garside (2020), the demand for SEOs for magnets was 43,733 tonnes of SEOs in 2019. Roskill (2020a) states that around 15 % were needed for consumer electronics, including sound converters. Below, it is assumed that the magnets are NdFeB magnets only as they are the most common, even if they could be replaced by SmCo magnets to a certain extent.

Table 3.77: Global production (BGR 2021) and calculated neodymium demand for magnet applications in consumer electronics, in tonnes

Raw material	Production in 2018	Demand in 2018	Demand foresight for 2040		
			SSP1 Sustainability	SSP2 Middle of the Road	SSP5 Fossil Path
Neodymium	23,900 (R)	5,620	19,630	20,340	24,270

Note: Demand for rare earths for magnet applications for traction engines in vehicles and generators for wind turbines is covered in 3.1.2 and 3.3.8.

R: Refinery production (tonnes of metal content)

For the sake of simplicity, it is also assumed that the NdFeB magnets for consumer electronics do not contain any heavy rare earths (Dy/Tb). This is because they are not necessary for these applications and are unlikely to be used due to their scarcity and high price.

Table 3.77 shows the demand for neodymium in 2040 based on the scenarios. According to the Federal Institute for Geosciences and Natural Resources (2021), the aggregate production volume for rare earths was 151,200 tonnes of metal content in 2018.

3.3.9.5 Recycling, resource efficiency and substitution

According to expert opinion, it will not be possible to develop a magnetic material with comparable properties which does not require any rare earth elements in the foreseeable future despite intensive research efforts. It is more likely that there will be gradual improvements to NdFeB magnets, primarily optimisation of manufacturing methods and a reduction in the proportion of heavy rare earth elements, especially dysprosium. However, the unexpected discovery of new suitable magnetic materials could lead to new products within a few years thanks to intensive development efforts worldwide.

NdFeB magnets are not collected separately in Germany at the present time (Bast et al. 2015). Production waste is sent to China for recycling since there are no suitable plants in Europe. In addition to the further development of technical expertise, especially on reducing rare earths (oxides) to rare earth elements (metals), the creation of functioning and profitable collection infrastructures is also a fundamental requirement for future recycling. Other conditions include dismantling methods suitable for handling recycling on a massive scale, which needs to be taken into account at the design stage of devices (design for recycling). This is all the more crucial the smaller the magnetic content is for the individual application concerned. In consumer electronics, each individual application usually contains tiny amounts difficult to recover but add up to sizeable quantities due to the large number of devices (Bookhagen et al. 2020).

According USGS (2021b), permanent magnets are only recycled to a limited extent. The substitution of the rare earth magnets is possible in many applications but this affects performance. Roskill (2020a), however, considers it likely that the future increase in demand for xEV will lead to substitutions and savings in other, price-sensitive sectors.

3.3.10 Synthetic fuels

3.3.10.1 Technology description

One sector which cannot easily be decarbonised is transport. Although electric transport exists in the form of battery-powered passenger cars and in trolley truck demonstration projects, there are yet to be convincing concepts for ships and, especially, aircraft. One possibility for these means of transport and passenger cars is synthetic fuels. These will be produced without CO_2 emissions in the mid-term and their carbon content will come from sources such as biomass or from the air. This means that only the CO_2 conducted in the circuit during combustion in the engine will escape to the atmosphere and will not increase the concentration.

One often cited advantage of synthetic fuels over the use of hydrogen or large electric drives, which require the expansion of power grids, is the utilisation of the existing infrastructure (petrol stations and combustion engines among other things. This is why they are also called drop-in fuels (Steinfort 2020). One disadvantage often indicated is the substantial conversion losses before production of these fuels, also known as e-fuels, is complete: the production chain for the vehicle ranging from renewable electricity and green hydrogen through to liquid fuel synthesis can lead to GHG emissions which are three times as high as for battery electric vehicles (Agora Verkehrswende 2019b).

Synthetic fuels are produced using methods based on liquid conversion technologies: GTL technology (gas-to-liquid) based on natural gas as the raw material, CTL (coal-to-liquid) with coal and BTL technology (biomass-to-liquid) when biomass such as wood, straw or organic waste from agriculture and forestry are used. The similar term power-to-x has also been coined. During these

processes, electricity is used to produce hydrogen by electrolysis and then produce liquids with CO using Fischer Tropsch reactions.

Liquid conversion technologies are at different stages in their technological development. Coal liquefaction (CTL) has the longest history.Hans Tropsch and Franz Fischer developed Fischer-Tropsch (FT) synthesis for coal liquefaction at the Kaiser Wilhelm Institute for Coal Research in Mülheim an der Ruhr in 1925. It declined in importance when petrochemistry began to flourish. South Africa is the only country to use the technology commercially to produce fuels from coal (CTL) and natural gas (GTL), a consequence of its need to cope with embargoes during apartheid. Production started in 1950. Expertise gained during many years' development and use allowed the South African company Sasol to become one of the global technology leaders in CTL and GTL processes. Its Secunda CTL plant built in 1980/84 has a production capacity of 160,000 barrels per day (BPD). Shell is also regarded as one of the international experts. The company has operated a GTL plant producing 14,800 BPD in the Malaysian town of Bintulu since 1993 and its Pearl GTL plant in Qatar producing 260,000 BPD since 2012. A BTL process is being operated in the bioliq pilot plant at the Karlsruhe Institute of Technology (KIT) in Karlsruhe (Eberhard et al. 2018).

All liquid conversion processes are based on the same process principle: during the first step, the raw materials used (coal, natural gas, biomass or hydrogen and CO_2) produce a synthesis gas, a mix between hydrogen (H_2) and carbon monoxide (CO). After the gas is purified, the high-purity synthesis gas is converted into fuel using Fischer-Tropsch synthesis directly or using intermediates such as dimethyl ether, waxes or similar. During the process, the synthesis can be carried out in such a way that custom-made fuels can be produced (optimized chain lengths, without aromatic compounds, sulphur-free).

3.3.10.2 Raw material content

Plants for producing liquid conversion fuels are built using normal steel. In this analysis, the focus is therefore on the catalyst in the Fischer-Tropsch reactor. Group 8 metals such as iron, cobalt, nickel and ruthenium can be used. However, nickel produces too much methane and ruthenium is too expensive for practical use (Dry 2002).

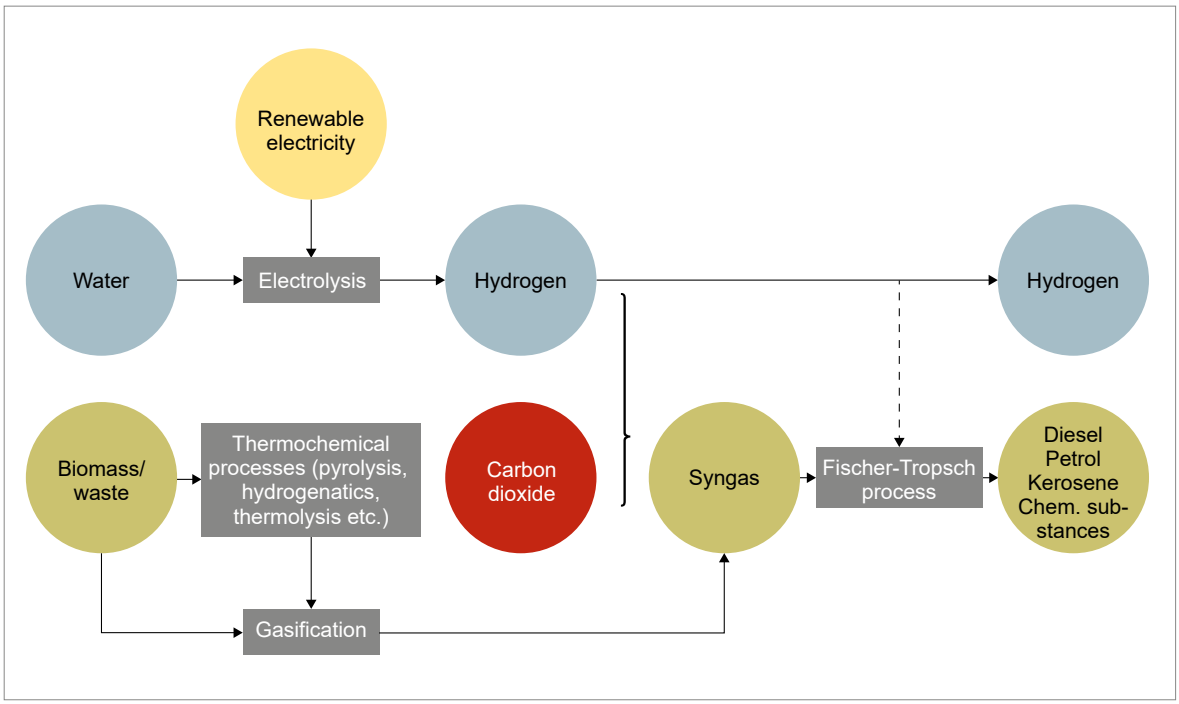

Figure 3.82: Methods of generating PtL (source: Wydra & Schwarz 2021)

Iron and cobalt catalysts are used instead. One advantage of iron is its activity during the water-gas shift reaction (1). The disadvantages are its kinetic hindrance due to the release of water (2) and its low catalytic selectivity.

(1) $CO + H_2O \rightleftharpoons CO_2 + H_2$

(2) $n\ CO + (2\ n + 1)\ H_2 \rightarrow CnH_{2n+2} + n\ H_2O$

Compared to iron, cobalt catalysts become active even at lower temperatures and ensure a longer service life (Dry 2002). Due to their low activity during the reaction (1), cobalt catalysts are particularly suitable for H_2:CO_2 gas compositions to produce the desired alkanes (Klerk 2008). Cobalt catalysts contain low quantities of rhenium or a platinum metal such as platinum, ruthenium, palladium or rhodium as promoters which improve the reduction process and are intended to keep the surface of the cobalt active (Dry 2002). The promoters account for a percentage by mass of less than 1 %. Due to its high price, attempts are made to keep the amount of cobalt in the catalyst low or maximise the available surface of the cobalt. This is achieved by applying cobalt dispersions to frame materials with large surfaces such as aluminium oxide, silicon dioxide or titanium dioxide, or by using specific catalyst geometries (Calderone et al. 2013). The mass fraction of cobalt within the total catalyst weight is a percentage by mass of 20 % (Dry 2002). Table 3.78 lists different compositions.

The specifications for the specific catalyst quantity required for the FT unit varies. The rule of thumb is 100–200 tonnes of cobalt for a 10,000 BPD plant (CDI 2006).

3.3.10.3 Foresight industrial use

The best available technology at present is a large GTL plant producing up to 120,000 BPD. Such plants are too large to use of biomass or electrolysis hydrogen and CO_2 from point sources. Work is being carried out to create smaller plant concepts (Kirsch et al. 2020).

The three SSP scenarios use very different raw materials for synthetic fuel and oil production; see Table 3.79. In SPP1-19 (Sustainability), fossil oil

Table 3.78: Composition of a Fischer-Tropsch catalyst from Johnson Matthey (source: COMBES et al. 2016)

Figures in %	Co	Al	Mg	Ru
Example 1a	17.18	36.86	0.26	0.06
Example 1b	19.58	33.28	2.06	0.06
Reference specimen A	18.26	31.07	4.13	0.5

Table 3.79: Trend in production of synthetic fuels in the various scenarios

XtLs (raw material) [EJ/a]	2020	2030	2040
SSP1-19 (Biomass)	2.18	11.73	19.45
SSP1-19	**2.18**	**11.73**	**19.45**
SSP2-26 (Biomass)	3.58	3.01	7.22
SSP2-26 (Coal)	1.10	2.18	1.62
SSP2-26 (Gas)	0.83	1.77	2.00
SSP2-26	**5.51**	**6.96**	**10.84**
SSP5-Baseline (Biomass)	4.23	3.58	2.35
SSP5-Baseline (Coal)	0.05	1.05	8.78
SSP5-Baseline	**4.28**	**4.63**	**11.12**

products are reduced overall and are replaced by liquid products from biomass (BTL or P2X with the biomass acting as the source of CO_2) from 2020 onwards, meaning more biomass-based fluids will be produced than fossil products by 2060. In SSP2-26 (Middle of the Road), there is also a reduction in liquid fuel consumption from 2040 onwards. Biomass is used but gas is too and also lower quantities of coal will be used until 2060. In the fossil fuelled development scenario SSP5, coal is increasingly being used as a raw material from around 2020 onwards. Around 2090, more coal-based energy sources will be produced than oil-based ones. Publications do not reveal exactly how CTL, GTL and BTL fuels will be produced or what proportion of the hydrogen produced in the scenarios will be used in PTL production (Bauer et al. 2017b).

3.3.10.4 Foresight raw material demand

If it is assumed that there will be linear development of plants built for the total production of the different synthetic fuels, the values for this expansion in 2040 will be between 0.47 and 0.96 EJ energy content in fuels and oils. This corresponds to between 11.2 and 22.9 Mtoe and between 82 and 168 million barrels of oil, which is between 225,400 and 460,500 BPD; see Table 3.80.

According to the aforementioned rule of thumb, around 100–200 tonnes of cobalt are required for a 10,000 BPD plant (CDI 2006). Other sources assume 50 tonnes of cobalt (Brumby et al. 2005). If we assume 100 tonnes, the requirement quantities for 2040 shown in Table 3.81 are based on the

Table 3.80: Cumulative and annual production quantities for XtL in 2040

XtLs 2040	SSP1 Sustainability	SSP2 Middle of the Road	SSP5 Fossil Path
Total production 2040 [EJ/a]	19.45	10.84	11.12
Additional production in 2040 [EJ]	0.96	0.47	0.93
Additional production in 2040 [Mtoe]	22.93	11.21	22.29
Additional production in 2040 [million barrels]	168.07	82.28	162.82
Additional production in barrels per day [bpd]	460,500	225,400	446,100
1 EJ = 23,884,589 toe; 1 toe = 7.33 barrels of oil equivalent (BOE)			

Table 3.81: Global production (BGR 2021) and calculated raw material demand for synthetic fuels, in tonnes

Raw material	Production in 2018	Demand in 2018	Demand foresight for 2040		
			SSP1 Sustainability	SSP2 Middle of the Road	SSP5 Fossil Path
Cobalt	151,060 (M) 126,019 (R)	low	4,600	2,250	4,460
Aluminium	63,756,000 (R)	–	7,600	3,700	7,360
Magnesium	948,963 (R)	–	460	225	450
Ruthenium	33[1] (R)	–	13.8	6.8	13.4

M: Mine production (tonnes of metal content)
R: Refinery production (tonnes of metal content)

[1] *Source: JM 2020*

BPD figures in Table 3.80. These quantities are critical for ruthenium compared to world production in 2018.

Since no sizeable liquid conversion plant was put into operation in 2018, the demand for cobalt was low.

3.3.10.5 Recycling, resource efficiency and substitution

Catalysts are used for about five years and must then be replaced (GÜTTEL et al. 2007; KLERK 2008). Catalysts containing precious metal are treated in advanced recycling processes, during which recovery rates of 97 % and higher are achieved (HASSAN & RICHTER 2002; BRUMBY et al. 2005) and the metals are reused. The indicated service life of GTL and CTL plants is 30 years (IEA ETSAP 2010).

3.4 Cluster: Recycling and water management

3.4.1 Sea water desalination

3.4.1.1 Technology description

On average, sea water is made up of 3.5 % (35 g/kg or 35 000 ppm) salt. Man can tolerate a maximum of 0.5 % (5000 ppm) of salt in drinking water, meaning that unless treated, sea water cannot be used as drinking water. Even more desalination of process water is needed for some industrial plants. According to the International Desalination Association (IDA 2020), there were around 17,000 desalination plants worldwide in 2019. These had a daily capacity of around 107 million m³ and produced around 66.5 million m³ of water a year.

Desalination takes place on an industrial scale using methods perfected by industry, which use 61 % sea water and 21 % brackish water. River water (8 %), waste water (6 %) and even raw water (4 %, for industrial purposes requiring a high water quality) are also treated (JONES et al. 2019).

Thermal and membrane-based methods are used. The most common are (see Figure 3.83):

– MSF method (Multi-Stage-Flash): This method involves heating sea water and vaporising it in several interlinked chambers under ever decreasing levels of pressure and temperature. Fresh sea water is fed through the chambers to the heater in parallel to this. The vapour from the heated sea water settles on the banks of tubes in which the fresh sea water is flowing through the system to the heater (RÖMPP 2020).

– RO (Reverse Osmosis): In reverse osmosis, a pump is used to press water through a semi-permeable membrane, which retains the

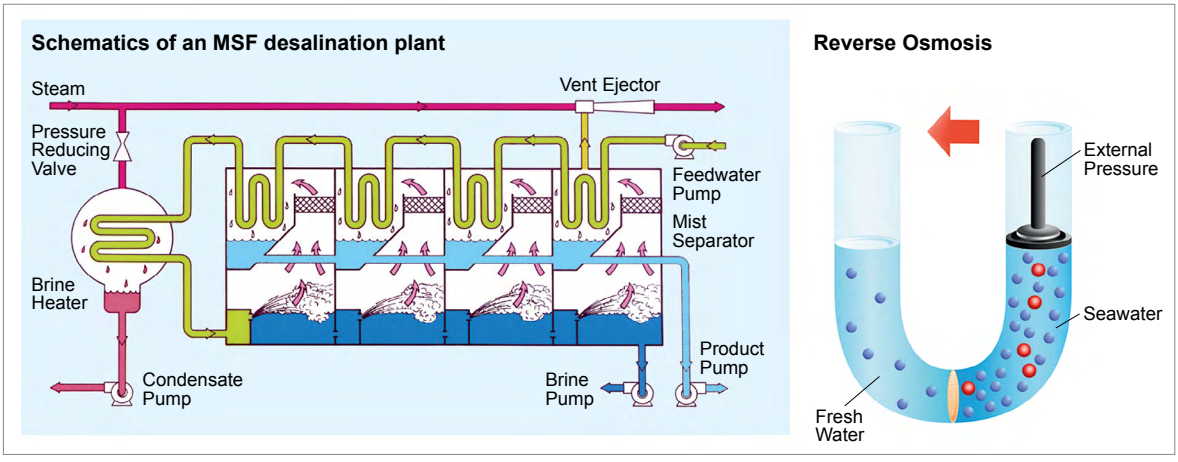

Figure 3.83: Process diagram of the most important sea water desalination methods (sources: left: Sasakura Engineering Co., Ltd, right: shutterstock.com/Designua)

ions of the dissolved substances. The pump pressure must be above the natural osmotic pressure of the water. High-pressure pumps can generate pressure of between 5.4 and 8.2 MPa (54–82 bar). The yield of desalinated water is between 30 and 45 % (RÖMPP 2020).

While the distillation method was the leading technology deployed up until 1995, membrane-based methods have displaced this technology due to lower investment costs, the need for less energy and environmental impacts. Today, around 70 % of all plants use reverse osmosis and only 25 % use thermal methods (JONES et al. 2019), compare Figure 3.84. Other technologies include electrodialysis (ED) and Multi-Effect Distillation (MED).

In principle, the desalination of sea water can also be linked to renewable sources of energy. In April 2020, the United States Department of Energy offered a prize for the development of a technically viable method (DOE 2020).

One potential future method for producing drinking water is capacitive deionisation (CDI). With this method, the ions to be separated can be concentrated into the anode or cathode depending on their charge. This allows salts and metals of interest to commerce to be produced while also generating drinking water.

3.4.1.2 Raw material content

In terms of raw material demand for the desalination of sea water, corrosion-resistant materials, membranes and water chemicals (for anti-fouling, anti-scaling, controlling corrosion) are needed.

The corrosive process environment with its high chloride content and high temperatures places considerable demands on materials. When developing materials, the providers of desalination plants have attempted to keep the corrosion resistance requirements consistent with low investment costs. When desalination was first deployed, the evaporators in Multi-Stage-Flash (MSF) and

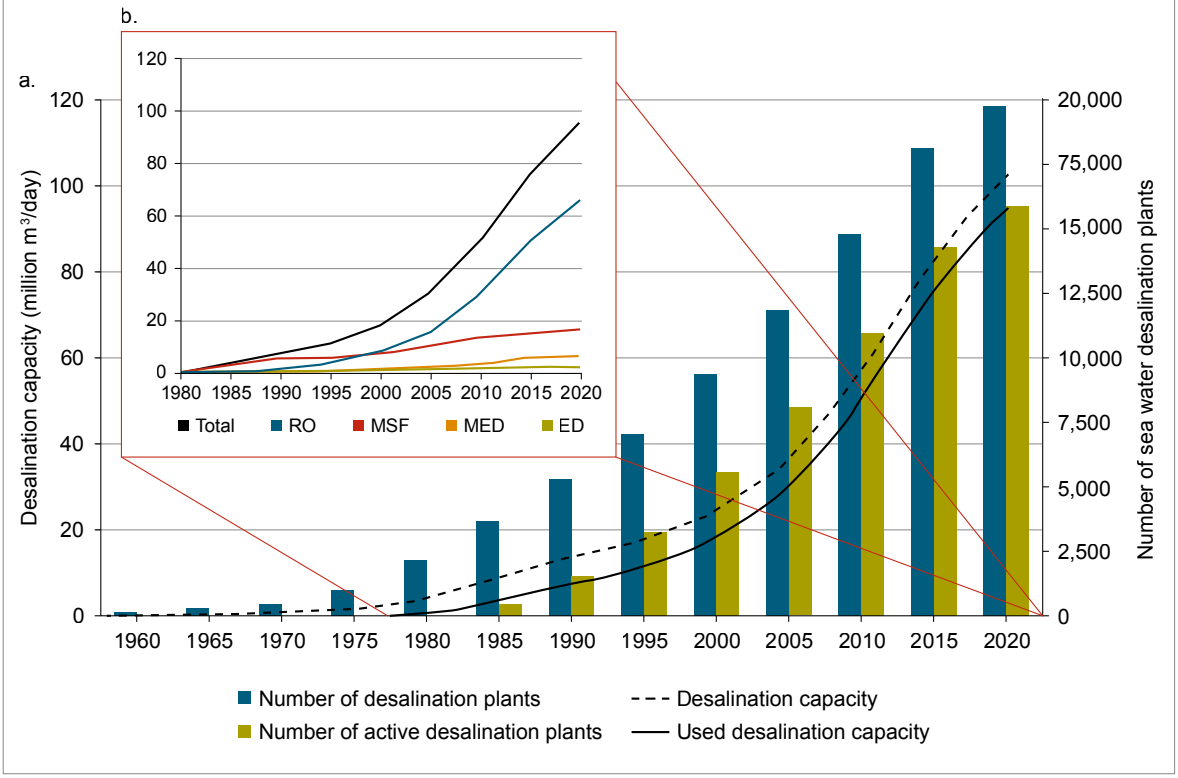

Figure 3.84: Trends in global sea water desalination by (a) number and capacity of all and operational desalination plants and (b) operating capacity by desalination technology (source: JONES et al. 2019)

Multi-Effect (MED) desalination plants were made from construction steel and later on MSF evaporators were typically covered with 316L austenitic stainless steel. MED chambers were initially covered with epoxy and then with stainless steel (IMOA 2014). These have a minimum chromium content of 12 %. The chromium forms a thin passive layer, which seals itself again if damaged.

Duplex stainless steels have mainly be used since 2003. These have a two-phase microstructure, comprising a ferrite matrix with islands made of austenitic phases. This results in higher strength levels – twice as high as with standard austenitic grades – combined with good resistance to corrosion. As a result, duplex stainless steel evaporators can be constructed with thinner panels, which requires less material and less welding work. The breakthrough for the duplex stainless steel concept came in 2003, when duplex stainless steel was chosen as the 2205 grade for solid duplex evaporators, which were to be installed in the Melittah MSF plant and the Zuara MED plant in Libya.

Since 2004, two different kinds of stainless duplex steel have been used in evaporator structures: highly corrosion-resistant 2205 for parts subject to the most severe conditions, and 2304 for parts subject to less harsh conditions. Three MSF plants have been constructed in line with this DualDuplex concept using a combination of 2205 and UNS S32101: Taweelah B (Abu Dhabi), Jebel Ali L2 (Dubai) and Ras Abu Fontas B2 (Qatar) (IMOA 2014).

As the proportion of chromium used increases and nickel and molybdenum are added, resistance to corrosion is yet further improved. The plant manufacturer Outokumpu, for example, uses 4501 quality and SAF 2507® with 25 % chromium, see Table 3.82 (Outokumpu 2020).

Titanium alloys are one basic alternative to steel. The company Allegheny Ludlum uses this, for example. At temperatures below 250 °C and pH values above 1, palladium-alloyed titanium materials are not subject to crevice corrosion. Titanium can mainly be found in the category of thermal

Table 3.82: Materials for sea water desalination plants (source: MatWeb 2020)

Alloy [%]	Cr	Mo	Mn	Cu	Ni	Ti	Al	C	Fe
316	16–18	2–3	≤ 2.0		10–14			≤ 0.08	61.8–72
AK Steel 2205 Duplex Stainless steel	22	3.1			6,0			0.02	68.7
UNS S32101	21.5	0.3	5		1.5			0.03	71.4
Sandvik SAF 2304	21.5–24.5	0.05–0.6	2.5	0.05–0.6	3–5.5			0.03	65.2–71.8
Outokumpu 254 SMO® High Performance Austenitic Stainless Steel	20	6.1			18				55.7
Sandvik SAF 2507 Bar Steel	25	4	≤ 1.2	≤ 0.5	7			≤ 0.03	61.1
Outokumpu 4501 Duplex Stainless Steel (W 0.5 %)	25	3.8		0.5	7			0.02	62.9
Copper nickel 10 %, UNS C70600				88.7	9–11				1–1.8
ATI Allegheny Ludlum Grade 5 Titanium 6Al-4V (UNS R56400) (V 4 %)						90	≤ 6.5	≤ 0.08	≤ 0.03
ATI Allegheny Ludlum Grade 7 Titanium (Pd 0.2 %)						≥ 99.1		≤ 0.1	≤ 0.3

distillation, where it is used for tubes, valves and plate heat exchangers.

For example, titanium tubes were used in the Jebel Ali L sea water desalination plant, where 317,000 cubic metres of drinking water is produced a day from sea water (Thyssen-Krupp 2004). The 160 tonnes of titanium tubes were roll-formed from a strip and welded in an argon inert gas atmosphere. The tube wall is 0.5 millimetres thick and has a diameter of 30 millimetres. The challenge is that the heat exchanger tubes are each 23.4 metres long. For the tubes to remain equally straight over their entire length, they have to be handled with precision when roll-forming and welding and must be supported throughout the production process so that they do not bend. The 160-tonne titanium tubes for Jebel Ali L cover a total distance of 764 km (Thyssen-Krupp 2004).

In contrast, titanium has very limited application in reverse osmosis plants, where it is used mainly in pump heads. The prices for the main materials used for the desalination of sea water have risen sharply, so the development of alternative materials is an important area of research.

90/10 or modified 70/30 copper/nickel is also often used in aggressive operating conditions (Meroufel 2017). Given that there are so many potential materials, we can only provide a very rough estimate of the raw material demand for sea water desalination plants.

The raw material demand for reverse osmosis came from (Raluy et al. 2005), see Table 3.83. 316 L is presumed to be the stainless steel used, see Table 3.82.

On the basis of these values, the results were analysed in terms of demand for special steel and titanium alloy for six thermal sea water desalination plants in order to adapt the raw material demand for the thermal plant.

Details of material consumption were found in the references for six thermal sea water desalination plants (Yebel Ali L, Ras Al-Khair, All Hidd, MARAFIQ plant, Yanbu3 and Az-Zour North). The averages of the six plants are presented in Table 3.84. The demand for 90/10 copper/nickel was not published so we have presumed the same demand as for duplex steel.

Table 3.83: Raw material demand for RO sea water desalination plants (source: Raluy et al. 2005)

Raw material demand (in tonnes/1,000 hm³/year)	Reverse osmosis
Cement	1,240,000
Concrete	130,000
Reinforced concrete	48,750
Iron	650
Steel	87,750
Stainless steel	370
Titanium	–
Sand	65,000
Aromatic polyamides	370
Epoxy resin	23
Polyethylene	16,000

Table 3.84: Raw material demand for thermal sea water desalination plants

Raw material demand (in tonnes/1,000 hm³/year)	Average for thermal plants
Duplex	29,200
Titanium	12,040
Copper	(as duplex)

3.4.1.3 Foresight industrial use

No predictions have been published on how the sea water desalination market will develop in the longer term beyond the year 2027. Market studies assume an annual growth rate (CAGR) of around 9 % (Grand View Research 2020) or 9.5 % (Fisia Italimpianti S.p.A. 2020) for global development up until 2027. With estimated expenditure of $8.6 billion in 2019, the Middle East is the region making the greatest investment in water desalination, however the Asia-Pacific region is home to the highest growth rates of 10 % a year (Fisia Italimpianti S.p.A. 2020). In areas of world where water resources are very scarce, such as Algeria, Libya, Morocco and Egypt, waste water is treated in special purification plants to produce drinking water.

Table 3.85: New sea water desalination plants in 2040

	SSP1 Sustainability	SSP2 Middle of the Road	SSP5 Fossil Path
Capacity [million m³/d]	11.3	7.6	15.5

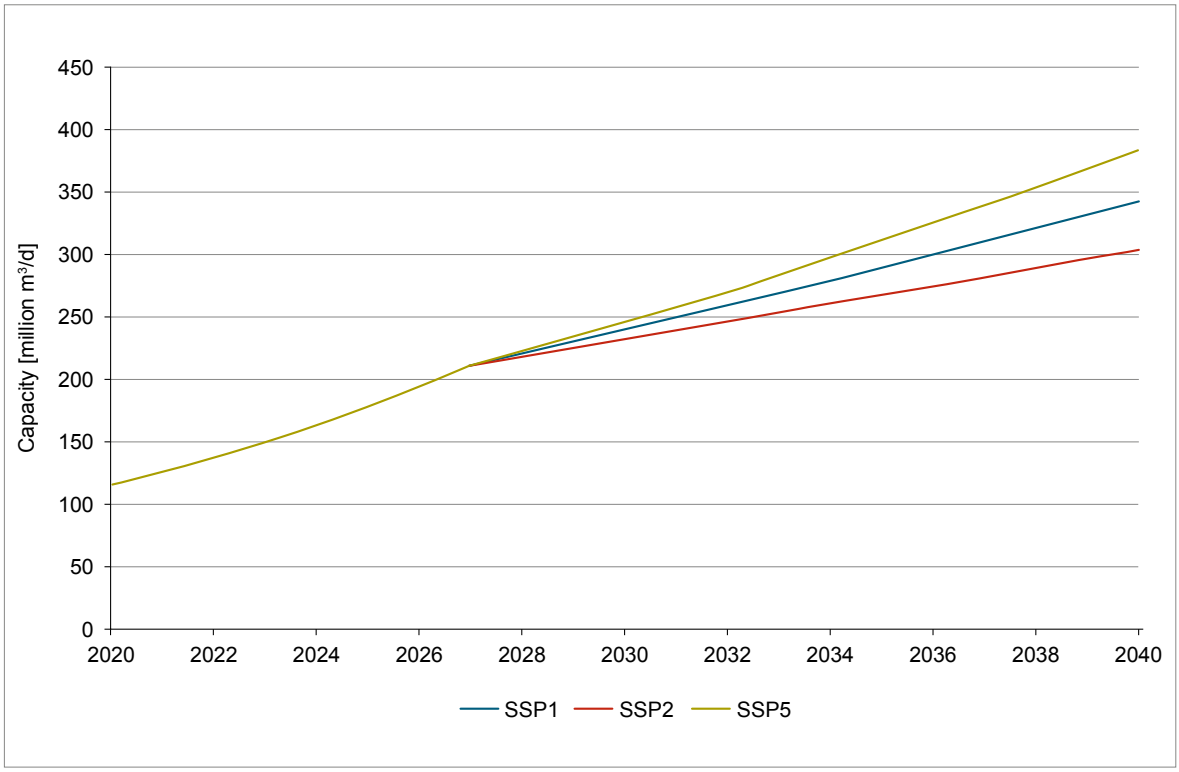

Figure 3.85: Estimated accumulated global desalination of sea water capacity, in million m³/d (source: own representation)

Because the sea water desalination market is also heavily dependent on industrial demand for water, growth of global GDP serves as the basis for estimating the market from 2027 onwards. For the three SSP scenarios, accumulated capacities of 305 (SSP2) to 385 billion m³/d (SSP5) therefore result for the year 2040, see Figure 3.85.

3.4.1.4 Foresight raw material demand

A mixture of 35 % UNS S32101, 35 % 2205 and 30 % 4501 is assumed in order to calculate the raw material demand for duplex steel. For titanium, half grade 5 and half grade 7 is assumed. We have also assumed that the proportion of thermal plants will continue to fall. In 2040, 20 % thermal and 80 % RO plants are anticipated.

Taking these assumptions and the data provided in Table 3.82 to Table 3.85 into account produces an estimated demand for 2040 which can be seen in Table 3.86. The presumed decline in thermal processes results in a decline in the corresponding steels and their metals and in titanium alloys in 2040 for SSP1 and SSP2. In SSP5, this shift to RO is compensated for by greater expansion of capacity. Demand for metals in 2040 is significantly lower than the production volumes for 2018.

3.4.1.5 Recycling, resource efficiency and substitution

The corrosion-resistant materials used in the desalination of sea water are easy to recycle (Outokumpu no date). Given the high growth rates seen in installation figures and the fact that

Table 3.86: Global production (BGR 2021) and calculated raw material demand for sea water desalination, in tonnes

Raw material	Production in 2018	Demand in 2018	Demand foresight for 2040		
			SSP1 Sustainability	SSP2 Middle of the Road	SSP5 Fossil Path
Iron	1,520,000,000 (M)	24,700	20,000	13,300	27,300
Titanium	260,548 (R)	12,500	9,400	6,300	12,900
Chromium	27,000,000 (M)	7,400	5,700	3,800	7,800
Nickel	2,327,500 (M)	4,100	3,200	2,100	4,400
Molybdenum	265,582 (M)	1,100	800	600	1,100
Copper	20,591,000 (M) 24,137,000 (R)	28,400	21,400	14,300	29,300
Manganese	20,300,000 (M)	1,100	800	500	1,100
Aluminium	63,756,000 (R)	400	300	200	410
Vanadium	90,661 (M)	260	200	130	270
Palladium	210 (M)	13	10	7	14

M: Mine production (tonnes of metal content)
R: Refinery production (tonnes of metal content)

the plants have lives in excess of 25 years, recycling will however only reduce the strain on primary raw material markets after a long delay.

Since we expect marked demand stimuli on the raw material markets for titanium metal and palladium, the question of a substitution arises. Palladium or titanium are not necessarily the only materials offering corrosion protection to sea water desalination plants.

3.4.2 Raw material recycling (of plastics)

3.4.2.1 Technology description

Raw material recycling for plastic is understood to mean procedures in which waste polymers are broken down into smaller chemical components. In the best-case scenario, these may be pure monomers, which can in turn be reused for polymerisation. In contrast, when recycling plastics, less energy is needed to sort, clean and reintegrate the materials into plastics processing. However, used plastics are not normally pure enough for the materials to be reused for the same purpose.

In terms of the processes used, a distinction is made between thermal and solvolysis methods. In the latter case, through the application of appropriate reaction conditions, condensation polymers are broken back down into their precursors, as is the case with polyethylene terephthalate (PET). Methanolysis is a catalytic process that employs high-temperature of up to 300 °C and high-pressure methanol of up to 40 bar to recover the raw materials for PET, which is basically the manufacturing process in reverse.

We will only consider thermal processes below because their demand for high-grade steels is greater.

Thermal raw material plastic recycling processes were originally developed in response to the 1973 oil price crisis, limited crude oil reserves, rising demand for plastics and the statutory framework conditions for recycling waste materials (Lechleitner et al. 2020).

Against the backdrop of a major drive to cut CO_2 emissions and reuse carbon in the chemical industry, recycling is again gaining in importance. The aim is to increase use of materials as much as possible because this makes a short cycle pos-

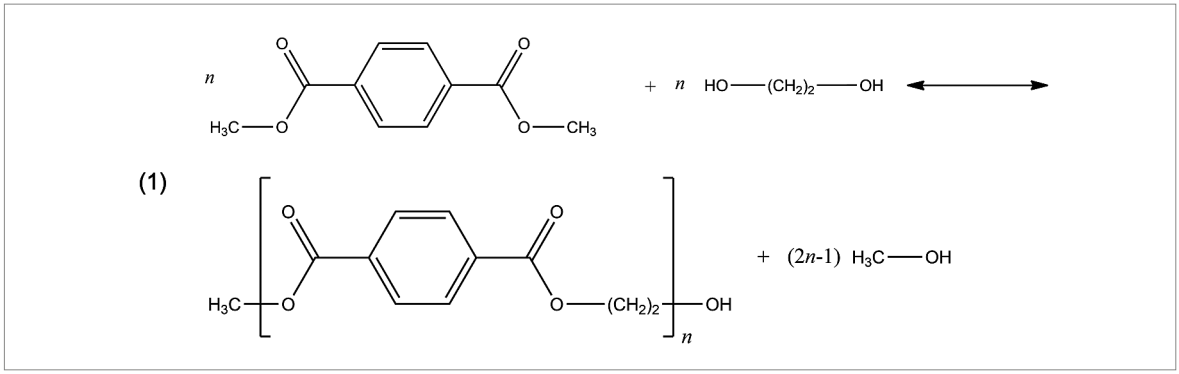

sible and in principle, CO_2 savings are then at their greatest. Where materials cannot be used, recycling should be deployed to recover chemical raw materials, see Figure 3.86. A second reason for why we need to recycle plastics is the fact that of the 359 million tonnes of plastics produced globally in 2018 (PLASTICSEUROPE 2019), a large proportion ended up in the environment where it is having a major impact on flora and fauna (EC 2018; DEUTSCHE UMWELTSTIFTUNG 2020). In 2016, the Ellen MacArthur Foundation published a study indicating that there will be more plastic in the oceans than fish in the year 2050 (ELLEN MACARTHUR FOUNDATION 2016).

A well-documented pyrolysis concept is the Hamburg fluidised-bed pyrolysis process, which is shown in Figure 3.87, where a thermal raw material process is illustrated by way of example. The process was developed in the 1970s at the University of Hamburg and tested between 1984–1988 in a project in a demonstration plant funded by the German Federal Ministry of Education and Research (KAMINSKY et al. 1979; SCHEIRS & KAMINSKY 2016).

This process used various input materials, which were taken into the reactor by an inlet screw conveyor, see Figure 3.87. Oxygen was excluded from the process. The reactor was designed as an

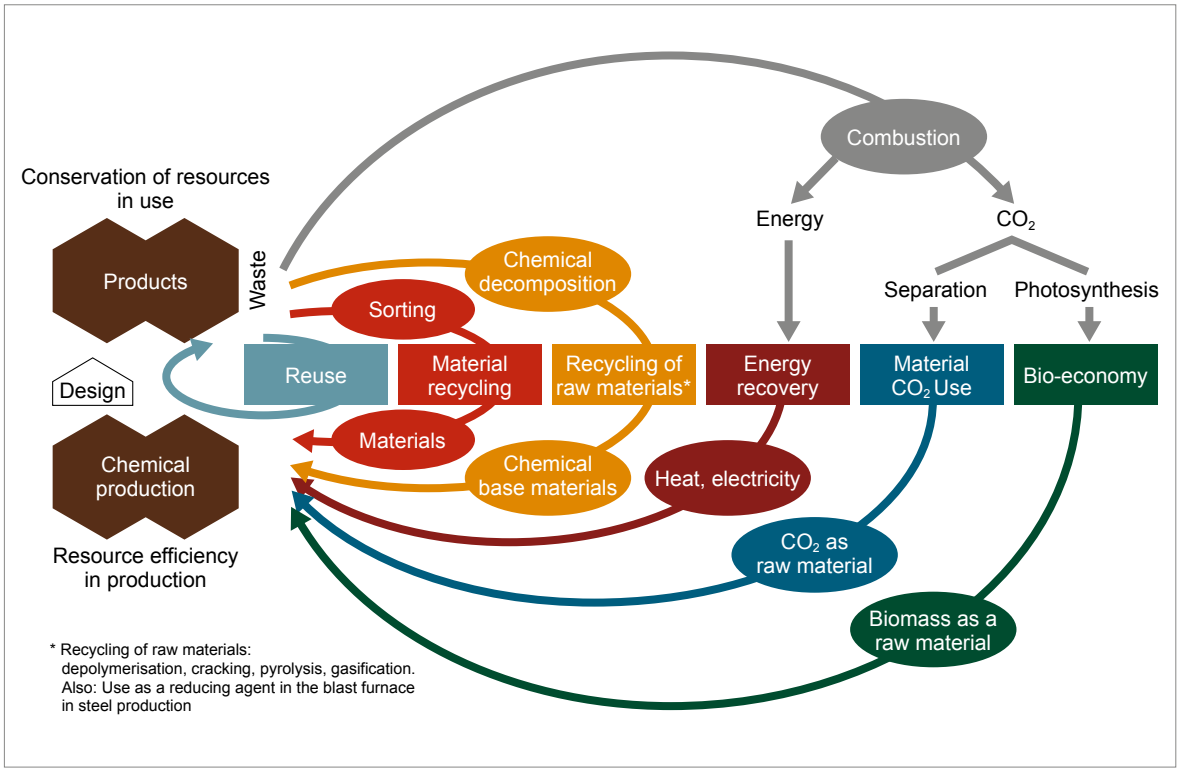

Figure 3.86: Possible cycles for carbon in the chemical industry (source: VCI 2018)

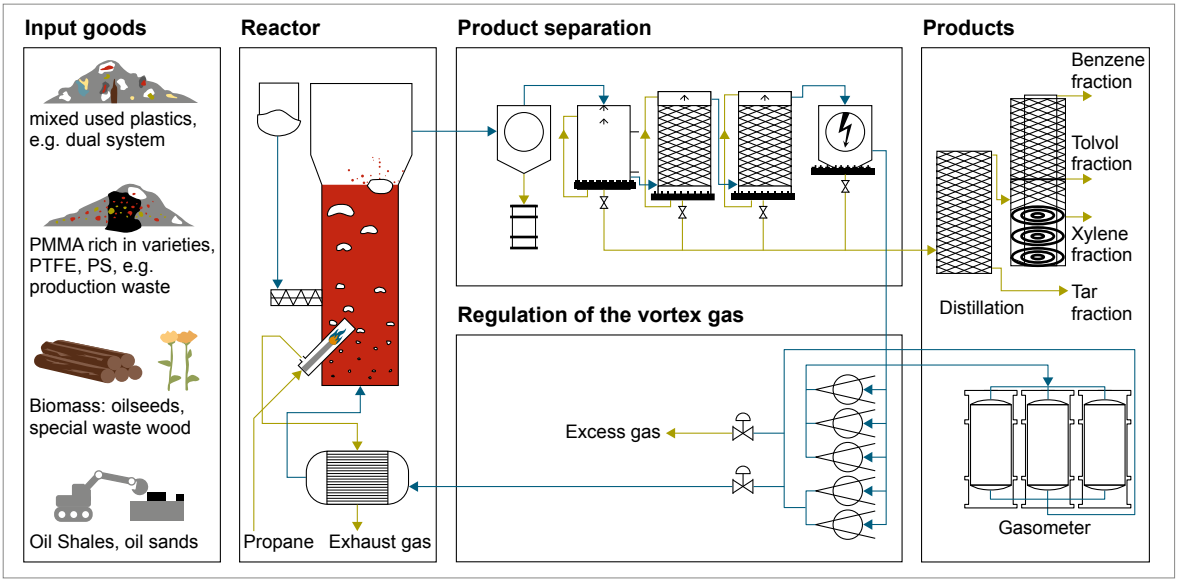

Figure 3.87: Plant schematic of the Hamburg pyrolysis process (source: Universität Hamburg 2012)

indirectly heated quartz sand fluidised bed, operated at temperatures of up to around 800 °C. The fluidising gas used in the circular operation was pyrolysis gas. Any solid matter was removed from the pyrolysis products along with the fluidising gas in a cyclone and the products were then cooled. The pyrolysis oils produced were separated into benzene, toluene, xylene and tar fractions by way of distillation. The pyrolysis gas was quenched with pyrolysis oil and stored in a gasometer before being again used as fluidising gas or heating gas for the jet burners. The main products of the Hamburg fluidised-bed pyrolysis process were the pyrolysis oils, which, depending on the input material and pyrolysis temperature, made up 40–60 % of the products. The other output was pyrolysis gas, which contained not just hydrocarbons but also a high proportion of hydrogen.

Many different variations of processes are used for thermal raw material recycling. Less time spent in the fluidised bed and moderate temperatures produce more fluids while long periods in the bed and high temperatures produce more gases. Rotary furnaces or typical stirrer vessels are also used as the reactors. As well as differ-

Table 3.87: Examples of raw material recycling processes (sources: BASF 2018, Ecoloop 2018, OMV 2018, Petrogas Gas-Systems B.V 2020, Quantafuel 2020, Monreal 2020)

Process	Operator	Feedstock	Capacity [tonnes/year]	Remarks
ReOil	OMV, Schwechat	Plastic waste	800	Used in refinery
BlueAlp™	Petrogas, Eindhoven	Polyolefins	15,000 to 20,000	Planned, plastic to oil
Quantafuel	Skive, DK	Plastic waste	20,000	Use of catalysts, oils at BASF
ChemCycling™	BASF	Oils from Recenso		Use of pyrolysis oil in steam cracker
Plastic Energy	Sevilla, Almeria		5,000	So-called TACOIL for refineries
Ecoloop	Traunstein, Germany	Sorting residue containing plastics	50,000	Updraught gasifier with lime

ent input materials, different target products are also possible and range from synthesis gas and olefins to synthetic oils or waxes, see Table 3.87. References also contain terms such as hydrogenation, gasification, thermal depolymerisation etc. The range of potential products can be expanded through the use of catalysts.

3.4.2.2 Raw material content

It is difficult to assume one specific raw material content for the different types of plants used for thermal raw material recycling. Our forecast is therefore made on the basis of one specific plant currently available on the market. This is the MIDI depolymerisation plant from Modis GmbH, which is able to turn around 6,000 tonnes/year of used plastic into new raw materials in an electrically heated rotary kiln. Steel is needed for the MIDI plant, see Table 3.88.

Table 3.88: Raw material demand for the Modis MIDI plant (source: Modis GmbH 2021)

Materials (plant with a capacity of 6,000 tonnes/year)	Demand in tonnes
Alloyed materials	2
1.4404 steel	15
1.0037 steel	50
Copper cable	3

The composition of the materials can be seen in Table 3.89. Data for alloy 601, a standard material for high-temperature applications, is provided for the alloy material in the rotary kilns (Special Metals 2021).

The data provided in Table 3.88 and Table 3.89 allows us to estimate the specific demand for steel refiners per 6,000 tonnes/year capacity of a thermal raw material plastic recycling plant. The results are displayed in Table 3.90.

While specific material demand is lower for larger plants, for plastic recycling plants in particular it makes more sense to use several smaller plants because it is not energy-efficient to transport the lightweight used plastics long distances without pretreatment.

3.4.2.3 Foresight industrial use

For the reasons stated above, raw material recycling is currently undergoing something of a renaissance (Auel et al. 2020). The way in which it will develop in the future depends on several factors: the extent to which a circular economy with no plastics emissions becomes the norm, whether plastics can be manufactured at net zero and whether consumers continue to accept such an approach.

One study investigated the measures which could be taken to reduce the amount of plastic waste entering the world's oceans (The Pew Charita-

Table 3.89: Materials for pyrolysis plants (source: MatWeb 2020)

Alloy [%]	Al	Cr	Cu	Mo	Mn	Ni	C	Fe
INCONEL® Alloy 601	1–1.7	21–25	≤ 1		≤ 1	58–63	≤ 0.1	13
4404 Cr-Ni-Mo Austenitic Stainless Steel		17.2		2.1		10.1	0.02	70.58
EN 1.0037 High Manganese Carbon Steel					≤ 1.4		≤ 0.17	≥ 98.3

Table 3.90: Specific materials for a pyrolysis plant with a capacity of 6,000 tonnes/year

Metalls	Al	Cr	Cu	Mo	Mn	Ni	C	Fe
Demand in t	0,027	3,04	3,02	0,32	0,72	2,73	0,09	60,00

BLE TRUSTS 2020). In a business-as-usual scenario, this study assumed that the production of plastic will increase to 430 million tonnes by the year 2040. In a system-change scenario, in contrast, it is assumed that 130 million tonnes of this can be eliminated and 71 million tonnes can be substituted by paper etc. Of the remaining 229 million tonnes, 13 million tonnes could be turned into plastics through raw material recycling (P2P chemical recycling-plastic to plastic) and 13 million tonnes could be turned into fuel (P2F-plastic to fuel) (LAU et al. 2020), compare Figure 3.88.

3.4.2.4 Foresight raw material demand

For the various scenarios presented in this report, we assume a capacity of 26 million tonnes for P2P and P2F processes in SSP2 for the year 2040. This corresponds to the system-change scenario shown in Figure 3.88.

The SSP1 scenario assumes that the volume of plastic waste produced by 2040 is reduced to just 200 million tonnes through approaches such as eliminating typical plastics and using “bio plastics”. 11 % of this is recycled, a similar percentage to that assumed in SSP2.

In the SSP5 scenario, only half of all used plastic is recycled, with more being incinerated instead. In order to estimate the raw material recycling capacities in 2040, we have assumed a linear expansion of capacities, see Table 3.91.

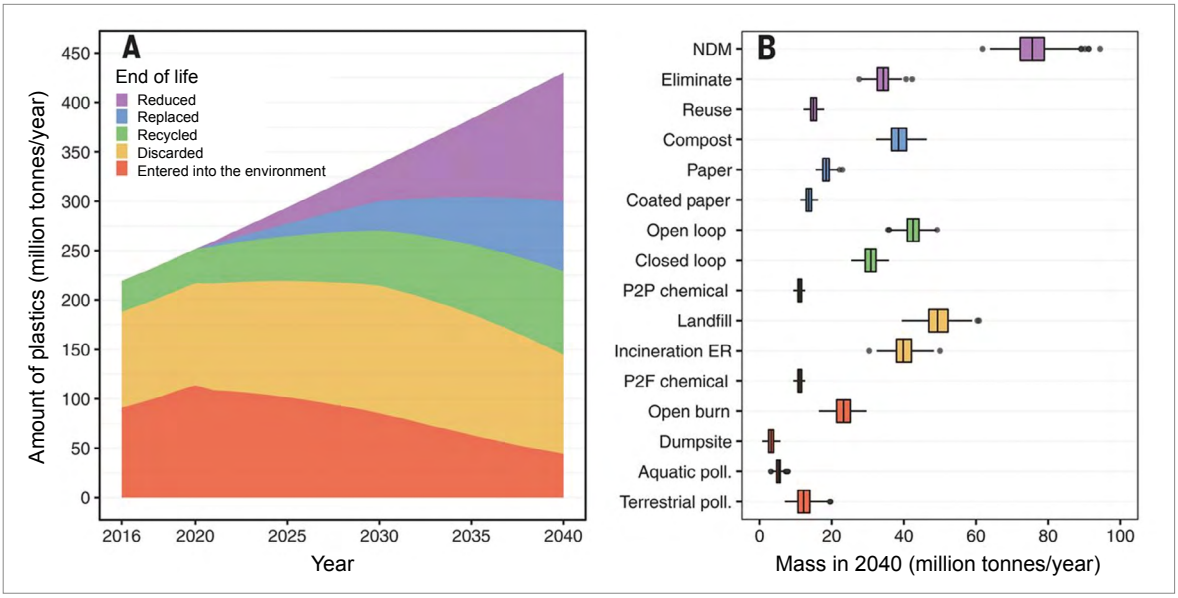

Figure 3.88: Fate of plastics in the system change scenario (source: LAU et al. 2020)

Table 3.91: Assumed amounts of plastic waste for the scenarios, in million tonnes

Figures in million tonnes	Assumptions for 2018	Assumptions for 2040		
		SSP1 Sustainability	SSP2 Middle of the Road	SSP5 Fossil Path
Total plastic waste	230	200	229	229
of which sent to raw material recycling (cumulative)	0.25	21	26	13
Raw material recycling (built in 2040)		3.8	4.9	2.1

Table 3.92: Global production (BGR 2021) and calculated raw material demand for raw material recycling of plastics, in tonnes

Raw material	Production in 2018	Demand in 2018	Demand foresight for 2040		
			SSP1	SSP2	SSP5
Aluminium	63,756,000 (R)	1	17	22	10
Chromium	27,000,000 (M)	127	1,940	2,500	1,080
Copper	20,591,000 (M) 24,137,000 (R)	126	1,930	2,490	1,080
Molybdenum	265,582 (M)	13	200	260	110
Manganese	20,300,000 (M)	30	460	590	260
Nickel	2,327,499 (M) 2,189,313 (R)	114	1.740	2,250	970
Iron	1,520,000,000 (M)	2,500	38,300	49,480	21,370

M: Mine production (tonnes of metal content)
R: Refinery production (tonnes of metal content)

As can be seen in Table 3.92, the plants do not require critical volumes of raw material for raw material recycling.

3.4.2.5 Recycling, resource efficiency and substitution

Industrial plants containing known materials are easy to recycle. Wherever possible, raw material recycling should be substituted by the recycling of materials. As mentioned above, high-quality material recycling is superior to raw material recycling because hydrocarbon bonds do not then have to be destroyed.

3.5 Cluster: Power and data networks

3.5.1 Expansion of the power grid

3.5.1.1 Technology description

Power grids transport and distribute electrical energy from the place of production to the place of consumption. They consist of networks which are nationally and regionally organised and structured, but normally interconnected, and which operate at different voltages. A distinction is made between transmission and distribution networks. Transmission networks allow electrical power to be transported over long distances at very high voltage (in Europe this is usually at 220 kV or 380 kV; in North America and Russia it may also be around 750 kV or up to 1,200 kV). Transmission grids are connected internationally by interconnecting lines that allow power to be imported and exported. Distribution networks handle regional distribution by means of increasingly small structures, from the transmission grid to larger and smaller industrial consumers and, finally, individual homes.As power is distributed through the network the voltage is gradually reduced, such that distribution grids consist of high-, medium- and low-voltage sections. The different voltage levels are connected by substations with transformers (Figure 3.89). It is estimated that the global power grid consists of over 70 million km of power lines, of which more than 90 % form distribution grids (IEA 2021).

Originally, power flowed in one direction from a small number of large producers such as hydroelectric, coal-fired or nuclear power plants, which fed very high-voltage electricity into the transmission grid, to a multitude of larger and smaller consumers, which drew power from the distribution grid in the high- to low-voltage range as required. Today, the growing integration of renewable energy sources is leading to a marked diversification of the electricity market and new demands on the power grid. A large number of different electricity producers, some with fluctuating capacity,

must be integrated at the various voltage levels. The challenges include large offshore wind farms that must be linked by long undersea cables, the electrification of the heat and transport sectors, and a large number of individual homes generating electricity from small roof-mounted photovoltaic systems which is fed into the low-voltage network (IZES gGmbH et al. 2011; Karimi et al. 2016; Protopapadaki & Saelens 2017; Thormann & Kienberger 2020).

Both transmission and distribution networks are normally operated with three-phase alternating current (AC). Single-phase AC is only used in a few cases, for example in rail networks. This is because three-phase operation offers a better ratio of capacity to material requirements (with a 120° phase shift and a symmetrical load, currents in the neutral wire are reduced, which means that this wire can be reduced in size or even dispensed with). However, in recent years and decades high-voltage direct current (HVDC) transmission lines have become increasingly important. The generators in power stations normally generate three-phase AC. Converting the power and transporting it as DC is uneconomical due to the technical effort involved and the losses that occur in rectifiers. However, as transport distances increase, these drawbacks of DC transmission can be offset by the absence of reactive power and lower material requirements (due to the reduction from three to two cables, or even one, and the higher power transport with the same cable diameter). In the case of underground cables this applies

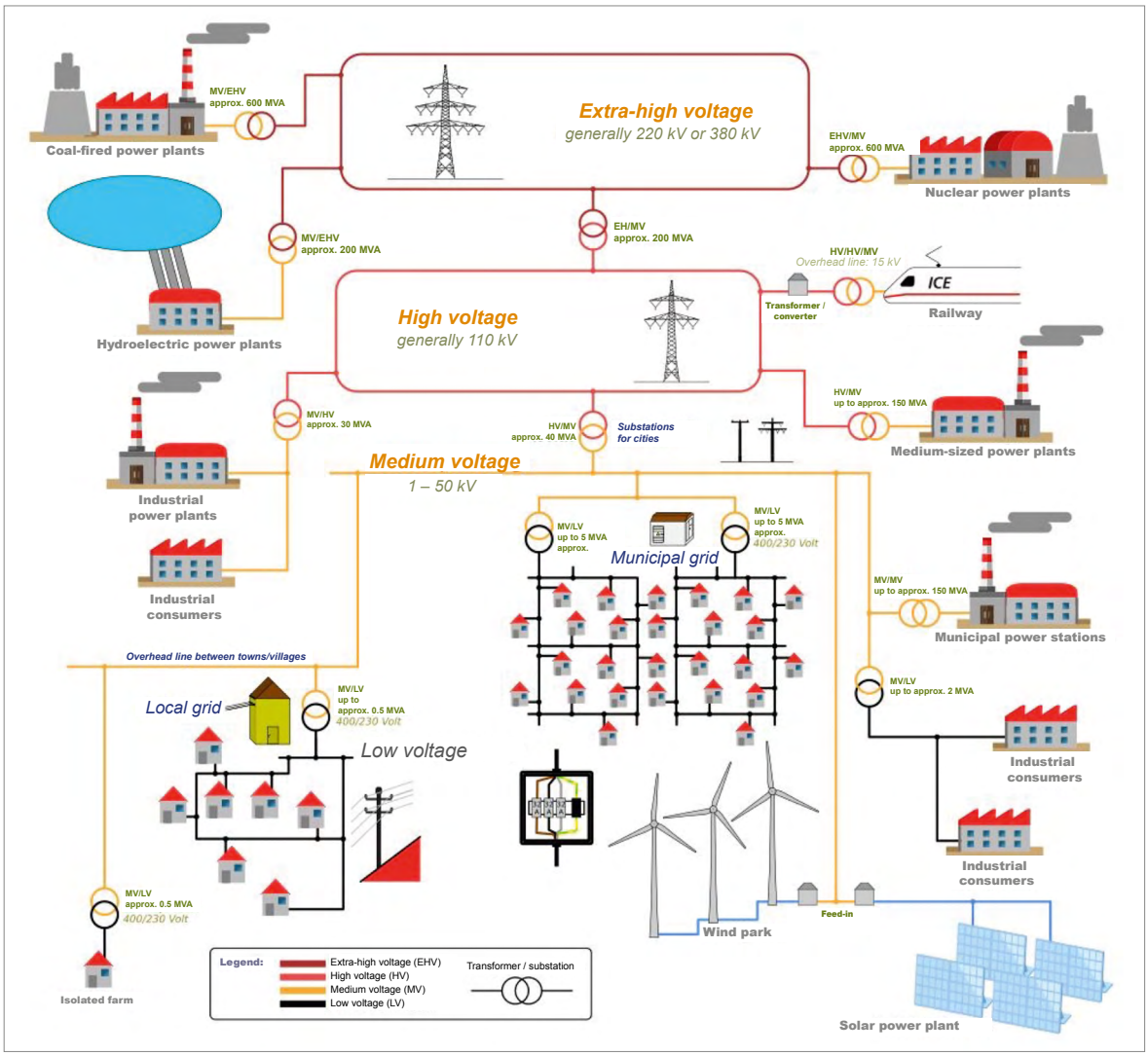

Figure 3.89: Schematic representation of the German power grid (source: Stefan Riepl, CC0, Wikimedia)

from a distance of a few tens of kilometres and in overhead lines from a few hundreds of kilometres. HVDC transmission lines are therefore often used when longer undersea cables are required. This includes connections between national networks, such as the Baltic Cable between Sweden and Germany or BritNed between Great Britain and the Netherlands, and links to offshore wind farms. On land there are lines over 1,000 km long, for example linking the USA and Canada and in DR Congo. But as well as transport over very long distances, HVDC lines can also be used to interconnect AC networks with asynchronous phases. Due to high transmission losses, these short lines are normally taken out of service as soon as AC networks can be synchronised. Unlike AC networks, HVDC lines allow power to flow in both directions in a controllable way, which can be exploited to ensure grid stability (Rudervall et al. 2000; Wietschel et al. 2015; Gellings 2015; Alassi et al. 2019). Although HVDC lines have been in use since the 1950s, their importance has significantly increased and installed line length has tripled in the last ten years (IEA 2021).

Power grids may be constructed by using overhead lines suspended on pylons or by laying underground cables. Both options can be used in all voltage ranges and for both AC and DC power. Underground cabling requires less space, is less vulnerable to external influences (such as weather damage, tampering or manipulation) and generally enjoys higher public acceptance. However, transmission losses through reactive power are higher and there is also more installation work involved than with overhead lines. In Germany there is a continuing trend towards the use of cables. In 2007, underground cables already accounted for a considerable 77.8 % of power lines in Germany, rising to 82.4 % by 2017. Similar figures apply in Austria and Switzerland (FSM, no date; IZES gGmbH et al. 2011; BDEW 2018; Energieallianz Austria GmbH 2019).

3.5.1.2 Raw material content

As explained above, in the construction of power grids a general distinction can be made between overhead lines and underground cables. The raw material requirements vary accordingly.

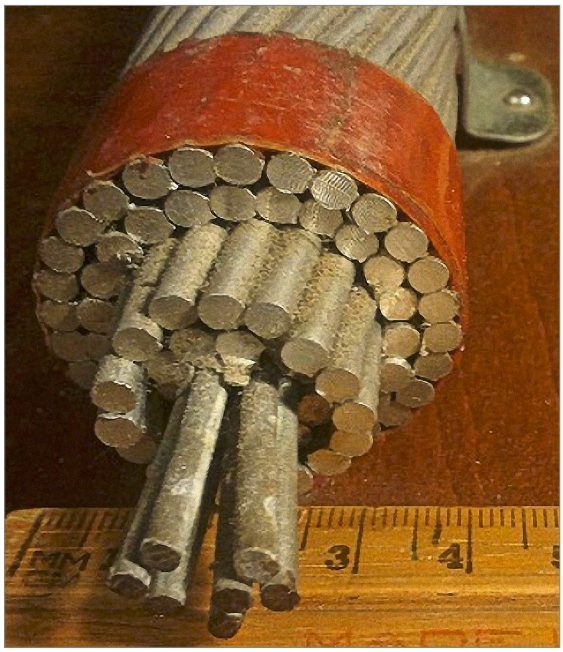

Figure 3.90: Steel-reinforced aluminium cable (source: Clark Mills, Sample cross-section of high tension power (pylon) line.jpg, CC BY-SA 3.0)

Overhead lines

In the case of overhead lines, the conductor ropes are suspended on pylons by means of insulators. Additionally, earth wires or neutral conductors may be used depending on requirements. If necessary a pylon can support multiple power circuits, which in the normal case of 3-phase AC consist of one conductor rope for each phase. Above a voltage of 220 kV, multiple conductor ropes known as bundles are required. Currently, conductor ropes are usually aluminium-conductor steel-reinforced cables (ACSR), in which the aluminium strands are wrapped around a steel core for greater mechanical stability (Figure 3.90). They may also be made of pure aluminium or aluminium alloys with magnesium, silicon and iron (known as Aldrey alloys). Although copper is more conductive, it is not used in standard overhead lines as the smaller material requirement does not compensate for the higher price. This does not apply in the special case of overhead lines on railways. Here, the contact wire is made of copper or low-alloy copper (Mg, Ag, Sn) and the catenary wire of bronze. The insulators are made of plastic, glass, ceramic or porcelain. Pylons are usu-

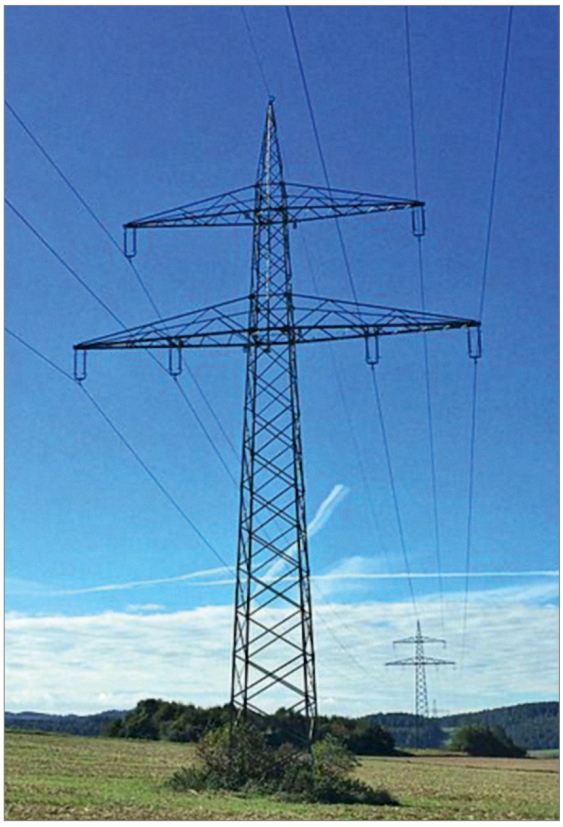

Figure 3.91: Danube pylon' with two 110 kV power circuits (left and right, each with three lines suspended from insulators) and earth wire on top of the pylon (source: Adl252, 110 kV Leitung Borken Lauterbach.jpg, CC BY-SA 4.0)

ally steel lattice structures but may also be made from concrete, wood or composite materials. The type of construction depends on the voltage level and technical requirements, as well as regional conventions and local circumstances. In Germany, steel lattice structures are widely used in high- and extra high-voltage lines. These are usually the types known as 'Danube pylons' with two cross-arms supporting two power circuits as well as an earth wire for earthing and lightning protection on top of the pylon (Figure 3.91). These are spaced 300 m to 500 m apart. In the medium- and low-voltage range in local networks, overhead lines are fairly unusual in Germany. For reasons of safety, avoidance of visual pollution, and public acceptance, extensive use is made of underground cabling. The situation in other countries is different (Amprion GmbH, no date b; Crastan 2015; Hofmann 2015).

Underground lines

Underground cables are mostly used in low- and medium-voltage areas of the power grid. In built-up areas, public acceptance plays a more important role and underground cables enjoy higher acceptance than visible overhead lines despite the considerable work involved in laying them. Underground cables are also protected against damage caused by tampering or the effects of weather, which helps to increase the reliability of energy supply. Together with the added safety of a power line which is inaccessible to the general public, this normally justifies the high costs of cabling incurred as a result of laying and difficult maintenance. In high- and extra high-voltage networks, cables are normally only used when overhead lines are not an option (e.g. undersea cables).

In underground cables, both copper and aluminium conductors are used. Because aluminium requires a larger conductor cross-section, more insulation material is needed for the cable, which cancels out the advantage of the lower price of aluminium. For underground cables carrying low- and medium-voltage power, both aluminium and copper conductors are therefore used. A cable consists of three conductors (3-phase AC) plus a neutral conductor if required. Each conductor may be a single solid wire or multiple wires, encased in an insulating plastic layer (PE, VPE, PVC or EPR). The inner conductor strands are cushioned by a rubber layer, which in turn is surrounded by either a concentric conductor or a copper screen. A plastic jacket (PE) forms the outermost protective layer.

In high- and extra high-voltage cables, only copper conductors are used as the material costs of insulating an aluminium cable would be too high. Each cable also contains just one conductor strand to allow more flexibility in cable laying. In high- and extra high-voltage areas of the grid, cables carrying AC power now also consist of plastic insulation surrounding the conductor, a copper wire screen and an outer plastic sheath. Originally used only in low-voltage areas, plastic insulation has gradually become more commonplace and is now used for voltages up to 500 kV. Due to the higher requirements for the insulating layer, cables that carry DC power still contain mass impregnated paper. The copper conductor

Table 3.93: Material demand per power kilometre for the German power grid (source: Wetzel 2016)

Raw material demand	Distribution grid	Transmission network (underground cables)	Transmission network (overhead lines)
Steel [tonnes/MWkm]	0.8836	0.0392	0.0406
Aluminium [tonnes/MWkm]	0.0276	–	0.0069
Plastic [tonnes/MWkm]	0.0084	0.0038	–
Glass [tonnes/MWkm]	0.0018	–	0.0008
Copper [tonnes/MWkm]	0.0259	0.0310	–
Zinc [tonnes/MWkm]	0.0006	–	0.0009
Lead [tonnes/MWkm]	–	0.0277	–

Table 3.94: Material demand for HVDC overhead lines or cables (source: Wetzel 2016)

Raw material demand	Overhead line 1,000 MW 400 kV	Overhead line 2,200 MW 600 kV	Overhead line 5,000 MW 800 kV	Cable 1,000 MW 400 kV	Cable 2,200 MW 600 kV	Cable 5,000 MV 800 kV
Concrete [tonnes/MWkm]	0.200	0.138	0.040			
Steel [tonnes/MWkm]	0.0508	0.0350	0.0163	0.0480	0.0326	0.0192
Aluminium [tonnes/MWkm]	0.0087	0.0060	0.0035			
Plastic [tonnes/MWkm]				0.0046	0.0031	0.0018
Copper [tonnes/MWkm]				0.0380	0.0258	0.0152
Lead [tonnes/MWkm]				0.0340	0.0231	0.0498

strand is wound in layers of paper saturated in an oil/resin compound which, for high-voltage cables, is also pressurised with gas or oil. The paper insulating layer is enclosed by a lead or aluminium plastic layer and a steel sheath. The outermost layer is a plastic jacket (Amprion GmbH no date; Crastan 2015).

Material composition

Material requirements per power kilometre for the German power grid can be found in Wetzel (2016). These are based on European life cycle analyses for power grid components (May 2005; Jorge et al. 2012a; Jorge et al. 2012b; Jorge & Hertwich 2013; Jorge & Hertwich 2014).

3.5.1.3 Foresight industrial use

Demand for electricity transport and therefore power grids is linked to electricity consumption. This has risen continuously in recent decades: global power consumption has more than doubled since 1990, increasing from 36 EJ or 10,116 TWh to 83 EJ or 23,103 TWh in 2019. A large proportion of this growth is due to rising electricity consumption in Asia (Enerdata 2020). There are three aspects that must be considered in connection with the rise in electricity use: global population growth, increasing per-capita consumption and the growing proportion of the population with access to electricity.

For decades, global electricity consumption per capita has been increasing almost linearly. In 1971 it was 1.2 MWh, increasing to 3.1 MWh by 2014 (World Bank 2014). This is due partly to economic growth and increasing affluence and partly to the growing electrification of our world. This trend is likely to continue or be amplified. Combatting climate change demands the decarbonisation of the world economy, which in many cases is associated with electrification. Prominent examples include the growth of electromobility and the transformation of the heating sector with the large-scale use of heat pumps instead of oil and gas heating (IEA 2020d).

In 2011, the United Nations and the World Bank launched the Sustainable Energy for All (SE4ALL) initiative to ensure that everyone had access to electricity by 2030 (World Bank 2013). Since then, the proportion of the world population with access to electricity has risen from 82 % to almost 90 % in 2019 (World Bank). It is now mainly rural areas, especially in sub-Saharan Africa, that remain unconnected to an electricity supply (Ciller & Lumbreras 2020). It does not always make sense to build a long-distance connection to a major power grid. So-called off-grid solutions are common for the purposes of initial provision, but these too require the basic technology and materials of a power grid. As regional development progresses, connection to or expansion of the grid can take place as a long-term objective.

When these factors are taken together, a significant rise in global electricity consumption may be expected. The magnitude of this growth depends on the assumptions applied in different scenarios; however, the basic trend is the same in all scenarios. Shown here are three SSP scenarios identified by the IPCC (Figure 3.92). Anticipated electricity consumption in 2040 ranges from just under 179 EJ in a heavily fossil-driven development scenario (SSP5) to an initially unchanged 83 EJ in the sustainability scenario (SSP1) (Riahi et al. 2017).

3.5.1.4 Foresight raw material demand

The future raw material demand of the global power grid is difficult to calculate as a whole. Unlike conventional emerging technologies, the power

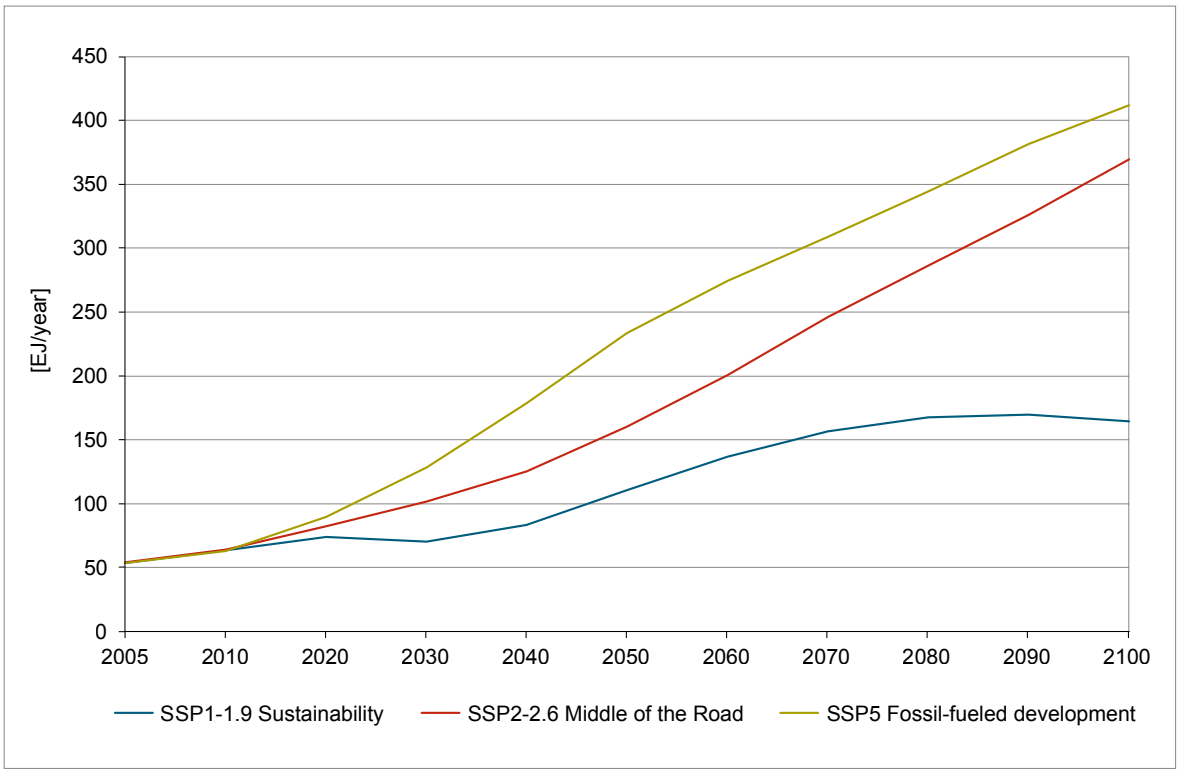

Figure 3.92: Expected demand for electrical energy based on the SSP scenarios of the IPCC (source: Riahi et al. 2017)

Table 3.95: Global production (BGR 2021) and calculated copper demand for transmission and distribution networks, in tonnes

Raw material	Production in 2018	Demand in 2018	Demand foresight for 2040		
			SSP1 Sustainability	SSP2 Middle of the Road	SSP5 Fossil Path
Copper	20,591,000 (M) 24,137,000 (R)	3,825,000	3,832,000	5,759,000	8,211,000

M: Mine production (tonnes of metal content)
R: Refinery production (tonnes of metal content)

grid has already existed as a global infrastructure for over a century. The technological configuration depends on various historical developments and local circumstances. For Europe and Germany somewhat better information is available, with data on grid length and average material content. Extrapolations can be found in Wetzel (2016) for Germany and in Moss et al. (2011) for Europe. At global level, the annual required material volume for replacing and expanding the world's transmission and distribution networks is known for copper (IWCC 2020). This can be used alongside the current annual energy demand (Enerdata 2020) and the forecasts for 2040 from the three SSP scenarios (Figure 3.92) to estimate the demand for copper for power grids in 2040 (Table 3.95). A calculation by the IEA (2021) arrives at similar results, forecasting a copper demand of 7.5 Mt to 10.0 Mt for the expansion and maintenance of global power grids for 2040 depending on the scenario. Demand for aluminium is estimated at 13 Mt to 16 Mt in 2040 for the two IEA scenarios. More detailed assumptions are not made public and so cannot be referred to or used for comparison here.

3.5.1.5 Recycling, resource efficiency and substitution

Recycling systems for components of the power grid are well developed and efficient due to the high material value, ease of collection and known, simple material composition. Copper cables are one of the most valuable sources of secondary copper and are therefore in high demand on the market. The high purity of the copper used in electrical conductors, combined with the ease of separating it from the insulating plastic layer, make it very cost-effective to recover the metal with a high quality. Recycling cables that contain lead is somewhat more difficult, as the lead sheath and any lubricants must first be removed. The quality of the secondary material obtained is somewhat lower. Other copper components, for example in transformers, also have a high material value and can be easily recycled (Langner 2011; Li et al. 2017). A similar situation applies with regard to aluminium, steel and zinc, which are used in large power grid components with a relatively simple material composition and are therefore easy to recycle. Foundation and insulator materials such as concrete, cement, ceramic and glass are however sent to landfill (Jorge et al. 2012a; Jorge et al. 2012b).

There have been various efforts in R&D for some time to optimise the transmission capacity of power grids, which equates to an increase in resource efficiency. Approaches include the use of high-temperature conductor ropes, overhead line monitoring and the use of flexible AC transmission systems (FACTS) and flexible AC distribution systems (FACDS), all of which are intended to make more efficient use of existing network structures. Transmission capacity is limited mainly by operating temperature and sagging of conductor ropes. By modifying the material composition and design of the conductors, the permissible operating temperature has been increased from 80 °C to around 200 °C in high-temperature conductor ropes. Overhead line monitoring allows transmission to be dynamically adjusted through monitoring of the lines and the analysis of weather data, which makes it possible to operate the network at close to capacity limit on a more continuous basis. Similarly, FACTS/FACDS uses power electronics in control and compensation systems in place of conventional variable transformers and static compensators to make grid operation more dynamic and achieve better capacity utilisation (Wietschel et al. 2015).

3.5.2 Fibre-optic cable

3.5.2.1 Technology description

As shown in Figure 3.93, fibre-optic cables are optical waveguides that can transmit light over long distances. Light is a form of electromagnetic radiation and therefore consists of both electrical and magnetic fields. The spatial variation of the electrical and magnetic field strength gives rise to different modes of vibration. The mode of vibration that a waveguide transports depends on its geometry and properties. Fibre-optic cables may be single-mode or multimode. Single-mode cables transmit only one light mode and can cover distances of several hundred kilometres without signal amplification. Multimode cables, on the other hand, transmit multiple light modes, which over long distances results in signal distortion due to interference. However, because they are cheaper than single-mode cables they are the preferred option for shorter transmission distances. Signal distortion in multimode fibres can also be reduced by means of graded-index fibres. Unlike the step-index fibres shown in Figure 3.93, which have an abrupt, step-like transition from one refractive index to the next, with graded-index fibres the refractive index changes gradually.

Light can be transmitted in wavelengths of between 350 nm and 2,500 nm (IR – UV). LEDs or lasers are used as light sources. Fibre-optic cables are, currently, the technically most important type of optical waveguide. There are also optical waveguides based partially or entirely on plastic polymers. These are mostly used for short-distance transmission and play a fairly minor role overall. Optical waveguides are enclosed in a protective coating, for example polyamide, silicone or acrylic, and a sheath (Figure 3.93). One fibre-optic cable may contain many optic fibres (up to 1,000). When stating quantities, it is therefore important to distinguish between cable kilometres and fibre kilometres.

Production

The production of optical fibres starts with a preform, from which fibres are then drawn. The preform of high-purity silica glass (SiO_2) is produced through chemical vapour deposition (CVD) of silicon tetrachloride ($SiCl_4$) and oxygen. The fibres are doped through an analogous process of deposition. This gives the preform the desired refractive index profile, which remains unchanged when the fibres are then drawn in a fibre drawing tower. Immediately after drawing, the outer protective layers are applied and cured (Petermann 2015).

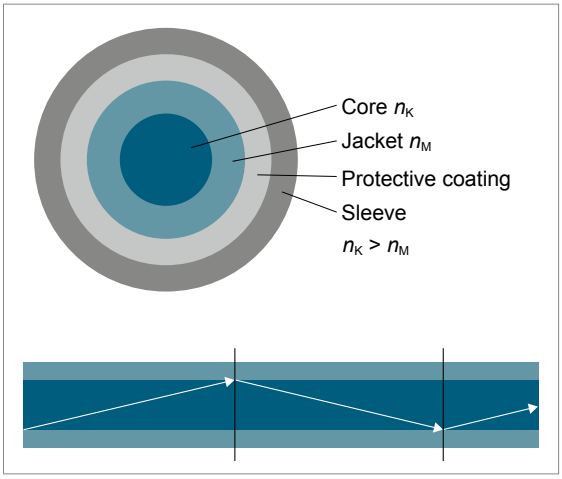

Figure 3.93: Design and working principle of a Fibre-optic cable (source: Fraunhofer ISI)

Note: The refractive index of the core is greater than that of the cladding ($n_K > n_M$), such that total reflection occurs at the boundary when light beams strike it at a shallow enough angle. This allows light to be transmitted through the core over long distances.

Application

Fibre-optic cables are primarily used as a transmission medium in telecommunications. Compared with conventional copper cables, they offer a longer range (up to several hundred kilometres without the need for repeaters) and higher transmission rate (gigabits to terabits).

For this reason, the backbones of modern communication networks, in which high transmission rates are required, consist almost exclusively of fibre-optic cable. Backbones include the core networks of telecommunications companies, cable TV network operators and energy suppliers. Energy companies lay fibre-optic cables together with other lines and operate them to monitor their lines and to rent them to telecommunications companies and cable TV network operators.

Fibre-optic cable is also increasingly being used to connect individual end customers. Different types of connection are named according to the destination, e.g. FTTN (fibre to the neighbourhood/node), FTTH (fibre to the home), FTTB (fibre to the building), FTTP (fibre to the premises), FITH (fibre in the home) and FTTD (fibre to the desk). The greatest obstacle to connections of this type is the cable's susceptibility to bending, which makes additional work necessary during cable laying and can lead to higher failure rates in the event of incorrect use (bending or applying pressure). Fibre-optic cables are also more susceptible to water and dust. In addition, bending will reduce the transmission rate of the fibres. For FTTx applications, special optical fibres have therefore been developed with lower bending losses – for example by adding a fluorine-doped layer at the core-cladding interface or by using nanostructures (Li et al. 2008). As well as telecommunications, optical fibres are used in measuring and medical technology and high-energy lasers.

3.5.2.2 Raw material content

Optical fibres are normally made of amorphous silicon dioxide (SiO_2), also known as silica glass or quartz glass. The refractive index profile is adjusted by doping. To increase the refractive index of the core, it can be doped with germanium dioxide (GeO_2) or phosphorus pentoxide (P_2O_5). The cladding can also be doped with boron or fluorine to reduce its refractive index (Petermann 2015). Normally either the core or the cladding is doped, with the other component consisting of pure SiO_2. Doping generally refers to very low concentrations of 100 ppm (parts per million), i.e. less than one doping atom per 10,000 atoms of the basic material.

The fact that different materials and doping substances are used, as well as the varying number of fibres per cable (100–1,000), makes it difficult to state the average material content per kilometre of cable laid. To estimate germanium demand, the number of kilometres of optical fibres laid per year, or 'fibre kilometres', is therefore more useful.

3.5.2.3 Foresight industrial use

There are several recent market studies on the growth of the optical fibre market. As there is no strict definition of this market, the various studies include different aspects, for example hardware (including cables, controllers and connectors), software and services (Fortune Business Insights 2019), resulting in different market volumes and growth rates. It is not possible to draw direct conclusions about the growth of fibre kilometres and germanium demand from this data:

– (Allied Market Research 2017): Global optical fibre market grows from USD 3,477 million in 2017 to USD 8,153 million in 2025, average annual growth rate (CAGR): 11.6 % from 2018 until 2025.

– (Fortune Business Insights 2019): Global optical fibre market grows from USD 4.48 billion in 2019 to USD 9.73 billion in 2027, CAGR: 10.3 % from 2019 until 2027.

– (Mordor Intelligence 2020a): Global optical fibre market grows from USD 9,236.5 million in 2020 to USD 20,832.6 million in 2026, CAGR: 14.85 % from 2018 until 2026.

– (Maximize Market Research 2020): Global optical fibre market grows from USD 9.38 billion in 2019 to USD 20.9 billion in 2027, CAGR: 11.51 % from 2020 until 2027.

However, these market studies do provide important insights into current trends and the drivers and inhibitors of future demand for fibre-optic cable, which are summarised below. Firstly, linking previously unconnected regions requires further expansion of the fibre-optic network (Allied Market Research 2017). This expansion will also be driven by new technology trends and the associated rising demands on bandwidth, or rather an increase in bandwidth resulting from network expansion will enable new technology trends that exploit this bandwidth; see 1.4 on digitisation scenarios. According to Mordor Intelligence (2020a), over the last ten years the growing fibre-optic network has satisfied the growing demand for bandwidth for Internet, e-commerce, networks and multimedia and will do the same for future technology trends. Further cost reductions in installation, operation and maintenance, as well

as investments in the fibre-optic infrastructure, are identified as key factors in further expansion (Allied Market Research 2017; Fortune Business Insights 2019). The major technological drivers of data transmission and therefore fibre-optic expansion are 5G, the Internet of Things (IoT), cloud computing, big data and FTTx (Allied Market Research 2017; Fortune Business Insights 2019). Although 5G involves wireless transmission, which to some extent is expected to diminish expansion of the cable network to the end user (Allied Market Research 2017), it may also be assumed that overall 5G will result in rising data traffic and therefore higher demands on the data transmission backbone structure (Allied Market Research 2017; Fortune Business Insights 2019; Mordor Intelligence 2020a). However, according to Finch (2020) the demand for fibre-optic cable for 5G provision cannot yet be reliably estimated because the spread of 5G technology is still in the early stages. FTTx connections, on the other hand, are comparatively widespread. In 2019 there were 972 million FTTP (fibre to the premises) or FTTB (fibre to the building) connections worldwide for 1,937 million households (Finch 2020). 481 million of these FTTP or FTTB connections are in China and 153 million in other countries in the Asia-Pacific region. Some European countries (e.g. Norway, Denmark, Sweden, Latvia and Lithuania) already have almost complete coverage with FTTH connections, which allow 4K video streaming, for example (Allied Market Research 2017). Several recent market studies identify the COVID-19 crisis as a growth inhibitor, due to delays and obstacles in production (Fortune Business Insights 2019) or more broadly a weakening of production, the market and financing (Mordor Intelligence 2020a). According to USGS (2021a) the decline in demand for germanium in the USA in 2020 caused by COVID-19 was mitigated by investments in the fibre-optic infrastructure.

The growth trend which had been ongoing since 2004 had already halted before the COVID-19 crisis, with the number of fibre kilometres laid falling in 2019 compared with 2018 (Finch 2020). Figure 3.94 shows data on fibre kilometres laid worldwide per year. The most important driver is the growing global market for broadband access, which has been observed since the early 2000s. Broadband access points create higher demands on data transmission than the previously widespread narrowband access points, with the result that narrowband had only a negligible impact on network expansion after broadband became prevalent; see 1.4 on digitisation scenarios. Since around 2008, fibre-optic expansion in China has had a particular impact on global demand. Between 2008 and 2018, demand for fibre-optic cable in China grew at an average of 21 % (CAGR) per year, resulting in overall growth of 556 % (Finch 2020). Between 2018 and 2019, demand in China then collapsed by a two-figure percentage. In the long term, however, China is expected to invest heavily in fibre-optic cable, as are other countries such as India and Indonesia (Mordor Intelligence 2020a). Consequently, the decline in 2019 cannot yet be

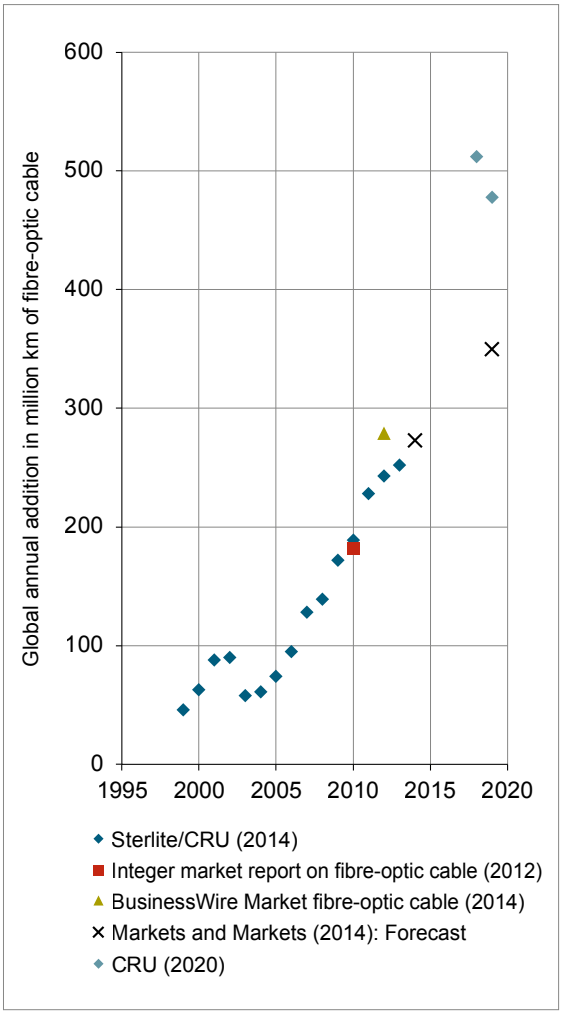

Figure 3.94: Global additional millions of km of fibre-optic cable laid per year (source: own representation based on Eveland 2011, Business Wire 2014, Gomatam 2014, Markets and Markets 2014, Finch 2020)

regarded as a reversal of the trend, and even a temporary drop due to obstacles caused by COVID-19 is unlikely to break the long-term trend towards a globally growing fibre-optic network. If the years prior to the decline in 2003 are included, then the CAGR for the 20 years between 1999 and 2019 is 12.4 %. High growth rates over a long period of time are therefore not unusual for this key infrastructure technology of digitisation and appear plausible for the next 20 years. For comparison, in the 20 years between 1997 and 2017 data traffic grew at a CAGR of 63 %; see 1.4. Between 2003 and 2019, the number of additional fibre kilometres laid per year grew at a CAGR of 14 % (Figure 3.94). Over this period, the growth rates for annual additional construction declined slightly. Between 2003 and 2008 the CAGR was 19 %, falling to 13 % between 2008 and 2013 and then 11 % between 2013 and 2019. Assuming that historical trends continue, it may be assumed that more fibre-optic cables will continue to be laid from year to year, but that the annual growth rate of this development will continue to gradually decrease.

According to StrategyR (2020), demand for germanium for fibre-optic cable will grow between 2020 and 2027 with a CAGR of 6.2 % to reach 90.3 tonnes in 2027. Demand for fibre-optic cable is therefore growing much faster than total demand for germanium, for which StrategyR (2020) predicts a growth from 173.1 tonnes in 2020 to 225.6 tonnes in 2027 (CAGR 3.9 %). These forecasts take the impact of the COVID-19 crisis into account, which means that in the long term, stronger growth is plausible.

In scenario SSP2, in keeping with the framework assumptions, it is assumed that historical trends will continue and the average growth rate between 2027 and 2040 is therefore estimated at CAGR 8 %. In scenario SSP5, however, faster and stronger expansion is anticipated. Previously unconnected areas are connected to the fibre-optic network at a rapid pace as low- and lower-income countries quickly catch up. However, the main growth driver is the steadily growing data transmission resulting from new technological possibilities such as 5G, IoT, cloud computing, AI, streaming and gaming; see above and 1.4. The CAGR is estimated at 9 %. Scenario SSP1 also assumes an acceleration compared with historical trends as regards technological development and catch-up on the part of low- and lower-income countries. In particular, the use of digital technologies for long-term applications in education, health and environmental protection advances rapidly and drives further expansion. However, in SSP1 consumption in high-income countries does not continue to grow unchecked, with streaming, gaming and social media in particular showing saturation in ever higher resolutions, such that further efficiency increases achieved through technical development result partially in actual savings (c.f. 1.4 on digitisation scenarios). For the period between 2027 and 2040, this results in a CAGR of 7.7 %.

3.5.2.4 Foresight raw material demand

Table 3.96 shows the demand for germanium in 2040 arising from the expansion scenarios described above in the various SSPs.

3.5.2.5 Recycling, resource efficiency and substitution

Given the very low concentration of germanium dioxide used in the doping of silica glass, it is difficult to recover germanium from fibre-optic cable. This, combined with the very long lifetime of the

Table 3.96: Global production (BGR 2021) and calculated germanium demand for fibre-optic cable, in tonnes

Raw material [tonnes]	Production in 2018	Demand in 2018	Demand in 2040		
			SSP1 Sustainability	SSP2 Middle of the Road	SSP5 Fossil Path
Germanium	143.1 (R)	59.3	237	246	277

R: Refinery production (tonnes of metal content)

cables and rising demand for them, means that this is not a promising secondary raw material source. However, a possible technique for recovering germanium from fibre-optic cable has been scientifically investigated (Chen et al. 2017b). In total, the USGS quotes a recycling rate of 30 % for germanium, which has been constant for some years, with 60 % of germanium used in electronics manufacturing being production waste or 'new scrap' which is directly reused (USGS 2021a).

3.5.3 5G (6G)

3.5.3.1 Technology description

3.5.3.1.1 Comparison of the capability of 5G and 6G

5G is the fifth generation of the mobile communications network. The term 5G does not refer to a single, clearly defined technology but to a standard that enables software, infrastructure and various technologies to work together to achieve particular targets. 5G is intended to enable 'real-time Internet'. The latency of a data packet is therefore to be reduced to between 1 ms and 10 ms, which requires a very high data transmission and processing speed. While the rollout of 5G has been underway since 2019 and is likely to be largely complete by 2025, the introduction of the next generation 6G is expected to begin in 2030, enabling even shorter latency times and even higher data rates. According to Ndip (2021b), 6G will build on and expand the functions first made possible by 5G. Table 3.97 shows differences between the various generations of mobile communications networks.

5G will enlarge the spectrum of frequencies used for mobile communications into the high-frequency range beyond the 2.6 GHz used for 4G, while 6G will expand into even higher frequency bands. Table 3.98 shows the frequency bands used for 5G and other mobile communications standards in Germany, which are to be used with greater flexibility in future, for 5G and later 6G.

With respect to the frequency bands shown in Table 3.98, it should be noted that both the 5G and 6G frequencies will be used only for communication and other data transfer, not exclusively but in addition to the currently used frequencies. Frequencies freed up from previous mobile communications standards such as 3G will be used for 5G and presumably also for 6G. 5G and 6G

Table 3.97: Comparison of typical latency times and data rates of various generations of mobile communications (sources: 5G-Anbieter 2021, elektroniknet.de 2021, Ndip 2021b)

Generation	2G	3G	4G	5G	6G
Latency (ms)	400 to 500	80 to 400	15 to 80	1 to 10	0.1
Max. data transfer rate (Mbit/s)	0.25	42.2	500	1,000 to 20,000	1,000,000
Time to download 4.5 GB (video)	1 d 16 h	14 min 33 s	1 min 13 s	3.7 s	0.074 s

Table 3.98: Frequency bands used for mobile communications in Germany (sources: Informationszentrum Mobilfunk 2020, LTEmobile 2021, Ndip 2021a)

Generation	2G	3G (UMTS)	4G (LTE)	5G	6G
Frequency bands (GHz)	0.89 to 0.915 0.935 to 0.96 1.71 to 1.785 1.805 to 1.88	1.92 to 1.98 2.11 to 2.17	0.7 0.8 1.8 2.0 2.6	3.4 to 3.7 26 Frequencies made available (e.g. when 3G is switched off)	110 to 170

can therefore be defined in terms of latency and data transfer rates but not in terms of the frequency bands used.

3.5.3.1.2 Network qualities for 5G and 6G and their implementation

According to Freund et al. (2020) and Informationszentrum Mobilfunk (2020), three different areas of application can be distinguished for the 5G network:

1. Ultrafast mobile broadband (Enhanced Mobile Broadband)

2. Communication between machines and applications (Massive Machine Type Communications, M2M)

3. High-reliability network with short response times (Ultra-Reliable and Low Latency Communications)

Freund et al. (2020) and Informationszentrum Mobilfunk (2020) state that the three areas of application are not three separate networks but can be offered through the same 5G-ready network by means of 'network slicing'. This technology splits the available network such that users with different needs can be offered connections with the quality features they require, e.g. with a guaranteed data capacity or latency.

With the help of dynamic spectrum sharing (DSS), the current expansion of communication networks with additional capacities for both 4G and 5G enables fast, demand-based allocation of the frequency bands in a mobile communications antenna between the 4G and 5G standards. For example, if 10 % of users in the mobile communications cell are using a 5G-ready device and 90 % of users a 4G device, then 10 % of the spectrum will be used to supply 5G services and 90 % for 4G/LTE. In principle, DSS works on all frequencies that might conceivably be used for 4G and 5G, allowing network operators to adapt the limited spectrum to actual demand. If the proportion of users with 5G-compatible devices increases, then provision with this newer standard can grow. In a single step, DSS enables operators to expand 5G network coverage while satisfying demand for 4G/LTE. No additional construction measures are normally required, as only existing communications resources are being opened up for the 5G standard (Informationszentrum Mobilfunk 2020).

3.5.3.1.3 Infrastructural requirements

According to (Informationszentrum Mobilfunk 2020, 5G and also 6G, presumably from 2030, will require expansion of the mobile infrastructure and fibre-optic networks (see 3.5.2) to equip base stations with fast connections. Data processing capacity in the base stations will also be increased to avoid long transmission routes to central data centres and to reduce the amount of data that needs to be sent there.

The number and density of base stations will no longer be based primarily on population or user density, but on user requirements in terms of different network qualities and so forth. Smaller networks or 'campus networks' will continue to develop, for example on university campuses and at airports and rail stations, providing spatially limited mobile communications connections. These must be equipped with the necessary transmission and receiving infrastructure, albeit on a smaller scale than networks covering large areas.

Multiple-input, multiple-output (MIMO) technology is already improving the quality and data rate of wireless connections in base stations and end devices for 4G (LTE). Two to eight antenna elements are used on the transmission and the receiving side. For the expansion of 5G and 6G, MIMO antennas are to be equipped with several hundred antenna elements[16], transforming them into 'massive MIMO' (mMIMO) antennas. Each antenna increases the data rate and the number of potential users in a cell.

The elements in a MIMO antenna bundle signals in the approximate direction of the receiver. This 'beamforming' ensures that signals reach their destination with greater accuracy, unlike the almost spherical signal propagation of other antennas.

[16] C.f. T-Systems, https://www.t-systems.com/de/blickwinkel/netze/multiple-input-multiple-output/massive-mimo-800124

3.5.3.1.4 Key technologies for 5G and 6G in relation to critical raw materials

Key technologies and construction elements for 5G and 6G in relation to critical raw materials include:

- Frequency filters with amplifiers based mostly on gallium arsenide (GaAs) for mobile devices and piezoelectric converters based on lithium niobate ($LiNbO_3$) and lithium tantalate ($LiTaO_3$) to make the long-wave high-frequency spectrum that goes beyond the current 4G[17] usable for 5G and later also 6G.
- Amplifiers based on gallium nitride (GaN) for use in base stations
- Photonic components, especially optical transceivers based on indium phosphide (InP), but also those based on GaAs, which are needed for fast signal transmission in base stations and the amplification of optical signals in fibre-optic cables (Tekin 2021). 6G could also operate with InP-based optical components, which use visible light to provide 'visible light communication' (Ndip 2021a).

Optical components are described in more detail in 3.2.3 (Optoelectronics/photonics) and the other components mentioned above in 3.2.5 (Radio frequency microchips).

3.5.3.2 Raw material content

The raw material content of the above-mentioned components is described in 3.2.4.2 (Raw material demand for optoelectronics/photonics) and 3.2.3.2 (Raw material demand for radio frequency microchips).

3.5.3.3 Foresight industrial use

3.5.3.3.1 Frequency filters with amplifiers in RF applications

According to Yole Développement (2020b), mobile ICT devices (mostly mobile phones) accounted for 93 % of the market for GaAs semiconductors entering the RF market. These semiconductors are used in amplifiers in frequency filters for the 3G, 4G, 4G+ and 5G standards, while silicon-based CMOS (complementary metal-oxide-semiconductor) technology is dominant in the 2G domain and is now also used for 3G. Since frequencies previously reserved for 3G as well as 4G frequencies are also to be used for 5G with the help of DSS, it would not be useful to calculate the use of GaAs-based semiconductors only for the new frequencies to be used for 5G and later 6G. The number of filters is increasing due to the expansion of 5G and may be expected to continue rising with 6G, as HF filters will be used in addition to the filters currently used in mobile phones and other mobile devices.

The new frequencies associated with 5G can be divided into the sub-6 GHz frequency band, with GaAs-based amplifiers in the HF filters, and the 'millimetre-wave band' with higher frequencies up to over 28 GHz, for which it has not yet been decided whether the amplifiers in the HF filters should be manufactured with GaAs- or silicon-based semiconductors.

3.5.3.3.2 Optical transceivers

Optical transceivers are used in connection with 5G and 6G in base stations to transmit signals more quickly to (opto)electrical circuits. They play an important role in achieving the short latency times desired in 5G and 6G networks. They are also used as amplifiers in fibre-optic cables. The number of base stations and the amount of fibre-optic cable correlate with the likely future data traffic, which will significantly determine the demand for optical transceivers beyond the expansion phases of 5G and 6G networks.

[17] High-frequency waves have a shorter wavelength than low-frequency waves, in accordance with the equation $c = \lambda \nu$ (c: speed of light; λ: wavelength; ν: frequency); the high frequencies used for 5G and 6G therefore have a longer wavelength ('millimetre waves') than low frequencies.

3.5.3.3.3 GaN-based amplifiers in base stations

In base stations and for campus networks, according to NDIP (2021a), for 5G and 6G GaN semiconductors are used as amplifiers that increase the transmission and receiving power of antenna elements in mMIMO antennas and allow them to be controlled. Two elements are connected to each GaN amplifier, with a range of around 10 m in the high frequencies used for 5G and just 5 m in the even higher frequencies for 6G, which means that the number of base stations will increase further for 6G to achieve the required spatial coverage with the necessary network quality.

As with optical transceivers, future demand for base stations correlates with the likely future data traffic, which will significantly determine the demand for GaN amplifiers beyond the expansion phases of 5G and 6G networks.

3.5.3.4 Foresight raw material demand

The raw material demand described below includes the use of critical resources for both 5G and 6G, which is mostly generated by frequency filters with GaAs-based amplifiers for mobile phones, GaN-based amplifiers for base stations, and InP- and GaAs-based optical transceivers. The corresponding quantities of raw materials are therefore already noted in 3.2.3 (Optoelectronics/photonics) and 3.2.5 (Radio frequency microchips) and in this section they are only summarised again specifically for the new 5G and 6G mobile communications standards.

3.5.3.4.1 Gallium, lithium, niobium and tantalum in frequency filters

According to YOLE DÉVELOPPEMENT (2020b), the demand for frequency filters with GaAs-based amplifiers is largely dependent on the number of mobile phones, as approximately 93 % of these filters are used in such devices. The number of mobile communications connections rose sharply and steadily in the past (STATISTA 2021a), but in the last ten years has shown a considerably reduced growth rate, with little growth since 2019. With approximately 8.2 billion connections, it exceeds the global population of approximately 7.8 billion people (STATISTA 2019b). The growth in connections in recent years has been driven primarily by countries in Asia and Africa. By contrast, in Europe and in North and Latin America the number of mobile communications connections has grown only slowly and saturation has now been reached.

Due to this development of the mobile phone market in recent years and due to the fact that the number of mobile phones considerably exceeds the world's population, it is assumed for the calculations of the raw material demand for GaAs-based amplifiers in mobile phones that the total number of mobile phones will increase with the population growth from 2026 onwards.

For GaAs semiconductors in mobile devices, YOLE DÉVELOPPEMENT (2020b) forecasts an average annual growth of 6 % between 2019 and 2025, prompted primarily by 5G. For the period 2019 to 2025, from sales forecasts for mobile phones of different generations (c.f. p. 111 in YOLE DÉVELOPPEMENT (2020b)) an average annual increase of 81 % was calculated for 5G mobile phones. This growth in 5G mobile phones is therefore behind the 6 % annual increase in GaAs amplifiers.

To calculate the demand for gallium in 2040 in the various scenarios, the Yole forecast was used as a basis for the period 2019 to 2025. On this basis, it is assumed that the different data traffic of the digitisation scenarios SSP1, SSP2 and SSP5 will determine the growth of 5G-capable mobile phones and thus GaAs semiconductors after 2025, when 5G networks are expected to be widely expanded. The following growth rates between 2025 and 2040 were assumed for the individual scenarios:

– SSP5: the share of 5G-enabled mobile phones in mobile phone sales increases by an average of 81 % annually from 2019 to 2025, starting with 19 million units. This continues after 2025 until market saturation, i.e. 100 % of new mobile phones sold are 5G-enabled. According to YOLE DÉVELOPPEMENT (2020b), this growth corresponds to an average annual increase in GaAs amplifiers of 6 %. By introducing 6G from 2030, these

growth rates are repeated, so that from 2039 all mobile phones sold are 6G-capable.

– Alternatively, since the amplifiers can also be manufactured with silicon technology for frequencies above 6 Hz, as of 2030 the growth in 5G/6G mobile phones is only expected to be 0.7 %, corresponding to annual global population growth in this period. The annual increase in GaAs semiconductors in this period is therefore 0.14 %.

– SSP2: After 2025, the proportion of mobile phones sold that are 5G-ready will grow by an average of 40 % per year until market saturation, if this is reached in the relevant periods. As of 2030 the proportion of mobile phones that are 6G-ready, starting at 9.5 million units, is expected to rise by an average of 40 % a year up to the maximum of market saturation.

– Alternatively, it is assumed that as of 2030 further growth will only correspond to global population growth, since 6G-specific frequencies beyond 6 GHz are implemented or integrated in silicon-based technology.

– SSP1: After 2025, the proportion of mobile phones that are 5G-ready will increase by only 0.7 % annually, corresponding to the growth in the global population (Statista 2019b). The introduction of 6G from 2030 to 2036 causes an annual increase of 40 % starting with 9.5 million units, as in SSP2. Thereafter the proportion of these phones will again grow analogously to global population in this period.
The alternative scenario described in SSP2 and SSP5 is also considered here, so that from 2030 continued annual growth in GaAs amplifiers is 0.14 %, resulting from the growth in global population.

Since amplifiers are an integral part of frequency filters as long as the amplifiers are not integrated, the above scenarios are also applied for the trends in demand for lithium, niobium and tantalum in frequency filters, although without the integration scenarios, which are not relevant in this context.

During the production of GaAs semiconductors, according to Clemm et al. (2016), only about 45 % of the gallium used goes into the product. Besides the gallium in the amplifiers, the quantities of gallium that end up in various production waste streams should therefore also be taken into account. According to Clemm et al. (2016), waste containing gallium is treated in recycling processes and gallium is also recovered in the process. However, this statement relates to an investigation at a German manufacturer. It is not known what recycling rates are achieved on a global scale for gallium from production waste. The demand for gallium shown in Table 3.99 therefore represents a worst-case scenario based on the

Table 3.99: Global production (BGR 2021) and calculated raw material demand for GaAs-based amplifiers in frequency filters, in tonnes

Raw material	Production in 2018	Demand in 2018	2040 (no integration)			2040 (with integration)		
			SSP1	SSP2	SSP5	SSP1	SSP2	SSP5
Gallium (total)	413 (R)	38	60	74	90	49	54	54
of which Ga in semiconductors		17	27	33	41	22	24	24
of which Ga in waste (min.)		21	33	41	50	27	30	30
Lithium	95,170 (M)	8	15	18	22	–	–	–
Niobium	68,200 (M)	5	12	15	18	–	–	–
Tantalum	1,832 (M)	194	356	435	531	–	–	–

M: Mine production (tonnes of metals content)
R: Refinery production (tonnes of metals content)

assumption that there is no or only very little recycling of gallium from production waste. Gallium in mobile phones and other electrical products is not recycled. The gallium content in the semiconductors thus represents the “best case” under the assumption that gallium is recycled from the production residues at very high rates and thus hardly any gallium is consumed net via the gallium demand in the GaAs semiconductors. Table 3.99 summarises the demand for gallium in the various scenarios for the year 2040; see also Figure 3.45 in Section 3.2.5.4.

The figures for gallium demand apply on the assumption that amplifiers for the frequencies previously used for 3G and 4G are not integrated on a silicon basis, which would reduce demand for gallium. For 2G this integration has already taken place – which is taken into account in the scenarios above – and for 3G it has already begun.

3.5.3.4.2 Indium and gallium in optical transceivers

The 5G and presumably also the 6G mobile communications standards will require more and faster base stations, which will need dozens of millions of transceivers. The same market trend is anticipated for the InP wafer market as for RF devices (see 3.2.5 Radio frequency microchips), as 5G is the main driver. Yole forecasts an annual growth of 9 % between 2019 and 2024 (Yole Développement 2019a). It is assumed that between 2025 and 2040, the growth in sales of InP wafers will follow the annual growth in mobile Internet data (see 1.4 Digitisation scenarios), proportional to the ratio of 0.3 for the growth in wafer sales and mobile Internet traffic in 2023 and 2024. For further details of the scenarios and how they are calculated, see 3.2.5.4 and 3.2.3.4.

Table 3.100 shows the resulting annual demand for gallium and indium for optical transceivers in 2018 and the predicted demand for 2040.

The amounts of gallium and arsenic are not expected to increase significantly in the future. They remain small compared to the RF market (see 3.2.5 Radio frequency microchips). However, demand for indium, which is essential for photodiodes and laser diodes, will more than triple by 2040. This forecast is based on a worst-case scenario in which InP technology will remain the main platform. Silicon photonics is currently replacing the InP platform to reduce costs and increase performance (see 3.2.3.5, under Substitution). If this trend continues, then demand for indium in 2040 will be lower than forecast.

3.5.3.4.3 Gallium in GaN-based amplifiers for antenna elements in base stations

Table 3.101 shows the demand for gallium for GaN amplifiers in the three SSPs. The calculations are based on the assumption that demand for GaN amplifiers will increase on a par with data volume in the scenarios. The figures given therefore represent a worst-case scenario to the extent that no efficiency increases are included and no increase in resource efficiency, for example through future integration or further miniaturisation. For further details of the calculation, see 3.2.5.

Table 3.100: Global production (BGR 2021) and calculated raw material demand for optical transceivers for 5G/6G, in tonnes

Raw material	Production in 2018	Demand in 2018	Demand foresight for 2040		
			SSP1 Sustainability	SSP2 Middle of the Road	SSP5 Fossil Path
Gallium	413 (R)	1	2	2	2
Arsenic	32,783 (M)	1	2	2	2
Indium	808 (R)	5	35	35	35

M: Mine production (tonnes of As_2O_3 content)
R: Refinery production (tonnes of metals content)

Table 3.101: Demand for gallium in 2040 for GaN amplifiers in base stations

	2040		
	SSP1 Sustainability	**SSP2 Middle of the Road**	**SSP5 Fossil Path**
SiC wafer units	3,810,284	5,216,810	5,734,869
Ga demand for production (kg)	659	902	992
Silicon wafer units	1,129,502	1,546,446	1,700,017
Ga demand for production (kg)	942	1,290	1,418
Total Ga demand (tonnes)	**1.6**	**2.2**	**2.4**

Despite these worst-case assumptions, the maximum demand calculated for 2040 is 2.4 tonnes, which is low given an annual gallium production of 413 tonnes in 2018.

3.5.3.5 Recycling, resource efficiency and substitution

Options for recycling and substitution are only briefly outlined here. For further information see 3.2.3 (Optoelectronics/photonics) and 3.2.5 (Radio frequency microchips).

3.5.3.5.1 Recycling and resource efficiency

Gallium is not currently recycled from old electrical products, either within or outside the EU. The gallium found in the amplifiers of mobile devices is therefore not recovered. The same may be assumed for Ga in the GaN amplifiers of antenna elements in base stations and for In in optical transceivers. The small quantities involved would be disproportionately complex and expensive to recycle, assuming that the task is technically possible at all.

As explained in the previous section, it is not known how much gallium is recycled on a global scale from the waste generated from GaAs semiconductor production. In addition to improvements in the semiconductor manufacturing process to increase the amount of gallium remaining in the product, production waste offers potential for reducing the demand for gallium through recycling. The situation regarding GaN semiconductors and their manufacturing is assumed to be comparable to that for GaAs semiconductors.

Indium in electrical and electronic products is not currently recycled. As the indium content in optical transceivers is low and the relevant parts would need to be separated out for recycling purposes, this situation is unlikely to change for economic and technical reasons. For further information see 3.2.3 (Optoelectronics/photonics) and 3.2.5 (Radio frequency microchips).

3.5.3.5.2 Substitution

Optical transceivers and indium

The market is currently dominated by InP-based transceivers. However, the proportion of silicon-based photonic parts is growing quickly, especially at higher data rates, because complex circuits can be made more compact and transceivers for higher data rates of 400 G and 800 G (G = gigabit/s) can presumably be manufactured more cheaply with this technology. Transceivers with silicon photonics nonetheless require InP lasers, which are integrated in the silicon-based technology (Tekin 2021). However, since the other parts of the transceiver (which would otherwise be solely InP-based) no longer rely on InP, less indium is required for such silicon-based transceivers. For further information, see 3.2.3.5.

Amplifiers for mobile devices and gallium

According to Yole Développement (2020a), amplifiers for the new frequency range for 5G

beyond the current 4G frequencies of up to 6 GHz could be integrated in silicon-based technologies, resulting in at least a marked reduction in demand for gallium. However, this integration cannot be expected until after 2025.

The future standard for frequencies above 6 GHz, which will be used for 5G and then for 6G, has not yet been defined, so it is undecided whether these amplifiers will also be based on GaAs or on silicon technology, which would significantly reduce or entirely avoid an additional need for gallium.

Amplifiers in base stations and gallium

Since the demand for gallium for GaN-based amplifiers proved to be negligible, possibilities for substitution were not investigated further.

3.5.4 Data centres

3.5.4.1 Technology description

Data centres are not a technology in themselves, but highly individual combinations of hardware and software tailored to a particular application. They may incorporate a wide range of different cross-cutting technologies and components, with widely varying designs and rapidly evolving technologies.

Due to the complexity of this area, this study focuses on the main component of data centres, the storage systems. Other key pillars of data centres that could be considered include the overall infrastructure (cooling, power, Internet provision) and the processors. Here, however, rather than providing a sketchy overview of all these areas, it was decided to examine in more detail the storage systems.

Storage systems are an important part of the data centre architecture. As the volumes of data that need to be stored continuously increase, storage is becoming ever more important to the smooth operation of data centres. Three types of storage are currently used: magnetic tape, hard disk drives (HDD) and solid state drives (SSD). Magnetic tape is preferred for long-term storage, archiving and backup. HDD and SSD are the standard types of drive used in data centres.

Magnetic tapes

Magnetic tape is primarily used to store data in tape drives for backup purposes. It consists of a flexible film to which a magnetic coating is applied. Digital data is then stored on the tapes by a process of magnetisation (Lipinski 2015). The magnetic coating consists of iron oxide or chromium oxide (Lipinski 2015); in more recent generations, efforts have been made to switch from barium ferrite to strontium ferrite (Mellor 2020b; Mantel 2020). Previously there were different standards for magnetic tape, but since 2016 only one format – known as Linear Tape-Open (LTO) – has continued in development (Labs 2020a). This open format is developed and maintained by an association of companies consisting of Hewlett Packard Enterprise, IBM Corporation and Quantum Corporation[18]. In 2015, the LTO-7 generation became available; this technology can store up to 15 terabytes (TB) of data per tape in compressed form (Ultrium LTO 2015).

Figure 3.95 shows the development of storage capacities in recent and planned future generations. It can be seen that further significant leaps in tape capacities are expected; in the past, capacity has doubled approximately every 2.3 years (Wesseler 2020). The LTO-9 generation was announced in 2020. The transition from generation 5 to 6 increased the compression rate from 2 to 2.5.

In data centres magnetic tapes are kept in tape libraries, in which a large number of tapes can be stored, automatically searched and fed into a reader (Coyne et al. 2017). Magnetic tape is very energy-efficient as it requires no additional energy between writing data to the tape and retrieving it. Tape should only be re-written up to 200 times, but the data can be stored for up to 30 years (Labs 2020a). This makes it especially useful for archiving and backup copies.

The costs per gigabyte are also only up to a sixth of the costs of HDD and SSD storage (Ultrium

[18] See https://www.lto.org/ (last accessed on 12/02/2021).

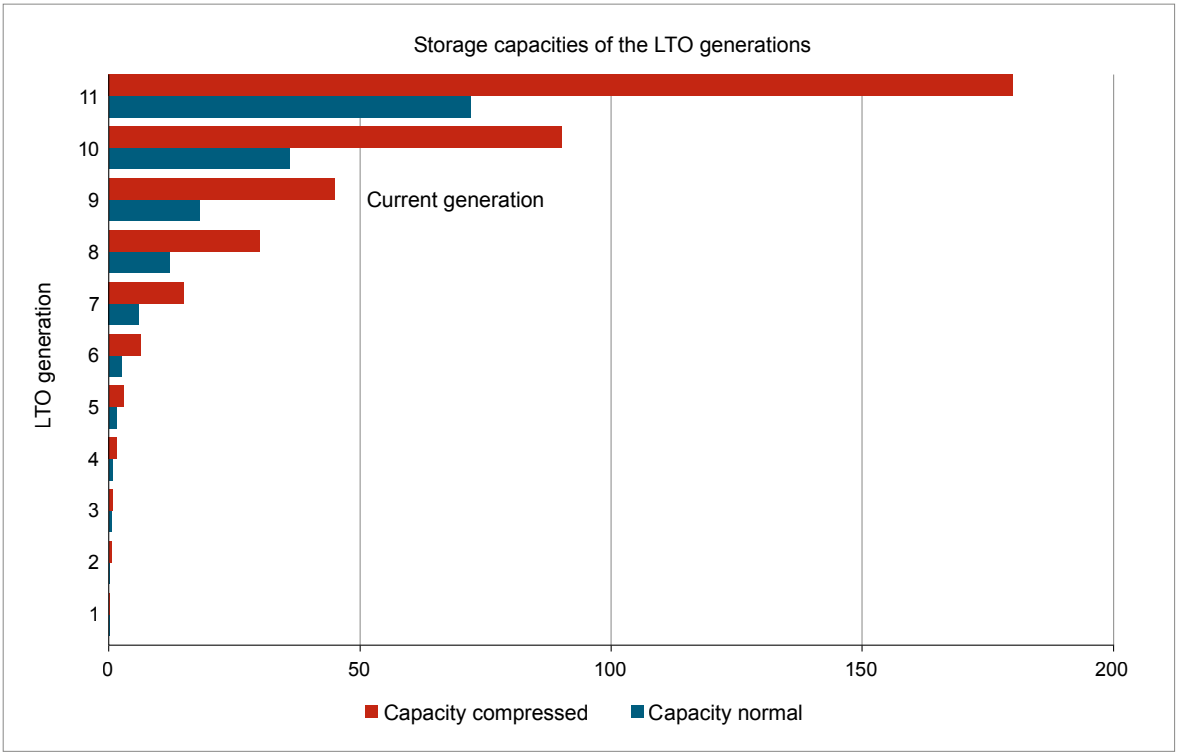

Figure 3.95: Past and planned band capacities of the LTO standard (source: Ultrium LTO 2020)

LTO 2015). For example, one gigabyte of storage on Fujitsu tape costs around USD 0.004 (Ostler 2019). Access speeds are lower, but the error rates of tape are four to five orders of magnitude lower than those of HDD and SSD, which makes them especially attractive as backup media. Magnetic tape is also comparatively secure, since the data stored on a cartridge can only be retrieved when the cartridge is physically placed in a tape drive. This makes it attractive as the final form of backup in a multilevel approach (Lantz 2020). Modern magnetic tapes can store up to 30 TB per cartridge, and there is still active research on tapes with larger storage volumes (Ostler 2019; Mellor 2020b; IBM Knowledge Center 2020). Tape is in widespread use, although there are few concrete figures on the extent of use in data centres. In 2015 a group of tape manufacturers known as the LTO Program stated that 90 % of Fortune 500[19] companies use magnetic tape as one of their data backup options (Ultrium LTO 2015). In its future report, consultancy firm IDC estimates that the amount of data transported on magnetic tapes (worldwide byte shipments) will continue to rise between now and 2025 (from 0.1 zettabyte (ZB) globally in 2018 to just short of 1 ZB in 2025) (Reinsel et al. 2018). It may be assumed that the majority of this data is stored by companies and data centres, as magnetic tape has mostly been pushed out of the consumer market. However, this does not include long-term backup copies, which may represent a much larger amount of data.

Hard disk and solid state drives

HDDs are also magnetic storage media. The housing contains a rotating disk with a magnetic surface that is magnetised when data is written to the disk. Data is read and written with an arm that moves across the disk (Bauer 2018a). These drives are typically 3.5 or 2.5 inches in size. HDDs normally incorporate a neodymium magnet (Linne 2020). The greatest advantage of HDDs is the low cost per gigabyte of stored data, which may be as much as ten times lower than for SSDs (USD 0.03 per GB compared with USD 0.20–0.30 per GB in 2018). This is the main reason that they continue to be frequently installed in data centres (Bauer 2018b).

[19] The Fortune 500 is a list that ranks the 500 US companies with the highest revenues in a given financial year.

SSDs are based on what is known as NAND flash storage technology, in which the individual storage cells are connected in series. SSDs (solid state disks) are electronic semiconductor-based storage media. Because they require no rotating parts, they are more resistant to shock (Bauer 2018a). SSDs are more robust and less prone to mechanical failures, but in terms of gigabytes of data stored they are currently much more expensive than HDDs. Their greatest advantage is the fact that they offer shorter access time and better read and write speeds than HDDs (Linne 2020). SSDs are also usually more energy-efficient (Bauer 2018b). The makeup of the storage media used in a data centre therefore varies depending on the individual application.

At present, most storage in data centres and companies is achieved with HDDs (Reinsel et al. 2018). There are various forecasts of the distribution of data between HDD and SSD over the next 20 years. It may be assumed that SSDs will gradually take over larger and larger shares of the data centre market. Some data analysts believe that HDDs will "soon" only be used in hyperscale data centres that store very large volumes of data, but are reserved about concrete timeframes (van Winkle 2019; Mellor 2020a).

IDC estimates that by 2025, 80 % of company data will still be stored on HDDs (Reinsel et al. 2018). The reason given for this is the low costs involved. However, in 2018 their estimate was over 90 %, with SSDs accounting for most of the change in distribution in this forecast (the rest being split between other NAND storage media).

Seagate estimates that it can maintain the price advantage of HDD over SSD until at least the mid-2030s (Mellor 2019). Coughlin Associates forecasts that the price per GB for HDD will fall to below USD 0.01 by 2024 (Coughlin 2019). Although the price of SSD is also falling, various experts predict that the price per GB for HDD will continue to be cheaper far into the next decade. Ramirez, Senior Director of Product Marketing and Data Center Devices at Western Digital, believes that the price difference will level off at around 6:1 and remain there until at least 2030 (van Winkle 2019). In this scenario HDDs would remain attractive, especially for data centres handling large data volumes.

The company Toshiba announced in 2019 that although SSDs will take over a larger share of the storage market, at the same time the absolute number of SSDs and HDDs will increase because the quantity of data to be stored is rising so rapidly (Kaese 2020). In terms of the raw materials required for storage systems in data centres, the magnets in HDDs therefore play a crucial role.

The most promising developments relating to storage systems are briefly described below.

Trends relating to storage systems

HAMR / MAMR

HAMR (heat-assisted magnetic recording) is a technology designed to increase the capacity of storage media. As data is written to a disk, the surface of the disk is heated by a high-precision laser. HAMR significantly increases the amount of data that can be stored on an HDD. The current maximum capacity is 20 TB, with further increases anticipated in the years ahead (Labs 2020b). HAMR technology is similar to MAMR (microwave-assisted magnetic recording), which exploits a similar principle using microwaves instead of a laser. Western Digital expects to see 40 TB HDDs with MAMR technology in 2025 (Bauer 2018b).

It is likely that the storage capacities of HDDs will increase dramatically over the next several years (Rao 2019), keeping them an attractive cost-effective solution for data centres.

Network interfaces

Over the next several years, new network interfaces are likely to become established in data centres, for example PCIe (Peripheral Component Interconnect Express). This is much faster than the SAS (Serial Attached Small Computer System Interface) often used today (Bauer 2018b).

QLC NAND

In terms of NAND flash memory, including SSDs, QLC NAND (quad-level cell) is a new trend that promises faster and denser SSDs, which could reduce the price per GB (Ramseyer 2018). This

technology can store four bits per physical memory cell, instead of one bit as with SLC (single-level cell) or two bits as with MLC (multi-level cell) (Bauer 2018b).

FLAPE

FLAPE combines flash and tape technologies. It exploits the advantage of rapid (temporary) flash storage combined with the low storage costs and fast writing and streaming speed offered by tape (Schadhauser & Graefen 2016). Numerous articles and publications on this technology appeared in 2016, after which the media resonance faded. In 2016 IBM launched a product series based on this method (IBM Systems 2016).

DNA-based storage technologies

DNA-based storage technology is currently on the threshold between feasibility and scaling up to industrial scale. It is not yet clear whether this threshold will be successfully crossed. The long-term stability of DNA makes it especially interesting as a storage medium. This technology involves converting digital data into adenine (A), cytosine (C), guanine (G) and thymine (T). The resulting DNA strands can be securely stored and read out at a later date.

Takahashi et al. (2019) demonstrated the basic feasibility of writing and reading digital data in artificial DNA strands on a laboratory scale. They stored the word “hello” – 5 bytes of data – in strands of artificial DNA and then read it out again. The write speed was around 21 hours and the read speed six minutes. To make the technology suitable for commercial use, these times would have to be significantly reduced. Other problems include costs and the automation of laboratory tasks (Ryon 2019).

The first application could potentially be long-term data archiving, as the storage density is extremely high. In an experiment to test the basic principle, researchers demonstrated a storage density of 215,000 TB/g, as reported by Erlich & Zielinski (2017). DNA molecules have the advantage of being highly stable, as demonstrated by the presence of intact DNA in archaeological finds. In 2016 the Microsoft team (The AI Blog 2016) achieved a record by storing 200 MB in DNA; the company reports that it has since stored 1 GB of data.

3.5.4.2 Foresight industrial use

For this study, three basic scenarios were developed on the basis of the Shared Socioeconomic Pathways (SSPs) (Fricko et al. 2017); see Section 1.4 on digitisation scenarios. To adapt these scenarios specifically for data centres, firstly a set of assumptions were made about the development of the global data volume in data centres and overall. These are based, among others, on the IDC Global DataSphere report (Reinsel et al. 2018) and the Cisco Global Cloud Index 2015–2020 (Cisco 2016).

For the scenarios, the three relevant storage technologies – magnetic tape, SSDs and HDDs – were identified. After an in-depth source study, assumptions were made about the development of each technology in data centres in the three scenarios. A redundancy factor was also included to represent the additional consumption of resources for failover protection.

The most favourable scenario (SSP1) is based on the assumption that the increase in data volume will be comparatively small while the increase in the efficiency of storage technologies is comparatively high, resulting in lower overall resource consumption.

The most resource-intensive scenario (SSP5) is based on the opposite assumption – that the global data volume in data centres will rise at a relatively high rate and the efficiency of storage media will rise at a much lower rate than in the most resource-efficient scenario. This scenario is therefore much more resource-intensive than the most favourable scenario.

The assumptions made in the baseline scenario (SSP2) fall between these two extremes.

Trend in total data volume in data centres

To calculate the total amount of data stored in data centres at the relevant points in time, the Cisco Global Cloud Index 2015–2020 (Cisco 2016) was used as a basis. Figure 3.96 shows various growth

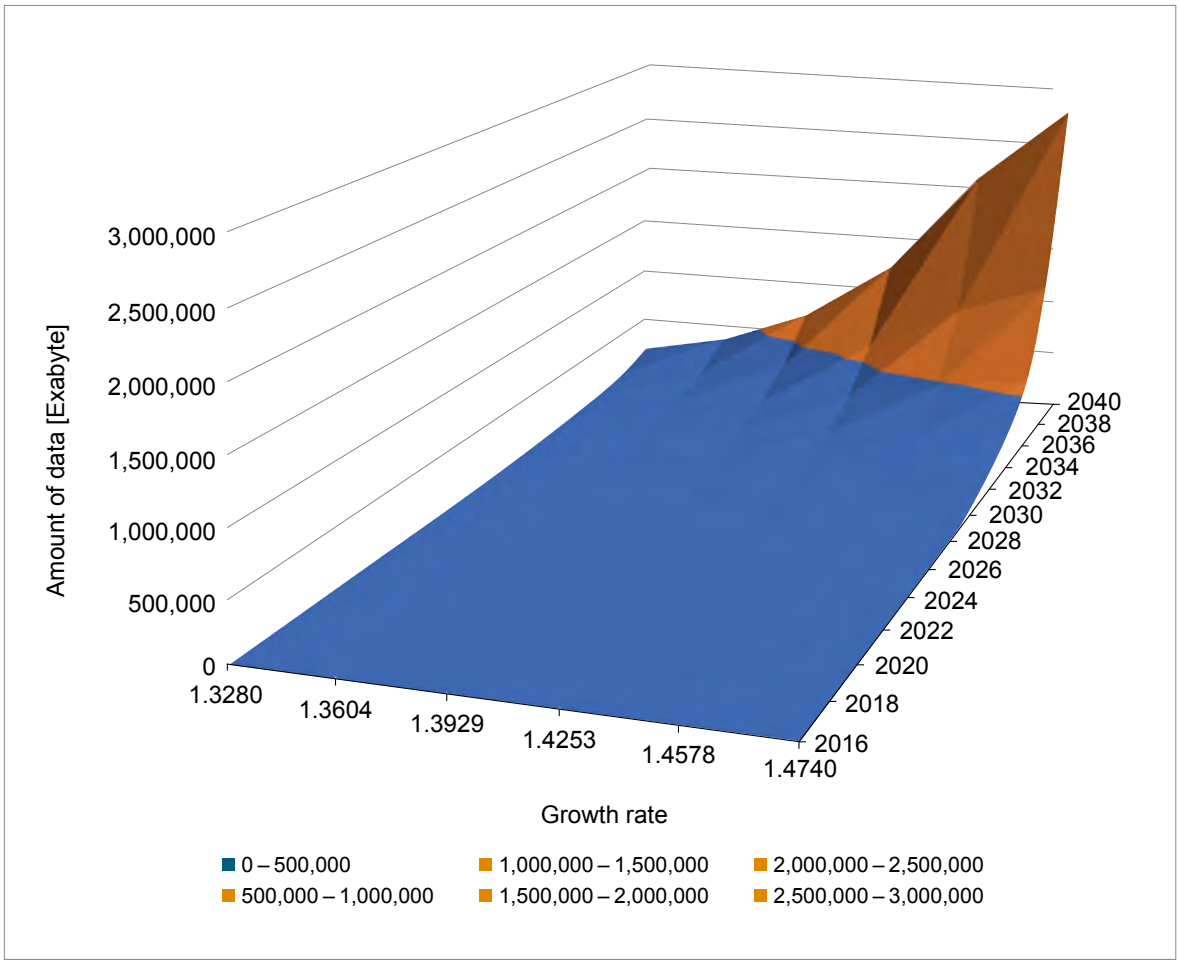

Figure 3.96: Various data growth scenarios until 2040 (source: own representation)

rates to 2040, all of which are within the rates considered for the scenarios. As can be clearly seen here, the figures in two decades' time are difficult to forecast due to exponential growth and deviations are immense. In the diagram, the area in which the calculated data volume for higher growth rates climbs into different orders of magnitude is shown in red. Nevertheless, a model was developed which, given the circumstances, shows a wide variation in potential outcomes in three scenarios.

From this forecast, three basic scenarios were identified for the development of data centres between now and 2040. The starting point was the data volume given by Cisco of 171 exabytes of data in 2015. Firstly a base growth rate was calculated using the least-squares method. The maximum and minimum growth rates were also calculated for the period examined in the Cisco study. The following scenarios were identified:

– **Baseline scenario (SSP2):**
  • The growth rate of 39 % calculated with the least-squares method continues until 2040.
– **Most resource-efficient scenario (SSP1):**
  • For the scenario with the lowest increase in data, the minimum growth rate for the Cisco data was calculated and applied up to the year 2040.
  • Minimum growth rate: 32 %
– **Most resource-intensive scenario (SSP5):**
  • Here, the maximum growth rate in the Cisco study of 47 % per year was applied.

To verify the validity of these growth rates, the IDC's Data Age 2025 report was also examined (Reinsel et al. 2018). This report forecasts the growth of the global datasphere between 2015 and 2025. Here too, the average growth and trend line were calculated. At 31 %, the average growth rate is similar to the Cisco data. Figure

3.97 shows a comparison of the estimated data volumes in the three scenarios for the years 2018 and 2040 in zettabytes. It can be clearly seen that, as expected, the differences in data volumes are still very small in 2018 but vast in 2040 due to exponential growth. In the most resource-efficient scenario, the estimated amount of data in data centres in 2040 is over 90 % lower than in the most resource-intensive scenario.

Storage medium quantities

The development of scenarios for the required storage medium quantities up to 2020 was divided into stages. Firstly, the three relevant technologies were identified and deployed for these growth forecasts. A 'drive type' factor was then determined to establish the distribution of the total required storage capacity between the various technologies. Finally, a redundancy factor was defined. Since sources from manufacturers only describe the most recent developments, the predicted developments were not applied to the scenarios directly but with a two-year delay, since it is assumed that by this time new developments will have reached data centres.

The relevant technologies are HDD, SSD and magnetic tape. Technological advances in storage media normally occur in leaps, making an annual analysis difficult. However, it is assumed that growth rates in storage capacity resulting from technology leaps can be described in terms of an average in the given annual growth rates.

HDD hard drives

The three scenarios for an increase in HDD storage capacity are based on various press releases from manufacturers which are judged to play a key role in the direction of development:

– **Baseline scenario:** According to a Seagate press release in 2017, the launch of HAMR and HDMR technologies can be expected to produce an annual growth of 30 % (Seagate Blog 2017).

– **Most resource-efficient scenario:** The most optimistic press release describes a doubling of the storage capacity of HDDs every 2.5 years, or an annual growth of approximately 35 %. This was used as the most resource-efficient scenario (Mellor 2018).

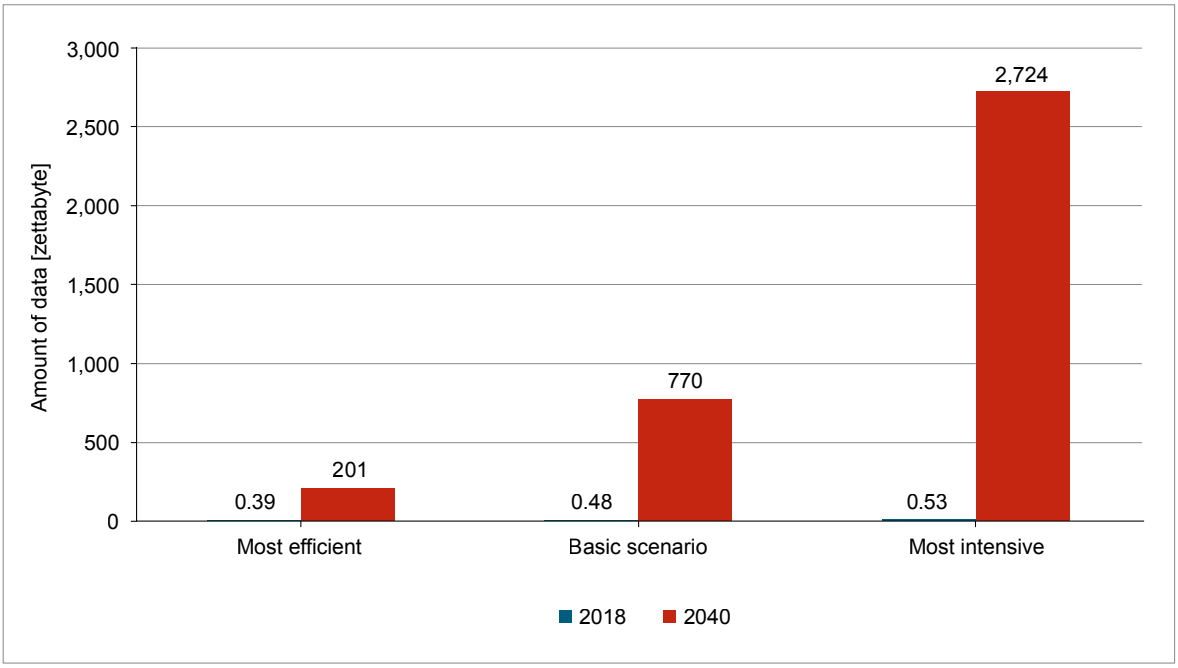

Figure 3.97: Comparison of data volumes in the various scenarios, 2018 and 2040 (source: own representation)

– **Most resource-intensive scenario:** This scenario is based on the assumption that the growth rates mentioned above are missed by a large margin and that the annual growth in storage capacity is only 10 %.

Figure 3.98 shows the results of these scenarios. As can be clearly seen, the exponential growth of capacities favours large differences in results by 2040.

SSD hard drives

The assumptions about the improvement in SSD storage capacity are based primarily on reports by Google at USENIX (The Advanced Systems Computing Association), with the extraction of data points and the extrapolation of growth factors (USENIX Association 2016; USENIX Association 2020).

– **Baseline scenario:** The capacity of SSDs increases by around 40 % per year.

– **Most resource-efficient scenario:** The capacity of SSDs increases by 65 % per year.

– **Most resource-intensive scenario:** The capacity of SSDs increases by 20 % per year.

Figure 3.99 shows the results of these scenarios. As can be clearly seen, the exponential growth of capacities once again favours large differences in results by 2040.

Magnetic tapes

The assumptions relating to magnetic tape are based on an estimate by Fujifilm on the development of tape over the next several years. In the source, a change of technology is anticipated every two to three years (Mellor 2020b).

– **Baseline scenario:** Here it is assumed that the next LTO technology will arrive on the market every three years and that no further development will take place after the announced version LTO-14 (in this scenario, in 2035).

– **Most resource-efficient scenario:** Here it is assumed that the next LTO technology will be developed every two years and developed continuously until 2040. This would result in LTO-19 by 2040, so LTO-18 is used for the calculation.

– **Most resource-intensive scenario:** Assumes that even the baseline scenario cannot be sustained and that LTO-14 will not appear on the market until 2040. Due to the

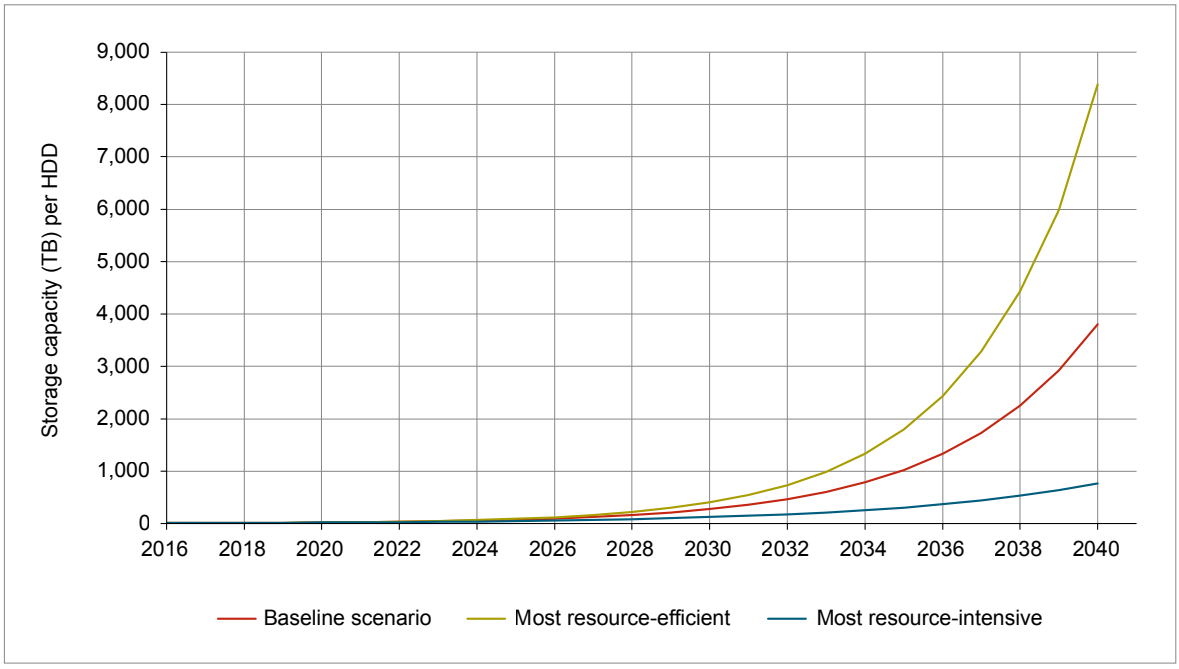

Figure 3.98: Comparison of scenarios for HDDs (source: own representation)

delay, LTO-13 is considered for this scenario. A new LTO technology would appear on the market every four years.

Figure 3.100 shows the results of these scenarios. As can be clearly seen, the exponential growth of capacities favours large differences in results by 2040. In contrast to HDD and SSD technologies, the capacity increase for magnetic tape advances in very noticeable leaps, resulting in the plateaus shown in the diagram.

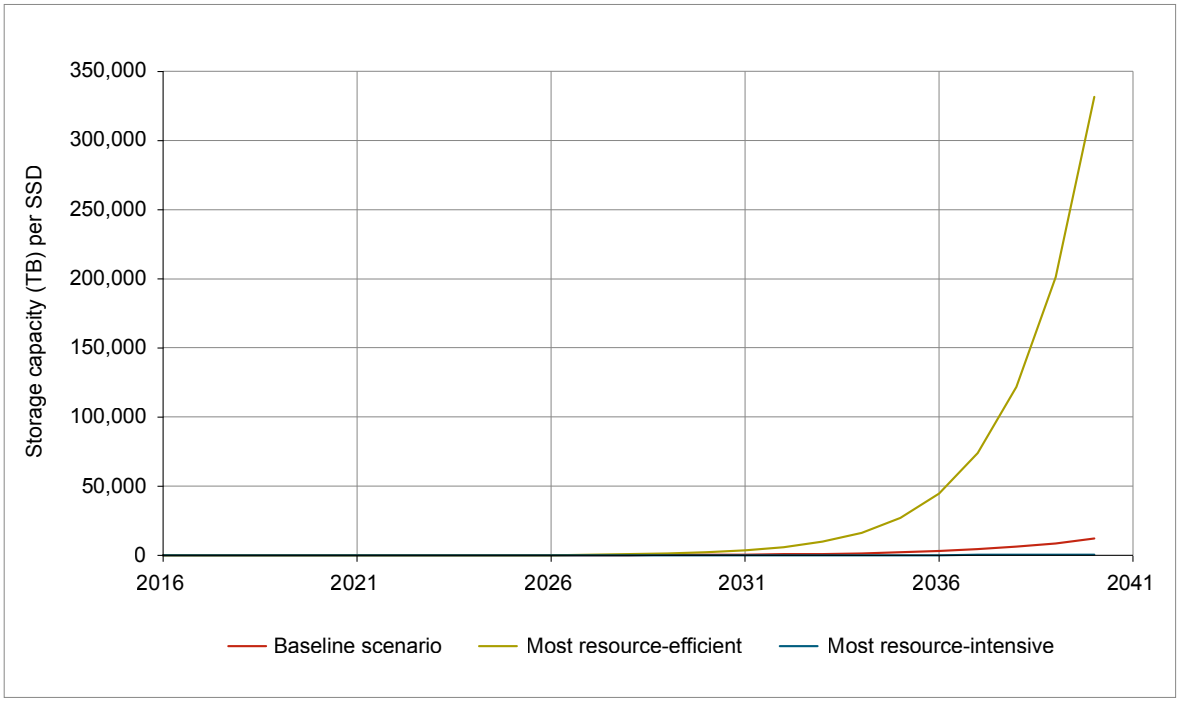

Figure 3.99: Comparison of scenarios for SSDs (source: own representation)

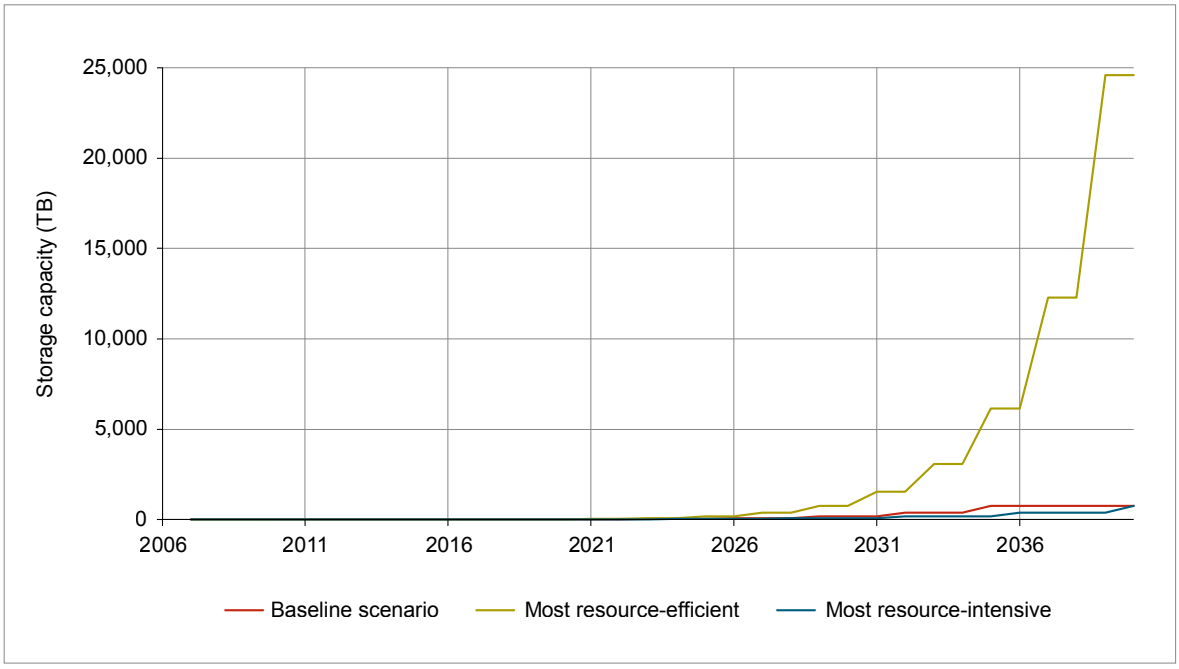

Figure 3.100: Comparison of scenarios for magnetic tape (source: own representation)

Storage medium distribution factor

The distribution of data volumes between different storage technologies is crucial to future raw material requirements. To create a predictive model, the percentage distribution of storage capacities in a data centre was combined with the global distribution. It was assumed that the quantity of magnetic tape given for the global distribution by Reinsel et al. (2018) is destined exclusively for data centres. Since a shift towards SSD in data centre storage dynamics has been predicted and has been foreseeable in recent years, this has also been represented (Plankers 2015; Viaud 2019; Mellor 2020a). Figure 3.101 shows the storage medium distribution factor for the three main storage media in 2018 and 2040. Figure 3.102 shows the overall distribution of storage media for 2018 and 2040. A clear proportional increase can be seen for SSD.

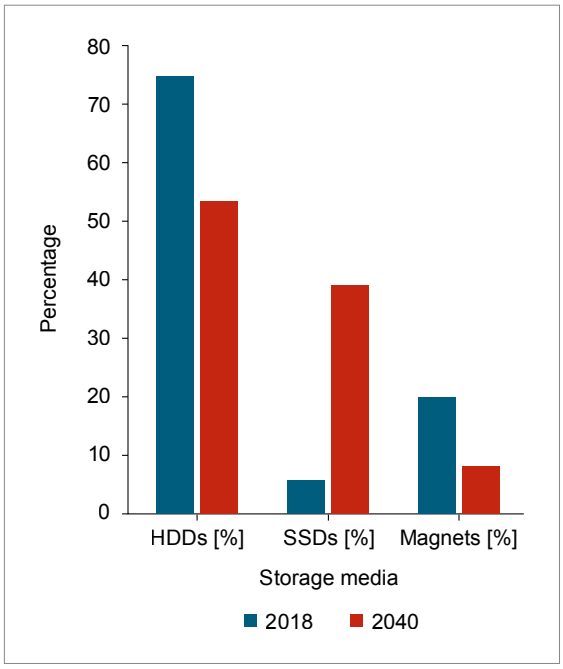

Figure 3.101: Distribution of storage media in 2018 and 2040 (source: own representation)

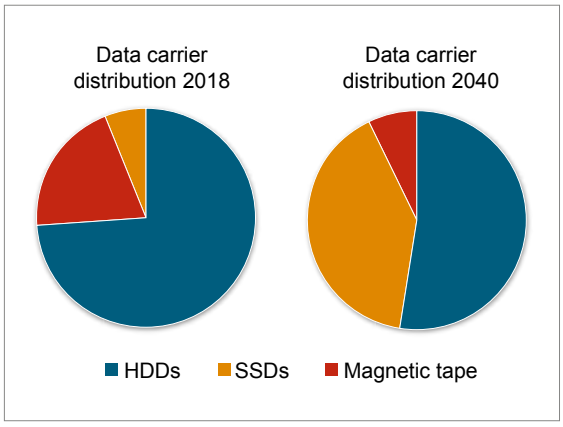

Figure 3.102: Overall distribution of storage media in 2018 and 2040 (source: own representation)

Redundancy factor

Since reliability and availability are important economic factors for data centres, they often operate with a high level of component redundancy to avoid outages. Since actual data on the redundancy factor of real data centres is difficult to obtain, a redundancy factor of 2 was assumed for all three scenarios. The resources required in the previous model are therefore doubled. In terms of possible redundancy factors, 2 (or 2N) is a defensive value that allows for high additional resource requirements. This assumption was made because data storage is one of the most important elements in a data centre and the failure of a data medium could quickly result in irreversible data loss (Allen 2014). However, since the redundancy factor is only incorporated linearly in the model (the data media being doubled), it does not have an significant impact on the forecasts compared with other factors such as data volume growth and increase in storage capacity, which are exponential.

Complete scenarios

From the partial scenarios outlined above three complete scenarios were developed, which are combined below. The drive type factors and redundancy remain the same for all three scenarios:

– **Most resource-efficient scenario:**
  - This is the scenario in which the smallest amount of resources is used, since a low increase in data volume and a high increase in storage capacity result in less data having to be stored than in the other scenarios.
  - The amount of global data in data centres is growing at a rate of 32 % per year.

Table 3.102: Number of storage media by scenario

Raw material	Volume in 2018			Forecast for 2040		
	SSP1	SSP2	SSP5	SSP1	SSP2	SSP5
Data carriers (million units, rounded)	109	134	149	71	602	26,339
HDDs (million units, rounded)	60	73	82	49	372	5,555
SSDs (million units, rounded)	23	28	31	1.3	187	19,596
Magnetic tapes (million units, rounded)	27	33	36	21	44	1,188

  - Storage media:
    Annual growth of 35 % is assumed for HDD hard drives.
    For SSD hard drives, annual growth by a factor of 1.65 is assumed.
    For magnetic tape, the technology develops continuously to LTO-18 by 2040, which corresponds to around 13 petabytes of data per tape.

– **Baseline scenario:**
  - In this scenario fewer resources are used than in scenario 3, but more than in scenario 1.
  - The amount of global data in data centres is growing at a rate of 39 % per year.
  - Storage media:
    Annual growth of 30 % is assumed for HDD hard drives. For SSD hard drives, annual growth by a factor of 1.4 is assumed. Magnetic tape technology develops to LTO-14, corresponding to around 800 TB of data storage per tape.

– **Most resource-intensive scenario:**
  - This is the scenario in which the largest amount of resources is used, since a high increase in data volume and a low increase in storage capacity result in more data having to be stored than in the other scenarios.
  - The amount of global data in data centres is growing at a rate of 47 % per year.
  - Storage media:
    Annual growth of 10 % is assumed for HDD hard drives. For SSD hard drives, annual growth by a factor of 1.2 is assumed. For magnetic tape, development ends at LTO-13 with just under 400 TB.

These scenarios produce the results in Table 3.102. As can be seen, the exponential growth in data and storage medium capacity results in enormous differences between the scenarios. In the most resource-efficient scenario the total number of data carriers actually falls between 2018 and 2040 due to the assumed strong capacity increase, while in the most resource-intensive scenario there is a dramatic increase in the number of data carriers. The same trend can be seen for the individual technologies. The most marked rise is in SSDs, followed by HDDs. The number of magnetic tapes sees a comparatively moderate increase.

3.5.4.3 Foresight raw material demand

HDD hard drives

The following information was taken from Ku (2018): To examine the critical raw materials used in HDDs, it is necessary to consider the various components. In an HDD, data is stored on a thin magnetic cobalt-chromium-platinum (CoCrPt) layer. HDDs also contain magnets for the read/write process, which are partly made of neodymium. Neodymium-iron-boron magnets are commonly used. In some cases ruthenium is used for nonmagnetic separating layers between data layers or in the manufacturing of the disks. This results in the following ranges for critical raw materials in HDDs, in tonnes/zettabyte:

– Cobalt (Co): 0.34–1.0 tonnes/ZB
– Chromium (Cr): 0.03–0.09 tonnes/ZB

– Platinum (Pt): 0.18–0.55 tonnes/ZB
– Ruthenium (Ru): 0.3–0.4 tonnes/ZB
– Neodymium (Nd): 342–480 tonnes/ZB

A significant efficiency increase in the storage capacity of the hardware is expected between now and 2040. This was calculated using historical increases and expected future drive capacities on a scenario-specific basis. For neodymium it is assumed that this will result in a consumption lower than 342–480 tonnes/ZB, as a read/write head will continue to be installed as drive capacity increases (JM, no date). The demand for neodymium in the scenarios is divided by the anticipated increase in efficiency. For the other raw materials it is assumed that consumption will rise in correlation with increasing drive capacity. This results in the raw material demands shown in Table 3.103. In almost all scenarios, raw material demand increases significantly between 2018 and 2040. It can be seen that differences in demand are relatively large both between the scenarios and between the minimum and maximum values. Even in the most resource-intensive scenario, chromium is only needed in relatively small amounts compared with the other materials considered. It is clear that neodymium, in particular, is consumed in large amounts due to HDD production. Here the differences between the minimum and maximum values are also comparatively small. The increase in demand for neodymium between 2018 and 2040 is especially noticeable in the most resource-intensive scenario, with the predicted annual maximum demand being around one third of current global production. The differences between the scenarios are also marked. In the most sustainable scenario (SSP1), annual demand for neodymium falls to around one third of current consumption in 2040 (2040 maximum value).

SSD hard drives

The following information was taken from Ku (2018): To examine the critical raw materials in SSDs, it is important to consider the basic structure of an SSD. SSDs are flash memory devices. They often use a multilayer NAND floating gate transistor structure. The most commonly used architecture contains silicon in the form of silicon nitride and silicon oxide and is known as SONOS (silicon-oxide-nitride-oxide-silicon). An alternative to floating gate structures is TANOS structures, which contain tantalum (tantalum nitride-aluminium oxide-nitride-oxide-silicon) (Tan et al. 2008). This alternative offers better scalability and higher performance.

This results in the following raw materials in HDDs, in tonnes/zettabyte:

– Silicon (Si): 0.02 tonnes/ZB
– Tantalum (Ta): 0.6 tonnes/ZB

Table 3.103: Raw material requirements for HDDs by scenario and year, in tonnes

Raw material	SSP1 Sustainability		SSP2 Middle of the Road		SSP5 Fossil Path	
	2018	2040	2018	2040	2018	2040
Cobalt, min.	0.10	37	0.12	142	0.14	500
Cobalt, max.	0.30	109	0.37	418	0.41	1,480
Chromium, min.	0.01	3.2	0.01	12	0.01	44
Chromium, max.	0.03	9.8	0.03	38	0.04	133
Platinum, min.	0.05	20	0.07	75	0.07	266
Platinum, max.	0.16	60	0.20	230	0.22	813
Ruthenium, min.	0.09	33	0.11	125	0.12	444
Ruthenium, max.	0.12	44	0.15	167	0.16	592
Neodymium, min.	51	44	63	376	70	6,570
Neodymium, max.	72	62	88	530	98	9,220

Table 3.104: Raw material demand for SSDs by scenario and year, in tonnes

Raw material	SSP1 Sustainability		SSP2 Middle of the Road		SSP5 Fossil Path	
	2018	2040	2018	2040	2018	2040
Silicon	0.0005	1.6	0.0006	6.1	0.0006	21.6
Tantalum	0.0136	47.8	0.0167	184	0.0186	650

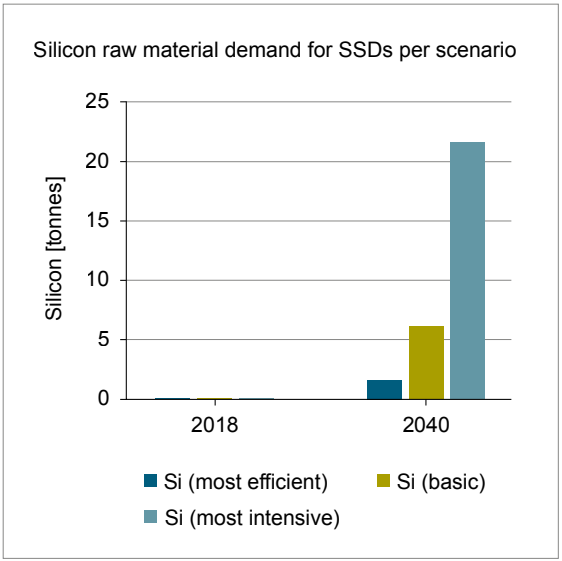

Figure 3.103: Demand for silicon for SSDs in tonnes by scenario and year (source: own representation)

This results in the following requirements for silicon and tantalum (Table 3.104). For both materials there is a clear increase across the scenarios and over time. The amount of these materials required in 2040 is many times the demand in 2018. Figure 3.103 shows this using silicon as an example.

Magnetic tapes

The magnetic layer of a tape may contain critical raw materials. Known magnetic coatings include iron, chromium, strontium and barium. The thickness of the oxide crystal layer is less than 10 nm (Lipinski 2015). With the commonly used tape length of 960 m and width of 12.65 mm, this means that each cartridge contains a maximum of 0.7 g of metal oxide. Using the data in the literature referred to, it is not possible to state the extent to which each type of magnetic coating is used. The calculation cannot therefore be broken down any further. However, it may be assumed that any market scarcity could be overcome by substituting the magnetic coating with another material. In the case of magnetic tape, the reading and writing devices are also relevant from a resource perspective. The literature is unclear in this regard and no valid values could be found for the read/write heads in tape libraries. For this technology synopsis it is assumed that the use of magnetic type tends to have a mitigating effect on material scarcity compared with SSDs and HDDs.

Consolidation

The difference between the minimum and maximum requirements in the outlook results from the range of raw material requirements for SSDs and HDDs according to Ku (2018). There is a particularly large increase in demand for neodymium, but demand for platinum and tantalum also sees a noticeable rise, such that a significant proportion of current tantalum production would be needed and more than current production in the case of platinum. In SSP5, demand for neodymium in 2040 reaches around one third of today's global production.

Data centres are highly diverse technology clusters, designed differently according to the application. Because they store sensitive data, confidentiality requirements also apply. This makes it difficult to assess what hardware is actually on the market and how it is used. The composition of the storage media used will vary depending on the use of the data centre, and this in turn affects the raw material requirements. The amount of data involved is also highly variable due to factors such as new digital trends, new forms of data compression, coding, security rules and standards. All these uncertainties give rise to widely diverging results. Ensuring that materials are recycled at the end of a component's service life and reconditioning used components could be an important part

Table 3.105: Global production (BGR 2021) and calculated raw material demand for storage media in data centres, in tonnes

Raw material	Production in 2018	Demand in 2018	Demand foresight for 2040					
			SSP1 Sustainability		SSP2 Middle of the Road		SSP5 Fossil Path	
			Min.	Max.	Min.	Max.	Min.	Max.
Cobalt	151,060 (M) 126,019 (R)	0.1	37	109	142	418	503	1,479
Chromium	27,000,000 (M)	0.02	3	10	13	38	44	133
Platinum	190 (M)	0.1	20	60	75	230	266	813
Ruthenium	33[1] (R)	0.1	33	44	125	167	444	592
Neodymium	23,900 (R)	180	44	62	376	528	6,570	9,220
Tantalum	1,832 (M)	0.01	48		185		649	

M: Mine production (tonnes of metal content)
R: Refinery production (tonnes of metal content)
[1] Source: JM 2020

of protecting material supplies. Government policies could also perceptibly alter actual raw material demand in relation to data centres.

3.5.4.4 Recycling, resource efficiency and substitution

Data centres are major components of the IT infrastructure with no direct physical link to end users. When equipment is upgraded or dismantled, legal requirements relating to methods of disposal are likely to be fully complied with. Recycling rates may be higher than average for European waste, as it is possible to collect larger quantities of presorted materials. Data carriers are highly sensitive waste and appropriate efforts are made to wipe them of data. Physical destruction of the storage medium is a reliable way of doing this, but the storage medium cannot then be reused. There are specialist companies which recondition used components from data centres (such as storage media, racks and servers) and offer maintenance beyond the period of normal warranty agreements (Schlücker 2016).

The lifetime of individual data centre components is difficult to assess, as any upgrades are always driven by progress, the aim being to keep pace with the latest technologies and ensure reliability through preventive maintenance. In principle it is conceivable that equipment or storage media is replaced before it is technically obsolete or faulty. This could provide leverage for increasing resource efficiency. In such cases there could be a conflict between energy efficiency and resource efficiency, for example if new processors consume much less energy.

In this section, the focus has been on storage media in data centres. HDDs, SSDs and magnetic tape have been identified as essential and established technologies. Since the substitution of individual critical raw materials would require a technology shift, the calculated future requirements for raw materials would probably be difficult to replace with other materials.

3.5.5 Inductive transfer of electrical energy

3.5.5.1 Technology description

Today, electrical energy is normally transferred by cable. This conductive power transfer can take place through a permanent connection, as in an oven, through a cable with a plug, as with a refrigerator, or through contacts, as in a power tool. But electrical power can also be transferred without the need for a cable, be it through electromagnetic, optical, capacitive or inductive means. Electromagnetic and optical methods can only be

used for small amounts of power. For example, electromagnetic waves are used to exchange data between an RFID transponder and a reader. Capacitive transfer is energy-inefficient because it involves high spreading loss. This technology is used for data transmission. Inductive transfer is the preferred contactless method for transferring medium to high amounts of electrical power. This method, in which electrical power is transferred from a primary to a secondary coil, is suitable for many purposes and has already become established in some applications, such as charging electric toothbrushes and pacemakers or in driverless forklift trucks in factories.

The contactless transfer of electrical energy is based on the physical principle of electromagnetic induction, discovered in 1831 by Michael Faraday. If a loop of electrically conductive material is moved through a magnetic field with a flux Φ, the voltage U is induced in the loop. This voltage can be measured at the open ends of the loop. The induced voltage is proportional to the change in the magnetic flux over time:

$$U = \frac{d\Phi}{dt}$$

It does not matter whether the magnetic flux changes over time in a loop at rest or the loop is moved through a fixed magnetic field.

In 1820, Hans Christian Ørsted realised that when current passes through a wire a magnetic field is produced. If the wire is formed into a coil as shown in Figure 3.104, when the current flows a rotationally symmetrical magnetic field is created around the axis of the coil. Inductive energy transfer is based on a combination of this phenomenon and Faraday's law of induction. When an alternating current flows through the primary coil, an alternating magnetic field is produced. If parts of this primary magnetic field pass through a second coil of conductive material, an electrical voltage is induced in this secondary coil.

If a consumer is connected to the secondary coil with an ohmic resistance R_2, the current $I_2 = U_2/R_2$ flows and the power $P_2 = I_2 \cdot U_2$ is transmitted, which can be used to charge a battery, for example. The energetic quality of the transfer is characterised by the efficiency with which supplied energy is converted into usable energy. This efficiency depends on a number of factors. The first

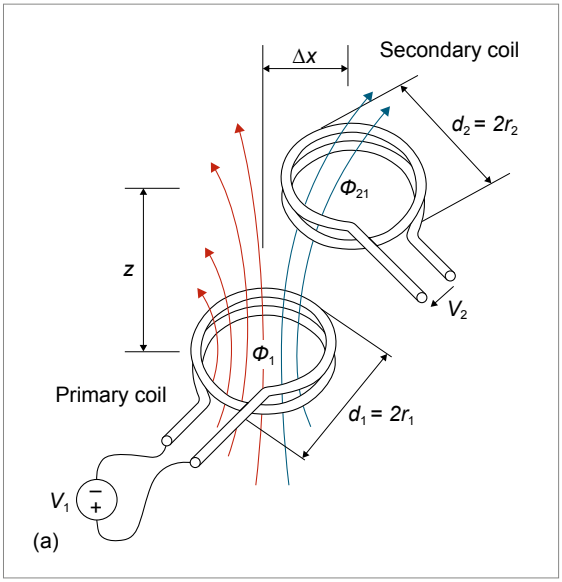

Figure 3.104: Induction principle (source: own representation based on Wambsganss & Parspour 2010)

aim is to capture as much of the primary magnetic field as possible with the secondary coil to minimise spreading loss. This is achieved by positioning the coils one on top of the other without significant lateral offset Δx. The gap between the coils (air gap z) has an important effect on spreading loss. Loss can be reduced with the use of shielding, for example ferrite sheets placed underneath the coils. Increasing the frequency of the primary alternating field concentrates the magnetic field and increases the efficiency.

In practical applications, transfer frequencies of 20 kHz–400 kHz are used (IFAK 2011). To achieve international and cross-manufacturer interoperability, the transfer frequency for electric vehicles is defined in ISO 19363 as 85 kHz.

The overall efficiency of contactless charging systems is given by WiTricity (2018) as 90 %–93 % and transfer capacities of up to 11 kW have been achieved for cars (WiTricity 2018). In the future, inductive transfer systems could be almost as efficient as conductive systems, which typically have an efficiency of over 97 % (IFAK 2011). Recent research indicates that inductive charging systems, like conductive charging systems, can be used bidirectionally. This means that energy can be fed back from the vehicle into the power

grid, helping to stabilise the grid (Tachikawa et al. 2018).

In practice, for the reasons explained above, inductive power transfer does not take place at the grid frequency of 50 Hz but is raised to the transfer frequency by an inverter. Figure 3.105 shows the power electronics components of the circuit within the overall system. In the case of electric vehicle charging, the primary side (on the left in the diagram) corresponds to the charging station, while the secondary side (right) is inside the vehicle.

A few years ago, the chances of wireless power transfer were still being assessed fairly pessimistically (Schraven et al. 2010). The technology has made huge strides in recent years and is now viewed as an emerging technology, with the potential to replace conventional conductive power transfer in many applications. The power range achievable today ranges from a few watts to several hundred kilowatts. A study by the German Aerospace Center (DLR) in partnership with other institutions concluded that it is technically feasible to operate high-speed trains with inductive sections integrated in the track system, without the use of overhead contact lines. To achieve the maximum operating speed of 400 km/h, 25 MW of electrical power needs to be inductively transferred (DLR 2014). Smartphones and other electronic devices are also increasingly being equipped with inductive charging systems.

The inductive charging of electric vehicles is set to become more important in future. This is supported by the fact that all OEMs in the automotive industry already have programmes to research or develop contactless charging (Tachikawa et al. 2018). Below, this application is examined in more detail as one example from the wide spectrum of potential areas of use.

There are two different types of inductive charging for electric vehicles: static and dynamic charging. With static charging, power transfer takes place while the vehicle is stationary – for example in a private or public parking space. Dynamic charging involves charging the vehicle while it is being driven, by installing primary coils in the road surface. There are already numerous research and development projects devoted to static inductive charging. For example, BMW already offers an inductive charging system for end users. Designed for the plug-in hybrid vehicle 530e, the system has a maximum charging power of 3.7 kW and an efficiency of 85 % (Oleg Satanovsky 2019).

Dynamic inductive charging has also been successfully tested, with a power of 8.5 kW and an efficiency of over 91 % being achieved over a distance of 20 m (Werwitzke 2019). This application of the technology could counter the low ranges of battery-powered electric vehicles. However, given that the estimated costs of installing charging coils in the road amount to USD 460,000 to USD 760,000 per kilometre, it is unlikely that dynamic inductive charging for electric vehicles will become widespread in the near future (Suh & Cho 2017). For this reason, only static inductive charging systems are considered in what follows.

The advantages of contactless charging are obvious. There is no need for charging stations or a cable to connect the vehicle to the power grid. It also dispenses with the manual process of han-

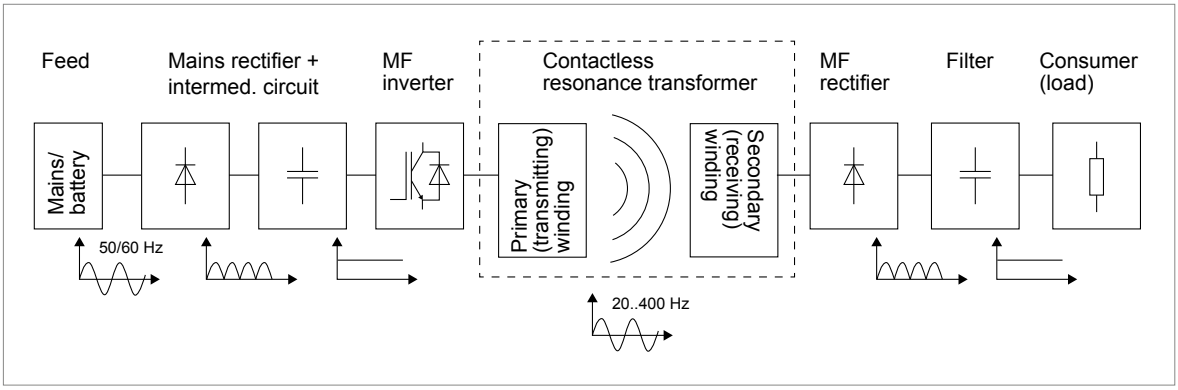

Figure 3.105: Components of a wireless system to transfer electrical power (source: IFAK 2011)

dling a charging cable. This makes electric vehicles much more convenient, especially in comparison with conventional vehicles with an internal combustion engine, which need to be regularly refuelled. The primary coil can be inconspicuously integrated in parking areas, which also reduces the risk of charging cables or stations becoming targets for vandalism. The secondary system inside the vehicle is automatically and accurately positioned over the primary system with the help of the parking assistant. It is virtually maintenance-free, with no wear and tear to plugs or cables, the regular replacement of which represents a significant cost factor for charging stations. However, the high-frequency stray electromagnetic fields must be shielded by ferrite. At high charging outputs, foreign object detection is also required to ensure that there are no electrically conductive objects between the primary and secondary coils, as eddy current losses could cause these to heat up. Any danger to living objects is also prevented by monitoring the air gap. If required, power transfer is stopped by a protective circuit. The vehicle and the charging station communicate via WLAN to ensure that the primary field is only switched on once the secondary coil is correctly positioned. This prevents the formation of an open magnetic circuit.

3.5.5.2 Raw material content

To keep ohmic losses low and achieve efficient power transfer, the current-carrying parts of conductive and inductive charging systems are made of copper wire. The wires are made of individual copper strands which are insulated from one another to improve efficiency. Most of the copper is needed for the primary and secondary coils. Ferrite is also used to shield the magnetic field. The signal and power electronics components contain a large number of elements in the periodic table, albeit in noncritical amounts.

In conductive transfer systems, copper is mostly used in charging cables and the wiring of the charging station and vehicle. Plastic and steel are required for the charging station's housing. Conductive charging systems also use small quantities of many other raw materials for the power electronics. Copper should be regarded as a quantitatively critical material.

As part of a research project on wireless charging for electric vehicles, researchers evaluated a series of funded development projects on inductive charging, recreated test systems and assessed the current state of development and future prospects through empirical surveys (IFAK 2011). The team reconstructed a stationary inductive charging system with an output of 3.6 kW and concluded that the required weight of copper for the two coils amounted to 1.3 kg. A 5-core, 4-metre-long standard charging cable for a conductive charging station contains 1.2 kg of copper. In addition, there is the weight of the copper wiring in charging stations themselves, which was not examined in more detail. The Institute for Automation and Communication concludes that the amount of copper is approximately comparable in the two charging systems (IFAK 2011). The copper requirement for inductive charging systems rises roughly in proportion to the maximum transferable power. However, it is expected that inductive charging will mostly be used in the low and medium power range. Because vehicles remain stationary for extended periods, an extensive inductive charging infrastructure could ensure even with low charging power that a vehicle was always sufficiently charged.

3.5.5.3 Foresight industrial use

The future dissemination of stationary inductive charging systems will be crucially dependent on their costs. They are in competition with conventional conductive charging systems. In Germany, the inductive charging system for the plug-in BMW 530e is already available as a special equipment item. The costs of the secondary side in the vehicle are €890. Purchasing and installing the primary side, i.e. the infrastructure-side charging pad, costs an additional €2,315 (Schaal 2019). Given the total additional costs of €3,205, it is safe to assume that in the near future inductive charging will remain limited to the premium car segment. However, with increasing market penetration of this technology, costs may be expected to fall considerably as research and development costs are more widely distributed and large quantities can be manufactured more efficiently.

Bi et al. (2017) compared the total system costs of conductive and inductive charging for electric buses in a life cycle cost analysis. In this study it

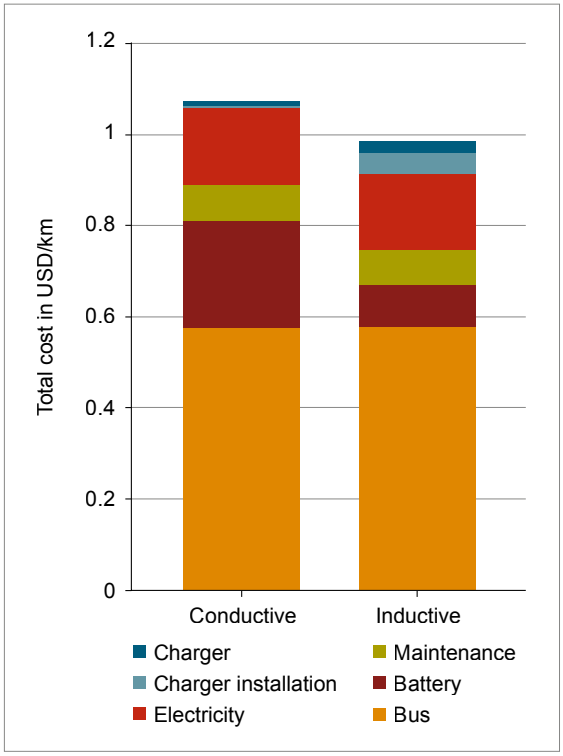

Figure 3.106: Comparison of total costs for buses with conductive and inductive charger per kilometre travelled (source: Bi et al. 2017)

was assumed that buses make regular use of contactless charging while stationary at stops, while conductive buses can only be charged at the depot. This means that a bus with inductive charging can be equipped with a smaller battery. There would however be significantly higher investment costs for the charging station infrastructure. The energy saved through contactless charging as a result of the vehicle being lighter is cancelled out by the lower charging efficiency, resulting in almost no net difference. However, the study concluded that due to the lower battery costs, the total costs over the lifetime of contactless charging are lower for buses than with cable-based charging. A comparison of the costs of both technologies can be seen in Figure 3.106.

3.5.5.4 Foresight raw material demand

For new registrations of electric vehicles the SSP1, SSP2 and SSP5 scenarios described by IIASA were used; these are described in more detail in Section 1.3 Mobility scenarios. Both fully electric and plug-in hybrid vehicles are considered, as both require charging systems. In the scenarios for inductive and conductive charging, it is assumed that only one or the other technology is used so as to make the difference in raw material requirements clear. According to DENA (2020), the German federal government's target is that one charging point will be installed for every eight to nine electric vehicles. Here, this ratio is used to calculate the number of newly installed charging points from the number of electric vehicle registrations. In scenario SSP1 there are 8.9 million new charging systems installed in 2040. In SSP2 there are 6.3 million and in SSP5, 2.4 million.

The total copper demand for an inductive charging system is mostly split equally between the vehicle and the charging station. It is assumed that inductive charging systems transfer 3.6 kW of power, resulting in a copper demand of 0.65 kg for both sides. In the inductive charging scenario it is assumed that every electric vehicle is equipped with the secondary side of an inductive charging system. For conductive charging, it is assumed that the only requirement for copper is in the charging station. The copper demand for both

Table 3.106: Global production (BGR 2021) and calculated copper demand for electric vehicle charging systems, in tonnes

Charging system	Copper production in 2018	Demand in 2018	Demand foresight for 2040		
			SSP1 Sustainability	SSP2 Middle of the Road	SSP5 Fossil Path
Inductive	20,591,000 (M) 24,137,000 (R)	0	54,960	38,760	14,990
Conductive		195	10,680	7,530	2,910

M: Mine production (tonnes of metal content)
R: Refinery production (tonnes of metal content)

systems and global copper production in 2018 are shown in Table 3.106. It is assumed that in the reference year of 2018, no copper is required for inductive charging systems as this technology is not yet established on the market.

The annual copper demand for inductive charging systems exceeds that of conductive systems by around a factor of 5, since every vehicle must be fitted with a charging coil. The same goes for the copper inventory, such that the conductive charging system is much more resource-efficient. However, this must be balanced against the fact that the charging cables and connectors used in conductive systems are subject to wear and must be regularly replaced. An inductive system, on the other hand, is virtually maintenance-free and not vulnerable to vandalism. It does not require steel or plastic for the housing of a charging station.

3.5.5.5 Recycling, resource efficiency and substitution

Copper is the most electrically conductive material after silver. For cost reasons, the use of silver is not a realistic alternative for the power transfer infrastructure. In principle, aluminium could also be used a conductor if certain technical properties of this metal were taken into account (Dittrich et al. 2018). This would have advantages in terms of resource efficiency, weight and costs. However, because aluminium wires are less conductive it is unlikely that this substitution would be widely used.

Copper from charging systems is very easy to recycle. After the electrolysis stage, secondary copper does not differ in quality from primary copper. There are efficient disposal and recycling systems in place for steel and plastic components. Recycling the power and signal electronics is more problematic. Although considerable progress has been made, material recovery from electronic scrap recycling is unsatisfactory for economic and technical reasons. The majority of substances are therefore lost from the economic cycle.

4 Synopses of raw materials

4.1 Gallium

Gallium is in the third main group, the boron group, of the periodic table of the elements directly below aluminium. It was discovered in 1875, but only gained industrial significance from 1970 onwards with the discovery of its applications in the production of semiconductors (Greber 2012).

4.1.1 Properties

Gallium is a soft, silvery blue lustrous metal. With its relatively low melting point of 29.8 °C and a very high boiling point of 2,403 °C, gallium has the largest liquid interval of all metals (Table 4.1). Some gallium alloys, e.g. the alloys with aluminium, form at normal temperatures. These properties are taken advantage of industrially, but complicate the storage and transport of gallium, which requires refrigeration and special packaging to ensure the purity of the metal and the integrity of the transport packaging (Quadbeck-Seeger 2007; Greber 2012; Liedtke & Huy 2018).

Table 4.1: Gallium properties

Density	5.9 g/cm³
Melting point	29.8 °C
Electric conductivity	7.1 · 10⁶ S/m
Thermal conductivity	29 W/(m · K)

4.1.2 Deposits and production

Gallium is not a rare element, but it is rarely found in higher concentrations in the earth's crust. Amongst the minerals containing gallium, the very rare copper-gallium sulphide gallite has the highest gallium content of up to 35.3 %. The gallium content in West African germanite ranges between 0.1 and 1 %. In many other minerals, including bauxite, sphalerite and anthracite, gallium is only present as a trace element. Bauxite, for example, has an average gallium content of about 50 ppm. Fly ash can also contain traces of gallium (Römpp o. J; Greber 2012; Rongguo et al. 2016; Liedtke & Huy 2018).

Gallium is obtained as a by-product of aluminium production (from bauxite) and to a much lesser extent as a by-product of zinc production (e.g.

Table 4.2: Gallium supply situation in 2010, 2013 and 2018 (sources: BGR 2021, USGS 2011a, USGS 2014a, USGS 2019a, USGS 2020c)

	2010	2013	2018
Primary production [tonnes of metal content]	182	369	413
Refinery production [tonnes of metal content]	161	200	205
Reserve [tonnes of metal content]	–	–	–
Resources [tonnes of metal content]	> 1,000,000	> 1,000,000	> 1,000,000
Most important countries for production	Germany 49 %[1] Kazakhstan 26 %[1] Russia 18 %[1]	China 81 % Germany 10 % Ukraine 4 %	China 96 % Russia 2 % Ukraine 1 %
Most important countries for refining	–	–	–
Country concentration – Primary production[2]	–	6,747	9,244
Country concentration – Refinery production	–	–	–
Weighted country risk – Primary production[2]	–	-0.30	-0.31
Weighted country risk – Refinery production	–	–	–
Price[3] [USD/kg]	469.15	279.41	191.82

[1] *2011 data*
[2] *For a colour legend, please refer to the HHI and GLR entries in the "Abbreviations and glossary" section.*
[3] *min. 99.99 % fob China*

from sphalerite). It is found in particular in the sodium aluminate created in aluminium production and in residues produced in zinc smelters (Liedtke & Huy 2018; USGS 2020c).

China's share of the world's primary gallium production capacity is around 80 %. It is estimated that 97 % of the primary gallium produced globally in 2019 was produced in China. The main producers of refined (high-purity) gallium are China, Japan, Slovakia and the USA. Extensive gallium resources worldwide are bound up in bauxite and zinc ores. The gallium resources in bauxite alone amount to more than one million tonnes. However, less than 10 % of the gallium resources bound in bauxite and zinc ores have the potential to be exploited. There are also large reserves (in low concentrations) contained in phosphate ores and various types of coal. There is currently no estimate of current gallium reserves (Ronggguo et al. 2016; USGS 2020c). The supply situation for gallium is shown in Table 4.2.

4.1.3 Applications

Owing to the properties that made it industrially important in semiconductor production from 1970 onwards, integrated circuits represent the most important area of application for gallium today. The large liquid interval of gallium is used for the design of special thermometers. The areas of application of gallium in the EU are shown in Table 4.3.

Table 4.3: Gallium usage in the EU (source: European Commission 2020a)

Area of application	2012–2016 [%]
Integrated circuits	70
LEDs	25
Solar technologies	5
Total	**100**

Emerging technologies

The most important emerging technologies with a high growth potential that make use of gallium are:

– Radio frequency microchips
– Thin-film photovoltaics

4.1.4 Gallium demand in 2040

The additional raw material demands estimated on the basis of the technology synopses are shown in Table 4.4 and Figure 4.1. The demand for the emerging technologies segment examined was about 11 % of the refined gallium production in 2018. Depending on the scenario, the amount of gallium required for the emerging technologies examined in 2040 may grow to up to 22 % of the 2018 refinery production.

Table 4.4: Gallium demand for selected emerging technologies, in tonnes

Technology	Demand in 2018	Demand in 2040		
		SSP1 Sustainability	SSP2 Middle of the Road	SSP5 Fossil Path
Optoelectronics / photonics	1	2	2	2
Radio-frequency microchips	38	60	74	90
Thin-film photovoltaics	5	26	3	0
Demand (accumulated)	**44**	**88**	**79**	**92**
Demand / Primary production in 2018	6 %	12 %	11 %	13 %
Demand / Refinery production in 2018	11 %	21 %	19 %	22 %

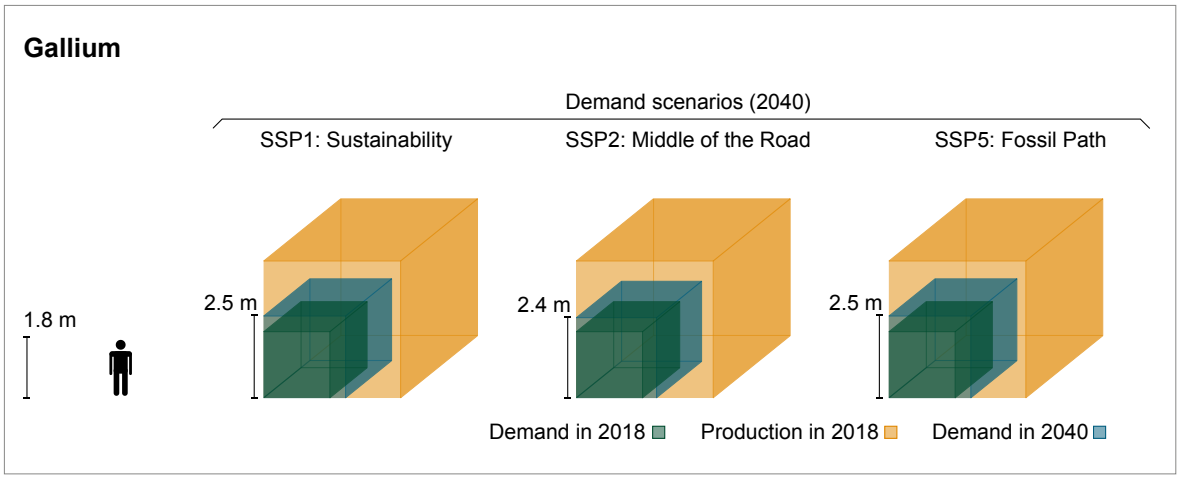

Figure 4.1: Gallium primary production in 2018 and demand for emerging technologies in 2018 and 2040

4.2 Germanium

Germanium is in the fourth main group, the carbon group, of the periodic table of the elements below silicon. It was first isolated in 1886 and gained industrial significance from 1947 onwards with its use in transistor production (Scoyer et al. 2012).

4.2.1 Properties

Germanium is a grey-white, metallic lustrous semimetal. It has semiconducting properties and is transmissive for infrared light (Table 4.5). Its physical properties are generally strongly dependent on temperature. Germanium crystals are susceptible to thermal shocks. For end-use applications, germanium is used, amongst other things, in the form of various chemicals whose storage and transport can be associated with relatively high packaging costs due to their sometimes corrosive properties (as in the case of germanium tetrachloride) and high quality requirements of the intended areas of application (Wagner 1958; Scoyer et al. 2012).

Table 4.5: Germanium properties

Density	5.3 g/cm^3
Melting point	938.3 °C
Electric conductivity	2 · 10^3 S/m
Thermal conductivity	60 W/(m · K)

4.2.2 Deposits and production

Germanium is a relatively rare element and dispersed in the earth's crust. Minerals with a relatively high germanium content include stottite (approx. 29 %), schaurteite (approx. 14 %), briartite (13–17 %), germanite (5–10 %) and renierite (6.3–7.7 %). Germanium enrichments are found in certain zinc and zinc-lead-copper sulphide deposits and are also bound to organic matter in coals and lignites (Römpp no date; Scoyer et al. 2012; USGS 2020d).

While germanite and renierite used to be amongst the main sources of germanium, today germanium is mainly extracted as a by-product in the production of other metals, above all zinc. Pulverised fuel ash from coal combustion is also used for the extraction of germanium (Elsner et al. 2010; Scoyer et al. 2012; USGS 2017b).

Exact data on primary production of germanium are not available, since the few producers that exist (especially in the USA) keep their data confidential. China is the largest refinery producer, accounting for 75 % of global refinery production. Secondary production (recycling) meets roughly 30 % of global germanium demand (USGS 2020d). An overview of the supply situation for germanium is shown in Table 4.6.

Table 4.6: Germanium supply situation in 2010, 2013 and 2018 (source: BGR 2021)

	2010	2013	2018
Mine production [tonnes of metal content]	–	–	–
Refinery production [tonnes of metal content]	129	140	143
Reserve [tonnes of metal content]	–	–	–
Resources [tonnes of metal content]	–	–	–
Most important countries for mining	–	–	–
Most important countries for refining	China 62 % Canada 19 % Finland 9 %	China 70 % Finland 12 % Canada 11 %	China 75 % Canada 5 % Russia 4 %
Country concentration – Mine production	–	–	–
Country concentration – Refinery production[1]	4,365	5,182	5,661
Weighted country risk – Mine production	–	–	–
Weighted country risk – Refinery production[1]	0.16	0.03	–0.14
Price[2] [USD/kg]	640.23	1,317.71	1,102.39

[1] *For a colour legend, please refer to the HHI and GLR entries in the "Abbreviations and glossary" section.*
[2] *Germanium dioxide, min. 99.99 %, MB free market, in warehouse*

4.2.3 Applications

Germanium has lost importance in its original industrial area of application, transistor production. Its main applications today are in the field of optics. Owing to its infrared light transmission, germanium is used in optics for night vision devices, thermal imaging cameras and the like. Data on the worldwide use of germanium are provided in Table 4.7.

Table 4.7: Worldwide application of germanium (source: European Commission 2020a)

Area of application	2016 [%]
Polymerisation catalysts	31
Optical fibres	24
Infrared optics	23
Solar applications	12
Other applications	10
Total	**100**

Emerging technologies

The most important emerging technology with a high growth potential that makes use of germanium is:

– Fibre-optic cables

4.2.4 Germanium demand in 2040

The additional raw material demands estimated on the basis of the technology synopses are shown in Table 4.8 and Figure 4.2. The most important emerging technology for germanium is its use in fibre-optic cables; its demand accounted for 41 % of refinery production in 2018. In 2040, germanium demand for fibre-optic cables is estimated to grow to 195 % of 2018 refinery production, depending on the scenario.

Table 4.8: Germanium demand for selected emerging technologies, in tonnes

Technology	Demand in 2018	Demand in 2040		
		SSP1 Sustainability	SSP2 Middle of the Road	SSP5 Fossil Path
Aircraft for 3D mobility (eVTOL)	–	0.76	1.3	1.5
Fibre-optic cables	59	237	246	277
Demand (accumulated)	**59**	**237.8**	**247.3**	**278.5**
Demand / Refinery production in 2018	41 %	166 %	173 %	195 %

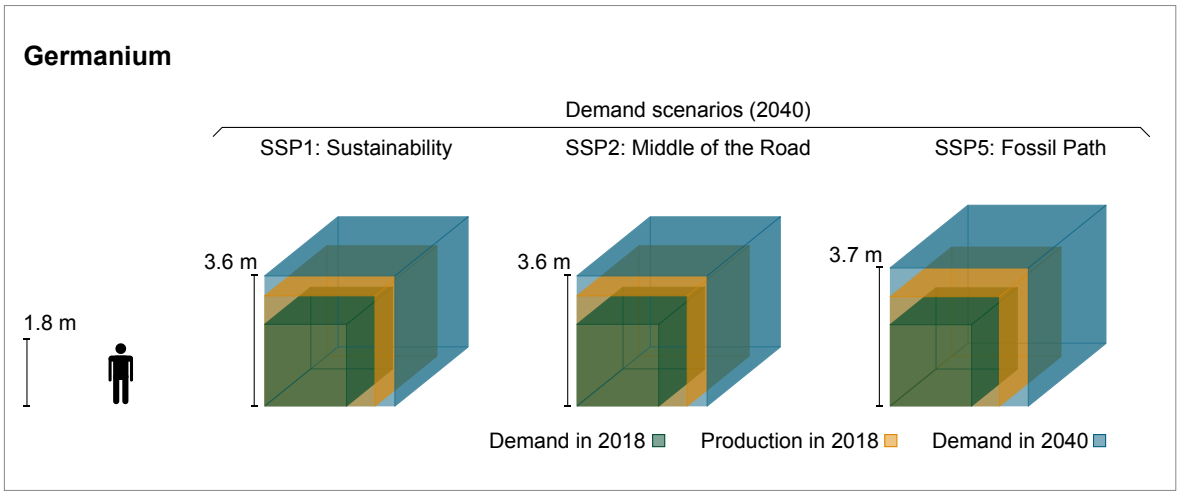

Figure 4.2: Germanium production in 2018 and demand for emerging technologies in 2018 and 2040

4.3 Graphite

Graphite is a stable modification of carbon, which is in the fourth main group, the carbon group, of the periodic table of the elements (Römpp no date). There is evidence that graphite was used to produce refractory ceramics as early as 2,800 years ago. It was used as a pencil material from the middle of the 16th century. The proof that graphite is a form of carbon came in 1779. From the beginning of the 20th century, graphite electrodes were increasingly used in electrolytic and electrothermal processes (Römpp no date; Frohs et al. 2012).

4.3.1 Properties

Graphite is a grey to grey-black, metallic, lustrous, crystalline form of carbon. It is hardly combustible, chemically very resistant, has no melting point under normal pressure and sublimates at approx. 3,750 °C. Due to the special parallel layer structure of its crystal lattice, graphite exhibits anisotropic properties (Table 4.9). This applies in particular to electrical and thermal conductivity: Parallel to the layers of its crystal lattice, graphite is (at room temperature) a good electrical and thermal conductor. Perpendicular to the layers, however, graphite is almost an electrical insulator. The fact that graphite is relatively soft and can be used in pencils or as a lubricant can also be explained by its layered structure. The layers can easily be displaced against each other (Römpp no date; Frohs et al. 2012; Robinson et al. 2017).

Table 4.9: Graphite properties

Density	2.1–2.3 g/cm³
Melting point	–
Electric conductivity	anisotropic
Thermal conductivity	anisotropic

4.3.2 Deposits and production

The graphite market consists of mined natural graphite and synthetic graphite produced from carbonaceous raw materials by complex processes in blast furnaces. Natural graphite can be further subdivided into macrocrystalline graphite

Table 4.10: Graphite supply situation in 2010, 2013 and 2018 (sources: BGR 2021, USGS 2011b, USGS 2014b, USGS 2019b)

	2010	2013	2018
Mine production [tonnes of materials]			
– natural graphite	1,719,400	1,055,800	1,700,000
… thereof flake graphite	860,700	731,900	1,156,300
Production [tonnes of materials]			
– synthetic graphite	1,428,000	1,514,000	1,573,000
Reserve [tonnes of materials]			
– natural graphite	71,000,000	130,000,000	300,000,000
Resources [tonnes of materials]			
– natural graphite	> 800,000,000	> 800,000,000	> 800,000,000
Most important countries for mining			
– natural graphite	China 90 % Brazil 5 % Canada 1 %	China 80 % Brazil 9 % India 3 %	China 74 % Mozambique 6 % Brazil 6 %
– flake graphite	China 81 % Brazil 11 % Canada 2 %	China 74 % Brazil 13 % India 4 %	China 69 % Mozambique 9 % Brazil 8 %
Most important countries for production			
– synthetic graphite	China 42 % Japan 22 % USA 14 %	China 43 % Japan 21 % USA 13 %	China 49 % Japan 19 % USA 10 %
Country concentration – Mine production[1]			
– natural graphite	8,054	6,423	5,938
– flake graphite	6,658	5,537	4,961
Country concentration – Production[1,2]			
– synthetic graphite	3,287	3,199	3,556
Weighted country risk – Mine production			
– natural graphite	-0.51	-0.46	-0.35
– flake graphite	-0.5	-0.49	-0.28
Weighted country risk – Production[1,2]			
– synthetic graphite	0.19	0.16	0.21
Price[3] [USD/tonne]	1,329.84	1,170.83	1,025.94

[1] *For a colour legend, please refer to the HHI and GLR entries in the "Abbreviations and glossary" section.*
[2] *Based on 92 % of global production*
[3] *Crystalline fine, 94–97 % C, +100 – 80 mesh, CIF European Port FCL*

(flake graphite), microcrystalline (amorphous) graphite and gangue graphite. Natural graphite ores and concentrates require a number of preparation and further processing steps depending on the respective end application; in the production of synthetic graphite, the desired properties can be systematically modified during the production process. The graphite products available on the market differ in terms of carbon content, structure and purity. Notably, natural graphite and synthetic graphite are not identical materials (Damm & Zhou 2020).

The world's natural graphite resources are estimated at 800 milion tonnes and include both flake and amorphous graphite. Most of the reserves are located in China, Turkey and Brazil. It can be assumed that with regard to the use as anode material in lithium-ion batteries, only a part of these resources can be processed to grades suitable for batteries. Currently, the most important mining country for natural graphite is China; the country also holds a leading position in the mining of flake graphite (USGS 2019b; Damm & Zhou 2020). China currently also dominates the production of synthetic graphite (cf. Table 4.10).

4.3.3 Applications

With about 60 %, refractory materials in various industrial applications or processes, e.g. steel, iron, glass and ceramics production are the main applications of natural graphite (Jara et al. 2019; Roskill 2019; Damm & Zhou 2020). Other areas of application include aerospace composites, lubricants in high-temperature applications and friction materials in brake pads; graphene and electrode materials for fuel cells represent niche applications.

Around 14 % of the global demand for natural graphite is currently used for lithium-ion batteries, where graphite is used as anode material (see Table 4.11). Flake graphite is predominantly used for this purpose; the grades required for use in batteries are achieved in a series of further processing steps. The quality of the starting ore is decisive in this respect. It should also be noted that the actual demand is lower, as losses occur during the further processing of flake graphite into battery-grade spherical graphite.

The main area of application for synthetic graphite is in metallurgical applications (Mordor Intelligence 2020c). Synthetic graphite is also used as anode material in lithium-ion batteries. A mix of both graphite types is common, especially in batteries for high-end applications.

Table 4.11: Worldwide application of natural graphite (sources: Damm & Zhou 2020, Roskill 2019)

Area of application	2018 [%]
Refractory materials	46
Foundries	14
Batteries	14
Friction materials (e.g. for brake pads)	6
Lubricants	5
Other	15
Total	**100**

Emerging technologies

The most important emerging technology with a high growth potential that makes use of graphite is:

– Lithium-ion high-performance electricity storage

4.3.4 Graphite demand in 2040

In 2018, 2 % of flake graphite production were used for lithium-ion high-capacity storage. Depending on the scenario, this quantity may increase to up to 88 % of the 2018 production in 2040, compare Table 4.12 and Figure 4.3.

Table 4.12: Graphite demand for selected emerging technologies, in tonnes

Technology	Demand in 2018	Demand in 2040		
		SSP1 Sustainability	SSP2 Middle of the Road	SSP5 Fossil Path
Lithium-ion high-performance electricity storage	21,900	1,019,000	886,400	196,000
Demand (accumulated)	**21,900**	**1,019,000**	**886,400**	**196,000**
Demand / Primary production flake graphite in 2018	2 %	88 %	77 %	17 %

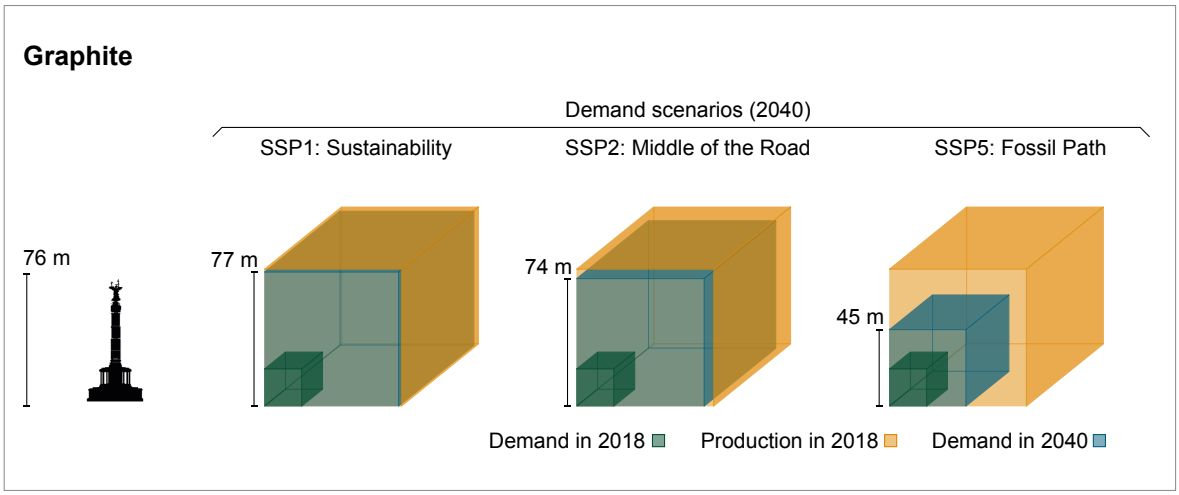

Figure 4.3: Graphite production in 2018 and demand for emerging technologies in 2018 and 2040

4.4 Indium

Indium is in the third main group, the boron group, of the periodic table of the elements under gallium. It was discovered in 1863 and found its first major area of application in the 1940s as a bearing coating material in high-performance aircraft engines (Jorgenson & George 2005; Felix 2012).

4.4.1 Properties

Indium is a silvery-white, highly lustrous and very soft metal. It retains its high ductility and plasticity even at very low temperatures. It can form alloys with most metals, increasing hardness and corrosion resistance even in low concentrations. Indium wets glass and forms a more corrosion-resistant mirror surface than silver with equally good reflective properties (Römpp no date; Quadbeck-Seeger 2007; Felix 2012).

Table 4.13: Indium properties

Density	7.31 g/cm^3
Melting point	156.6 °C
Electric conductivity	12.5 · 10^6 S/m
Thermal conductivity	81.6 W/(m · K)

4.4.2 Deposits and production

Indium is relatively rare and dispersed in the earth's crust. Rare indium minerals such as indite ($FeIn2S_2$) and roquesite ($CuInS_2$) have high indium contents in the range between about 45 % and 60 %. Indium is also contained as a trace ele-

ment in many polymetallic ores/minerals, such as in sulphidic zinc ores, especially sphalerite, copper ores, e.g. chalcopyrite and bornite, tin ores, e.g. stannite and cassiterite, and lead ores, especially galena (RÖMPP no date; ANTHONY et al. 2001a; ANTHONY et al. 2001b; FELIX 2012).

Indium is largely obtained as a by-product from processing and smelting residues as well as dusts and gases generated during zinc extraction and smelting. Sphalerite serves as the indium/zinc source with indium contents ranging between 1 and 100 ppm. The remaining portion of indium production is from tin and copper processing residues (USGS 2017c; PRADHAN et al. 2018; USGS 2020e).

With a share of 50 to 60 % of the worldwide refined indium production, China is the leading producer. The data on the supply situation for indium are shown in Table 4.14. Due to the relatively small indium market, these figures are not deemed very reliable.

4.4.3 Applications

Thin films of indium tin oxides (ITO) are used in the production of liquid crystal displays (LCD) and flat screens. Due to the wide range of applications for these screens in consumer electronics (e.g. in mobile phones, notebooks and televisions) and the high demand, this is the most important area of application for indium in terms of quantity. Depending on the literature source, the share of indium used in this area is estimated to be up to approx. 80 % of the total indium demand, because indium lost in the production process is also taken into account. Further applications can be found, amongst others, in the field of high-purity low-temperature alloys. An overview of indium applications in the EU is shown in Table 4.15.

Table 4.15: Indium usage in the EU (source: EUROPEAN COMMISSION 2020a)

Area of application	2012–2016 [%]
Flat screens	60
Solders	11
Photovoltaics	9
Thermally conductive materials	7
Batteries	6
Alloys	4
Semiconductors and LEDs	3
Total	**100**

Table 4.14: Indium supply situation in 2010, 2013 and 2018 (source: BGR 2021)

	2010	2013	2018
Mine production [tonnes of metal content]	–	–	–
Refinery production [tonnes of metal content]	669	825	808
Reserve [tonnes of metal content]	–	–	–
Resources [tonnes of metal content]	–	–	–
Most important countries for mining	–	–	–
Most important countries for refining	China 50 % Rep. of Korea 22 % Japan 10 %	China 50 % Rep. of Korea 21 % Japan 9 %	China 60 % Rep. of Korea 12 % Japan 9 %
Country concentration – Mine production	–	–	–
Country concentration – Refinery production[1]	3,235	3,153	3,914
Weighted country risk – Mine production	–	–	–
Weighted country risk – Refinery production[1]	0.232	0.233	0.263
Price[2] [USD/kg]	567.26	595.54	291.16

[1] *For a colour legend, please refer to the HHI and GLR entries in the "Abbreviations and glossary" section.*
[2] *Indium ingots, min. 99.97 %, MB free market, in warehouse*

Emerging technologies

The most important emerging technologies with a high growth potential that make use of iridium are:

– Indium tin oxide (ITO) in display technology
– Thin-film photovoltaics

4.4.4 Indium demand in 2040

The additional raw material demands estimated on the basis of the technology synopses are shown in Table 4.16 and Figure 4.4. The greatest demand for indium is in display technology. The emerging technologies segment examined required around 26 % of the refinery output in 2018. This amount may increase to 50 % by 2040 relative to 2018 refinery production, depending on the scenario.

4.5 Cobalt

Cobalt is in the 9th group, the cobalt group, of the periodic table of the elements before rhodium and iridium. It was first isolated in 1735 and identified as a distinct element in 1780. Although it has been used as a dye for thousands of years, the increased industrial use of cobalt did not begin until its applications in alloys and magnets were developed in the early 20th century (Donaldson & Beyersmann 2012).

Table 4.16: Indium demand for selected emerging technologies, in tonnes

Technology	Demand in 2018	Demand in 2040		
		SSP1 Sustainability	SSP2 Middle of the Road	SSP5 Fossil Path
Indium tin oxide (ITO) in display technology	185	297	297	297
Optoelectronics / photonics	5	35	35	35
Thin-film photovoltaics	17	92	10	0
Demand (accumulated)	**207**	**424**	**342**	**332**
Demand / Refinery production 2018	26 %	52 %	42 %	41 %

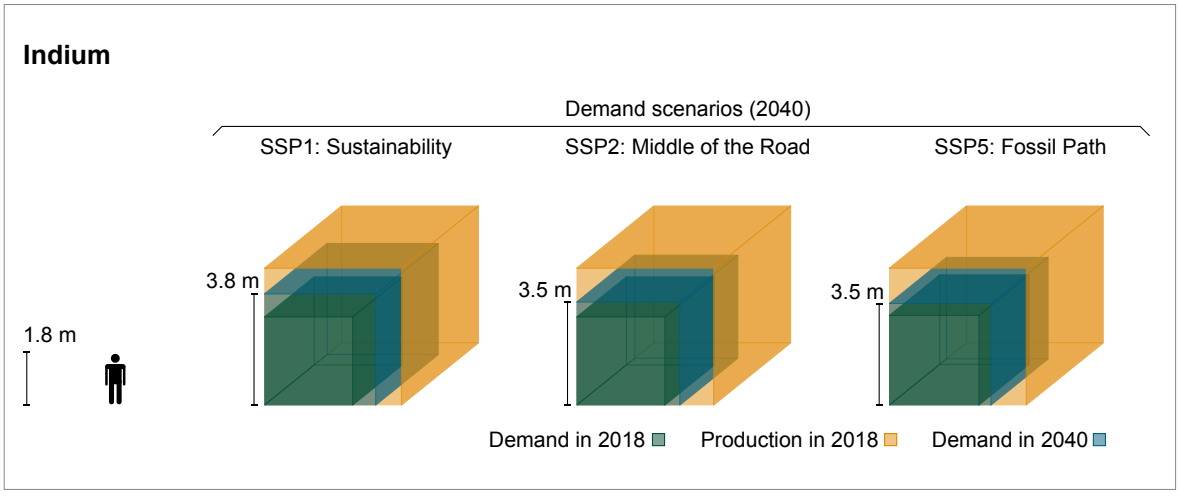

Figure 4.4: Indium production in 2018 and demand for emerging technologies in 2018 and 2040

4.5.1 Properties

Pure cobalt is grey-silvery and lustrous. With its high degree of purity and optimum thermal conditions, it is hard and particularly tough, like other transition metals. It is stronger than steel. In addition to these mechanical and ferromagnetic properties – cobalt retains its magnetism up to 1,121 °C – the properties of the cobalt chemicals also play an important role in its current areas of application (Table 4.17). For example, lithium can intercalate very well in the layered structure of lithium cobalt dioxide, leading to a high energy density of lithium cobalt dioxide cathodes in lithium-ion batteries (Römpp no date; Truebb & Rüetschi 1998; Quadbeck-Seeger 2007; Donaldson & Beyersmann 2012).

Table 4.17: Cobalt properties

Density	8.89 g/cm^3
Melting point	1,495 °C
Electric conductivity	16.7 · 10^6 S/m
Thermal conductivity	100 W/(m · K)

4.5.2 Deposits and production

Cobalt, which is less abundant than nickel and copper in the upper crust, is widespread and dispersed on Earth. It can be found in many different minerals and the environment, mostly as a trace element. Minerals that have high concentrations of cobalt include heterogenite (40–60 %), linnite (approx. 58 %), cattierite (approx. 48 %), cobaltine (approx. 36 %), and skutterudite (approx. 21 %) – the data in parentheses refer to the cobalt content of the minerals (Römpp no date; Donaldson & Beyersmann 2012; Al Barazi 2018; Petavratzi et al. 2019).

Major cobalt deposits include stratabound synsedimentary cobalt-bearing copper deposits, liquid magmatic sulphide nickel (copper) deposits and cobalt-bearing nickel laterite deposits. For example, nickel and copper ores, from which cobalt is extracted as a by-product, currently serve as the main source of cobalt production. In addition, cobalt arsenide ores are used for cobalt extraction (Römpp no date; Donaldson & Beyersmann 2012; Al Barazi 2018; Petavratzi et al. 2019).

Table 4.18: Cobalt supply situation in 2010, 2013 and 2018 (source: BGR 2021)

	2010	2013	2018
Mine production [tonnes of metal content]	105,100	118,502	151,060
Refinery production [tonnes of metal content]	79,457	87,232	126,019
Reserve [tonnes of metal content]	7,302,000	7,203,000	6,875,200
Most important countries for mining	Congo 70 % Zambia 5 % Australia 5 %	Congo 65 % Australia 6 % Zambia 5 %	Congo 72 % Australia 4 % Russia 4 %
Most important countries for refining	China 45 % Finland 12 % Zambia 6 %	China 41 % Finland 12 % Canada 6 %	China 62 % Finland 10 % Belgium 5 %
Country concentration – Mine production[1]	4,922	4,276	5,316
Country concentration – Refinery production[1]	2.368	2,066	4,061
Weighted country risk – Mine production[1]	–1.12	–0.92	–1.15
Weighted country risk – Refinery production[1]	0.14	0.29	0.23
Price[2] [USD/kg]	45.33	29.01	82.52

[1] *For a colour legend, please refer to the HHI and GLR entries in the "Abbreviations and glossary" section.*
[2] *high grade (min. 99.8 %), MB free market, in warehouse*

Approximately 70 % of the cobalt mined worldwide currently comes from the DRC. China is the largest refinery producer. Terrestrial cobalt resources amount to approximately 25 million tonnes and are predominantly distributed amongst stratabound cobalt-bearing copper deposits, stratabound cobalt-bearing nickel laterite deposits and nickel-copper sulphide deposits. Marine manganese nodules and crusts make up an estimated cobalt resource of 120 million tonnes (USGS 2020a). An overview of the supply situation is shown in Table 4.18.

4.5.3 Applications

The original main application of cobalt as a (blue) dye for ceramics and glass, amongst other things, plays only a minor role today. The areas of application in the field of alloys and magnets, which were established at the beginning of the 20th century, are still important today. For example, the hard and particularly tough cobalt is used in highly resilient iron alloys such as razor blades, drills and tools and, thanks to its ferromagnetic properties, it is used to manufacture permanent magnets, e.g. SmCo magnets (Quadbeck-Seeger 2007). However, alloys and magnets are no longer the most important areas of application for cobalt. Instead, just under half of the world's cobalt production is used to make batteries. In these, cobalt is used as a cathode material, e.g. in the form of lithium nickel manganese cobalt oxide, and is used in electric vehicles, stationary energy storage systems, computers and telecommunications equipment. An overview of the main areas of application of cobalt worldwide is shown in Table 4.19.

Table 4.19: Worldwide application of cobalt (source: Petavratzi et al. 2019)

Area of application	2017 [%]
Batteries	46
Super alloys	17
Hard metals	8
Catalysts	7
High-speed steel / other alloys	6
Dyes	5
Magnets	5
Other	6
Total	**100**

Table 4.20: Cobalt demand for selected emerging technologies, in tonnes

Technology	Demand in 2018	Demand in 2040		
		SSP1 Sustainability	SSP2 Middle of the Road	SSP5 Fossil Path
Super alloys	37,000	68,000	63,000	88,000
Lithium-ion high-performance electricity storage	12,750	311,000	270,400	59,830
Solid-state batteries	–	109,000	28,000	3,000
Additive manufacturing of metal components ("3-D printing")	4	139	116	93
Water electrolysis	0	160	40	8
SOFC – Stationary fuel cell	1	63	35	7
CCS – Carbon capture and storage	–	200	700	0
Synthetic fuels	–	4,600	2,250	4,460
Data centres	0	110	420	1,480
Demand (accumulated)	**49,755**	**493,272**	**364,961**	**156,878**
Demand / Primary production 2018	33 %	327 %	242 %	104 %
Demand / Refinery production 2018	39 %	391 %	290 %	124 %

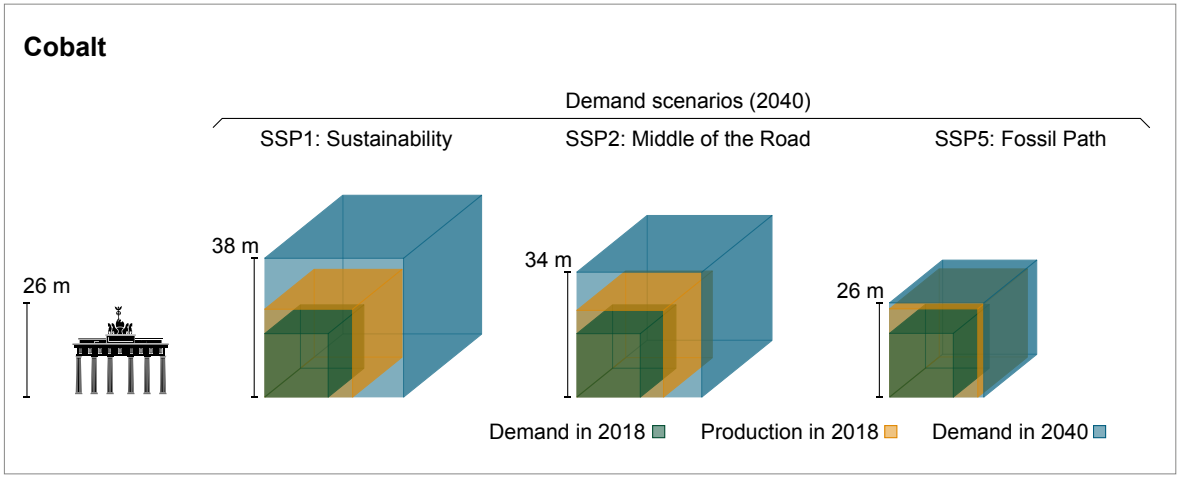

Figure 4.5: Cobalt refinery production in 2018 and demand for emerging technologies in 2018 and 2040

Emerging technologies

The most important emerging technologies with a high growth potential that make use of cobalt are:

- Lithium-ion high-performance electricity storage
- Solid-state batteries
- Super alloys

4.5.4 Cobalt demand in 2040

The additional raw material demands estimated on the basis of the technology synopses are shown in Table 4.20 and Figure 4.5. The demand for the emerging technologies segment under study was about 39 % of the refined cobalt production in 2018. This volume could grow to as much as 391 % of the 2018 refinery production by 2040, depending on the scenario.

Even though 46 % of cobalt production is already used in battery production today, this amount will increase significantly by 2035 depending on the diffusion of electromobility.

4.6 Copper

Copper, together with silver and gold, is in the 11th group, the copper group, of the periodic table of the elements. There is evidence that copper was used more than 9,000 years ago. It has been widely used over various periods (e.g. during the Copper Age 2000-1800 BC), with use increasing greatly in the last century. Major technological advances in the copper industry have been made in the last 140 years (Römpp no date; Lossin 2012).

4.6.1 Properties

Pure copper is a bright red, heavy and easily malleable metal. It is characterised by its high ductility. Like other transition metals, it can be relatively hard and very tough (depending on its purity and thermal pretreatment). It retains its strength even at temperatures below 0 °C. As a semiprecious metal, it is not corroded by air, largely due to the formation of a protective oxide layer. It also forms a patina of copper salts (Cu sulphates) under moist and acidic conditions. Of all metals, copper has the highest electrical and thermal conductivity after silver (Table 4.21). However, cold (massive) forming reduces the electrical conductivity of copper to a certain degree (Römpp no date; Quadbeck-Seeger 2007; Lossin 2012).

Table 4.21: Copper properties

Density	8.92 g/cm^3
Melting point	1,085 °C
Electric conductivity	58.1 · 10^6 S/m
Thermal conductivity	400 W/(m · K)

4.6.2 Deposits and production

Copper occurs in native form and has been extracted and processed in this form throughout human history. It is contained in numerous minerals, sometimes in high proportions, and occurs as a trace element in the environment. It is about twice as abundant as cobalt in the earth's upper crust. Minerals with high copper contents include cuprite (approx. 89 %), tenorite (approx. 80 %), chalcocite (approx. 80 %), digenite (approx. 78 %) and covelline (approx. 67 %) (Römpp no date; Lossin 2012).

Copper is mined on all continents in different geological formations. Of great economic importance are chalcopyrite – a copper ore/mineral with a copper content of about 35 % – as well as porphyry and stratabound copper deposits, which account for the majority of the world's copper supply. The largest countries for mining are Chile, Peru and China; the largest refinery producer is China; the largest copper reserves are found in Chile, Peru and Australia. More than half of the world's identified resources in porphyry and stratabound copper deposits are located in North and South America. In addition to mine production, copper recycling is also an important source of copper, which is why refined copper production significantly exceeds mine production (Lossin 2012; Johnson et al. 2014; Sun et al. 2015; Dorner 2020; USGS 2020b). An overview of the copper supply situation is shown in Table 4.22.

4.6.3 Applications

Although copper can be alloyed with many other metals to produce products with specific properties, unlike many other metals it is often used in its non-alloyed form. Thanks to its properties mentioned above (high ductility and electrical conductivity), it can be processed into many forms (especially sheet, foil and wire) and used for electrical applications, which account for about 79 % of copper use (Dorner 2020). For example, copper is used for electricity distribution (in buildings) and in electrical infrastructure; it is found in transformers and electric motors and is installed in cable harnesses in automobiles. It is also used in electronics and, thanks to its high thermal conductivity, in cooling systems (cf. Römpp no date; Copper Alliance 2019). Table 4.23 summarises the most important global applications of copper.

Table 4.22: Copper supply situation in 2010, 2013 and 2018 (sources: BGR 2021, USGS 2020b)

	2010	2013	2018
Mine production [tonnes of metal content]	16,123,946	18,321,082	20,590,587
Refinery production [tonnes of metal content]	19,070,226	21,084,422	24,136,955
Reserve [tonnes of metal content]	635,000,000	685,000,000	826,000,100
Resources [billion tonnes of metal content]	2.1–3.5	2.1–3.5	2.1–3.5
Most important countries for mining	Chile 34 % Peru 8 % China 7 %	Chile 32 % China 9 % Peru 8 %	Chile 28 % Peru 12 % China 8 %
Most important countries for refining	China 24 % Chile 17 % Japan 8 %	China 32 % Chile 13 % Japan 7 %	China 38 % Chile 10 % Japan 7 %
Country concentration – Mine production[1]	1,444	1,343	1,182
Country concentration – Refinery production[1]	1,063	1,341	1,739
Weighted country risk – Mine production[1]	0.44	0.40	0.25
Weighted country risk – Refinery production[1]	0.34	0.20	0.16
Price[2] [USD/tonne]	7,534.18	7,332.19	6,524.80

[1] *For a colour legend, please refer to the HHI and GLR entries in the "Abbreviations and glossary" section.*
[2] *Copper: Grade A, LME, cash, in LME warehouse*

Table 4.23: Worldwide application of copper (source: Copper Alliance 2019)

Area of application	2018 [%]
Building construction	28
Electrical infrastructure and telecommunications networks	16
Transport (automobiles and other)	13
Industrial machinery and equipment	12
Cooling systems	8
Electronics	5
Other (instruments, tools, coins, etc.)	18
Total	**100**

Emerging technologies

The most important emerging technologies with a high growth potential that make use of copper are:

– Expansion of the power grid
– Electrical traction engines for motor vehicles
– Wind turbines
– Solid-state batteries

4.6.4 Copper demand in 2040

The additional raw material demands estimated on the basis of the technology synopses are shown in Table 4.24 and Figure 4.6. The emerging technologies segment under study currently requires about 19 % of 2018 copper production. This volume will multiply and could grow to as much as 45 % of 2018 mine production by 2035, depending on the scenario.

Table 4.24: Copper demand for selected emerging technologies, in tonnes

Technology	Demand in 2018	Demand in 2040		
		SSP1 Sustainability	SSP2 Middle of the Road	SSP5 Fossil Path
Electrical traction engines for motor vehicles	33,200	800,000	816.000	772,600
Alloys for lightweight airframe construction	11,000	12,000	13,000	18,000
Aircraft for 3D mobility (eVTOL)	–	150	390	390
Solid-state batteries	–	261,000	76,000	8,000
Quantum computers	3	1,150	1,150	1,150
Thin-film photovoltaics	14	79	8	0
Water electrolysis	29	110,400	31,300	5,800
CCS – Carbon capture and storage	–	22,300	61,100	0
Wind turbines	95,100	355,000	317,000	121,000
Desalination of sea water	28,400	21,400	14,300	29,300
Raw material recycling (of plastics)	126	1,930	2,490	1,080
Expansion of the power grid	3,825,000	3,832,000	5,759,000	8,211,000
Inductive transfer of electrical energy	195	65,640	46,290	17,900
Demand (accumulated)	**3,993,067**	**5,483,049**	**7,138,028**	**9,186,220**
Demand / Primary production 2018	19 %	27 %	35 %	45 %
Demand / Refinery production 2018	17 %	23 %	30 %	38 %

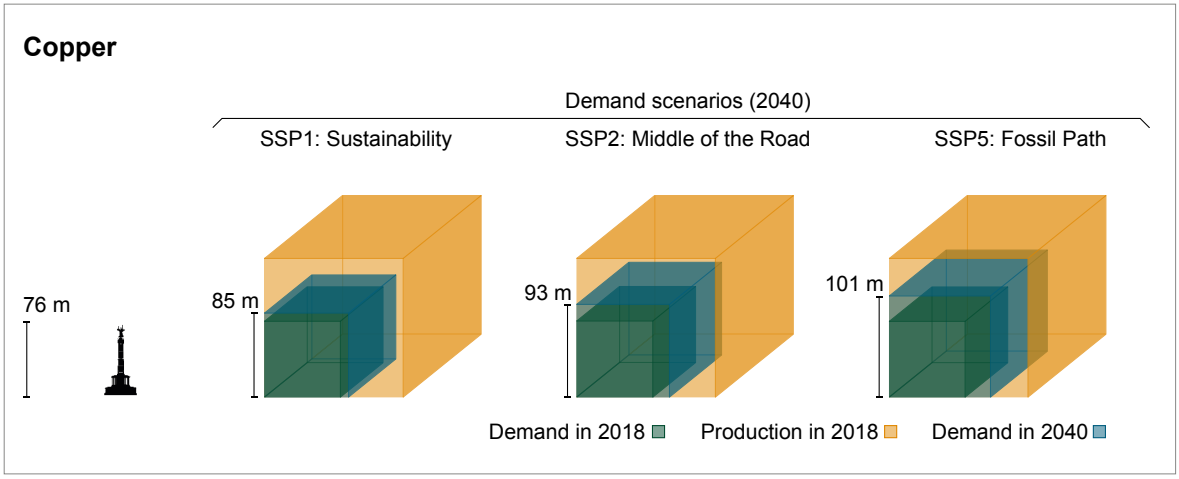

Figure 4.6: Copper refinery production in 2018 and demand for emerging technologies in 2018 and 2040

4.7 Lithium

Lithium is in third place in the first main group, the alkali metal group, of the periodic table of the elements. It was discovered in 1817 and gained industrial significance about a century later due to the demand for bearing metal for railways, for which lithium was needed as an alloying component (Wietelmann & Steinbild 2013).

4.7.1 Properties

Lithium is a silvery-white lustrous metal. It belongs to the group of light metals and has the lowest density of all solid elements (at room temperature) (Table 4.25). It is also very soft and easy to work into wire or very thin sheets. Lithium has good electrical conductivity. It is comparable to that of iron. Like all alkali metals, lithium has a high reactivity. Amongst all metals, it has the lowest redox potential (Römpp no date; Quadbeck-Seeger 2007; Wietelmann & Steinbild 2013; Schmidt 2017).

Table 4.25: Lithium properties

Density	0.53 g/cm^3
Melting point	180.5 °C
Electric conductivity	10.6 · 10^6 S/m
Thermal conductivity	85 W/(m · K)

4.7.2 Deposits and production

In the upper continental crust lithium is not as common as copper, but more common than zinc or lead. Due to its high reactivity, lithium is not found in nature as an element, but it is a component of numerous minerals. Some rare minerals have relatively high lithium contents, e.g. zabuyelite (Li_2CO_3) with a lithium content of approx 18.79 %. In contrast, the lithium contents of the technologically and economically important lithium minerals (amblygonite, eucryptite, lepidolite, petalite and spodumene) are in the range between approx. 2 % and 5.5 %. Lithium is not only found in bedrock but also in salt lakes, bottom waters of oil reservoirs, continental deep waters and clays such as hectorite (Römpp no date; Quadbeck-Seeger 2007; Bradley et al. 2017; Schmidt 2017).

The most important sources of lithium include lithium-bearing brines from salt lakes and the minerals contained in pegmatites (especially spodumene). Lithium concentrate, hydroxide, carbonate and chloride are extracted from them and then processed into other chemicals, reduced to metal or fed directly into end products. Most of the lithium produced worldwide comes from mining in Australia and China and from lithium brines in Argentina, Chile and China. Global lithium resources are estimated at 80 million tonnes. Two-thirds of these are located in the Americas, particularly Bolivia, Argentina, Chile and (to a lesser extent) the USA

Table 4.26: Lithium supply situation in 2010, 2013 and 2018 (sources: BGR 2021, USGS 2011c, USGS 2014c, USGS 2020f)

	2010	2013	2018
Mine production [tonnes of metal content]	26,044	30,718	95,170
Refinery production [tonnes of metal content]	–	–	–
Reserve [tonnes of metal content]	12,565,000	13,017,000	13,919,000
Resources [tonnes of metal content]	33,000,000	39,500,000	80,000,000
Most important countries for mining	Chile 37 % Australia 33 % Argentina 12 %	Australia 38 % Chile 37 % Argentina 8 %	Australia 61 % Chile 19 % China 7 %
Most important countries for refining	–	–	–
Country concentration – Mine production[1]	2,694	2,956	4,184
Country concentration – Refinery production	–	–	–
Weighted country risk – Mine production[1]	0.91	1.01	1.16
Weighted country risk – Refinery production	–	–	–
Price[2] [USD/tonne]	5,180.87	6,899.44	16,812.50

[1] *For a colour legend, please refer to the HHI and GLR entries in the "Abbreviations and glossary" section.*
[2] *Lithium: Lithium-carbonate, large contracts, USA, del. continental*

(Bradley et al. 2017; Schmidt 2017; Sun et al. 2017; USGS 2020f). An overview of the lithium supply situation is shown in Table 4.26.

4.7.3 Applications

The most noteworthy development in terms of lithium use is the massive shift in the demand structure towards batteries. The battery sector's share of total lithium demand has almost tripled in the last ten years and is now 65 %. This structural change was driven, amongst other factors, by the increasing demand for electronic mobile devices that use lithium-ion batteries. This trend will continue in the future, especially thanks to rising demand for batteries for e-mobility.

Ceramics and glasses, which were the main areas of application for lithium a few years ago, now account for only 18 % of total demand. Lithium concentrate (mainly α-spodumene) flows directly into the production of ceramics and reduces the sensitivity of the corresponding end products (including ceramic hobs) to strong and sudden temperature changes. An overview of the main areas of application of lithium is shown in Table 4.27.

Table 4.27: Worldwide application of lithium in 2010, 2013, 2019 (sources: USGS 2011c, USGS 2014c, USGS 2020f)

Area of application	2010 [%]	2013 [%]	2019 [%]
Glass and ceramics	31	35	18
Batteries	23	29	65
Greases	9	9	5
Polymers and pharmaceuticals	6	5	3
Air treatment	6	5	1
Aluminium melts	6	1	
Continuous casting	4	6	3
Other applications	15	10	5
Total	**100**	**100**	**100**

Emerging technologies

The most important emerging technologies with a high growth potential that make use of lithium are:

- Lithium-ion high-performance electricity storage
- Solid-state batteries

4.7.4 Lithium demand in 2040

The additional raw material demands estimated on the basis of the technology synopses are shown in Table 4.28 and Figure 4.7. The demand of the examined segment of emerging technologies was about 8 % of lithium production in 2018. This amount could increase to as much as 587 % of 2018 lithium production by 2040 as demand for electric vehicles with lithium-ion batteries increases, depending on the scenario.

4.8 PGM (ruthenium, iridium, platinum)

Platinum Group Metals (PGM) is a collective term for the six elements ruthenium, rhodium and palladium as well as osmium, iridium and platinum, all of which are precious metals. While the first three elements are light platinum metals (atomic numbers 44-46, density approx. 12 g/cm^3), osmium, iridium and platinum are heavy platinum metals (atomic numbers 76-78, density approx. 22 g/cm^3).

There is evidence that platinum was used more than 2,600 years ago. It was not scientifically described in Europe until 1750. Palladium and rhodium were first discovered around 1803 by Wil-

Table 4.28: Lithium demand for selected emerging technologies, in tonnes

Technology	Demand in 2018	Demand in 2040		
		SSP1 Sustainability	SSP2 Middle of the Road	SSP5 Fossil Path
Alloys for lightweight airframe construction	–	4,200	4,400	6,200
Aircraft for 3D mobility (eVTOL)	–	210	660	1,630
Lithium-ion high-performance electricity storage	7,460	377,300	328,100	72,600
Solid-state batteries	–	177,000	47,000	5,000
Radio frequency microchips	8	15	18	22
Demand (accumulated)	**7,468**	**558,725**	**380,178**	**85,452**
Demand / Primary production 2018	8 %	587 %	399 %	90 %

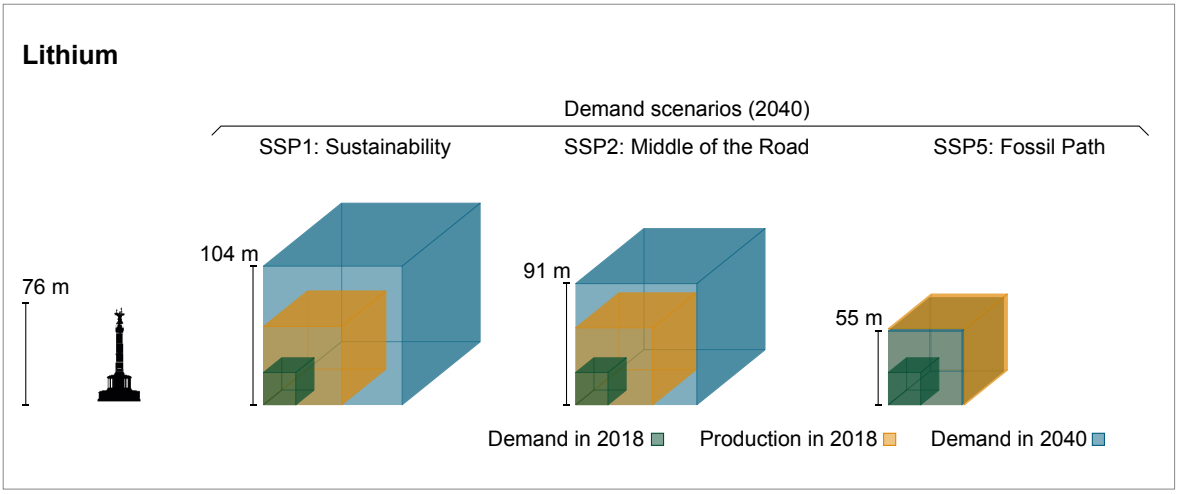

Figure 4.7: Lithium production in 2018 and demand for emerging technologies in 2018 and 2040

liam Hyde Wollaston, iridium and osmium around 1804 by Smithson Tennant and ruthenium even later, around 1844 by Carl Ernst Claus (RÖMPP no date; RENNER et al. 2018).

4.8.1 Properties

The chemical and physical properties of PGMs are very similar (Table 4.29). All PGMs are grey to highly silvery precious metals. In particular the outstanding catalytic properties of PGMs find industrial application, e.g. in the field of automotive exhaust catalysts (RÖMPP no date; RENNER et al. 2018).

Table 4.29: Ruthenium, iridium and platinum properties

	Ruthenium	Iridium	Platinum
Density	12.4 g/cm³	12.6 g/cm³	21.5 g/cm³
Melting point	2,334 °C	2,466 °C	3,827 °C
Electric conductivity	14.1 · 10⁶ S/m	19.7 · 10⁶ S/m	9.43 · 10⁶ S/m
Thermal conductivity	120 W/(m · K)	150 W/(m · K)	72 W/(m · K)

Table 4.30: PGM supply situation in 2010, 2013 and 2018 (sources: BGR 2021, JM 2020, JM 2021a, JM 2021b, USGS 2011d, USGS 2014d, USGS 2020g)

	2010	2013	2018
Mine production [tonnes of metal content]			
– Platinum	194	195	190
Refinery production [tonnes of metal content]			
– Ruthenium	29.4	25.8	33
– Iridium	10.5	6.2	6.8
Reserve [1] [tonnes of metal content]	66,110	66,110	69,310
Resources[1] [tonnes of metal content]	> 100,000	> 100,000	> 100,000
Most important countries for mining	South Africa 76 % Russia 13 % Zimbabwe 4 %	South Africa 70 % Russia 13 % Zimbabwe 7 %	South Africa 72 % Russia 11 % Zimbabwe 8 %
Most important countries for refining	–	–	–
Country concentration – Mine production[2,3]	5,999	5,999	5,402
Country concentration – Refinery production	–	–	–
Weighted country risk – Mine production[2,3]	0.09	0.09	0.06
Weighted country risk – Refinery production	–	–	–
Price for ruthenium[4] [USD/troz]	197.52	75.75	240.94
Price for iridium[5] [USD/troz]	641.49	836.14	1,283.77
Price for platinum[6] [USD/troz]	1,611.73	1,487.31	879.75

[1] *Figures for platinum group metals*
[2] *Figures for platinum*
[3] *For a colour legend, please refer to the HHI and GLR entries in the "Abbreviations and glossary" section.*
[4] *Johnson Matthey base price (unfab) USD per troy oz (09.00 hrs)*
[5] *Johnson Matthey base price (unfab) USD per troy oz*
[6] *99.95%, London, morning, in warehouse*

4.8.2 Deposits and production

PGMs are amongst the rarest metals. They occur in native form and in various minerals, e.g. laurite (RuS_2), osmiridium (Os–Ir) and sperrylite ($PtAs_2$). The majority of global PGM primary production and identified PGM primary resources can be attributed to two deposit types and three locations, respectively. On the one hand, there are the PGM-dominated deposits, especially mafic to ultramafic magmatic intrusions (Bushveld Complex in South Africa and Great Dyke in Zimbabwe) that serve as PGM sources. On the other hand, PGMs are extracted as by-products from nickel-copper dominated deposits, in particular from nickel-copper PGM mineralizations/intrusions (in the Russian Norilsk-Talnakh region) bound to rift zones and continental flood basalts. Approximately 26 % of the platinum demand is covered by recycling (Schmidt 2015; Zientek et al. 2017; Renner et al. 2018; JM 2021). An overview of the supply situation is shown in Table 4.30.

4.8.3 Applications

The majority of ruthenium demand is for chemical applications, e.g. the caprolactam and adipic acid industries, and the electronics sector, where ruthenium is mainly used in the manufacture of hard disks and chip-grade resistors. Iridium is largely used in electrochemical applications, e.g. chloralkali electrolysis, and in the electronics sector (as a crucible material in the production of crystals for electronics applications). As a versatile catalyst, platinum is mainly used as a catalyst. The jewellery industry also accounts for a large part of the platinum demand. The third most important use category for platinum is as a capital good or vehicle for storing wealth (JM 2021). Further areas of application are listed in Table 4.31.

Emerging technologies

The most important emerging technologies with a high growth potential that make use of PGM are:

– Data centres
– Water electrolysis
– Super alloys

4.8.4 PGM demand in 2040

Based on the analysis of the presented emerging technologies, the additional raw material demands for the PGMs ruthenium, iridium and platinum in Table 4.32 to Table 4.34 have been estimated and are shown in Figure 4.8 to Figure 4.10. For ruthenium, there was a demand of about 37 % of production in 2018 for the emerging technologies examined; for platinum and iridium, there was almost no demand in 2018 for the aforemen-

Table 4.31: Worldwide application of ruthenium, iridium and platinum in 2019 (source: JM 2021)

Area of application	Ruthenium [%]	Iridium [%]	Platinum [%]
Automotive catalysts			34
Jewelry			24
Investments			13
Chemical applications	37	9	8
Glass			5
Petrochemistry			3
Medical and biomedical sciences			3
Electronics	37	21	3
Electrochemical applications	13	35	
Other applications	13	36	7
Total	**100**	**100**	**100**

tioned emerging technologies. Demand could grow for ruthenium up to 1,922 % of 2018 refined metal production by 2040, depending on the scenario, driven primarily by the demand of data centres. Demand for platinum and iridium could also increase.

Table 4.32: Ruthenium demand for selected emerging technologies, in tonnes

Technology	Demand in 2018	Demand in 2040		
		SSP1 Sustainability	SSP2 Middle of the Road	SSP5 Fossil Path
Super alloys	12	22	21	29
Synthetic fuels	0	13.8	6.8	13.4
Data centres	0.1	44	167	592
Demand (accumulated)	**12**	**80**	**195**	**634**
Demand / Refinery production 2018	37 %	242 %	590 %	1,922 %

Table 4.33: Iridium demand for selected emerging technologies, in tonnes

Technology	Demand in 2018	Demand in 2040		
		SSP1 Sustainability	SSP2 Middle of the Road	SSP5 Fossil Path
Water electrolysis	0.01	34	20	2
Demand (accumulated)	**0.01**	**34**	**20**	**2**
Demand / Refinery production 2018	0 %	500 %	294 %	29 %

Table 4.34: Platinum demand for selected emerging technologies, in tonnes

Technology	Demand in 2018	Demand in 2040		
		SSP1 Sustainability	SSP2 Middle of the Road	SSP5 Fossil Path
Water electrolysis	0.01	6	2	0.33
Data centres	0.1	60	230	810
Demand (accumulated)	**0.11**	**66**	**232**	**810**
Demand / Primary production 2018	0 %	35 %	122 %	426 %

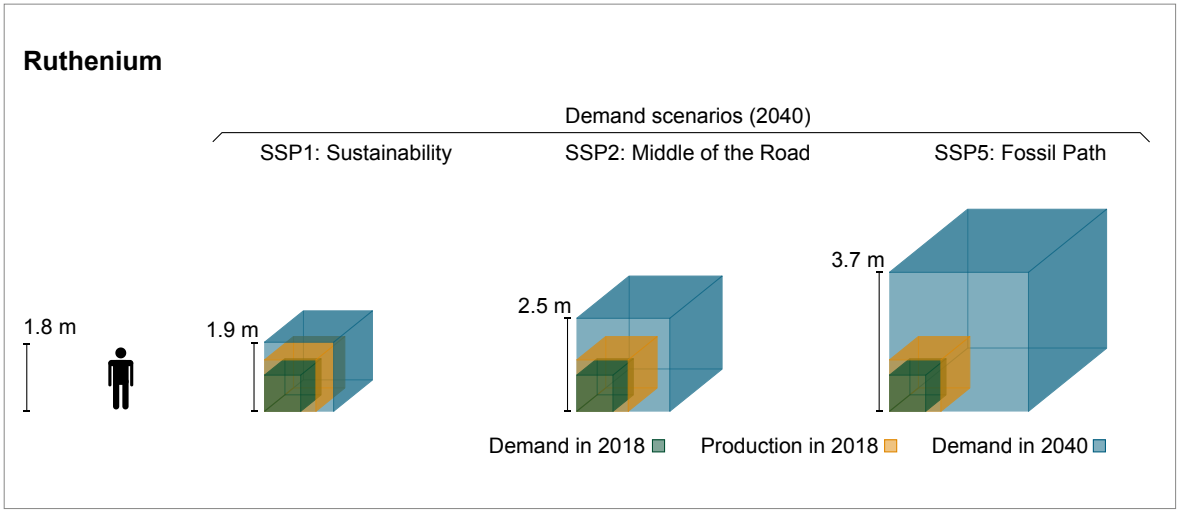

Figure 4.8: Ruthenium production in 2018 and demand for emerging technologies in 2018 and 2040

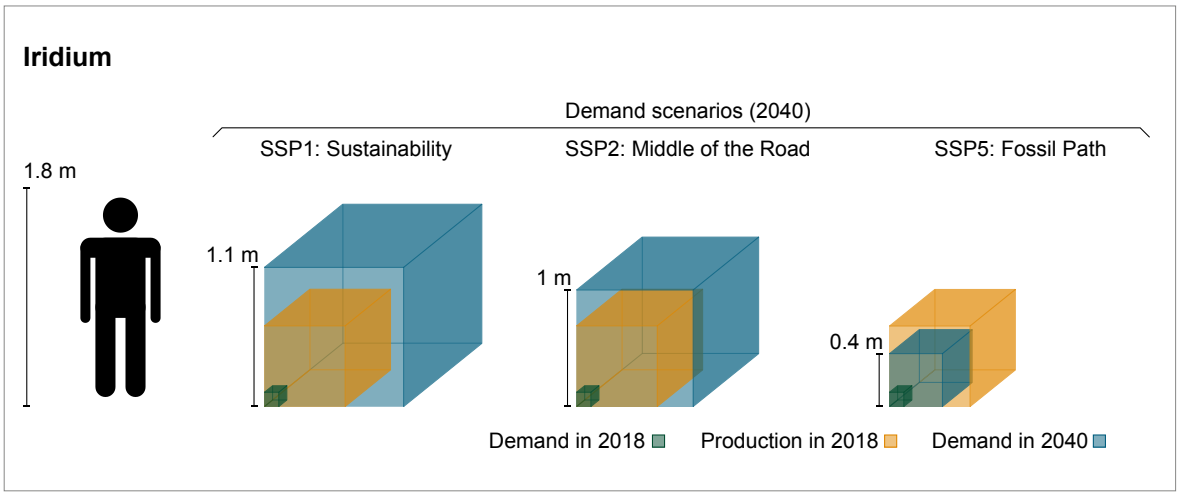

Figure 4.9: Iridium production in 2018 and demand for emerging technologies in 2018 and 2040

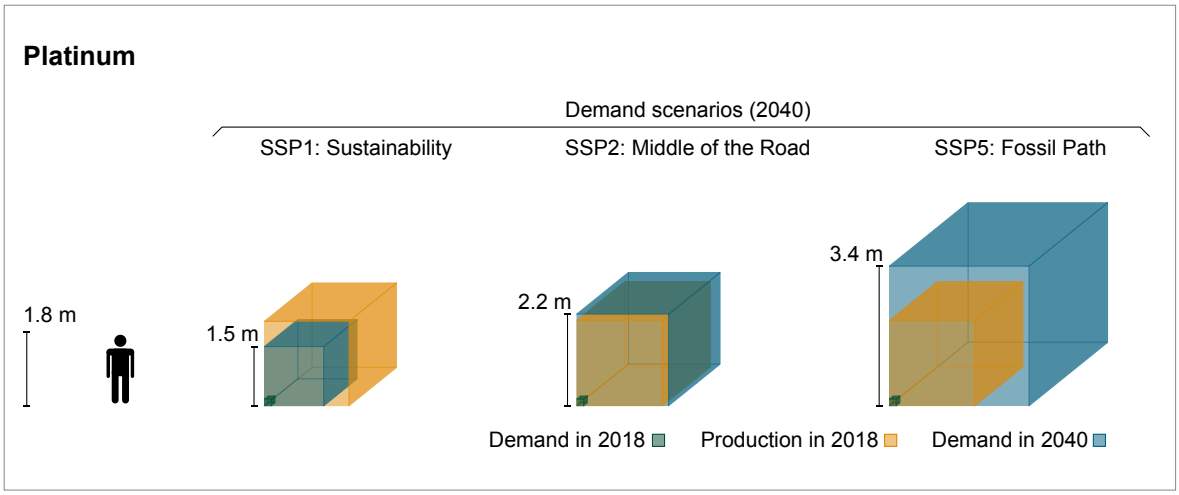

Figure 4.10: Platinum production in 2018 and demand for emerging technologies in 2018 and 2040

4.9 Rhenium

Together with manganese and technetium, rhenium is in the 7th subgroup, the manganese group, of the periodic table of the elements. It was predicted in 1871 but not isolated until 1925, making it the last natural element to be discovered. The first industrial rhenium production started in the 1930s, but due to high production costs rhenium did not become industrially important (as an alloying material) until the 1950s (RÖMPP n.d.; NADLER 2003; JOHN 2015; MMTA 2015; USGS 2020j).

4.9.1 Properties

Rhenium is a silvery-white transition metal. It has a catalytic effect, high density and is (sometimes) counted amongst the precious metals. Of all metals, it has the highest boiling point (5,596 °C) and the second highest melting point (after tungsten) (Table 4.35). In general, it has similar properties to molybdenum. As an alloy component, rhenium increases, inter alia, ductility at low temperatures and strength at high temperatures (RÖMPP o. J; NADLER 2003; QUADBECK-SEEGER 2007; JOHN et al. 2017).

Table 4.35: Rhenium properties

Density	21.0 g/cm³
Melting point	3,186 °C
Electric conductivity	5.56 · 10⁶ S/m
Thermal conductivity	48 W/(m · K)

4.9.2 Deposits and production

In the continental crust rhenium is one of the rarest elements. Native rhenium (in trace form) and the rhenium mineral rheniite (ReS_2) occur rarely. Rhenium-rich minerals (especially tarkianite with a rhenium content of about 54 %) are economically insignificant. The main source of rhenium is molybdenite (MoS_2) in which rhenium occurs as a substitute for molybdenum in widely varying concentrations (KOJONEN et al. 2004; JOHN 2015; JOHN et al. 2017).

Rhenium is mainly a by-product of copper mining and in particular of molybdenum extraction. For this porphyry but also stratabound copper deposits are used. Large quantities of rhenium are recycled and serve as a secondary source of rhenium. Of the primary rhenium produced globally

Table 4.36: Rhenium supply situation in 2010, 2013 and 2018 (sources: BGR 2021, USGS 2011e, USGS 2014e, USGS 2020i)

	2010	2013	2018
Mine production [tonnes of metal content]	45	49	50
Refinery production [tonnes of metal content]	–	–	–
Reserve [tonnes of metal content]	2,453	2,453	2,372
Resources [tonnes of metal content]	11,000	11,000	11,000
Most important countries for mining	Chile 55 % USA 14 % Poland 10 %	Chile 51 % Poland 15 % USA 15 %	Chile 54 % Poland 18 % USA 16 %
Most important countries for refining	–	–	–
Country concentration – Mine production[1]	3,439	3,165	3,552
Country concentration – Refinery production	–	–	–
Weighted country risk – Mine production[1]	0.81	0.81	0.81
Weighted country risk – Refinery production	–	–	–
Price[2] [USD/kg]	4,828.53	3,400.21	1,519.17

[1] *For a colour legend, please refer to the HHI and GLR entries in the "Abbreviations and glossary" section.*
[2] *In warehouse Rotterdam, duty unpaid, APR catalytic grade*

in 2019, (an estimated) 55 % comes from Chile; other significant producers include Poland and the USA. Germany and the USA are leading in the production of secondary rhenium. The world's rhenium reserves are largely distributed amongst Chile, the USA, Russia and Kazakhstan (John et al. 2017; USGS 2017e; USGS 2020i). Table 4.36 contains an overview of the worldwide rhenium supply situation.

4.9.3 Applications

Due to the previously described (thermal and catalytic) properties of rhenium, it is an important component of heat-resistant materials/ super alloys and catalysts. For example, rhenium is used in the production of turbine blades, which are installed in aircraft, and catalysts, which are used in oil refinery processes (for reforming). Rhenium alloys are also found in numerous other products, including electrical contacts, electromagnets, semiconductors and electron tubes (Quadbeck-Seeger 2007; USGS 2017e; USGS 2020i). Worldwide, 80 % of rhenium demand is for super alloys (European Commission 2020a). An overview of the areas of application in the EU is provided in Table 4.37.

Table 4.37: Rhenium usage in the EU (sources: European Commission 2020a, European Commission 2020b)

Area of application	2012–2016 [%]
Aerospace	83
Catalysts (for the petroleum industry)	17
Total	**100**

Emerging technologies

The most important emerging technology with a high growth potential that makes use of rhenium is:

– Super alloys

4.9.4 Rhenium demand in 2040

The additional raw material demand estimated on the basis of the technology synopses are shown in Table 4.38 and Figure 4.11. The emerging technologies examined here already require about 30 % of total refinery production today. Rhenium demand for super alloys could grow to as much as 72 % of 2018 mine production by 2040, depending on the scenario.

Table 4.38: Rhenium demand for selected emerging technologies, in tonnes

Technology	Demand in 2018	Demand in 2040		
		SSP1 Sustainability	SSP2 Middle of the Road	SSP5 Fossil Path
Super alloys	15	28	26	36
Demand (accumulated)	**15**	**28**	**26**	**36**
Demand / Primary production 2018	30 %	56 %	52 %	72 %

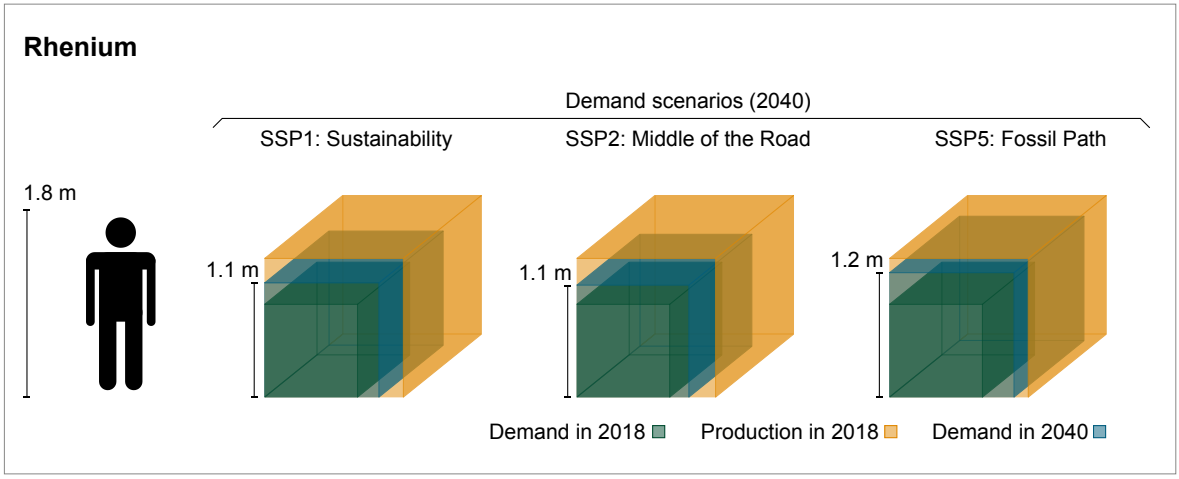

Figure 4.11: Rhenium production in 2018 and demand for emerging technologies in 2018 and 2040

4.10 Scandium

Scandium is in the third subgroup, the scandium group, of the periodic table of the elements. It was discovered in 1879, but received little scientific attention over the following decades due to difficulties in obtaining it in sufficient quantity and purity. It was not until 1937 that (95 % pure) scandium was first produced in its metallic form. From the 1950s onwards, there was increased research into scandium – thanks in part to its extractability from nuclear fission processes – which, along with discoveries in the area of application of alloys in the 1960s/70s, paved the way for its (current) industrial use (Horovitz 1975; Bünzli & Mcgill 2018).

4.10.1 Properties

Scandium is a silvery-white, soft metal. It is counted amongst the light, transition and (mostly) rare earth metals. It is almost as light as aluminium, is combustible as a powder and has catalytic properties. Similar to aluminium, it forms a protective oxide layer in the air. For a long time, the alloying properties of scandium were of primary economic interest: A scandium addition of 0.1-0.5 % increases the strength and melting point of aluminium without a (significant) increase in weight; the resulting alloy is weldable (Römpp no date; Enghag 2004; Emsley 2014; Binnemans et al. 2018).

Table 4.39: Scandium properties

Density	2.98 g/cm³
Melting point	1,541 °C
Electric conductivity	1.81 · 10⁶ S/m
Thermal conductivity	16 W/(m · K)

4.10.2 Deposits and production

Scandium is relatively widespread in the earth's crust; it is more abundant than, for example, lead, but it occurs dispersed. It is rarely found in commercially viable concentrations. Scandium (rich) minerals include thortveitite ($Sc_2Si_2O_7$), sterrettite ($ScPO_4{\cdot}2H_2O$) and kolbeckite ($(Sc,Be,Ca)(SiO_4,PO_4){\cdot}2H_2O$). Scandium also occurs in low concentrations combined with numerous other minerals (in the form of solid solutions). Tungsten ores (especially wolframite) and tin ores (especially cassiterite) may contain up to 1 % scandium. In contrast, uranium ores used commercially as a source of scandium have much lower concentrations. Scandium occurs as a trace element in most rare earth minerals (Römpp no date; Emsley 2014; Bünzli & Mcgill 2018; USGS 2020k).

Due to the low concentrations in which it primarily occurs, scandium is only recovered as a by-product of the extraction processes of iron ore, rare

earths, titanium, zirconium, uranium, cobalt, nickel and apatite. As the properties of scandium are similar to those of aluminium, the element also occurs in stronger concentrations in some laterites, for example in Australia. Methods and feasibility studies for the extraction of scandium as a by-product of aluminium mining, processing and refining are being developed or are underway (Elsner et al. 2010; Al Barazi et al. 2016; USGS 2020k).

Compared to other metal markets, the scandium market is relatively small; the annual demand for scandium is estimated at 10 to 15 tonnes. The leading producers are China, Philippines and Russia. Detailed information on country concentrations or country risks cannot be provided, as the quantities of scandium produced are not published (Elsner et al. 2010; USGS 2020k).

Information on reserves and resources is also not available in any detail or is incomplete (cf. Table 4.40). Scandium reserves are reported for Australia and the Philippines, amongst others. Scandium resources are extensive and are found in Australia, Canada, China, Kazakhstan, Madagascar, Norway, Philippines, Russia, Ukraine and the USA (USGS 2020k).

4.10.3 Applications

According to Grandfield (2018), the solid oxide fuel cell (SOFC) sector accounted for approximately three-quarters of the scandium market in 2017. In SOFCs, scandium-stabilised zirconium dioxide is used as an electrolyte, amongst other things, and allows lower operating temperatures and thus a longer service life of the SOFC compared to the usual alternatives. In addition, scandium is used as an alloying material for the construction of sports equipment (e.g. bicycles) and in the aerospace industry (Binnemans et al. 2018; CM 2018; Grandfield 2018). Table 4.41 classifies these areas of application quantitatively.

Table 4.41: Scandium applications 2017 (source: Grandfield 2018)

Area of application	2017 [%]
Solid oxide fuel cells (SOFCs)	74
Sports equipment	10
Aerospace industry	3
Other	13
Total	**100**

Table 4.40: Scandium supply situation in 2010, 2013 and 2018 (source: BGR 2021)

	2010	2013	2018
Mine production [tonnes of Sc_2O_3 content]	8.2	9.6	14 (9.1 tonnes of metal content)
Refinery production [tonnes of metal content]	–	–	–
Reserve [tonnes of metal content]	–	–	–
Resources [tonnes of metal content]	–	–	–
Most important countries for mining	–	–	–
Most important countries for refining	–	–	–
Country concentration – Mine production	–	–	–
Country concentration – Refinery production	–	–	–
Weighted country risk – Mine production	–	–	–
Weighted country risk – Refinery production	–	–	–
Price for scandium oxide[1] [RMB/kg]	11,500.00	22,507.94	7,025.44

[1] *Scandium oxide, min. 99.5%, China*

Emerging technologies

The most important emerging technology with a high growth potential that makes use of scandium is:

– SOFC – Stationary fuel cell

4.10.4 Scandium demand in 2040

The additional raw material demands estimated on the basis of the technology synopses are shown in Table 4.42 and Figure 4.12. It is assumed in the technology scenario that Sc-Al alloys will hardly play a role in aviation in the long term. Scandium demand for the emerging technologies segment under study was 55 % of mine production in 2018 and could be as high as 791 % in 2040 in terms of 2018 production, depending on the scenario.

4.11 Rare earth metals

Various definitions and subgroupings of rare earth metals are used in the literature. In the following, the rare earth metals are defined as a group of 16 metals that includes lanthanum and the 14 elements that follow lanthanum in the periodic table, the lanthanides, as well as yttrium. The rare earth metals are divided into the light rare earth metals and the heavy rare earth metals. The subgroup of light rare earth metals includes lanthanum, cerium, praseodymium, neodymium, promethium, samarium and europium (cerium group). The heavy rare earth subgroup includes yttrium, gadolinium, terbium, dysprosium, holmium, erbium, thulium, ytterbium and lutetium. The division into light and heavy rare earth metals is also not consistent in the literature. Europium, for example, is sometimes classified as a heavy rare earth rather than a light rare earth (Elsner 2011; Binnemans et al. 2018; Bünzli & Mcgill 2018).

Table 4.42: Scandium demand for selected emerging technologies, in tonnes

Technology	Demand in 2018	Demand in 2040		
		SSP1 Sustainability	SSP2 Middle of the Road	SSP5 Fossil Path
Water electrolysis	0.01	24	7	1
SOFC – Stationary fuel cell	5	48	27	5
Demand (accumulated)	**5**	**72**	**34**	**6**
Demand / Primary production 2018	55 %	791 %	374 %	66 %

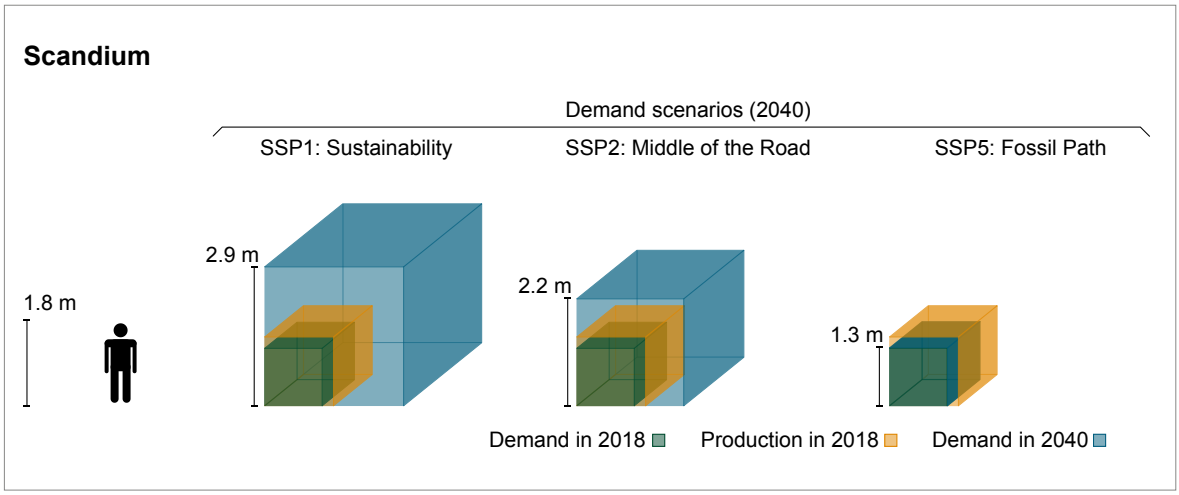

Figure 4.12: Scandium production in 2018 and demand for emerging technologies in 2018 and 2040

The discovery of rare earth metals took place over a period of more than 100 years. Yttrium was the first to be discovered, in 1794, and lutetium the last, in 1907. The first industrial applications emerged at the end of the 19th century in the metal/alloy sector (including the invention of “misch metal”). Around the middle of the 20th century, in a second wave of development, many new areas of application were added, e.g. in glass and in the field of catalytic cracking (petroleum processing). As a result, a strong growth in the industrial use of rare earth metals occurred from the mid-1960s and continued until the 2000s thanks to the development of new areas of application (including in the field of automotive exhaust catalysts, FCC catalysts, magnets, batteries, etc.) (Bünzli & Mcgill 2018; Wang et al. 2020).

4.11.1 Properties

Rare earth metals in elemental form are iron-grey to lustrous silver. They are relatively soft and their degree of elasticity increases with the degree of purity. Within the rare earth group, the melting point varies in the range between 798 °C (cerium) and 1,663 °C (lutetium). Most rare earth metals are strongly paramagnetic; the heavier rare earth metals are ferromagnetic at low temperatures. In general, rare earth metals are very reactive and rather base metals. They are flammable at elevated temperatures; finely powdered they are often pyrophoric. All oxidise rapidly in air, can absorb much hydrogen in powder form, and dissolve rapidly when exposed to weak acids. (Individual) rare earth metals and their chemical compounds have many other industrially important properties (including optical, catalytic and alloying properties). For an overview, see e.g. Bünzli & Mcgill (2018). In general, rare earth metals are similar in their chemical properties because they all have the same external electron number (Römpp no date; Quadbeck-Seeger 2007; Bünzli & Mcgill 2018).

4.11.2 Deposits and production

Despite their name, which is due to their historical classification in the 18th and 19th centuries, rare earth metals are not necessarily rare. In fact, the elemental abundance varies greatly within the rare earth metal group. For example, promethium does not have a stable isotope and therefore does not occur naturally (apart from stores resulting, for example, from spontaneous nuclear fission of uranium-238). The proportion of promethium in rare earth minerals is less than 10^{-19} %. Although lutetium and thulium do not fall into this extreme category, they are nevertheless very rare – their abundance in the earth’s upper crust is comparable to that of silver. Other rare earth metals are by all

Table 4.43: Properties of selected light rare earth metals

	Lanthanum	Praseodymium	Neodymium
Density	6.2 g/cm³	6.5 g/cm³	7.0 g/cm³
Melting point	920 °C	935 °C	1.024 °C
Electric conductivity	1.63 · 10^6 S/m	1.43 · 10^6 S/m	1.56 · 10^6 S/m
Thermal conductivity	13 W/(m · K)	13 W/(m · K)	17 W/(m · K)

Table 4.44: Properties of selected heavy rare earth metals

	Yttrium	Terbium	Dysprosium
Density	4.4 g/cm³	8.2 g/cm³	8.6 g/cm³
Melting point	1,526 °C	1,356 °C	1,407 °C
Electric conductivity	1.66 · 10^6 S/m	0.87 · 10^6 S/m	1.08 · 10^6 S/m
Thermal conductivity	17 W/(m · K)	11 W/(m · K)	11 W/(m · K)

means less rare. The most abundant of these in the (upper) continental crust is cerium. It is more common than, for example, cobalt, copper or lead. In general, light rare earth metals occur more frequently than heavy rare earth metals (Elsner 2011; van Gosen et al. 2017; Binnemans et al. 2018; Bünzli & Mcgill 2018; USGS 2020h).

Rare earth metals occur in numerous minerals, most of which belong to the group of silicates, oxides, carbonates or phosphates. A categorization of the rare earth minerals is also possible on the basis of the rare earth subgroups dominating in them (or forming their main component). This way three categories can be defined: 1. Minerals in which light rare earth metals predominate. 2. Minerals in which heavy rare earth metals dominate. 3. Complex minerals in which both light and heavy rare earth metals may be dominant. Representative minerals of these three categories are bastnaesite and monazite, xenotime as well as fergusonite, all of which have relatively high rare earth contents (Römpp no date; Dostal 2017; van Gosen et al. 2017; Bünzli & Mcgill 2018).

Amongst the most important rare earth minerals are bastnaesite, monazite and xenotime; a large part of the rare earth resources is bound in them. In addition to these three, several other rare earth minerals are economically exploitable, including synchisite, loparite and eudialyte. The most important deposits of rare earth metals include, for example, carbonatites containing bastnaesite, monazite/xenotime-bearing placer deposits, magmatic alkali rocks in which loparite is found, and ion adsorption rocks in lateritic weathering crusts. The latter are a major source of heavy rare earth metals; light rare earth metals are mainly derived from carbonatites and the aforementioned placer deposits (Römpp no date; Schorn no date; Adler & Müller 2014; Dostal 2017; USGS 2017d; van Gosen et al. 2017; Bünzli & Mcgill 2018; Balaram 2019).

The production, in other words extraction and processing, and supply situation are characterised by three (interrelated) properties of rare earth metals/minerals: Rare earth metals are similar in their chemical properties and occur together in deposits/minerals in sometimes very different concentrations; the rare earth minerals mainly used today contain significant amounts of uranium and thorium. These circumstances give rise to the central characteristics of rare earth metal production: rare earth metals are to a large extent produced as by-products – they are not only by-products of the extraction process of non-rare earth metals (e.g. iron ore, heavy minerals and tin ore), but can also be understood as by-products of each other (see below). In production, the separation of rare earth elements (from each other) plays a central role; from a chemical point of view, the extraction is challenging and the methods used for this are not very selective. The uranium/thorium content of rare earth minerals not only poses a production challenge from an environmental point of view, but also leads to the partial non-utilisation of some minerals in specific deposits. In general, these production characteristics result in a complex supply situation, which is characterised by a high country concentration in mine production (see Table 4.45), “criticality” of rare earth metals and imbalances between the demand structure and the geological-technical production-supply structure in the rare earth market. The latter problem in particular is triggered by the strong coupling of the production of the individual rare earth metals, which means that some rare earth metals that occur in ores in high concentrations have excess production to meet the demand for other rare earth metals that occur in rather low concentrations (Elsner 2011; van Gosen et al. 2017; Binnemans et al. 2018; Bünzli & Mcgill 2018).

Today, China’s share of global (documented) rare earth production is about 65 %, much smaller than it was a few years ago. Other major countries for production are the USA, Myanmar and Australia, which together account for about 33 %. The majority of rare earth reserves are distributed amongst China, Brazil, Vietnam and Russia. Their cumulative share of global reserves is 83 % (USGS 2016; USGS 2020h). Table 4.45 provides an overview of the supply situation.

4.11.3 Applications

Rare earth metals have numerous applications that can be classified into the following areas: Magnets (in hard drives, speakers, headphones, motors, generators), catalysts (FCC, automotive catalysts), metallurgy/alloys (increasing hot workability, copper and aluminium alloys), energy (fuel cells, metal hydrides in batteries), glass and ceramics (UV blockers, colourants/pigments, polishing agents for glass), electronics (screens/displays, capacitors,

Table 4.45: Rare earth metals supply situation in 2010, 2013 and 2018 (source: BGR 2021)

	2010	2013	2018
Mine production[1] [tonnes of SEO]	139,393	92,884	173,800
Refinery production [tonnes of metal content]			
– Dysprosium	–	–	1,000
– Lanthanum	–	–	35,800
– Neodymium	–	–	23,900
– Praseodymium	–	–	7,500
– Terbium	–	–	280
– Yttrium	–	–	7,600
Reserve [1] [1,000 tonnes of SEO]	113,778	136,230	111,731
Resources [1,000 tonnes of SEO]	–	–	–
Most important countries for mining[1]	China 85 % Vietnam 8 % Thailand 4 %	China 90 % USA 4 % Vietnam 2 %	China 69 % Australia 10 % Myanmar 9 %
Most important countries for refining[1]	–	–	–
Country concentration – Mine production[1,2]	7,357	8,066	4,997
Country concentration – Refinery production[1,2]	–	–	–
Weighted country risk – Mine production[1,2]	–0.54	–0.46	–0.08
Weighted country risk – Refinery production[1,2]	–	–	–
Price for dysprosium[3] [USD/kg]	310.29	698.65	261.97
Price for neodymium[3] [USD/kg]	60.74	90.93	63.72
Price for praseodymium[3] [USD/kg]	62.21	104.59	114.48
Price for terbium[3] [USD/kg]	718.26	1,356.06	604.25

[1] All rare earth metal oxides
[2] For a colour legend, please refer to the HHI and GLR entries in the "Abbreviations and glossary" section.
[3] min. 99 % fob China

thermistors, semiconductors), photonics (phosphors, lasers in medicine, telecommunication systems), etc. For a more in-depth overview of these and other application areas, see Bünzli & Mcgill (2018). The most important applications (in terms of quantity) for rare earth metals are magnets and catalysts. They account for more than half of the rare earth demand (see Table 4.46).

Emerging technologies

The most important emerging technologies with a high growth potential that make use of rare earth metals are:

- Electrical traction engines for motor vehicles
- Wind turbines
- High-performance permanent magnets

Table 4.46: Worldwide application of rare earth metals in 2018 (source: Gao et al. 2019)

Area of application	2018 [%]
Magnets	34
Catalysts	17
Polishing agents (powder)	11
Batteries (NiMH)	6
Other (metallurgy/alloys, glass/ceramics, luminescent materials)	32
Total	**100**

4.11.4 Rare earth metal demand in 2040

The additional raw material demands estimated on the basis of the technology synopses are shown in Table 4.47 to Table 4.50 and are illustrated in Figure 4.13 to Figure 4.16.

For light rare earth metals, demand in neodymium and praseodymium applications could increase up to 227 % of 2018 primary production by 2040, depending on the scenario (Table 4.48). As for heavy rare earth metals, total demand could increase up to 687 % of 2018 refined metal production by 2040 for dysprosium and terbium (Table 4.50). The demands for lanthanum are shown in Table 4.47 and for yttrium in Table 4.49.

Table 4.47: Lanthanum demand for selected emerging technologies, in tonnes

Technology	Demand in 2018	Demand in 2040		
		SSP1 Sustainability	SSP2 Middle of the Road	SSP5 Fossil Path
Solid-state batteries	–	38,000	11,000	1,200
Water electrolysis	0.1	370	100	20
SOFC – Stationary fuel cell	2	270	150	29
Demand (accumulated)	**2.1**	**38,640**	**11,250**	**1,249**
Demand / Refinery production 2018	0 %	108 %	31 %	3 %

Table 4.48: Light rare earth metals demand for selected emerging technologies, in tonnes

Technology	Elements	Demand 2018	Demand in 2040		
			SSP1 Sustainability	SSP2 Middle of the Road	SSP5 Fossil Path
Electrical traction engines for motor vehicles	Pr, Nd	1,430	34,050	31,350	31,960
Autonomous driving of motor vehicles	Pr, Nd	0	15	16	22
Aircraft for 3D mobility (eVTOL)	Pr, Nd	–	11	30	70
Wind turbines	Nd	2,430	13,470	8,900	3,180
Wind turbines	Pr	390	2,420	1,480	520
High-performance permanent magnets	Pr, Nd	5,620	19,630	20,340	24,270
Data centres	Pr, Nd	180	62	530	9,220
Demand (accumulated)		**10,050**	**69,658**	**62,646**	**69,242**
Demand / Refinery production 2018	Pr, Nd	32 %	222 %	200 %	221 %

Table 4.49: Yttrium demand for selected emerging technologies, in tonnes

Technology	Demand in 2018	Demand in 2040		
		SSP1 Sustainability	SSP2 Middle of the Road	SSP5 Fossil Path
Autonomous driving of motor vehicles	0	930	1,050	1,400
Water electrolysis	0.7	2,800	800	150
SOFC – Stationary fuel cell	2	840	470	90
Demand (accumulated)	**2.7**	**4,570**	**2,320**	**1,640**
Demand / Refinery production 2018	0 %	60 %	31 %	22 %

Table 4.50: Heavy rare earth metals (dysprosium, terbium) demand for selected emerging technologies, in tonnes

Technology	Elements	Demand 2018	Demand in 2040		
			SSP1 Sustainability	SSP2 Middle of the Road	SSP5 Fossil Path
Electrical traction engines for motor vehicles	Dy, Tb	500	5,140	7,530	7.680
Wind turbines	Dy	270	1,370	970	350
Wind turbines	Tb	77	480	290	100
Demand (accumulated)		**847**	**6,990**	**8,790**	**8,130**
Demand / Refinery production 2018	Dy, Tb	66 %	546 %	687 %	635 %

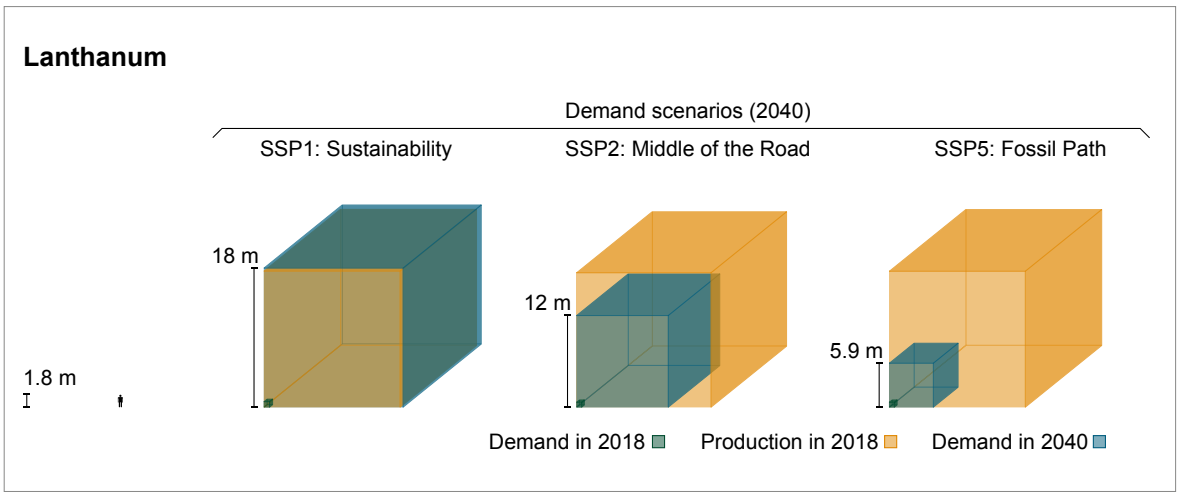

Figure 4.13: Lanthanum production in 2018 and demand for emerging technologies in 2018 and 2040

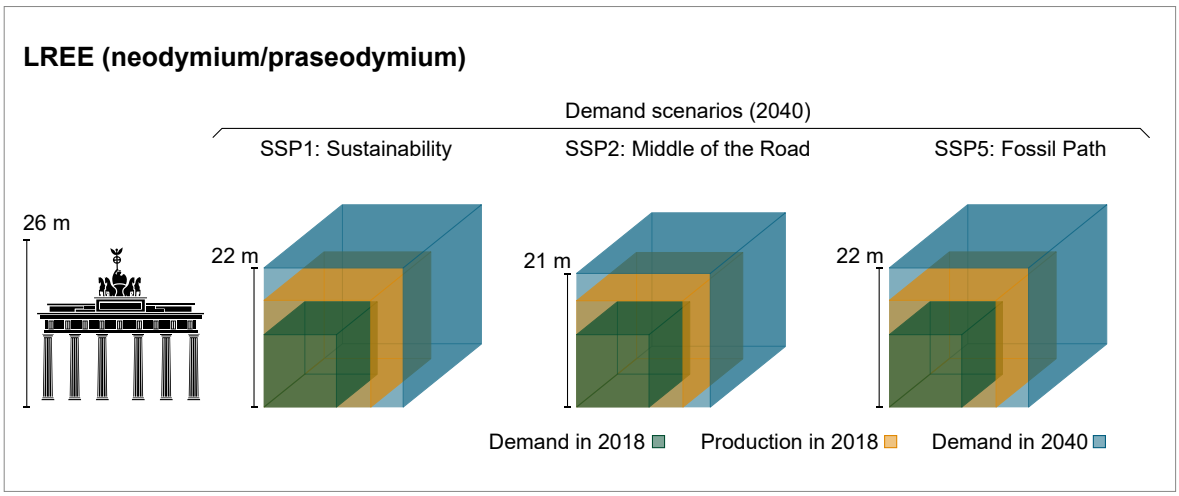

Figure 4.14: Neodymium / praseodymium production in 2018 and demand for emerging technologies in 2018 and 2040

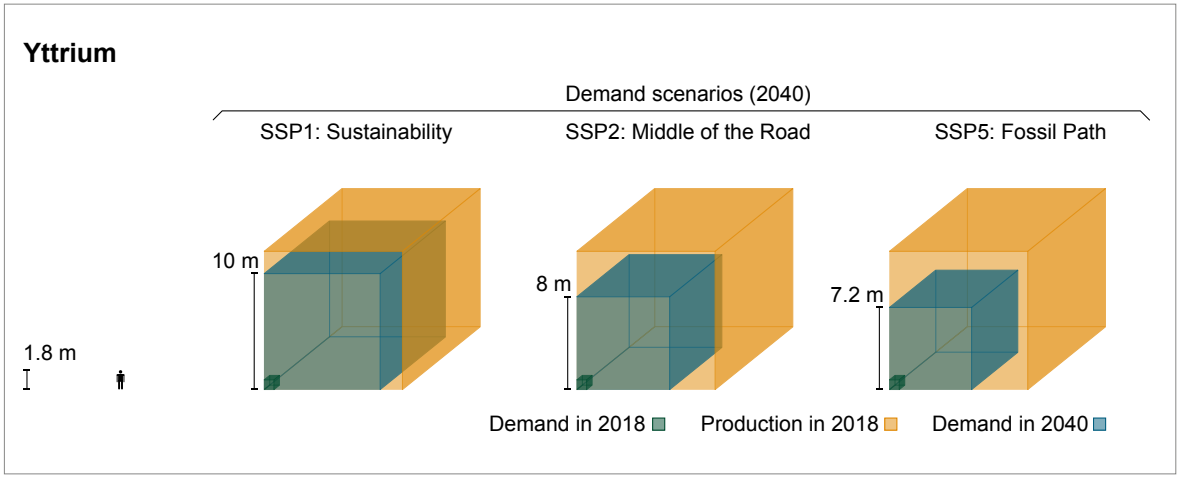

Figure 4.15: Yttrium production in 2018 and demand for emerging technologies in 2018 and 2040

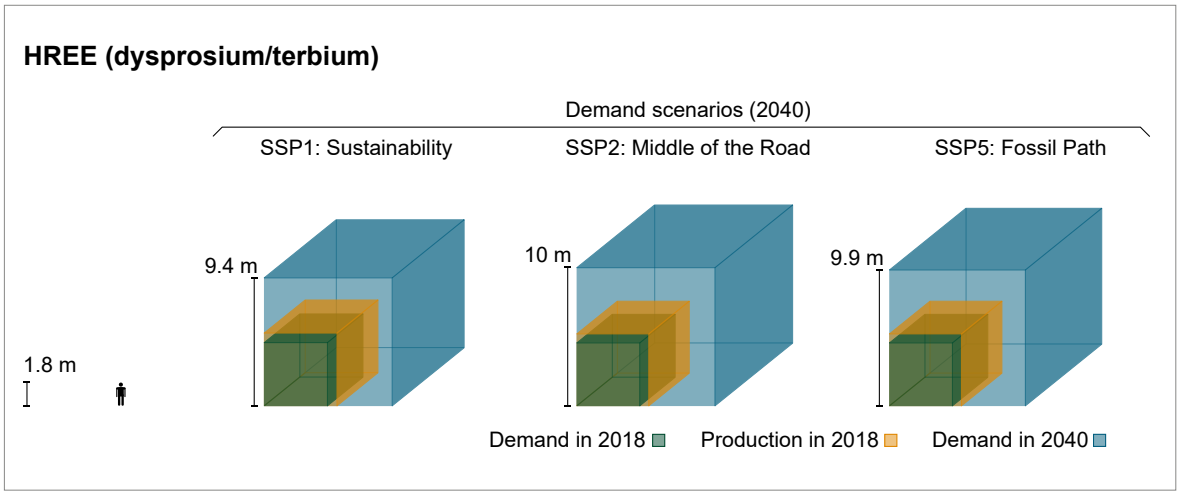

Figure 4.16: Dysprosium / terbium production in 2018 and demand for emerging technologies in 2018 and 2040

4.12 Tantalum

Tantalum is in the 5th subgroup of the periodic table of the elements below vanadium and niobium. It was discovered in 1802 (as an oxide) and isolated for the first time in 1903. In the 20th century, tantalum was used for various areas of application that, among other properties, took advantage of its heat and corrosion resistance and hardness. Amongst other things, the development of tantalum electrolytic capacitors in the 1950s, which resulted in a strong growth in demand in this area, is significant for the current use structure of tantalum (RÖMPP no date; ALBRECHT et al. 2012; TERCERO ESPINOZA 2012).

4.12.1 Properties

Tantalum is a platinum-grey metal. In addition to its high melting and boiling points and high thermal and electrical conductivity, it is very strong and ductile (Table 4.51). A thin, but very dense, stable layer of tantalum pentoxide (Ta_2O_5) is responsible for the passivation, which provides corrosion resistance to most acids. As a refractory metal, it resembles titanium and niobium in many respects and can partly replace them in applications (RÖMPP no date; ALBRECHT et al. 2012; SCHULZ et al. 2017).

Table 4.51: Tantalum properties

Density	16.7 g/cm³
Melting point	2,996 °C
Electric conductivity	7.6 · 10⁶ S/m
Thermal conductivity	57 W/(m · K)

4.12.2 Deposits and production

Tantalum occurs almost exclusively together with niobium. Both have similar physical and chemical properties, although tantalum is about ten times rarer than niobium (20 ppm), averaging 2 ppm in the earth's crust. It does not occur naturally in solid form. The most important tantalum and niobium compounds in terms of economic value are oxides, and the minerals of the columbite-tantalite solid solution series are particularly important for mining. Examples of tantalum minerals/ores with Ta_2O_5 contents ranging from 40 % to 85 % are tantalite ($(Fe,Mn)Ta_2O_6$), vodginite ($(Mn,Sn,Ti)Ta_2O_6$), microlite ($Ca_2Ta_2O_6(O,OH,F)$) and tapiolite ($FeTa_2O_6$); columbite ($(Fe,Mn)(Nb,Ta)_2O_6$) has a Ta_2O_5 content ranging from 1 % to 40 % (Römpp no date; Albrecht et al. 2012; Schulz et al. 2017; Damm 2018).

Tantalum is largely extracted from tantalite and columbite-tantalite mix ore ("coltan"). Cassiterite, loparite and tantalum-bearing tin slags obtained as a by-product are also used. The (economically) most important tantalum deposits are rare-metal granites and rare-metal pegmatites; the majority of the world's resources are bound up in them (Römpp no date; Albrecht et al. 2012; Schulz et al. 2017; USGS 2017a; Damm 2018).

The majority of the world's tantalum resources are located in South America, particularly Brazil and Australia. Significant reserves are also reported for these countries. The most important countries for mining are currently the DRC, Rwanda and Brazil; 67 % of the world's mined tantalum comes from these three countries (USGS 2017a; Damm 2018; USGS 2020l). An overview of the Tantalum supply situation is contained in Table 4.52.

4.12.3 Applications

Today, capacitors, which are used in entertainment and telecommunications technology, amongst other areas of application, represent the largest area of application for tantalum. The coating processes in which tantalum is used are also used to manufacture products (e.g. displays) used in electronic end products. Two other important areas of application of tantalum in terms of quantity are super alloys, which are used in gas turbines and other applications, and chemicals,

Table 4.52: Tantalum supply situation in 2010, 2013 and 2018 (source: BGR 2021)

	2010	2013	2018
Mine production [tonnes of metal content]	739	1,265	1,832
Refinery production [tonnes of metal content]	–	–	–
Reserve [tonnes of metal content]	108,200	98,001	110,001
Resources [tonnes of metal content]	–	–	–
Most important countries for mining	Rwanda 23 % Brazil 19 % DR Congo 14 %	Rwanda 44 % Brazil 15 % DR Congo 13 %	DR Congo 27 % Rwanda 20 % Brazil 20 %
Most important countries for refining	–	–	–
Country concentration – Mine production[1]	1,453	2,566	1,720
Country concentration – Refinery production	–	–	–
Weighted country risk – Mine production[1]	–0.48	–0.45	–0.65
Weighted country risk – Refinery production	–	–	–
Price[2] [USD/kg Ta_2O_5]	121.18	236.73	203.03

[1] *For a colour legend, please refer to the HHI and GLR entries in the "Abbreviations and glossary" section.*
[2] *Tantalite: concentrate, 30 % Ta_2O_5, cif China*

which have broad applications as intermediates in optoelectronics and optical glass, amongst others (Nassar 2017; Damm 2018; USGS 2020l). An overview of the applications of tantalum is contained in Table 4.53.

Table 4.53: Worldwide application of tantalum (source: USGS 2017a)

Area of application	2016 [%]
Capacitors	33
Super alloys	18
Sputtering targets for coating process	14
Rolled products	9
Carbide-containing tool and cutting steels	8
Chemicals	18
Total	**100**

Emerging technologies

The most important emerging technologies with a high growth potential that make use of tantalum are:

- Microelectronic capacitors
- Data centres
- Super alloys
- Radio frequency microchips

4.12.4 Tantalum demand in 2040

The additional raw material demands estimated on the basis of the technology synopses are shown in Table 4.54 and Figure 4.17. Tantalum demand for the emerging technologies segment under study was 65 % of mine production in 2018. Demand could grow to as much as 207 % of 2018 mine production by 2040, depending on the scenario.

Table 4.54: Tantalum demand for selected emerging technologies, in tonnes

Technology	Demand in 2018	Demand in 2040		
		SSP1 Sustainability	SSP2 Middle of the Road	SSP5 Fossil Path
Super alloys	260	470	440	610
Microelectronic capacitors	740	1,720	1,460	2,010
Radio frequency microchips	194	360	430	530
Data centres	0.01	48	185	650
Demand (accumulated)	**1,194**	**2,598**	**2,515**	**3,800**
Demand / Primary production 2018	65 %	142 %	137 %	207 %

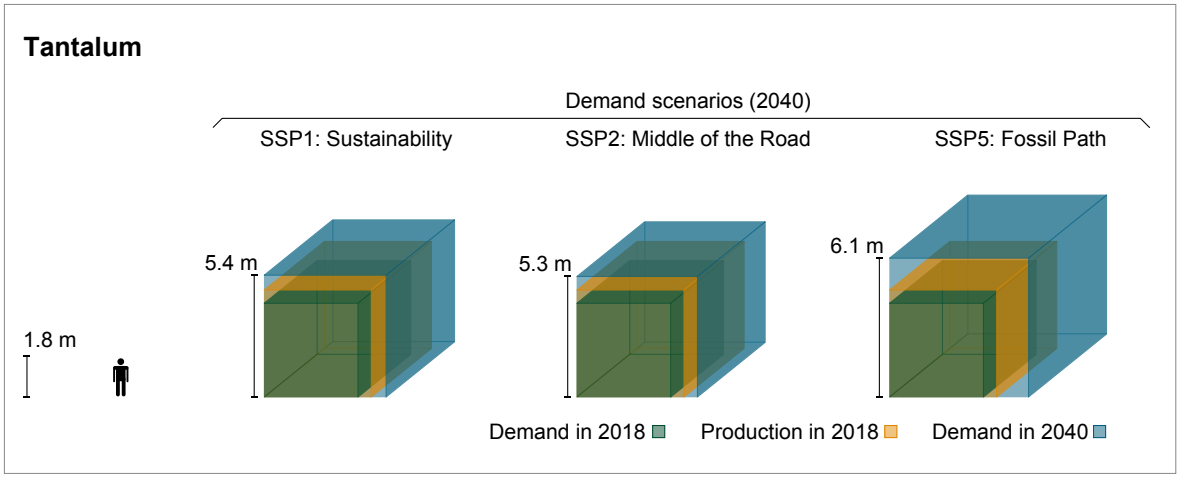

Figure 4.17: Tantalum mine production in 2018 and demand for emerging technologies in 2018 and 2040

4.13 Titanium

Titanium is in the 4th subgroup, the titanium group, of the periodic table of the elements above zirconium and hafnium. It was discovered in the late 18th century and isolated (in high grade form) in 1910. The development of the Kroll process in the late 1930s enabled large-scale industrial production, which began in 1946 (Römpp no date; Woodruff & Bedinger 2013; Sibum et al. 2017; Woodruff et al. 2017).

4.13.1 Properties

Titanium in its pure form is a lustrous silvery-white metal. It belongs to the light, transition and refractory metals. Metallic titanium is relatively light and has a high mechanical strength and a relatively high melting point (Table 4.55). Pure titanium is ductile (it can be cold rolled), but even with small impurities it is brittle and hard. In general, many characteristics of titanium, including mechanical properties and electrical and thermal conductivity, are strongly dependent on the degree of purity and thermal and mechanical pretreatment. The hardness and strength of titanium and its resistivity increase with decreasing degree of purity (and by cold working). For example, titanium is available in various degrees of purity, which can be used for different applications depending on the requirements profile (degree of hardness, corrosion resistance, conductivity, etc.). Titanium is a base metal; it forms a protective oxide layer that increases its resistance to corrosion. The corrosion resistance of titanium can be increased by small additions of other/precious metals (alloys). Titanium powder is pyrophoric (Römpp no date; Quadbeck-Seeger 2007; Sibum et al. 2017).

Table 4.55: Titanium properties

Density	4.5 g/cm^3
Melting point	1,941 °C
Electric conductivity	2.5 · 10^6 S/m
Thermal conductivity	22 W/(m · K)

4.13.2 Deposits and production

Titanium is one of the most abundant metals in nature. In the upper earth's crust it is more abundant than, for example, carbon or nitrogen. It occurs in pure form as well as in numerous minerals (also associated with rare earth metals). The most important titanium minerals/ores include two of the naturally occurring titanium oxide modifications, anatase (TiO_2) and rutile (TiO_2) as well as ilmenite ($FeTiO_3$), which can have a TiO_2 content of up to 53 %. Leucoxene is a weathering product of ilmenite or titanomagnetite and consists, amongst other things, of rutile and anatase in addition to ferruginous phases and phases of silicon oxide. The TiO_2 content is 76–90 %. Ilmenite, which is mined from placer deposits, accounts for a large proportion of the world's titanium resources and 89 % of the world's titanium mineral demand (Römpp no date; Fang et al. 2013; Sibum et al. 2017; Woodruff et al. 2017; USGS 2020n).

In 2018, ilmenite was mined in China, South Africa, Australia and Canada, amongst other countries. The ilmenite output of these countries accounts for more than half of the 2018 global cumulative ilmenite and rutile production. The largest ilmenite and rutile reserves are reported for Australia, China and India, all of which have ilmenite reserves (USGS 2020n). An overview of the titanium supply situation is shown in Table 4.56.

4.13.3 Applications

As mentioned above, titanium (metal) is available in various degrees of purity. Titanium of the highest purity, grade 1, is used in applications where strength is less important than corrosion resistance, conductivity and cold formability, e.g. in electrical applications. Grade 4 is used when the strength/hardness of titanium is to be utilised, such as in aerospace and some medical applications. In addition, various titanium alloys are used which have improved properties (e.g. higher corrosion resistance) compared to pure titanium. Almost all titanium metal demand is for aerospace, alloys and other industrial applications. Other, non-industrial applications, e.g. medical applications, account for only a small share of titanium metal demand. However, all applications of titanium metal play only a minor role compared to the applications of titanium oxide. The majority (95 %) of the titanium ores mined are not processed into titanium metal but into titanium oxide. Thanks to its high light refraction, it is widely used as a white pigment in paints, plastics, paper, etc. Other tita-

Table 4.56: Titanium supply situation in 2010, 2013 and 2018 (sources: BGR 2021, USGS 2012, USGS 2015, USGS 2020l, USGS 2020n)

	2010	2013	2018
Mine production[1] [tonnes of TiO_2]	6,400,000	7,400,500	7,460,000
Refinery production [tonnes of metal content]			
– Titanium sponge	152,400	190,900	198,050
– Titanium metal (primary / secondary refinery production)	–	217,992	260,548
Reserve [1] [1,000 tonnes of metal content]	690,000	770,000	820,000
Resources [1,000 tonnes of TiO_2]	2,000,000	2,000,000	2,000,000
Most important countries for mining	Australia 23 % Canada 18 % South Africa 18 %	Australia 18 % Canada 16 % South Africa 16 %	South Africa 17 % Australia 13 % Norway 9 %
Most important countries for refining			
– Titanium sponge	–	China 40 % Russia 22 % Japan 21 %	China 36 % Japan 25 % Russia 22 %
– Titanium metal (primary / secondary refinery production)	–	USA 30 % China 28 % Russia 25 %	USA 33 % China 29 % Russia 23 %
Country concentration – Mine production	–	–	–
Country concentration – Refinery production[2]			
– Titanium sponge	2,339	2,646	2,565
– Titanium metal (primary / secondary refinery production)	–	2,423	2,509
Weighted country risk – Mine production	–	–	–
Weighted country risk – Refinery production[2]			
– Titanium sponge	–0.07	–0.07	0.08
– Titanium metal (primary / secondary refinery production)	–	0.17	0.30
Price[3] [USD/kg]	8.95	9.06	9.17

[1] *Titanium mineral concentrate made from ilmenite and rutile*
[2] *For a colour legend, please refer to the HHI and GLR entries in the "Abbreviations and glossary" section.*
[3] *Titanium sponge, 99.7 % Ti, ex-works China*

nium applications include catalysts, ceramics, fabric/fibre coatings, etc. (Quadbeck-Seeger 2007; Sibum et al. 2017; DERA 2019; USGS 2020m). An overview of the application of titanium within the EU is contained in Table 4.57.

Table 4.57: Titanium usage in the EU (source: European Commission 2020a)

Area of application	2012–2016 [%]
Paints	54
Plastics	24
Aerospace	8
Medical equipment	6
Motor vehicles	3
Alloys	2
Other	3
Total	**100**

Emerging technologies

The most important emerging technology with a high growth potential that makes use of titanium is:

– Desalination of sea water

4.13.4 Titanium demand in 2040

The additional raw material demands estimated on the basis of the technology synopses are shown in Table 4.58 and Figure 4.18. The emerging technologies examined required about 29 % of titanium metal production in 2018. Demand could grow to as much as 55 % of 2018 production by 2040, depending on the scenario.

4.14 Vanadium

Vanadium is the first element of the 5th subgroup of the periodic table of the elements. It was discovered in 1801 and isolated in a very pure form in 1867. The first major application was in 1903 in the production of a vanadium steel alloy and subsequently in the automotive industry (RÖMPP no date; BAUER et al. 2017a).

Table 4.58: Titanium demand for selected emerging technologies, in tonnes

Technology	Demand in 2018	Demand in 2040		
		SSP1 Sustainability	SSP2 Middle of the Road	SSP5 Fossil Path
Alloys for lightweight airframe construction	57,000	75,000	80,000	110,000
Super alloys	5,000	8,500	8,000	11,100
Solid-state batteries	–	15,000	4,400	500
Additive manufacturing of metal components (“3-D printing”)	308	6,460	7,000	6,900
Water electrolysis	4	13,600	3,900	720
Desalination of sea water	12,500	9,400	6,300	12,900
Demand (accumulated)	**74,812**	**127,960**	**109,600**	**142,120**
Demand / production of titanium sponge in 2018	38 %	65 %	55 %	72 %
Demand / production of titanium metal in 2018	29 %	49 %	42 %	55 %

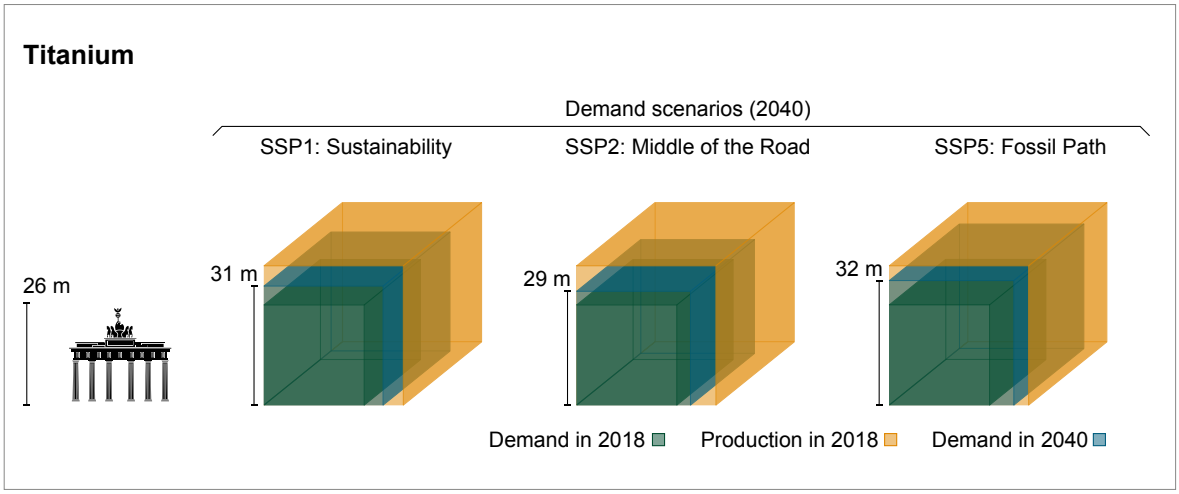

Figure 4.18: Titanium metal refinery production in 2018 and titanium demand for emerging technologies in 2018 and 2040

4.14.1 Properties

Vanadium is a steel-grey and bluish shimmering metal. Its mechanical properties depend strongly on the degree of purity: relatively pure vanadium is ductile and can be forged and rolled when cold; when contaminated with e.g. oxygen or carbon, ductility decreases and hardness/strength increases. At low room temperatures, vanadium is relatively corrosion resistant. It is readily alloyable with various metals (Römpp no date; Bauer et al. 2017a).

Table 4.59: Vanadium properties

Density	6.11 g/cm³
Melting point	1,910 °C
Electric conductivity	5 · 10⁶ S/m
Thermal conductivity	31 W/(m · K)

4.14.2 Deposits and production

Vanadium is not rare; it is more abundant in the earth's crust than nickel or copper. It is also to be found natively. Important vanadium minerals include montroseite ((V,Fe)OOH), corvusite ($(V_2^{4+} \cdot V_{12}^{5+}\ 0_{34} \cdot nH_20$) und roscoelite ($[KV_2(OH)_2/AlSi_3O_{10}]$), which have vanadium contents of about 45.5 %, 40.8 % and 11.2–14 % respectively. Vanadium deposits are found in titanomagnetite ore, phosphate rock, uranium-bearing sandstone and siltstone, bauxite and carbonaceous materials, e.g. coal and petroleum (Römpp no date; Ostrooumov & Taran 2016; Bauer et al. 2017a; Kelley et al. 2017; USGS 2020o).

Titanomagnetite deposits, where magnetite (Fe_3O_4) and ilmenite ($FeTiO_3$) are the main vanadium-bearing minerals, serve as the main source for today's vanadium production. In the production of vanadium from titanomagnetite, vanadium is obtained as a primary product from titanomagnetite and as a by-product from the slag produced during the smelting of titanomanetite into pig iron. Secondary production includes vanadium from vanadium-containing pulverised fuel ash, spent catalysts and industrial waste products. In 2018, vanadium was mined in China, Russia and South Africa, amongst other countries. The largest reserves have been reported for China, Russia and Australia (Römpp no date; Bauer et al. 2017a; Kelley et al. 2017; USGS 2017f; USGS 2020o). An overview of the supply situation is contained in Table 4.60.

Table 4.60: Vanadium supply situation in 2010, 2013 and 2018 (sources: BGR 2021, USGS 2011f, USGS 2014f, USGS 2020o)

	2010	2013	2018
Mine production [tonnes of metal content]	54,714	61,600	90,661
Refinery production [tonnes of metal content]	–	–	–
Reserve [tonnes of metal content]	13,645,100	13,645,100	20,275,000
Resources [tonnes of metal content]	> 63,000,000	> 63,000,000	> 63,000,000
Most important countries for mining	China 47 % South Africa 33 % Russia 18 %	China 55 % South Africa 26 % Russia 18 %	China 58 % Russia 19 % South Africa 16 %
Most important countries for refining	–	–	–
Country concentration – Mine production[1]	3,595	4,062	4,104
Country concentration – Refinery production	–	–	–
Weighted country risk – Mine production[1]	–0.29	–0.36	–0.30
Weighted country risk – Refinery production	–	–	–
Price[2] [USD/kg]	30.06	27.70	81.37

[1] *For a colour legend, please refer to the HHI and GLR entries in the "Abbreviations and glossary" section.*
[2] *Ferro-Vanadium, basis min. 78 %, free delivered duty paid, consumer plant, 1st grade Western Europe*

4.14.3 Applications

Vanadium is largely used as a component of steel and other (e.g. titanium) alloys. The addition of vanadium increases tensile strength, high-temperature strength and corrosion resistance, amongst other things. Alloys containing vanadium have a wide range of applications from tools to vehicles and ships to pipelines and bridges. Vanadium is also used in energy storage devices (e.g. vanadium redox batteries) and numerous chemicals (used e.g. as catalysts) (Bauer et al. 2017a; Kelley et al. 2017; USGS 2017f; USGS 2020o).

Emerging technologies

The most important emerging technology with a high growth potential that makes use of vanadium is:

– Redox flow batteries

Table 4.61: Worldwide application of vanadium (source: TNT Limited no date)

Area of application	2017 [%]
Steel	86
Non-iron alloys	5
Energy storage	5
Chemicals	4
Total	**100**

4.14.4 Vanadium demand in 2040

The additional raw material demands estimated on the basis of the technology synopses are shown in Table 4.62 and Figure 4.19. Vanadium demand for the emerging technologies segment under study was approximately 0.4 % of mine production in 2018. Demand could grow to as much as 77 % of 2018 mine production by 2040, depending on the scenario.

Table 4.62: Vanadium demand for selected emerging technologies, in tonnes

Technology	Demand in 2018	Demand in 2040		
		SSP1 Sustainability	SSP2 Middle of the Road	SSP5 Fossil Path
CCS – Carbon capture and storage	–	3,200	8,800	0
Redox flow batteries	60	60,500	60,500	60,500
Desalination of sea water	260	200	130	270
Demand (accumulated)	**320**	**63,900**	**69,430**	**60,770**
Demand / Primary production 2018	0.4 %	70 %	77 %	67 %

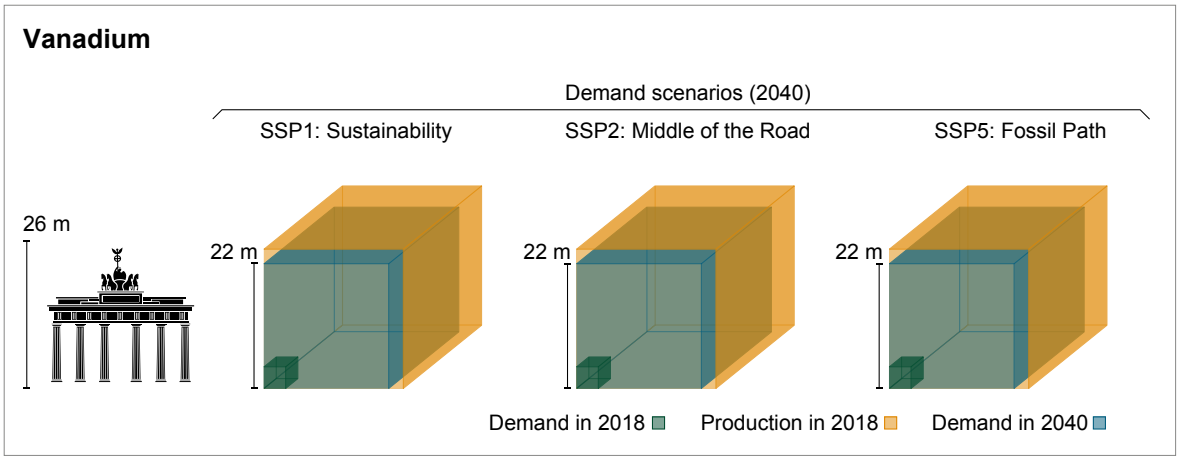

Figure 4.19: Vanadium mine production in 2018 and demand for emerging technologies in 2018 and 2040

5 Conclusions

In the previous studies from 2009 and 2016 (Angerer et al. 2009; Marscheider-Weidemann et al. 2016), electromobility and thin-film photovoltaics had the greatest impact on the raw materials presented as the most critical in each of the studies. Lithium-ion high-performance electricity storage, solid-state batteries and electrical traction engines generate significant demands in terms of lithium, cobalt and rare earth metals in this study too. In thin-film PV, better efficiencies, thinner absorber layers and more resource-efficient manufacturing processes have led to a reduction in the need for gallium.

The 33 technologies examined in this study were selected because they are essential to the clusters analysed. These clusters are “Mobility and aerospace”, “Digitisation and Industry 4.0”, “Energy technologies and decarbonisation”, “Recycling and water management” and “Power and data networks”. Fibre-optic cables or data centres, for example, are essential infrastructure technologies that are needed for the Digitisation and Industry 4.0 cluster. In data centres, the large amounts of data stored result in a large demand for HDD hard drives, for which ruthenium and platinum are needed. Due to the “unrestrained use of data” in SSP5, the demand for ruthenium in 2040 will be 19 times higher than the production from 2018, while the demand for platinum will be four times higher. However, with SSD hard drives, technology is available that can be used to substitute HDDs. Since this is significantly more expensive than HDDs, however, it is not gaining acceptance on the market as quickly as previously assumed, so HDDs will still be of considerable importance in 2040.

In the Energy technologies and decarbonisation cluster, water electrolysis plays a major role in producing CO_2-free hydrogen with renewable electricity. The technologies available on the market or being researched are alkaline electrolysis (AEL), polymer electrolyte membrane electrolysis (PEMEL) and solid oxide electrolysis (SOEL). While base metals are used in AEL, PEMEL usually uses iridium in the anode and platinum in the cathode. In SOEL, scandium and yttrium, among others, are used in the solid electrolyte. Since SOEL works similarly to a SOFC (solid oxide fuel cell), the same raw materials are used here.

In the previous studies, it was a challenge to make scenario assumptions that applied as far as possible to all the technologies investigated. This unified view of development was only partially successful, e.g. by using a common model for the market distribution of electric cars. In this study, the Shared Socioeconomic Pathways (SSPs) were used, which were created from 2011 onwards within the framework of the 5th Assessment Report of the Intergovernmental Panel on Climate Change (IPCC) for climate policy issues (Kriegler et al. 2012). Three SSPs were selected, representing different global socioeconomic developments for the 21st century: SSP1 “Sustainability – Taking the green road”, SSP2 “Middle of the road” and SSP5 “Fossil-fueled development – Taking the highway”.

Where possible, the narratives and data from the models developed for the SSPs were used for the technology chapters, for example on global GDP, energy consumption or population development (IIASA n.d.). Where there were no statements in the SSPs on the development of indicators necessary for the technologies market, the narratives were supplemented and backed up with figures. This was particularly necessary in the area of electromobility and digitisation, as there are no direct statements from the SSP publications for these sectors.

Results for the various SSPs

Depending on the development path, the quantities of raw materials required in 2040 for the technologies studied differ, in some cases very significantly.

Given the sustainable development in SSP1, decarbonisation in particular is being pursued, leading to high raw material demand for scandium, lithium, heavy and light rare earth metals, iridium and cobalt, see Figure 5.1. The demand results primarily from hydrogen technologies, lithium-ion high-performance storage, solid-state batteries, electrical traction engines, wind turbines and high-performance permanent magnets. In the area of digitisation, SSP1 assumes that everyone should participate in this development, so that ruthenium (HDDs) and germanium (fibre-optic cables) also exhibit high demand.

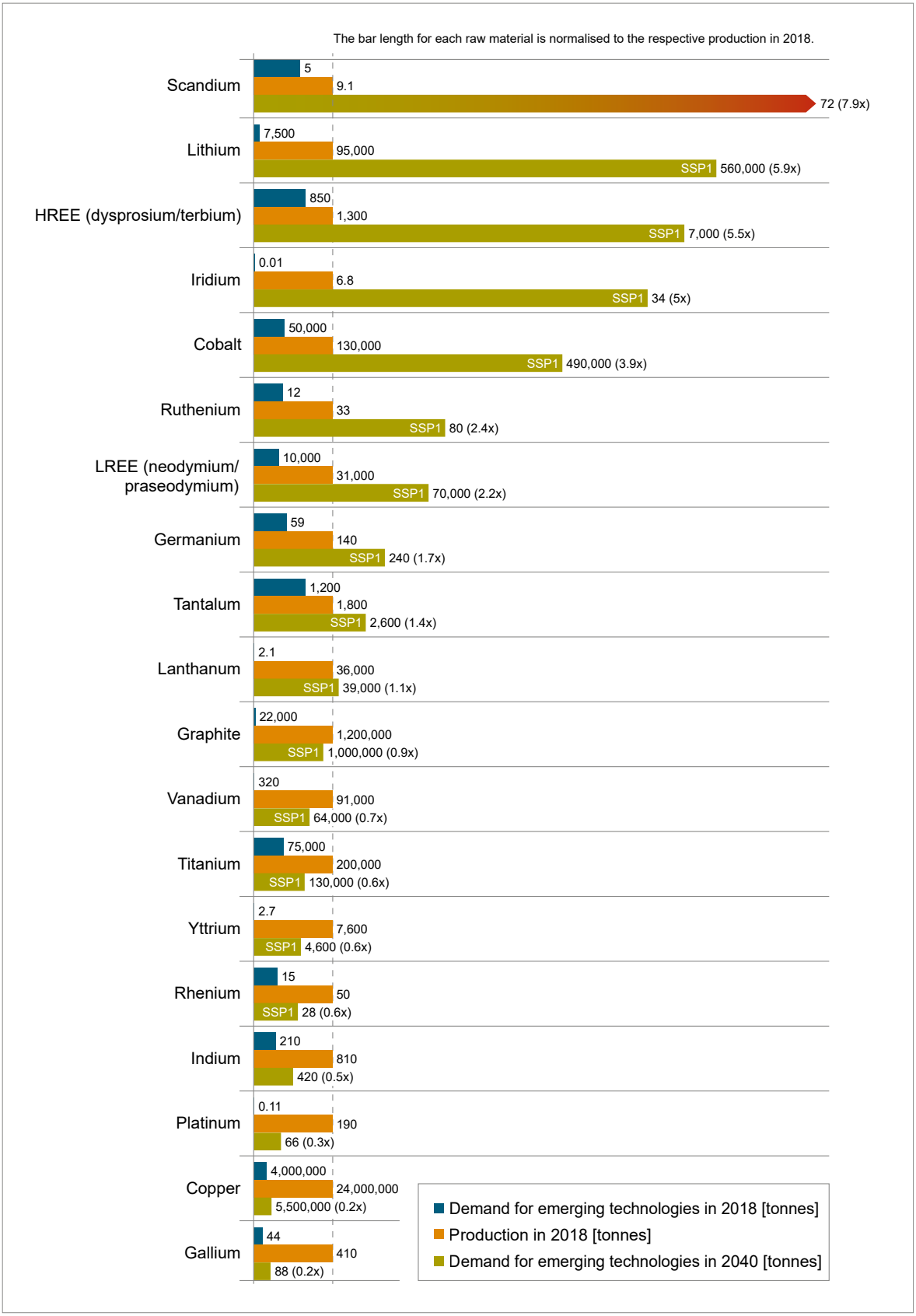

Figure 5.1: Demand for different raw materials for selected emerging technologies in 2018 and in the SSP1 in 2040 compared to the primary production of the respective raw materials in 2018

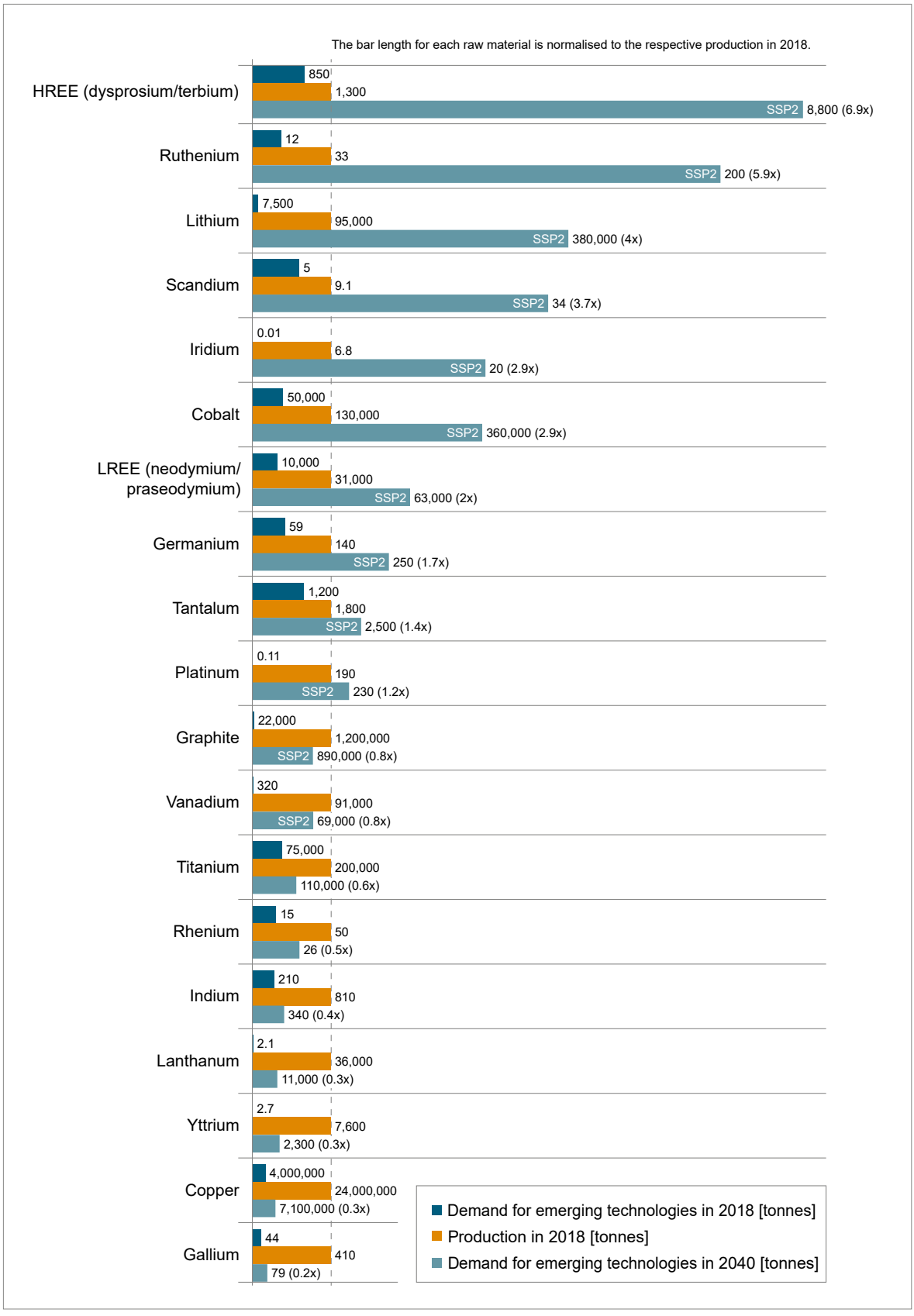

Figure 5.2: Demand for different raw materials for selected emerging technologies in 2018 and in the SSP2 in 2040 compared to the primary production of the respective raw materials in 2018

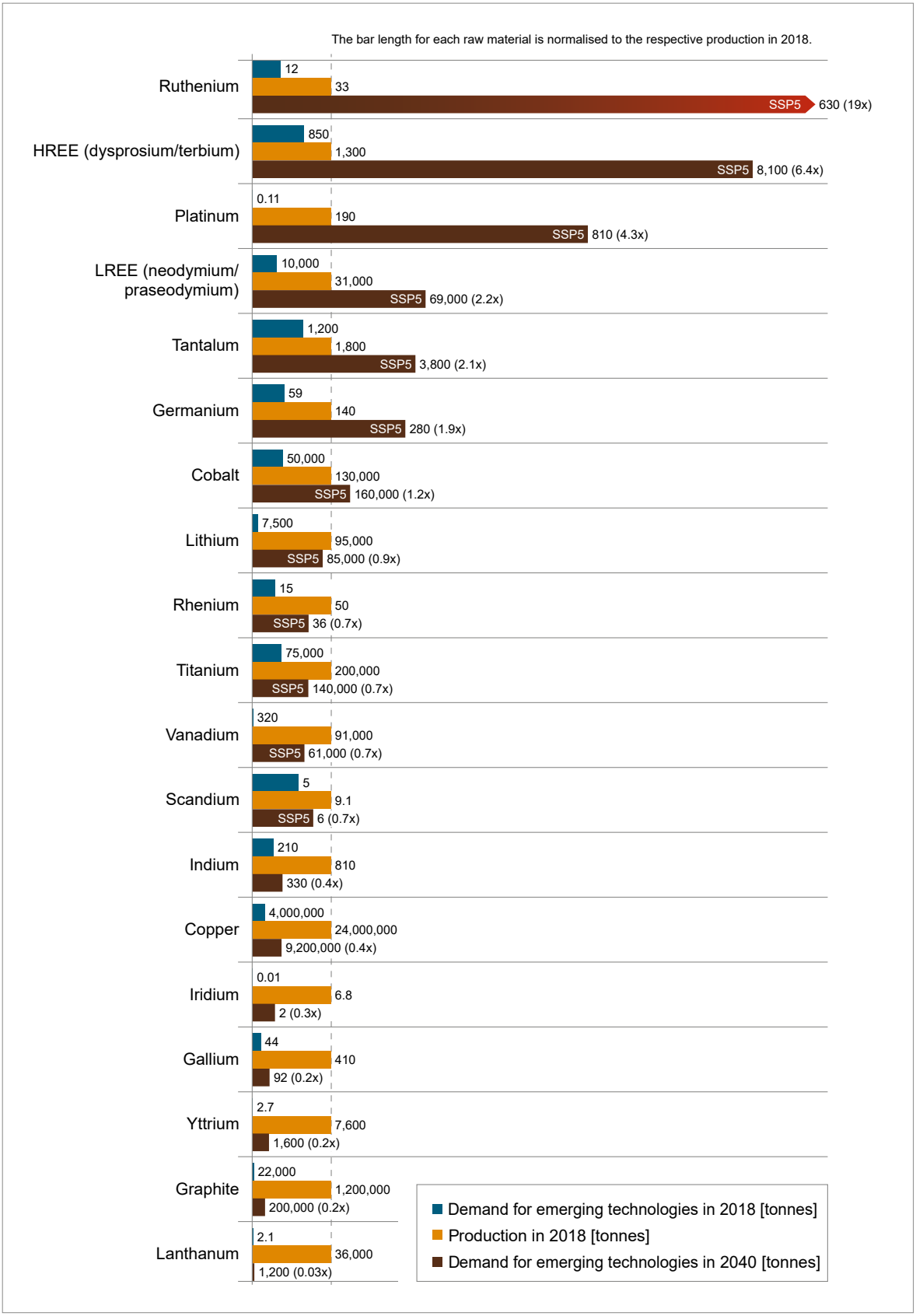

Figure 5.3: Demand for different raw materials for selected emerging technologies in 2018 and in the SSP5 in 2040 compared to the primary production of the respective raw materials in 2018

In SSP5, the high demand for ruthenium is particularly noticeable and is caused by the high storage requirements in the data centres, see Figure 5.3. This results from an “unrestrained” use of digitisation assumed in SSP5 through streaming services in high resolutions, extensive backup data, etc. The demand for raw materials for electromobility and decarbonisation in 2040 is significantly lower and in some cases below the production levels from 2018.

SSP2 offers a mixed picture, compare Figure 5.2. The raw material requirements are not as extreme as in SSP1 and SSP5, but require a doubling to about a sevenfold increase in the relevant 2018 production for seven metals – namely the light rare earth metals, cobalt, iridium, scandium, lithium, ruthenium and the heavy rare earth metals – to meet them.

Overall, the SSPs paint a broad picture of future development, each of them setting different priorities in technology development.

6 References

5G providers (2021): 5G Ping. – URL: https://www.5g-anbieter.info/speed/5g-ping.html [Rev.: 31/05/2021].

Abuelsamid, S. (2019): New vehicles keep getting heavier? – Or are they? – URL: https://www.forbes.com/sites/samabuelsamid/2019/01/03/new-vehicles-keep-getting-heavier-or-are-they/#fc3ac8145186 [Rev.: 07/09/2020].

ACEA (2020): Association Registration Statistics. – URL: https://www.acea.be/ [Rev.: 12/06/2020].

Aceto, G., Persico, V. & Pescape, A. (2019): A Survey on Information and Communication Technologies for Industry 4.0: State-of-the-Art, Taxonomies, Perspectives, and Challenges. – IEEE Commun. Surv. Tutorials, 21: 3467–3501.

Adler, B. & Müller, R. (2014): Seltene Erdmetalle. Gewinnung, Verwendung und Recycling. – Ilmenau.

Agora Verkehrswende (2019a): Klimabilanz von Elektroautos. Einflussfaktoren und Verbesserungspotenzial. – URL: https://www.agora-verkehrswende.de/fileadmin/Projekte/2018/Klimabilanz_von_Elektroautos/Agora-Verkehrswende_22_Klimabilanz-von-Elektroautos_WEB.pdf [Rev.: 05/05/2021].

Agora Verkehrswende (2019b): Klimabilanz von strombasierten Antrieben und Kraftstoffen. – URL: https://static.agora-verkehrswende.de/fileadmin/Projekte/2019/Klimabilanz_Batteriefahrzeugen/32_Klimabilanz_strombasierten_Antrieben_Kraftstoffen_WEB.pdf [Rev.: 10/02/2021].

AIRBUS (2018): Metals and composites: finding the right material for each application. – URL: https://www.airbus.com/newsroom/stories/metals-and-composites--finding-the-right-material-for-each-appli.html [Rev.: 25/06/2020].

AIRBUS (2019a): Cities, Airports & Aircraft. Global Market Forecast 2019-2038. – [Rev.: 26/06/2020].

AIRBUS (2019b): Airbus achieves new commercial aircraft delivery record in 2018.

AIRBUS GROUP (2015): Scalmalloy: Aluminum-Magnesium-Scandium Alloy. – URL: http://www.technology-licensing.com/etl/int/en/What-we-offer/Technologies-for-licensing/Metallics-and-related-manufacturing-technologies/Scalmalloy.html [Rev.: 14/11/2015].

AIRWISE (2013): Aluminium Makers Fight Plastic Planes With New Alloys. – URL: http://news.airwise.com/story/view/1371778684.html [Rev.: 14/11/2015].

Al Barazi, S. (2018): Rohstoffrisikobewertung – Kobalt. – DERA Rohstoffinformationen 36: 120 S., Berlin. – URL: https://www.bgr.bund.de/DE/Gemeinsames/Produkte/Downloads/DERA_Rohstoffinformationen/rohstoffinformationen-36.html [Rev.: 28/07/2020].

Al Barazi, S., Elsner, H., Kärner, K., Liedtke, M., Schmidt , M., Schmitz, M. & Szurlies, M. (2016): Mineralische Rohstoffe in Australien. Investitions- und Lieferpotenziale. – DERA Rohstoffinformationen 29, Berlin. – URL: https://www.deutsche-rohstoffagentur.de/DERA/DE/Downloads/studie-australien-rosit-29.pdf?__blob=publicationFile&v=6 [Rev.: 30/07/2020].

Alassi, A., Bañales, S., Ellabban, O., Adam, G. & MacIver, C. (2019): HVDC Transmission: Technology Review, Market Trends and Future Outlook. – Renewable and Sustainable Energy Reviews, 112: 530–554.

Albrecht, S., Cymorek, C., Andersson, K., Reichert, K. & Wolf, R. (2012): Tantalum and Tantalum Compounds. – Ullmann's encyclopedia of industrial chemistry [Rev.: 25/07/2020].

Allen, M. (2014): Data Center Redundancy N+1, N+2 vs. 2N vs. 2N+1. – URL: https://www.datacenters.com/news/redundancy-n-1-n-2-vs-2n-vs-2n-1 [Rev.: 09/12/2020].

Allied Market Research (2017): Global Optical Fiber Market by Mode (Single Mode and Multi-Mode), Type (Glass Optical Fiber and Plastic Optical Fiber), and Industry Vertical (Telecom & IT, Public Sector, Healthcare, Energy & Utilities, Aerospace & Defense, Manufacturing, and Others): Opportunity Analysis and Industry Forecast, 2018 – 2025. – URL: https://www.alliedmarketresearch.com/optical-fiber-market [Rev.: 22/02/2021].

AltfahrzeugV (2016): Verordnung über die Überlassung, Rücknahme und umweltverträgliche Entsorgung von Altfahrzeugen.

Aluminium-Messe (2014): Flugzeug-Hersteller fliegen auf Aluminium. – URL: https://www.aluminium-messe.com/Pressemitteilung/Flugzeug-Hersteller-fliegen-auf-Aluminium/n71/ [Rev.: 14/11/2015].

Amato, A. & Beolchini, F. (2018): End of life liquid crystal displays recycling: A patent review. – Journal of environmental management, 225: 1–9.

Amato, A. & Beolchini, F. (2019): End-of-life CIGS photovoltaic panel: A source of secondary indium and gallium. – Prog Photovolt Res Appl, 27: 229–236.

Amprion GmbH (no date): Erdkabel. Aufbau. – URL: https://www.amprion.net/%C3%9Cbertragungsnetz/Technologie/Erdkabel/Aufbau-einer-Kabelanlage.html [Rev.: 06/07/2020].

Amprion GmbH (no date): Freileitungen. – URL: https://www.amprion.net/%C3%9Cbertragungsnetz/Technologie/Freileitung/ [Rev.: 06/07/2020].

Andrae, A. & Edler, T. (2015): On Global Electricity Usage of Communication Technology: Trends to 2030. – Challenges, 6: 117–157.

Angerer, G., Marscheider-Weidemann, F., Lüllmann, A., Erdmann, L., Scharp, M., Handke, V. & Marwede, M. (2009): Rohstoffe für Zukunftstechnologien. – Einfluss des branchenspezifischen Rohstoffbedarfs in rohstoffintensiven Zukunftstechnologien auf die zukünftige Rohstoffnachfrage. 2nd edition, Stuttgart.

Antão, L., Pinto, R., Reis, J. P. & Gonçalves, G. (2018): Requirements for Testing and Validating the Industrial Internet of Things.

Anthony, J. W., Bideaux, R. A., Bladh, K. W. & Nichols, M. C. (2001a): Handbook of Mineralogy. Indite. – URL: http://www.handbookofmineralogy.org/ [Rev.: 14/07/2020].

Anthony, J. W., Bideaux, R. A., Bladh, K. W. & Nichols, M. C. (2001b): Handbook of Mineralogy. Roquesite. – URL: http://www.handbookofmineralogy.org/ [Rev.: 14/07/2020].

Apworks (no date): As ductile as titanium, as light as aluminium. – URL: https://apworks.de/en/scalmalloy/.

Aravindan, V., Lee, Y.-S. & Madhavi, S. (2017): Best Practices for Mitigating Irreversible Capacity Loss of Negative Electrodes in Li-Ion Batteries. – Adv. Energy Mater., 7: 1602607.

Arconic (2020): Lighter, Stronger and Bigger Than Ever. – URL: https://www.arconic.com/aluminum-lithium/ [Rev.: 06/07/2020].

Argus Media (2020): Aerospace crisis drags on high-temp metal prices. – URL: https://www.argusmedia.com/en/news/2119363-aerospace-crisis-drags-on-hightemp-metal-prices.

Asenbauer, J., Eisenmann, T., Kuenzel, M., Kazzazi, A., Chen, Z. & Bresser, D. (2020): The success story of graphite as a lithium-ion anode material – fundamentals, remaining challenges, and recent developments including silicon (oxide) composites. – Sustainable Energy Fuels, 4: 5387–5416.

Audi (2017): Die Audi Space Frame-Technologie – Meilensteine seit 1994. – URL: https://www.audi-mediacenter.com/de/karosserieentwicklung-bei-audi-innovation-qualitaet-und-praezision-7559/die-audi-space-frame-technologie-meilensteine-seit-1994-7563 [Rev.: 07/09/2020].

Auel, C., Falter, W., Jansz, J. & Sudau, C. (2020): Kunststoffabfälle – das neue Gold. – CHEManager: 9–10.

Auer, J. (2019): 3D-Druck: Starkes Wachstum in der Nische.

AUVSI (2013): The Economic Impact of Unmanned Aircraft Systems Integration in the United States. – URL: http://www.auvsi.org/auvsiresources/economicreport [Rev.: 16/04/2015].

Aviation Safety Bureau (2007): FAA Definitions. – URL: http://www.faa-aircraft-certification.com/faa-definitions.html.

Avnet Abacus (2020): MLCCs Vs Polymer Capacitors. Replacing MLCCs with polymer capacitors. – URL: https://www.avnet.com/wps/portal/abacus/solutions/technologies/passive/capacitors/replacing-mlccs-with-polymer-capacitors/ [Rev.: 17/12/2020].

AVX (2021): Highest CV/cc Conductive Polymer Chip Capacitors Undertab. – URL: https://www.mouser.de/datasheet/2/40/TCN_Undertab-934935.pdf [Rev.: 15/01/2021].

AXT (2020): URL: http://www.axt.com/site/index.php?q=node/36.

Balaram, V. (2019): Rare earth elements: A review of applications, occurrence, exploration, analysis, recycling, and environmental impact. – Geoscience Frontiers, 10: 1285–1303.

Bareiss, K., La Rua, C. de, Möckl, M. & Hamacher, T. (2019): Life cycle assessment of hydrogen from proton exchange membrane water electrolysis in future energy systems. – Applied Energy, 237: 862–872.

Bartos, R. (2014): Leichtere Autos aus Stahl – die Kombination macht's! – URL: http://www.stahl-blog.de/index.php/leichtere-autos-aus-stahl-die-kombination-machts/ [Rev.: 07/09/2020].

BASF (2018): ChemCycling™. Chemisches Recycling von Kunststoffabfällen. – URL: https://www.basf.com/global/de/who-we-are/sustainability/we-drive-sustainable-solutions/circular-economy/mass-balance-approach/chemcycling.html.

Bass, F. M. (1969): A new product growth for model consumer durables. – Management Science, 15: 215–227.

Bast, U., Blank, R., Buchert, M., Elwert, T., Finsterwalder, F., Hörnig, G., Klier, T., Langkau, S., Marscheider-Weidemann, F., Müller, J.-O., Thürigen, C., Treffer, F. & Walter, T. (2015): Abschlussbericht zum Verbundvorhaben „Recycling von Komponenten und strategischen Metallen aus elektrischen Fahrantrieben". – password: MORE (Motor Recycling).

Battery University (2020): Types of lithium-ion. – URL: https://batteryuniversity.com/index.php/learn/article/charging_lithium_ion_batteries [Rev.: 19/08/2020].

Bauer, G., Güther, V., Hess, H., Otto, A., Roidl, O., Roller, H., Sattelberger, S., Köther-Becker, S. & Beyer, T. (2017a): Vanadium and Vanadium Compounds. – Ullmann's encyclopedia of industrial chemistry [Rev.: 27/07/2020].

Bauer, N., Calvin, K., Emmerling, J., Fricko, O., Fujimori, S., Hilaire, J., Eom, J., Krey, V., Kriegler, E., Mouratiadou, I., Sytze de Boer, H., van den Berg, M., Carrara, S., Daioglou, V., Drouet, L., Edmonds, J. E., Gernaat, D., Havlik, P., Johnson, N., Klein, D., Kyle, P., Marangoni, G., Masui, T., Pietzcker, R. C., Strubegger, M., Wise, M., Riahi, K. & van Vuuren, D. P. (2017b): Shared Socioeconomic Pathways of the Energy Sector\textendash Quantifying the Narratives. – Global Environmental Change, 42: 316–330.

Bauer, R. (2018a): HDD vs SSD: What Does the Future for Storage Hold? – URL: https://www.backblaze.com/blog/ssd-vs-hdd-future-of-storage/ [Rev.: 08/12/2020].

Bauer, R. (2018b): HDD vs SSD: What Does the Future for Storage Hold? Part 2. – URL: https://www.backblaze.com/blog/hdd-vs-ssd-in-data-centers/ [Rev.: 08/12/2020].

BDEW (2018): Zahl der Woche. 1,84 Millionen Kilometer Stromleitungen vernetzen Deutschland. – Berlin.

BDI (2016): Implikationen des 3D-Drucks für die Rohstoffsicherung der deutschen Industrie. – URL: http://bdi.eu/media/themenfelder/rohstoffe/publikationen/20151022_Positionspapier_3D-Druck_Rohstoffsicherung.pdf.

Bedder, J. & Baylis, R. (2013): Into the melting pot: the superalloy market and its impact on minor metals. – Minor Metals Conference 28.2.2013. – URL: https://roskill.com/news/download-roskills-paper-on-the-superalloy-and-minor-metal-markets/ [Rev.: 08/11/2015].

Beiderbeck, R., Ngo, K., Rolon, J. E. C., Tudgay, J., Villarreal, F. C., Zwemmer, E. & Coyne, L. (2020): IBM TS4500 R6 Tape Library Guide.

Belkhir, L. & Elmeligi, A. (2018): Assessing ICT global emissions footprint: Trends to 2040 & recommendations. – Journal of Cleaner Production, 177: 448–463.

Beretta, D., Neophytou, N., Hodges, J. M., Kanatzidis, M. G., Narducci, D., Martin-Gonzalez, M., Beekman, M., Balke, B., Cerretti, G., Tremel, W., Zevalkink, A., Hofmann, A. I., Müller, C., Dörling, B., Campoy-Quiles, M. &

Caironi, M. (2019): Thermoelectrics: From history, a window to the future. – Materials Science and Engineering: R: Reports, 138: 100501.

Berwald, A., Faninger, T., Bayramoglu, S., Tinetti, B. & Mudgal, S. (2015): Preparatory study for implementing measures of the Ecodesign Directive 2009/125/EC – DG ENTR Lot 9 – Enterprise servers and data equipment.

BGR (2021): Fachinformationssystem Rohstoffe. – unpublished. Hanover, Germany [Rev.: March 2021].

Bhutto, G. M. & Jalbani, A. H. (2012): Life cycle assessment of Autoliv's Night vision camera. – Journal of Environmental Sciences, 3: 498–508.

Bi, Z., Kleine, R. de & Keoleian, G. A. (2017): Integrated Life Cycle Assessment and Life Cycle Cost Model for Comparing Plug-in versus Wireless Charging for an Electric Bus System. – Journal of Industrial Ecology, 21: 344–355.

Bicer, Y. & Khalid, F. (2020): Life cycle environmental impact comparison of solid oxide fuel cells fueled by natural gas, hydrogen, ammonia and methanol for combined heat and power generation. – International Journal of Hydrogen Energy, 45: 3670–3685.

BINE Informationsdienst (2011): Supraleiter für große Windenergieanlagen. Die Abhängigkeit von seltenen Erden lässt sich vermindern. – URL: http://www.bine.info/ [Rev.: 30/04/2014].

Binnemans, K., Jones, P. T., Müller, T. & Yurramendi, L. (2018): Rare Earths and the Balance Problem: How to Deal with Changing Markets? – J. Sustain. Metall., 4: 126–146.

Birnbaum, K. U., Steinberger-Wilckens, R. & Zapp, P. (2019): Solid Oxide Fuel Cells: Sustainability Aspects. – In: Lipman, T. E. & Weber, A. Z. (editors): Fuel Cells and Hydrogen Production. New York, NY.

Blagoeva, D., Pavel, C., Wittmer, D., Huisman, J. & Pasimeni, F. (2019): Materials dependencies for dual-use technologies relevant to Europe's defence sector [er]. – Background report. Luxemburg.

Blankenbach, K. (2016): Die Zukunft von Display-Technologien. »Früher war alles besser, sogar die Zukunft«. – URL: https://www.elektroniknet.de/automotive/elektromobilitaet/frueher-war-alles-besser-sogar-die-zukunft.131691.html [Rev.: 06/01/2021].

BloombergNEF (2020): Electric Vehicle Sales to Fall 18 % in 2020 but Long-term Prospects Remain Undimmed. – URL: https://about.bnef.com/blog/electric-vehicle-sales-to-fall-18-in-2020-but-long-term-prospects-remain-undimmed/ [Rev.: 15/06/2020].

BMVI (2020): Entwurf eines Gesetzes zur Anpassung nationaler Regelungen an die Durchführungsverordnung (EU) 2019/947 der Kommission vom 24. Mai 2019 über die Vorschriften und Verfahren für den Betrieb unbemannter Luftfahrzeuge. – URL: https://www.bmvi.de/SharedDocs/DE/Anlage/Gesetze/Gesetze-19/entwurf-gesetz-anpassung-nationaler-regelungen-unbemannte-luftfahrzeuge.pdf?__blob=publicationFile.

BMWi (2007): Trends der Angebots- und Nachfragesituation bei mineralischen Rohstoffen. – [Rev.: 20/09/2012].

Boeing (2019a): Commercial Market Outlook 2019-2038. – [Rev.: 26/06/2020].

Boeing (2019b): Boeing sets new airplane delivery records, expands order backlog. Strong finish to 2018 results in delivery records.

Boeing (2020): Commercial Market Outlook 2020–2039. – [Rev.: 02/03/2021].

Bombardier (2017): Market forecast. 2017–2036. – [Rev.: 26/06/2020].

Bonesmart.org (2015): Total knee replacement implants. – URL: http://bonesmart.org/knee/total-knee-replacement-implants/ [Rev.: 17/11/2015].

Böni, H., Wäger, P., Thiebaud, E., Du, X., Figi, R., Nagel, O., Bunge, R., Stäubli, A., Spörry, A., Wolfensberge-Malo, M., Brechbühler-Peskova, M. & Grösser, S. (2015): Rückgewinnung von kritischen Metallen aus Elektronikschrott am Beispiel von Indium und Neodym. – Projekt e-Recmet.

Bookhagen, B., Bastian, D., Buchholz, P., Faulstich, M., Opper, C., Irrgeher, J., Prohaska, T. & Koeberl, C. (2020): Metallic resources in smartphones. – Resources Policy, 68: 101750.

Bookhagen, B., Obermaier, W., Opper, C., Koeberl, C., Hofmann, T., Prohaska, T. & Irrgeher, J. (2018): Development of a versatile analytical protocol for the comprehensive determination of the elemental composition of smartphone compartments on the example of printed circuit boards. – Anal. Methods, 10: 3864–3871.

Bosch (2014): Doppelbatterie für den Stromspeicher Braderup. – Press release on 27/05/2014. – URL: http://www.bosch-presse.de/presseforum/details.htm?txtID=6876&locale=de [Rev.: 13/08/2015].

Bourhis, F., Kerbrat, O., Hasco, J.-Y. & Mognol, P. (2013): Sustainable manufacturing: evaluation and modeling of environmental impacts in Additive manufacturing. – The International Journal of Advanced Manufacturing Technology, 69: 1927–1939.

Bradley, D. C., Stillings, L. L., Jaskula, B.W., Munk, L. & McCauley, A. D. (2017): Lithium. Chapter K of Critical Mineral Resources of the United States – Economic and Environmental Geology and Prospects for Future Supply. [Rev.: 14/07/2020].

Bradshaw, A. M., Reuter, B. & Hamacher, T. (2013a): The Potential Scarcity of Rare Elements for the Energiewende. – Green, 3: 93–111.

Bradshaw, A. M., Reuter, B. & Hamacher, T. (2013b): The Potential Scarcity of Rare Elements for the Energiewende. – Green, 3: 93–111.

Broadcom (2020): Optical transceiver. – Product description.

Brumby, A., Verhelst, M. & Cheret, D. (2005): Recycling GtL – a New Challange. – Catalysis Today, 106: 166–169.

Buchert, M. (2011): Rare Earths – a Bottleneck for Future Wind Turbine Technologies? – Wind turbine supply chain and logistics (2011).

Buchert, M., Manhart, A., Bleher, D. & Pingel, D. (2012): Recycling kritischer Rohstoffe aus Elektronik-Altgeräten.

Budde, F. & Volz, D. (2019): The next big thing? Quantum computing's potential impact on chemicals. – URL: https://www.mckinsey.com/industries/chemicals/our-insights/the-next-big-thing-quantum-computings-potential-impact-on-chemicals [Rev.: 31/08/2020].

Bughin, J., Seong, J., Manylka, J., Chui, M. & Joshi, R. (2018): Notes from the frontier: modeling the impact of AI on the world economy.

Bünzli, J.-C. G. & Mcgill, I. (2018): Rare Earth Elements. – Ullmann's encyclopedia of industrial chemistry [Rev.: 20/07/2020].

Burkhardt, Y., Schleicher, K. & Klöpzig, M. (2014): A novel hybrid excited synchronous machine for (H)EV applications. – IEEE.

Business Wire (2014): Research and Markets. – URL: http://www.businesswire.com/news/home/20130704005265/en/Research-Markets-Global-Chinese-Optical-Fiber-Preform#.VHSbtWMhBHc [Rev.: 05/04/2016].

Butaud, E., Tavel, B., Ballandras, S., Bousquet, M., Drouin, A., Huyet, I., Courjon, E., Ghorbel, A., Reinhardt, A., Clairet, A., Bernard, F. & Bertrand, I. (2020): Smart Cut™ Piezo On Insulator (POI) substrates for high performances SAW components. – 2020 IEEE International Ultrasonics Symposium (IUS): 1–4.

Calderone, V. R., Shiju, N. R., Curulla-Ferré, D., Chambrey, S., Khodakov, A., Rose, A., Thiessen, J., Jess, A. & Rothenberg, G. (2013): De novo design of nanostructured iron-cobalt Fischer-Tropsch catalysts. – Angewandte Chemie (International ed. in English), 52: 4397–4401.

Carbon Engineering (2019): CE expanding capacity of commercial Direct Air Capture plant. – URL: https://carbonengineering.com/news-updates/expanding-dac-plant/.

Carmo, M., Keeley, G. P., Holtz, D., Grube, T., Robinius, M., Müller, M. & Stolten, D. (2019): PEM water electrolysis: Innovative approaches towards catalyst separation, recovery and recy-

cling. – International Journal of Hydrogen Energy, 44: 3450–3455.

Carrara, S., Alves Dias, P., Plazzotta, B. & Pavel, C. (2020): Raw materials demand for wind and solar PV technologies in the transition towards a decarbonised energy system. Luxemburg. – URL: https://op.europa.eu/en/publication-detail/-/publication/19aae047-7f88-11ea-aea8-01aa75ed71a1/language-en [Rev.: 23/04/2020].

Caviezel, C., Grünwald, R., Ehrenberg-Silies, S., Kind, S., Jetztke, T. & Bovenschulte, M. (2017): Additive Fertigungsverfahren (3-D-Druck). – Innovationsanalyse. Berlin.

CDI (2006): Cobalt Facts. Cobalt in Chemicals. – URL: http://www.thecdi.com/cdi/images/documents/facts/COBALT_FACTS-Chemicals%202015.pdf [Rev.: 22/10/2015].

Champier, D. (2017): Thermoelectric generators: A review of applications. – Energy Conversion and Management, 140: 167–181.

Chandler, D. (2918): Cell-sized robots can sense their environment. Made of electronic circuits coupled to minute particles, the devices could flow through intestines or pipelines to detect problems. – URL: https://news.mit.edu/2018/cell-sized-robots-sense-their-environment-0723.

Chau, K. T. & Li, W. (2014a): Overview of electric machines for electric and hybrid vehicles. – International Journal of Vehicle Design, 64: 46–71.

Chau, K. T. & Li, W. (2014b): Overview of electric machines for electric and hybrid vehicles. – 64.

Chen, J., Cranton, W. & Fihn, M. (2016): Handbook of Visual Display Technology. – Cham.

Chen, K. & Jiang, S. P. (2016): Review – Materials Degradation of Solid Oxide Electrolysis Cells. – J. Electrochem. Soc., 163: F3070-F3083.

Chen, Q., Chen, Z., Shi, L., Li, X., Zhou, G. & Zhang, Y. (1996): Preparation of zinc sulfide thin films by the hydrothermal method. – Thin Solid Films, 272: 1–3.

Chen, R., Kim, S. & Chang, Z. (2017a): Redox Flow Batteries: Fundamentals and Applications. – In: Khalid, M. A. A. (editor): Redox – Principles and Advanced Applications.

Chen, W.-C., Chang, B.-C. & Chiu, K. L. (2017b): Recovery of germanium from waste Optical Fibers by hydrometallurgical method. – Journal of Environmental Chemical Engineering, 5: 5215–5221.

Chiang, M. & Zhang, T. (2016): Fog and IoT: An Overview of Research Opportunities. – IEEE Internet of Things Journal, 3: 854–864.

Cichy, M. (2017): Kritische mineralische Ressourcen von Photovoltaik-Dünnschicht-Technologien. – Eine Analyse unter Betrachtung der technologischen und marktwirtschaftlichen Entwicklung (2017-02-16). Vienna.

Ciller, P. & Lumbreras, S. (2020): Electricity for all: The contribution of large-scale planning tools to the energy-access problem. – Renewable and Sustainable Energy Reviews, 120: 109624.

Cisco (2016): Cisco Global Cloud Index 2015–2020. – URL: https://www.cisco.com/c/dam/m/en_us/service-provider/ciscoknowledgenetwork/files/622_11_15-16-Cisco_GCI_CKN_2015-2020_AMER_EMEAR_NOV2016.pdf.

Cisco (2017): Cisco Visual Networking Index.

Cisco (2018): Cisco Global Cloud Index: Forecast and Methodology, 2016–2021. – White Paper.

Cisco (2019): Cisco Visual Networking Index: Global Mobile Data Traffic Forecast Update, 2017–2022. – [Rev.: 22/03/2021].

Clemm, C., Bugge, F., Rothenbacher, S., Dethlefs, N., Ferkinghoff, C., Bergunde, T. & Lang, K.-D. (editors) (2017): Material flow of gallium arsenide and risk analysis in the III-V semiconductor industry in Germany.

Clemm, C., Emmerich, J. & Dethlefs, N. (2016): Toxikologische, physikalisch-chemische und gesellschaftliche Erforschung innovativer Materialien und Prozesse der Optoelektronik (TEMPO). Stoffflussanalysen, Lebenzyklusbetrachtung und Freisetzungspotenziale in Produktionsprozessen und Produkten. – Public report. – URL: https://www.tmp.tu-berlin.de/menue/forschung/stoffstromanalysen_fuer_elektronik/projekt_tempo/parameter/en/font3/maxhilfe/.

Clifton, A. (2013): Material Challenges for the Aerospace Sector. Presentation for COST Symposium: Materials in a resource-constrained world. – URL: http://www.cost.eu/events/materials [Rev.: 17/08/2015].

CM (2018): Outlook for the global Scandium market to 2028. – URL: https://www.cmgroup.net/reports/outlook-for-the-global-scandium-market/.

CMBlue Energy AG (2020): Organic-Flow-Batterien: Stromspeicher für die Energiewende. – Alzenau, Germany.

Colomina, I. & Molina, P. (2014): Unmanned aerial systems for photogrammetry and remote sensing: A review. – ISPRS Journal of Photogrammetry and Remote Sensing, 92: 79–97.

Colthorpe (2020): High safety level, ease of recyclability makes flow batteries 'very promising' in circular economy.

Columbus, L. (2018): 2018 Roundup Of Internet Of Things Forecasts And Market Estimates. – URL: https://www.forbes.com/sites/louiscolumbus/2018/12/13/2018-roundup-of-internet-of-things-forecasts-and-market-estimates/#767e94c67d83.

Combes, G. B., Claridge, J. B., Gallagher, J. R., Rosseinsky, M. J. & Boldrin, P. (2016): Fischer Tropsch Catalyst comprising Cobalt, Magnesium and precious Metal. – US2016/0222301 [Rev.: 10/03/2021].

Constellium (no date): Airware®, our aluminium-lithium alloy solutions. – URL: https://www.constellium.com/markets-applications/aerospace/products-and-solutions [Rev.: 06/07/2020].

Constellium (2013): Airware®. – URL: http://www.constellium.com/aluminium-innovation/aluminium-innovation-success-stories/airware-r [Rev.: 14/11/2015].

Constellium (2017a): Airware® 2050-T84 plate. – URL: https://www.constellium.com/sites/default/files/markets/airware_2050_t84_plate.pdf [Rev.: 06/07/2020].

Constellium (2017b): Airware® 2065-T84 extrusions. – URL: https://www.constellium.com/sites/default/files/markets/airware_2065_t84_extrusions.pdf [Rev.: 06/07/2020].

Constellium (2017c): Airware® 2098-T8 sheet. – URL: https://www.constellium.com/sites/default/files/markets/airware_2098_t8_sheet.pdf [Rev.: 06/07/2020].

Constellium (2017d): Airware® 2195-T84 plate. – URL: https://www.constellium.com/sites/default/files/markets/airware_2195_t84_plate.pdf.

Constellium (2017e): Airware® 2196-T8511 extrusions. – URL: https://www.constellium.com/sites/default/files/markets/airware_2196_t8511_extrusions.pdf [Rev.: 06/07/2020].

Constellium (2017f): Airware® 2198-T8 fuselage sheet. – URL: https://www.constellium.com/sites/default/files/markets/airware_2198_t8_fuselage_sheet.pdf [Rev.: 06/07/2020].

Constellium (2017g): Airware® 2297-T87 plate. – URL: https://www.constellium.com/sites/default/files/markets/airware_2297_t87_plate.pdf [Rev.: 06/07/2020].

Copper Alliance (2019): Global 2019 Semis End Use Data. – URL: https://copperalliance.org/trends-and-innovations/data-set/.

Cormos, C.-C., Vatopoulos, K. & Tzimas, E. (2013): Assessment of the consumption of water and construction materials in state-of-the-art fossil fuel power generation technologies involving CO_2 capture. – Energy, 51: 37–49.

Coughlin, T. (2019): CQ3 2019 Hard Disk Drive Results. – Forbes (2019-11-14). – URL: https://www.forbes.com/sites/tomcoughlin/2019/11/14/cq3-2019-hard-disk-drive-results/?sh=33f0192f1236#4390fbc31236 [Rev.: 08/12/2020].

Coyne, L., Browne, S. & Engelbrecht, M. (2017): IBM Tape Library Guide for Open Systems.

Cramer, C. L., Wang, H. & Ma, K. (2018): Performance of Functionally Graded Thermoelectric Materials and Devices: A Review. – Journal of Elec Materi, 47: 5122–5132.

Crastan, V. (2015): Elektrische Energieversorgung 1. Netzelemente, Modellierung, stationäres Verhalten, Bemessung, Schalt- und Schutztechnik. – 4th edition, Berlin, Heidelberg.

Cremer, C. (2007): Zukunftsmarkt CO_2-Abscheidung und -Speicherung. – Fallstudie im Auftrag des Umweltbundesamtes im Rahmen des Forschungsprojektes Innovative Umweltpolitik in wichtigen Handlungsfeldern. – URL: http://www.umweltbundesamt.de/en/publikationen/zukunftsmarkt-co2-abscheidung-speicherung [Rev.: 16/11/2015].

Crespo Cuaresma, J. (2017): Income projections for climate change research: A framework based on human capital dynamics. – Global Environmental Change, 42: 226–236.

Culver, S. P., Koerver, R., Zeier, W. G. & Janek, J. (2019): On the Functionality of Coatings for Cathode Active Materials in Thiophosphate-Based All-Solid-State Batteries. – Adv. Energy Mater., 9: 1900626.

Da Silva, F. S. & Souza, T. M. de (2017): Novel materials for solid oxide fuel cell technologies: A literature review. – International Journal of Hydrogen Energy, 42: 26020–26036.

D'Alessandro, D. M., Smit, B. & Long, J. R. (2010): Carbon dioxide capture: prospects for new materials. – Angewandte Chemie, 49: 6058–6082.

Damm, S. (2018): Rohstoffrisikobewertung – Tantal. – DERA Rohstoffinformationen 31, Berlin. – URL: https://www.bgr.bund.de/DE/Gemeinsames/Produkte/Downloads/DERA_Rohstoffinformationen/rohstoffinformationen-31.html [Rev.: 25/07/2020].

Damm, S. (2020): Tantalmarkt. – personal message.

Damm, S. & Zhou, Q. (2020): Supply and Demand of Natural Graphite. – DERA Rohstoffinformationen 43, Berlin. – URL: https://www.deutsche-rohstoffagentur.de/DERA/DE/Downloads/Studie%20Graphite%20eng%202020.pdf?__blob=publicationFile&v=3 [Rev.: 24/02/2021].

DatacenterDynamics (2015): Investitionen in Rechenzentren weltweit in den Jahren 2010 bis 2014 und Prognose für 2020. – URL: datacenterdynamics.com.

David, M., Ocampo-Martínez, C. & Sánchez-Peña, R. (2019): Advances in alkaline water electrolyzers: A review. – Journal of Energy Storage, 23: 392–403.

Deal, W. R. (2014): InP HEMT for Sub-Millimeter Wave Space Applications: Status and Challenges. – 39th International Conference on Infrared, Millimeter, and Terahertz waves (IRMMW-THz).

Dellink, R., Chateau, J., Lanzi, E. & Magné, B. (2017): Long-term economic growth projections in the Shared Socioeconomic Pathways. – Global Environmental Change, 42: 200–214.

DENA (2020): Privates Ladeinfrastrukturpotenzial in Deutschland. – URL: file:///C:/Users/rol/Downloads/dena-STUDIE_Privates_Ladeinfrastrukturpotenzial_in_Deutschland.pdf [Rev.: 14/07/2020].

DePuy Orthopaedics (2008): DePuy Hips Designed to Restore Your Motion and Reduce Your Pain. – URL: https://www.hipreplacement.com/technology/depuy_hipimplants [Rev.: 18/11/2015].

DERA (2019): Chart des Monats, Oktober 2019. – URL: https://www.deutsche-rohstoffagentur.de/DERA/DE/Downloads/DERA%202019_cdm_10_Titan.pdf [Rev.: 26/07/2020].

Deutsche Umweltstiftung (2020): Raus aus der Kunststofffalle. Kunststoffverpackungen – das unterschätzte Problem.

Deutz, S. & Bardow, A. (2020): How (Carbon) Negative Is Direct Air Capture? Life Cycle Assessment of an Industrial Temperature-Vacuum Swing Adsorption Process.

DGUV – Deutsche Gesetzliche Unfallversicherung (2015): DGUV Information 209-074 „Industrieroboter". – Berlin.

Di Cioccio, L., Jalaguier, E. & Letertre, F. (2005): III–V layer transfer onto silicon and applications. – physica status solidi (a): 509–515.

Díaz-Ramírez, M. C., Ferreira, V. J., García-Armingol, T., López-Sabirón, A. M. & Ferreira, G. (2020): Environmental Assessment of Electrochemical Energy Storage Device Manufacturing to Identify Drivers for Attaining Goals of Sustainable Materials 4.0. – Sustainability, 12: 342.

Diermann, R. (2019): Forscher erreichen mit ultradünner Galliumarsenid-Zelle Wirkungsgrad

von fast 20 Prozent. – (06/08/2019). – URL: https://www.pv-magazine.de/2019/08/06/forscher-erreichen-mit-ultraduenner-galliumarsenid-zelle-wirkungsgrad-von-fast-20-prozent/ [Rev.: 26/11/2020].

Ding, Y., Cano, Z. P., Yu, A., Lu, J. & Chen, Z. (2019): Automotive Li-Ion Batteries: Current Status and Future Perspectives. – Electrochem. Energ. Rev., 2: 1–28.

Display Daily (2020a): Flat Panel Display Area Demand Comes Roaring Back to Robust Growth, with a 9.1 Percent Expansion Expected in 2020. – URL: https://www.displaydaily.com/article/press-releases/flat-panel-display-area-demand-comes-roaring-back-to-robust-growth-with-a-9-1-percent-expansion-expected-in-2020 [Rev.: 11/01/2021].

Display Daily (2020b): Q2 OLED Supply/Demand Update – Oversupply in Phones to Persist to 2025. – URL: https://www.displaydaily.com/article/press-releases/q2-oled-supply-demand-update-oversupply-in-phones-to-persist-to-2025 [Rev.: 11/02/2021].

Dittmeyer, R., Klumpp, M., Kant, P. & Ozin, G. (2019): Crowd oil not crude oil. – Nature communications, 10: 1818.

Dittrich, M., Kämper, C., Ludmann, S., Ewers, B., Giegrich, J., Sartorius, C., Hummen, T., Marscheider-Weidemann, F. & Schoer, K. (2018): Strukturelle und produktionstechnische Determinanten der Ressourceneffizienz. – Untersuchung von Pfadabhängigkeiten, strukturellen Effekten und technischen Potenzialen auf die zukünftige Entwicklung der Rohstoffproduktivität (DeteRess). Dessau-Roßlau.

DJI (2020): Vergleich Hobby Drohnen. – URL: https://www.dji.com/de/products/compare-consumer-drones.

Djukanovic, G. (2017): Are Aluminium-Scandium Alloys the Future? – URL: https://aluminiuminsider.com/aluminium-scandium-alloys-future/ [Rev.: 06/07/2020].

DLR (2014): Fahrdrahtlose Energieübertragung bei Schienenfahrzeugen des Vollbahnverkehrs. – URL: http://elib.dlr.de/90435/1/20140423_Abschlussbericht_Fahrdrahtlose_Energie%C3%BCbertragung_Langfassung.pdf [Rev.: 14/07/2020].

DOE (2020): American-Made Challenges – Solar Desalination Prize. – URL: https://www.energy.gov/eere/solar/american-made-challenges-solar-desalination-prize.

Donaldson, J. D. & Beyersmann, D. (2012): Cobalt and Cobalt Compounds. – Ullmann's encyclopedia of industrial chemistry [Rev.: 14/07/2020].

Dorin, T., Ramajayam, M., Vahid, A. & Langan, T. (2018): Aluminium Scandium Alloys. – In: Lumley, R. N. (editor): Fundamentals of aluminium metallurgy. Recent advances. United Kingdom.

Dorner, U. (2020): Rohstoffrisikobewertung – Kupfer. – DERA Rohstoffinformationen 45, Berlin. URL: https://www.bgr.bund.de/DE/Gemeinsames/Produkte/Downloads/DERA_Rohstoffinformationen/rohstoffinformationen-45.html [Rev.: 26/05/2021].

Dostal, J. (2017): Rare Earth Element Deposits of Alkaline Igneous Rocks. – Resources, 6: 34.

DRONEII (2020): The Drone Industry Barometer 2020: Consolidating New Trends and Perspectives of the Commercial Drone Industry.

Dry, M. E. (2002): The Fischer-Tropsch process: 1950–2000. – Catalysis Today, 71: 227–241.

Du, Y., Xu, J., Paul, B. & Eklund, P. (2018): Flexible thermoelectric materials and devices. – Applied Materials Today, 12: 366–388.

Duan, J., Tang, X., Dai, H., Yang, Y., Wu, W., Wei, X. & Huang, Y. (2020): Building Safe Lithium-Ion Batteries for Electric Vehicles: A Review. – Electrochem. Energ. Rev., 3: 1–42.

Dubbel (1983): Taschenbuch für den Maschinenbau. – Heidelberg.

Durmus, Y. E., Zhang, H., Baakes, F., Desmaizieres, G., Hayun, H., Yang, L., Kolek, M., Küpers, V., Janek, J., Mandler, D., Passerini, S. & Ein-Eli, Y. (2020): Side by Side Battery Technologies with Lithium-Ion Based Batteries. – Adv. Energy Mater., 10: 2000089.

Dursun, T. & Soutis, C. (2014): Recent developments in advanced aircraft aluminium alloys. – Materials & Design (1980-2015), 56: 862–871.

Dutta, S. & Lanvin, B. (2019): The Network Readiness Index 2019. Towards a Future-Ready Society.

Duwe, D., Keicher, L., Ruess, P. & Klausmann, F. (2019): QUO VADIS 3D MOBILITY. Technological readiness, urban and rural use cases & urban integration of flying cars and passenger drones. – Stuttgart.

D-Wave Systems Inc. (2015): The D-Wave 2X(TM) Quantum Computer. Technology Overview. – URL: https://www.dwavesys.com/sites/default/files/D-Wave%202X%20Tech%20Collateral_0915F.pdf [Rev.: 31/08/2020].

E4tech (UK) Ltd (2016): The Fuel Cell Industry Review 2016. – URL: www.FuelCellIndustryReview.com.

E4tech (UK) Ltd (2019a): Study on Value Chain and Manufacturing Competitiveness Analysis for Hydrogen and Fuel Cells Technologies. – FCH contract 192. Evidence Report. – URL: www.e4tech.com.

E4tech (UK) Ltd (2019b): The Fuel Cell Industry Review 2019. – URL: www.FuelCellIndustryReview.com.

EAFO (2020): Vehicles & Fleet data. – URL: https://www.eafo.eu/ [Rev.: 12/06/2020].

Eberhard, M., Santo, U., Böning, D., Schmid, H., Michelfelder, B., Zimmerlin, B., Günther, A., Weigand, P., Müller-Hagedorn, M., Stapf, D. & Kolb, T. (2018): Der bioliq®-Flugstromvergaser – ein Baustein der Energiewende. – Chemie Ingenieur Technik, 90: 85–98.

EC (2018): A European Strategy for Plastics in a Circular Economy. – URL: https://ec.europa.eu/environment/strategy/plastics-strategy_en [Rev.: 04/02/2021].

EcoGraf (2020): Significant Battery Recycling Results. – Recovered high-purity battery anode material supports the global efforts to increase recycling of lithium-ion batteries.

Ecoloop (2018): Ecoloop Recycle to Gas. – URL: https://www.ecoloop.eu/wp-content/uploads/2019/05/Ecoloop-Prospekt_02-2019_deutsch.pdf.

Eichenseer, M. (2003): Aufbau und Charakterisierung eines hochstabilen Nd:YAG Lasers für ein Indium Frequenznormal. – Dissertation. Ludwig-Maximilians-Universität.

Electronicsnotes (2021): Photodiode structures. – URL: https://www.electronics-notes.com/articles/electronic_components/diode/photodiode-detector-structures-fabrication-materials.php.

elektroniknet.de (2021): Ab 2020: 5G lässt GaAs-Chips kräftig wachsen. – URL: https://www.elektroniknet.de/markt-technik/halbleiter/5g-laesst-gaas-chips-kraeftig-wachsen-167102.html.

Ellen MacArthur Foundation (2016): The New Plastics Economy. Rethinking the future of plastics. – URL: https://www.ellenmacarthurfoundation.org/assets/downloads/EllenMacArthur Foundation_TheNewPlasticsEconomy_Pages.pdf [Rev.: 08/02/2021].

Elsner, H. (2011): Kritische Versorgungslage mit schweren Seltenen Erden. Entwicklung „Grüner Technologien“ gefährdet? – Commodity Top News, 36: 8. Hanover, Germany.

Elsner, H., Melcher, F., Schwarz-Schampera, U. & Buchholz, P. (2010): Elektronikmetalle – zukünftig steigender Bedarf bei unzureichender Versorgungslage. – Commodity Top News, 33: 13. Hanover, Germany.

Emsley, J. (2014): Unsporting scandium. – Nature chemistry, 6: 1025.

Enerdata (2020): Global Enerergy Statistical Yearbook 2020. Electricity domestic consumption. – URL: https://yearbook.enerdata.net/electricity/electricity-domestic-consumption-data.html [Rev.: 22/01/2021].

Energieallianz Austria GmbH (2019): Weniger Stromausfälle in Österreich. – URL: https://www.energieallianz.com/de/at/ueber-eaa/presse/aktuelles/weniger-stromausfaelle-in-oesterreich.html [Rev.: 19/01/2021].

Enghag, P. (2004): Encyclopedia of the elements. Technical data, history, processing, applications. – Weinheim, Germany.

Enlitech (no date): VCSEL structure. – URL: https://www.enlitechnology.com/show/application-semiconductor.htm.

EnOcean (2020): EnOcean – The World of Energy Harvesting Wireless Technology.

EnOcean (2021): Products. – URL: https://www.enocean.com/en/products/.

Environment Park SPA, UNIVERZA V LJUBLJAN, Fundación Hidrógeno Aragón, Fundación IMDEA Energía & Industrias López Soriano SA (2018): HyTechCycling – New technologies and strategies for fuel cells and hydrogen technologies in the phase of recycling and dismantling. – WP2 Regulatory analysis, critical materials and components identification and mapping of recycling technologies D2.2 Existing end-of-life technologies applicable to FCH products. Grant No. 700190. – URL: https://ec.europa.eu/research/participants/documents/downloadPublic?documentIds=080166e5b9d244af &appId=PPGMS.

Environment Park SPA, UNIVERZA V LJUBLJAN, Fundación Hidrógeno Aragón, Fundación IMDEA Energía & Industrias López Soriano SA (2019): HyTechCycling – New technologies and strategies for fuel cells and hydrogen technologies in the phase of recycling and dismantling. – WP4 LCA for FCH technologies considering new strategies & technologies in the phase of recycling and dismantling D4.3 Case studies with new strategies in dismantling and recycling stage. Grant No. 700190. – URL: https://ec.europa.eu/research/participants/documents/downloadPublic?documentIds=080166e5b9d244af&appId=PPGMS.

EOS (2020): EOS Materials Metal: Portfolio Overview. – URL: https://www.eos.info/03_system-related-assets/material-related-contents/material_pdf/eos_materials_overview_metal_en.pdf.

Erlich, Y. & Zielinski, D. (2017): DNA Fountain enables a robust and efficient storage architecture. – Science (New York, N.Y.), 355: 950–954.

ESS (2017): Technical White Paper. All-Iron Flow Battery – Overview. – URL: https://www.essinc.com/white-papers/ [Rev.: 16/07/2020].

EuRIC aisbl (2020): Metal Recycling Factsheet. – URL: https://www.euric-aisbl.eu/position-papers/download/591/335/32.

European Commission (2019): The European Green Deal. – Brussels, Belgium.

European Commission (2020a): Study on the EU's list of Critical Raw Materials (2020). – Factsheets on Critical Raw Materials. Brussels. – URL: https://op.europa.eu/en/publication-detail/-/publication/ff34ea21-ee55-11ea-991b-01aa75ed71a1/language-en [Rev.: 24/02/2021].

European Commission (2020b): Study on the EU's list of Critical Raw Materials (2020). – Factsheets on Non-critical Raw Materials. Brussels. – URL: https://op.europa.eu/en/publication-detail/-/publication/ff34ea21-ee55-11ea-991b-01aa75ed71a1/language-en [Rev.: 24/02/2021].

European Commission (2020c): Proposal for a Regulation of the European Parliament and of the Council concerning batteries and waste batteries, repealing Directive 2006/66/EC and amending Regulation (EU) 2019/1020.

European Union (2020): A silver lining lights the way to thinner, more efficient solar cells. Advanced aRchitectures for ultra-thinhigh-efficiency CIGS solar cells with highManufacturability. – URL: https://cordis.europa.eu/article/id/396756-a-silver-lining-lights-the-way-to-thinner-more-efficient-solar-cells.

European Commission (2015): Carbon Capture and Storage. – URL: https://setis.ec.europa.eu/mis/technology/carbon-capture-and-storage [Rev.: 12/11/2015].

European Commission (2020a): Critical materials for strategic technologies and sectors in the EU – a foresight study. – URL: https://ec.europa.eu/docsroom/documents/42881 [Rev.: 18/11/2020].

European Commission (2020b): Study on the EU's list of Critical Raw Materials.

EUWID (2015): Illegale Exporte von Altautos kritisiert. – Euwid Recycling und Entsorgung, 8: 17.

EV Sales Blog (2020): EV Sales. – URL: http://ev-sales.blogspot.com/ [Rev.: 08/06/2020].

Eveland, K. (2011): Fibre optic cable growth continues in 2012. – Integer Research Limited. – URL: https://www.integer-research.com/integer-alert/fibre-optic-cable-growth-continues-in-2012 [Rev.: 09/12/2015].

FAA (2020): Unmanned Aircraft Systems. – URL: https://www.faa.gov/uas/.

Falk, F. (2006): Physik und Technologie von Solarzellen. – Lecture script. – URL: www.ipht-jena.de/fileadmin/user_upload/redaktion/Lehre/Vorlesungsscripte/PVtot_deutsch.pdf [Rev.: 11/08/2015].

Fan, Z., Zhang, Y., Pan, L., Ouyang, J. & Zhang, Q. (2021): Recent developments in flexible thermoelectrics: From materials to devices. – Renewable and Sustainable Energy Reviews, 137: 110448.

Fang, Q., Bai, W., Yang, J., Rong, H., Shi, N., Li, G., Xiong, M. & Ma, Z. (2013): Titanium, Ti, A New Mineral Species from Luobusha, Tibet, China. – Acta Geologica Sinica, 87: 1275–1280.

Fasihi, M., Efimova, O. & Breyer, C. (2019): Techno-economic assessment of CO_2 direct air capture plants. – Journal of Cleaner Production, 224: 957–980.

Feldman, S. (2019): 20 Years of Quantum Computing Growth. – URL: https://www.statista.com/chart/17896/quantum-computing-developments/ [Rev.: 31/08/2020].

Felix, N. (2012): Indium and Indium Compounds. – Ullmann's encyclopedia of industrial chemistry [Rev.: 14/07/2020].

Ferraro, E. & Prati, E. (2020): Is all-electrical silicon quantum computing feasible in the long term? – Physics Letters A, 384.

Fialka, J. (2021): Mining the sky for CO_2 with metal trees, towers and pumps. – URL: https://www.eenews.net/stories/1063721733 [Rev.: 20/01/2021].

Finch, M. (2020): Optical fibre and cable industry review. Highlights from 2019 and what's hot or not in 2020. – URL: https://www.crugroup.com/knowledge-and-insights/spotlights/2020/optical-fibre-and-cable-industry-review/ [Rev.: 23/02/2021].

Fischedick, M., Esken, A., Luhmann, H.-J., Schüwer, D. & Supersberger, N. (2007): Geologische CO_2-Speicherung als klimapolitische Handlungsoption. – Technologien, Konzepte, Perspektiven. Wuppertal, Germany.

Fischedick, M., Görner, K. & Thomeczek, M. (editors) (2015): CO_2: Abtrennung, Speicherung, Nutzung. – Ganzheitliche Bewertung im Bereich von Energiewirtschaft und Industrie. Berlin.

Fisia Italimpianti S.p.A. (2020): Desalination: a growing market. – URL: https://www.fisiait-the-future-of-water.com/en/facts-data/desalination-a-growing-market.html.

Fortune Business Insights (2019): Fiber Optics Market Size, Share and Industry Analysis. – URL: https://www.fortunebusinessinsights.com/fiber-optics-market-102904 [Rev.: 22/02/2021].

FPV (2020): Best 6S LiPo Battery Comparison Table. – URL: https://fpvcompare.com/6s-lipo-battery-comparison-matrices/.

Fraunhofer ICT (2015): Großprojekt »Redox-Wind«. – URL: http://www.ict.fraunhofer.de/de/komp/ae/rfb/redoxwind.html#tabpanel-3 [Rev.: 13/08/2015].

Fraunhofer IPM (2017): Thermoelektrik: Abwärmenutzung. – [Rev.: 05/03/2021].

Fraunhofer ISE (2020): Photovoltaics Report. – URL: https://www.ise.fraunhofer.de/content/dam/ise/de/documents/publications/studies/Photovoltaics-Report.pdf [Rev.: 23/09/2020].

Freer, R. & Powell, A. V. (2020): Realising the potential of thermoelectric technology: a Roadmap. – J. Mater. Chem. C, 8: 441–463.

Freiberger Compound Materials (2020a): URL: https://freiberger.com/en/products/specifications/.

Freiberger Compound Materials (2020b): Wireless Communication. – URL: https://freiberger.com/en/products/applications/wireless-communication/ [Rev.: 09/12/2020].

Freund et al. (2020): 5G-Datentransport mit Höchstgeschwindigkeit. – URL: https://link.springer.com/chapter/10.1007/978-3-662-55890-4_7 [Rev.: 06/10/2020].

Fricko, O., Havlik, P., Rogelj, J., Klimont, Z., Gusti, M., Johnson, N., Kolp, P., Strubegger, M., Valin, H., Amann, M., Ermolieva, T., Forsell, N., Herrero, M., Heyes, C., Kindermann, G., Krey, V., McCollum, D., Obersteiner, M., Pachauri, S., Rao, S., Schmid, E., Schoepp, W. & Riahi, K. (2017): The marker quantification of the Shared Socioeconomic Pathway 2: A middle-of-the-road scenario for the 21st century. – Global Environmental Change, 42: 251–267.

Friedrich, H. E. (editor) (2013): Leichtbau in der Fahrzeugtechnik. – Wiesbaden, Germany, s.l.

Frohs, W., Sturm, F. von, Wege, E., Nutsch, G. & Handl, W. (2012): Carbon, 3. Graphite. – Ullmann's encyclopedia of industrial chemistry.

Frost & Sullivan (2016): Lightweighting in Aerospace. – Future of Composites [Rev.: 25/06/2020].

Frost & Sullivan (2019): Composite Material Use in Global Commercial Aerospace. – [Rev.: 25/06/2020].

Frost & Sullivan (2020a): Cobots Transforming the Global Industrial Robotics Market. – Opportunities Forecast. Santa Clara.

Frost & Sullivan (2020b): Growth Opportunities for Superalloys. – Increasing Focus on Technology Developments and Application Extension Drive Growth of Superalloys.

FSM: Technik – Stromversorgung. Das schweizerische Stromversorgungsnetz. – URL: https://www.emf.ethz.ch/de/emf-info/themen/technik/stromversorgung/das-schweizerische-stromversorgungsnetz/?text=&author=964 [Rev.: 19/01/2021].

Fthenakis, V. (2009): Sustainability of photovoltaics: The case for thin-film solar cells. – Renewable and Sustainable Energy Reviews, 13: 2746–2750.

Gambhir, A. & Tavoni, M. (2019): Direct Air Carbon Capture and Sequestration: How It Works and How It Could Contribute to Climate-Change Mitigation. – One Earth, 1: 405–409.

Gandiglio, M., Sario, F. de, Lanzini, A., Bobba, S., Santarelli, M. & Blengini, G. A. (2019): Life Cycle Assessment of a Biogas-Fed Solid Oxide Fuel Cell (SOFC) Integrated in a Wastewater Treatment Plant. – Energies, 12: 1611.

Gao, A., Wietlisbach, S. & Schlag, S. (2019): Rare earth elements – The vitamins of modern industry. – URL: https://ihsmarkit.com/research-analysis/rare-earth-elements--the-vitamins-of-modern-industry.html.

Gao, Y., Wang, C., Zhang, J., Jing, Q., Ma, B., Chen, Y. & Zhang, W. (2020): Graphite Recycling from the Spent Lithium-Ion Batteries by Sulfuric Acid Curing–Leaching Combined with High-Temperature Calcination. – ACS Sustainable Chem. Eng., 8: 9447–9455.

Garside, M. (2020): Demand for rare earth oxides worldwide by application 2019 & 2025. – URL: https://www.statista.com/statistics/449722/rare-earth-estimated-demand-globally-by-application/ [Rev.: 15/03/2021].

Gartner (2020): Prognose zu den weltweiten IT-Ausgaben für Datencenter-Systeme von 2012 bis 2021. – URL: gartner.com.

Gärtner, M., Hermes, W., Marudhachalam, P., Schidleja, M. & Schierle-Arndt, K. (2003): Thermoelectricity. – In: Ullmann's encyclopedia of industrial chemistry. 6th edition, Weinheim, Germany.

Gellings, C. W. (2015): Let's Build a Global Power Grid. With a little DC wizardry and a lot of cash, we could swap power across continents. – IEEE Spectrum (2015-07-28). – URL: https://spectrum.ieee.org/energy/the-smarter-grid/lets-build-a-global-power-grid [Rev.: 26/06/2020].

Geoengineering Monitor (2018): Direct Air Capture. – [Rev.: 15/06/2020].

Georgescu, I. (2020): Trapped ion quantum computing turns 25. – Nature Reviews Physics, 2: 278.

Ghaffarzadeh, K. (2018): ITO alternatives 2018-2028: progress review of technology options. – URL: https://www.linkedin.com/pulse/ito-alternatives-2018-2028-progress-review-technology-ghaffarzadeh/ [Rev.: 07/01/2020].

Gille, G. & Meier, A. (2012): Recycling von Refraktärmetallen. – In: Thomé-Kozmiensky, K. J. & Goldmann, D. (editors): Recycling und Rohstoffe. Neuruppin, Germany.

Global CCS Institute (2019): Global Status Report. Targeting Climate Change.

Global CCS Institute (2020): Remove: Carbon capture and Storage. – URL: https://www.globalccsinstitute.com/wp-content/uploads/2020/11/Remove-Carbon-Capture-and-Storage-6.pdf [Rev.: 17/02/2021].

Global Data (2018): Internet of Things. Hot Topic Report GDTMT-TR-S176. – URL: https://hot-topics.globaldata.com/internet-of-things/.

Global Data (2019): Drones. Report GDTMT-TR-S206. – URL: https://hot-topics.globaldata.com/drones/.

Glöser-Chahoud, S. & Tercero Espinoza, L. (2015): Dynamische Materialfluss-Analyse von Neodym und Dysprosium als Magnetwerkstoffe.

Gok, A. (2020): Reliability and ecological aspects of photovoltaic modules. – London.

Gomatam, B. (2014): Optical Communications Infrastructure, Investment and Emerging Markets. State of the Industry. – OFC 2014 Marketwatch Panel.

Gossart, C. (2015): Rebound Effects and ICT: A Review of the Literature. – In: ICT Innovations for Sustainability.

Götz, U. (2018): Sobald sie über einen Schutzzaun nachdenken müssen, springen die Meisten schon ab. – URL: https://www.blog.kuka.com/2018/09/07/collaboration-and-coexistence/.

Gouveia, J., Mendes, A., Monteiro, R., Mata, T. M., Caetano, N. S. & Martins, A. A. (2020): Life cycle assessment of a vanadium flow battery. – Energy Reports, 6: 95–101.

Graedel, T. E., Gunn, G. & Tercero Espinoza, L. (editors) (2014): Metal resources, use and criticality.

Grand View Research (2019): Commercial Drone Market Size, Share & Trends Analysis Report. – URL: https://www.grandviewresearch.com/industry-analysis/global-commercial-drones-market.

Grand View Research (2020): Water Desalination Equipment Market Size. – URL: https://www.grandviewresearch.com/industry-analysis/water-desalination-equipment-market.

Grandfield, J. (2018): CM 10-Year Outlook for the Global Scandium Market to 2028. – (2018-11-26). Berlin, Germany.

Grandl, G., Ostgathe, M., Cachay, J., Doppler, S., Salib, J. & Ross, H. (2018): The Future of Vertical Mobility Sizing the market for passenger, inspection, and goods services until 2035. – A Porsche Consulting Study.

Greber, J. F. (2012): Gallium and Gallium Compounds. – Ullmann's encyclopedia of industrial chemistry [Rev.: 14/07/2020].

Green Car Congress (2019): TeraWatt Technology solid-state battery prototype tests showing 432 kWh/kg. – URL: https://www.greencarcongress.com/2019/08/20190822-tera.html.

Green Car Congress/Adamas Intelligence (2020): Adamas: "Unfathomable" rare earth demand growth awaits post-2030. – URL: https://www.greencarcongress.com/2020/09/20200929-adamas.html [Rev.: 15/03/2021].

Groesser, S. & Brechbuehler-Peskova, M. (2015): Rückgewinnung von Indium aus Bildschirmen: Ist das sinnvoll?

Grumbling, E. & Horowitz, M. (2019): Quantum Computing. – Washington, D.C.

Grünwald, R. (2007): CO_2-Abscheidung und -Lagerung bei Kraftwerken. – Arbeitsbericht des Büros für Technikfolgenabschätzung des Deutschen Bundestages Nr. 120.

Guina, M., Rantamäki, A. & Härkönen, A. (2017): Optically pumped VECSELs: review of technol-

ogy and progress. – J. Phys. D: Appl. Phys., 50: 383001.

Güttel, R., Kunz, U. & Turek, T. (2007): Reaktoren für die Fischer-Tropsch-Synthese. – Chemie Ingenieur Technik, 79: 531–543.

GWEC (2019): Global wind market development – Supply side data 2018. – Brussels.

Häfele, S., Hauck, M. & Dailly, J. (2016): Life cycle assessment of the manufacture and operation of solid oxide electrolyser components and stacks. – International Journal of Hydrogen Energy, 41: 13786–13796.

Harmsen, J., Roes, A. L. & Patel, M. K. (2013): The impact of copper scarcity on the efficiency of 2050 global renewable energy scenarios. – Energy, 50: 62–73.

Hassan, A. & Richter, S. (2002): Kreislaufführung von verbrauchten aus der chemischen Industrie. – Chemie Ingenieur Technik, 74: 219–227.

HEATRECAR Consortium (2013): Reduced Energy Consumption by Massive Thermoelectric Waste Heat Recovery in Light Duty Trucks. – URL: https://cordis.europa.eu/project/id/218541/reporting [Rev.: 05/03/2021].

Heckmann, D. (2020): Urban Air Mobility – Ein neuer Markt für Automobilakteure. – URL: https://magazine.fev.com/de/urban-air-mobility-ein-neuer-markt-fuer-automobilakteure/.

Heer, C. (2020): Top Trends Robotics 2020. – Frankfurt.

Hegmann, G. (2019): Lilium-Jet gegen Volocopter – Duell um das Billionen-Flugtaxi. – URL: https://www.welt.de/wirtschaft/article202308066/Flugtaxis-Lilium-und-Volocopter-kaempfen-um-Millionenmarkt.html.

Herweijer, C., Combes, J. & Gillham, J. (2020): How AI can enable a sustainable future. – URL: https://www.pwc.de/de/nachhaltigkeit/how-ai-can-enable-a-sustainable-future.pdf.

Heske, C., Lincot, D., Powalla, M., Salome, P., Schlatmann, R., Tiwari, A., Linden, H., Melkonyan, K., Petrova-Koch, V., Wade, A., Dalibor, T., Dimmler, B., Lundberg, O., Petroncini, S., Poplavskyy, D., Rühle, U., Schneider, H., Fischer, M. & Jaremalm, Eric, Reinhardt, Hannes (2019): CIGS_White_Paper_2019_online. – CIGS White Paper 2019.

Hettesheimer, T., Hirzel, S. & Ross, H. B. (2018): Energy savings through additive anufacturing: an analysis of selective laser sintering for automotive and aircraft components. – Energy Efficiency, 11: 1227–1245.

Hilbert, M. (2014): How much of the global information and communication explosion is driven by more, and how much by better technology? – Journal of the Association for Information Science and Technology, 65: 856–861.

Hilbert, M. (2015): Quantifying the Data Deluge and the Data Drought. Background note for the World Development Report 2016. World Bank, Washington, DC. – URL: https://papers.ssrn.com/sol3/papers.cfm?abstract_id=2984851 [Rev.: 22/03/2021].

Hilbert, M. (2019): Digital Data Divide Database. – URL: https://papers.ssrn.com/sol3/papers.cfm?abstract_id=3345756 [Rev.: 22/03/2021].

Hilbert, M. & López, P. (2011): The world's technological capacity to store, communicate, and compute information. – Science (New York, N.Y.), 332: 60–65.

Hildenbrand, P. (2019): Entwicklung einer Methodik zur Herstellung von Tailored Blanks mit definierten Halbzeugeigenschaften durch einen Taumelprozess. – FAU Studien aus dem Maschinenbau. Band 318. FAU University Press.

Hirsch-Kreinsen, H., Ittermann, P. & Niehaus, J. (editors) (2018): Digitalisierung industrieller Arbeit. Die Vision Industrie 4.0 und ihre sozialen Herausforderungen. – Baden-Baden, Germany.

Hochschule Landshut (2020): Kostengünstige Stromspeicher für die Welt. – URL: https://www.haw-landshut.de/aktuelles/news/news-detailansicht/article/kostenguenstige-stromspeicher-fuer-die-welt.html [Rev.: 17/07/2020].

Hoenderdaal, S. Tercero Espinoza, L. Marscheider-Weidemann, F. Graus, W. (2013): Can

a dysprosium shortage threaten green energy technologies? – Energy, 49: 344–355.

Hofmann, L. (2015): Einsatz von Erdkabeln und Freileitungen in Hochspannungs-Drehstrom- und -Gleichstromübertragungssystemen. – Hanover, Germany. [Rev.: 05/05/2015].

Horovitz, C. T. (editor) (1975): Scandium Its Occurrence, Chemistry Physics, Metallurgy, Biology and Technology. – London.

Horowitz, K. A. W., Remo, T., Smith, B. & Ptak, A. (2018): A Techno-Economic Analysis and Cost Reduction Roadmap for III-V Solar Cells.

Hovde, D. C. Prouty, M.D. Hrvoic, I. Slocum, R.E. (2013): Commercial Magnetometers and their Application. – Cambridge.

Huang, R., Riddle, M., Graziano, D., Warren, J., Das, S., Nimbalkar, S., Cresko, J. & Masanet, E. (2016): Energy and emissions saving potential of additive manufacturing: the case of lightweight aircraft components. – Journal of Cleaner Production: 1559–1570.

Hussain, S. & Yangping, L. (2020): Review of solid oxide fuel cell materials: cathode, anode, and electrolyte. – Energy Transit, 4: 113–126.

IBM (no date): Quantum technology & computing. – URL: https://www.zurich.ibm.com/st/quantum/alternativeplatforms.html [Rev-: 31/08/2020].

IBM Knowledge Center (2020): IBM TS4500 documentation. 3592 tape drives. – URL: https://www.ibm.com/support/knowledgecenter/en/STQRQ9/com.ibm.storage.ts4500.doc/ts4500_ipg_drives_3592.html [Rev.: 08/12/2020].

IBM Systems (2016): Tape goes high speed. Technical White Paper. – URL: https://www.ibm.com/downloads/cas/Q8BZDXZE [Rev.: 15/02/2021].

ICA (2020): EV motors boost copper demand. – URL: https://copperalliance.org/wp-content/uploads/2020/03/COR-04-Copper-motors2403.pdf.

IDA (2020): Desalination and Water Reuse by the Numbers. – URL: https://idadesal.org/ [Rev.: 18/06/2020].

IDC (2019): The Growth in Connected IoT Devices Is Expected to Generate 79.4ZB of Data in 2025, According to a New IDC Forecast. – URL: https://www.idc.com/getdoc.jsp?containerId=prUS45213219.

IEA (2012): Barriers to implementation of CCS: capacity Constraints. – URL: https://www.globalccsinstitute.com/archive/hub/publications/103746/barriers-implementation-ccs-capacity-constraints.pdf [Rev.: 16/11/2015].

IEA (2013a): Technology Roadmap. Carbon Capture and StorageCarbon Capture and Storage. – URL: https://www.iea.org/reports/technology-roadmap-carbon-capture-and-storage-2013 [Rev.: 16/11/2015].

IEA (2013b): World Energy Outlook 2013. – URL: http://www.worldenergyoutlook.org/weo2013/ [Rev.: 20/01/2015].

IEA (2013c): World Energy Outlook 2013. Renewable Energy Outlook.

IEA (2015): Storing CO_2 through Enhanced Oil Recovery. Paris. – URL: https://nachhaltigwirtschaften.at/resources/iea_pdf/reports/iea_ghg_storing_co2_trough_enhanced_oil_recovery.pdf [Rev.: 21/01/2021].

IEA (2016): 20 Years of Carbon Capture and Storage – Accelerating Future Deployment. – International Energy Agency.

IEA (2019): World Energy Outlook 2019.

IEA (2020a): Direct Air Capture. – URL: https://www.iea.org/reports/direct-air-capture.

IEA (2020b): Global electrolysis capacity becoming operational annually, 2014-2023, historical and announced. IEA hydrogen project database (2020). – URL: https://www.iea.org/data-and-statistics/charts/global-electrolysis-capacity-becoming-operational-annually-2014-2023-historical-and-announced.

IEA (2020c): Hydrogen Projects Database. – URL: https://www.iea.org/reports/hydrogen-projects-database.

IEA (2020d): World Energy Outlook 2020.

IEA (2021): The Role of Critical Minerals in Clean Energy Transitions. – URL: https://www.iea.org/reports/the-role-of-critical-minerals-in-clean-energy-transitions [Rev.: 12/05/2021].

IEA ETSAP (2010): Liquid Fuels Production from Coal & Gas. IEA ETSAP – Technology Brief S02. – URL: https://iea-etsap.org/E-TechDS/PDF/S02-CTL&GTL-GS-gct.pdf [Rev.: 27/11/2015].

IFAK (2011): Begleitforschung zum kabellosen Laden von Elektrofahrzeugen. – Chancen und Risiken beim kabellosen Laden von Elektrofahrzeugen, Technologiefolgenabschätzung für eine Schlüsseltechnologie in der Durchbruchphase der Elektromobilität. Abschlussbericht (Final Report). – URL: https://www.erneuerbar-mobil.de/sites/default/files/publications/abschlussbericht-justpark_1.pdf [Rev.: 14/07/2020].

IFR (2020): Executive Summary World Robotics. Industrial Robots. – URL: https://ifr.org/img/worldrobotics/Executive_Summary_WR_2020_Industrial_Robots_1.pdf.

IHS Markit (2019): News Release | IHS Markit Online Newsroom. – URL: https://news.ihsmarkit.com/prviewer/release_only/slug/technology-flat-panel-display-demand-increased-double-digits-2018-first-time-four-year [Rev.: 11/02/2021].

IIASA (no date): SSP Database, 2012 – 2018. – URL: https://tntcat.iiasa.ac.at/SspDb [Rev.: 13/05/2021].

Imarc (2020): Rare Earth Magnet Market: Global Industry Trends, Share, Size, Growth, Opportunity and Forecast 2021-2026. – URL: https://www.imarcgroup.com/rare-earth-magnet-manufacturing-plant [Rev.: 15/03/2021].

IMOA (2014): Practical Guidelines for the Fabrication of Duplex Stainless Steels. – URL: https://www.imoa.info/download_files/stainless-steel/Duplex_Stainless_Steel_3rd_Edition.pdf [Rev.: 20/10/2020].

Informationszentrum Mobilfunk (2020): Infobaukasten Mobilfunk 2/4 – Infrastruktur und Technik. DOKUMENTATION NO 156. – URL: https://www.informationszentrum-mobilfunk.de/sites/default/files/medien/Informationsbaustein%20Infrastruktur%20und%20Technik%20DStGB.pdf.

International Telecommunication Union & WEEE Forum (2020): Internet Waste. – A thought paper for International E-Waste Day 2020. Geneva. – URL: https://www.itu.int/en/ITU-D/Environment/Documents/Publications/2020/Internet-Waste%202020.pdf?csf=1&e=iQq5Zi.

Ionic Materials (2020): Breakthrough Innovation – Our solid polymer is the first of its kind to conduct ions at room temperature. – URL: https://ionicmaterials.com/.

IonQ (no date): Atoms make better quantum computers. – URL: https://ionq.com/technology [Rev.: 09/05/2021].

IÖW (2014): Dezentrale Produktion, 3D-Druck und Nachhaltigkeit. Trajektorien und Potenziale innovativer Wertschöpfungsmuster zwischen Maker-Bewegung und Industrie 4.0. Schriftenreihe des IÖW 206/14. Berlin.

IPCC (2005): IPCC Special Report on Carbon Dioxide Capture and Storage. – Working Group III of the Intergovernmental Panel on Climate Change. Cambridge, New York.

Irena (2017): Electricity Storage and Renewables: Costs and markets to 2030. – Abu Dhabi.

Irena (2019): Future of wind: Deployment, investment, technology, grid integration and socioeconomic aspects. – A Global Energy Transformation paper. Abu Dhabi.

Irena (2020a): Green Hydrogen Cost Reduction. Scaling up Electrolysers to Meet the 1.5 °C Climate Goal. Abu Dhabi. – URL: https://forum.xumuk.ru/applications/core/interface/file/attachment.php?id=47419.

Irena (2020b): Renewable Energy Technologies. – URL: https://www.irena.org/Statistics/View-Data-by-Topic/Capacity-and-Generation/Technologies [Rev.: 12/06/2020].

Irena (2020c): Wind Energy. – URL: https://www.irena.org/wind [Rev.: 09/12/2020].

ISO/IEC 20924 (2018): Information technology – Internet of Things (IoT) – Vocabulary.

IWCC (2020): Global Copper Semis End-Use Reports. – End use summary – copper content. – URL: http://www.coppercouncil.org/iwcc-statistics-and-data [Rev.: 25/02/2021].

IZES gGmbH, BET GmbH & PowerEngS (2011): Ausbau elektrischer Netze mit Kabel oder Freileitung unter besonderer Berücksichtigung der Einspeisung Erneuerbarer Energien. – Eine Studie im Auftrag des Bundesministeriums für Umwelt, Naturschutz und Reaktorsicherheit. Saarbrücken, Germany. – URL: https://www.bet-energie.de/fileadmin/redaktion/PDF/Studien_und_Gutachten/BET-Studie_Netzausbau_bf_BMU.pdf [Rev.: 19/01/2021].

Jara, A. D., Betemariam, A., Woldetinsae, G. & Kim, J. Y. (2019): Purification, application and current market trend of natural graphite: A review. – International Journal of Mining Science and Technology, 29: 671–689.

Jaziri, N., Boughamoura, A., Müller, J., Mezghani, B., Tounsi, F. & Ismail, M. (2020): A comprehensive review of Thermoelectric Generators: Technologies and common applications. – Energy Reports, 6: 264–287.

Jetzke, T. (2018): Flugtaxis – bemannte, vollelektrische Senkrechtstarter. – URL: https://www.tab-beim-bundestag.de/de/pdf/publikationen/themenprofile/Themenkurzprofil-021.pdf [Rev.: 27/04/2021].

Jiang, L. & O'Neill, B. C. (2017): Global urbanization projections for the Shared Socioeconomic Pathways. Global Environ. Change. – URL: https://www.sciencedirect.com/science/article/abs/pii/S0959378015000394.

JM (no date): Hard Disks. – URL: http://www.platinum.matthey.com/about-pgm/applications/industrial/hard-disks [Rev.: 17/05/2021].

JM (2019): Pgm Market Report. May 2019. – URL: http://www.platinum.matthey.com/documents/new-item/pgm%20market%20reports/pgm_market_report_may_19.pdf [Rev.: 17/12/2020].

JM (2020): Pgm Market Report. February 2020. – URL: http://www.platinum.matthey.com/documents/new-item/pgm-market-reports/pgm_market_report_february_2020.pdf [Rev.: 16/03/2021].

JM (2021): Pgm market report. May 2021. – URL: http://www.platinum.matthey.com/documents/new-item/pgm-market-reports/pgm-market-report-may-21.pdf [Rev.: 27/05/2021].

John, D. (2015): Rhenium – A Rare Metal Critical to Modern Transportation. – [Rev.: 15/07/2020].

John, D. A., Seal II, R. R. & Polyak, D. E. (2017): Rhenium. Chapter P of Critical Mineral Resources of the United States – Economic and Environmental Geology and Prospects for Future Supply. – [Rev.: 15/07/2020].

Johnson, K. M., Hammarstrom, J. M., Zientek, M. L. & Dicken, C. L. (2014): Estimate of Undiscovered Copper Resources of the World, 2013. – Global Mineral Resource Assessment [Rev.: 14/07/2020].

Jones, E., Qadir, M., van Vliet, M. T. H., Smakhtin, V. & Kang, S.-M. (2019): The state of desalination and brine production: A global outlook. – The Science of the total environment, 657: 1343–1356.

Jonge, M. M. de, Daemen, J., Loriaux, J. M., Steinmann, Z. J. & Huijbregts, M. A. (2019): Life cycle carbon efficiency of Direct Air Capture systems with strong hydroxide sorbents. – International Journal of Greenhouse Gas Control, 80: 25–31.

Joosting, J.-P. (2020): Soitec to produce POI substrates for Qualcomm 5G RF filters. – eeNEWS Europe, 2020 2020 (2020-07-08). – URL: https://www.eenewseurope.com/news/soitec-produce-poi-substrates-qualcomm-5g-rf-filters.

Jorge, R. S., Hawkins, T. R. & Hertwich, E. G. (2012a): Life cycle assessment of electricity transmission and distribution – part 1: power lines and cables. – Int J Life Cycle Assess, 17: 9–15.

Jorge, R. S., Hawkins, T. R. & Hertwich, E. G. (2012b): Life cycle assessment of electricity transmission and distribution – part 2: transformers and substation equipment. – Int J Life Cycle Assess, 17: 184–191.

Jorge, R. S. & Hertwich, E. G. (2013): Environmental evaluation of power transmission in Norway. – Applied Energy, 101: 513–520.

Jorge, R. S. & Hertwich, E. G. (2014): Grid infrastructure for renewable power in Europe: The environmental cost. – Energy, 69: 760–768.

Jorgenson, J. D. & George, M. W. (2005): Indium. Mineral Commodity Profile. – [Rev.: 14/07/2020].

Jouhara, H., Żabnieńska-Góra, A., Khordehgah, N., Doraghi, Q., Ahmad, L., Norman, L., Axcell, B., Wrobel, L. & Dai, S. (2021): Thermoelectric generator (TEG) technologies and applications. – International Journal of Thermofluids, 9: 100063.

JPCIC (2020): LCD Panel Project of Gongzhuling. – URL: http://www.jl.gov.cn/szfzt/tzcj/zdxm/english/dzxxjgxjs/202004/t20200423_7150649.html [Rev.: 11/02/2021].

Kaese, R. W. (2020): Storage Trends 2019. – URL: https://www.toshiba-storage.com/trends-technology/its-not-raining-data-its-pouring-storage-trends-2019/ [Rev.: 08/12/2020].

Kamalasanan, M. N. (1996): Sol-gel synthesis of ZnO thin films. – Thin Solid Films, 288: 112–115.

Kaminsky, W., Sinn, H. & Janning, J. (1979): Technische Prototypen für die Altreifen- und Kunststoff-Pyrolyse. – Chemie Ingenieur Technik, 51: 419–429.

Kampker, A., Vallée, D. & Schnettler, A. (2018): Elektromobilität. – Berlin, Heidelberg.

Kane, M. (2020): Tesla Model 3's IPM-SynRM electric motor explained. – URL: https://uk.motor1.com/news/462107/video-tesla-model-3-electric-motor-explained/ [Rev.: 17/03/2021].

Karimi, M., Mokhlis, H., Naidu, K., Uddin, S. & Bakar, A. (2016): Photovoltaic penetration issues and impacts in distribution network – A review. – Renewable and Sustainable Energy Reviews, 53: 594–605.

Kc, S. & Lutz, W. (2017): The human core of the shared socioeconomic pathways: Population scenarios by age, sex and level of education for all countries to 2100. – Global Environmental Change, 42: 181–192.

Keith, D. W., Holmes, G., St. Angelo, D. & Heidel, K. (2018): A Process for Capturing CO_2 from the Atmosphere. – Joule, 2: 1573–1594.

Kelley, K. D., Scott, C. T., Polyak, D. E. & Kimball, B. E. (2017): Vanadium. – Chapter U of Critical Mineral Resources of the United States – Economic and Environmental Geology and Prospects for Future Supply [Rev.: 27/07/2020].

Kendall, K. & Kendall, M. (2016): High-Temperature Solid Oxide Fuel Cells for the 21st Century.

Khan, M. A., Zhao, H., Zou, W., Chen, Z., Cao, W., Fang, J., Xu, J., Zhang, L. & Zhang, J. (2018): Recent Progresses in Electrocatalysts for Water Electrolysis. – Electrochem. Energ. Rev., 1: 483–530.

Khavarian, K. & Kockelman, K. M. (2020): Life-cycle Analysis of Electric Vertical Take-Off and Landing Vehicles.

Kim, T., Song, W., Son, D.-Y., Ono, L. K. & Qi, Y. (2019): Lithium-ion batteries: outlook on present, future, and hybridized technologies. – J. Mater. Chem. A, 7: 2942–2964.

Kirsch, H., Brübach, L., Loewert, M., Riedinger, M., Gräfenhahn, A., Böltken, T., Klumpp, M., Pfeifer, P. & Dittmeyer, R. (2020): CO_2-neutrale Fischer-Tropsch-Kraftstoffe aus dezentralen modularen Anlagen: Status und Perspektiven. – Chemie Ingenieur Technik, 92: 91–99.

KIT (2012): Miniatur-Radar mit Millimeter-Genauigkeit. – URL: http://www.pro-physik.de/details/news/2559291/Miniatur-Radar_mit_Millimeter-Genauigkeit.html [Rev.: 15/04/2015].

Klein, B. (2012): Leichtbau-Konstruktion. Berechnungsgrundlagen und Gestaltung. – 9th edition, Wiesbaden.

Klerk, A. de (2008): Fischer-Tropsch Refining. – A thesis submitted in partial fulfillment of the requirements for the degree Philosophiae Doctor (Chemical Engineering). University of Pretoria. – URL: https://repository.up.ac.za/bitstream/handle/2263/26754/Complete.pdf [Rev.: 15/02/2021].

Kluy, L. (2020): Was verspricht der Einsatz von Cobots? – URL: https://www.vdi.de/news/detail/was-verspricht-der-einsatz-von-cobots [Rev.: 16/12/2020].

Köhler, A. R., Gröger, J. & Liu, R. A. (2018): Energie- und Ressourcenverbräuche der Digitalisierung. – Berlin.

Koiwanit, J. (2018): Analysis of environmental impacts of drone delivery on an online shopping system. – Advances in Climate Change Research, 9: 201–207.

Koj, J. C., Schreiber, A., Zapp, P. & Marcuello, P. (2015): Life Cycle Assessment of improved high pressure alkaline electrolysis.

Koj, J. C., Wulf, C., Schreiber, C. & Zapp, P. (2017): Site-Dependent Environmental Impacts of Industrial Hydrogen Production by Alkaline Water Electrolysis. – Energies, 10: 860.

Kojonen, K. K., Roberts, A. C., Isomäki, O.-P., Knauf, V. V., Johnason, B. & Pakkanen, L. (2004): Tarkanite, (Cu,Fe)(Re,Mo)4S8, A new mineral species from the hitura mine, nivala, Finland. – The Canadian Mineralogist, 42: 539–544.

König, J., Tarantik, K., Heuer, J. & Bartholomé K. (2015): Thermoelectric research and developments at Fraunhofer IPM. Thermoelectrics: Ready for Progress to industrialization. – Symposium on waste heat recovery, 24.02.2015. Tokio.

Konter, M. (2012): Gas Turbine Materials with Focus on Re and RE Utilization and Trends. – The MMTA's International Minor Metals Conference. Cologne, Germany.

Kopacek, B. & Kopacek, P. (2013): End of life management of industrial robots. – Elektrotech. Inftech., 130: 67–71.

Korthauer, R. (2013): Handbuch Lithium-Ionen-Batterien. – Berlin, Heidelberg.

Kowsar, A., Rahaman, M., Islam, M. S., Imam, A. Y., Debnath, S. C., Sultana, M., Hoque, M. A., Sharmin, A., Mahmood, Z. H. & Farhad, S. (2019): Progress in Major Thin-film Solar Cells: Growth Technologies, Layer Materials and Efficiencies. – International Journal of Renewable Energy Research (2019).

Krail, M., Dütschke, E., Hellekes, J., Schneider, U., Schellert, M., Rüdiger, D., Steindl, A., Luchmann, I., Wassmuth, V., Flämig, H., Schade, W., Mader, S. & Wagner, U. (2019): Energie- und Treibhausgaswirkungen des automatisierten und vernetzten Fahrens im Straßenverkehr. – Karlsruhe, Germany.

Krapp, M. (2020): SONAR. Modelling for the search for new active materials for redox flow batteries. – URL: https://www.sonar-redox.eu/en/About.html [Rev.: 08/07/2020].

Krause, T., Strauss, O., Scheffler, G., Kett, H., Lehmann, K. & Renner, T. (2017): IT-Plattformen für das Internet der Dinge (IoT). Basis intelligenter Produkte und Services.

Kräusslich, W. (2020): Alles Wissenswerte zu Robotern: Geschichte, Typen, Anwendung. – URL: https://www.kollegeroboter.de/industrie/alles-wissenswerte-zu-robotern-geschichte-typen-einsatzbereiche-101.html#cobots.

Kreft, S. & Jackel, F. (2019): 3D Printing and the World of Metal Powders (2019).

Kreiger, M. & Pearce, J. M. (2013): Environmental Life Cycle Analysis of Distributed Three-Dimensional Printing and Conventional Manufacturing of Polymer Products. – ACS Sustainable Chem. Eng., 1: 1511–1519.

Kriegler, E., Bauer, N., Alexander, P., Humpenöder, F., Leimbach, M., Strefler, J., Baumstark, L., Bodirsky, B., Hilaire, J., Klein, D., Mouratiadou, I., Weindl, I., Bertram, C., Dietrich, JP., Luderer, G., Pehl, M., Pietzcker, R., Piontek, F., Lotze-Campen, H., Biewald, A., Bonsch, M., Giannousakis, A., Kreidenweis, U., Müller, C., Rolinski, S., Schultes, A., Schwanitz, J., Stevanovic, M., Calvin, K., Emmerling, J., Fujimori, S. & Edenhofer, O. (2017): Fossil-fueled development (SSP5): An energy and resource intensive scenario for the 21st century. – Global Environmental Change, 42: 297–315.

Kriegler, E., O'Neill, B. C., Hallegatte, S., Kram, T., Lempert, R. J., Moss, R. H. & Wilbanks, T. (2012): The need for and use of socio-economic scenarios for climate change analysis: a new approach based on shared socioeconomic pathways. – Global Environmental Change, 22: 807–822.

Ku, A. Y. (2018): Anticipating critical materials implications from the Internet of Things (IOT): Potential stress on future supply chains from emerging data storage technologies. – Sustainable Materials and Technologies, 15: 27–32.

Kuckshinrichs, W. (editor) (2013): CO_2-Abscheidung, -Speicherung und -Nutzung. Technische, wirtschaftliche, umweltseitige und gesellschaftliche Perspektive. – Jülich.

KUKA (2021): Industrieroboter. – personal message.

Kuroki, T., Murai, R., Makino, K., Nagano, K., Kajihara, T., Kaibe, H., Hachiuma, H. & Matsuno, H. (2015): Research and Development for Thermoelectric Generation Technology Using Waste Heat from Steelmaking Process. – Journal of Elec Materi, 44: 2151–2156.

Kurzweil, P. & Dietlmeier, O. K. (2018): Elektrochemische Speicher. – Wiesbaden, Germany.

Labs, L. (2020a): Grundlagen Bandlaufwerke. – Heise (2020-03-27). – URL: https://www.heise.de/select/ct/2020/8/2006413101160501970 [Rev.: 14/02/2021].

Labs, L. (2020b): Seagate: HAMR-Festplatte mit 20 TByte kommt im Dezember. – heise Online (24/09/2020). – URL: https://www.heise.de/news/Seagate-HAMR-Festplatte-mit-20-TByte-kommt-im-Dezember-4912052.html [Rev.: 14/02/2021].

Lambert, F. (2018): Tesla motor designer explains Model 3's transition to permanent magnet motor. – URL: https://electrek.co/2018/02/27/tesla-model-3-motor-designer-permanent-magnet-motor/ [Rev.: 17/03/2021].

Lang, P. (2019): Mehr Reichweite und Power dank Model-3-Antrieb. – URL: https://www.auto-motor-und-sport.de/elektroauto/tesla-model-s-x-synchronmotor-facelift-reichweite-leistung/ [Rev.: 17/03/2021].

Langione, M., Tillemann-Dick, C., Kumar, A. & Taneja, V. (2019): Where Will Quantum Computers Create Value – and When? – URL: https://www.bcg.com/publications/2019/quantum-computers-create-value-when [Rev.: 31/08/2020].

Langner, B. E. (2011): Understanding copper. Technologies, markets, business. – Winsen, Germany.

Lantz, M. (2020): Why the Future of Data Storage is (Still) Magnetic Tape – IEEE Spectrum. – URL: https://spectrum.ieee.org/computing/hardware/why-the-future-of-data-storage-is-still-magnetic-tape [Rev.: 08/12/2020].

Laschi, C., Mazzolai, B. & Cianchetti, M. (2016): Soft robotics: Technologies and systems pushing the boundaries of robot abilities. – Science robotics, 1.

Lau, W. W. Y., Shiran, Y., Bailey, R. M., Cook, E., Stuchtey, M. R., Koskella, J., Velis, C. A., Godfrey, L., Boucher, J., Murphy, M. B., Thompson, R. C., Jankowska, E., Castillo Castillo, A., Pilditch, T. D., Dixon, B., Koerselman, L., Kosior, E., Favoino, E., Gutberlet, J., Baulch, S., Atreya, M. E., Fischer, D., He, K. K., Petit, M. M., Sumaila, U. R., Neil, E., Bernhofen, M. V., Lawrence, K. & Palardy, J. E. (2020): Evaluating scenarios toward zero plastic pollution. – Science (New York, N.Y.), 369: 1455–1461.

Lechleitner, A., Schwabl, D., Schubert, T., Bauer, M. & Lehner, M. (2020): Chemisches Recycling von gemischten Kunststoffabfällen als ergänzender Recyclingpfad zur Erhöhung der Recyclingquote. – Österr Wasser- und Abfallw, 72: 47–60.

Lee, G. C., Cushner, F. D., Cannella, L. Y. & Scott, W. N. (2005): The effect of total knee arthroplasty on body weight. – Orthopedics, 28: 321–323.

Lee, Y. D. (2015): Thermodynamic, economic and environmental evaluation of solid-oxide fuel-cell hybrid power-generation systems. – Dissertation. Technische Universität Berlin. – URL: https://opus4.kobv.de/opus4-tuberlin/files/6857/lee_young_duk.pdf [Rev.: 25/10/2015].

Lee, Y.-G., Fujiki, S., Jung, C., Suzuki, N., Yashiro, N., Omoda, R., Ko, D.-S., Shiratsuchi, T., Sugimoto, T., Ryu, S., Ku, J. H., Watanabe, T., Park, Y., Aihara, Y., Im, D. & Han, I. T. (2020): High-energy long-cycling all-solid-state lithium metal batteries enabled by silver–carbon composite anodes. – Nat Energy, 5: 299–308.

Leimbach, M., Kriegler, E., Roming, N. & Schwanitz, J. (2017): Future growth patterns of world regions – a GDP scenario approach. – Global Environmental Change, 42: 215–225.

Li, L., Liu, G., Pan, D., Wang, W., Wu, Y. & Zuo, T. (2017): Overview of the recycling technology for copper-containing cables. – Resources, Conservation and Recycling, 126: 132–140.

Li, M.-J., Tandon, P., Bookbinder, D. C., Bickham, S. R. & McDermott, M. A. (2008): Ultra-low Bending Loss Single-Mode Fiber for FTTH. – Journal of Lightwave Technology, 2008: 376–382.

Li, Q. & Lau, K. M. (2017): Epitaxial growth of highly mismatched III-V materials on (001) silicon for electronics and optoelectronics. – Progress in crystal growth and characterization of materials: 105–120.

Lian, B., Sun, X.-Q., Vaezi, A., Qi, X.-L. & Zhang, S.-C. (2018): Topological quantum computation based on chiral Majorana fermions. – Proceedings of the National Academy of Sciences of the United States of America, 115: 10938–10942.

Licht, C., Peiró, L. T. & Villalba, G. (2015): Global Substance Flow Analysis of Gallium, Germanium, and Indium: Quantification of Extraction, Uses, and Dissipative Losses within their Anthropogenic Cycles. – Journal of Industrial Ecology, 19: 890–903.

Liedtke, M. & Huy, D. (2018): Rohstoffrisikobewertung – Gallium. DERA Rohstoffinformationen 35, Berlin.

Lilley, P. D., Erdle, E. & Gross, F. (1989): Market potential of solid oxide fuel cells (SOFC). – European Commission.

Linne, K. (2020): Was ist eine Festplatte? Einfach erklärt. – URL: https://praxistipps.chip.de/was-ist-eine-festplatte-einfach-erklaert_41663 [Rev.: 08/12/2020].

Lipinski, K. (2015): Magnetband. – URL: https://www.itwissen.info/Magnetband-magnetic-tape-MT.html [Rev.: 08/02/2021].

Liu, C. M., Sandhu, N. K., McCoy, S. T. & Bergerson, J. A. (2020a): A life cycle assessment of greenhouse gas emissions from direct air capture and Fischer–Tropsch fuel production. – Sustainable Energy Fuels, 4: 3129–3142.

Liu, J. & Chinnasamy, C. (2012): Rare Earth Magnet Recycling. – Rare Earth Elements Workshop, 10/05/2012. Colorado.

Liu, K., Yang, S., Luo, L., Pan, Q., Zhang, P., Huang, Y., Zheng, F., Wang, H. & Li, Q. (2020b): From spent graphite to recycle graphite anode for high-performance lithium ion batteries and sodium ion batteries. – Electrochimica Acta, 356: 136856.

López de Lacalle, L. Norberto, Campa, F. J. & Lamikiz, A. (2011): Milling. – In: Davim, J. (editor): Modern Machining Technology.

Lossin, A. (2012): Copper. – Ullmann's encyclopedia of industrial chemistry [Rev.: 14/07/2020].

Lotrič, A., Sekavčnik, M., Kuštrin, I. & Mori, M. (2021): Life-cycle assessment of hydrogen technologies with the focus on EU critical raw materials and end-of-life strategies. – International Journal of Hydrogen Energy, 46: 10143–10160.

LTEmobile (2021): 5G Frequenzen und Frequenzbänder. – URL: https://ltemobile.de/5g-frequenzen-und-frequenzbaender/ [Rev.: 31/05/2021].

Lutsey, N. (2010): Review of technical literature and trends related to automobile mass-reduction technology. Davis. – URL: https://escholarship.org/uc/item/9t04t94w [Rev.: 07/09/2020].

Lutz, C., Becker, L., Ulrich, P. & Distelkamp, M. (2019): Sozioökonomische Szenarien als Grundlage der Vulnerabilitätsanalysen für Deutschland. Teilbericht des Vorhabens „Politikinstrumente zur Klimaanpassung". – Dessau-Rosslau, Germany. – URL: https://www.umweltbundesamt.de/sites/default/files/medien/1410/publikationen/2019-05-29_cc_25-2019_soziooekonomszenarien.pdf.

Mahmoudi, S., Huda, N., Alavi, Z., Islam, M. T. & Behnia, M. (2019): End-of-life photovoltaic modules: A systematic quantitative literature review. – Resources, Conservation and Recycling, 146: 1–16.

Mantel, M. (2020): Magnetbänder: Fujifilm stellt 400-TByte-Tapes in Aussicht. – heise Online (06/07/2020). – URL: https://www.heise.de/news/Magnetbaender-Fujifilm-stellt-400-TByte-Tapes-in-Aussicht-4836606.html [Rev.: 12/02/2021].

Market Research Future (2021): Global Data Center Market. By Type (Corporate data centers, Web hosting data centers), Density (Low, Medium, High, Extreme), and Verticals (Banking & Financial Services, Telecom & IT, Government, Healthcare) – Forecast to 2023. – URL: https://www.marketresearchfuture.com/reports/data-centre-market-4721 [Rev.: 23/03/2021].

Markets and Markets (2014): Fiber Optics Market by Application (Telecom & Broadband, Utilities, Oil & Gas, Private Data Networks, Military/Aerospace, Cable Television & Others) – Global Trends & Forecasts to 2019. – URL: http://www.marketsandmarkets.com/Market-Reports/fiber-optics-market-238443438.html [Rev.: 20/11/2015].

MARKLINES CO Ltd (2020): Automotive Industry Portal. – URL: http://www.marklines.com [Rev.: 12/06/2020].

Marscheider-Weidemann, F., Langkau, S., Hummen, T., Erdmann, L., Tercero Espinoza, L. A., Angerer, G., Marwede, M. & Benecke, S. (2016): Rohstoffe für Zukunftstechnologien 2016. – DERA Rohstoffinformationen 28: 353 S., Berlin. – URL: https://www.bgr.bund.de/DERA/DE/Downloads/Studie_Zukunftstechnologien-2016.pdf;jsessionid=69AF2CA7D87C8AEE74782EFF3D20DB15.1_cid284?__blob=publicationFile&v=5.

Marti, P., Lampus, F., Benevento, D. & Setacci, C. (2019): Trends in use of 3D printing in vascular surgery: a survey. – Int Angiol., 38: 418–424.

Martin, D., Johnson, K., Stolberg, A., Zhang, X. & De Young, C. (2017): Carbon Dioxide Removal Options. – A Literature Review Identifying Carbon Removal Potentials and Costs.

Marwede, M. (2013): Cycling critical absorber materials of CdTe- and CIGS-photovoltaics: Material efficiency along the life-cycle. – Dissertation. University of Augsburg. – URL: http://opus.bibliothek.uni-augsburg.de/opus4/frontdoor/index/index/docId/2440 [Rev.: 23/06/2015].

Marwede, M. & Reller, A. (2014): Estimation of Life Cycle Material Costs of Cadmium Telluride- and Copper Indium Gallium Diselenide-Photovoltaic Absorber Materials based on Life Cycle Material Flows. – Journal of Industrial Ecology, 18: 254–267.

Marx, A., Hoess, J. & Uhlig K. (2014): Dry Dilution Refrigerator for Experiments on Quantum Effects in the Microwave Regime. – URL: https://arxiv.org/abs/1412.3619 [Rev.: 31/08/2020].

Massa, N. (2000): Fundamentals of photonics. – Module 1.8. Fiber Optic telecommunication.

Massimo, R., Thaker, A. & Suhare, A. (2018): The Coming Quantum Leap in Computing. – URL: https://www.bcg.com/publications/2018/coming-quantum-leap-computing [Rev.: 31/08/2020].

Matthews, N. (2018): Additive metal technologies for aerospace sustainment. – Aircraft Sustainment and Repair: 845–862.

Mattke, S. (2020): Luftnummer Lilium? – URL: https://www.heise.de/tr/artikel/Luftnummer-Lilium-4665642.html.

MatWeb (2020): Material Property Data. – URL: http://www.matweb.com [Rev.: 10/10/2020].

Maximize Market Research (2020): Global Optical Fiber Market Industry Analysis and Forecast (2020-2027) – by Mode, by Type, by Industry Vertical, by Application, and by Geography. – URL: https://www.maximizemarketresearch.com/market-report/global-optical-fiber-market/23623/ [Rev.: 22/02/2021].

May, N. (2005): Ökobilanz eines Solarstromtransfers von Nordafrika nach Europa. – Diploma thesis. Technische Universität Braunschweig. – URL: https://www.dlr.de/tt/Portaldata/41/Resources/dokumente/institut/system/publications/Oekobilanz_eines_Solarstromtransfers.pdf [Rev.: 09/06/2020].

Mayyas, A., Steward, D. & Mann, M. (2019): The case for recycling: Overview and challenges in the material supply chain for automotive li-ion batteries. – Sustainable Materials and Technologies, 19: e00087.

McKinsey & Company (2008): Carbon Capture & Storage. Assessing the Economics. – McKinsey Climate Change Initiative. – URL: https://assets.wwf.ch/downloads/mckinsey2008.pdf [Rev.: 16/11/2015].

McKinsey & Company (2019): Growing opportunities in the Internet of Things. – URL: https://www.mckinsey.com/industries/private-equity-and-principal-investors/our-insights/growing-opportunities-in-the-internet-of-things#.

Meetham, G. W. (2012): High-Temperature Materials. – Ullmann's encyclopedia of industrial chemistry.

Mehmeti, A., McPhail, S. J., Pumiglia, D. & Carlini, M. (2016): Life cycle sustainability of solid oxide fuel cells: From methodological aspects to system implications. – Journal of Power Sources, 325: 772–785.

Mekki, K., Bajic, E., Chaxel, F. & Meyer, F. (2019): A comparative study of LPWAN technologies for large-scale IoT deployment. – ICT Express, 5: 1–7.

Mellor, C. (2018): Seagate HAMRs out a roadmap for future hard drive recording tech. – The Register (2018-11-02). – URL: https://www.theregister.com/2018/11/02/seagate_hamr_roadmap/ [Rev.: 09/12/2020].

Mellor, C. (2019): Seagate: our disk drives are safe from SSDs for at least 15 years. – URL: https://blocksandfiles.com/2019/09/23/seagate-assumes-ssds-wont-kill-disk-drives/ [Rev.: 08/12/2020].

Mellor, C. (2020a): Hard disk drives will disappear from your data centre – unless you work for a hyperscaler. – URL: https://blocksandfiles.com/2020/02/07/hard-disks-disappear-small-data-centres/ [Rev.: 08/12/2020].

Mellor, C. (2020b): Fujifilm points to 400 TB tape cartridge on the horizon. – URL: https://blocksandfiles.com/2020/06/29/fujifilm-400tb-magnetic-tape-cartridge-future/ [Rev.: 09/12/2020].

Merklein, M., Johannes, M., Lechner, M. & Kuppert, A. (2014): A review on tailored blanks – Production, applications and evaluation. – Journal of Materials Processing Technology, 214: 151–164.

Meroufel, A. (2017): Controlling corrosion in Saudi Arabia's desalination plants. – URL: https://www.stainless-steel-world.net/webarticles/2017/07/04/controlling-corrosion-in-saudi-arabias-desalination-plants.html [Rev.: 10/10/2020].

Mertens, A. & Koch, M. (2003): Tailored Blank: Geschichte eines Erfolgs. – Stuttgarter Lasertage (Stuttgart Laser Technology Forum, STL), 2003: 169–172.

Merwerth, J. (2014): The hybrid-synchronous machine of the new BMW i3 and i8. – URL: http://hybridfordonscentrum.se/wp-content/uploads/2014/05/20140404_BMW.pdf [Rev.: 17/03/2021].

MetalAM (2020): Constellium launches Aheadd® high-performance aluminium powders. – URL: https://www.metal-am.com/constellium-launches-aheadd-high-performance-aluminium-powders/ [Rev.: 07/07/2020].

Meteyer, S., Xub, X., Perryc, N. & Zhaob, Y. F. (2014): Energy and Material Flow Analysis of Binder-jetting Additive Manufacturing Processes. – Procedia CIRP, 15: 19–25.

Mewawalla, C. (2019): Robotics. – Thematic Research at GlobalData.

Michaels, K. (2018): Overlooked: Looming Threats In The Aerospace Raw Material Supply Chain. – URL: https://www.linkedin.com/pulse/overlooked-looming-threats-aerospace-raw-material-supply-michaels/ [Rev.: 08/07/2020].

Micke, P., Stark, J., King, S. A., Leopold, T., Pfeifer, T., Schmöger, L., Schwarz, M., Spiess, L. J., Schmidt, P. O. & Crespo López-Urrutia, J. R. (2019): Closed-cycle, low-vibration 4 K cryostat for ion traps and other applications. – The Review of scientific instruments, 90: 65104.

MIT (2015): Power Plant Carbon Dioxide Capture and Storage Projects. Pilot Projects. – URL: https://sequestration.mit.edu/tools/projects/index_pilots.html [Rev.: 11/11/2015].

MMTA (2015): Re – Rhenium. – URL: http://www.mmta.co.uk/metals/Re [Rev.: 02/02/2016].

Modis GmbH (2021): personal message.

Monreal, C. (2020): Chemical recycling in Practice. – (2020-10-13).

Moore, S. K. & Nordrum, A. (2018): Intel's New Path to Quantum Computing. Intel's director of quantum hardware, Jim Clarke, explains the company's two quantum computing technologies. – URL: https://spectrum.ieee.org/nanoclast/computing/hardware/intels-new-path-to-quantum-computing [Rev.: 31/08/2020].

Mordor Intelligence (2020a): Fiber Optic Cable Market – Growth, Trends, COVID-19 Impact, and Forecasts (2021–2026). – URL: https://www.mordorintelligence.com/industry-reports/fiber-optic-cable-market [Rev.: 22/02/2021].

Mordor Intelligence (2020b): Rare Earth Elements Market – Growth, Trends, COVID-19 Impact, and Forecasts (2021 – 2026). – URL: https://www.mordorintelligence.com/industry-reports/rare-earth-elements-market [Rev.: 15/03/2021].

Mordor Intelligence (2020c): Synthetic Graphite Market – Growth, Trends, COVID-19 Impact, and Forecasts (2021 – 2026). – URL: https://www.mordorintelligence.com/industry-reports/synthetic-graphite-market.

Morimoto, T., Kobayashi, S., Nagao, Y. & Iwahori, Y. (2017): A new cost/weight trade-off method for airframe material decisions based on variable fuel price. – Cogent Engineering, 4: 17.

Morrish, J. (2020): Global IoT market to grow to $1.5 tn annual revenue by 2030. – URL: https://www.iot-now.com/2020/05/20/102937-global-iot-market-to-grow-to-1-5trn-annual-revenue-by-2030/.

Moss, R. L., Tzimas, E., Kara, H., Willis, P. & Kooroshy, J. (2011): Critical Metals in Strategic Energy Technologies. Assessing Rare Metals as Supply-Chain Bottlenecks in Low-Carbon Energy Technologies. – European Commission. – URL: http://publications.jrc.ec.europa.eu/repository/handle/JRC65592 [Rev.: 15/11/2012].

MPIF & APMI International (2020): Powder Metallurgy Fact Sheet. – URL: https://www.mpif.org/Resources/IndustryFacts.aspx.

Mraz, S. (2014): Basics of Aerospace Materials: Aluminum and Composites. – URL: https://www.machinedesign.com/materials/article/21831769/basics-of-aerospace-materials-aluminum-and-composites.

Mulligan, J. & Lashof, D. (2019): A CO_2 Direct Air Capture Plant Will Help Extract Oil in Texas. Could This Actually Be Good for the Climate? – URL: https://www.wri.org/blog/2019/07/co2-direct-air-capture-plant-will-help-extract-oil-texas-could-actually-be-good-climate [Rev.: 20/01/2021].

Münder, P. (2017): Mit dem Auto über die Wolken: Verkehr der Zukunft. – URL: https://www.zeit.de/mobilitaet/2017-05/verkehr-zukunft-flugtaxi-flugzeug-luftverkehr/seite-2.

Murata (2007): Choosing between ceramic and tantalum capacitors. – URL: http://www.dataweek.co.za/news.aspx?pklnewsid=27008 [Rev.: 21/12/2015].

Mutig, A. (2010): High Speed VCSELs for Optical Interconnects. – PhD Thesis.

Nadler, H. G. (2003): Rhenium and Rhenium Compounds. – In: Ullmann's encyclopedia of industrial chemistry. 6th edition, Weinheim, Germany.

Nakamura, K. (2012): Ultrasonic Transducers Materials and Design for Sensors, Actuators and Medical Applications. – Part 1 – chapter 3: Piezoelectric ceramics for transducers.

NASA (2018): URBAN AIR MOBILITY (UAM) MARKET STUDY. – URL: https://www.nasa.gov/sites/default/files/atoms/files/uam-market-study-executive-summary-v2.pdf.

Nassar, N. T. (2015): Limitations to elemental substitution as exemplified by the platinum-group metals. – Green Chem, 17: 2226–2235.

Nassar, N. T. (2017): Shifts and trends in the global anthropogenic stocks and flows of tantalum. – Resources, Conservation and Recycling, 125: 233–250.

National Academies of Sciences, Engineering, and Medicine (2019): Negative Emissions Technologies and Reliable Sequestration. – A Research Agenda.

Ndip (2021a): 5G und 6G: Schlüsseltechnologien und -bauelemente, Trends. – Interview Dr. Otmar Deubzer mit Dr. Ivan Ndip.

Ndip (2021b): »6G kommt, um die Erwartungen zu erfüllen, die 5G geweckt hat«. – Interview mit Dr. Ivan Ndip, Fraunhofer IZM. – URL: https://www.elektroniknet.de/kommunikation/mobilfunk/6g-kommt-um-die-erwartungen-zu-erfuellen-die-5g-geweckt-hat.182475.html [Rev.: 18/01/2021].

NETL (2019): Assessing the Export Potential for High-Performance Materials. – URL: https://www.netl.doe.gov/sites/default/files/2019-05/2019_Annual_Reports/Tuesday/Materials%20and%20Modeling/3%20-%202300.202.015_High%20Performance%20Materials%20Final%20Slide%20Deck%20-%20Shuster.pdf [Rev.: 03/03/2021].

Neumeier, S. (2020): MRK – Hype oder Erfolgsmodell für die Automobilindustrie? – URL: https://www.blog.kuka.com/2020/10/28/mrk-hype-oder-erfolgsmodell-fuer-die-automobilindustrie/ [Rev.: 15/02/2021].

Noll, R., Bergamos, M., Bergmann, K., Brumm, H., Eschen, M., Fricke-Begemann, C., Gorewoda, T., Makowe, J., Saenz, J., Schreckenberg, F., Torim, A. & Veglia, F. (2020): Process Line for the Automated Dismantling and Sorting of Valuable Components from Printed Circuit Boards. – In: Thomé-Kozmiensky, E., Holm, O., Friedrich, B. & Goldmann, D. (editors): Recycling und Sekundärrohstoffe, Band 13. Nietwerder.

NOW GmbH (2018): Industrialisierung der Wasserelektrolyse in Deutschland: Chancen und Herausforderungen für nachhaltigen Wasserstoff für Verkehr, Strom und Wärme. – Studie IndWEDe.

O'Donnell, N. (2020): ABB makes manufacturing more sustainable by recycling and remanufacturing thousands of old robots. – URL: https://new.abb.com/news/detail/64305/remanufacturing-old-robots [Rev.: 02/02/2021].

O'Neill, B. C., Kriegler, E., Ebi, K. L., Kemp-Benedict, E., Riahi, K., Rothman, D. S., van Ruijven, B. J., van Vuuren, D. P., Birkmann, J., Kok, K., Levy, M. & Solecki, W. (2017): The roads ahead: Narratives for shared socioeconomic pathways describing world futures in the 21st century. – Global Environmental Change, 42: 169–180.

OECD (2021): OECD Science, Technology and Innovation Outlook 2021. Times of Crisis and Opportunity. – Paris.

Oertel, D. (2008): Energiespeicher – Stand und Perspektiven. Sachstandsbericht zum Monitoring „Nachhaltige Energieversorgung". – URL: http://www.tab-beim-bundestag.de/de/pdf/publikationen/berichte/TAB-Arbeitsbericht-ab123.pdf [Rev.: 05/05/2014].

OICA (2020): Production statistics. – URL: http://www.oica.net/category/production-statistics/2013-statistics/ [Rev.: 12/06/2020].

Ojo, M. O., Giordano, S., Procissi, G. & Seitanidis, A. I. N. (2018): A Review of Low-End, Middle-End, and High-End Iot Devices. – IEEE Access, 6.

Ökopol GmbH (2016): Recyclingpotenzial strategischer Metalle (ReStra). – Abschlussbericht (Final Report).

Oleg Satanovsky (2019): BMW Expands 530e Sedan Inductive Charging Pilot Program to U.S. – URL: https://www.press.bmwgroup.com/usa/article/detail/T0299828EN_US/bmw-expands-530e-sedan-inductive-charging-pilot-program-to-u-s.

OMV (2018): Factsheet ReOil. – URL: https://www.omv.com/services/downloads/00/omv.com/1522138335117/Factsheet%20ReOil_de.

Oppenheimer, S. (2020): Elektromotoren: Es gibt drei Arten – doch die Zukunft gehört wohl dieser Technik. – URL: https://www.24auto.de/technik/antriebsarten/elektromotor-e-auto-stromer-permanenterregter-synchronmotor-rotor-stator-90066208.html [Rev.: 17/03/2021].

Or, T., Gourley, S. W. D., Kaliyappan, K., Yu, A. & Chen, Z. (2020): Recycling of mixed cathode lithium-ion batteries for electric vehicles: Current status and future outlook. – Carbon Energy, 2: 6–43.

Orth, M. (2014): Experimentelle Untersuchung des Chemical Looping Verfahrens an einer 1 MW Versuchsanlage. – Darmstadt. – Ph.D. Thesis.

Ostler, U. (2019): Warum das Tape im Datacenter noch lange nicht am Ende ist. Die Rolle von LTO Tape Libraries in einer Storage-Architektur. – URL: https://www.datacenter-insider.de/warum-das-tape-im-datacenter-noch-lange-nicht-am-ende-ist-a-855997/ [Rev.: 08/12/2020].

Ostrooumov, M. & Taran, Y. (2016): Vanadium, V – a new native element mineral from the Colima volcano, State of Colima, Mexico, and implications for fumarole gas composition. – Mineralogical Magazine, 80: 371–382.

Oubbati, M. (2007): Robotik. – Lecture notes. Ulm, Germany.

Outokumpu (no date): Produktlebenszyklus. – URL: http://www.outokumpu.com/de/nachhaltigkeit/nachhaltiger-produkte/produktlebenszyklus/Seiten/default.aspx.

Outokumpu (2020): The stainless steel family – introducing the different categories and grades. – URL: https://www.outokumpu.com/expertise/2020/the-stainless-steel-family [Rev.: 10/10/2020].

Pachauri, R. K. & Meyer, L. A. (2014): Climate Change 2014: Synthesis Report. – Contribution of Working Groups I, II and III to the Fifth Assessment Report of the Intergovernmental Panel on Climate Change. Geneva, Switzerland.

PATHION (2020): Lithium-ion Rich Anti-Perovskite (LiRAP)™. – URL: https://www.pathion.com/li-rap/.

Peither, M. (2020): VoltStorage. – Aktuelle Entwicklungen zu Redox-Flow-Batterien.

Perpetua (2021): Use Cases. Thermoelectric delivers power for all industries. – URL: https://perpetuapower.com/use-cases/ [Rev.: 04/03/2021].

Pervaiz, S., Anwar, S., Qureshi, I. & Ahmed, N. (2019): Recent Advances in the Machining of Titanium Alloys using Minimum Quantity Lubrication (MQL) Based Techniques. – Int. J. of Precis. Eng. and Manuf.-Green Tech., 6: 133–145.

Petavratzi, E., Gunn, G. & Kresse, C. (2019): BGS Commodity Review – Cobalt. – [Rev.: 14/07/2020].

Petermann, K. (2015): Herstellung von Lichtwellenleitern (TECH). Einführung in die optische Nachrichtentechnik.

Petrogas Gas-systems B.V (2020): Plastic to Chemicals. – URL: https://www.petrogas.nl/process-systems/plastic-to-oil/ [Rev.: 08/02/2021].

Plankers, B. (2015): The data center SSD takeover is well underway. – TechTarget (2015-04-14). – URL: https://searchdatacenter.techtarget.com/feature/The-data-center-SSD-takeover-is-well-underway [Rev.: 09/12/2020].

PlasticsEurope (2019): Plastics – the Facts 2019.

Podbregar, N. (2019): Kühlen ohne Kältemittel. Forscher optimieren die Kälteerzeugung durch Magnete. – URL: https://www.scinexx.de/news/technik/kuehlen-ohne-kaeltemittel/ [Rev.: 15/03/2021].

Pontes, J. (2021): 2020 Sales by OEM. – URL: http://ev-sales.blogspot.com/2021/02/2020-sales-by-oem.html [Rev.: 17/03/2021].

Powalla, M., Paetel, S., Ahlswede, E., Wuerz, R., Wessendorf, C. D. & Magorian Friedlmeier, T. (2018): Thin-film solar cells exceeding 22 % solar cell efficiency: An overview on CdTe-, Cu(In,Ga)Se 2 –, and perovskite-based materials. – Applied Physics Reviews, 5: 41602.

Pradhan, D., Panda, S. & Sukla, L. B. (2018): Recent advances in indium metallurgy: A review. – Mineral processing and extractive metallurgy review, 39: 167–180.

Priemer, B. (2015): Selbstversuch mit BMW i3 Remote Parking. Auto Motor Sport Online. – URL: http://www.auto-motor-und-sport.de/news/selbstversuch-bmw-i3-remote-parking-parken-mit-hang-zur-perfektion-9143838.html [Rev.: 19/02/2015].

Princeton Optronics (no date): Vertical-Cavity Surface-Emitting Laser Technology.

Protopapadaki, C. & Saelens, D. (2017): Heat pump and PV impact on residential low-voltage distribution grids as a function of building and district properties. – Applied Energy, 192: 268–281.

Prouvé, T., Godfrin, H., Gianèse, C., Triqueneaux, S. & Ravex, A. (2007): Pulse-Tube Dilution Refrigeration Below 10 mK. – Journal of Low Temperature Physics, 148: 909–914.

Quadbeck-Seeger, H.-J. (2007): Die Welt der Elemente – Die Elemente der Welt.

Quantafuel (2020): Plants and Projects. – URL: https://www.quantafuel.com/map-over-projects [Rev.: 08/02/2021].

Radziukynas, V. (2020): EnergyKeeper. – URL: http://www.energykeeper.eu/ [Rev.: 09/07/2020].

Rahimzei, E., Sann, K. & Vogel, M. (2015): Kompendium: Li-Ionen-Batterien. – Frankfurt.

Raluy, R. G., Serra, L., Uche, J. & Valero, A. (2005): Life Cycle Assessment of Water Production Technologies – Part 2: Reverse Osmosis Desalination versus the Ebro River Water Transfer (9 pp). – Int J Life Cycle Assess, 10: 346–354.

Ramseyer, C. (2018): Intel SSD 760p And 660p QLC Leak Online. – URL: https://www.tomshardware.com/news/intel-760p-660p-700p-specifications,36335.html [Rev.: 08/12/2020].

Rao, A. S. & Verweij, G. (2017): Sizing the prize. What's the real value of AI for your business and how can you capitalise?

Rao, M. (2019): The Future Of Data Centers. – URL: https://www.cbinsights.com/research/future-of-data-centers/ [Rev.: 08/12/2020].

Rasenack, K. & Goldmann, D. (2014): Herausforderungen des Indium-Recyclings aus LCD-Bildschirmen und Lösungsansätze. – Recycling und Rohstoffe.

Ravikumar, D., Seager, T., Sinha, P., Fraser, M. P., Reed, S., Harmon, E. & Power, A. (2020): Environmentally improved CdTe photovoltaic recycling through novel technologies and facility location strategies. – Prog Photovolt Res Appl, 28: 887–898.

Reinhardt, R., Amante García, B., Canals Casals, L. & Gassó Domingo, S. (2019): A Critical Evaluation of Cathode Materials for Lithium-Ion Electric Vehicle Batteries. – In: Ayuso Muñoz, J. L., Yagüe Blanco, J. L. & Capuz-Rizo, S. F. (editors): Project Management and Engineering Research. Cham.

Reinhold, J. (2020): Recyclingpotenzial von W, Ta und Nd aus Smartphones. – Bachelorarbeit. TU Berlin.

Reinsel, D., Gantz, J. & Rydning, J. (2018): The Digitization of the World – From Edge to Core.

Renner, H., Schlamp, G., Kleinwächter, I., Drost, E., Lüschow, H. M., Tews, P., Panster, P., Diehl, M., Lang, J., Kreuzer, T., Knödler, A., Starz, K. A., Dermann, K., Rothaut, J., Drieselmann, R., Peter, C., Schiele, R., Coombes, J., Hosford, M. & Lupton, D. F. (2018): Platinum Group Metals and Compounds. – Ullmann's encyclopedia of industrial chemistry [Rev.: 14/07/2020].

Research and Markets (2019): Rare Earth Elements: The Future of the Market to 2024 – High Demand from Emerging Economies. – URL: https://www.prnewswire.com/news-releases/rare-earth-elements-the-future-of-the-market-to-2024---high-demand-from-emerging-economies-300877742.html [Rev.: 15/03/2021].

Research Interfaces (2020): What do we know about next-generation NMC 811 cathode? – URL: https://researchinterfaces.com/know-next-generation-nmc-811-cathode/ [Rev.: 19/08/2020].

Reuter, Benjamin, Hendrich, A., Hengstler, J., Kupferschmid, S. & Schwenk, M. (2019): Rohstoffe für innovative Fahrzeugtechnologien. Herausforderungen und Lösungsansätze. – URL: https://www.e-mobilbw.de/fileadmin/media/e-mobilbw/Publikationen/Studien/Material-Studie_e-mobilBW.pdf.

rggroup (2020): COBOTS Vs. Industrial Robots: What's the Difference? – URL: https://www.rg-group.com/resources/blog/cobots-vs-industrial-robots.

Riahi, K., van Vuuren, D. P., Kriegler, E., Edmonds, J., O'Neill, B. C., Fujimori, S., Bauer, N., Calvin, K., Dellink, R., Fricko, O., Lutz, W., Popp, A., Crespo Cuaresma, J., Kc, S., Leimbach, M., Jiang, L., Kram, T., Rao, S., Emmerling, J., Ebi, K., Hasegawa, T., Havlik, P., Humpenöder, F., Da Silva, L. A., Smith, S.,

Stehfest, E., Bosetti, V., Eom, J., Gernaat, D., Masui, T., Rogelj, J., Strefler, J., Drouet, L., Krey, V., Luderer, G., Harmsen, M., Takahashi, K., Baumstark, L., Doelman, J., Kainuma. M., Klimont, Z., Marangoni, G., Lotze-Campen, H., Obersteiner, M., Tabeau, A. & Tavoni, M. (2017): The Shared Socioeconomic Pathways and their energy, land use, and greenhouse gas emissions implications: An overview. – Global Environmental Change, 42: 153–168.

Robinson, G. R., Hammarstrom, J. M. & Olson, D. W. (2017): Graphite. Chapter J of Critical Mineral Resources of the United States—Economic and Environmental Geology and Prospects for Future Supply. – [Rev.: 24/02/2021].

Rohrig, K. (2014): Windenergie Report Deutschland 2013. –

Römpp (no date): Chemisches Lexikon. – URL: https://roempp.thieme.de/ [Rev.: 08/04/2016].

Römpp (2020): Meerwasserentsalzung. – Römpp-online. – URL: https://roempp.thieme.de.

Rongguo, C., Juan, G., Liwen, Y., Huy, D. & Liedtke, M. (2016): Supply and Demand of Lithium and Gallium. – URL: https://www.deutsche-rohstoffagentur.de/EN/Themen/Min_rohstoffe/Downloads/studie_Li_Ga.pdf;jsessionid=4A572FB6D71EB86041EAEEB3A0E5138B.2_cid321?__blob=publicationFile &v=4 [Rev.: 14/07/2020].

Roskill (2011): Rare Earths & Yttrium: Market Outlook to 2015. – London, England.

Roskill (2018): Tantalum: Global Industry, Markets and Outlook to 2028. – 14th Edition. – URL: http://roskill.cn/Uploads//20190503/5ccb197ab69fa.pdf [Rev.: 17/12/2020].

Roskill (2019): Natural and synthetic graphite: Global Industry, Markets & Outlook. – London.

Roskill (2020a): Rare Earths. Outlook to 2030. – 20th Edition. – URL: https://roskill.com/market-report/rare-earths/ [Rev.: 15/03/2021].

Roskill (2020b): Roskill: Tantalum industry to be shaped by supply over next decade. – URL: https://www.globenewswire.com/news-release/2020/04/16/2017499/0/en/Roskill-Tantalum-industry-to-be-shaped-by-supply-over-next-decade.html [Rev.: 14/12/2020].

Roskill (2020c): Tantalum Outlook to 2029. 15th Edition. – URL: https://www.globenewswire.com/news-release/2020/04/16/2017499/0/en/Roskill-Tantalum-industry-to-be-shaped-by-supply-over-next-decade.html.

Roskill Information Services (2011): Rare Earths & Yttrium: Market Outlook to 2015. A quick introductory guide to rare earths.

Rozier, P. & Tarascon, J. M. (2015): Review – Li-Rich Layered Oxide Cathodes for Next-Generation Li-Ion Batteries: Chances and Challenges. – J. Electrochem. Soc., 162: A2490-A2499.

RP Photonics Encyclopedia (2019): Avalanche Photodiodes. – URL: https://www.rp-photonics.com/avalanche_photodiodes.html [Rev.: 18/01/2021].

Rudervall, R., Charpentier, J. P. & Sharma, R. (2000): High Voltage Direct Current (HVDC) Transmission Systems Technology Review Paper.

Ruffo, G. H. (2019): Imec Doubles Its Solid-State Battery Energy Density. They now reach 400 Wh/liter, enough for a 100 kWh EV battery pac. – URL: https://insideevs.com/news/360300/imec-energy-density-solidstate-batteries/.

Ryon, B. (2019): With a “hello,” Microsoft and UW demonstrate first fully automated DNA data storage. – Microsoft (2019-03-21). – URL: https://news.microsoft.com/innovation-stories/hello-data-DNA-storage/ [Rev.: 09/12/2020].

Sainathan, P. (2018): Supply Chain Visibility Evolution: Barcodes, RFID, NFC, BLE Beacons. – URL: https://blog.roambee.com/supply-chain-technology/evolution-in-supply-chain-visibility-barcodes-to-rfid-to-ble-beacons#:~:text=The%20most%20unique%20difference%20between,which%20is%20highly%20energy%2Defficient.&text=High%20Read%2DRange%3A%20Beacons%20have,nature%20of%20the%20BLE%20technology.

Salehi, A., Fu, X., Shin, D.-H. & So, F. (2019): Recent Advances in OLED Optical Design. – Adv. Funct. Mater., 29: 1808803.

Sander, K., Schilling, S., Wambach, K., Schlenker, S., Müller, A., Springer, J., Fouquet, D., Jelitte, A., Stryi-Hipp, G. & Chrometzka, T. (2007): Studie zur Entwicklung eines Rücknahme- und Verwertungssystems für Photovoltaische Produkte. – URL: http://epub.sub.uni-hamburg.de/epub/volltexte/2012/12655/pdf/Gesamtbericht_PVCycle_de.pdf [Rev.: 30/06/2015].

Sander, K., Otto, S.J., Rödig L., Wagner, L (2018): Behandlung von Elektroaltgeräten (EAG) unter Ressourcen- und Schadstoffaspekten. – 2018. edition, Dessau-Rosslau, Germany.

Sashank, S. S., Rajakumar, S., Karthikeyan, R. & Nagaraju, D. S. (2020): Weldability, Mechanical Properties and Microstructure of Nickel Based Super Alloys: a review. – E3S Web Conf., 184: 1040.

Savage, N. (2018): Building Quantum Computers With Photons. Silicon chip creates two-qubit processor. – URL: https://spectrum.ieee.org/tech-talk/computing/hardware/building-quantum-computers-with-photons [Rev.: 31/08/2020].

Schaal, S. (2019): Induktives Laden. BMW startet Pilotprojekt in den USA. – URL: https://www.electrive.net/2019/08/12/induktives-laden-bmw-startet-pilotprojekt-in-den-usa/.

Schadhauser, W. & Graefen, R. (2016): Was ist Flape? – Storage-Insider (2016-03-22). – URL: https://www.storage-insider.de/stichwort-flape-a-526963/ [Rev.: 15/02/2021].

Scheirs, J. & Kaminsky, W. (editors) (2016): Feedstock Recycling and Pyrolysis of Waste Plastics. – Converting waste Plastics into Diesel and other Fuels. Chichester et al.

Schlücker, I. (2016): Tapes und Disks besser jährlich wechseln. Lebenszyklus von Storage und Server. – URL: https://www.it-zoom.de/it-mittelstand/e/tapes-und-disks-besser-jaehrlich-wechseln-14555/ [Rev.: 12/02/2021].

Schmal, V. (2010): Neodym-Nachfrage für Zukunftstechnologien. – Diploma thesis. Baden-Wuerttemberg Cooperative State University (DHBW)

Schmidt, M. (2015): Rohstoffrisikobewertung – Platingruppenmetalle. Platin, Palladium, Rhodium. 2014. – DERA Rohstoffinformationen 26, Berlin. – URL: https://www.deutsche-rohstoffagentur.de/DERA/DE/Downloads/studie_Platin_2015.pdf?__blob=publicationFile&v=2.

Schmidt, M. (2017): Rohstoffrisikobewertung – Lithium. – DERA Rohstoffinformationen 33, Berlin. – URL: https://www.deutsche-rohstoffagentur.de/DERA/DE/Downloads/Studie_lithium_2017.pdf?__blob=publicationFile&v=3 [Rev.: 29/07/2020].

Schmidt, U. (2020): Elektromobilität und Klimaschutz: Die große Fehlkalkulation. – Kiel Policy Brief. – URL: https://www.ifw-kiel.de/fileadmin/Dateiverwaltung/IfW-Publications/-ifw/Kiel_Policy_Brief/2020/KPB_143.pdf [Rev.: 06/05/2021].

Schmirgel, V. (2021): Written exchange about industrial robotics: personal message.

Schorn, S. (no date): Mineralienatlas – Fossilienatlas. Seltene Erden. Lagerstätten und Vorkommen. – URL: https://www.mineralienatlas.de/lexikon/index.php/Mineralienportrait/Seltene%20Erden/Lagerst%C3%A4tten%20und%20Vorkommen#Lagerst.24.24ttentypen.

Schraven, S., Kley, F. & Wietschel, M. (2010): Induktives Laden von Elektromobilen. Eine technoökonomische Bewertung. – Working Paper Sustainability and Innovation.

Schuh, G., Dumitrescu, R., Krüger, A., Anderl, R. & Hompel, M. ten (2020): Industrie 4.0 Maturity Index. – Die digitale Transformation von Unternehmen gestalten – UPDATE 2020 – (acatech STUDIE). UPDATE 2020. Munich.

Schüler, D., Buchert, M., Liu, R., Dittrich, S. & Merz, C. (2011): Study on Rare Earths and Their Recycling. – Study conducted by the German Öko-Institut e. V. for The Greens/EFA Group in the European Parliament. – URL: www.oeko.de/oekodoc/1112/2011-003-en.pdf [Rev.: 13/04/2016].

Schulz, K., Piatak, N. M. & Papp, J. F. (2017): Niobium and Tantalum. – Chapter M of Critical Mineral Resources of the United States-Economic and Environmental Geology and Prospects for Future Supply [Rev.: 25/07/2020].

Scoyer, J., Guislain, H. & Wolf, H. U. (2012): Germanium and Germanium Compounds. – Ullmann's encyclopedia of industrial chemistry [Rev.: 14/07/2020].

Seagate Blog (2017): HAMR: the Next Leap Forward is Now | Seagate Blog. – URL: https://blog.seagate.com/craftsman-ship/hamr-next-leap-forward-now/ [Rev.: 09/12/2020].

Seiler, E. & Woidasky, J. (2013): Recycling von Windkraftanlagen (2013-02-06). – HamburgT.R.E.N.D.

Selenium-Tellurium Development Association (2021): Se & Te. – URL: https://stda.org/pages/SE-%26-TE.html.

SESAR (2016): European Drones Outlook Study: Unlocking the value for Europe.

Shah, A. (2020): Solar Cells and Modules. – 1st Edition. DOI 10.1007/978-3-030-46487-5

Shiva Kumar, S. & Himabindu, V. (2019): Hydrogen production by PEM water electrolysis – A review. – Materials Science for Energy Technologies, 2: 442–454.

Sibum, H., Güther, V., Roidl, O., Habashi, F., Uwe Wolf, H. & Siemers, C. (2003-2020): Titanium, Titanium Alloys, and Titanium Compounds. – In: Ullmann's encyclopedia of industrial chemistry. 7th edition, Weinheim, Germany.

Sibum, H., Güther, V., Roidl, O., Habashi, F., Uwe Wolf, H. & Siemers, C. (2017): Titanium, Titanium Alloys, and Titanium Compounds. – Ullmann's encyclopedia of industrial chemistry [Rev.: 26/07/2020].

Simon, R. W., Hammond, R. B., Berkowitz, S. J. & Willemsen, B.A. (2004): Superconducting microwave filter systems for cellular telephone base stations. – Proc. IEEE, 92: 1585–1596.

Sloan, J. (2020): The markets: Aerospace (2020). – URL: https://www.compositesworld.com/articles/the-markets-aerospace.

Slussarenko, S. & Pryde, G. J. (2019): Photonic quantum information processing: A concise review. – Applied Physics Reviews, 6: 41303.

Smit, M., Williams, K. & van der Tol, J. (2019): Past, present, and future of InP-based photonic integration. – APL Photonics, 4: 50901.

Smith, F. (2013): The Use of composites in aerospace: Past, present and future challenges. – URL: https://avaloncsl.files.wordpress.com/2013/01/avalon-the-use-of-composites-in-aerospace-s.pdf [Rev.: 02/07/2020].

Smith, L., Ibn-Mohammed, T., Yang, F., Reaney, I. M., Sinclair, D. C. & Koh, S. L. (2019): Comparative environmental profile assessments of commercial and novel material structures for solid oxide fuel cells. – Applied Energy, 235: 1300–1313.

Sojka, R., Pan, Q. & Billmann, L. (2020): Comparative study of Li-ion battery recycling processes. – URL: https://accurec.de/wp-content/uploads/2021/04/Accurec-Comparative-study.pdf.

Sparks, P. (2017): The route to a trillion devices: The outlook for IoT investment to 2035.

Special Metals (2021): Inconel nickel-chromium-iron alloy 601. – URL: https://www.specialmetals.com/assets/smc/documents/alloys/inconel/inconel-alloy-601.pdf [Rev.: 08/03/2021].

Srivastava, R. R., Kim, M., Lee, J., Jha, M. K. & Kim, B.-S. (2014): Resource recycling of superalloys and hydrometallurgical challenges. – J Mater Sci, 49: 4671–4686.

Staffell, I., Scamman, D., Velazquez Abad, A., Balcombe, P., Dodds, P. E., Ekins, P., Shah, N. & Ward, K. R. (2019): The role of hydrogen and fuel cells in the global energy system. – Energy Environ. Sci., 12: 463–491.

Statista (2018): Revenue of Internet of Things subsystems worldwide from 2012 to 2018.

Statista (2019a): Absatz von Industrierobotern weltweit nach Branchen in den Jahren 2018 und 2019. – URL: https://de.statista.com/statistik/daten/studie/188246/umfrage/installationen-von-industrierobotern-durch-robotik-seit-1998/.

Statista (2019b): Development of the world population until 2050 – URL: https://www.statista.com/statistics/262875/development-of-the-world-population/ [Rev.: 26/01/2021].

Statista (2019c): Quantum computing global market projections and forecast comparison 2017 to 2030 (in m USD). – URL: https://www.statista.com/statistics/936010/quantum-computing-future-market-outlook-forecast/.

Statista (2020): Umsatz mit Industrierobotern weltweit in den Jahren von 2018 bis 2025. – URL: https://de.statista.com/statistik/daten/studie/870571/umfrage/umsatz-von-industrie robotern-weltweit/.

Statista (2021a): Anzahl der Mobilfunkanschlüsse weltweit von 1993 bis 2020. – URL: https://de.statista.com/statistik/daten/studie/2995/umfrage/entwicklung-der-weltweiten-mobilfunk teilnehmer-seit-1993/.

Statista (2021b): Global new installed solar PV capacity from 2000 to 2019. – URL: https://www.statista.com/statistics/280200/global-new-installed-solar-pv-capacity/ [Rev.: 10/06/2021].

Steffen, A. D. (2020): Toyota's Solid-State Battery Set To Revolutionize EVs And Electronics. – URL: https://www.intelligentliving.co/toyotas-solid-state-battery/.

Steinfeldt, M., Gleich, A. von, Petschow, U., Haum, R., Chudoba, T. & Haubold, S. (2004): Nachhaltigkeitseffekte durch Herstellung und Anwendung nanotechnologischer Produkte. – TATuP, 13: 34–41.

Steinfort, T. (2020): Der Effizienzbegriff in der klimapolitischen Debatte zum Strassenverkehr. – URL: https://www.mwv.de/wp-content/uploads/2020/12/201026-Frontier-Studie-deutsch-NEU.pdf [Rev.: 10/03/2021].

Stengel, O., van Looy, A. & Wallaschkowski, S. (editors) (2017): Digitalzeitalter – Digitalgesellschaft. Das Ende des Industriezeitalters und der Beginn einer neuen Epoche. – Wiesbaden, Germany.

Stenzel, M. (2021): Tantalbedarf. – personal message.

Stiftung ear (no date): Kategorien des ElektroG Jedes Elektrogerät,. – https://www.stiftung-ear.de/de/themen/elektrog/herstellerbevollmaechtigte/kategorien. – URL: https://www.stiftung-ear.de/de/themen/elektrog/herstellerbevollmaechtigte/kategorien.

Stone, P., Brooks, R., Brynjolfsson, E., Calo, R., Etzioni, O., Hager, G., Hirschberg, J., Kalyanakrishnan, S., Kamar, E., Kraus, S., Leyton-Brown, K., Parkes, D., Press, W., Saxenian, A., Shah, J., Tambe, M. & Teller, A. (2016): Artificial Intelligence and Life in 2030. One Hundred Year Study on Artificial Intelligence. – Report of the 2015-2016 Study Panel. Stanford, CA. – URL: http://ai100.stanford.edu/2016-report.

Strassburg, F. W. (2019): Nickel Alloys. – In: Ullmann's Encyclopedia of Industrial Chemistry.

StrategyR (2020): Germanium. Global Markez Trajectory & Analytics. MCP-2637. – URL: https://www.strategyr.com/market-report-germanium-forecasts-global-industry-analysts-inc.asp.

Strazza, C., Del Borghi, A., Costamagna, P., Gallo, M., Brignole, E. & Girdinio, P. (2015): Life Cycle Assessment and Life Cycle Costing of a SOFC system for distributed power generation. – Energy Conversion and Management, 100: 64–77.

Suh, N. P. & Cho, D. H. (2017): The On-line Electric Vehicle. – Cham.

Sun, L. & He, Y. (2014): Research Progress of High Temperature Superconducting Filters in China. – IEEE Trans. Appl. Supercond., 24: 1–8.

Sun, W., Huang, R., Li, H., Hu, Y., Zhang, C., Sun, S., Zhang, L., Ding, X., Li, C., Zartman, R. E. & Ling, M. (2015): Porphyry deposits and oxidized magmas. – Ore Geology Reviews, 65: 97–131.

Sun, X., Hao, H., Zhao, F. & Liu, Z. (2017): Tracing global lithium flow: A trade-linked material flow analysis. – Resources, Conservation and Recycling, 124: 50–61.

Sweeney, S. J. & Mukherjee, J. (2017): Optoelectronic Devices and Materials. – In: S. Kasap, P. C. (editor): Springer Handbook of Electronic and Photonic Materials. Perspectives on electronic and photonic materials. Cham.

Tachikawa, K., Kesler, M. & Atasoy, O. (2018): Feasibility Study of Bi-directional Wireless Charging for Vehicle-to-Grid. – In: SAE Technical Paper Series.

Takada, K. (2013): Progress and prospective of solid-state lithium batteries. – Acta Materialia, 61: 759–770.

Takahashi, C. N., Nguyen, B. H., Strauss, K. & Ceze, L. (2019): Demonstration of End-to-End Automation of DNA Data Storage.

Tan, D. H. S., Banerjee, A., Chen, Z. & Meng, Y. S. (2020a): From nanoscale interface characterization to sustainable energy storage using all-solid-state batteries. – Nature nanotechnology, 15: 170–180.

Tan, D. H. S., Xu, P., Yang, H., Kim, M., Nguyen, H., Wu, E. A., Doux, J.-M., Banerjee, A., Meng, Y. S. & Chen, Z. (2020b): Sustainable design of fully recyclable all solid-state batteries. – MRS Energy & Sustainability, 7.

Tan, Y. N., Wen, H. C., Park, C., Gilmer, D. C., Young, C. D., Heh, D., Sivasubramani, P., Huang, J., Majhi, P., Kirsch, P. D., Lee, B. H., Tseng, H. H. & Jammy, R. (2008): Tunnel Oxide Dipole Engineering in TANOS Flash Memory for Fast Programming with Good Retention and Endurance. – In: 2008 International Symposium on VLSI Technology, Systems and Applications (VLSI-TSA).

TEC Microsystems (2021): Miniature thermoelectric generators. – URL: https://www.tec-microsystems.com/products/thermoelectric-generators/index.html.

Technavio (2019): Global Data Center Market Outlook 2019-2023. – URL: https://www.businesswire.com/news/home/20190823005139/en/Global-Data-Center-Market-Outlook-2019-2023-17 [Rev.: 23/03/2021].

Technavio (2020): Research Report: Global Rare Earth Metal Market 2020-2024 | Rising Demand For Electronic Appliances to boost the Market Growth | Technavio. – URL: https://finance.yahoo.com/news/research-report-global-rare-earth-233000385.html [Rev.: 15/03/2021].

TEGnology (2021): Products. – URL: https://www.tegnology.dk/.

Tekin (2021): Photonische Bauelemente und deren materielle Basis für 5G und 6G. – Interviews und schriftliche Kommunikation Dr. Otmar Deubzer mit Dr. Tolga Tekin, Fraunhofer IZM.

TeraWatt Technology (2020): Ultra-high energy density cells that work at scale. – URL: https://terawatt-technology.com.

Tercero Espinoza, L. (2012): Case study: Tantalum in the world economy: History, uses and demand. – [Rev.: 25/07/2020].

Terryn, S., Brancart, J., Lefeber, D., van Assche, G. & Vanderborght, B. (2017): Self-healing soft pneumatic robots. – Science robotics, 2.

The AI Blog (2016): Microsoft and University of Washington researchers set record for DNA storage. – URL: https://blogs.microsoft.com/ai/synthetic-dna-storage-milestone/#sm.0000k81a37qr6dijzdl15reujpheo [Rev.: 09/12/2020].

The Pew Charitable Trusts (2020): Breaking the Plastic Wave.

The Quantum Daily (2020): TQD Exclusive: A Detailed Review of Qubit Implementations for Quantum Computing. – URL: https://thequantumdaily.com/2020/05/21/tqd-exclusive-a-detailed-review-of-qubit-implementations-for-quantum-computing/ [Rev.: 31/08/2020].

Thellaputta, G. R., Chandra, P. S. & Rao, C. (2017): Machinability of Nickel Based Superalloys: A Review. – Materials Today: Proceedings, 4: 3712–3721.

Thielmann, A., Neef, C., Fenske, C. & Wietschel, M. (2018): Energiespeicher-Monitoring 2018. – Leitmarkt- und Leitanbieterstudie: Lithium-Ionen-Batterien für die Elektromobilität. Karlsruhe, Germany.

Thielmann, A., Neef, C. & Hettesheimer, T. (2019): All solid state batteries – What is the benchmark for a future commercialization? (2019).

Thielmann, A., Neef, C., Hettesheimer, T., Döscher, H., Wietschel, Prof Dr Martin & Tübke, Prof Dr Jens (2017): Energiespeicher-Roadmap. – Update 2017. Karlsruhe, Germany.

Thielmann, A., Sauer, A. & Wietschel, M. (2015): Gesamt-Roadmap Energiespeicher für die Elektromobilität 2030. – Karlsruhe, Germany.

Thormann, B. & Kienberger, T. (2020): Evaluation of Grid Capacities for Integrating Future E-Mobility and Heat Pumps into Low-Voltage Grids. – Energies, 13: 5083.

Thyssen-Krupp (2004): Großauftrag für Titanrohre zur Meerwasserentsalzung. – URL: https://www.thyssenkrupp.com/de/newsroom/pressemeldungen/gro-auftrag-fuer-titanrohre-zur-meerwasserentsalzung-2446.html [Rev.: 20/10/2020].

TIC (2020a): Applications for tantalum. – [Rev.: 17/12/2020].

TIC (2020b): The T.I.C. annual statistics presentation and data. – URL: https://www.tanb.org/images/T_I_C__Bulletin_no_180_(January%202020).pdf [Rev.: 04/01/2020].

TIC (2020c): Tantalum: a market overview by DERA. – URL: https://www.tanb.org/images/T_I_C__Bulletin_no_181_(April%202020).pdf [Rev.: 04/01/2021].

Titanium Asia (2018): Titanium Asia 2018. – Executive Summary.

Titanium USA (2018): Titanium USA 2018. – Executive Summary.

TNT Limited (no date): About Vanadium. – based on data provided by Vantitec. – URL: https://www.tmtlimited.com.au/about-vanadium.

Truebb, L. F. & Rüetschi, P. (1998): Batterien und Akkumulatoren. – Mobile Energiequellen für heute und morgen.

TWI2050 (2018): Transformations to Achieve the Sustainable Development Goals. The World in 2050. – Laxenburg, Austria. – URL: http://pure.iiasa.ac.at/id/eprint/15347/1/TWI2050_Report081118-web-new.pdf [Rev.: 22/05/2021].

Ugweje, O. (2004): The Internet Encyclopedia. Radio Frequency and Wireless Communications Security.

Ultrium LTO (2015): LTO-7: Questions & Answers. – URL: https://www.lto.org/2015/10/lto-7-specifications-questions-answers/ [Rev.: 01/11/2020].

Ultrium LTO (2020): Roadmap | Ultrium LTO. – URL: https://www.lto.org/roadmap/ [Rev.: 12/02/2021].

United Nations (2015): Paris Agreement. – URL: https://treaties.un.org/Pages/ViewDetails.aspx?src=IND&mtdsg_no=XXVII-7-d&chapter=27&clang=_en [Rev.: 24/03/2021].

United Nations (2019): World Population Prospects 2019.

Universität Hamburg (2012): Pyrolyse Gruppe. – URL: http://www.chemie.uni-hamburg.de/tmc/kaminsky/html/pyrolyse-gruppe.html [Rev.: 04/02/2020].

Urlings, H. (2019): EMEA Page Industry Trends – News Analysis – Market Intelligence and Opportunities Satellite IoT: A Game Changer for the Industry? How New Space and Old Space are Moving Into the New IoT Era. – URL: http://satellitemarkets.com/satellite-iot-game-changer-industry.

USENIX Association (2016): FAST '16. 14th USENIX Conference on File and Storage Technologies. Berkeley, CA.

USENIX Association (2020): FAST 20. 18th USENIX Conference on File and Storage Technologies. Santa Clara, CA.

USGS (2011a): Gallium. – Mineral Commodity Summaries [Rev.: 28/07/2020].

USGS (2011b): Graphite (natural). – Mineral Commodity Summaries [Rev.: 24/02/2021].

USGS (2011c): Lithium. – Mineral Commodity Summaries [Rev.: 29/07/2020].

USGS (2011d): Platinum-group metals. – Mineral Commodity Summaries [Rev.: 29/07/2020].

USGS (2011e): Rhenium. – Mineral Commodity Summaries [Rev.: 29/07/2020].

USGS (2011f): Vanadium. – Mineral Commodity Summaries [Rev.: 31/07/2020].

USGS (2012): Titanium mineral concentrates. – Mineral Commodity Summaries [Rev.: 31/07/2020].

USGS (2014a): Gallium. – Mineral Commodity Summaries [Rev.: 28/07/2020].

USGS (2014b): Graphite (natural). – Mineral Commodity Summaries [Rev.: 24/02/2021].

USGS (2014c): Lithium. – Mineral Commodity Summaries [Rev.: 29/07/2020].

USGS (2014d): Platinum-group metals. – Mineral Commodity Summaries [Rev.: 29/07/2020].

USGS (2014e): Rhenium. – Mineral Commodity Summaries [Rev.: 29/07/2020].

USGS (2014f): Vanadium. – Mineral Commodity Summaries [Rev.: 31/07/2020].

USGS (2015): Titanium Mineral Concentrates. – Mineral Commodity Summaries [Rev.: 31/07/2020].

USGS (2016): Rare Earths. – Mineral Commodity Summaries [Rev.: 23/07/2020].

USGS (2017a): Tantalum [Advance Release].– Minerals Yearbook [Rev.: 25/07/2020].

USGS (2017b): Germanium [Advance Release]. – Minerals Yearbook Minerals Yearbook [Rev.: 28/07/2020].

USGS (2017c): Indium [Advance Release]. – Minerals Yearbook [Rev.: 28/07/2020].

USGS (2017d): Rare Earths. – Minerals Yearbook [Rev.: 23/07/2020].

USGS (2017e): Rhenium [Advance Release]. – Minerals Yearbook [Rev.: 29/07/2020].

USGS (2017f): Vanadium [Advance Release]. – [Rev.: 27/07/2020].

USGS (2019a): Gallium. – Mineral Commodity Summaries [Rev.: 28/07/2020].

USGS (2019b): Graphite (natural). – Mineral Commodity Summaries [Rev.: 24/02/2021].

USGS (2020a): Cobalt. – Mineral Commodity Summaries [Rev.: 14/07/2020].

USGS (2020b): Copper. – Mineral Commodity Summaries [Rev.: 14/07/2020].

USGS (2020c): Gallium. – Mineral Commodity Summaries. – URL: https://pubs.usgs.gov/periodicals/mcs2020/mcs2020-gallium.pdf [Rev.: 14/07/2020].

USGS (2020d): Germanium. – Mineral Commodity Summaries [Rev.: 14/07/2020].

USGS (2020e): Indium. – Mineral Commodity Summaries [Rev.: 14/07/2020].

USGS (2020f): Lithium. – Mineral Commodity Summaries [Rev.: 14/07/2020].

USGS (2020g): Platinum Group Metals. – Mineral Commodity Summaries [Rev.: 14/07/2020].

USGS (2020h): Rare Earths. – Mineral Commodity Summaries [Rev.: 22/07/2020].

USGS (2020i): Rhenium. – Mineral Commodity Summaries [Rev.: 29/07/2020].

USGS (2020j): Rhenium Statistics and Information. – URL: https://www.usgs.gov/centers/nmic/rhenium-statistics-and-information.

USGS (2020k): Scandium. – Mineral Commodity Summaries [Rev.: 20/07/2020].

USGS (2020l): Tantalum. – Mineral Commodity Summaries [Rev.: 25/07/2020].

USGS (2020m): Titanium and Titanium Dioxide. – Mineral Commodity Summaries [Rev.: 26/07/2020].

USGS (2020n): Titanium Mineral Concentrates. – Mineral Commodity Summaries [Rev.: 26/07/2020].

USGS (2020o): Vanadium. – Mineral Commodity Summaries. [Rev.: 26/07/2020].

USGS (2021a): Germanium. – URL: https://pubs.usgs.gov/periodicals/mcs2021/mcs2021-germanium.pdf [Rev.: 23/02/2021].

USGS (2021b): Rare Earths. – URL: https://pubs.usgs.gov/periodicals/mcs2021/mcs2021-rare-earths.pdf [Rev.: 15/03/2021].

van Gosen, B. S., Verplanck, P. L., Seal, R. R., II, Long, K. R. & Gambogi, J. (2017): Rare-Earth Elements. – Chapter O of Critical Mineral Resources of the United States—Economic and Environmental Geology and Prospects for Future Supply [Rev.: 22/07/2020].

van Vuuren, D. P., Stehfest, E., David E.H.J. Gernaat, Jonathan C. Doelman, Maarten van den Berg, Mathijs Harmsen, Harmen Sytze de Boer, Lex F. Bouwman, Vassilis Daioglou, Oreane Y. Edelenbosch, Bastien Girod, Tom Kram, Luis Lassaletta, Paul L. Lucas, Hans van Meijl, Christoph Müller, Bas J. van Ruijven, Sietske van der Sluis & Andrzej Tabeau (2017): Energy, land-use and greenhouse gas emissions trajectories under a green growth paradigm. – Global Environmental Change, 42: 237–250.

van Winkle, W. (2019): The death of disk? HDDs still have an important role to play. – URL: https://venturebeat.com/2019/09/02/the-death-of-disk-hdds-still-have-an-important-role-to-play/ [Rev.: 08/12/2020].

Vatopoulos, K. & Tzimas, E. (2012): Assessment of CO_2 capture technologies in cement manufacturing process. – Journal of Cleaner Production, 32: 251–261.

VCI (2018): VCI-Position zu Kreisläufen für Kohlenstoff. Zirkuläre Wirtschaft: Kohlenstoff. – URL: https://www.vci.de/themen/energie-klima-rohstoffe/rohstoffe/vci-position-kreislaeufe-fuer-kohlenstoff.jsp [Rev.: 05/02/2020].

VDI (2014): Additive Fertigungsverfahren – Grundlagen, Begriffe, Verfahrensbeschreibungen. – 3405. – URL: https://www.vdi.de/richtlinien/details/vdi-3405-additive-fertigungsverfahren-grundlagen-begriffe-verfahrensbeschreibungen.

VDI ZRE (2014): Ressourceneffizienz von Windenergieanlagen. – VDI ZRE Publikationen: Kurzanalyse Nr. 9.

VDI-Gesellschaft Technologies of Life Sciences (2013): Bionik; Bionische Roboter. – URL: https://term.vdi-online.de/index.php/definition/updateDefinition/519/15286/show [Rev.: 22/10/2020].

Velázquez-Martínez, Valio, Santasalo-Aarnio, Reuter & Serna-Guerrero (2019): A Critical Review of Lithium-Ion Battery Recycling Processes from a Circular Economy Perspective. – Batteries, 5: 68.

Velodyne (2020): High Definitian Lidar HDL-64E. – URL: http://hypertech.co.il/wp-content/uploads/2015/12/HDL-64E-Data-Sheet.pdf [Rev.: 09/12/2020].

Verhoefa, L. A., Budde, B. W., Chockalingam, C., Nodar, B. G. & van Wijk, A. J. (2018): The effect of additive manufacturing on global energy demand: An assessment using a bottom-up approach. – Energy Policy: 349–360.

VGB (2011): Pre-Engineering Study “NRW Power Plant 700 °C”. – URL: https://www.vgb.org/en/research_project297.html [Rev.: 23/02/2021].

Viaud, A. (2019): Dominating the data center – the rise of SSD technology. – URL: https://www.datacenterdynamics.com/en/opinions/dominating-data-center-rise-ssd-technology/ [Rev.: 09/12/2020].

Viebahn, P., Arnold, K., Friege, J., Krüger, C., Nebel, A., Ritthoff, M., Samadi, S., Soukup, O., Teubler, J. & Wiesen, K. (2014): KRESSE – Kritische mineralische Ressourcen und Stoffstroeme bei der Transformation des deutschen Energieversorgungssystems. Abschlussbericht (Final Report). – URL: https://epub.wupperinst.org/frontdoor/deliver/index/docId/5419/file/5419_KRESSE.pdf.

Viebahn, P., Scholz, A. & Zelt, O. (2019): The Potential Role of Direct Air Capture in the German Energy Research Program—Results of a Multi-Dimensional Analysis. – Energies, 12: 3443.

Villanueva, J. C. (2009): How Many Atoms Are There in the Universe? – URL: https://www.universetoday.com/36302/atoms-in-the-universe/ [Rev.: 31/08/2020].

Vollmers, F. (2008): „Tailored Blanks“ senken Autogewicht um 20 Prozent. – URL: https://www.handelsblatt.com/unternehmen/mittelstand/massgeschneiderter-stahl-tailored-blanks-senken-autogewicht-um-20-prozent/2937592.html?ticket=ST-13416288-IULM7rnNJK7aaHinpSkD-ap5 [Rev.: 07/09/2020].

volterion (2020): Technical Specifications. – URL: file:///C:/Users/rol/Downloads/VOLT_power-RFB_Productsheet.pdf [Rev.: 09/07/2020].

VoltStorage GmbH: Voltstorage Smart. Weiterführende Informationen. – URL: https://voltstorage.com/wp-content/uploads/2020/06/VoltStorage-SMART-Weiterführende-Produktinformationen.pdf [Rev.: 08/07/2020].

Von Ardenne GmbH (2020): Einblicke in die Praxis der Herstellung von Dünnschichtphotovoltaik: personal message.

Wagner, M. (2020): Tailored Blanks: personal message.

Wagner, M., Jahn, A., Brenner, B. & Beyer, E. (2014): Innovative joining technologies for multi-material lightweight car body structures. – URL: https://www.iws.fraunhofer.de/content/dam/iws/en/documents/projects/joining/component_design/Paper_IABC2014_Fraunhofer_IWS_Dresden.pdf [Rev.: 24/06/2020].

Wagner, R. S. (1958): Production of Dislocations in Germanium by Thermal Shock. – Journal of Applied Physics, 29: 1679–1682.

Wambsganss, P. & Parspour, N. (2010): Kontaktlose Energieübertragung: Stromversorgung aus dem HF-Feld. – URL: https://www.elektroniknet.de/elektronik/power/stromversorgung-aus-dem-hf-feld-1644.html [Rev.: 14/07/2020].

Wang, J., Guo, M., Liu, M. & Wei, X. (2020): Long-term outlook for global rare earth production. – Resources Policy, 65: 101569.

Wang, Y., Yang, L., Shi, X.-L., Shi, X., Chen, L., Dargusch, M. S., Zou, J. & Chen, Z.-G. (2019): Flexible Thermoelectric Materials and Generators: Challenges and Innovations. – Advanced materials (Deerfield Beach, Fla.), 31: e1807916.

WBGU (2019): Unsere gemeinsame digitale Zukunft.

Weidner, E., Ortiz Cebolla, R. & Davies, J. (2019): Global deployment of large capacity stationary fuel cells. Drivers of, and barriers to, stationary fuel cell deployment. – Luxemburg.

Weltenergierat – Deutschland e. V. & Frontier Economics (2018): International aspects of a Power-to-X roadmap. – A report prepared for the World Energy Council Germany.

Werwitzke, C. (2019): ElectReon: Renault Zoe lädt induktiv während der Fahrt. – URL: https://www.electrive.net/2019/09/23/electreon-renault-zoe-laedt-induktiv-waehrend-der-fahrt/ [Rev.: 14/07/2020].

Wesseler, B. (2020): Ultrium9-Kassetten speichern 18 Terabyte. – URL: https://www.it-zoom.de/dv-dialog/e/ultrium9-kassetten-speichern-18-terabyte-26601/ [Rev.: 12/02/2021].

Wetzel, M. (2016): Materialbilanzen und Auswirkungen von Materialverfügbarkeit auf europäische Energieszenarien unter Berücksichtigung von Importen regelbaren Solarstroms. – Master thesis. Stuttgart University. – URL: https://elib.dlr.de/110449/1/Wetzel_Materialbilanzen_Materialverf%C3%BCgbarkeit.pdf [Rev.: 09/06/2020].

Wietelmann, U. & Steinbild, M. (2013): Lithium and Lithium Compounds. – Ullmann’s encyclopedia of industrial chemistry [Rev.: 14/07/2020].

Wietschel, M. (2020): Stellungnahme zum Policy Brief Elektromobilität und Klimaschutz: Die große Fehlkalkulation. – URL: https://www.isi.fraunhofer.de/content/dam/isi/dokumente/cce/2020/Stellungnahme_IfW-Langfassung.pdf [Rev.: 06/05/2021].

Wietschel, M., Arens, M., Dötsch, C. & Herkel, S. (2010): Energietechnologien 2050 – Schwerpunkte für Forschung und Entwicklung. – Technologienbericht. – Stuttgart, Germany.

Wietschel, M., Ullrich, S., Markewitz, P., Schulte, F. & Genoese, F. (editors) (2015): Energietechnologien der Zukunft. – Wiesbaden, Germany.

Wilts, H., Lucas, R., Gries, N. von & Zirngiebl, M. (2014): Recycling in Deutschland – Status quo, Potenziale, Hemmnisse und Lösungsansätze. – URL: https://www.kfw.de/PDF/Download-Center/Konzernthemen/Research/PDF-Dokumente-Studien-und-Materialien/SuM-Recycling-in-Deutschland-Wuppertal-Institut-Januar-2015.pdf [Rev.: 13/08/2015].

Winkel, P., Borisov, K., Grünhaupt, L., Rieger, D., Spiecker, M., Valenti, F., Ustinov, A. V., Wernsdorfer, W. & Pop, I. M. (2020): Implementation of a Transmon Qubit Using Superconducting Granular Aluminum. – Phys. Rev. X, 10: 4.

WiTricity (2018): The Next Wireless Revolution: Electric Vehicle Wireless Charging. Power and Efficiency.

Wittenauer, R., Smith, L. & Aden, K. (2013): Background Paper 6.12. Osteoarthritis. – URL: http://www.who.int/medicines/areas/priority_medicines/BP6_12Osteo.pdf.

Woidasky, J. & Jeanvré, S. (2015): Flugzeuge in der Kreislaufwirtschaft. – Wasser und Abfall, 2015: 36–40.

Woidasky, J., Klinke, C. & Jeanvré, S. (2017): Materials Stock of the Civilian Aircraft Fleet. – Recycling, 2: 21.

Wolf, J., Brüning, R., Nellesen, L. & Schiemann, J. (2017): Anforderungen an die Behandlung spezifischer Elektroaltgeräte unter Ressourcen- und Schadstoffaspekten.

Woodhouse, M. & Goodrich, A. (2013): A Manufacturing Cost Analysis Relevant to Single-and Dual-Junction Photovoltaic Cells Fabricated with III-Vs and III-Vs Grown on Czochralski Silicon. – (Presentation), NREL (National Renewable Energy Laboratory).

Woodruff, L. & Bedinger, G. (2013): Titanium –Light, Strong, and White. – [Rev.: 26/07/2020].

Woodruff, L. G., Bedinger, G. M. & Piatak, N. M. (2017): Titanium. Chapter T of Critical mineral resources of the United States – Economic and environmental geology and prospects for future supply. – [Rev.: 26/07/2020].

World Bank: Access to electricity. – URL: https://data.worldbank.org/indicator/EG.ELC.ACCS.ZS [Rev.: 22/01/2021].

World Bank (2013): Sustainable Energy for All. – URL: https://www.worldbank.org/en/topic/energy/brief/sustainable-energy-for-all [Rev.: 24/02/2021].

World Bank (2014): Electric power consumption (kWh per capita). – URL: https://data.worldbank.org/indicator/EG.USE.ELEC.KH.PC [Rev.: 22/01/2021].

World Economic Forum (2018): Harnessing Artificial Intelligence for the Earth.

Wu, F., Maier, J. & Yu, Y. (2020): Guidelines and trends for next-generation rechargeable lithium and lithium-ion batteries. – Chemical Society reviews, 49: 1569–1614.

Wuppertal Institut, Fraunhofer ISI & IZES (editors) (2017): Technologien für die Energiewende. – Teilbericht 2 an das Bundesministerium für Wirtschaft und Energie (BMWi). Wuppertal, Karlsruhe, Saarbrücken.

Wydra, S. & Schwarz, A. (2021): Synthetic fuels. – URL: https://ati.ec.europa.eu/sites/default/files/2021-02/PtGL%20Synthetic%20fuels.pdf [Rev.: 14/03/2021].

Xu, E. (2020): The future of transportation: White Paper on Urban Air Mobility Systems.

Yang, B., Murali, A., Nirmalchandar, A., Jayathilake, B., Prakash, G. K. S. & Narayanan, S. R. (2020): A Durable, Inexpensive and Scalable Redox Flow Battery Based on Iron Sulfate and Anthraquinone Disulfonic Acid. – J. Electrochem. Soc., 167: 60520.

Ying, P., He, R., Mao, J., Zhang, Q., Reith, H., Sui, J., Ren, Z., Nielsch, K. & Schierning, G. (2021): Towards tellurium-free thermoelectric

modules for power generation from low-grade heat. – Nature communications, 12: 1121.

Yole Développement (2019a): InP Wafer and Epiwafer Market Version 2019 – Photonics and RF Applications.

Yole Développement (2019b): Power GaN2019: Epitaxy, Devices, Applications & Technology Trends. – Market and Technology Report 2019.

Yole Développement (2020a): 5G's impact on RF front-end and connectivity for cellphones.

Yole Développement (2020b): GaAs Wafer and Epiwafer Market Version 2020 RF, Photonics, LED, Display and PV Applications. – Market and Technology Report 2020.

Yole Développement (2020c): Optical transceivers for datacom and telecom. – Market and technology report.

Yole Développement (2020d): Quantum Technologies. – Market and technology report.

Yusuf, S. M., Cutler, S. & Gao, N. (2019): Review: The Impact of Metal Additive Manufacturing on the Aerospace Industry. – Metals, 9.

Zednicek, T. (2006): Trends in Tantalum and Niobium Capacitors. – URL: https://www.researchgate.net/publication/228895537_Trends_in_Tantalum_and_Niobium_Capacitors.

Zednicek, T. (2019): Tantalum and niobium global trade statistics. Tantalum capacitors: current trends and potential future.

Zendehdel, M., Yaghoobi Nia, N. & Yaghoubinia, M. (2020): Emerging Thin Film Solar Panels. – In: Gok, A. (editor): Reliability and Ecological Aspects of Photovoltaic Modules.

Zhang, H., Li, X., Fang, Z., Yao, R., Zhang, X., Deng, Y., Lu, X., Tao, H., Ning, H. & Peng, J. (2018): Highly Conductive and Transparent AZO Films Fabricated by PLD as Source/Drain Electrodes for TFTs. – Materials (Basel, Switzerland), 11.

Zhang, J., Lenser, C., Menzler, N. H. & Guillon, O. (2020): Comparison of solid oxide fuel cell (SOFC) electrolyte materials for operation at 500 °C. – Solid State Ionics, 344: 115138.

Zhang, Y. & Park, N.-G. (2020): A thin film (<200 nm) perovskite solar cell with 18 % efficiency. – J. Mater. Chem. A, 8: 17420–17428.

Zhao, T. (2018): Sustainable Developement Strategy for EV Battery.

Zhou, H. & Lee, T.-W. (2020): From Foldable Phones to Stretchy Screens. – URL: https://spectrum.ieee.org/consumer-electronics/portable-devices/from-foldable-phones-to-stretchy-screens [Rev.: 07/01/2021].

Zientek, M. L., Loferski, P. J., Parks, H. L., Schulte, R. F. & Seal, R. R., II (2017): Platinum-Group Elements. – Chapter N of Critical Mineral Resources of the United States – Economic and Environmental Geology and Prospects for Future Supply [Rev.: 14/07/2020].

Zogbi, D. (2013): A Passion for Tantalum. – URL: https://www.ttii.com/content/ttii/en/marketeye/articles/categories/passives/me-zogbi-20130911.html [Rev.: 15/01/2021].

Zubi, G., Dufo-López, R., Carvalho, M. & Pasaoglu, G. (2018): The lithium-ion battery: State of the art and future perspectives. – Renewable and Sustainable Energy Reviews, 89: 292–308.

Zuser, A. & Rechberger, H. (2011): Considerations of resource availability in technology development strategies: The case study of photovoltaics. – Resources, Conservation and Recycling, 56: 56–65.

ZVEI (2003): Umbrella Specification. Passive Components: Ceramic Capacitors. – URL: http://www.zvei.org/fileadmin/user_upload/Fachverbaende/Electronic_Components/Umbrella_Specs/Passive_Components/Ceramic_Capacitors/USpecs_MLCC_DR_Ver02.pdf [Rev.: 06/10/2008].

ZVEI (2019): Technologie-Roadmap "Next Generation". Elektronische Komponenten und Systeme. – URL: https://www.zvei.org/fileadmin/user_upload/Presse_und_Medien/Publikationen/2019/November/ZVEI_Technologie-Roadmap_Next_Generation/ZVEI_Technologie-Roadmap_Next_Generation.pdf.

7 Abbreviations and glossary

3D	Three-dimensional
A	
ABS	Antilock brake system for motor vehicles
ACC	Adaptive Cruise Control
ACP	Adhesive Conductive Paste
AG	Asynchrounous generator
Ah	Ampere hours
AIM	Association for Automatic Identification and Mobility
Al	Aluminium
AM	Asynchronous motor
As	Arsenic
a-Si	Amorphous silicon
ASR	Traction control
ATO	Antimony tin oxide
B	
B	Boron
Ba	Barium
Barrel	Volumetric unit (1 barrel = 159 litres)
BEV	Battery-electric vehicle (battery-powered motor vehicle with purely electric drive)
BGR	Federal Institute for Geosciences and Natural Resources
Bi	Bismuth
BIPV	Building-integrated photovoltaics
BMU	Federal Ministry for the Environment, Nature Conservation and Nuclear Safety
bn	billion
bpd	barrels per day
BSCCO	Bismuth strontium calcium copper oxide
BST	Barium Strontium Titanate
BtL	Biomass to liquid
C	
C	Carbon
C_2H_5OH	Ethanol
Ca	Calcium
CA	Canada
CAD	Computer Aided Design
CAGR	Compound Annual Growth Rate
CCS	Carbon Capture and Storage
Cd	Cadmium
CDA	Copper Development Association
CdTe	Cadmium telluride
Ce	Cerium
CFRTP	Carbon-fibre-reinforced thermoplastic
CFRP	Carbon Fiber Reinforced Plastics
CIGS	Copper indium gallium (di)selenide
CIS	Copper indium (di)selenide
Cl	Chlorine
CIS	Commonwealth of Independent States (successor states of the Soviet Union)
CLC	Chemical Looping Combustion
CMOS	Complementary metal oxide semiconductor
CNT	Carbon nanotubes
Co	Cobalt
CO	Carbon monoxide
CO_2	Carbon dioxide
Cr	Chromium
CRT	Cathode Ray Tube
Cs	Caesium
CSP	Concentrating solar power
CtL	Coal to liquid
Cu	Copper
CVD	Chemical Vapor Deposition
D	
DC	Direct Current
DD	Direct Drive
DED	Direct Energy Deposition
DeNOx	Conversion of nitrogen oxides of flue gases to nitrogen by reduction (“denitrogenization”)
DLAR	Double Layer Anti Reflection
DLR	German Aerospace Center (Deutsches Zentrum für Luft- und Raumfahrt)
DNA	Desoxyribonucleic acid

DR Congo	Democratic Republic of Congo
DSSC	Dye-sensitized solar cell
dt	Time difference
Dy	Dysprosium
E	
ED	Electrodialysis
EDLC	Electrochemical Double Layer Capacitor
EE	Electrical and electronic (products)
EG	Electronic Grade (silicon)
EnEV	Energy-saving regulations
EoL-RR	End of Life Recycling Rate
EOR	Enhanced Oil Recovery
Er	Erbium
ESC	Electronic stability control for vehicles
ETF	Exchange-Traded Fund, London
Ethanol	C_2H_5OH
EU	European Union
eV	Electronvolt (unit of energy: 10^{19} eV = 1.6 Joule)
EV	Electric vehicles
EVA	Ethylene-Vinyl Acetate
F	
F	Fluor
F	Faraday (unit of electrical charge of electrical capacitors)
FCEV	Fuel-Cell-Electric-Vehicle
Fe	Iron
FED	Field Emitter Display
FHG IZM	Fraunhofer Institute for Reliability and Microintegration
FIR	Far infrared
ft	foot (1 ft = 30.48 cm)
FT	Fischer-Tropsch (fuel synthesis process)
FTTB	Fibre to the Building
FTTH	Fibre to the Home
FTTP	Fibre to the Premises
G	
g	Grammes
Ga	Gallium
Gd	Gadolinium
GDP	Gross Domestic Product
GE	General Electric Company
Ge	Germanium
GFRP	Glass-fiber reinforced plastic (fibreglass)
GLR	The weighted country risk of mining (GLR) is calculated as the sum of the shares of all countries in mining production, multiplied by the country risk (LR). The weighted country risk generally fluctuates between +1.5 and –1.5. Values above +0.5 are classified as low (green). Values between +0.5 and –0.5 indicate a medium risk (yellow). Values below –0.5 are considered critical (red).
GNP	Gross National Product
GoI	Germanium on Insulator
GPS	Global Positioning System (navigation satellite system of the U.S. military)
GtL	Gas to liquid
GWp	Gigawatt peak power (Power rating for solar cells)
H	
H_2	Hydrogen
H_2O	Water (vapour)
HAWT	Horizontal axis wind turbine
HCCI	Homogeneous Charge Compression Ignition
HDL	High definition laser
HEV	Hybrid-electric vehicle
HF	High Frequency
Hg	Mercury
HHI	Herfindahl-Hirschmann Index. The HHI is a ratio that indicates the concentration on a market. The index assumes values of between 0 and 10,000. With an HHI below 1,500, a market is considered to have a low concentration (green), between 1,500 and 2,500 points moderate (yellow) and above 2,500 a high concentration (red).
HPDL	High-power diode laser
HPMSR	Hybrid permanent-magnet excited and synchronous reluctance machine
Hz	Hertz (frequency unit)

I	
IC	Integrated Circuit
ICE	Internal Combustion Engine
ICT	Information and Communication Technology
IEA	International Energy Agency
IGCC	Integrated Gasification Combined Cycle
IGFC	Integrated Gasification Fuel Cell Cycle
In	Indium
InGaAs	Indium gallium arsenide semiconductor
IP	Internet Protocol
IPM	Inset-mounted permanent magnets
IPTV	Internet Protocol Television
IR	Infrared radiation (wavelength over 800 nm)
ISI	Fraunhofer Institute for Systems and Innovation Research
ISO	International Organization for Standardization
IT	Information Technology
ITO	Indium Tin Oxide

K	
K	Kelvin
kg	kilogramme
KIT	Karlsruhe Institut for Technology
km	kilometer
ksi	kilo-pound per square inch (1000 psi)
kt	kilotonne (1,000 tonnes)

L	
La	Lanthanum
LAN	Local Area Network
Laser	Light Amplification by Stimulated Emission of Radiation
Latency	“Ping”, run time of a data packet from the client (e.g. smartphone user) to the target server (e.g. a website) and back
lb	pound (weight unit) 1 lb = 0.454 kg
LCD	Liquid Crystal Display
LEDs	Light Emitting Diode
Li	Lithium
LiCAF	$LiCaAlF_6$
LiDAR	Light detection and ranging
LiLuF	$LiLuF_4$
LiSAF	$LiSrAlF_6$
LiSGAF	$LiSrGaF_6$
Li-ions	Lithium-ion high-performance electricity storage (rechargeable battery system)
LME	London Metal Exchange
LNA	Low Noise Amplifier
LR	The country risk (LR) is evaluated using the indicators from the World Bank on governance (Worldwide Governance Indicators, WGI)

M	
m	million
MBCCO	Mercury barium calcium copper oxide
MED	Multi-Effekt-Destillation
MEMS	Microelectromechanical systems
Mg	Magnesium
m(MIMO)	(massive) input massive output, multi-antenna communications system
MIV	Motorised private transport
MLCC	Multi Layer Ceramic Capacitor
MMIC	Monolithic Microwave Integrated Circuit
Mn	Manganese
Mo	Molybdenum
MOCVD	Metal Organic Chemical Vapor Deposition
Mono-coque	Self-supporting vehicle body
MSF	Multi-Stage Flash
MW	Megawatts (1 m Watts)
µm	micrometers (10^{-6} meters)

N	
N	Newton (unit of force, 1 N = 1 kg m/s^2)
N	Nitrogen
n/a	not applicable
n. a.	not available

n. s.	not specified
Nb	Niobium
Nd	Neodymium
Nd: YAG laser	Neodymium-doped yttrium aluminum garnet laser
NEDC	New European driving cycle
NFC	Near field communication
NGCC	Natural gas combined cycle
Ni	Nickel
Ni-Cd	Nickel cadmium (rechargeable battery system)
Ni-MH	Nickel-metal hydride (rechargeable battery system)
NIR	Near infrared
Nm	Newtonmeter (unit of torque)
nm	nanometer (1 nm = 10^{-9} meters)
O	
O	Oxygen
OCR	Optical Character Recognition
OCT	Optical coherence tomography
OECD	Organisation for economic cooperation and development
OICA	International Organization of Motor Vehicle Manufacturers, Paris
OLED	Organic Light-Emitting Diode
Os	Osmium
P	
P	Phosphorus
Pa	Pascal (1 Pa = 1 N/m^2)
PAN	Polyacrylonitrile
Pb	Lead
PBB	Polybrominated biphenyls
PBDE	Polybrominated diphenyl ethers
PBF	Powder Bed Fusion
PCB	Polychlorinated biphenyls
PC	Polycarbonate
Pd	Palladium
PDP	Plasma Display Panel
PECVD	Plasma Enhanced Chemical Vapor Deposition
PEM	Proton-exchange membrane (polymer-electrolyte membrane)
PET	Polyethylene terephthalate
PET	Positron emission tomography
PHEV	Plug-in hybrid vehicle (mains-chargeable electric hybrid vehicle)
pin	positive intrinsic negative diode
PJ	Petajoule (10^{15} Joule)
PC	Passenger car
PLA	Polylactic acid
plc	public limited company
Pm	Promethium (radioactive element)
PM	Permanent magnet
PP	Polypropylene
Pr	Praseodymium
PS	Polystyrene
psi	pounds per square inch (1 psi = 6,894.76 N/mm^2)
Pt	Platinum
PV	Photovoltaics
PVC	Polyvinyl chloride
PVD	Physical Vapour Deposition (coating process)
R	
R&D	Research and Development
Radar	Radio detection and ranging
Re	Rhenium
REM	Rare Earth Metals
REEV	Range-Extended Electric Vehicle
RFID	Radio Frequency Identification
Rh	Rhodium
RO	Reverse osmosis
RoHS	Restriction of the use of certain Hazardous Substances (Directive 2002/95/EC)
ROW	Rest Of the World
rpm	Revolutions per minute (60 rpm = 1 Hz)
RTD&E	Research, Development, Test & Evaluation
Ru	Ruthenium
S	
S	Sulphur
Sb	Antimony

Sc	Scandium
SCR	Selective Catalytic Reduction (reduction of nitrogen oxides)
ScSZ	Scandia-stabilized zirconia
Se	Selenium
SEO	Rare Earth Metal Oxides
SED	Surface Conduction Electron Emitter Display
SG	Synchronous generator
Si	Silicon
SiGe	Silicon germanium semiconductor
Sm	Samarium
SM	Synchronous motor
SMD	Surface Mounted Device (pluggable electronic components)
Sn	Tin
SOFC	Solid Oxid Fuel Cell
SPECT	Single Photon Emission Computed Tomography
SPM	Surface-mounted Permanent Magnets
Sr	Strontium
SR	Switched Reluctance
STC	Silicon tetrachloride
SWOT	Strength, Weakness, Opportunities and Threats
T	
T	Tesla (unit of magnetic field strength)
t	tonne
Ta	Tantalum
tag	Smart Label, Smart Ticket, Smart Card (RFID Transponder)
Tailored Blanks	Body panel welded together from various panel thicknesses of different steel quality
Tb	Terbium
TBCCO	Thallium barium calcium copper oxide
TCO	Transparent Conducting Oxide
Te	Tellurium
TEG	Thermoelectric generators
Ti	Titanium
TIC	Tantalum-Niobium International Study Center
TJ	Terajoule (10^{12} Joule)
Tm	Thulium
tn	trillion
tonnes of materials/ tonnes of metal content	Tonnes of the element / metal in question
t/a	tonnes per year
U	
UAE	United Arab Emirates
UBA	German Environment Agency
UBSW	University of New South Wales, Sydney, Australia
UHF	Ultra High Frequency
UHMWPE	Ultra High Molecular Weight PolyEthylene
Ultra-sound	Sound at frequencies above 16 kHz
UMTS	Universal Mobile Telecommunications System
USD	US Dollars
US	United States of America (country code)
USGS	United States Geological Survey
UV	Ultraviolet
V	
V	Vanadium
VAWT	Vertical axis wind turbine type
VCI	German Association of the Chemical Industry
VDA	German Association of the Automotive Industry
VDE	German Association for Electrical, Electronic & Information Technologies
VDI	Association of German Engineers
V-RFB	Vanadium Redox Flow Batteries
W	
W	Tungsten
WEEE	Waste Electric and Electronic Equipment (EU Directive 2002/96/EC)
WiFi	Wireless Ethernet Compatibility Alliance
WLAN	Wireless Local Area Network

WLED	White Light Emitting Diode
WT	Wind turbine
wt%	Percentage by mass
X	
XtL	Collective term for GtL, CtL and BtL processes
Y	
Y	Yttrium
YAG	$Y_3Al_5O_{12}$ (yttrium aluminium garnet)
Yb	Ytterbium
YBCO	Yttrium barium copper oxide
YGO	Yttrium gadolinium oxide
YLF	$YLiF_4$
YSZ	Yttria-stabilized zirconia
Z	
Zn	Zinc
Zr	Zirconium
ZVEI	German Association of the electro and digital industry

Deutsche Rohstoffagentur
Bundesanstalt für Geowissenschaften und Rohstoffe

Deutsche Rohstoffagentur (DERA) in der
Bundesanstalt für Geowissenschaften und Rohstoffe (BGR)

Wilhelmstr. 25–30
13593 Berlin
Phone: +49 30 36993 226
dera@bgr.de
www.dera.bund.de

ISBN: 978-3-948532-61-1 (print version)
ISBN: 978-3-948532-62-8 (pdf)
ISSN: 2193-5319